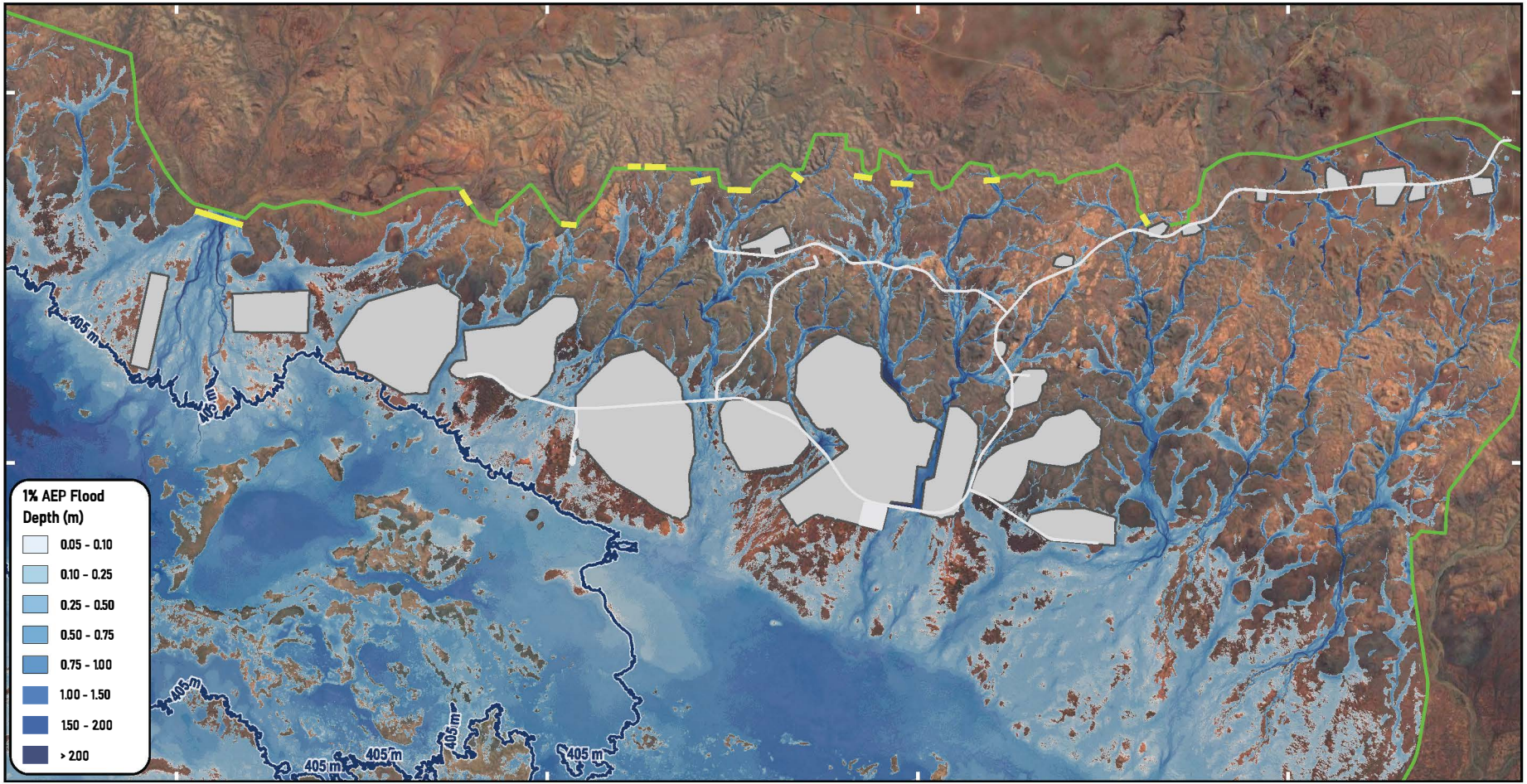

N

2 4 km

GDA94 / MGA zone 50

Legend

- Model Inflow
- Rain On Grid Model Boundary
- 1% AEP Claypan Flood Level (405 mRL)
- Proposed Haul Road
- Surface Water Containment Area

- Predicted maximum flood depths from a 2D HEC RAS model developed using LIDAR data from 2023, plus terrain modifications to simulate the impacts of surface water containment areas and project haul roads
- Flood depths <0.05m not shown
- The purpose of the model was to simulate hydrological conditions within, and immediately downstream of, mine development areas associated with the Mulga Downs Project.
- Inflow hydrographs were input around the boundary of the model and rain-on-grid calculations used to simulate runoff across the model domain.
- Flood depths upstream of the inflow boundary conditions are not valid.
- Depths of ponded water within the valley floor (e.g., in the claypans) are likely to be underpredicted as not all runoff from within the model will have drained by the end of the simulation period
- Maximum water levels resulting from rainfall-runoff (modelled depths) and claypan storage (contour) are unlikelyto occur simultaneously as they will be driven by different magnitude and duration rainfall events.

Data sources: Background Image: Base map and data from Google. © https://www.google.com/

P:\17764 GIS\Workspaces\493a_Figures\Appendix B.qgz: Figure B6 - 1% Depth (dark)

AQ2

Hydrology Figure C6 Developed Scenario 1% AEP Flood Depth

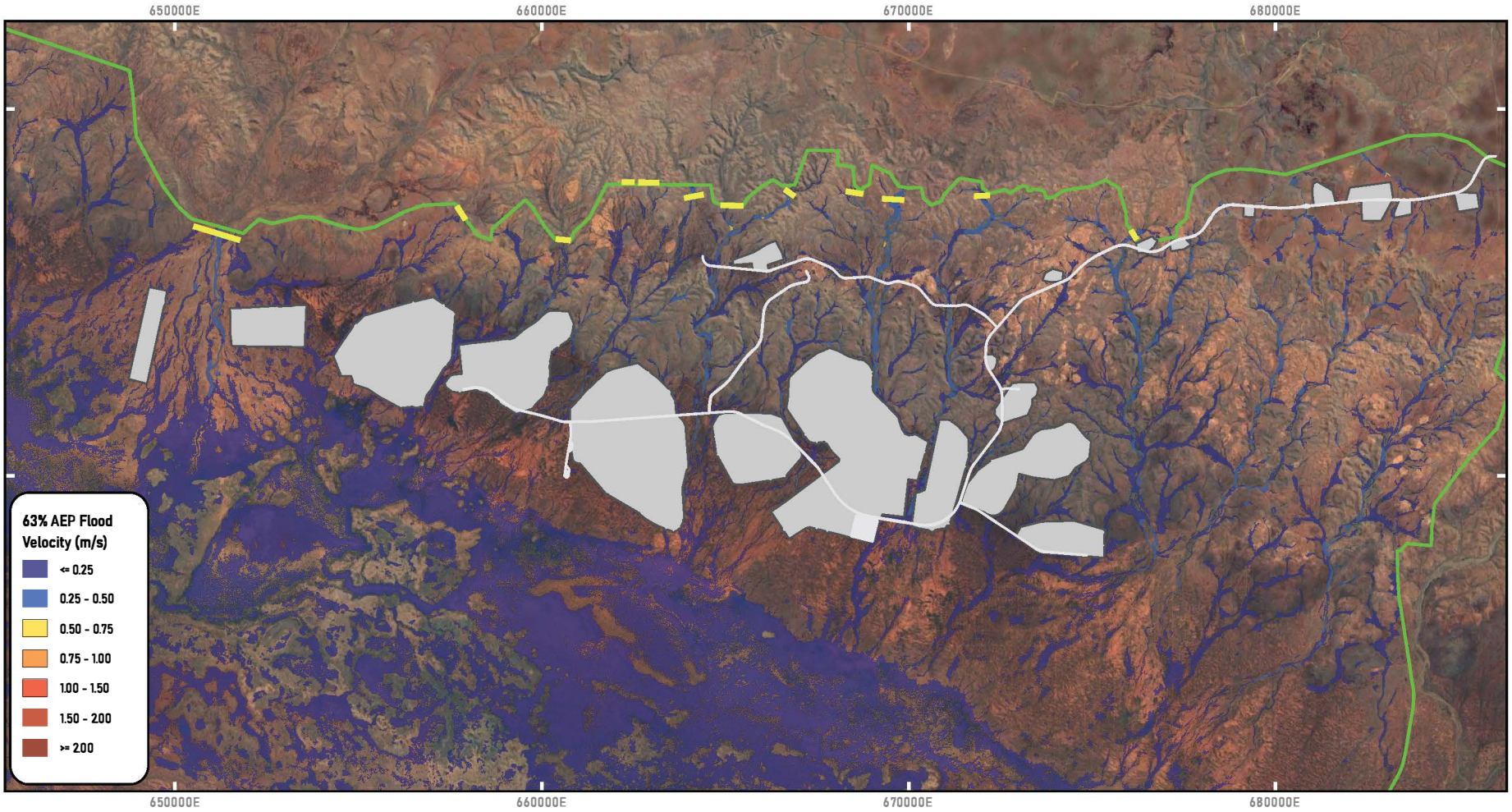

N

2 4 km

GDA94 / MGA zone 50

Legend

- Model Inflow
- Rain On Grid Model Boundary
- Proposed Haul Road
- Surface Water Containment Area

- Predicted maximum flood velocities are from the simulation period of a 2D HEC RAS model developed using LIDAR data from 2023
- The purpose of the model was to simulate hydrological conditions within, and immediately downstream of, mine development areas associated with the Mulga Downs Project.
- Inflow hydrographs were input around the boundary of the model and rain-on-grid calculations used to simulate runoff across the model domain.
- Flood velocities upstream of the inflow boundary conditions are not valid
- The claypan extent has been output from water balance modelling.

Data sources: Background Image: Base map and data from Google. © https://www.google.com/

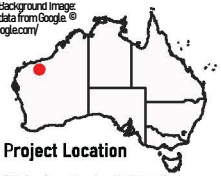

P:\17114 GIS\Workspaces\493a_Figures\Appendix B.qgz: Figure B7 - 63% Velocity (plan)

AQ2

Hydrology Figure C7
Developed Scenario
63% AEP Flood Velocity

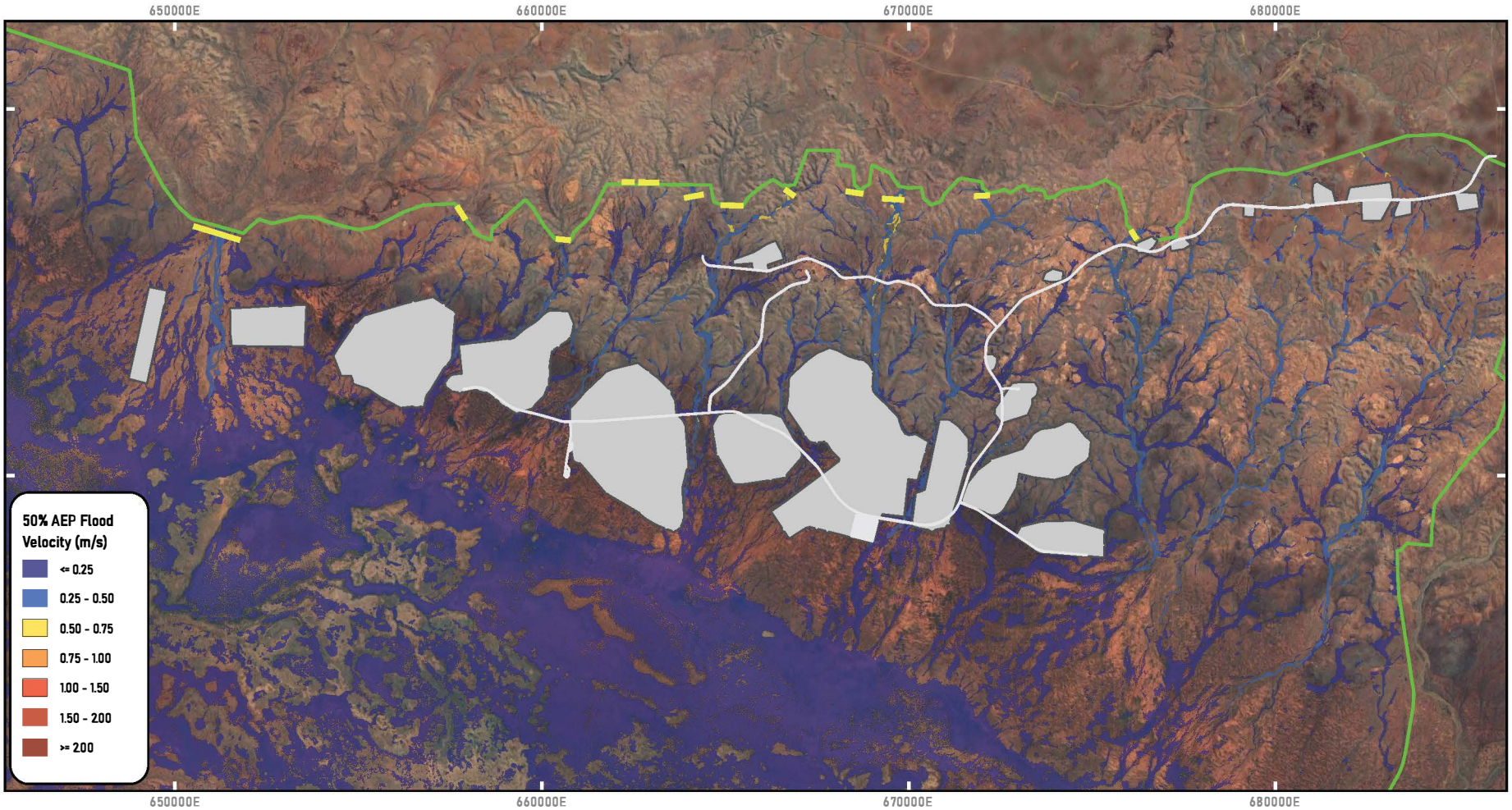

N

2 4 km

GDA94 / MGA zone 50

Legend

- Model Inflow
- Rain On Grid Model Boundary
- Proposed Haul Road
- Surface Water Containment Area

- Predicted maximum flood velocities are from the simulation period of a 2D HEC RAS model developed using LIDAR data from 2023
- The purpose of the model was to simulate hydrological conditions within, and immediately downstream of, mine development areas associated with the Mulga Downs Project.
- Inflow hydrographs were input around the boundary of the model and rain-on-grid calculations used to simulate runoff across the model domain.
- Flood velocities upstream of the inflow boundary conditions are not valid
- The claypan extent has been output from water balance modelling.

Data sources: Background Image: Base map and data from Google. © https://www.google.com/

P:\17114 GIS\Workspaces\A93a_Figures\Appendix B.qgz: Figure B8 - 50% Velocity (plan)

AQ2

Hydrology Figure C8 Developed Scenario 50%AEP Flood Velocity

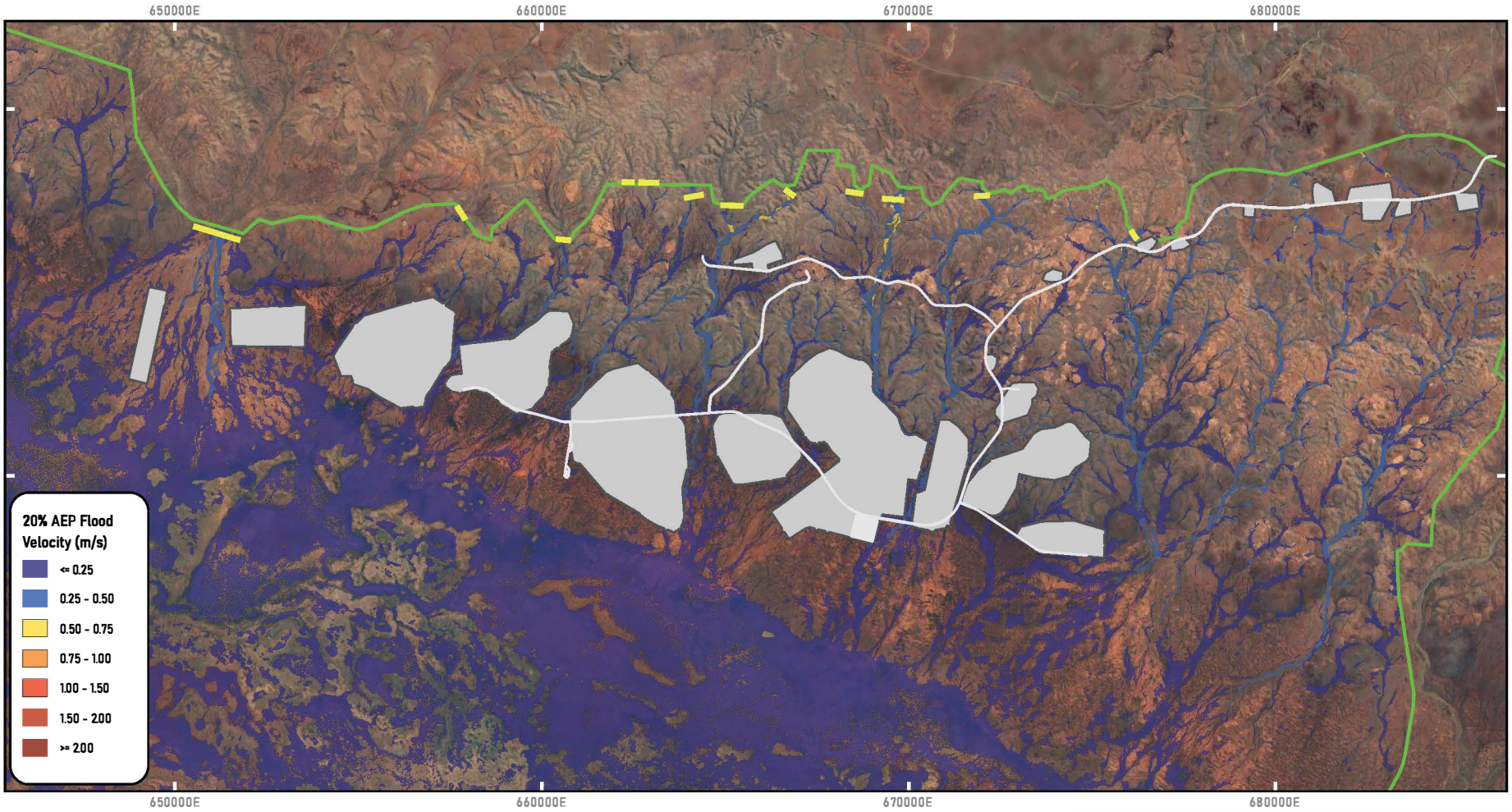

N

2 4 km

GDA94 / MGA zone 50

Legend

- Model Inflow
- Rain On Grid Model Boundary
- Proposed Haul Road
- Surface Water Containment Area

- Predicted maximum flood velocities are from the simulation period of a 2D HEC RAS model developed using LIDAR data from 2023
- The purpose of the model was to simulate hydrological conditions within, and immediately downstream of, mine development areas associated with the Mulga Downs Project.
- Inflow hydrographs were input around the boundary of the model and rain-on-grid calculations used to simulate runoff across the model domain.
- Flood velocities upstream of the inflow boundary conditions are not valid
- The claypan extent has been output from water balance modelling.

Data sources: Background Image: Base map and data from Google. © https://www.google.com/

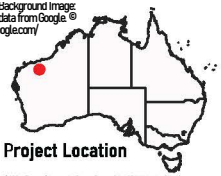

P:\17114 GIS\Workspaces\A93a_Figures\Appendix B.qgz: Figure B9 - 20% Velocity (plan)

AQ2

Hydrology Figure C9 Developed Scenario 20% AEP Flood Velocity

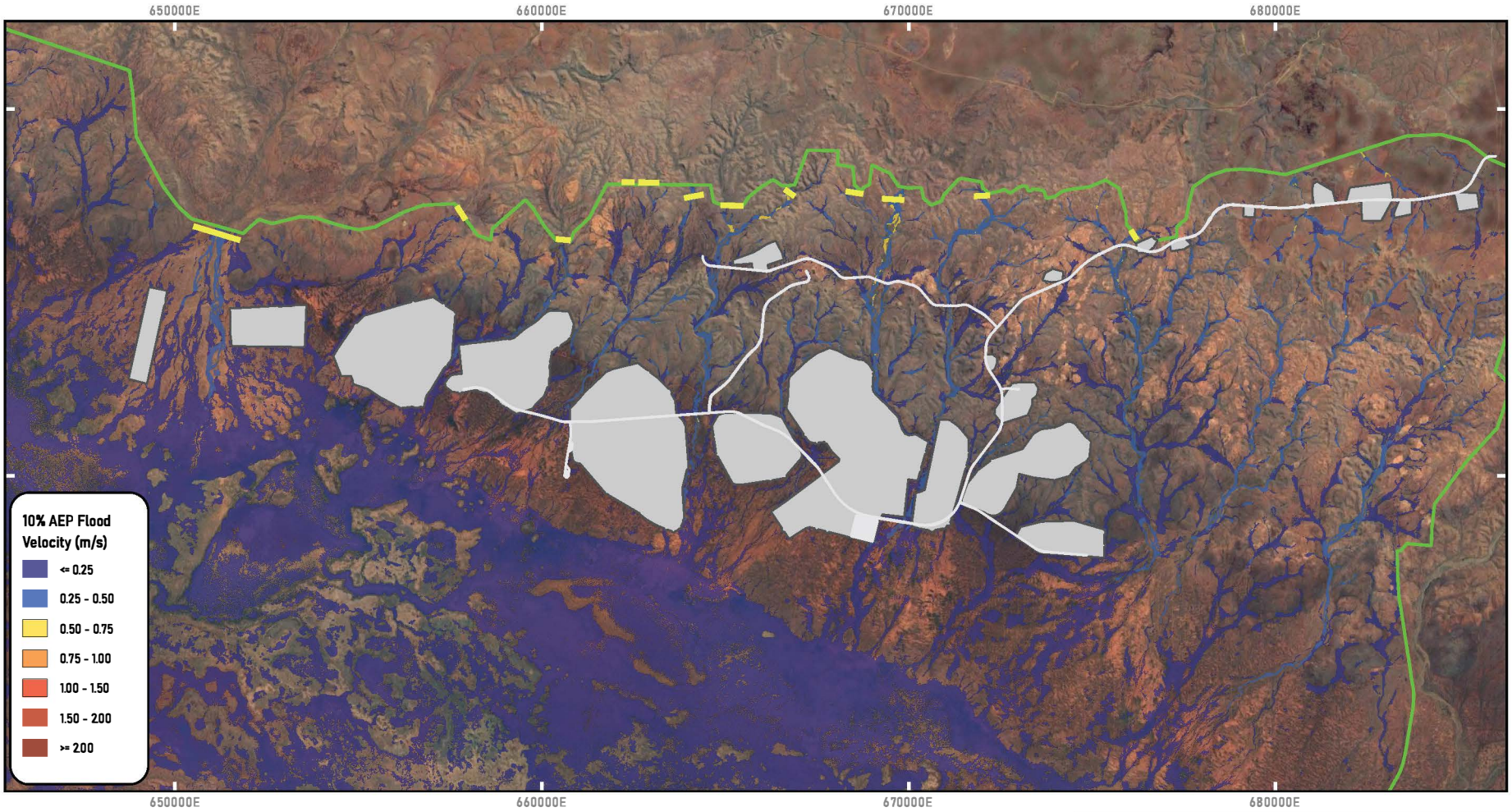

N

2 4 km

GDA94 / MGA zone 50

Legend

- Model Inflow
- Rain On Grid Model Boundary
- Proposed Haul Road
- Surface Water Containment Area

- Predicted maximum flood velocities are from the simulation period of a 2D HEC RAS model developed using LIDAR data from 2023
- The purpose of the model was to simulate hydrological conditions within, and immediately downstream of, mine development areas associated with the Mulga Downs Project.
- Inflow hydrographs were input around the boundary of the model and rain-on-grid calculations used to simulate runoff across the model domain.
- Flood velocities upstream of the inflow boundary conditions are not valid
- The claypan extent has been output from water balance modelling.

Data sources: Background Image: Base map and data from Google. © https://www.google.com/

P:\17114 GIS\Workspaces\A93a_Figures\Appendix B.qgz: Figure B10 - 10% Velocity (start)

AQ2

Hydrology Figure C10 Developed Scenario 10% AEP Flood Velocity

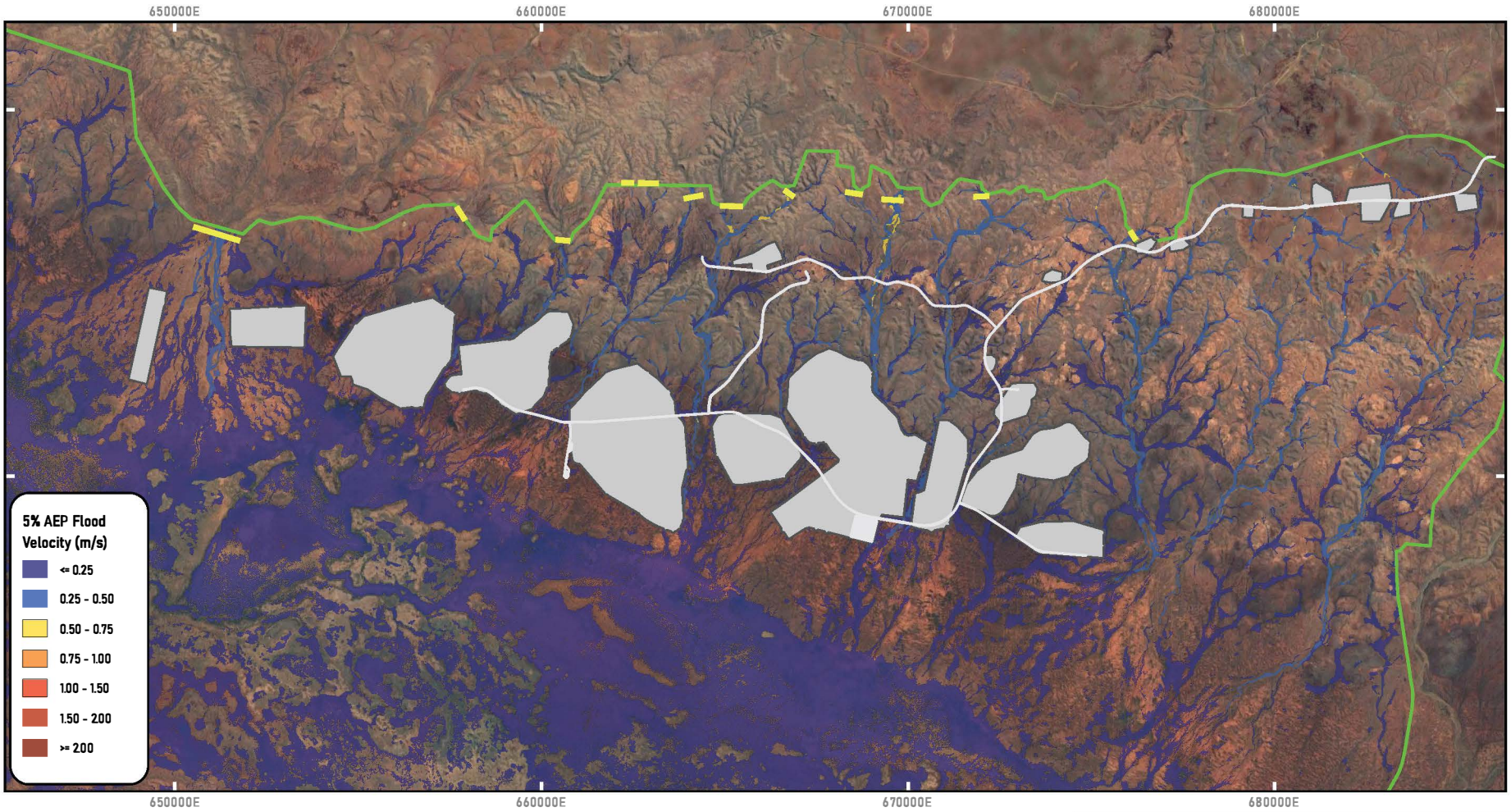

N

2 4 km

GDA94 / MGA zone 50

Legend

- Model Inflow
- Rain On Grid Model Boundary
- Proposed Haul Road
- Surface Water Containment Area

- Predicted maximum flood velocities are from the simulation period of a 2D HEC RAS model developed using LIDAR data from 2023
- The purpose of the model was to simulate hydrological conditions within, and immediately downstream of, mine development areas associated with the Mulga Downs Project.
- Inflow hydrographs were input around the boundary of the model and rain-on-grid calculations used to simulate runoff across the model domain.
- Flood velocities upstream of the inflow boundary conditions are not valid
- The claypan extent has been output from water balance modelling.

Data sources: Background Image: Base map and data from Google. © https://www.google.com/

P:\771\AGIS\Workspaces\493a_Figures\Appendix B.qgz: Figure B11 - 5% Velocity (plan1)

AQ2

Hydrology Figure C11
Developed Scenario
5% AEP Flood Velocity

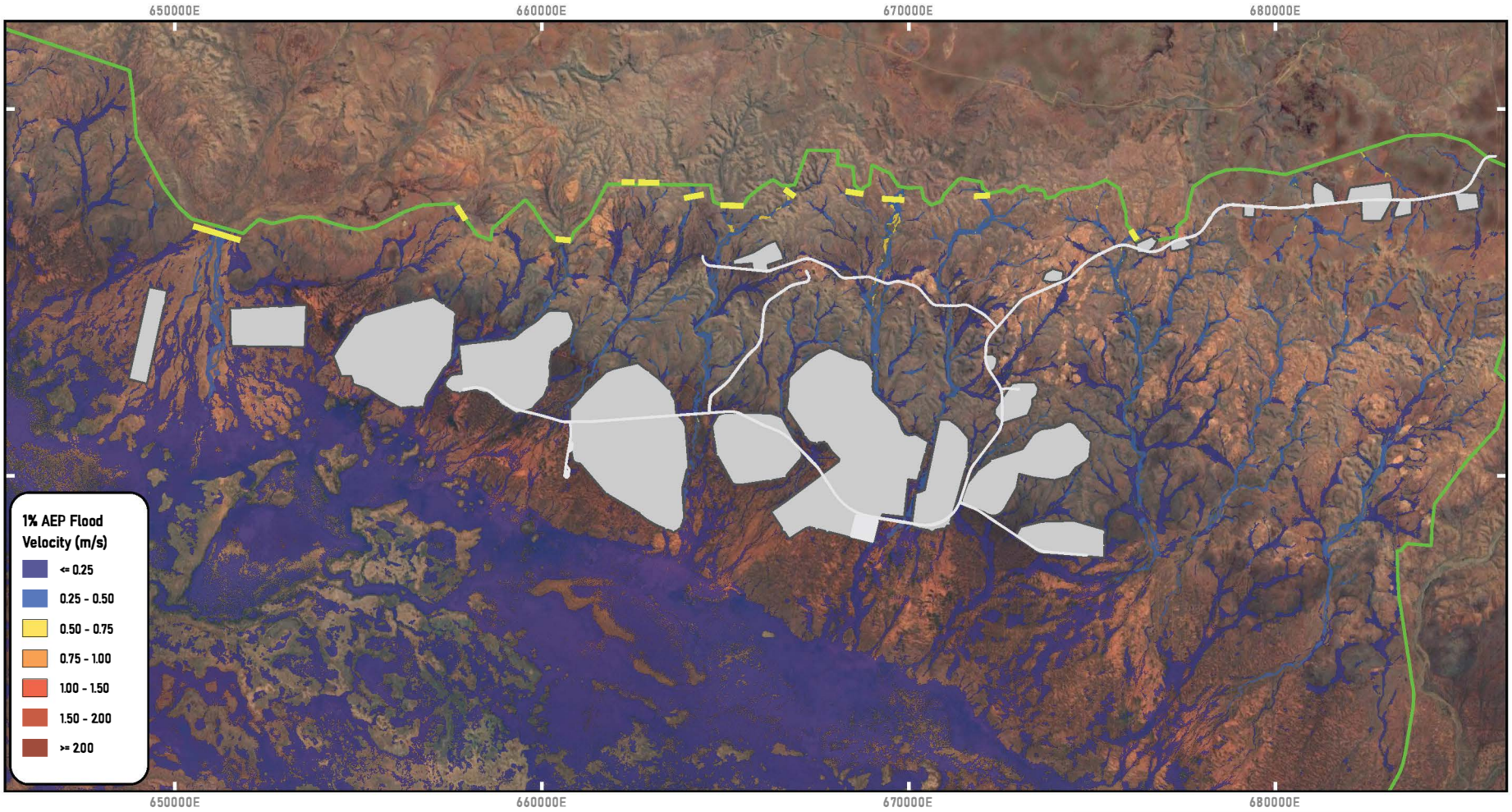

N

2 4 km

GDA94 / MGA zone 50

Legend

- Model Inflow
- Rain On Grid Model Boundary
- Proposed Haul Road
- Surface Water Containment Area

- Predicted maximum flood velocities are from the simulation period of a 2D HEC RAS model developed using LIDAR data from 2023
- The purpose of the model was to simulate hydrological conditions within, and immediately downstream of, mine development areas associated with the Mulga Downs Project.
- Inflow hydrographs were input around the boundary of the model and rain-on-grid calculations used to simulate runoff across the model domain.
- Flood velocities upstream of the inflow boundary conditions are not valid
- The claypan extent has been output from water balance modelling.

Data sources: Background Image: Base map and data from Google. © https://www.google.com/

P:\17114 GIS\Workspaces\A93a_Figures\Appendix B.qgz: Figure B12 – 1% Velocity (plan1)

AQ2

Hydrology Figure C12
Developed Scenario
1% AEP Flood Velocity

APPENDIX D
DIFFERENCE FLOOD MAPPING

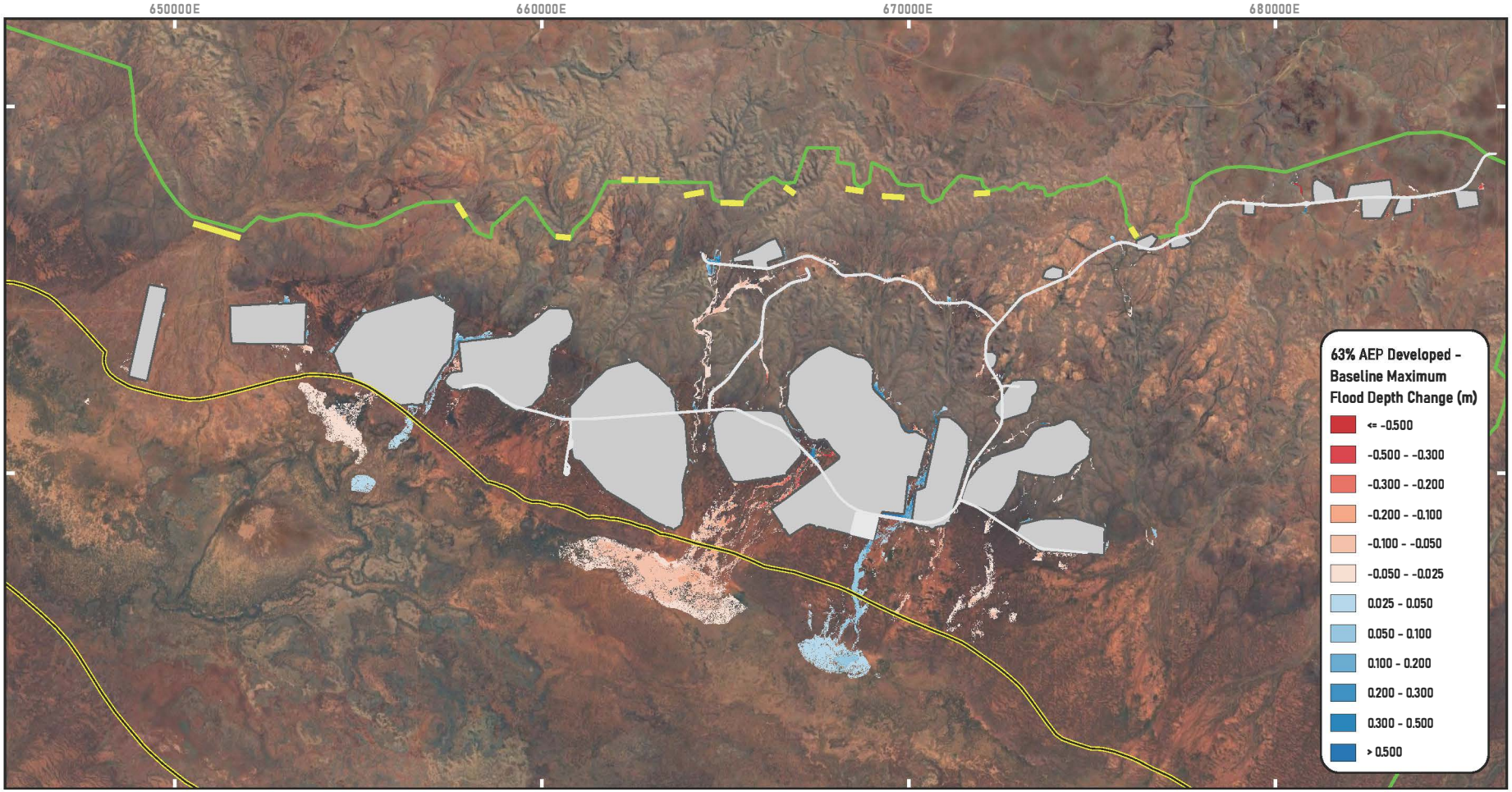

N

2 4 km

GDA94 / MGA zone 50

Legend

- Model Inflow
- Rain On Grid Model Boundary
- Proposed Haul Road
- Surface Water Containment Area
- Mungurrdu

- Difference between maximum predicted flood depths shown.
- A positive difference between flood depths indicates increased post-development flooding.
- Flood depth differences less than 0.05m are not shown.

Data sources: Background Image: Base map and data from Google. © https://www.google.com/

P:\1770A GIS\Workspaces\693a_Figures\Appendix C.qgz: Figure C1 - 63% Depth Diff (alert)

AQ2

Hydrology Figure D1
63% AEP Existing and Developed Maximum Flood Depth Difference Map

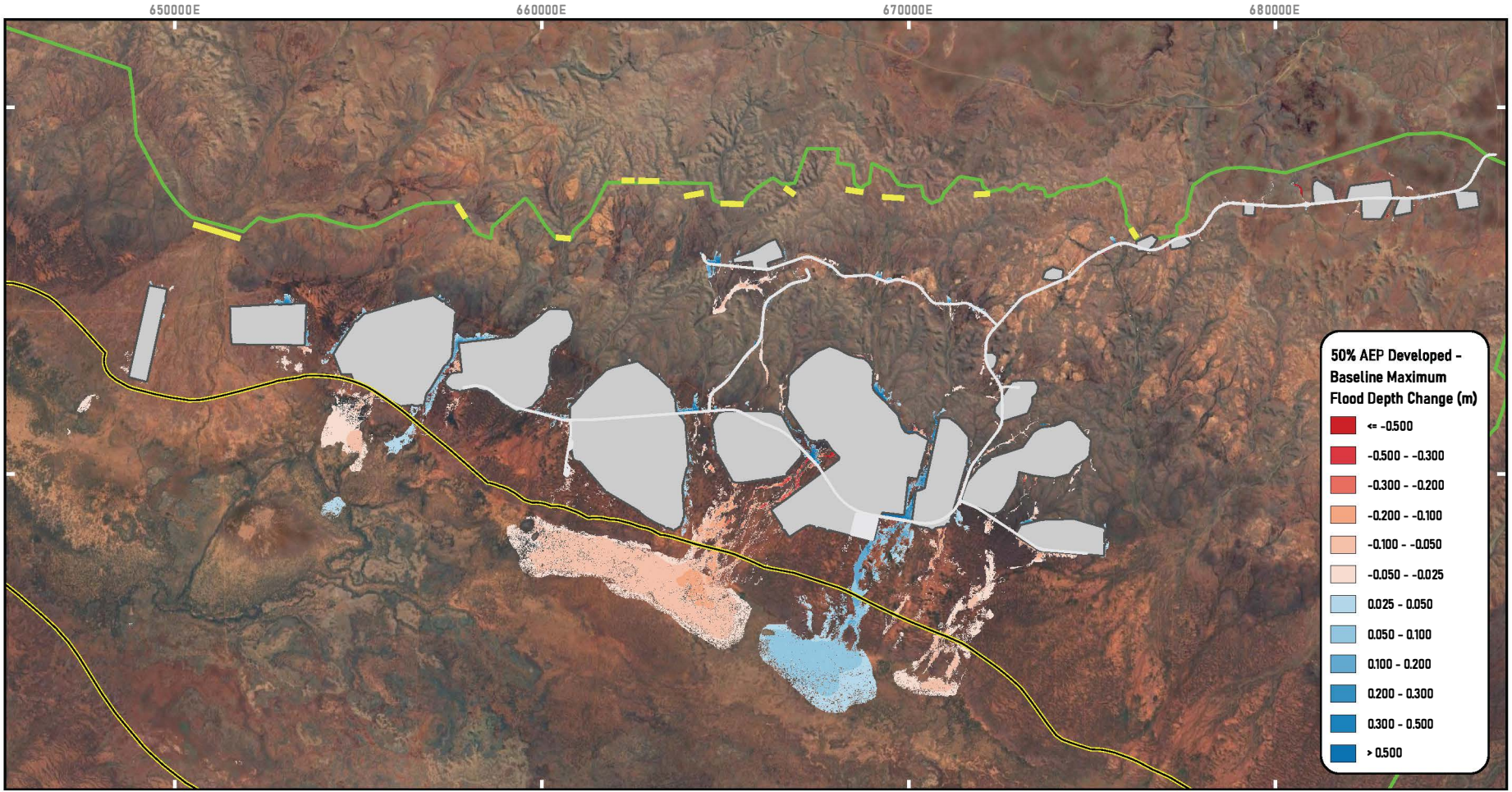

N

2 4 km

GDA94 / MGA zone 50

Legend

- Model Inflow
- Rain On Grid Model Boundary
- Proposed Haul Road
- Surface Water Containment Area
- Mungurrdu

- Difference between maximum predicted flood depths shown.
- A positive difference between flood depths indicates increased post-development flooding.
- Flood depth differences less than 0.05m are not shown.

Data sources: Background Image: Base map and data from Google. © https://www.google.com/

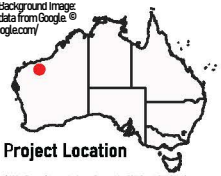

P:\17764 GIS\Workspaces\A93a_Figures\Appendix C.qgz: Figure C2 – 50% Depth Diff (plan1).

AQ2

Hydrology Figure D2
50% AEP Existing and Developed Maximum Flood Depth Difference Map

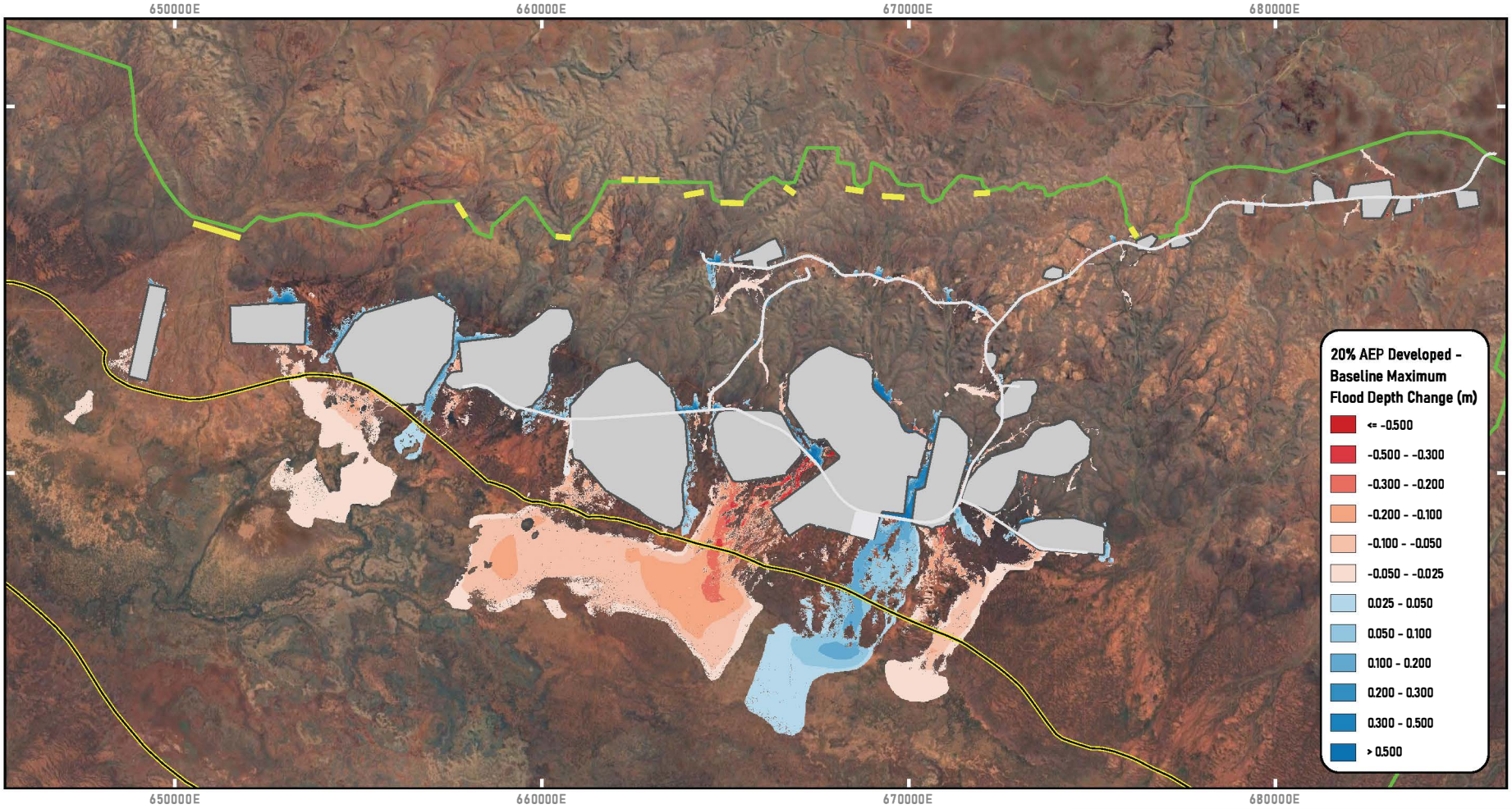

N

2 4 km

GDA94 / MGA zone 50

Legend

- Model Inflow
- Rain On Grid Model Boundary
- Proposed Haul Road
- Surface Water Containment Area
- Mungurrdu

- Difference between maximum predicted flood depths shown.
- A positive difference between flood depths indicates increased post-development flooding.
- Flood depth differences less than 0.05m are not shown.

Data sources: Background Image: Base map and data from Google. © https://www.google.com/

P:\17764 GIS\Workspaces\A93a_Figures\Appendix C.qgz: Figure C3 – 20% Depth Diff (plot)

AQ2

Hydrology Figure D3
20% AEP Existing and Developed Maximum Flood Depth Difference Map

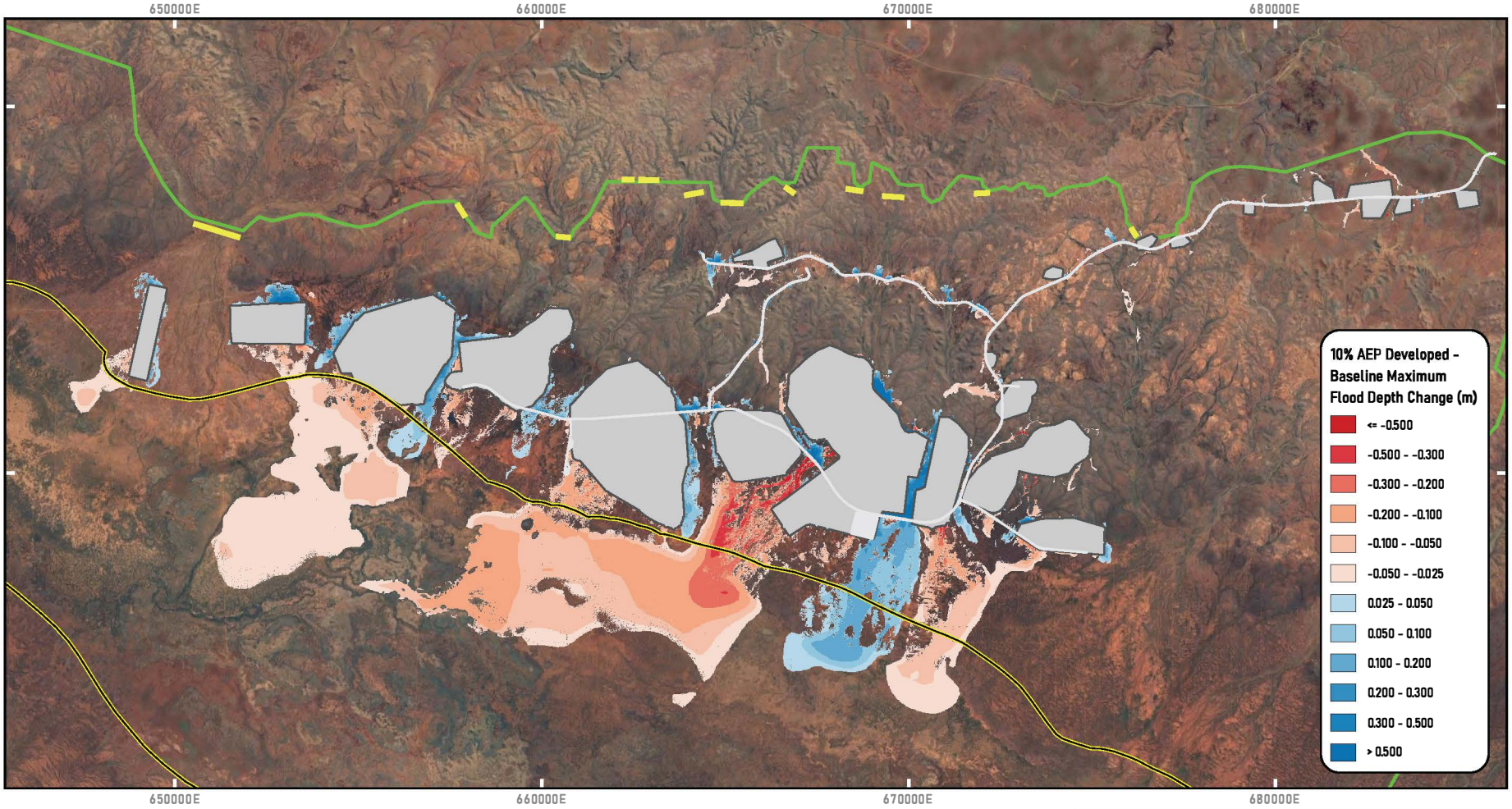

N

2 4 km

GDA94 / MGA zone 50

Legend

- Model Inflow
- Rain On Grid Model Boundary
- Proposed Haul Road
- Surface Water Containment Area
- Mungurrdu

- Difference between maximum predicted flood depths shown.
- A positive difference between flood depths indicates increased post-development flooding.
- Flood depth differences less than 0.05m are not shown.

Data sources: Background Image: Base map and data from Google. © https://www.google.com/

P:\17114 GIS\Workspaces\A93a_Figures\Appendix C.qgz: Figure C4 - 10% Depth Diff (dev)

AQ2

Hydrology Figure D4
10% AEP Existing and Developed
Maximum Flood Depth Difference Map

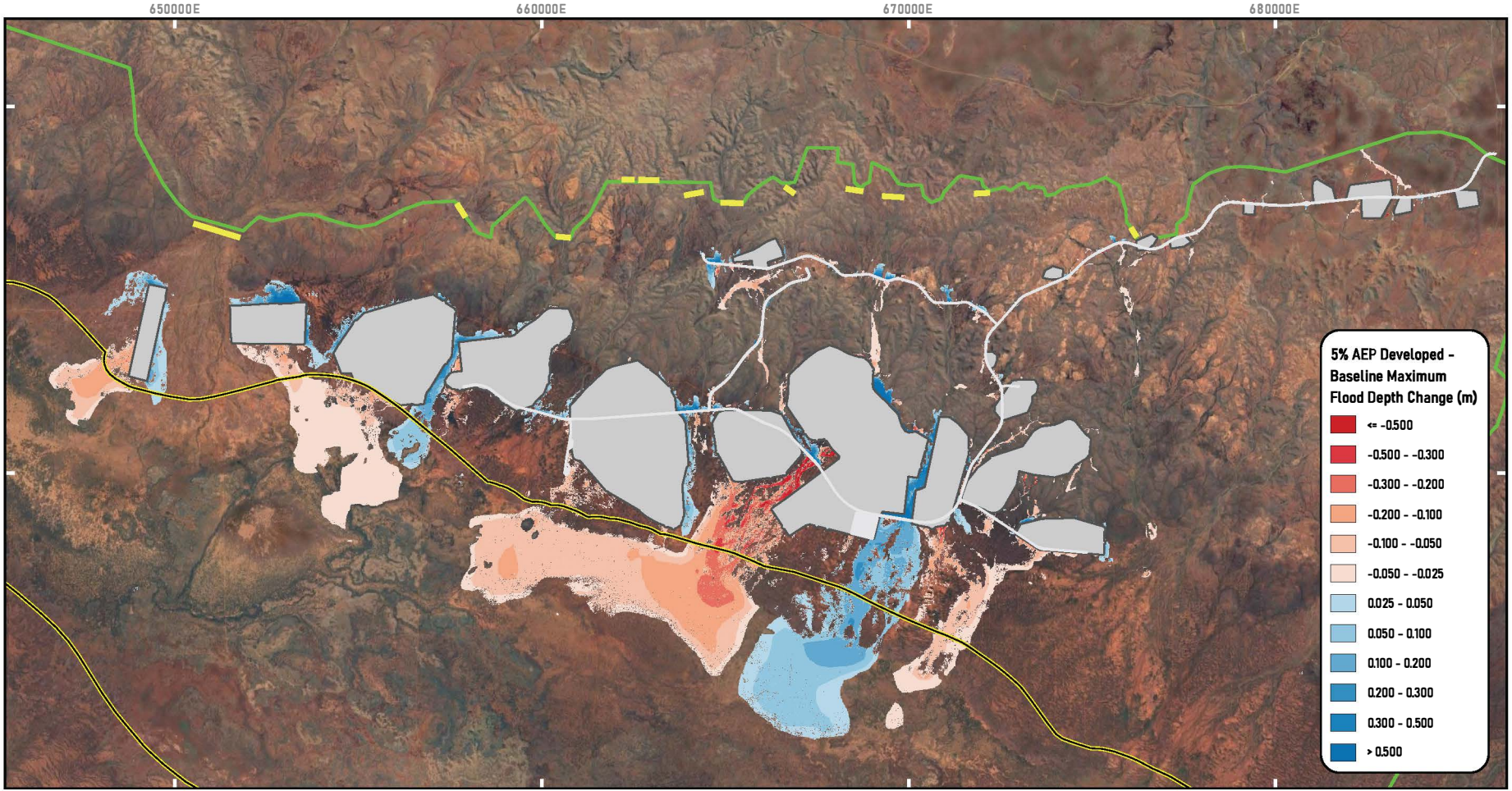

N

2 4 km

GDA94 / MGA zone 50

Legend

- Model Inflow
- Rain On Grid Model Boundary
- Proposed Haul Road
- Surface Water Containment Area
- Mungurrdu

- Difference between maximum predicted flood depths shown.
- A positive difference between flood depths indicates increased post-development flooding.
- Flood depth differences less than 0.05m are not shown.

Data sources: Background Image: Base map and data from Google. © https://www.google.com/

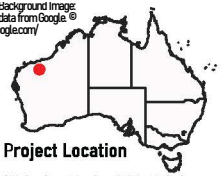

P:\17764 GIS\Workspaces\A93a_Figures\Appendix C.qgz: Figure C5 - 5% Depth Diff (start)

AQ2

Hydrology Figure D5
5% AEP Existing and Developed Maximum Flood Depth Difference Map

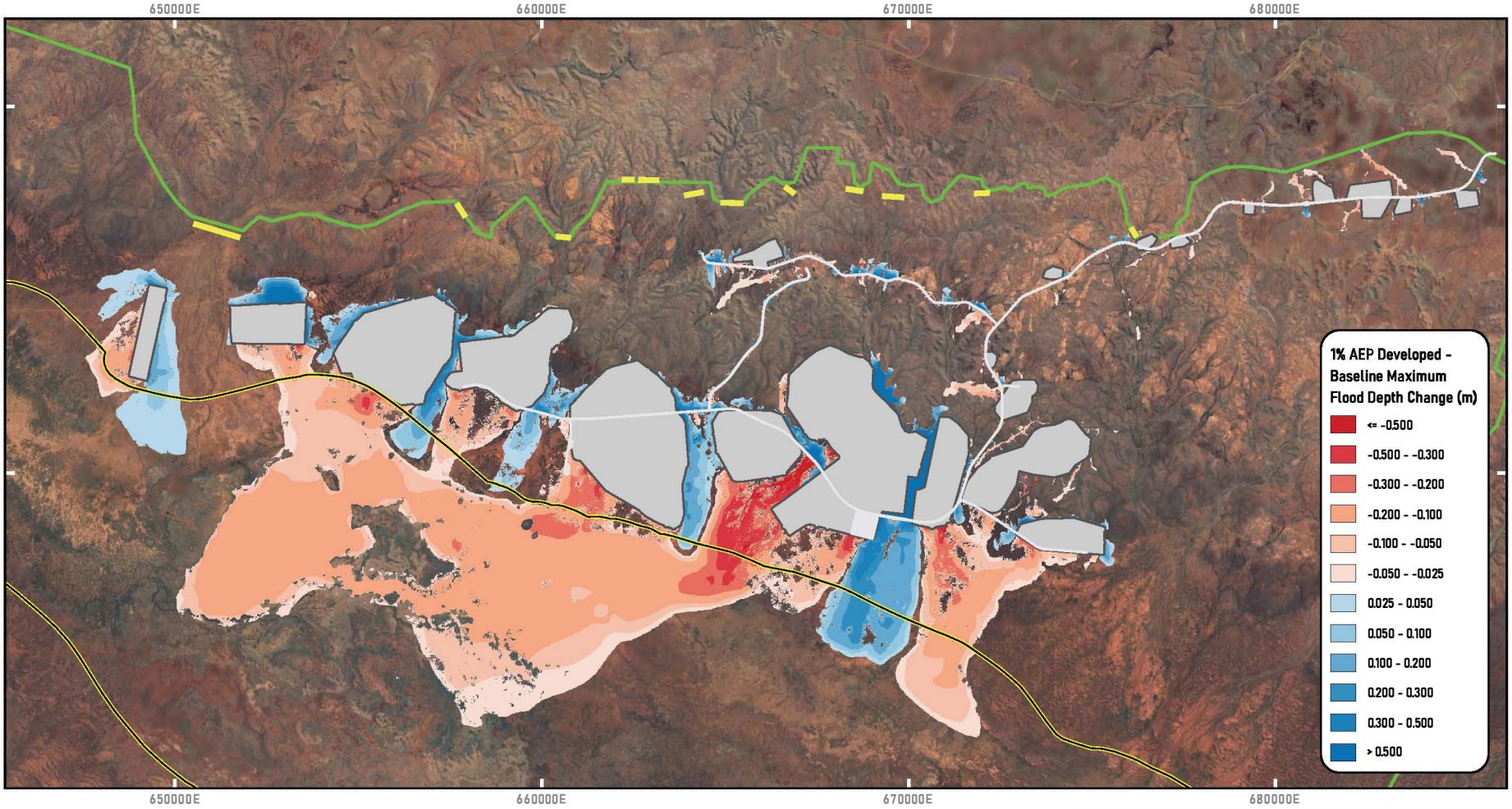

N

2 4 km

GDA94 / MGA zone 50

Legend

- Model Inflow
- Rain On Grid Model Boundary
- Proposed Haul Road
- Surface Water Containment Area
- Mungurrdu

- Difference between maximum predicted flood depths shown.
- A positive difference between flood depths indicates increased post-development flooding.
- Flood depth differences less than 0.05m are not shown.

Data sources: Background Image: Base map and data from Google. © https://www.google.com/

P:\17764 GIS\Workspaces\A93a_Figures\Appendix C.qgz: Figure C6 - 1% Depth Diff (start)

AQ2

Hydrology Figure D6

1% AEP Existing and Developed Maximum Flood Depth Difference Map

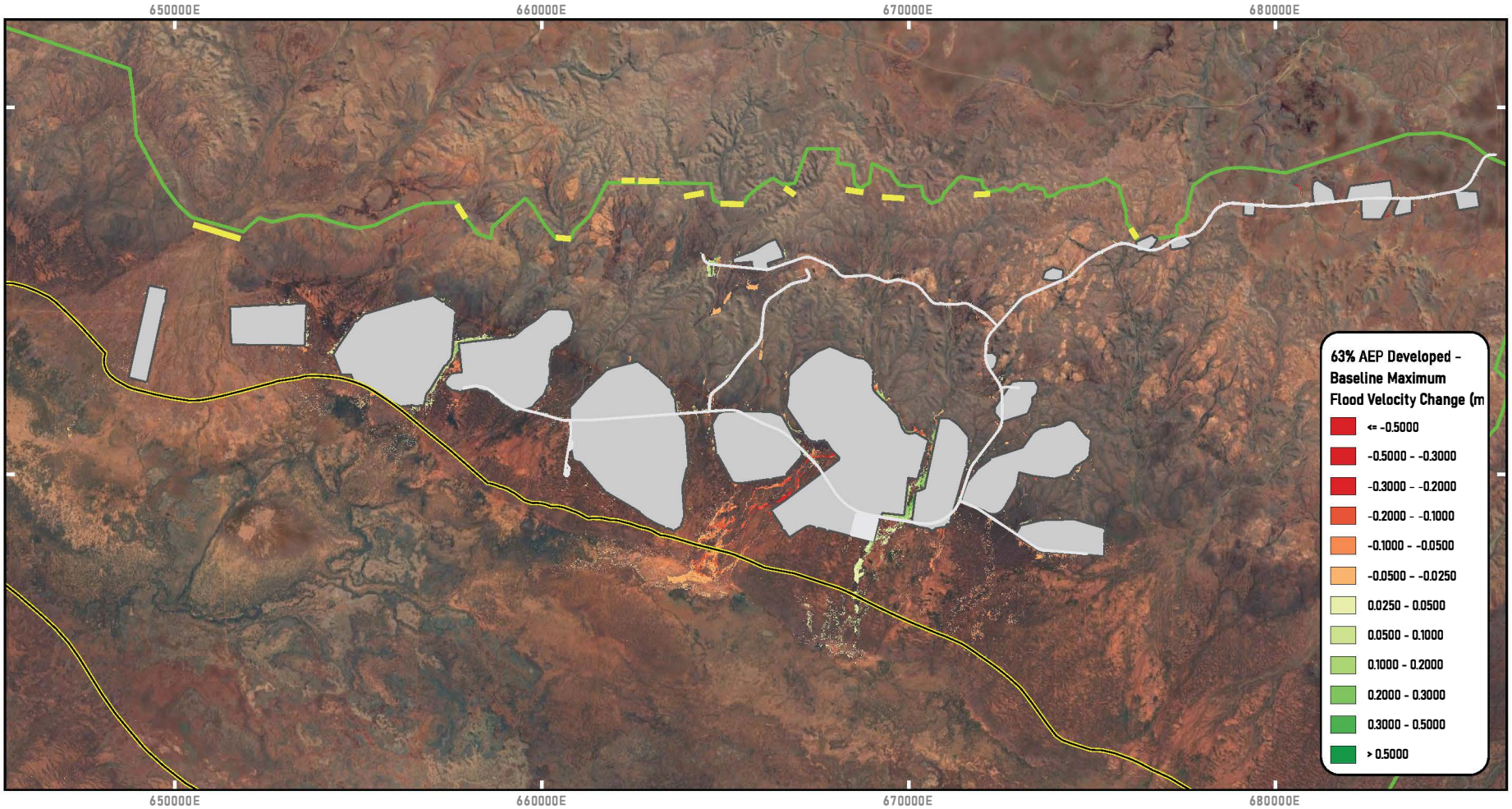

N

2 4 km

GDA94 / MGA zone 50

Legend

- Model Inflow
- Rain On Grid Model Boundary
- Proposed Haul Road
- Surface Water Containment Area
- Mungurrdu

- Difference between maximum predicted flood velocities shown.
- A positive difference between flood velocity indicates increased post-development flooding.
- Flood velocity differences less than 0.05m are not shown.

Data sources: Background Image: Base map and data from Google. © https://www.google.com/

P:\17764 GIS\Workspaces\AR3a_Figures\Appendix C.qgz: Figure C7 – 63% Velocity Diff (plan)

AQ2

Hydrology Figure D7

63% AEP Existing and Developed Maximum Flood Velocity Difference Map

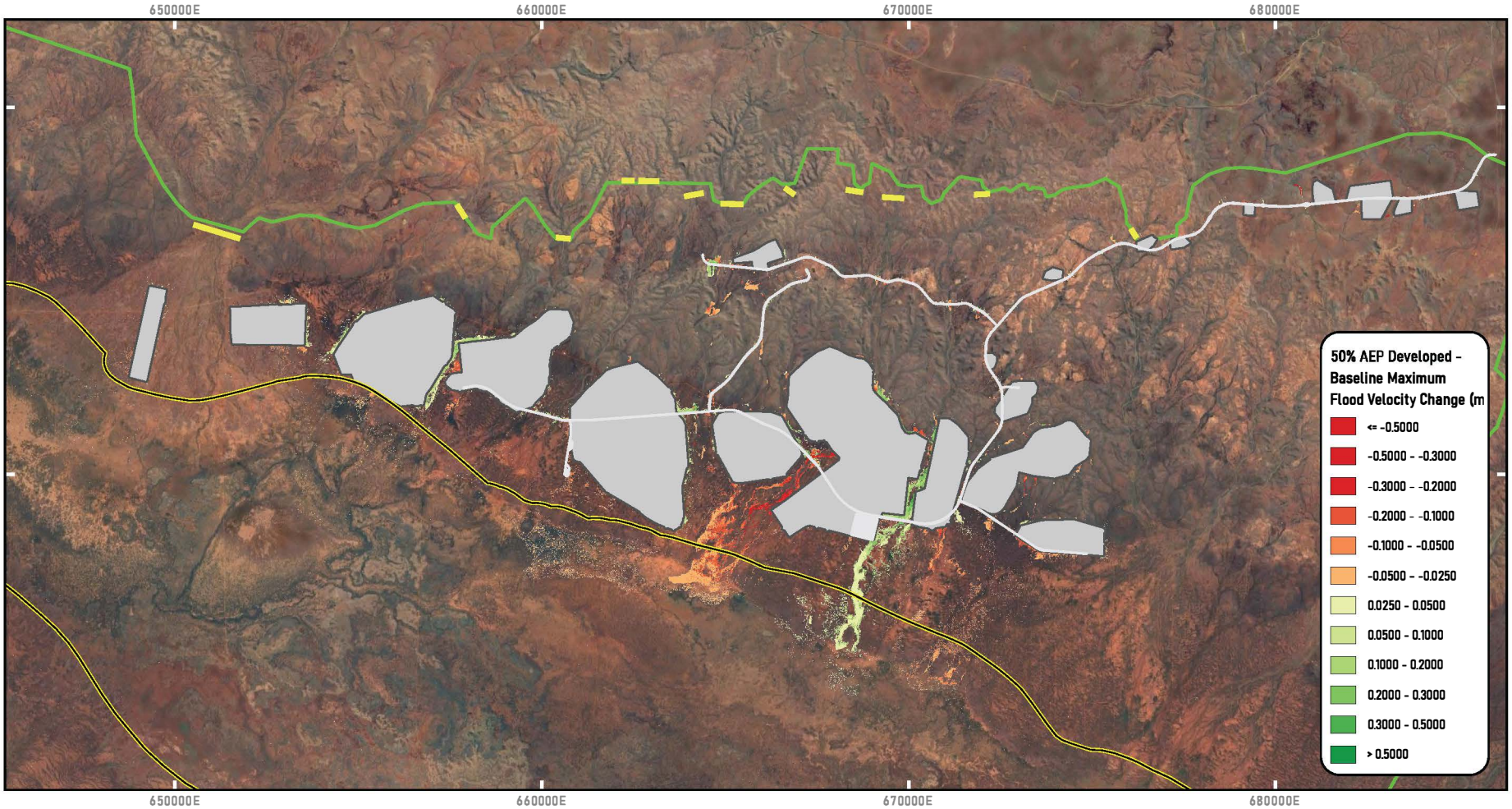

N

2 4 km

GDA94 / MGA zone 50

Legend

- Model Inflow
- Rain On Grid Model Boundary
- Proposed Haul Road
- Surface Water Containment Area
- Mungurrdu

- Difference between maximum predicted flood velocities shown.
- A positive difference between flood velocity indicates increased post-development flooding.
- Flood velocity differences less than 0.05m are not shown.

Data sources: Background Image: Base map and data from Google. © https://www.google.com/

P:\177A GIS\Workspaces\A93a_Figures\Appendix C.qgz: Figure C8 - 50% Velocity Diff (start)

AQ2

Hydrology Figure D8

50% AEP Existing and Developed Maximum Flood Velocity Difference Map

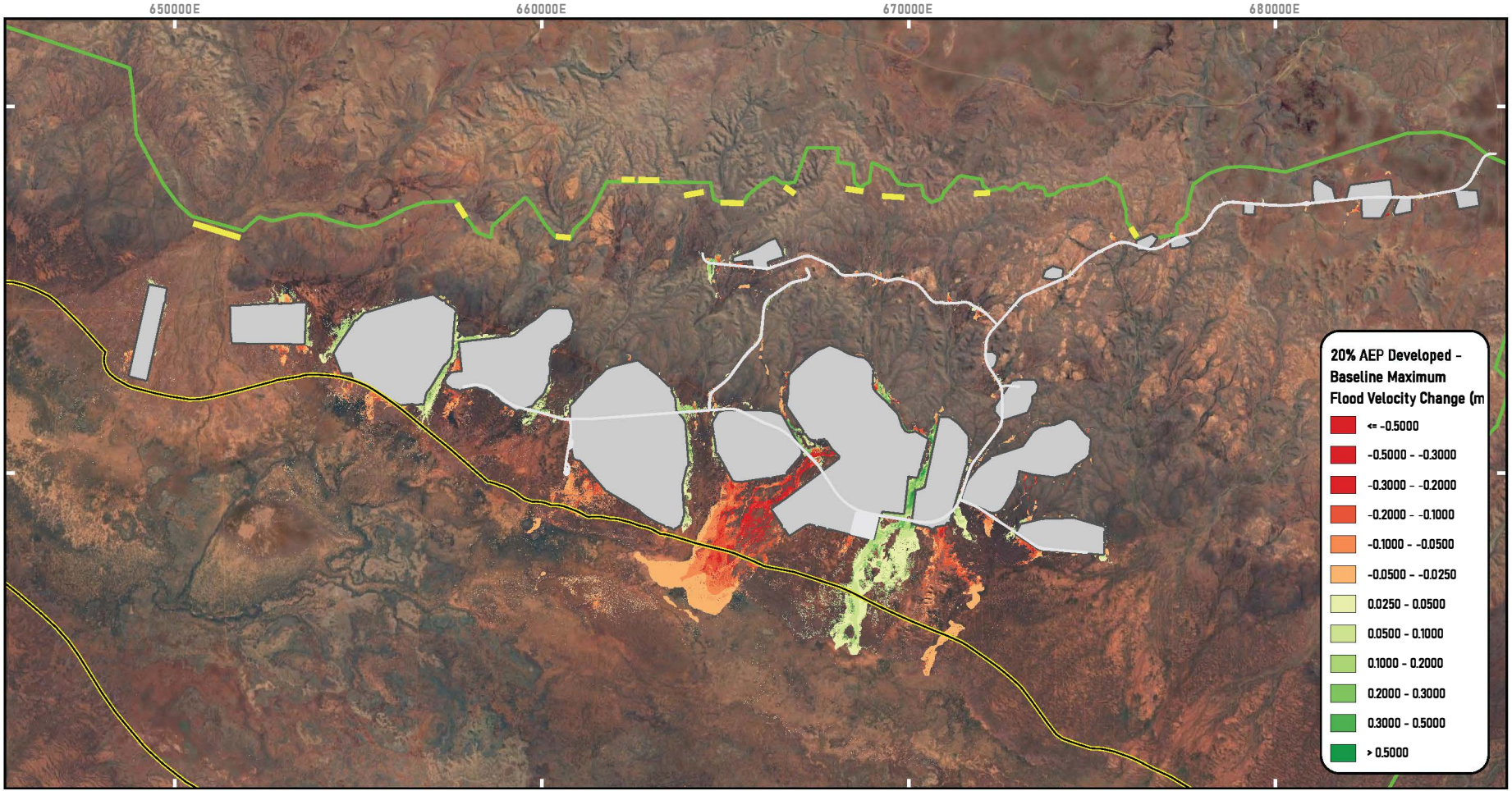

N

2 4 km

GDA94 / MGA zone 50

Legend

- Model Inflow
- Rain On Grid Model Boundary
- Proposed Haul Road
- Surface Water Containment Area
- Mungurrdu

- Difference between maximum predicted flood velocities shown.
- A positive difference between flood velocity indicates increased post-development flooding.
- Flood velocity differences less than 0.05m are not shown.

Data sources: Background Image: Base map and data from Google. © https://www.google.com/

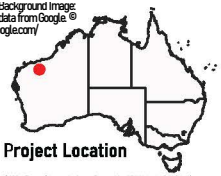

P:\177A GIS\Workspaces\A93a_Figures\Appendix C.qgz: Figure C9 - 20% Velocity Diff. (dan)

AQ2

Hydrology Figure D9

20% AEP Existing and Developed Maximum Flood Velocity Difference Map

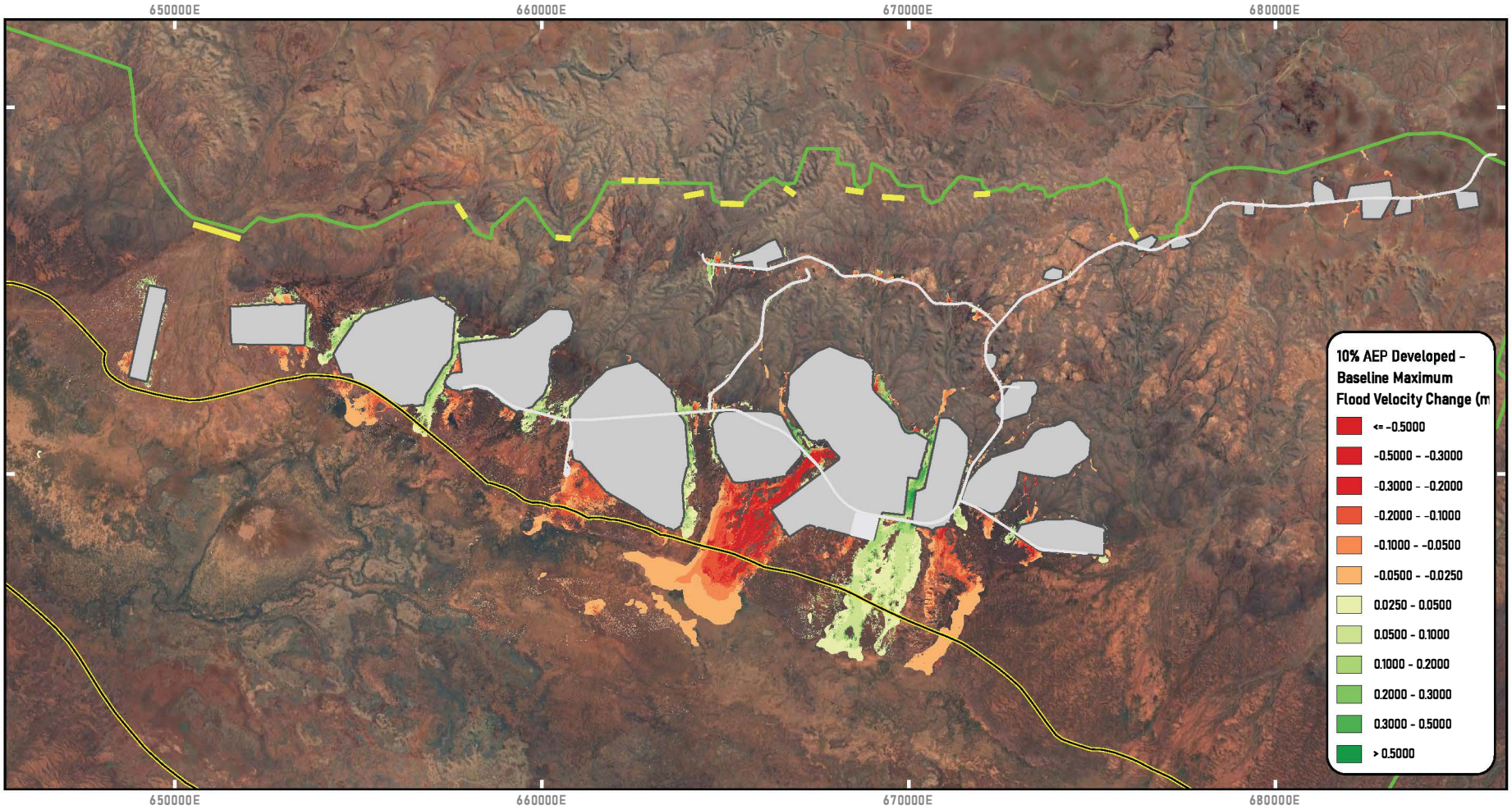

N

2 4 km

GDA94 / MGA zone 50

Legend

- Model Inflow
- Rain On Grid Model Boundary
- Proposed Haul Road
- Surface Water Containment Area
- Mungurrdu

- Difference between maximum predicted flood velocities shown.
- A positive difference between flood velocity indicates increased post-development flooding.
- Flood velocity differences less than 0.05m are not shown.

Data sources: Background Image: Base map and data from Google. © https://www.google.com/

P:\17114 GIS\Workspaces\A93a_Figures\Appendix C.qgz: Figure C10 - 10% Velocity Diff (plan)

AQ2

Hydrology Figure D10

10% AEP Existing and Developed Maximum Flood Velocity Difference Map

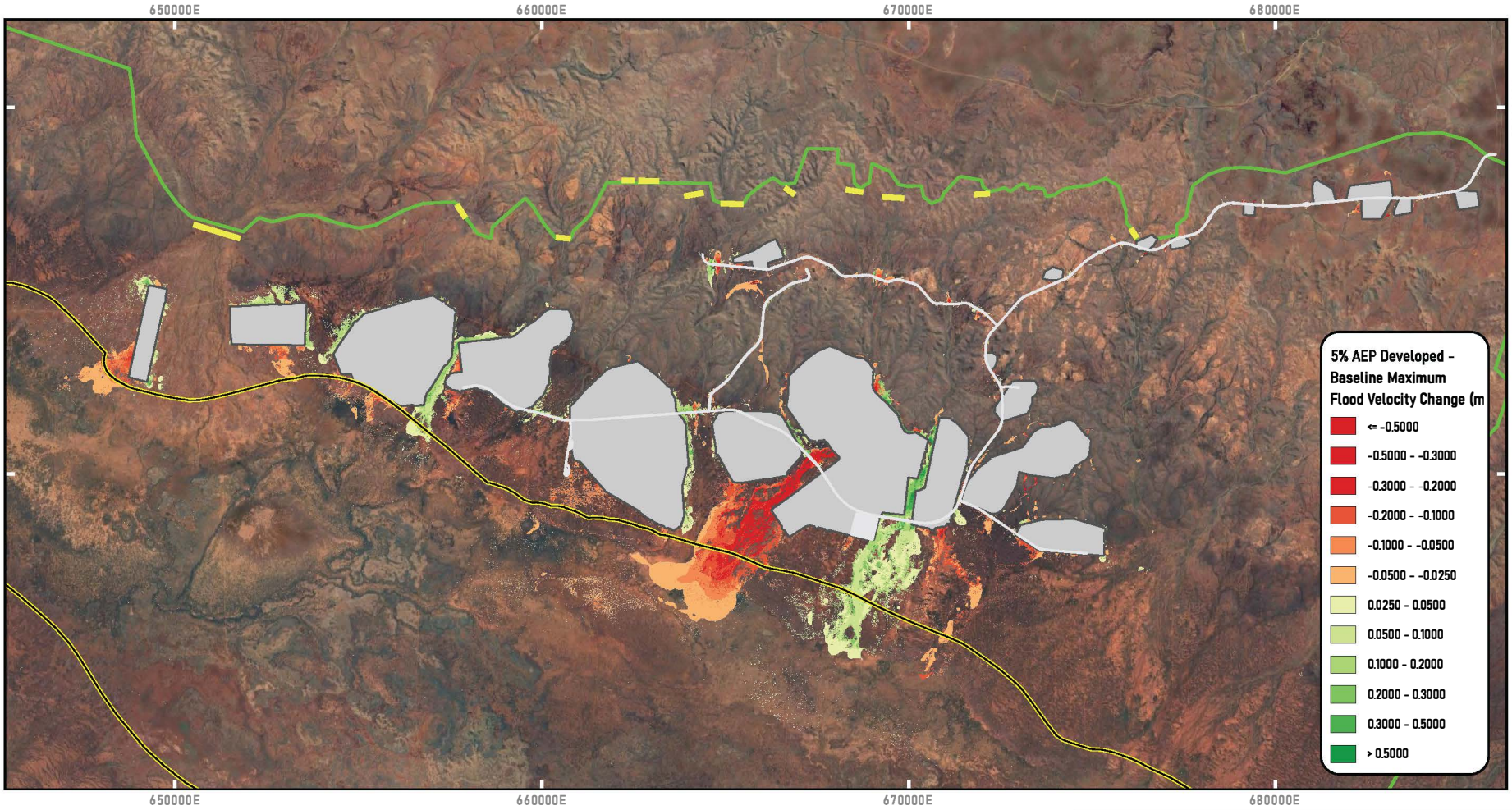

N

2 4 km

GDA94 / MGA zone 50

Legend

- Model Inflow
- Rain On Grid Model Boundary
- Proposed Haul Road
- Surface Water Containment Area
- Mungurrdu

- Difference between maximum predicted flood velocities shown.
- A positive difference between flood velocity indicates increased post-development flooding.
- Flood velocity differences less than 0.05m are not shown.

Data sources: Background Image: Base map and data from Google. © https://www.google.com/

P:\17114 GIS\Workspaces\A93a_Figures\Appendix C.qgz: Figure C11 – 5% Velocity Diff (dart)

AQ2

Hydrology Figure D11

5% AEP Existing and Developed Maximum Flood Velocity Difference Map

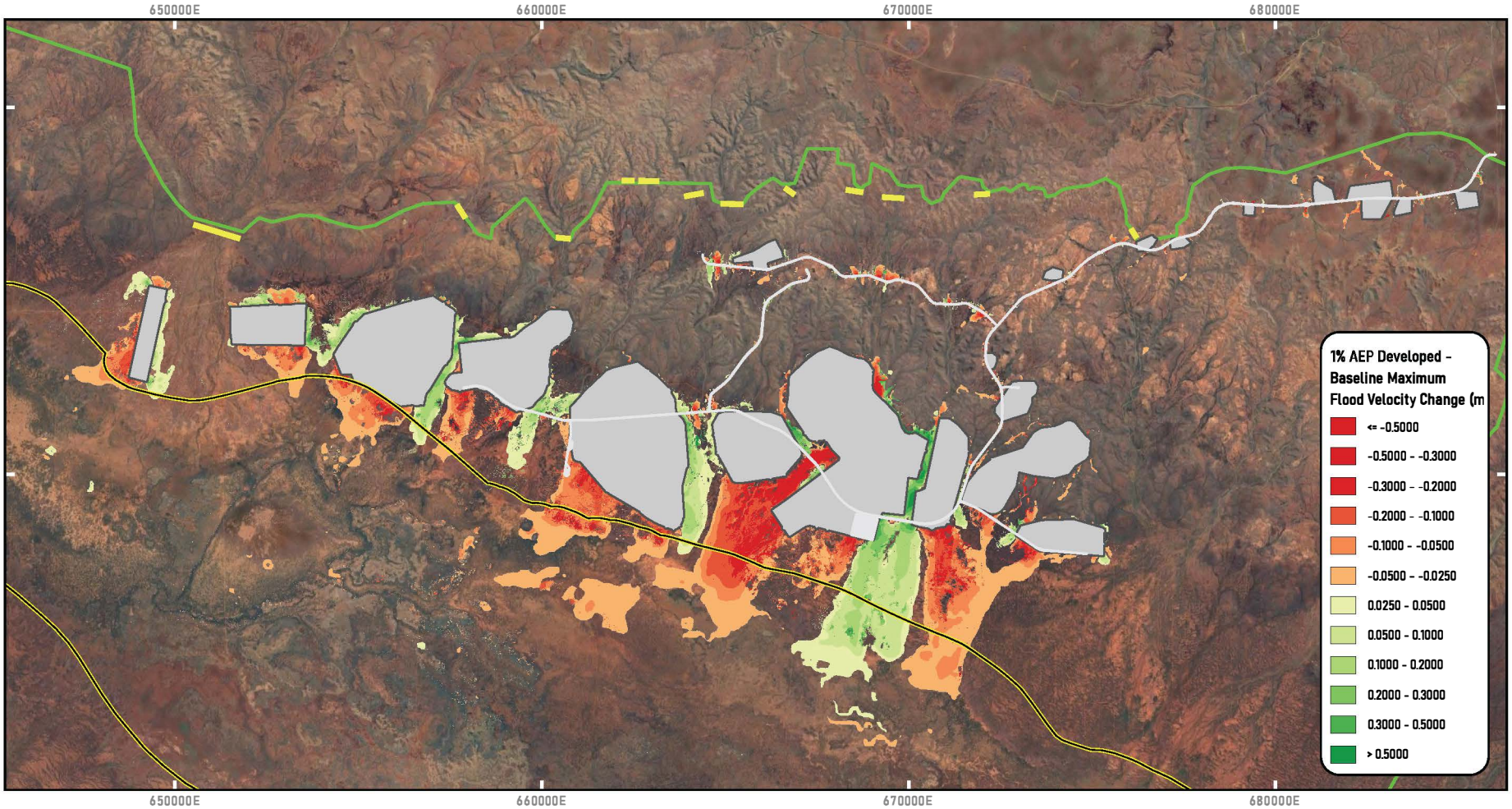

N

2 4 km

GDA94 / MGA zone 50

Legend

- Model Inflow
- Rain On Grid Model Boundary
- Proposed Haul Road
- Surface Water Containment Area
- Mungurrdu

- Difference between maximum predicted flood velocities shown.
- A positive difference between flood velocity indicates increased post-development flooding.
- Flood velocity differences less than 0.05m are not shown.

Data sources: Background Image: Base map and data from Google. © https://www.google.com/

P:\17114 GIS\Workspaces\A93a_Figures\Appendix C.qgz: Figure C12 - 1% Velocity Diff (start)

AQ2

Hydrology Figure D12

1% AEP Existing and Developed Maximum Flood Velocity Difference Map

APPENDIX E
NUMERICAL GROUNDWATER MODEL SET-UP

TABLE OF CONTENTS

Tables

Figures

1. INTRODUCTION

1.1 Background

The Mulga Downs Iron Ore Mine (the Project) is located in the Pilbara region of Western Australia. The Project encompasses the Murray's Hill and Mulga East Deposits within the Mulga East tenement (currently Retention Licence R47/12, with Mining Lease M47/1621 pending). Groundwater investigations to date have been focussed across the Mulga East and Malay Well (E47/2117) tenements, with limited (preliminary) investigations undertaken on the Mulga West tenement (E47/1315). A location plan is provided in Figure 1.1.

A numerical groundwater model for the Mulga Downs mine area and the surrounding groundwater catchment was developed in 2021 as part of a preliminary groundwater assessment (AQ2, 2021). The groundwater model was used to predict:

- Dewatering rates required to achieve dry mining conditions associated with a preliminary mine schedule and assumed pit designs.
- Regional groundwater drawdown and changes to the regional groundwater balance resulting from dewatering.
- Flow paths towards the proposed pit areas that develop over the life of the mine, to assess the potential for groundwater with higher salinity to be drawn into pit areas from the valley.

The groundwater model was updated in 2022 as part of the current water study to include:

- The findings of the 2021 hydrogeological drilling and testing programme (AQ2, 2024).
- Updates to the model calibration data set, including the groundwater level monitoring (up to December 2021).

This appendix covers the set-up and calibration of the model conducted by AQ2, together with the model prediction set-up. Model predictions were conducted by Groundwater Consulting Pty Ltd (GWC) under contract to Darkwater Consulting Pty Ltd (Darkwater) and are detailed in a separate report (GWC, 2024). The GWC report is presented as a separate appendix of the main report.

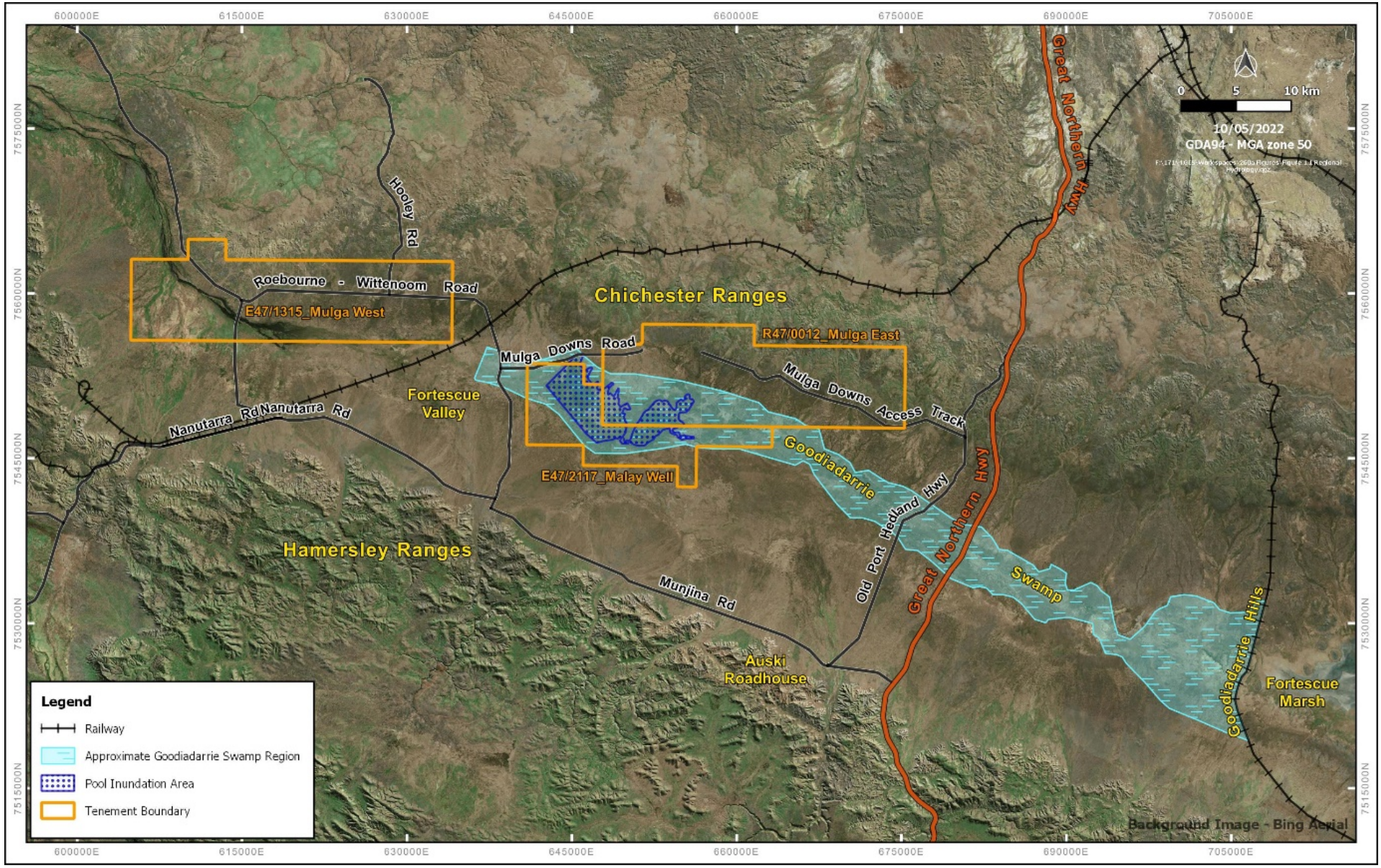

Figure 1.1 Location Map

1.2 Objectives

The overall aim of the current groundwater management assessment is to gain an understanding of the potential worst-case dewatering requirements, environmental impacts and other water management-related issues (i.e. related to water supply or disposal of excess water) associated with the proposed mining and ancillary activities. As such, the key objectives for the modelling assessment (inclusive of the predictions conducted by GWC) are as follows:

- Determine a feasible mining scenario with a viable dewatering and managed aquifer recharge (MAR) solution.
- Predict dewatering rates required to achieve dry mining conditions (i.e. groundwater levels at or just below the projected base of mining throughout the life of the mine which is the standard approach for this level of study).
- Predict regional groundwater drawdown / draw-up and changes to the regional groundwater balance resulting from dewatering and MAR.
- Predict potential changes to groundwater salinity resulting from dewatering and MAR.
- Predict the recovery of the groundwater system at the end of mining and dewatering, including the time taken for recovery of groundwater levels to a final equilibrium.

2. MODEL SET-UP

Features of the groundwater model are described in detail in the following sections and are summarised below. The model includes:

- The Tertiary / Quaternary aquifers that occur across the valley and along the lower slopes of the Chichester Range.
- Basement aquifers and aquitards, that occur outside of the valley areas, associated with the Marra Mamba and Jeerinah Formations. Higher permeability sub mineralised and mineralised / orebody areas in the Marra Mamba Formation are also represented (i.e. the Altered Marra Mamba unit referred to in the main body of this report).
- Recharge to the aquifer system from flow along surface water drainages and from incident rainfall.
- Groundwater inflows from upstream and groundwater outflow to downstream.
- Evaporation from shallow water tables and evapotranspiration from vegetation across the valley floor.
- Dewatering of open cut pits.
- MAR (via MAR bores) of excess dewatering water within the project area.

It should be noted that, as the model set-up was updated in 2021, all figures within this report show the proposed pits at that time.

2.1 Groundwater Model Setup and Extent

The groundwater model further developed and used for this assessment was originally developed for the Mulga East Preliminary Groundwater Management Assessment AQ2 (2021). The model uses the numerical groundwater flow modelling package Modflow SURFACT (Version 4.0, Hydrogeological Inc. 1996), operating under the Groundwater Vistas graphical user interface (Version 8, Environmental Science Simulations INC, 1996 to 2022). The model is used to simulate groundwater flow processes only. No transport processes are simulated however, particle tracking using MODPATH, (Pollock, 2016) is used to simulate long term flow paths across the modelled catchment. The Modflow SURFACT software was retained for the current project to expedite completion of the groundwater modelling assessment, based on the short time frame available to complete the modelling work.

The extent of the model domain and locations of the model boundaries are shown in Figure 2.1 and summarised in Table 2.1, with all associated data specified using the UTM (GDA94 / MGA Zone 50 – EPSG 28350) coordinate system. The model has been extended to the north (a maximum distance of 3.5 km) to allow simulation of the Jeerinah Formation upgradient of the Mulga Downs mining areas (i.e. the low permeability boundary units to the north).

The model grid is rotated 26 degrees to align it with the inferred direction of groundwater flow through the valley aquifer (approximately southeast to northwest). A minimum cell dimension of 100 m (or cell size of 100 m by 100 m) is assigned in the immediate mine area to allow simulation of the geometry of the orebody aquifers. A maximum cell dimension of 1,000 m (or cell size of up to 1,000 m by 1,000 m) is assigned away from the proposed mine area and close to model boundaries. Cell dimensions are shown in Figure 2.1. Between the zones shown in Figure 2.1, cell sizes increase at a maximum ratio of 1.5 (i.e. the larger cell is a maximum of 1.5 times bigger than the smaller adjacent cell). The model includes 156 rows and 301 columns over 11 model layers resulting in a total of 516,516 model cells and 445,753 active model cells.

Table 2.1 Extent of Model Domain (GDA94 / MGA Zone 50 – EPSG 28350 coordinate system)

	Easting (m)*	Northing (m)*
North West	627,220	7,582,019
North East	711,407	7,541,659
South West	607,409	7,541,684
South East	695,873	7,508,373

* Easting and northing in GDA94 / MGA Zone 50 – EPSG 28350 coordinate system

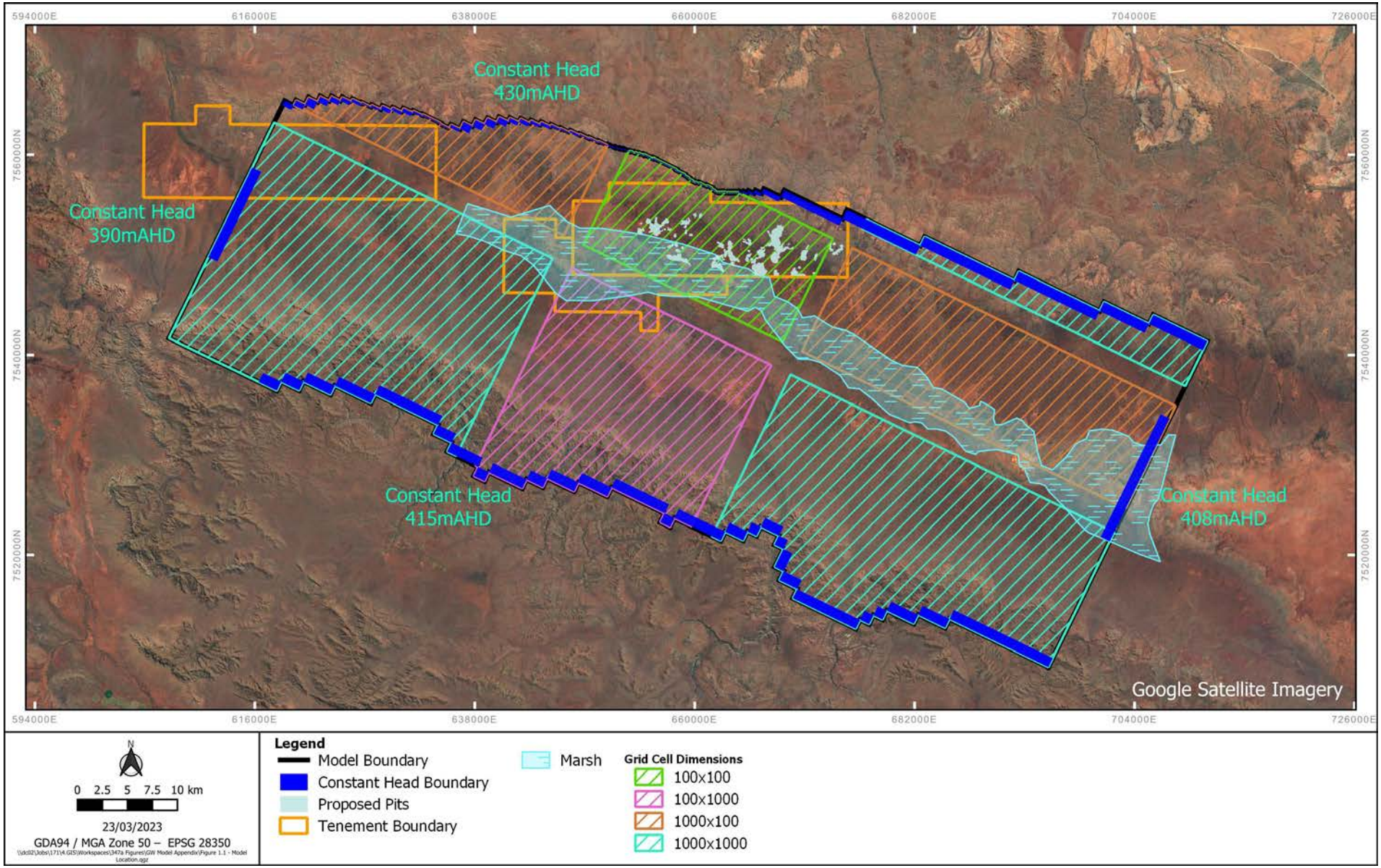

Figure 2.1 Extent of the Numerical Model

2.2 Groundwater Model Geometry

A Leapfrog (Sequent, 2022) geological model was constructed for the mine area, the valley and the surrounding groundwater catchment to allow the definition of key hydrogeological units outside of the immediate mine area where the impacts of groundwater development are expected to extend. This static model was used to define the thickness and extent of the aquifer and aquitard units across the mine and surrounding areas. Leapfrog is an industry standard geological modelling package. The geological model was developed using the following information:

- The elevation of the ground surface data was sourced from the NASA Shuttle Radar Topography Mission (SRTM) 1 arc-second elevation data (NASA, 2021). This data was used as the available LiDAR data set, at the time of model set-up, did not cover the extent the groundwater model. Attempts were made to combine the LiDAR and SRTM data sets, however these were unsuccessful due to the elevation differences between the data sets.
- Stratigraphic layers from the HPPL geological model, excluding the Malay Well area where the HPPL model was based on uniform layer thicknesses rather than interpretation of the HPPL exploration drilling.
- Geological logging from the HPPL drillhole database (particularly for the mapping of the Tertiary units and bedrock in the Malay Well area).
- Additional geological information for the Mulga East, Malay Well and Mulga West areas was taken from bore logs from previous hydrogeological investigations (MWH, 2009, 2012 & 2014 and AQ2, 2024).
- Information outside of the Mulga East, Malay Well and Mulga West areas was derived from 1:250,000 series geological maps of Western Australia (Roy Hill, Thorne et al, 1996 and Mount Bruce, Thorne et al, 1996).

Changes made to the Leapfrog model during this work include:

- Grouping of the lowermost (dolomitic) unit of the Nammuldi Member (HPPL code: DNAM) with the Jeerinah hydrostratigraphic unit.
- Inclusion of the West Angelas Member as a separate hydrostratigraphic unit (previously included as part of the Marra Mamba hydrostratigraphic unit).

The groundwater model used a total of 11 flat lying layers to simulate the geometry of the Leapfrog static model. Groundwater model layers are generally 10 m thick, with thicker layers (20 to 25 m in thickness) used to represent the lower lying units. Layer 1 also includes greater thicknesses (up to ~500 m) in areas of higher topographic elevation along the Chichester and Hamersley Ranges (refer Figure 1.1).

In addition to the geological framework assigned to the groundwater model from the Leapfrog model, the Marra Mamba / West Angela orebody mineralisation (40% or greater Fe) was used to define the extents of the orebody aquifers. A halo of sub mineralised ore between the orebody aquifers, with enhanced permeability / hydraulic connection was also assigned. This connection was assigned by including a zone around the mineralisation shell with a higher permeability than the surrounding weathered basement but lower than the Marra Mamba / West Angela orebody aquifers.

A schematic model section along the valley is shown in Figure 2.2. Model layer geometry is summarised in Table 2.2 with aquifer property zones for Layers 1 to 11 shown in Figure 2.3, Figure 2.4, Figure 2.5, Figure 2.6, Figure 2.7 and Figure 2.8. A single aquifer parameter zone is assigned to each aquifer unit. The extent of the model is such that the model is not set up to simulate local scale features, which will not be important for the prediction of groundwater inflows and catchment wide groundwater impacts.

Changes to the groundwater model setup include:

- Combining the Alluvium and Upper Calcrete zones (previously separate zones) into a single aquifer zone (referred to as Upper Calcrete). Noting the alluvium across the Project area is <4 m in thickness and unsaturated.
- Combining the 40% and 50% Mineralised zones into one Marra Mamba / West Angela Ore zone.
- Separation of the Unmineralised Marra Mamba into two zones:
  - A higher permeability Unmineralised / Fractured Marra Mamba Mulga East zone, and
  - A lower permeability Unmineralised Marra Mamba (Regional) zone.
- Additional aquifer zones, shown in Figures 2.3 to 2.8, including:
  - A low permeability Fresh Marra Mamba / Jeerinah zone in the north (based on the lowermost dolomitic unit of the Nammuldi Member mentioned above).
  - A separation of the Unmineralised / Fractured Marra Mamba into a high permeability Mulga East zone and a lower permeability regional zone.
  - A moderate permeability Weathered West Angela Member zone.
  - A high permeability West Angela Hardcap zone in the Malay Well area.
  - A very high permeability West Angela Hardcap zone (as observed at Bore MDPB0020) in the Malay Well area.
  - Low permeability Fresh Dolomite (Wittenoom Formation) zones in the Malay Well area to represent the identified juxtaposition of geological units, potentially resulting from faulting.

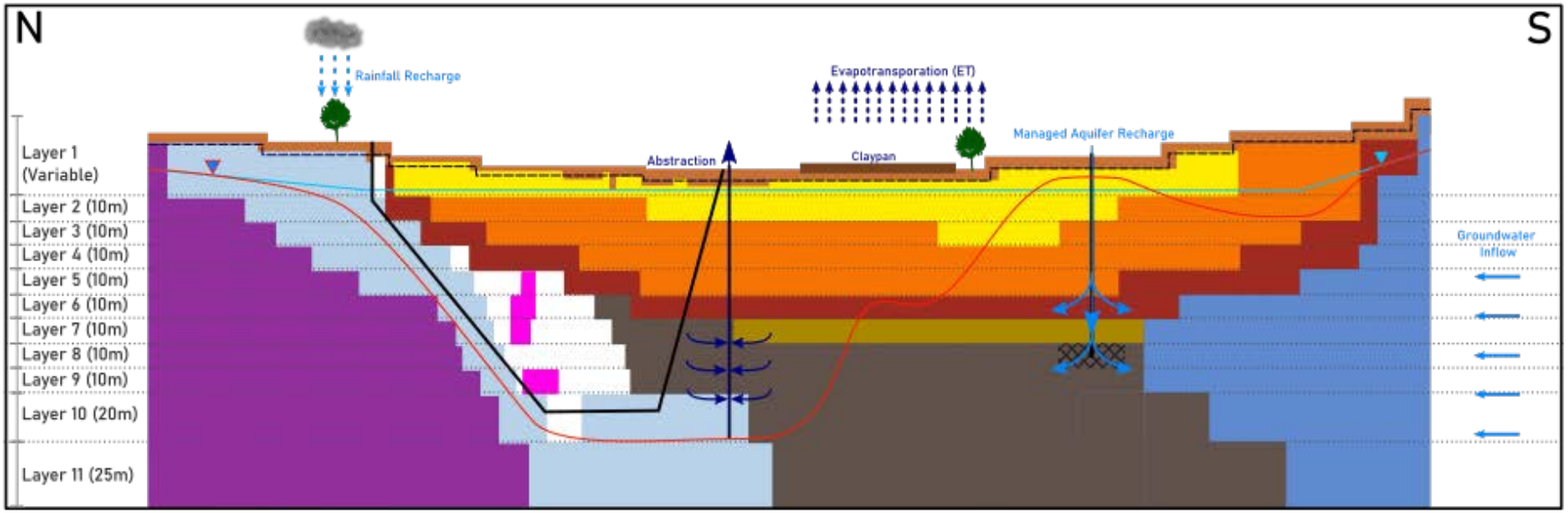

Figure 2.2 Schematic Model Section

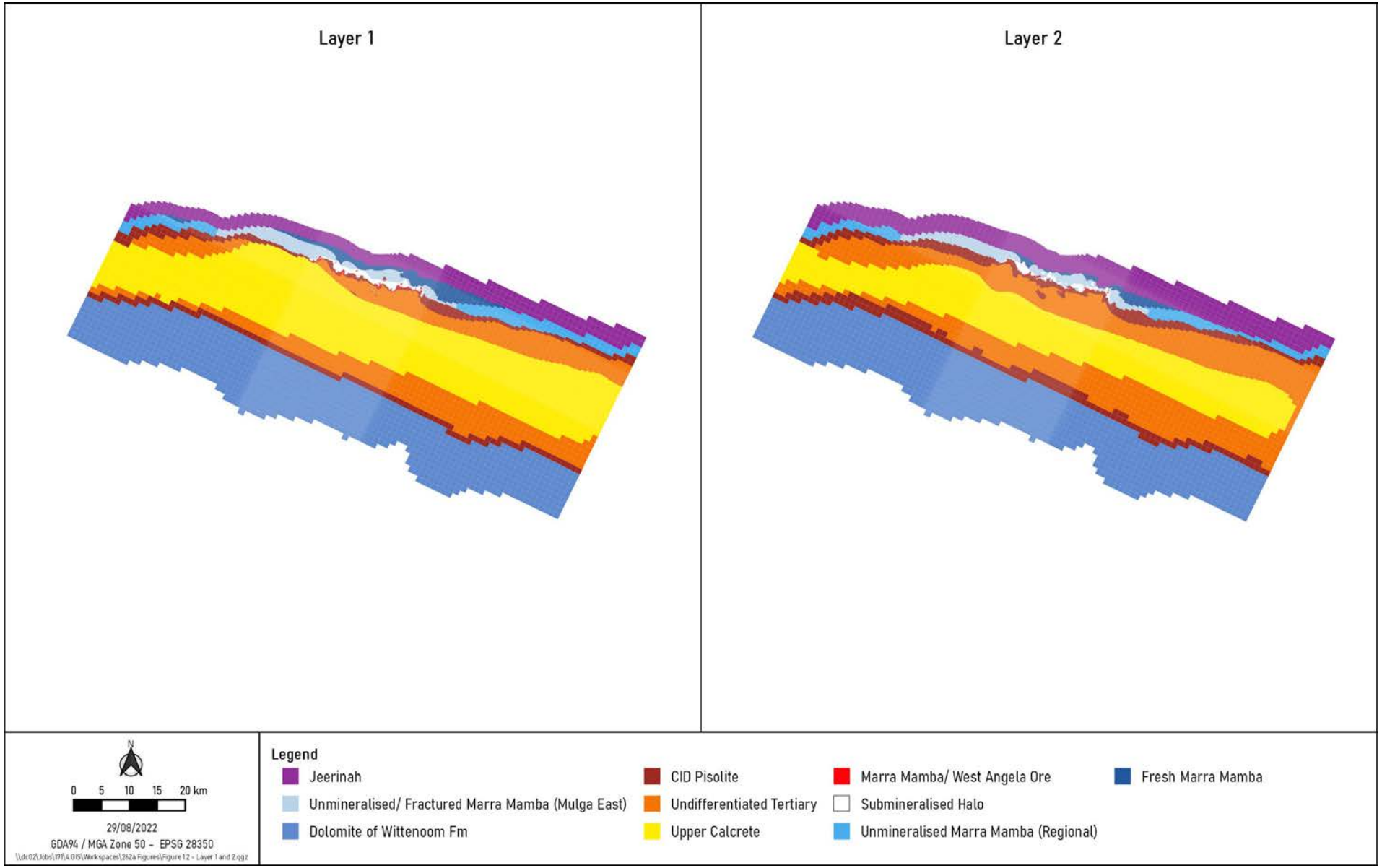

Figure 2.3 Model Layers 1 and 2

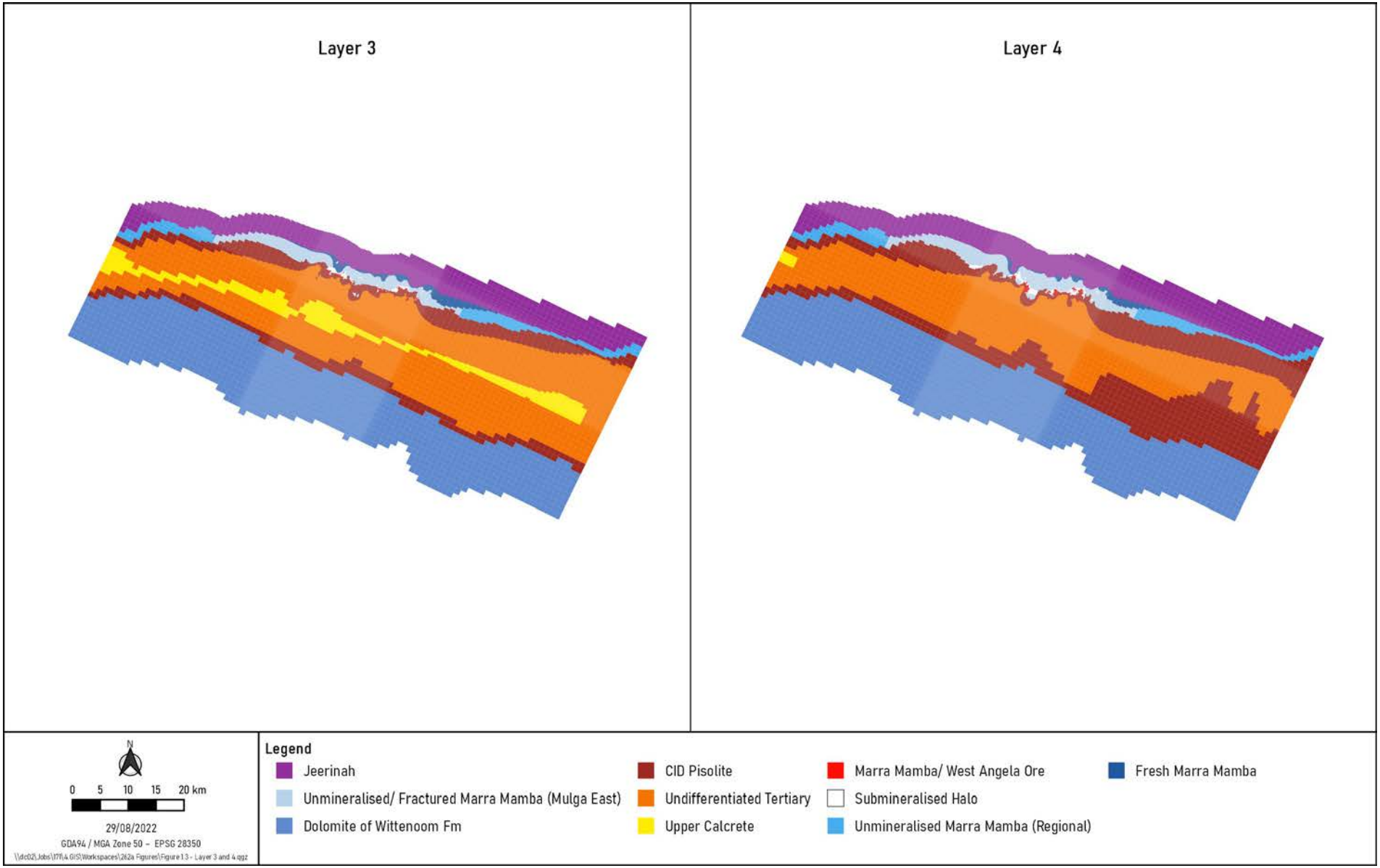

Figure 2.4 Model Layers 3 and 4

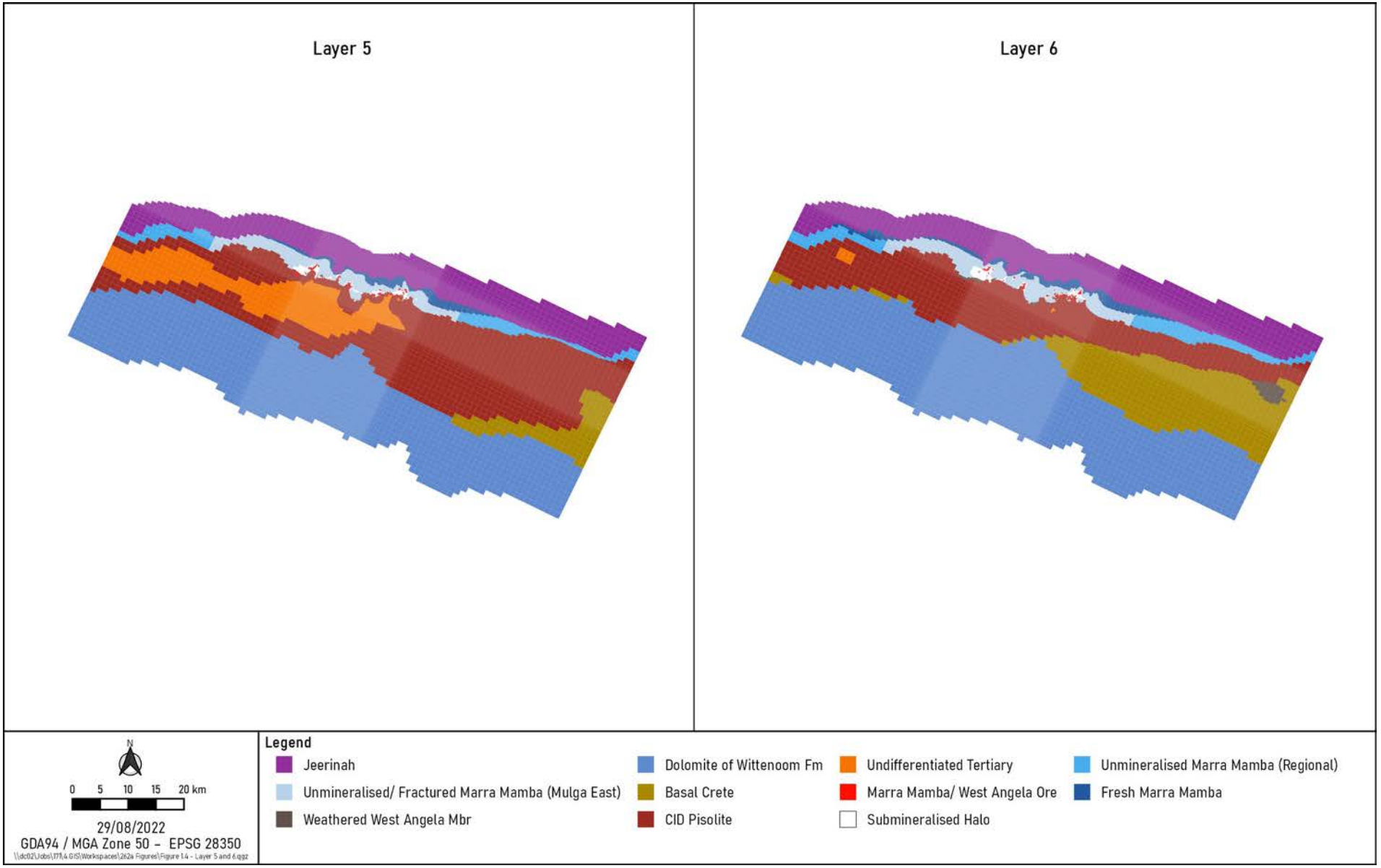

Figure 2.5 Model Layers 5 and 6

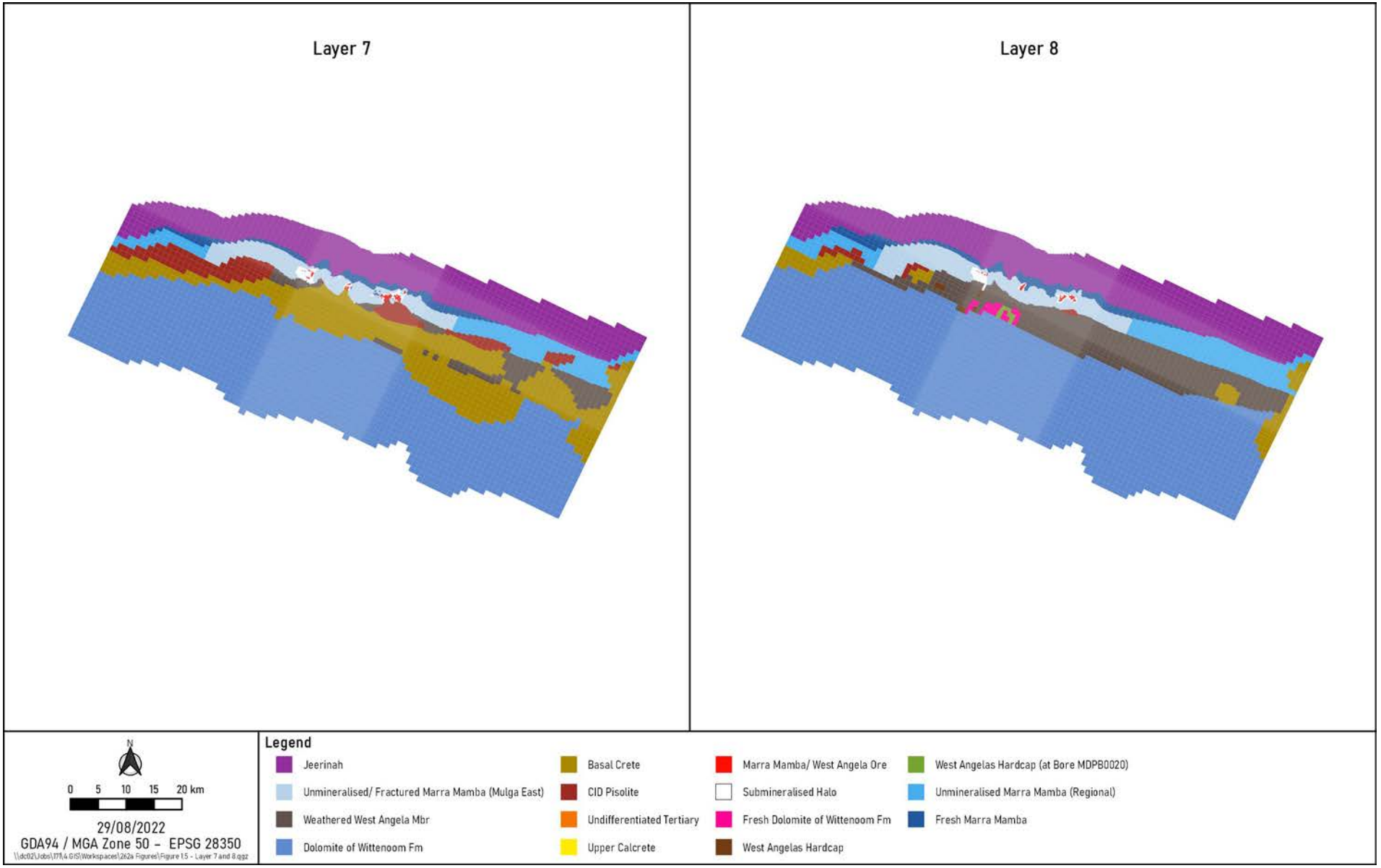

Figure 2.6 Model Layers 7 and 8

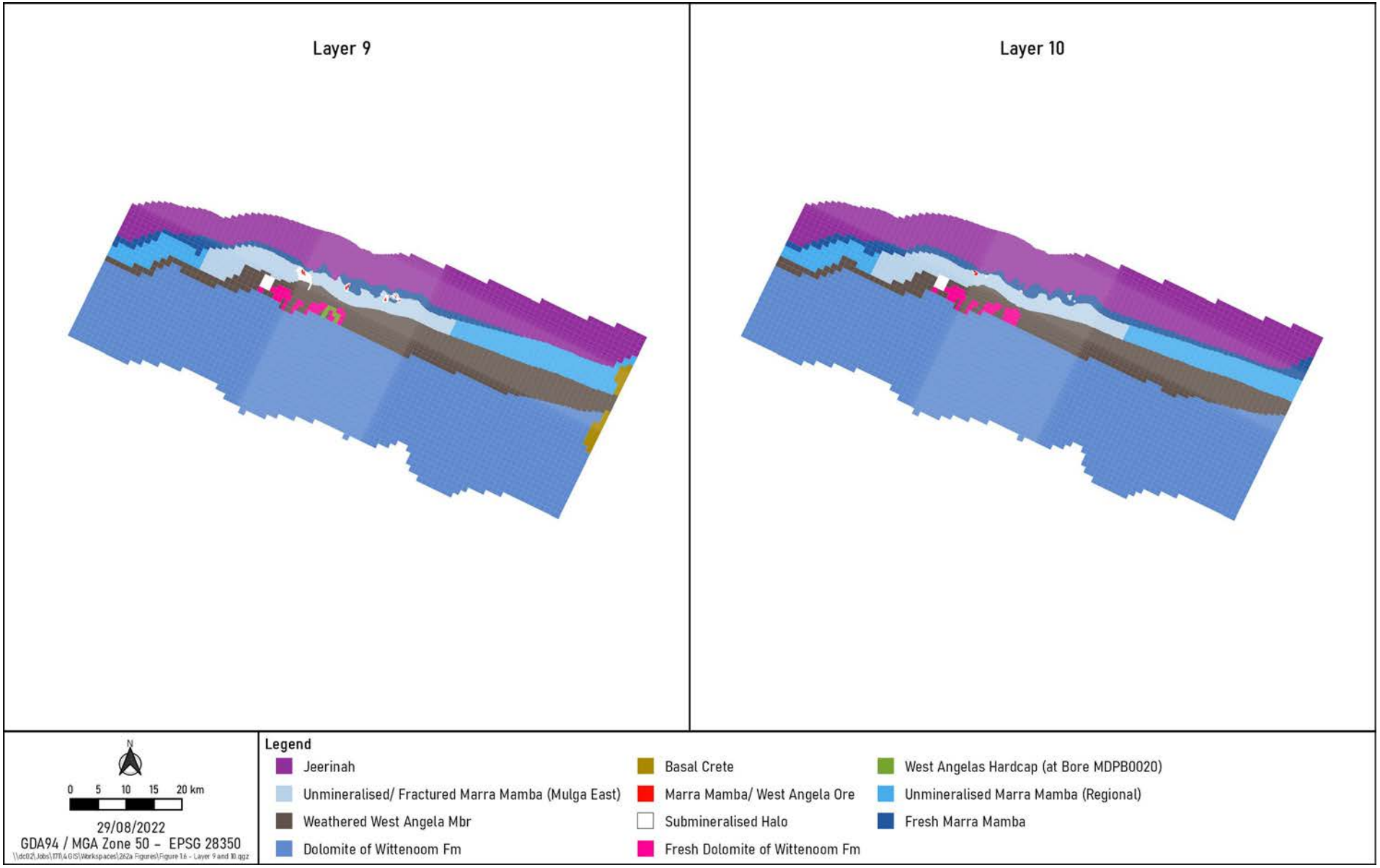

Figure 2.7 Model Layers 9 and 10

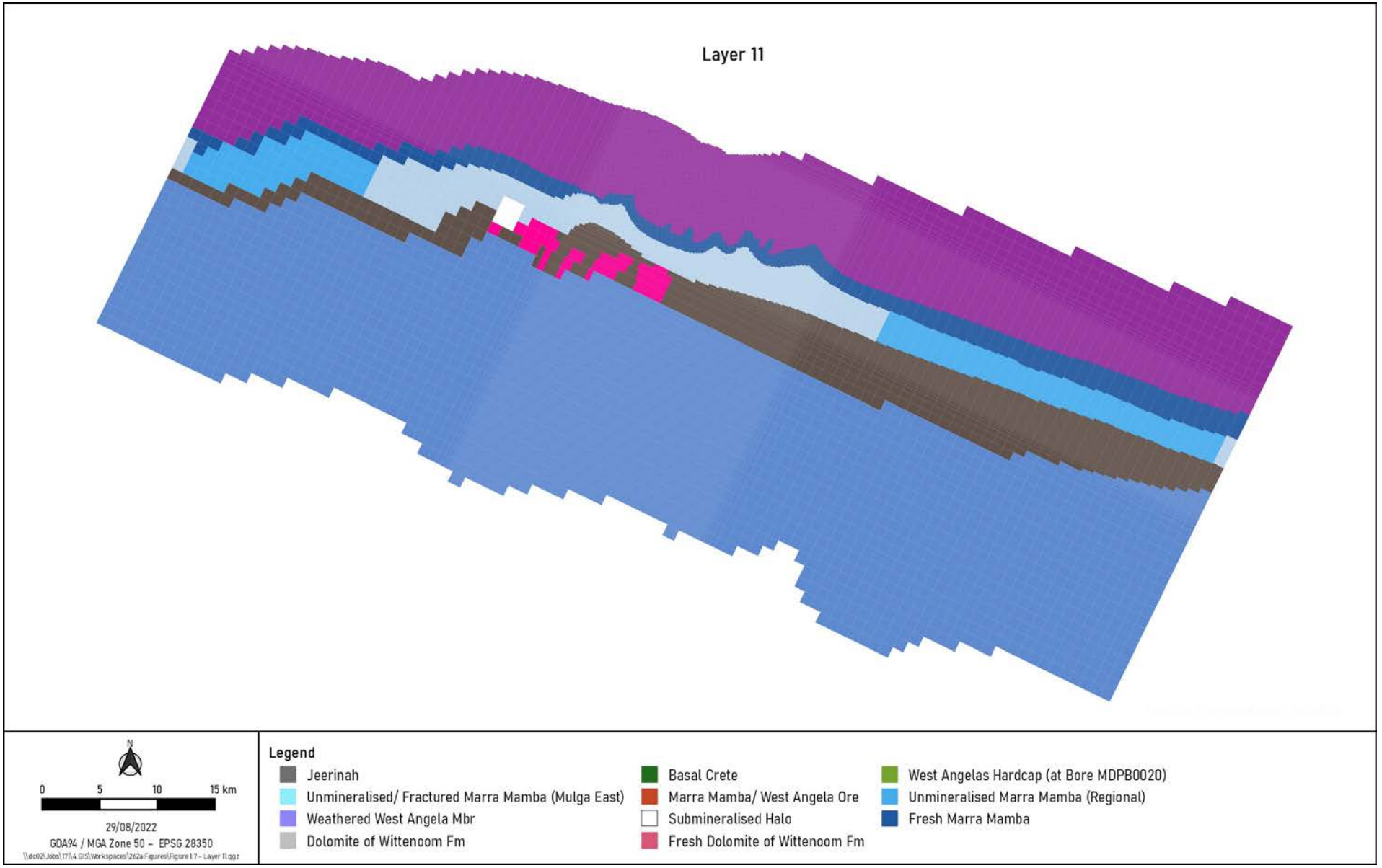

Figure 2.8 Model Layers 9 and 10

Table 2.2 Model Geometry

Layer	Aquifer Units	Description
1	Upper Calcrete Undifferentiated Tertiary Pisolite / CID Marra Mamba / West Angela Ore Submineralised Halo Fresh Dolomite of Wittenoom Fm Unmineralised / Fractured Marra Mamba (Mulga East) Unmineralised Marra Mamba (Regional) Fresh Marra Mamba / Jeerinah	Top of layer represents ground surface elevation with an elevation of between 397 mAHD to 973 mAHD. Base of layer set at between 397 mAHD and 400 mAHD resulting in a layer thickness of up to 570 m.
2	Upper Calcrete Undifferentiated Tertiary Pisolite / CID Marra Mamba / West Angela Ore Submineralised Halo Fresh Dolomite of Wittenoom Fm Unmineralised / Fractured Marra Mamba (Mulga East) Unmineralised Marra Mamba (Regional) Fresh Marra Mamba / Jeerinah	The base of layer is set to 390 mAHD resulting in a layer thickness of 10 m.
3	Upper Calcrete Undifferentiated Tertiary Pisolite / CID Marra Mamba / West Angela Ore Submineralised Halo Fresh Dolomite of Wittenoom Fm Unmineralised / Fractured Marra Mamba (Mulga East) Unmineralised Marra Mamba (Regional) Fresh Marra Mamba / Jeerinah	The base of layer is set to 380 mAHD resulting in a layer thickness of 10 m.
4	Upper Calcrete Undifferentiated Tertiary Pisolite / CID Marra Mamba / West Angela Ore Submineralised Halo Fresh Dolomite of Wittenoom Fm Unmineralised / Fractured Marra Mamba (Mulga East) Unmineralised Marra Mamba (Regional) Fresh Marra Mamba / Jeerinah	The base of layer is set to 370 mAHD resulting in a layer thickness of 10 m.
5	Undifferentiated Tertiary Pisolite / CID Basal Crete Fresh Dolomite of Wittenoom Fm Marra Mamba / West Angela Ore Submineralised Halo Unmineralised / Fractured Marra Mamba (Mulga East) Unmineralised Marra Mamba (Regional) Fresh Marra Mamba / Jeerinah	The base of layer is set to 360 mAHD resulting in a layer thickness of 10 m.

Layer	Aquifer Units	Description
6	Undifferentiated Tertiary Pisolite / CID Basal Crete Weathered West Angela Mbr Fresh Dolomite of Wittenoom Fm Marra Mamba / West Angela Ore Submineralised Halo Unmineralised / Fractured Marra Mamba (Mulga East) Unmineralised Marra Mamba (Regional) Fresh Marra Mamba / Jeerinah	The base of layer is set to 350 mAHD resulting in a layer thickness of 10 m.
7	Pisolite / CID Basal Crete Weathered West Angela Mbr Fresh Dolomite of Wittenoom Fm Marra Mamba / West Angela Ore Submineralised Halo Unmineralised / Fractured Marra Mamba (Mulga East) Unmineralised Marra Mamba (Regional) Fresh Marra Mamba / Jeerinah	The base of layer is set to 340 mAHD resulting in a layer thickness of 10 m.
8	Pisolite / CID Basal Crete West Angela Hardcap West Angela Hardcap (at Bore MDPB0020) Weathered West Angela Mbr Fresh Dolomite of Wittenoom Fm Marra Mamba / West Angela Ore Submineralised Halo Unmineralised / Fractured Marra Mamba (Mulga East) Unmineralised Marra Mamba (Regional) Fresh Marra Mamba / Jeerinah	The base of layer is set to 330 mAHD resulting in a layer thickness of 10 m
9	Basal Crete West Angela Hardcap (at Bore MDPB0020) Weathered West Angela Mbr Fresh Dolomite of Wittenoom Fm Marra Mamba / West Angela Ore Submineralised Halo Unmineralised / Fractured Marra Mamba (Mulga East) Unmineralised Marra Mamba (Regional) Fresh Marra Mamba / Jeerinah	The base of layer is set to 320 mAHD resulting in a layer thickness of 10 m.
10	Weathered West Angela Mbr Fresh Dolomite of Wittenoom Fm Marra Mamba / West Angela Ore Submineralised Halo Unmineralised / Fractured Marra Mamba (Mulga East) Unmineralised Marra Mamba (Regional) Fresh Marra Mamba / Jeerinah	The base of layer is set to 300 mAHD resulting in a layer thickness of 20 m.
11	Weathered West Angela Mbr Fresh Dolomite of Wittenoom Fm Submineralised Halo Unmineralised / Fractured Marra Mamba (Mulga East) Unmineralised Marra Mamba (Regional) Fresh Marra Mamba / Jeerinah	The base of layer is set to 275 mAHD resulting in a layer thickness of 25 m.

2.3 Groundwater Inflow and Outflow

2.3.1 Groundwater Throughflow

As described in the Baseline Assessment report (AQ2, 2024), groundwater gradients across the catchment generally follow the topographic gradient. Groundwater flows from south east to north west through the valley with groundwater flow also from topographic highs located to the north and south of the valley.

The locations of model boundaries are shown in Figure 2.1. The south eastern and north western model boundaries are assigned across the valley to simulate regional groundwater throughflow. These boundaries were set approximately 38 km upstream and 39 km downstream of the Mulga Downs mine area to limit boundary impacts and allow simulation of drawdown from mining activities along the valley aquifers. The upstream (southern eastern) model boundary is set just downstream of the surface water catchment boundary, that is defined by the Goodiadarrie Hills. Inflow across this upstream boundary includes outflow from the catchment immediately upstream plus any incident rainfall from the catchment boundary to the simulated model boundary. Skrzypek et al (2016) estimated that there is at least 2 GL/yr of outflow from the Fortescue Marsh (upstream) to the modelled groundwater catchment to maintain the groundwater salinities observed underlying the Fortescue Marsh (to the east of the modelled area).

The resulting model domain covers a distance of 94 km along the valley. The locations of the model boundaries also allow for the simulation of additional abstraction or re-injection away from the mining areas, if required. The southern model boundary, which simulates inflow from the Hamersley Range, was aligned with the Brockman Formation outcrop. The northern model boundary was assigned to simulate inflow from the Chichester Range. This boundary was set in the low permeability Jeerinah Formation, upstream of the Mulga Downs mine area. Flow through these boundaries is expected to be minimal compared to the overall catchment water balance due to the low permeability of these units (Brockman and Jeerinah Formations). Predicted inflows across these low permeability boundaries are discussed further in Section 2.56 (Model Calibration).

Groundwater inflow from the south east and groundwater outflow to the north west are simulated using constant head inflow and outflow boundaries. These boundaries are set at elevations of 390 mAHD (north western boundary) and 408 mAHD (south eastern boundary) respectively. The elevation of the north western boundary was set consistent with groundwater level monitoring data from Mulga West (Bore MDPZ5163). The elevation of the south eastern boundary was assigned consistent with monitoring data from the DWER data base (Bore 70810342 DWER, 2021) and data presented by Skrzypek et al (2016). The locations of these monitoring bores are shown in Figure 2.9.

Data from Skrzypek et al (2016) also suggests that the groundwater (water table) gradients from the most western part of the Fortescue Marsh and the Goodiadarrie Hills are very low.

The northern model boundary is assigned an elevation of 430 mAHD consistent with monitoring from the Mulga East area (Bore MDPZ7455, located to the north of the project). The southern model boundary is assigned at an elevation of 415 mAHD,) consistent with historical data from the DWER database (Bores 70870190 and 708010, located to the south of the project). The locations of these bores are also shown in Figure 2.9.

All other model boundaries are assigned as the no flow boundary type and are assigned where the model domain is aligned perpendicular to the inferred direction of groundwater flow.

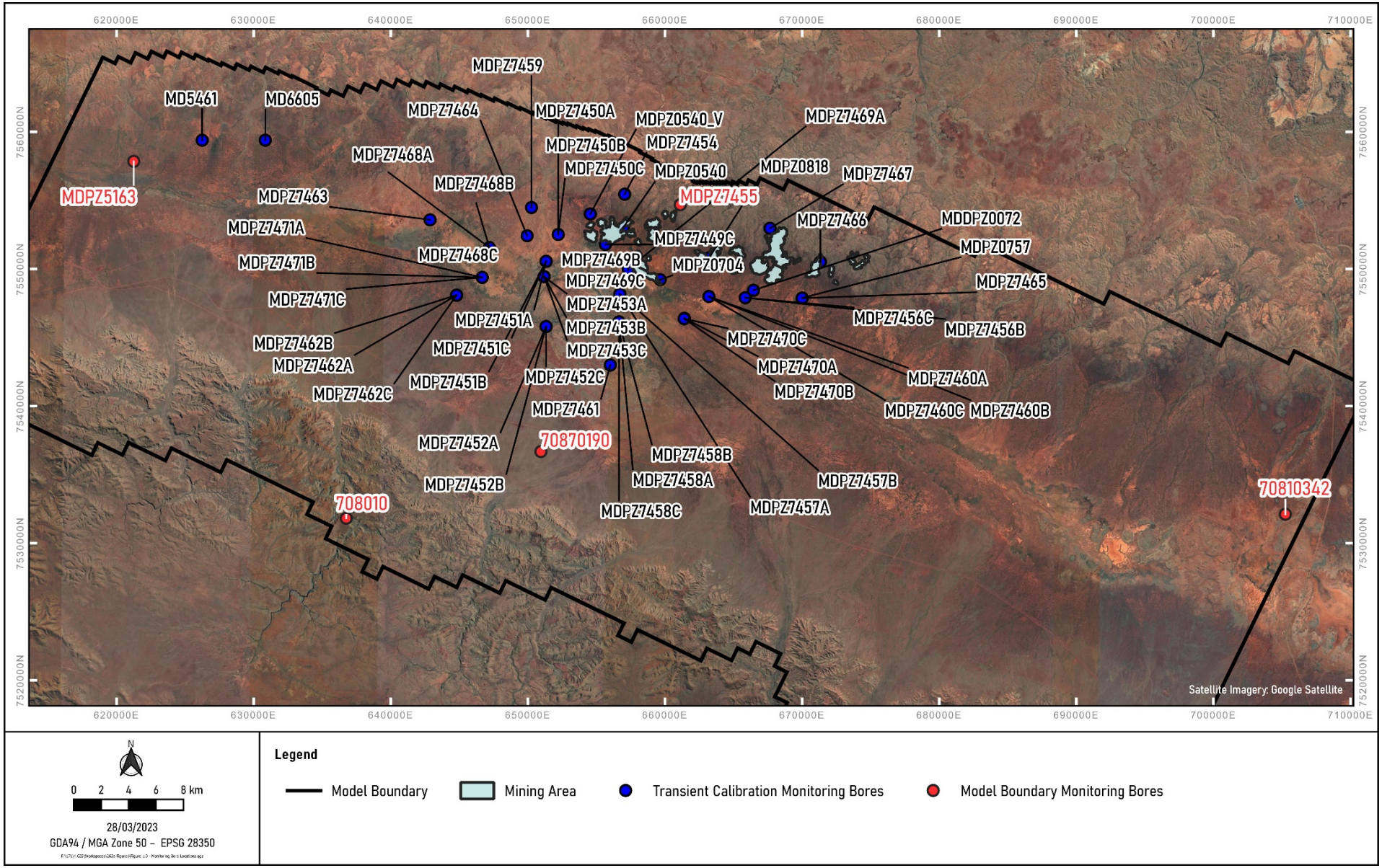

Figure 2.9 Monitoring Bores used in Model Calibration

2.3.2 Recharge

In addition to groundwater inflows from upstream and to downstream, the groundwater system is also recharged by incident rainfall from thunderstorms and cyclonic events. Rainfall recharge is assigned to creek zones and the valley as shown in Figure 2.10. Creek lines assigned recharge were mapped from the relevant 1:250,000 geological maps (Mount Bruce Thorne, 1992 and Roy Hill Thorne et al, 1996). No additional recharge was applied to the claypan areas (i.e. only valley recharge was assigned to the claypan areas).

Initially, a proportion of monthly rainfall, from the Scientific Information for Land Owners (SILO) data base (SILO station ID 19970526, SILO, 2022), which mostly falls between the months of December and March, was applied as recharge to the creek and valley recharge zones. This approach did not simulate the measured responses to rainfall events, suggesting that the antecedent rainfall conditions may be important in estimating rainfall recharge. To accommodate this, rainfall recharge to groundwater was simulated using an approach that assumes that recharge only occurs once the soil column above the water table has been raised to a moisture content close to field capacity. This approach assumes that no recharge occurs until cumulative rainfall over successive days exceeds a specified threshold. The cumulative threshold required to generate rainfall recharge and the percentage of incident rainfall assigned as recharge were adjusted as part of model calibration and is discussed further in Section 2.5.5.

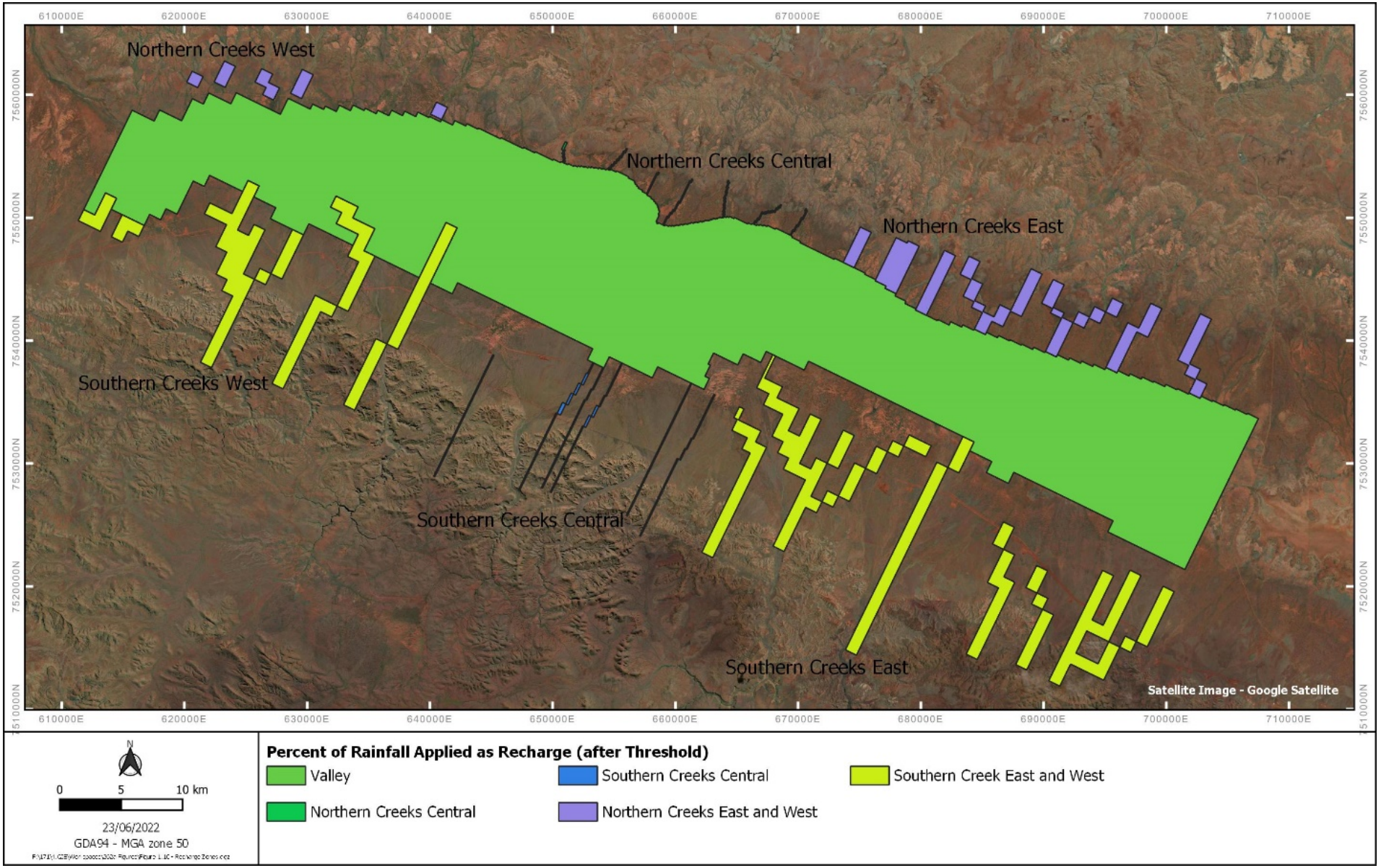

Figure 2.10 Recharge Zones used in the Model

2.3.3 Evapotranspiration

Evapotranspiration (ET) from the water table across the valley is simulated using the Evapotranspiration (EVT) package in Modflow SURFACT. The EVT package uses a depth dependant relationship such that if the predicted aquifer water levels are at or above a specified elevation (the ET surface), ET occurs at a maximum specified rate. If predicted aquifer water levels decrease to below the specified ET surface, the ET rate decreases linearly to zero as the predicted water level approaches an elevation equal to the ET surface, minus a specified extinction depth. This relationship is shown in Figure 2.11. Details of the parameters included in the EVT package are described below:

- ET losses are included over the model domain at a maximum rate of 1,095 mm/year (or 3 x 10^{-3} m/d). This is approximately 30% of long-term average annual potential evaporation of 3,372 mm/year (SILO station ID 19970526, SILO, 2022). While ET is modelled outside of the valley, there are no ET losses from areas where the depth to water exceeds the extinction depth (see below). The simulation of ET in the valley and along drainage lines is discussed further in Section 2.5.6.
- The ET surface was set equal to the ground surface.
- The ET extinction depth was set to 2 m below the ground surface across the model domain. Evaporative soil losses are only assumed to occur over this depth consistent with the direct evaporation of groundwater and to a lesser extent, evapotranspiration from vegetation (consistent with the root zone as estimated in a parallel ecohydrological study (AQ2, 2024)).
- Notwithstanding the above, modelled ET will not be directly comparable to the ET flux determined from the ecohydrological study. The former estimates the total volume of ET across the entire (regional) model domain. The latter estimated ET flux specifically for the flood plain vegetation community surrounding the claypans.

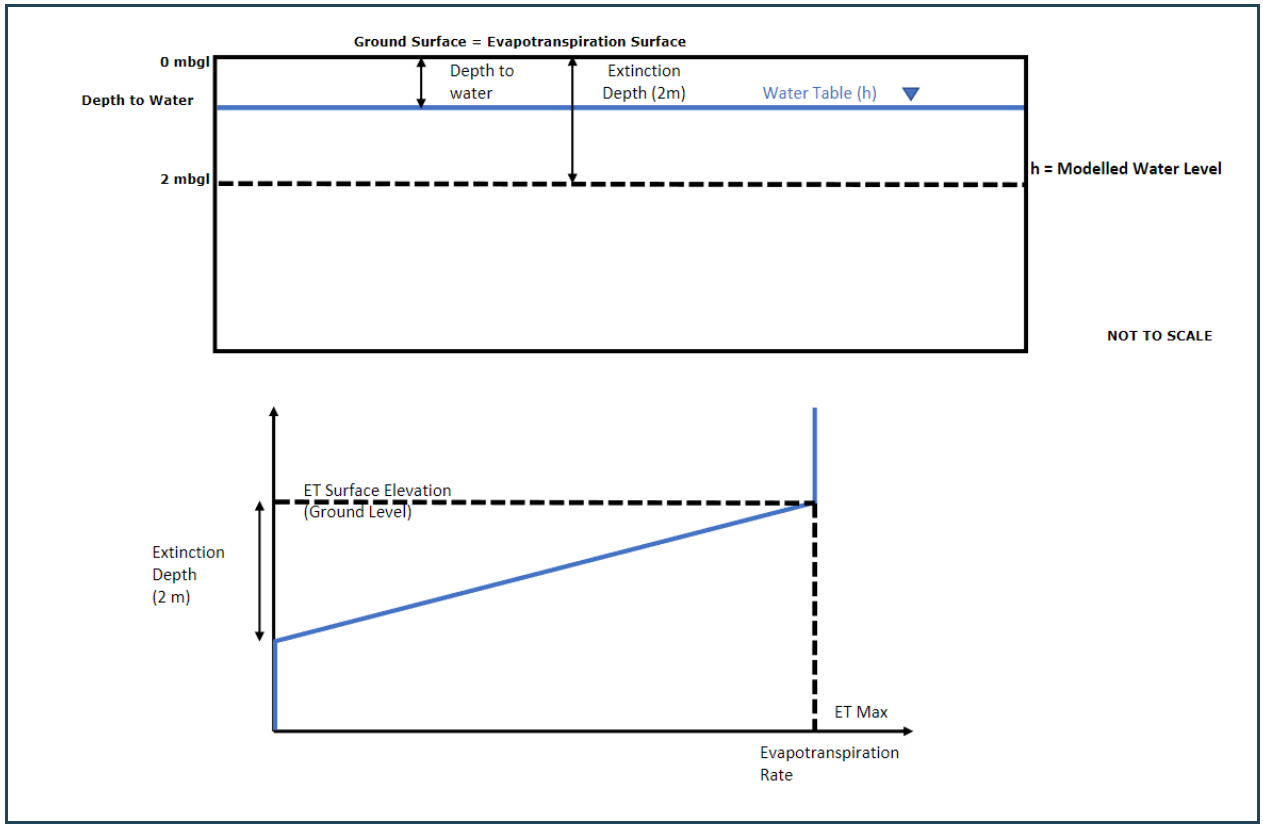

Figure 2.11 Evapotranspiration Conceptual Diagram

2.4 Model Calibration

2.4.1 Approach to Model Calibration

Model calibration is the process by which the parameters of a numerical model are adjusted, within realistic limits, to provide the best match to measured data. This process involved testing and refining the aquifer properties and boundary conditions of the model to improve the match between observed data and simulated values.

The groundwater level data available for model calibration was from several sources, including:

- Groundwater level data from aquifer testing completed between September and December 2021.
- Groundwater level monitoring for the Mulga East and Malay Well areas collected between 2008 and 2021.
- Groundwater level monitoring for Mulga West collected between 2019 and 2021.
- Groundwater water level monitoring from the DWER data base.

2.5 Model Calibration Performance

2.5.1 Aquifer Testing

The model was used to simulate the measured groundwater responses to five long-term aquifer tests conducted between September and December 2021 (AQ2 2024). Details of the five long-term aquifer tests conducted as part of the 2021 field investigations are outlined below:

- MDPB0018 was pumped for 5 days at 38 L/s (3,283 kL/d) with one day of measured water level recovery. Water level observations were taken at the pumping bore (MDPB0018) and at observation bores MDPZZ9206 and MDPZ7933.
- MDPB0019 was pumped for 4.25 days at 38 L/s (3,283 kL/d) with one day of measured water level recovery. Water level observations taken at the pumping bore (MDPB0019) and at observation bore MDPZ79207.
- MDPB0017 was pumped for 2.2 days at 40 L/s (3,456 kL/d) with one day of measured water level recovery. Water level observations taken at the pumping bore (MDPB0017) and at observation bores MDPZ9204, MDPZ7456A, MDPZ7456B and MDPZ7456C.
- MDPB0016 was pumped for 3.1 days at 40 L/s (3,456 kL/d) with one day of measured water level recovery. Water level observations taken at the pumping bore (MDPB0016) and at observation bores MDPZ7469A, MDPZ7469B and MDPZ7469C.
- MDPB0020 was pumped for 2 days at 20 L/s (1,728 kL/d) with one day of measured water level recovery. Water level observations taken at the pumping bore (MDPB0020) and at observation bores MDPZ9212D, MDPZ9212S and MDPZ5355.

Regional groundwater models, such as the one developed for Mulga Downs and surrounding groundwater catchment are generally not suitable to simulate the data collected during aquifer tests because:

- Drawdowns at pumping bores are influenced by bore losses that result from near bore characteristics (pumping losses and formation losses) that are not simulated by regional groundwater models.
- Observation bores are often located close to pumping bores, or in the case of regional groundwater models, only one to two cells away from pumping bores, or in the same cells. This limits the capacity of a regional finite difference groundwater flow model (used for the current study) to simulate the water level gradients that may develop around a pumping bore.

- Larger cells sizes, required for the development of a regional groundwater flow model, often contain significantly greater storage volumes than the entire volume of water removed during lower flow pumping tests.
- Aquifer testing is often short in duration (24 to 72 hours) although some longer tests were also conducted as part of the current investigations (up to 5 days duration).

In the absence of any longer term pumping, or aquifer stresses, the tests provide an opportunity to replicate the only available aquifer responses to pumping, as part of the model calibration processes. The regional groundwater flow model was used to simulate the general drawdown trends observed during the tests completed. A "trial and error approach" was used for the simulations, using the pumping test derived estimates of aquifer parameters as a set of narrow constraints. The locations of the pumped bores and monitoring bores used during testing are shown in Figure 2.12. The model was run to simulate the tests sequentially to include interactions between pumping locations.

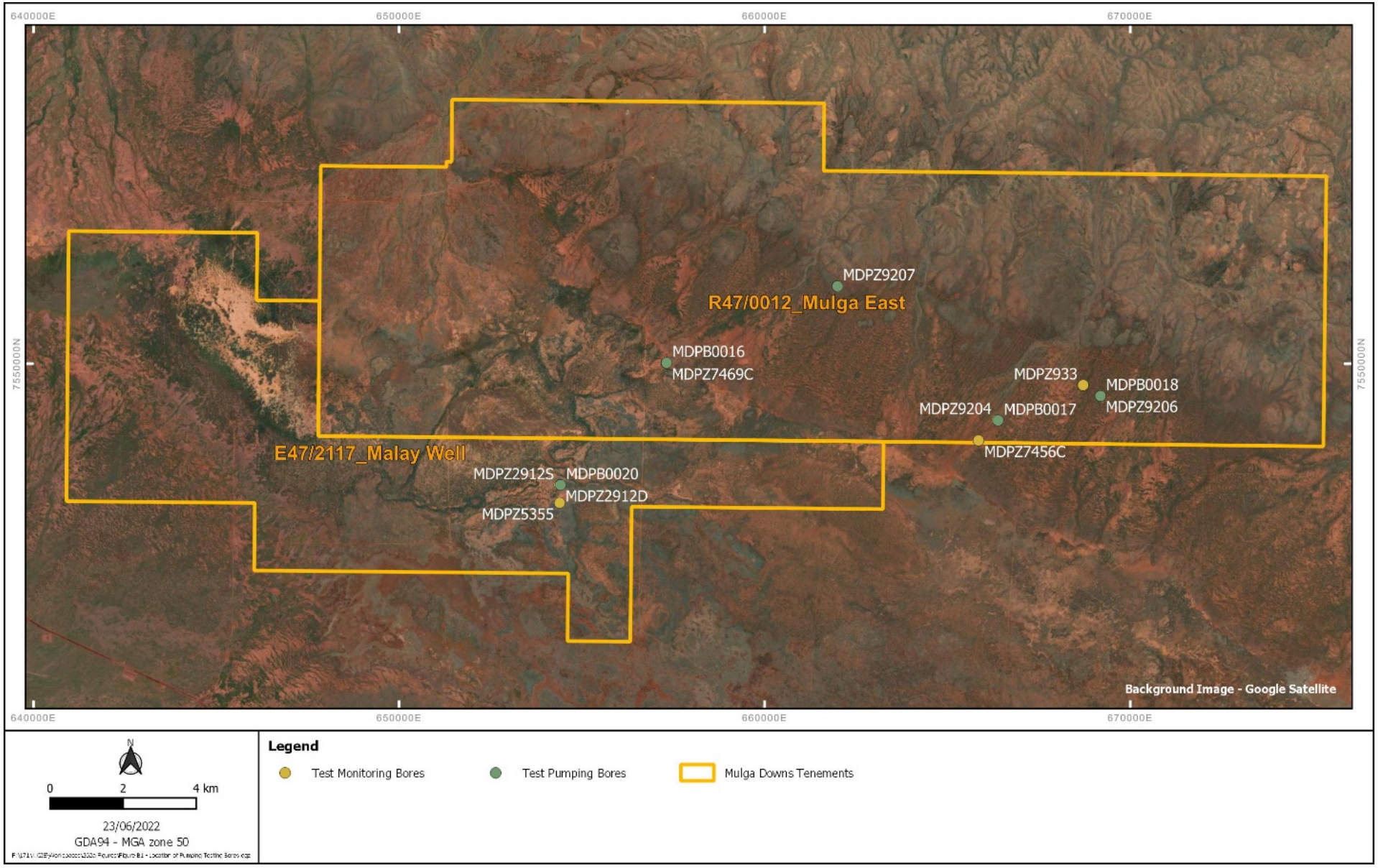

Figure 2.12 Location of Aquifer Testing Bores

The pumping test simulations were not designed to provide a range of aquifer parameters. Rather they were used to test the assumptions associated with the two potential conceptualisations. One conceptualisation (and associated parameter set) assumes that the orebody has a higher hydraulic conductivity than the CID / Pisolite. The alternate conceptualisation (and associated set of parameters) assumes that the CID/ Pisolite has a higher hydraulic conductivity than the orebody aquifer. With the current level of understanding it is not clear which of these cases is more likely and so two sets of calibrated aquifer parameters have been tested during the model calibration process.

Details of the aquifer parameters that provided the best match to pumping tests data, based on the two conceptualisations are outlined below:

- Base Case (Scenario 1): For this case, a higher hydraulic conductivity is included in the Marra Mamba / West Angela Ore (25 m/d) and a lower hydraulic conductivity for the CID / Pisolite (14 m/d). The hydraulic conductivity assigned to the Marra Mamba is based on the value estimated from the pumping tests at MDPB0018 and MDPB0016.
- Uncertainty Case (Scenario 2): For this case, a higher hydraulic conductivity was included for the CID / Pisolite (60 m/d based on the value estimated from the pumping test at MDPB0017), and a lower hydraulic conductivity was included for the Marra Mamba / West Angela Ore (12-13 m/d).

Observed and modelled drawdown responses from pumping tests are shown in Figure 2.13 to Figure 2.19. The Base Case and the Uncertainty Case test pumping simulations produced equally well matched responses to the measured drawdown. The difference in drawdown simulated for both cases was up to 1.5 m different. At most locations, the predicted drawdown differs by less than 1 m.

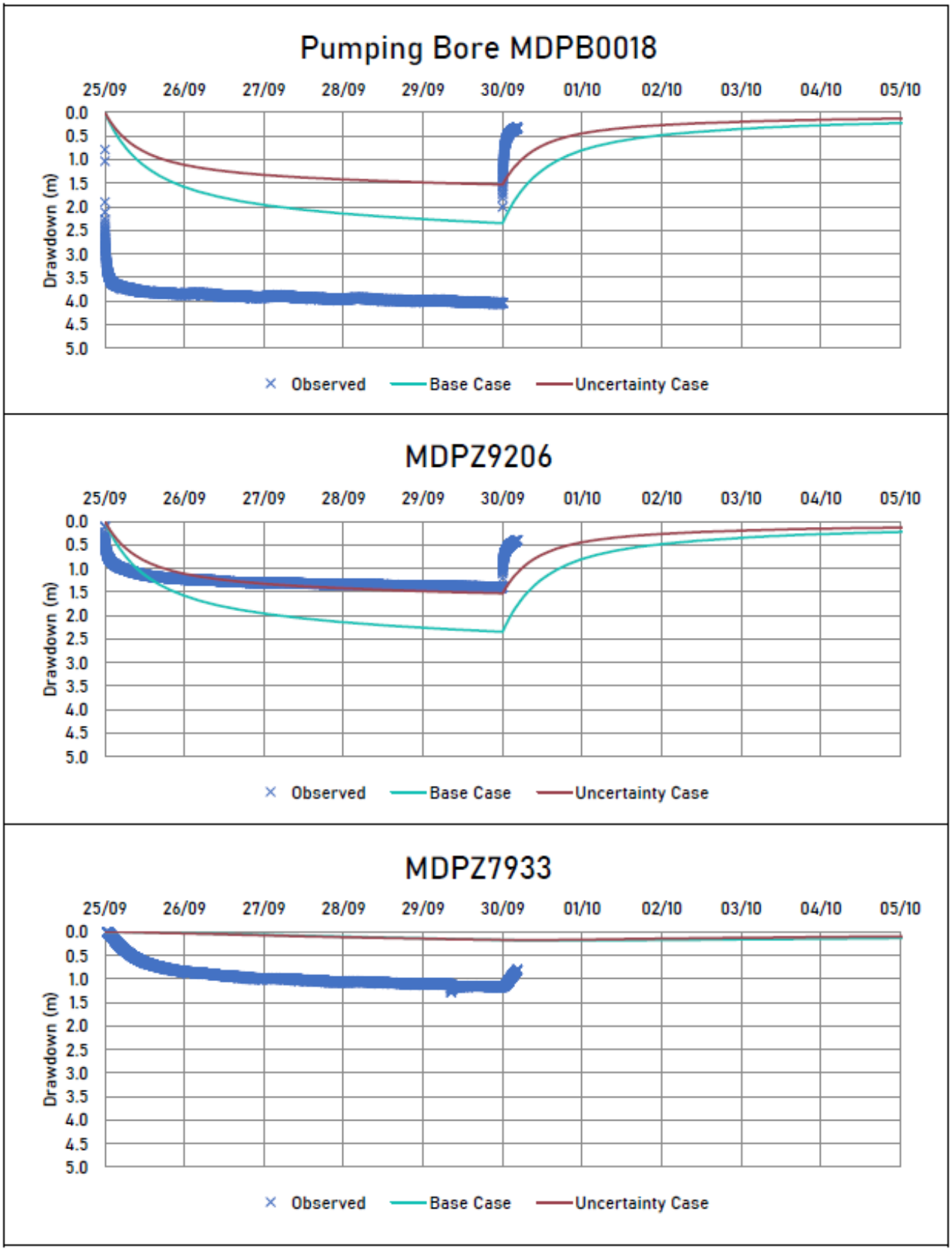

Figure 2.13 Test Pumping Calibration Hydrographs – MDPB0018

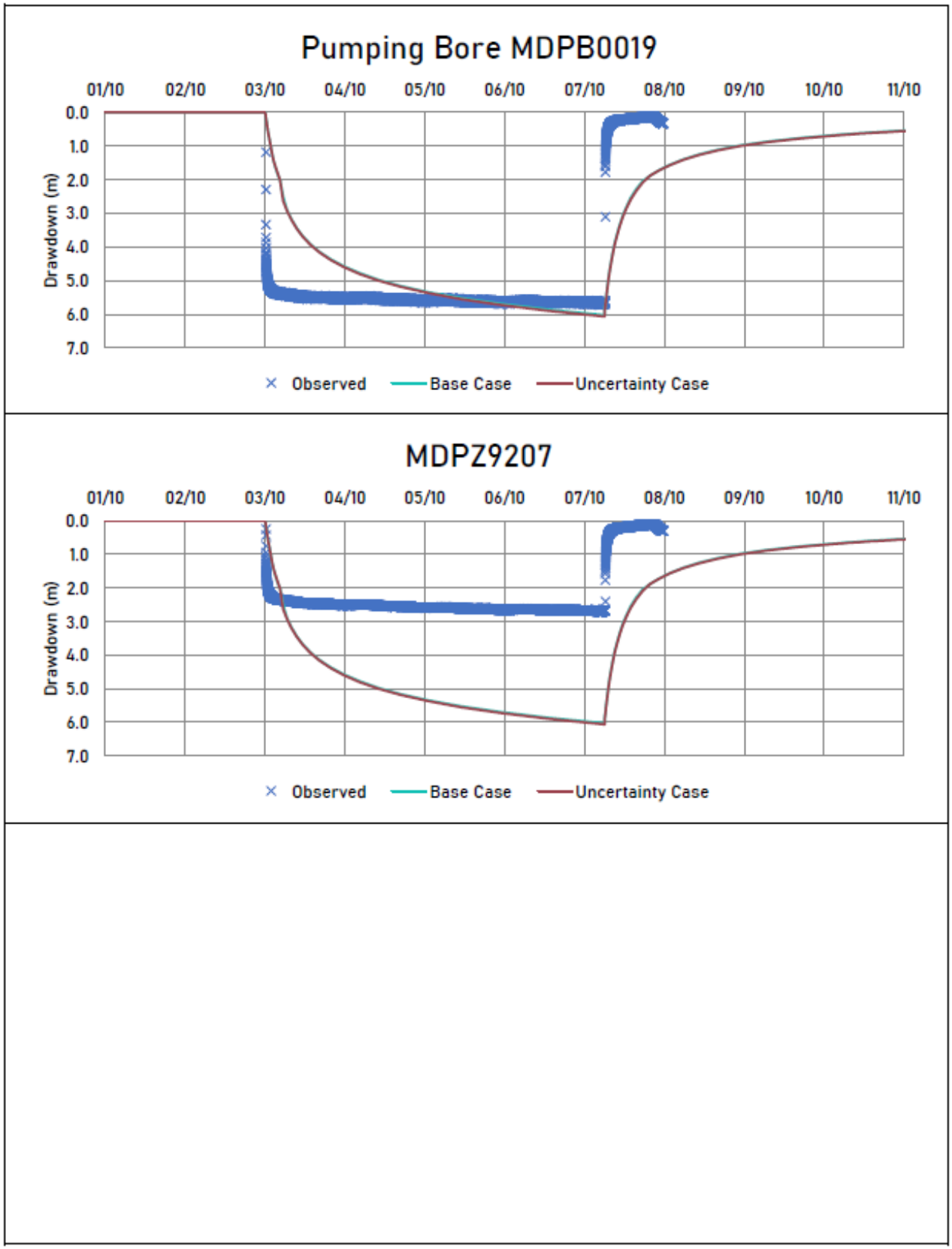

Figure 2.14 Test Pumping Calibration Hydrographs – MDPB0019

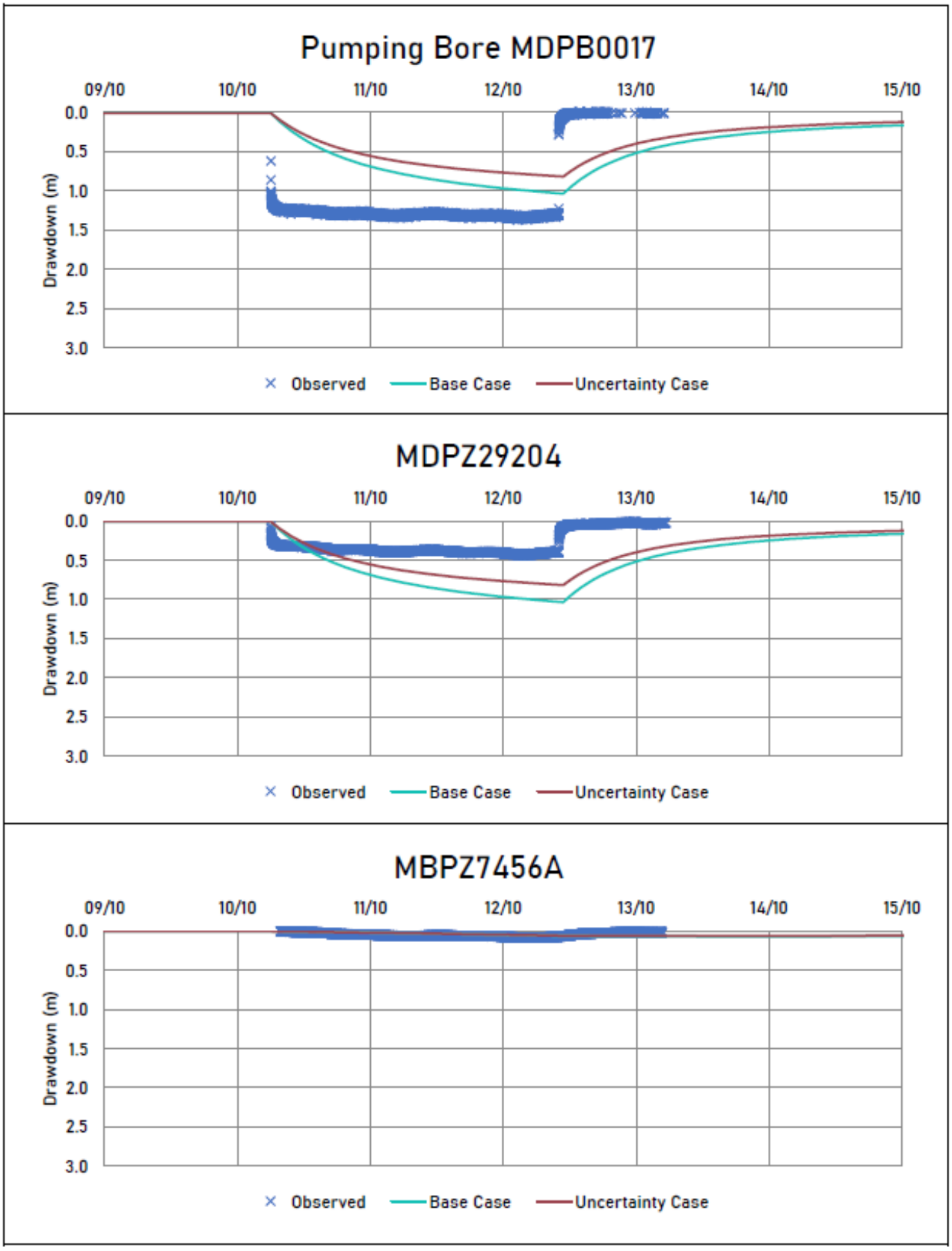

Figure 2.15 Test Pumping Calibration Hydrographs – MDPB0017

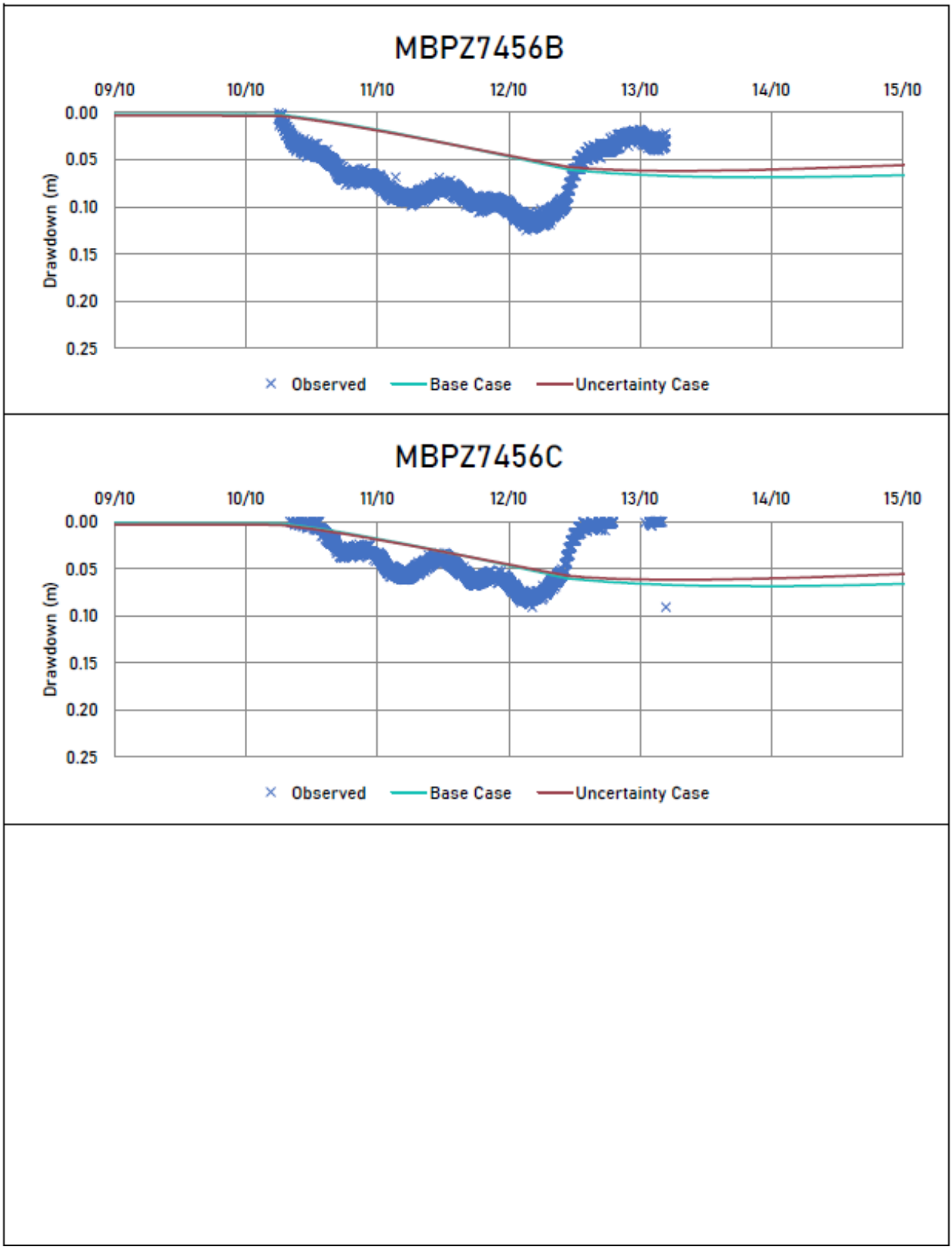

Figure 2.16 Test Pumping Calibration Hydrographs – MDPB0017 Observation bores

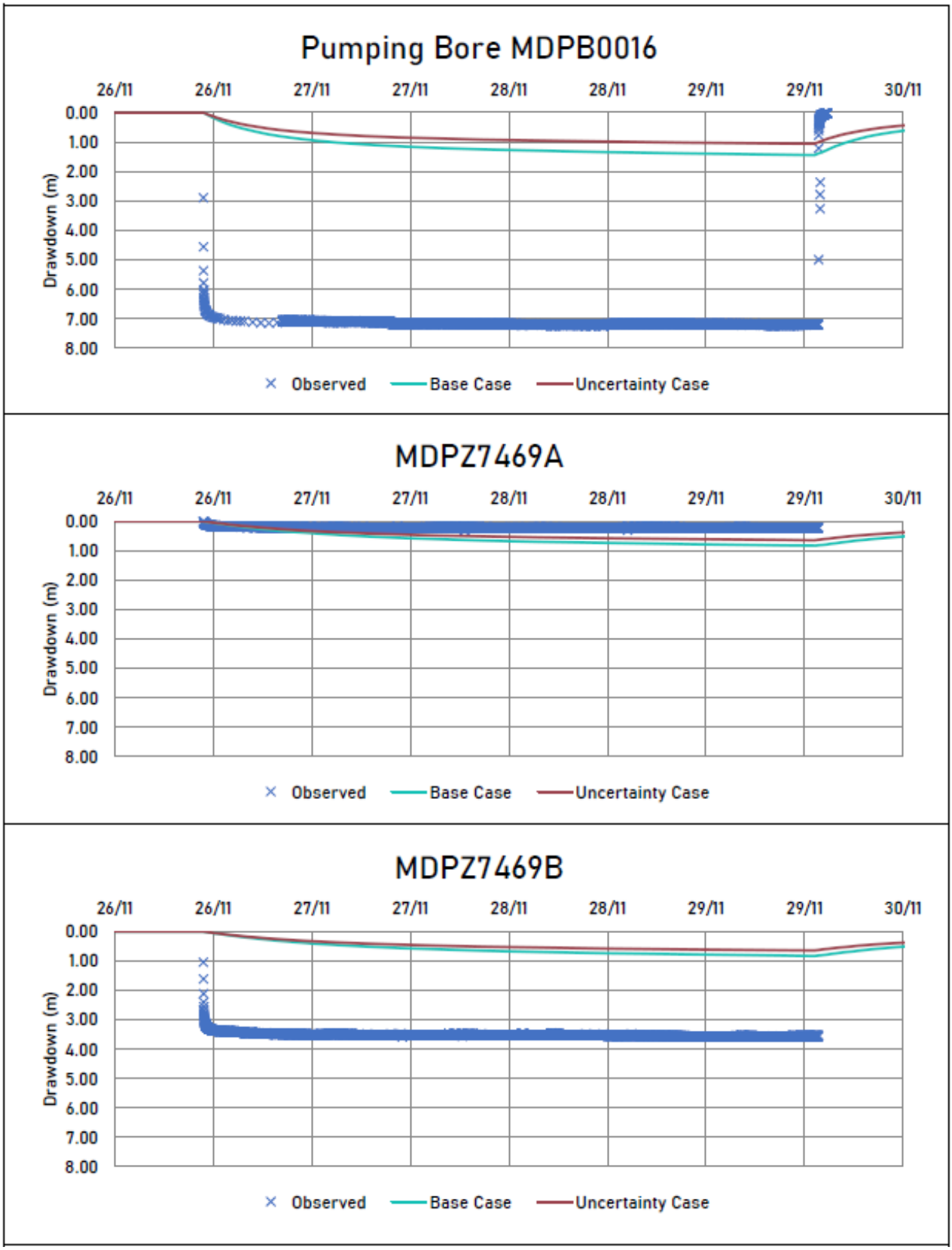

Figure 2.17 Test Pumping Calibration Hydrographs – MDPB0016

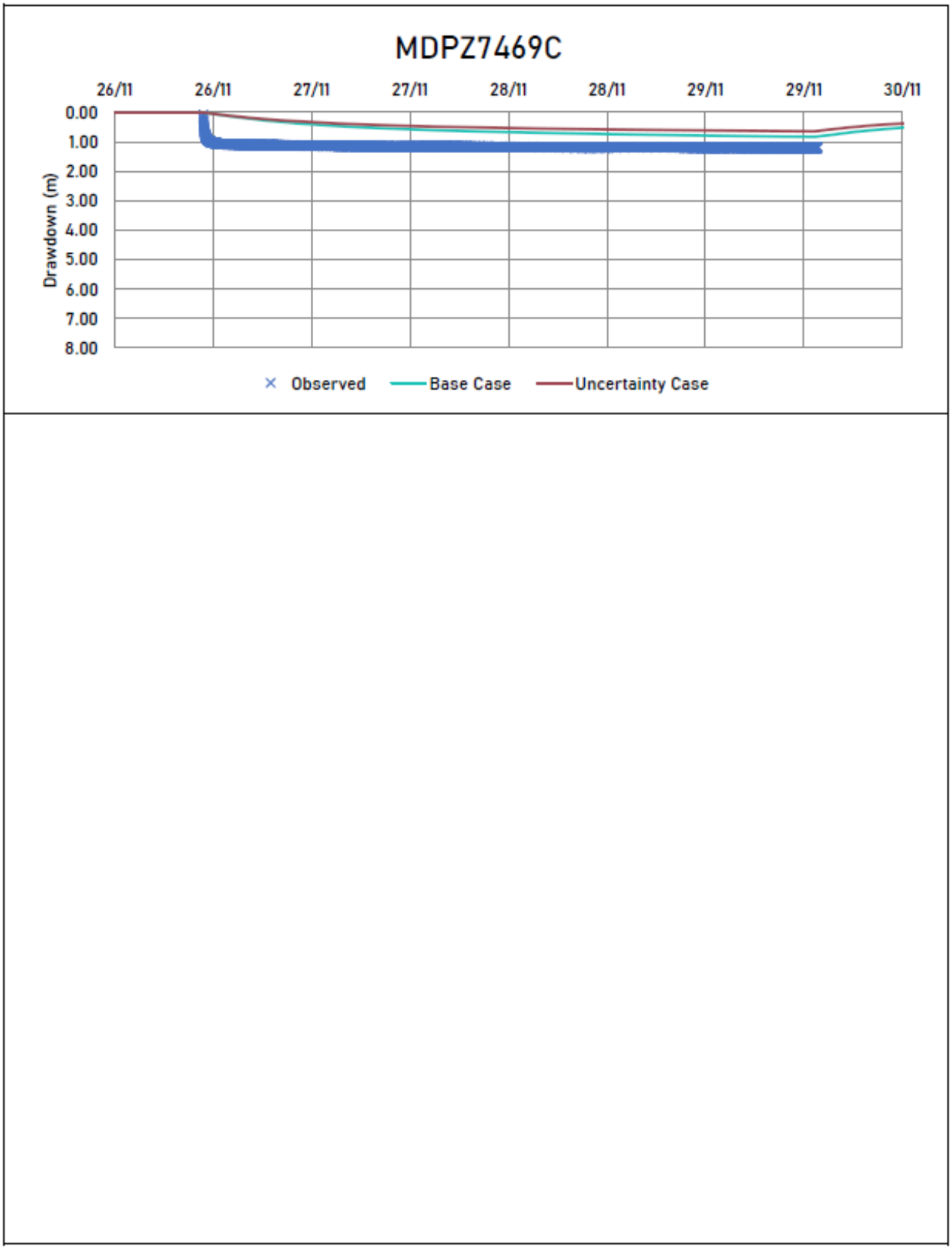

Figure 2.18 Test Pumping Calibration Hydrograph – MDPB0016 Observation bores

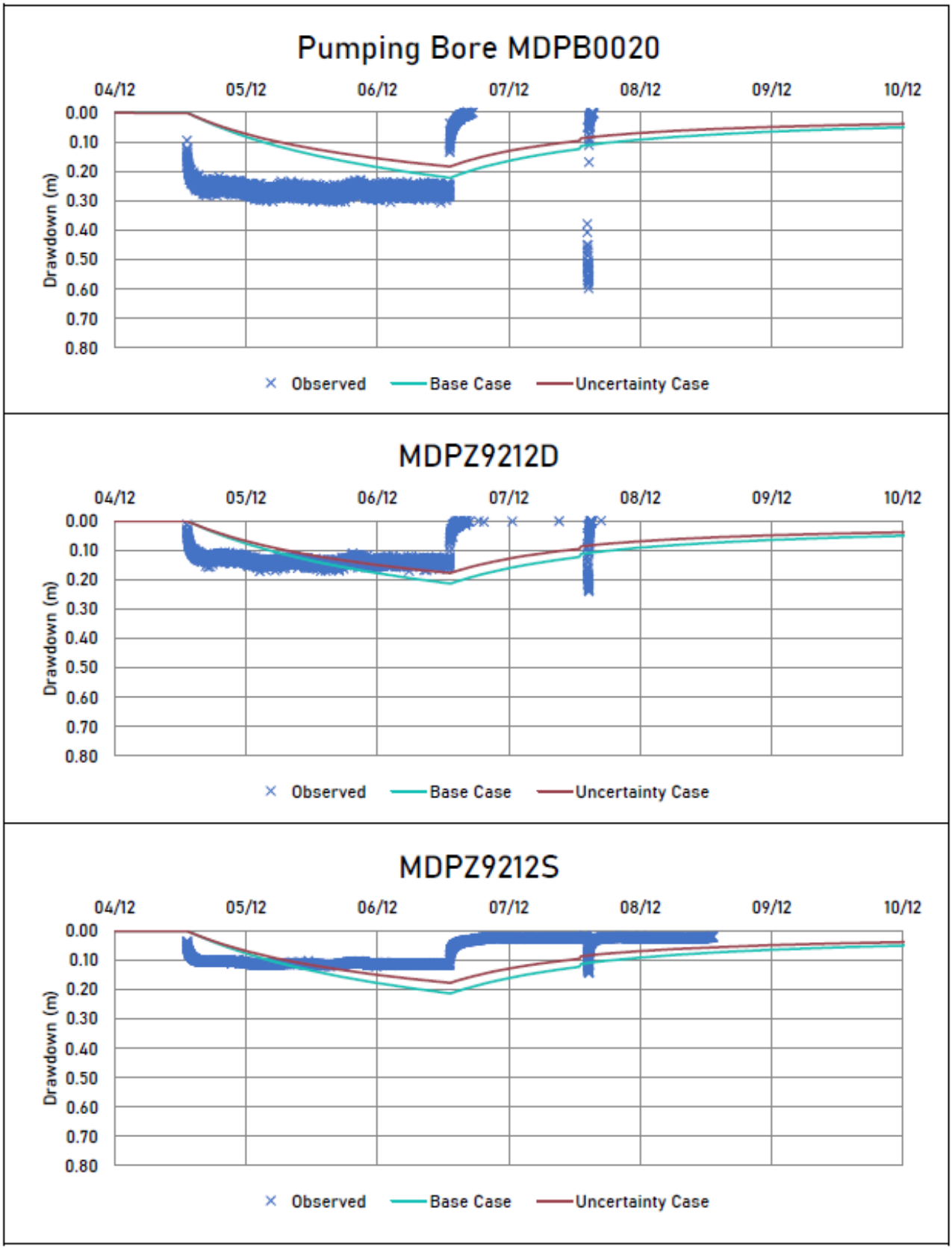

Figure 2.19 Test Pumping Calibration Hydrographs – MDPB0020

2.5.2 Calibration to Long Term Monitoring

Available groundwater monitoring, that extends back to 2008, at some monitoring locations, shows groundwater responses of several metres resulting from wet season rainfall followed by a recession (refer AQ2, 2024). In some cases, measured water levels show successive increases in water levels, with no intervening recession. Annual rainfall for Mulga Downs from 1900 onwards is shown presented in the Baseline Assessment report (AQ2, 2024). Since 1992, the long-term average rainfall for the area was 435 mm which is in excess of the longer term average of 400 mm (SILO, 2021).

As a result of the rainfall recharge conditions in the catchment, groundwater levels in the modelled catchment are not readily described by a long-term average or steady state water level calibration. To accommodate this, water level conditions for the catchment were simulated using a dynamic calibration process. The process involved running the model for a period of 62 years, from 1960 to 2022 using the rainfall recharge, groundwater throughflow and ET conditions described in the previous sections. A preliminary steady state model was developed to simulate a single set of initial conditions, however aside from the generation of these conditions, there was no further development or calibration of the steady state model.

The model data set was run for a 62-year period (or 732 monthly stress periods) to include the impacts of variable rainfall recharge). This process was used to simulate the dynamic water level conditions in the catchment under a range of climatic conditions. This process was also used to simulate the catchment water level response to variable rainfall conditions to check that the catchment would not "fill up" after several years or show no water level decline during drier periods (for example during the period 1960 to 1980) as a result of the applied recharge and discharge conditions.

From the results of the model simulation of the measured groundwater responses to aquifer tests, two sets of parameters (the Base Case or Scenario 1 and the Uncertainty Case or Scenario 2) were used for history matching or simulation of long term measured water levels. Some minor adjustments were made to aquifer parameters as part of model calibration to the extended long term data set. Significant model calibration effort was not required as part of the current study as detailed model calibration was completed as part of the Mulga East Preliminary Groundwater Management Assessment (AQ2, 2021) using a trial and error approach. As part of this previous assessment, changes were made to aquifer parameters, model boundary conditions and the rainfall recharge approximation to provide the best match to measured water levels.

The locations of the monitoring bores used in the history matching model calibration are shown in Figure 2.9, with hydrographs of observed and modelled water levels shown in Figure 2.20 to Figure 2.38. Water level monitoring data from recently installed bores show water level changes of the order of centimetres in response to rainfall recharge and the subsequent water level recession. Longer term monitoring from across the orebody areas, collected between 2008 and 2021 show variable water level responses in years with lower and higher than average rainfall. Water level responses to rainfall are limited between 2008 and 2010 when lower than average rainfall was recorded. Responses to rainfall recharge of between 0.2 and 1.5 m were measured between 2011 and 2021.

Model calibration performance is described below as a comparison between available measured and modelled water levels. The water level comparison is shown for the period over which monitoring data are available, and is variable between bores, even though the model calibration data set was run for a 62 year period (1960 to 2022). The comparison between measured water levels and the modelled responses for the Base Case (Scenario 1) and the Uncertainty Case (Scenario 2) are described below.

2.5.2.1 Mulga West

Hydrographs of measured and modelled water levels for the Base Case (Scenario 1) and the Uncertainty Case (Scenario 2), for bores MD5461 and MD6605 in Mulga West, are shown in Figure 2.20. Measured water

levels are available between August 2019 and December 2021 of the calibration period. At these monitoring locations, the water level magnitude is generally replicated by both models, with a maximum difference between observed and modelled water levels of 1.5 m and 0.5 m for the Base Case (Scenario 1) and the Uncertainty Case (Scenario 2) respectively. At this location, some of the seasonal water level responses are not matched by the model.

2.5.2.2 Mulga East – Northern Slopes

Hydrographs of measured and modelled water levels across the northern flanks of the Fortescue Valley (within the project area) are shown in Figure 2.20 to Figure 2.28 for Scenarios 1 and 2. At most locations data is only available from early 2019 to late 2021. At some locations, monitoring data is available for longer periods; from late 2008 to early 2014 at MDPZ0540 Figure 2.21) and from early 2015 to early 2020 at MDPZ0704 and MDPZ081 (Figure 2.25) and MDDPZ0072 (Figure 2.26).

At monitoring locations in this area, the measured water level trends are generally replicated by both the Base Case (Scenario 1) and the Uncertainty Case (Scenario 2). Measured and modelled responses are summarised below:

- At bore MDPZ7454 (Figure 2.20) measured water levels are under predicted by around 3.5 m and the seasonal trend is not well matched.
- At bore MPDZ0540 (Figure 2.21) the overall measured water level trend is generally matched. Between February 2012 and June 2013 there is a measured increase in water levels, however the magnitude of this water level change is not replicated by the model.
- Similarly, at MDPZ0757 (Figure 2.27) the overall trend is generally matched, with the exception of a water level increase and decrease observed between November 2016 to February 2017. At MDPZ7463 and MDPZ462A/B/C, for the Uncertainty Case (Scenario 2), the maximum difference between measured and modelled water levels was 0.5 m compared to 1.5 m for the Base Case (Scenario 1).
- At several locations, there is an overall rising water level trend, however the model simulates a water level change over a much shorter period. The magnitude of the water level rise is however similar in the measured and modelled responses (MDPPZ7457C, Figure 2.23, MDPZ7460C, Figure 2.25, MDPZ7456C, Figure 2.26).

2.5.2.3 Mulga Downs - Valley

Hydrographs of measured and modelled water levels in the valley area for Scenarios 1 and 2 are shown in Figure 2.28 to Figure 2.38. At some locations, measured water levels are available for part of 2019, with data from other locations available from early 2019 to late 2021.

At monitoring locations in this area, the measured water level trend is generally replicated by the model with a maximum difference of 2 m between observed and modelled water levels for Scenario 1 and 2. At bores MDPZ7462 (Figure 2.36), MDPZ7458B, MDPZ7458C and MDPZ7470A (Figure 2.37) the model simulates a small (less than 0.5 m) response to simulated rainfall that is not observed in the measured water levels. In the later months of 2021, however, a water level recession is measured at these locations, that is generally replicated by the model. At bore MDPZ7470C (Figure 2.38) there is a small increase in measured water level observed, however a greater increase in water level is simulated (~0.2 m simulated over a period of several months versus less than ~0.1 m measured over a period of around 4 months). This suggests that the long term water level fluctuations in the valley maybe controlled by long term seepage processes (from perched water or from the valley flanks) rather than direct rainfall recharge. The current simulations suggests that the model set up over estimates recharge to the valley which would provide conservatism in model results (i.e. predicted recharge is higher than would be expected). At present there is not sufficient data to explain the differences between measured and modelled water levels across the catchment. The requirement to update simulated recharge in the groundwater model as part of future modelling work is discussed further in Section 3.6.

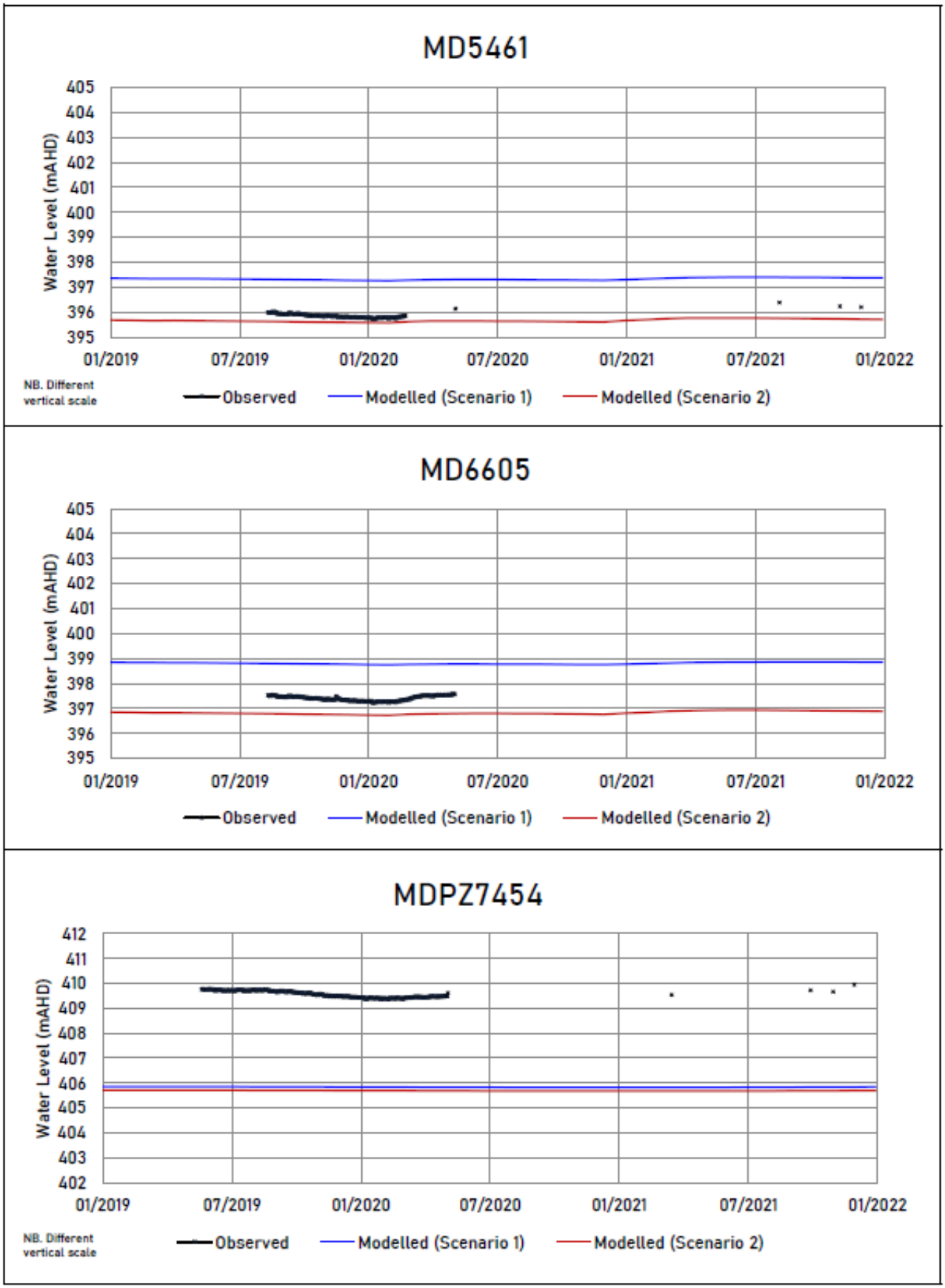

Figure 2.20 History Matching Calibration Hydrographs

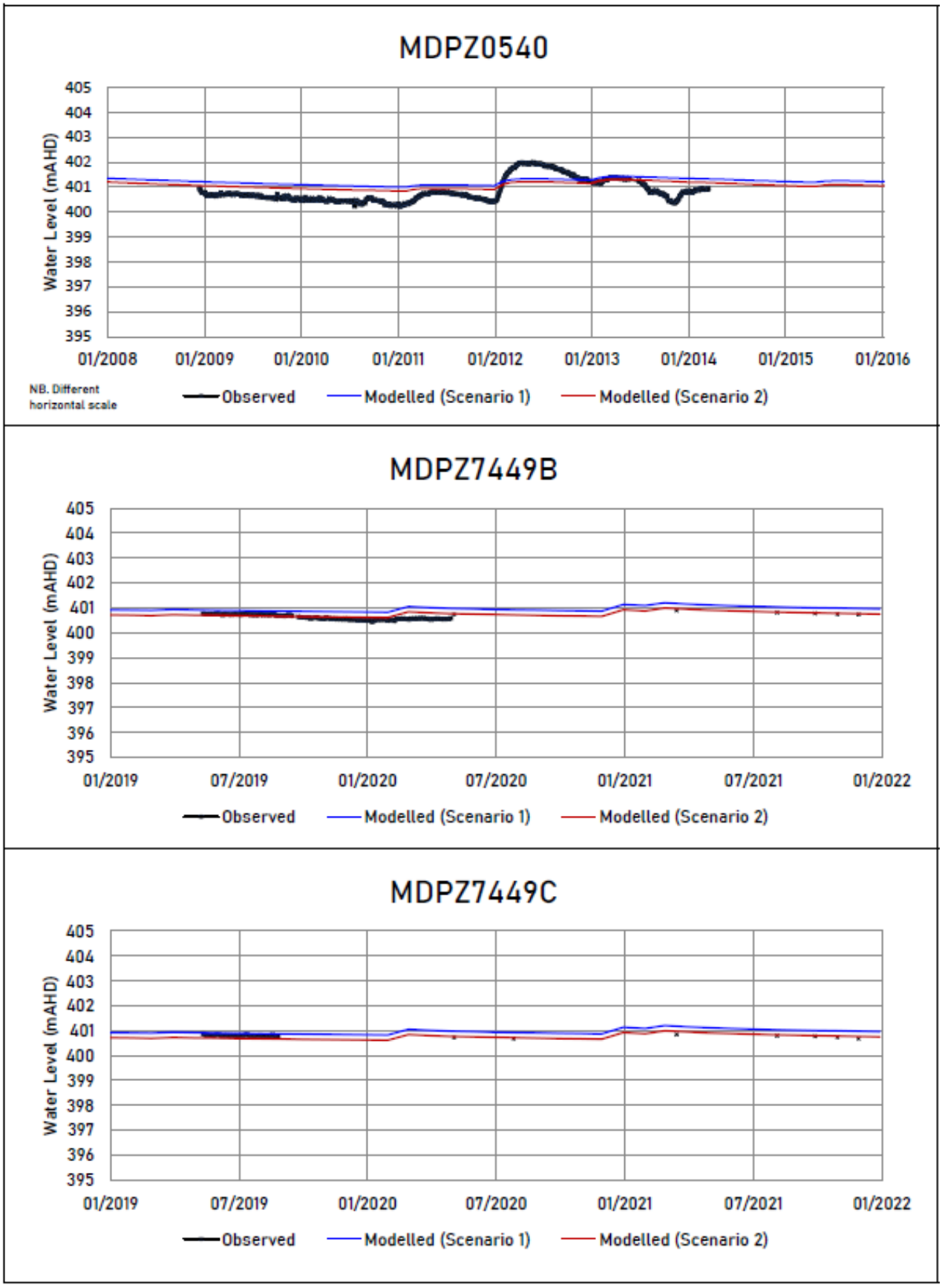

Figure 2.21 History Matching Calibration Hydrographs

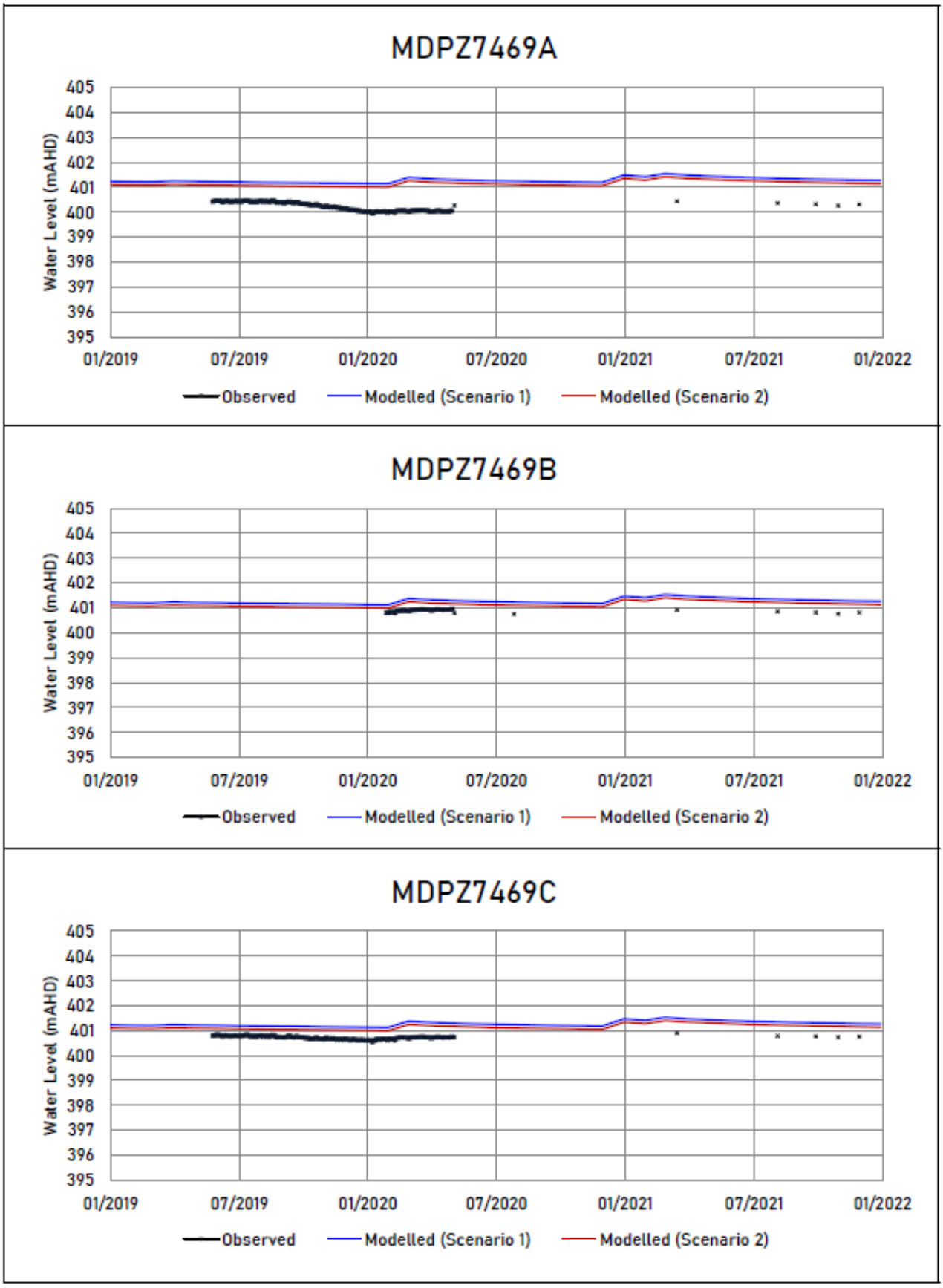

Figure 2.22 History Matching Calibration Hydrographs

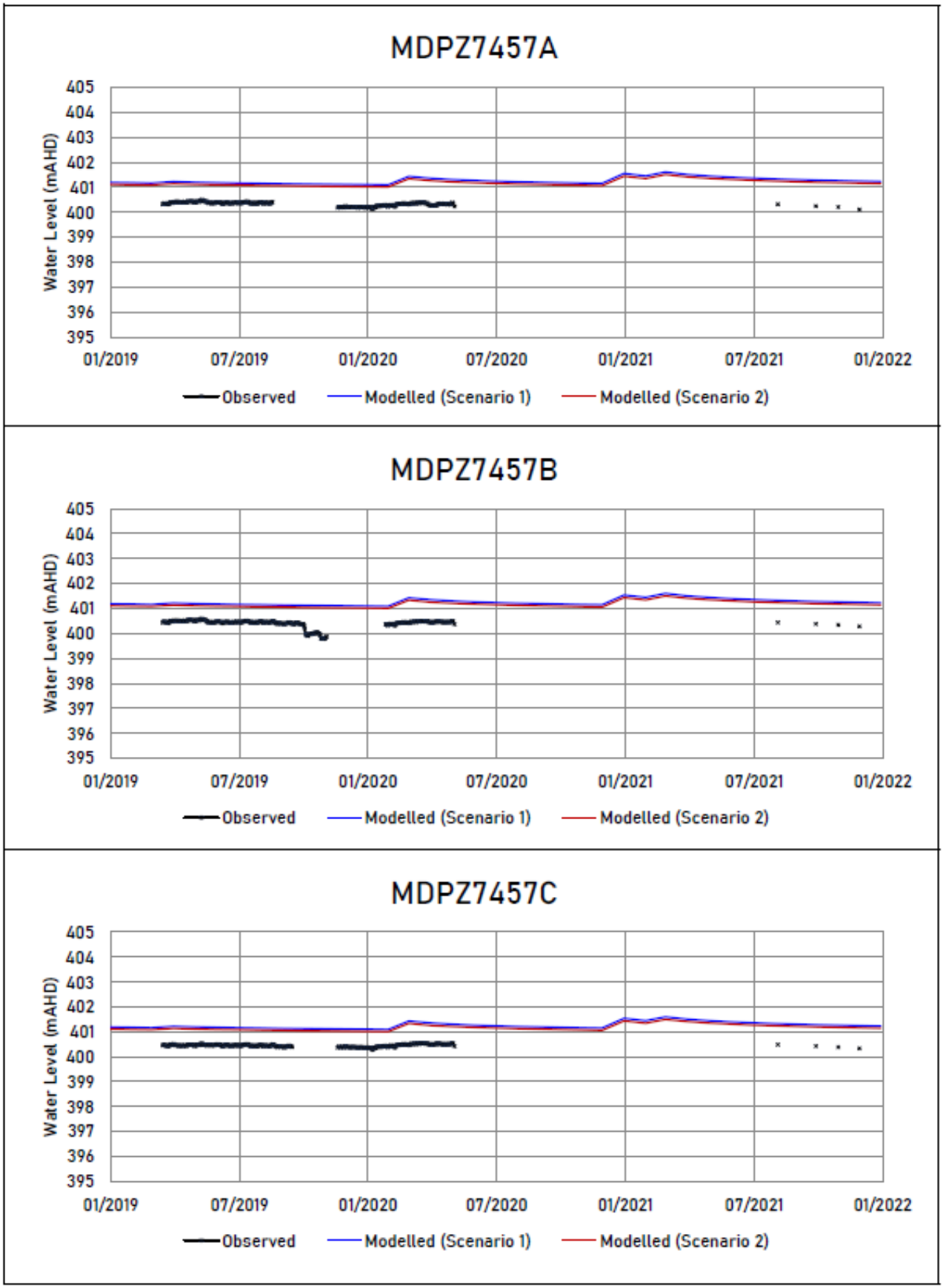

Figure 2.23 History Matching Calibration Hydrographs

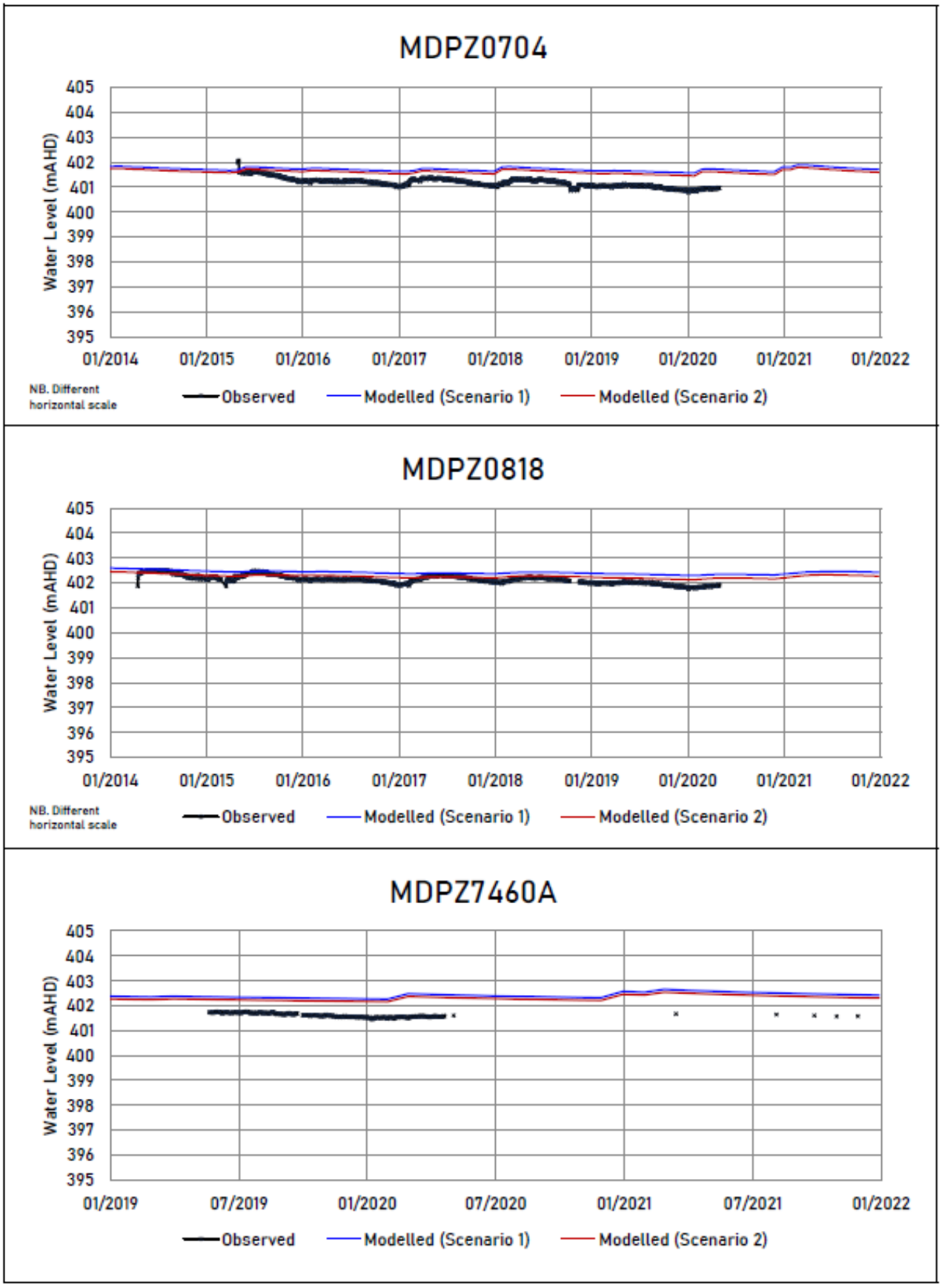

Figure 2.24 History Matching Calibration Hydrographs

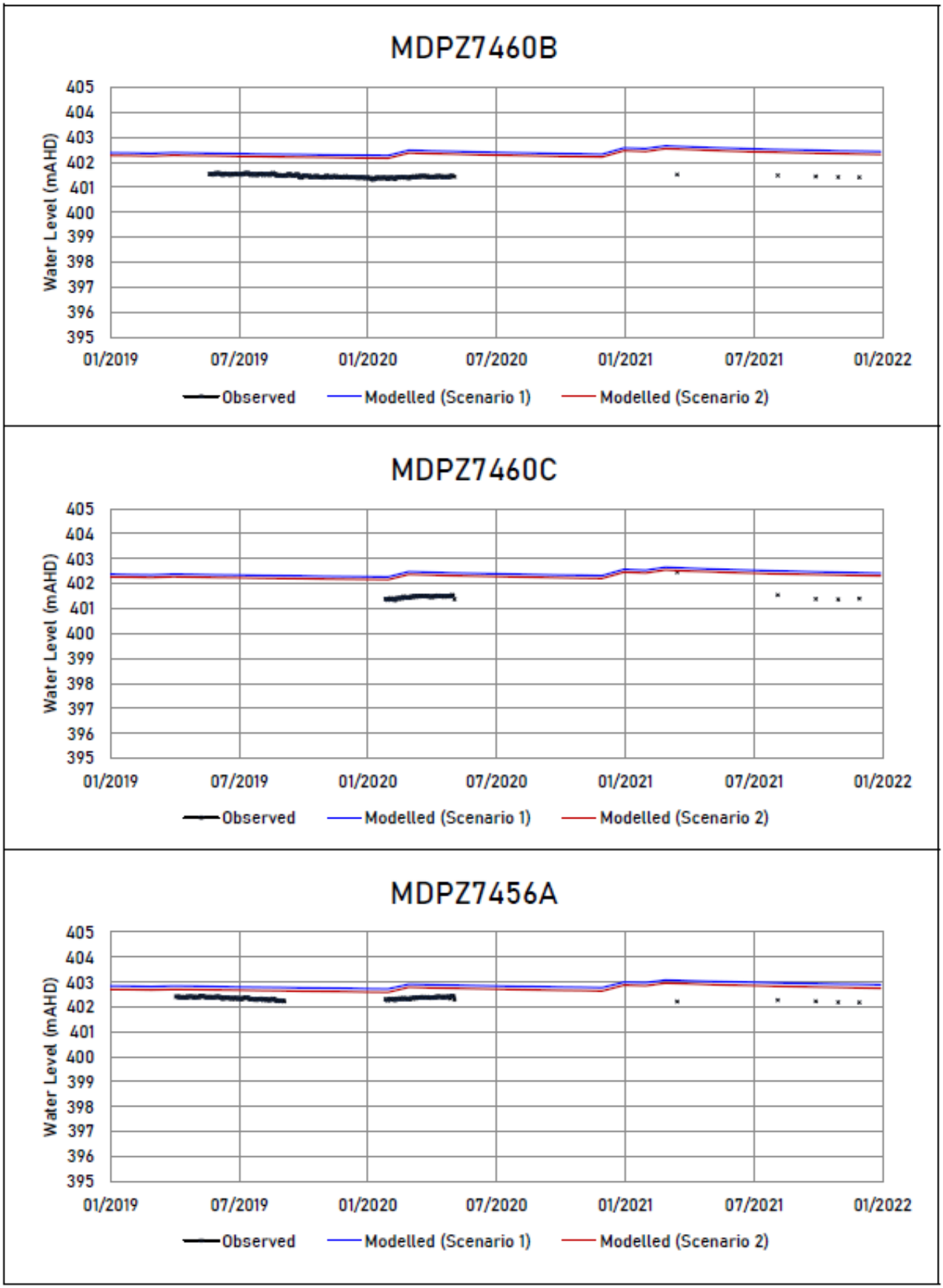

Figure 2.25 History Matching Calibration Hydrographs

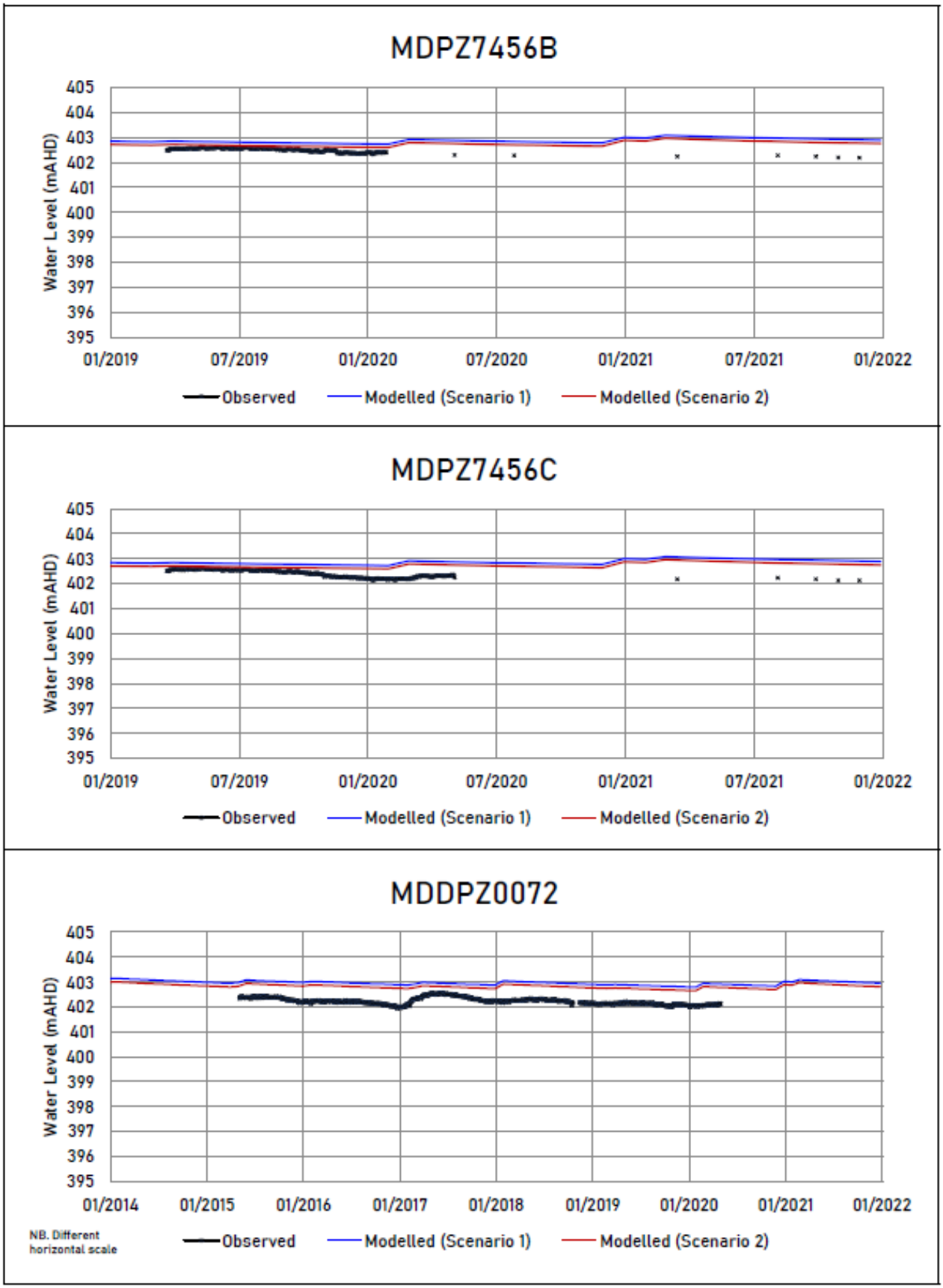

Figure 2.26 History Matching Calibration Hydrographs

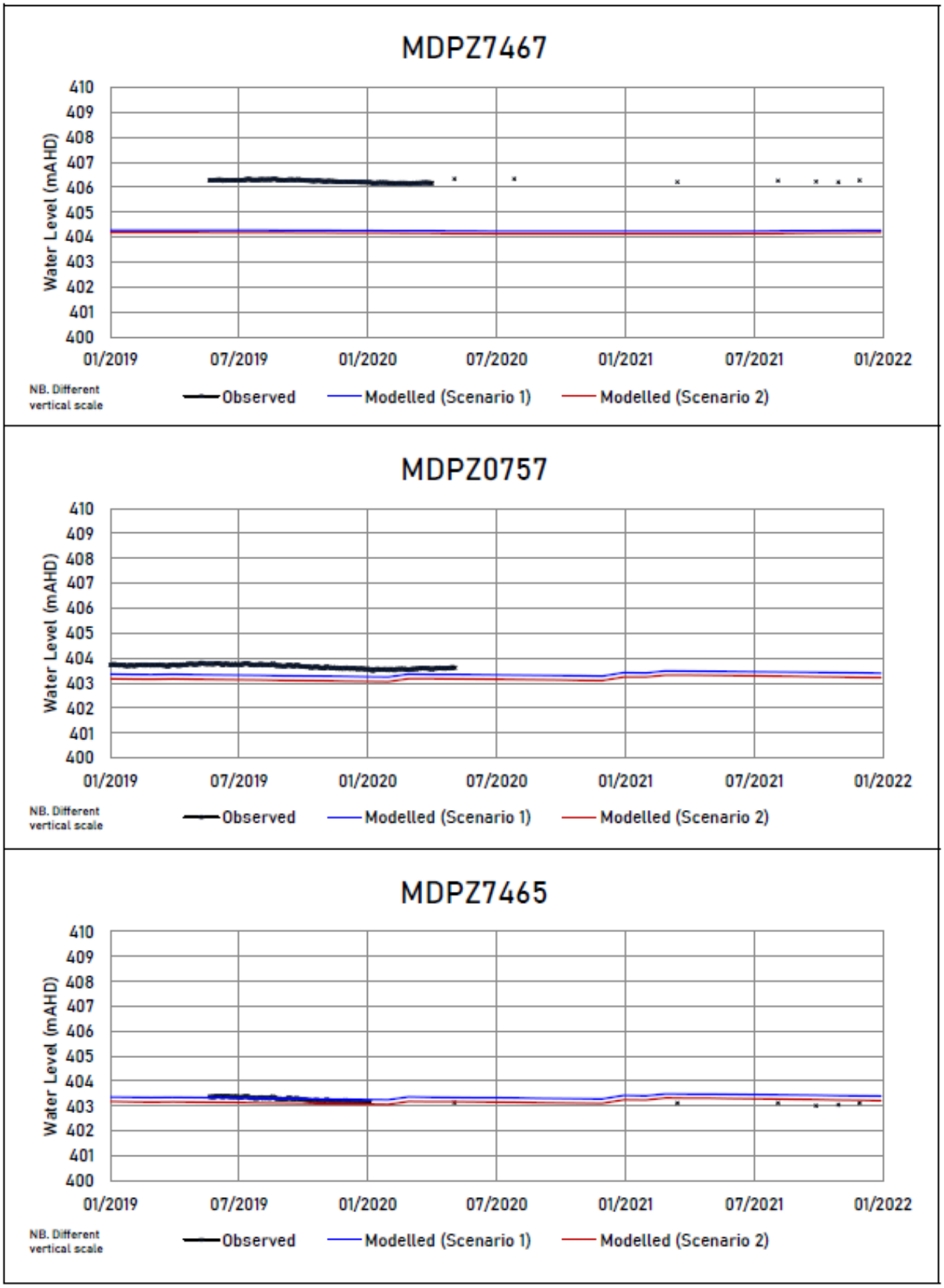

Figure 2.27 History Matching Calibration Hydrographs

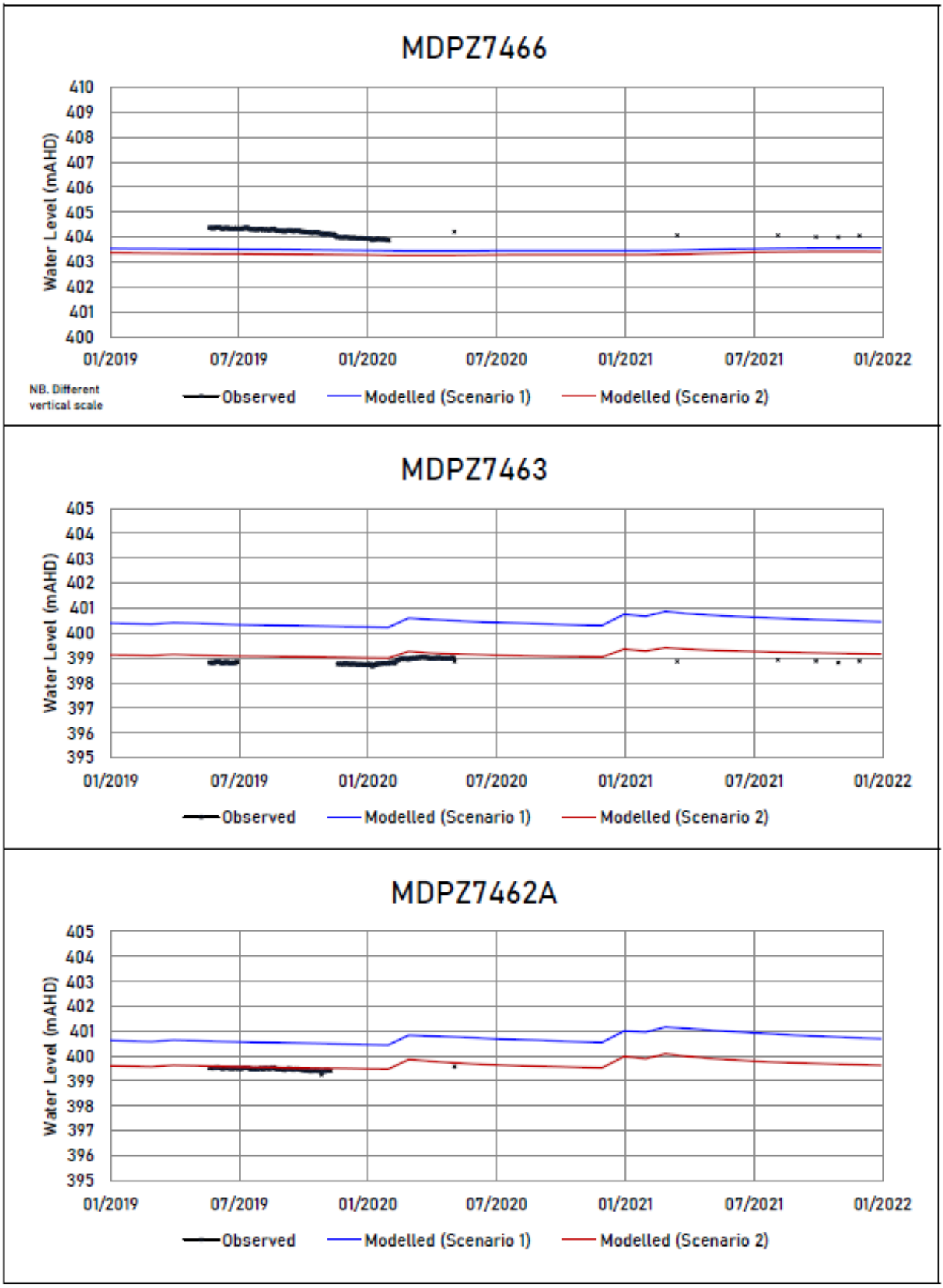

Figure 2.28 History Matching Calibration Hydrographs

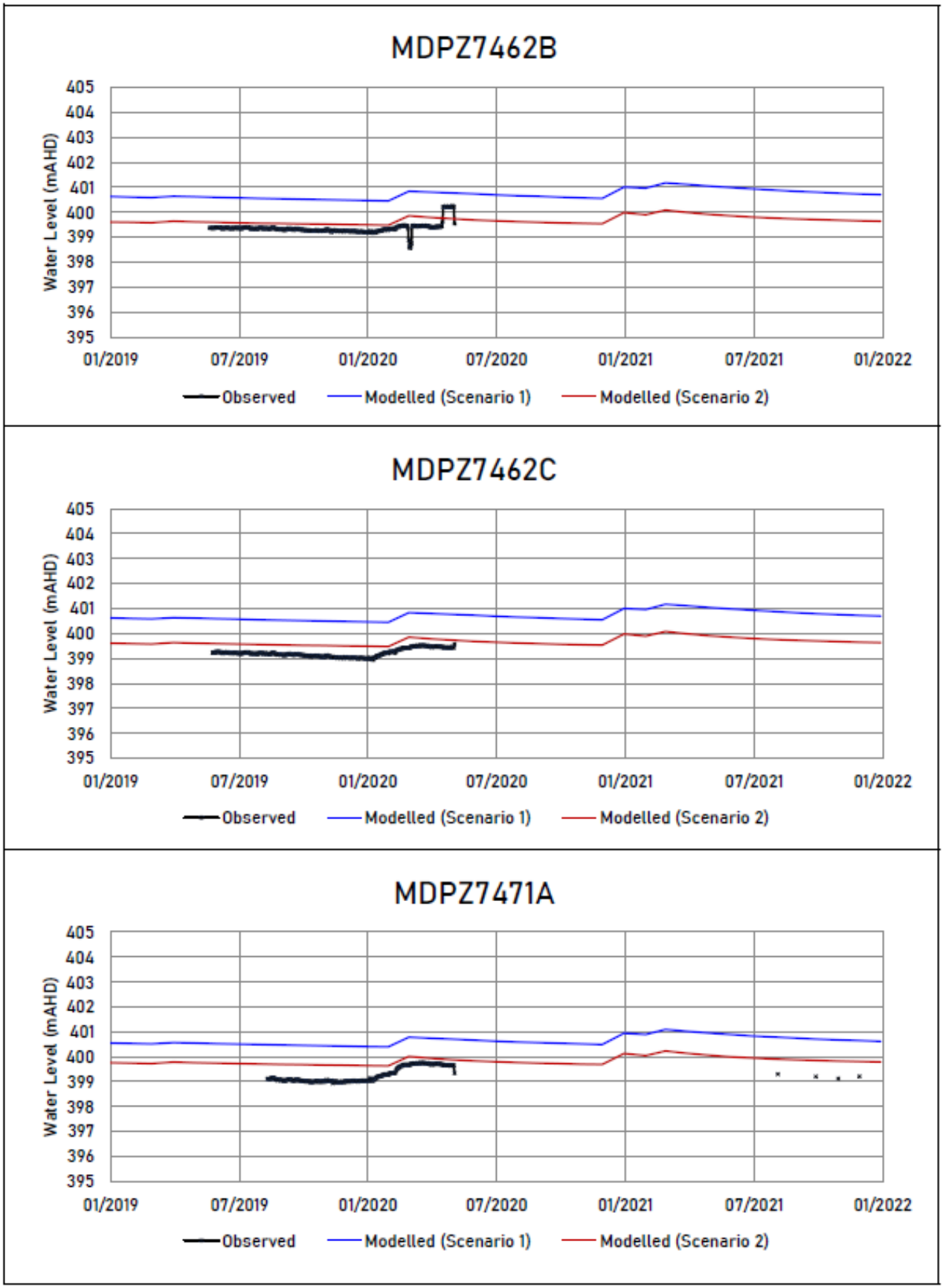

Figure 2.29 History Matching Calibration Hydrographs

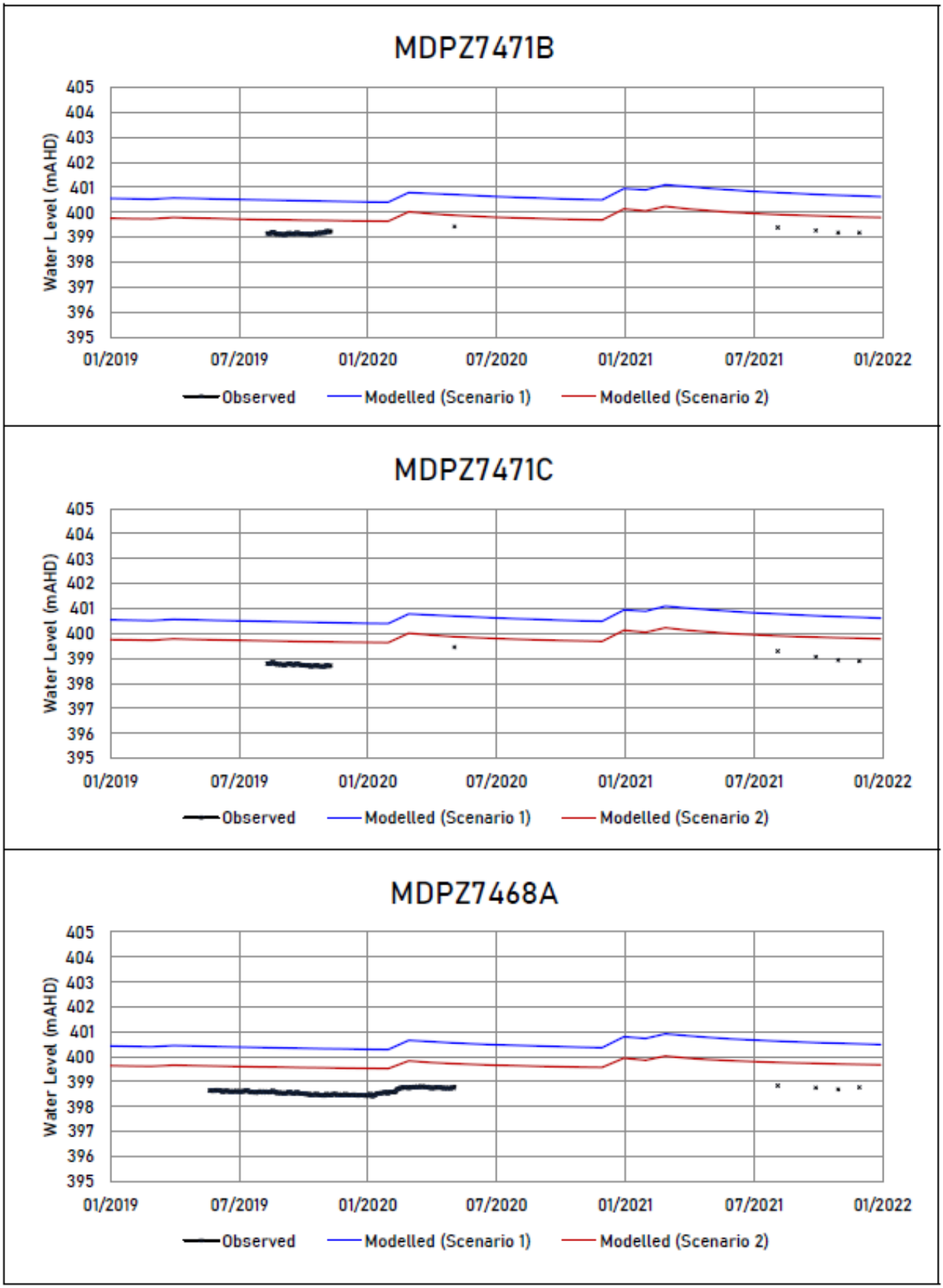

Figure 2.30 History Matching Calibration Hydrographs

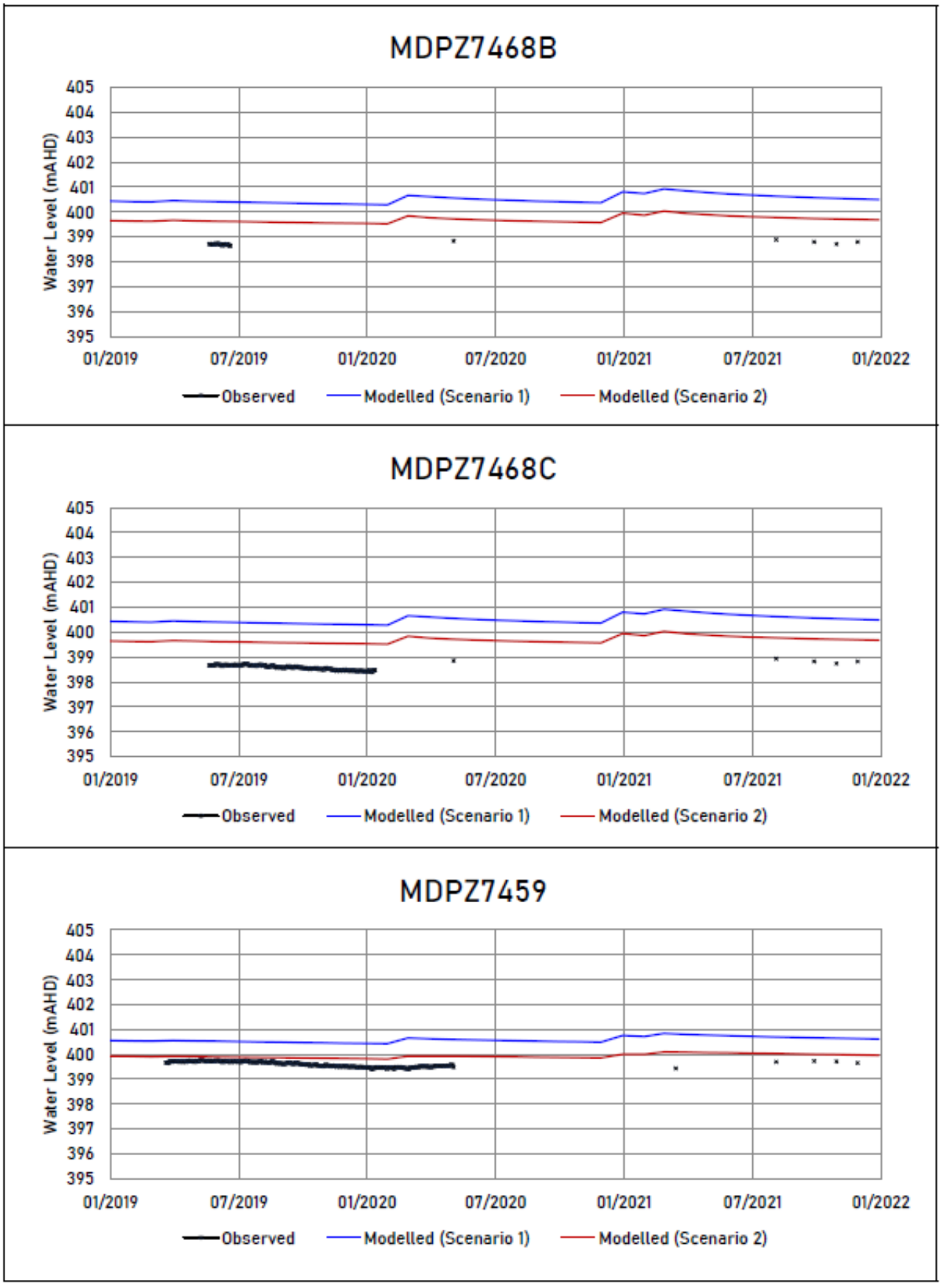

Figure 2.31 History Matching Calibration Hydrographs

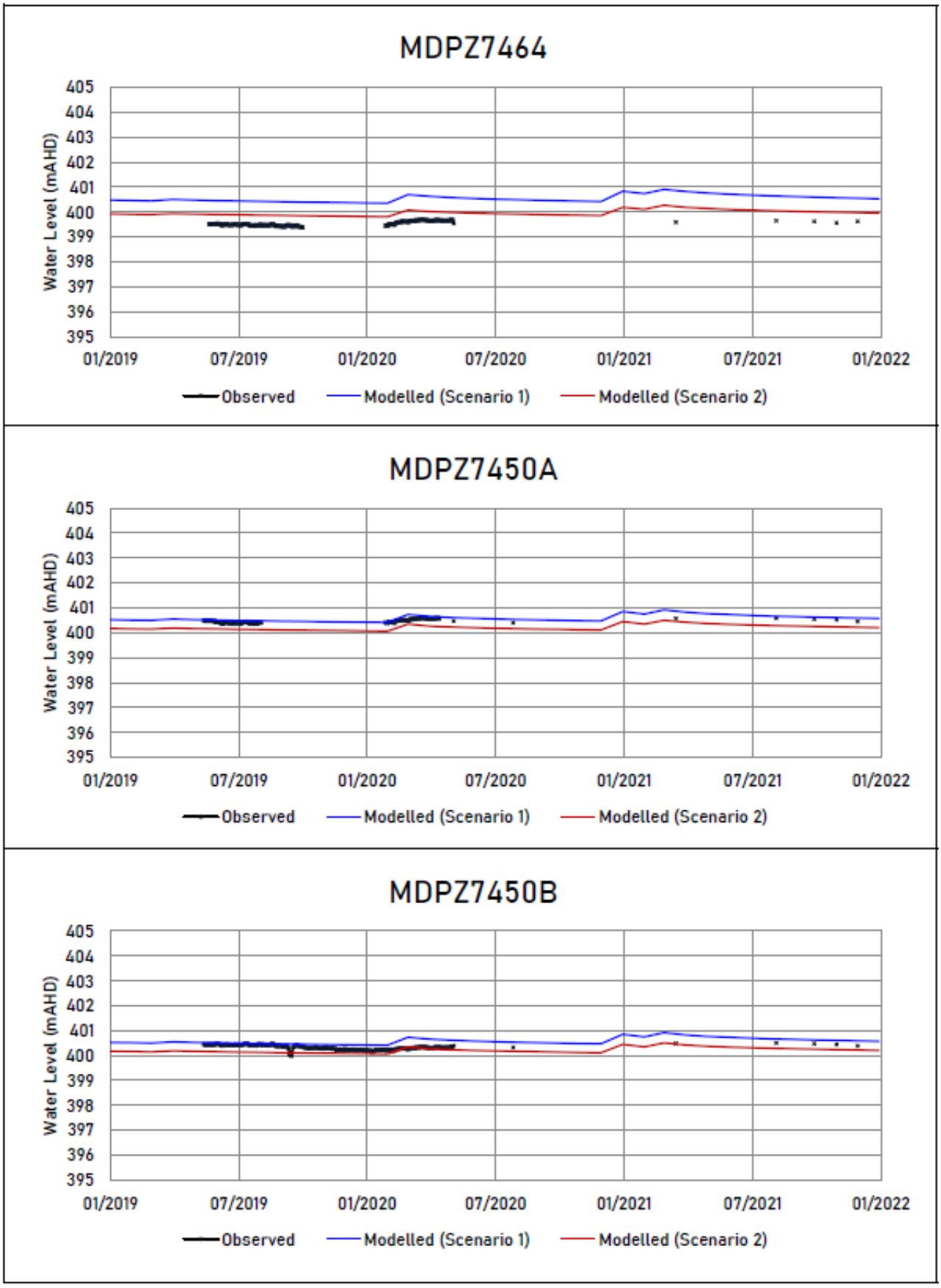

Figure 2.32 History Matching Calibration Hydrographs

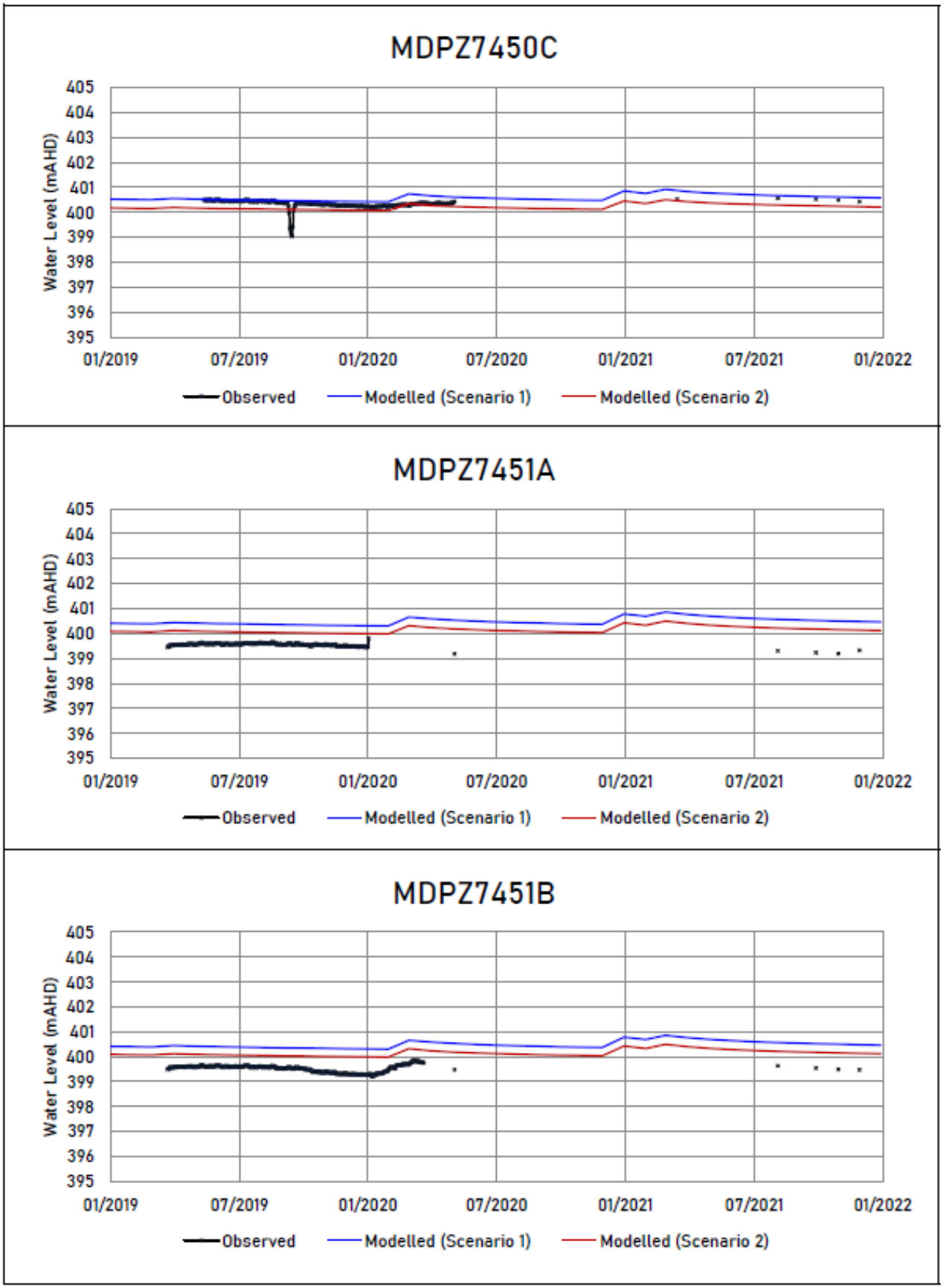

Figure 2.33 History Matching Calibration Hydrographs

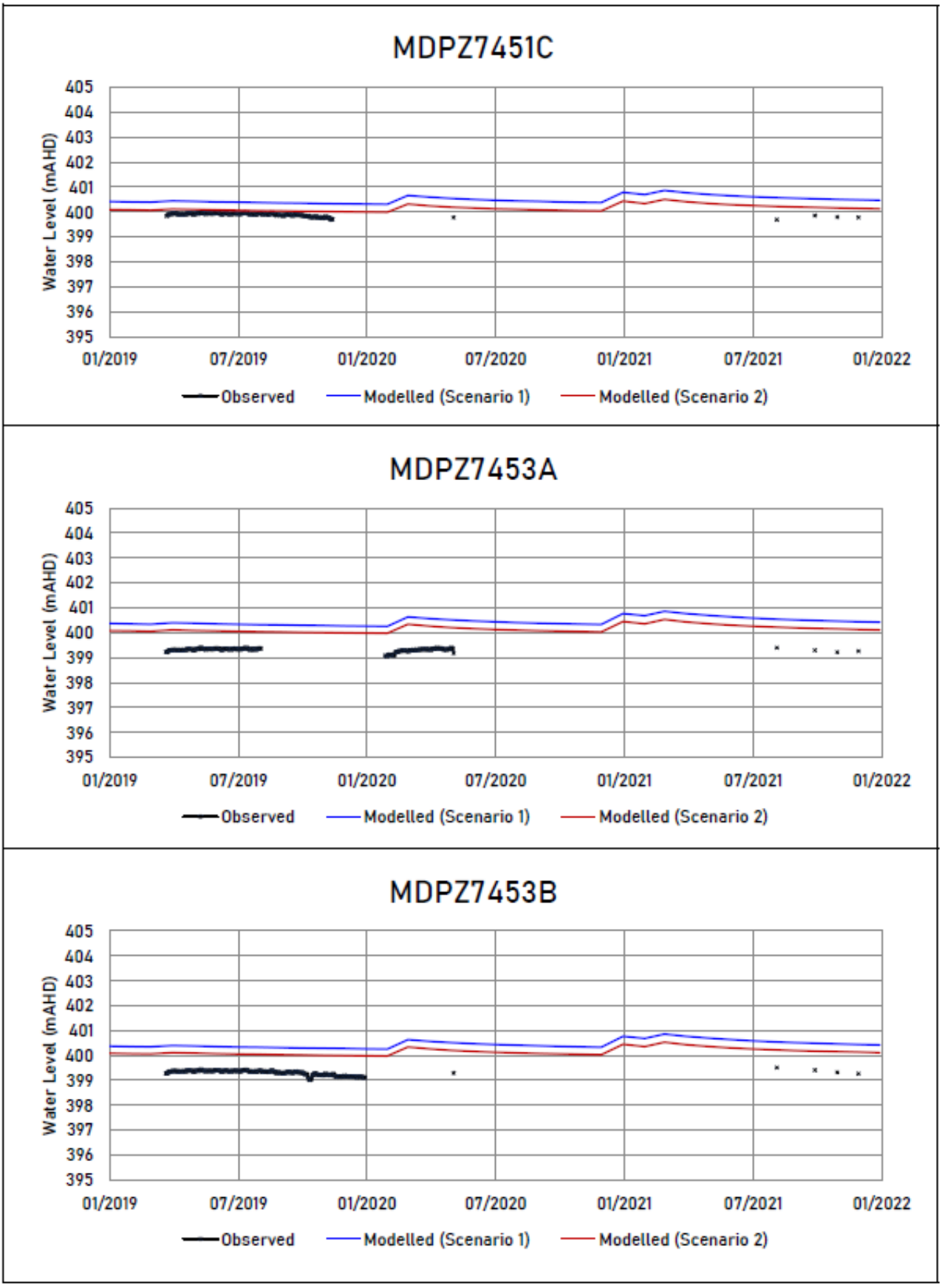

Figure 2.34 History Matching Calibration Hydrographs

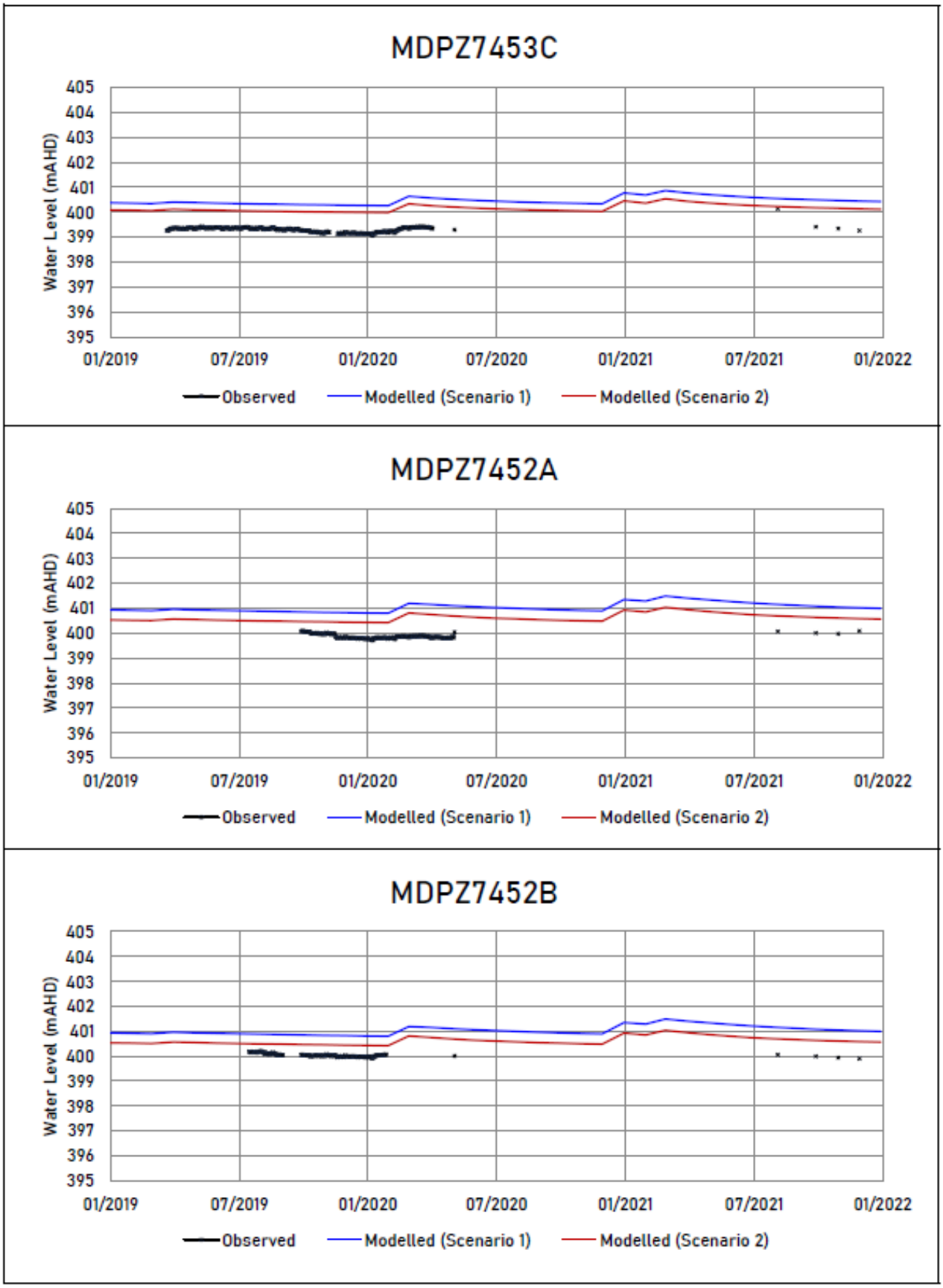

Figure 2.35 History Matching Calibration Hydrographs

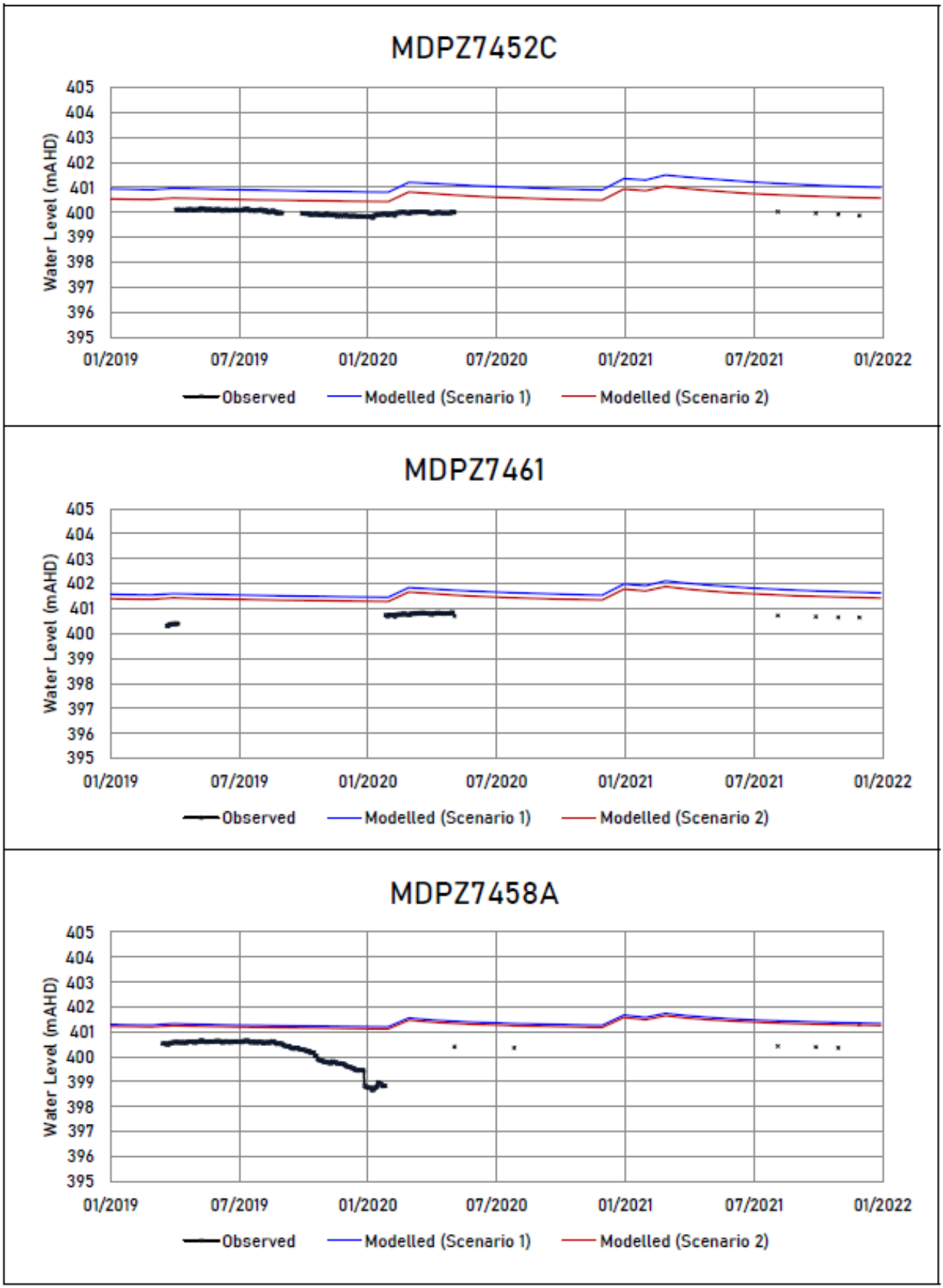

Figure 2.36 History Matching Calibration Hydrographs

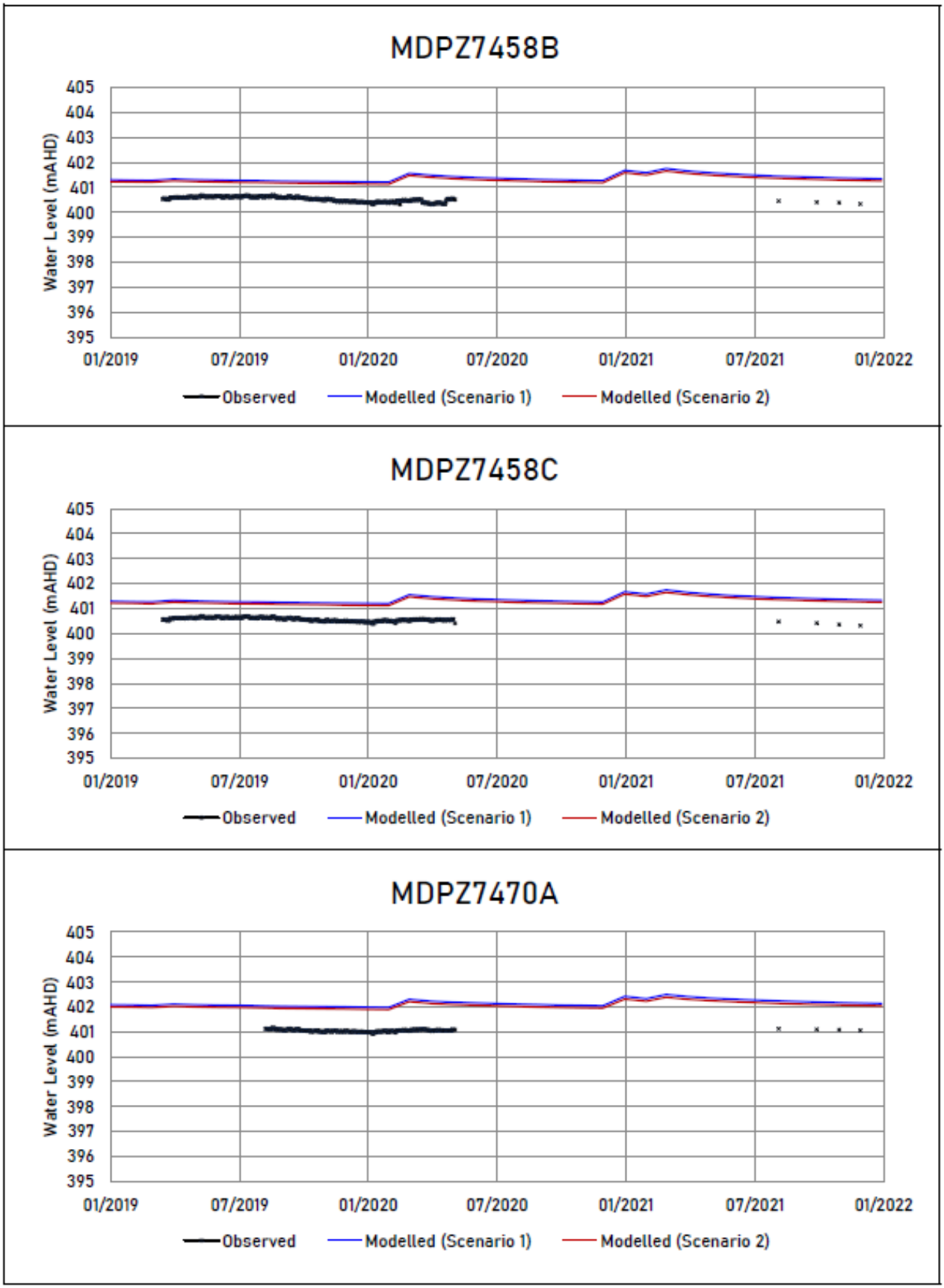

Figure 2.37 History Matching Calibration Hydrographs

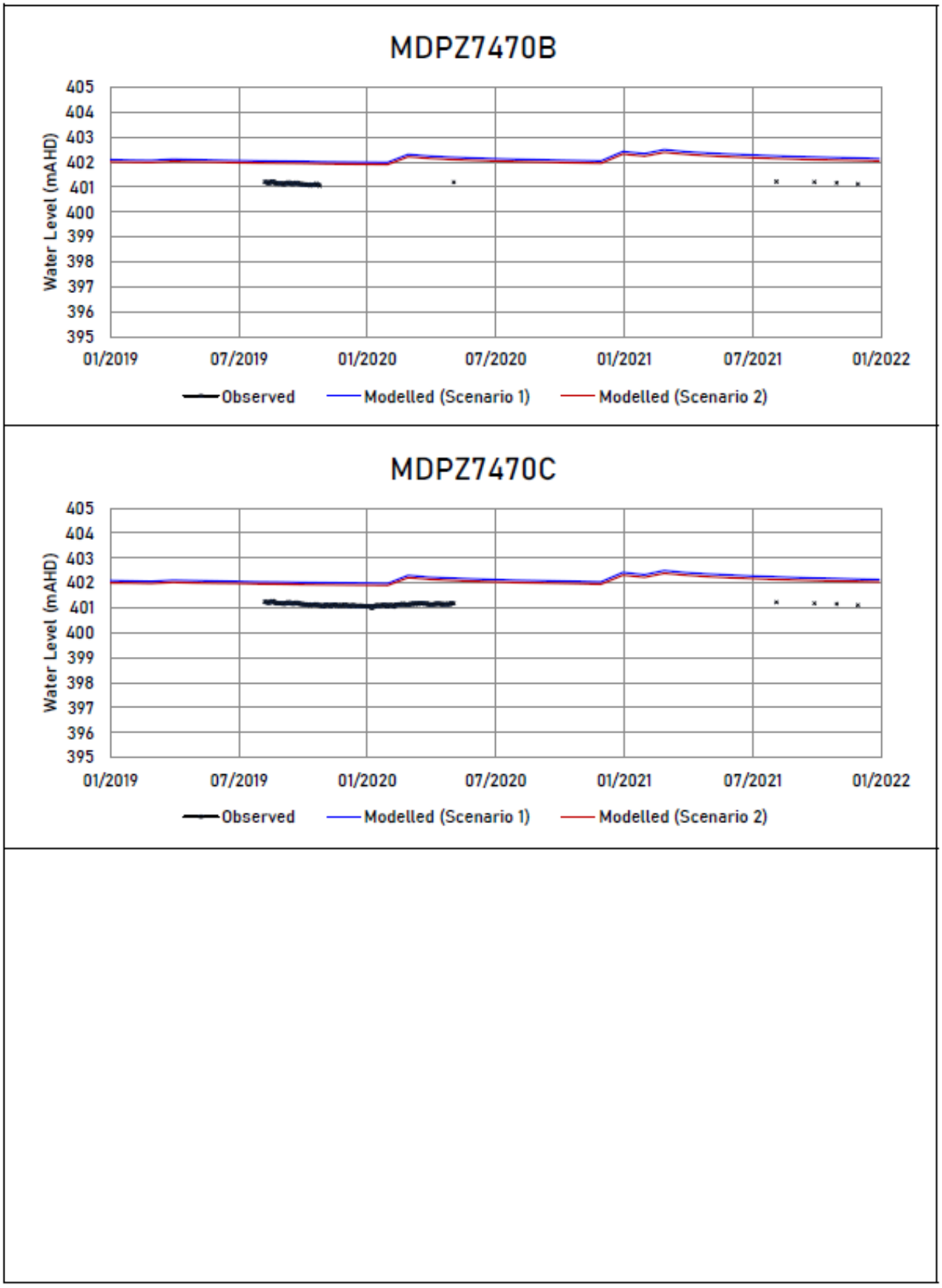

Figure 2.38 History Matching Calibration Hydrographs

2.5.3 Measured and Modelled Water Levels

Monthly measured and modelled water levels for the transient calibration (both the Scenario 1 Base Case and the Scenario 2 Uncertainty Case) are plotted together in Figure 2.39. These results show the following:

- The difference between measured and modelled water levels is less than 5 m for both cases. The maximum difference between measured and modelled water levels was 3.91 m and 4.06 m in the Base Case and Uncertainty Case respectively. This difference is simulated at MDPZ7454, located within the Mulga East – Northern Slopes area (calibration hydrograph shown in Figure 2.20.
- The Scaled Root Mean Squared (SRMS) error as a percentage of the range of measured heads is 7% for the Base Case and 6% for the Uncertainty Case. The absolute mean error is 0.78 m for the Base Case and 0.58 m for the Uncertainty Case.

Measured and modelled water levels for specific areas (i.e. Mulga West, Mulga East – Northern Slopes and Mulga Downs – Valley), also shown as monthly measured values, are shown in Figure 2.40 and discussed below.

- For the Mulga West area, the maximum difference between measured and modelled water levels is 1.54 m (MD5461) for the Base Case and 0.85 m (MD6605) for the Uncertainty Case. Available measured water levels in this area (from only two monitoring locations) are spread over a range of 0.7 m to 1.0 m whereas the modelled water levels are predicted over a range of less than this (approximately 0.5 m).
- For the Mulga East – Northern Slopes area, the maximum difference between measured and modelled water levels is 3.91 m and 4.06 m (MDPZ7454) for the Base Case and the Uncertainty Case respectively. This bore is located to the north of the mine (refer Figure 2.9). The measured and modelled water levels for this bore plot off the 1:1 measured versus modelled line on Figures 2.39 and 2.40 (2) (measured water level ~ 410 mRL and modelled around 406 mRL). Bore MDPZ7467 (on Figures 2.39 and Figure 2.40(2) measured water level ~ 406 mRL and modelled around 404 mRL) also plots off the 1:1 measured versus modelled line and form a straight line. A further group of bores located in the Northern Slopes area plot off the 1:1 line. These bores are MDPZ0757, MDPZ7466 and MDPZ7465 and these are located outside of the immediate mine areas. It is currently not clear why the measured trends or water level variations are not matched at these locations.
- For the Mulga Downs – Valley area predicted water levels are generally over predicted by up to 2 m. The maximum difference between measured and modelled water levels is 2.44 m and 2.36 m (MDPZ7458A) for the Base Case and the Uncertainty Case respectively.

Measured water levels and contours of modelled water levels for August 2021 are shown in Figure 2.41 for Scenario 1 (Base Case) and Scenario 2 (Uncertainty Case). The modelled water levels show the general direction of groundwater flow from the Hamersley and Chichester Ranges towards the valley and then to the north west along the valley. The transition from low permeability to high permeability units on the slopes of both sides of the valley can also be seen to result in the abrupt bends observed in the groundwater contours.

A plot of measured versus modelled water levels for August 2021 for Scenario 1 (Base Case) and Scenario 2 (Uncertainty Case) is shown in Figure 2.42.

For Scenario 1 (Base Case):

- The difference between measured and modelled water levels is equal or less than 2 m, with the maximum difference between measured and modelled water levels observed at MDPZ7467, where water levels are over predicted by 2.0 m.
- There is no systematic over or under prediction of measured water levels.
- The Scaled Root Mean Squared (SRMS) error as a percentage of the range of measured heads for August 2021 is 10% and the absolute mean error is 0.92 m.

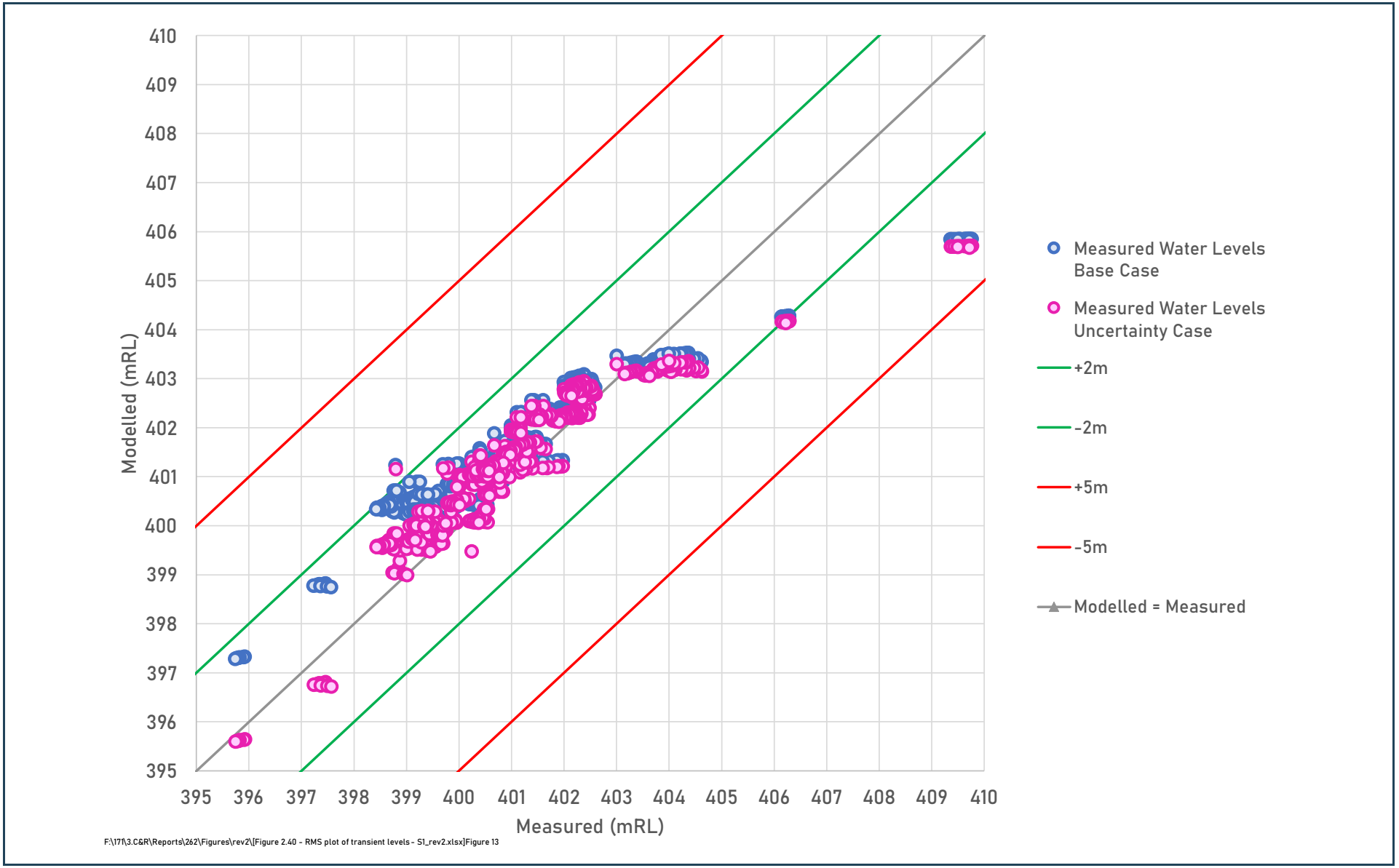

Figure 2.39 Transient Calibration Observed and Modelled Water Levels

1)

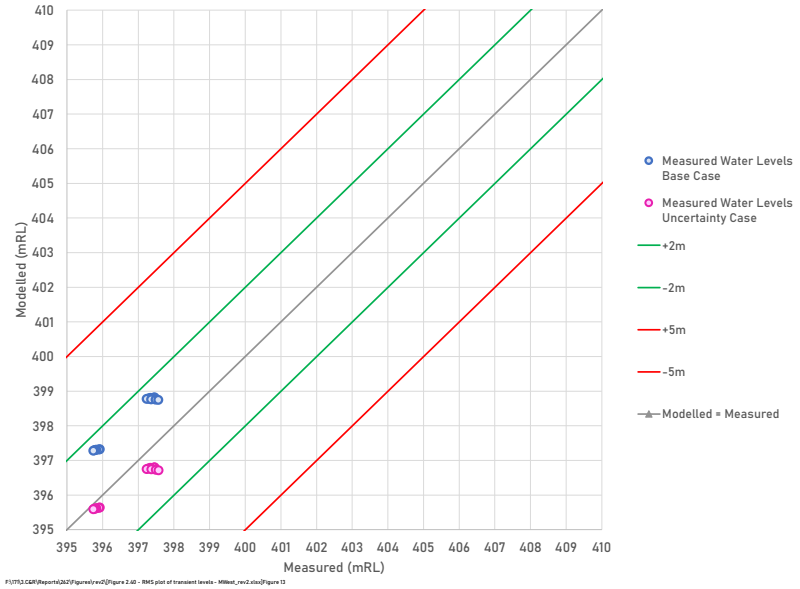

2)

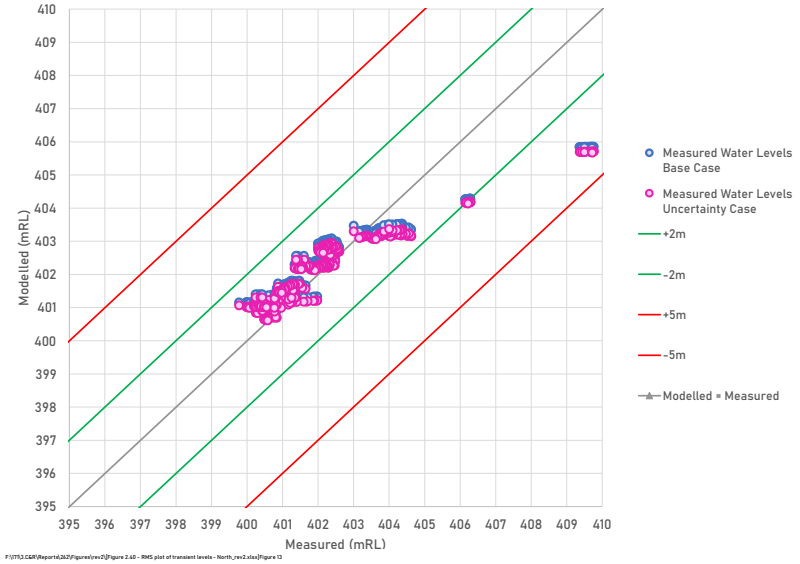

3)

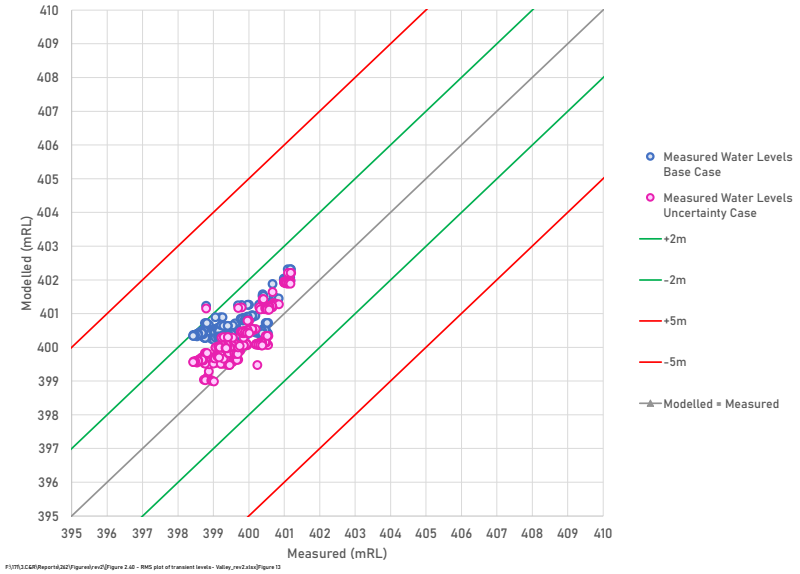

Figure 2.40 Transient Calibration All Observed and Modelled Water Levels by area: 1) Mulga West, 2) Mulga East – Northern Slopes and 3) Mulga Downs – Valley

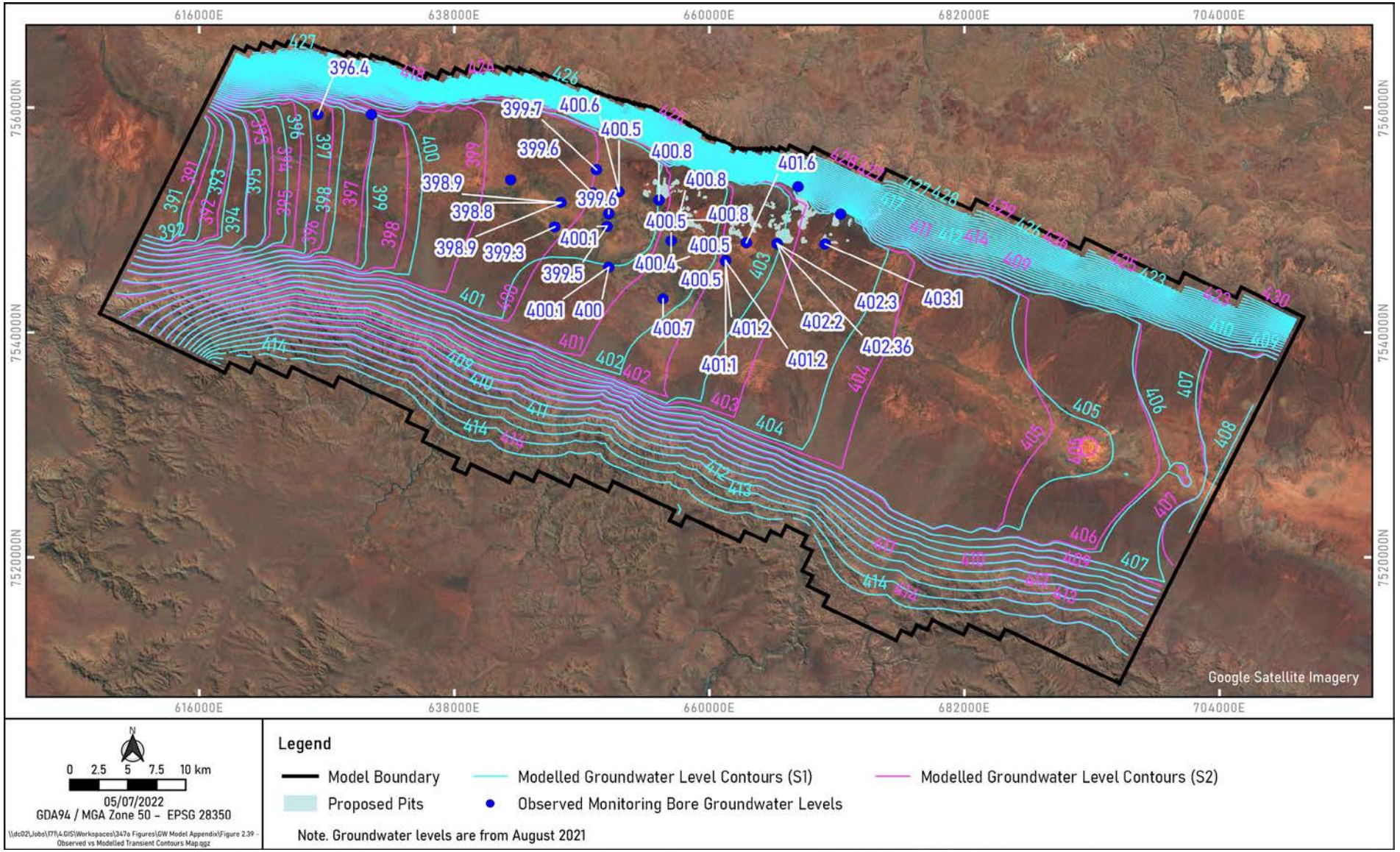

Figure 2.41 Transient Calibration August 2021 Observed and Modelled Water Level Map

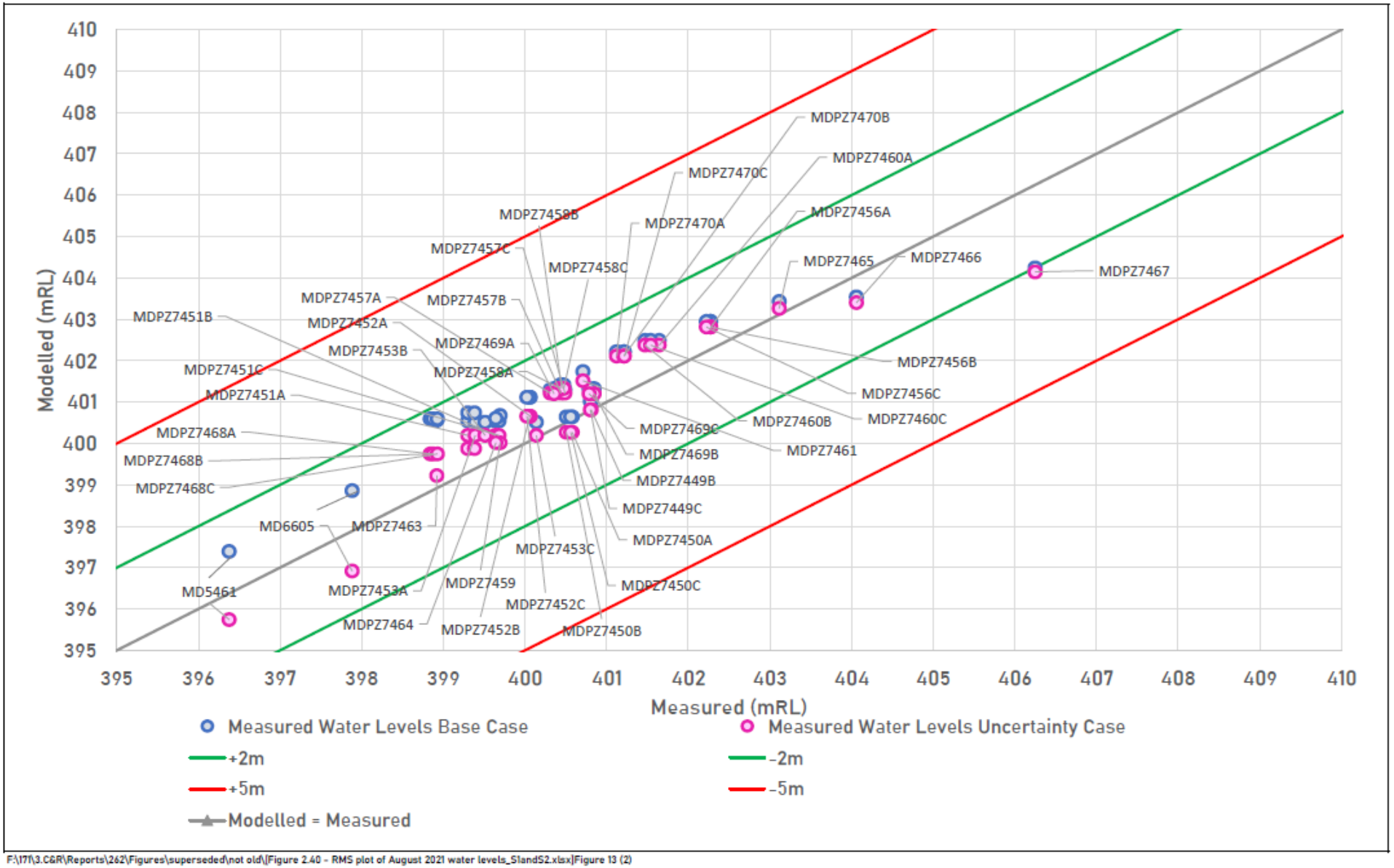

Figure 2.42 Transient Calibration August 2021 Observed and Modelled Water Level Plot

For Scenario 2 (Uncertainty Case):

- The difference between measured and modelled water levels is less than 2 m, with the exception of MDPZ7467, where water levels are over predicted by 2.10 m.
- There is no systematic over or under prediction of measured water levels.

The Scaled Root Mean Squared (SRMS) error as a percentage of the range of measured heads is 7% and the absolute mean error is 0.65m. The modelling guidelines (Barnett et al., 2012) do not specify SRMS criteria for this measure of model performance. There is, however, mention of ranges of SRMS error up to 10% that could be adopted if required and the current model performance is within this range. These criteria are considered with other model performance criteria including the use of realistic aquifer parameters. Aquifer parameters have been assigned uniformly across aquifer units to replicate the majority of measured water levels. Local scale features have not been added to achieve a better model calibration and in turn improve the SRMS or reduce the absolute error.

2.5.4 Aquifer Parameters

Aquifer parameters assigned to the Base Case (Scenario 1) and the Uncertainty Case (Scenario 2) calibrated models are summarised in Table 2.3. Calibrated aquifer parameters are consistent with values derived from the drilling and testing programmes conducted to date and similar hydrogeological environments in the Pilbara. The hydraulic conductivity values assigned to the mineralised and sub mineralised halo are consistent with the range of values derived for the mineralised Marra Mamba unit (AQ2, 2024), however, it should be noted that there has been limited drilling and testing to date to assess the potential variability in aquifer parameters for the sub mineralised halo unit (i.e. between the defined orebody areas). The distribution of aquifer parameter zones for Layer 1 to Layer 11 are shown in Figures 2.3 to 2.8.

Table 2.3 Calibrated Aquifer Parameters for the Base Case (Scenario 1) and Uncertainty Case (Scenario 2)

Unit		Horizontal Hydraulic Conductivity, Kh (m/d)	Vertical Hydraulic Conductivity, Kv (m/d)	Specific Yield, Sy (%)	Porosity, n (%)	Specific Storage, S (1/m)
Tertiary Cover	Upper Calcrete	10	1	1	10	1×10^{-6}
	Undifferentiated Tertiary	8	0.8	2	25	1×10^{-6}
	Pisolite / CID	14 *(60)*	1.4 *(6)*	5	15	1×10^{-6}
	Basal Crete	9	0.9	1	10	1×10^{-6}
Bedrock	Fresh Dolomite of Wittenoom Fm	0.01	0.001	0.1	5	1×10^{-6}
	Weathered West Angela Mbr	1	0.1	1	20	1×10^{-6}
	West Angela Hardcap	20	2	5	20	1×10^{-6}
	West Angela Hardcap (at BoreMDPB0020)	130	13	5	20	1×10^{-6}
	Marra Mamba / West Angela Ore (includes sub-mineralised halo)	25 *(13)*	2.5 *(1.3)*	3	15	1×10^{-6}
	Unmineralised / Fractured Marra Mamba (Mulga East)	10	1	1	8	1×10^{-6}
	Unmineralised Marra Mamba (Regional)	0.05	0.005	0.5	5	1×10^{-6}
	Fresh Marra Mamba / Jeerinah	0.01	0.001	0.1	1	1×10^{-6}

Italics = parameter changed for Uncertainty Case

Assigned porosity values are not calibrated or constrained by the model calibration completed to date. No calibration to porosity has been completed to support particle tracking and solute transport modelling via testing of a range of porosity values or the use of measured porosity values. The porosity assigned in the flow only model calibration does not impact the flow solution or resolve any uncertainties around the assigned values of porosity. Porosity values originally assigned to the model (AQ2 2021) were considered to be at the higher end of the expected range. Those values presented in Table 2.3 are considered more representative and have been adopted as Base Case parameters for the integrated flow and transport modelling detailed in the GWC report (GWC, 2024), with a sensitivity assessment undertaken to test both lower and higher values.

2.5.5 Other Calibrated Aquifer Parameters

As part of model calibration, a rainfall threshold total of 75 mm was observed to be consistent with the groundwater response to rainfall recharge. During most years, exceedance of the 75 mm threshold may occur over a month, however during cyclonic activity, this threshold could be exceeded over a period of days. Once the cumulative rainfall total was exceeded within a month, the following proportions of rainfall recharge were assumed to recharge groundwater as long as there was ongoing rainfall:

- Over the area along the valley, including the claypan areas, 4% of incident rainfall was assumed to recharge groundwater.
- Along drainage lines located on the northern side of the model domain, 0.7% of incident rainfall was assumed to recharge groundwater.
- Along drainage lines located on the southern side of the model domain, 0.35% of incident rainfall was assumed to recharge groundwater.

During drier years, the threshold is not exceeded, and no rainfall recharge is simulated.

Other assumptions of the recharge approach are outlined below:

- Daily rainfall data was sourced from SILO (station ID 19970526) for the period 1960 to 2021.
- Daily recharge totals calculated from the approach outlined above were summed into monthly recharge totals consistent with the time discretisation used in the model calibration and predictions and applied to the recharge zones (refer Figure 2.10 for the modelled recharge distribution).
- Once rainfall ceased, the cumulative threshold was reset and no further recharge to groundwater was calculated until the rainfall threshold of 75 mm was again reached (within a month).
- Creek recharge rates are scaled (down) for the east and west creek recharge zones to account for the increase in model cell size away from the Mulga East area.
- The maximum daily rainfall that could contribute to recharge to groundwater was 250 mm per day.

Over the model calibration period (1960 to 2021 or a period of 62 years), total annual recharge to the model domain varied from year to year. For 16 years of this period (close to 25% of the calibration period), total simulated recharge to groundwater was zero. For these years, annual rainfall totals varied from 151.9 mm in 1969 to 421.4 mm in 1968 as the current approach to estimating recharge accounts for the frequency of rainfall, rather than a rainfall total for a calendar year. Considering a 20 year sequence of annual rainfall (for example 1960 to 1979, 1961 to 1980 and so on) the current recharge simulation approach estimates that there are between 4 and 8 years in a 20 year sequence where no recharge to groundwater is simulated.

Over the calibration period, total recharge to groundwater, as a proportion of the total rainfall over the contributing surface water catchments to the valley, was up to 1.35%, with an average of 0.17% and a median of 0.15%.

2.5.6 Modelled Water Balance

Model predicted water balances for the calibrated model for the end of June and December are shown in Table 2.4 (for the Base Case Calibration). The years selected for detailed analysis (1967 and 1975) represent a dry year with annual rainfall of 334.9 mm and a very wet year with annual rainfall of 762 mm, (the long-term average annual rainfall is 365 mm). This wet year (1975) was chosen to allow assessment of the impact of recharge on dewatering and storage depletion / replenishment as part of model predictions (refer Sections 3.3.1.4 and 3.3.2.4). The larger annual rainfall total is reflected in the predicted recharge to groundwater for the wet season (December 1975) predicted water balance (high recharge and storage increase).

Table 2.4 Transient Calibration Predicted Wet and Dry Season Water Balances

Water Budget Component	June 1967		December 1967	
	In (kL/d)	Out (kL/d)	In (kL/d)	Out (kL/d)
North Catchment Inflow	1,200	-	1,200	-
South Catchment Inflow	120	-	120	-
Fortescue Valley East Inflow / Outflow	6,720	0	6,990	0
Fortescue Valley West Outflow	-	3,790	-	3,600
Storage	13,480	1,730	10,080	220
Rainfall Recharge	0	-	0	-
Evapotranspiration	-	16,000	-	14,570
Total	21,520	21,520	18,390	18,390
Water Budget Component	**June 1975**		**December 1975**	
	In (kL/d)	Out (kL/d)	In (kL/d)	Out (kL/d)
North Catchment Inflow	1,200	-	1,200	-
South Catchment Inflow	120	-	120	-
Fortescue Valley East Inflow / Outflow	7,250	0	2,640	1,610
Fortescue Valley West Outflow	-	3,360	-	6,820
Storage	7,840	30	260	487,480
Rainfall Recharge	0	-	529,070	-
Evapotranspiration	-	13,020	-	37,380
Total	16,410	16,410	533,290	533,290

- Denotes no water balance flow component

The model predicted water balances show that rainfall recharge (and the associated increase in groundwater storage) and ET losses from the water table are the greatest components of the modelled water balance. During the dry season there is some inflow to the valley from the south east which is higher than that estimated by Skrzypek et al (2016). During the wetter periods analysed, this flow is predicted to reverse to an outflow as the valley areas immediately downstream are filled with catchment recharge. In the event that the valley area, downstream of the Goodiadarrie Hills was recharged during a particularly wet period, the Fortescue Marsh immediately upstream would also show an increase in water level. Consistent with the flat gradient measured from the western part of the Fortescue Marsh towards the Goodiadarrie Hills, the water levels over this entire area would be expected to increase. This increase

is not simulated by the current fixed head model boundary. Predicted inflows (and outflows) across this boundary simulated during model predictions are discussed in the GWC report.

In comparison to the remainder of the water balance components, predicted groundwater inflows through the northern and southern model boundaries are minimal. Inflows from the northern catchment (aligned with the Jeerinah Formation outcrop) and the southern catchment (aligned with the Brockman Formation outcrop) are the smallest parts of the model predicted water balances. These inflows are not predicted to change as a result of the simulated climate conditions (i.e. they are the same during simulated periods that include wet and dry conditions). The model predicted water balances from preliminary predictions also suggest that inflows through these boundaries are unchanged over the duration of predictions that included both dewatering and MAR. Predicted inflows across these boundaries simulated during model predictions are discussed in the GWC report.

The cumulative predicted water balances over the 62 year period simulated for both Scenarios 1 and 2 are shown in Table 2.5. The percentage error for the overall cumulative water balances is less than 0.01%.

Table 2.5 Transient Calibration Cumulative Predicted Water Balance for the Base Case (Scenario 1) and Uncertainty Case (Scenario 2)

Water Budget Component	Cumulative Total Base Case (Scenario 1)		Cumulative Total Uncertainty Case (Scenario 2)	
	In (kL)	Out (kL)	In (kL)	Out (kL)
North Catchment Inflow	27,193,590	0	27,390,140	0
South Catchment Inflow	2,724,980	7,250	2,718,290	7,380
Fortescue Valley East Inflow / Outflow	153,818,180	126,940	214,087,040	52,990
Fortescue Valley West Outflow	0	83,398,290	0	150,775,810
Storage	251,813,300	252,895,360	255,655,300	255,890,500
Rainfall Recharge	243,868,860	-	243,868,860	-
Evapotranspiration	-	343,012,990	-	337,176,740
Total	679,418,910	679,440,830	743,719,630	743,903,420

Predicted monthly ET rates for the valley and flank areas (over the 62 year calibration simulation period) are shown in Figure 2.43 and suggest that ET is restricted to the valley areas only. An example of the distribution of ET across the valley (for January 2012) is shown in Figure 2.44 and shows that ET is limited to the valley areas. Figure 2.44 shows areas of ET simulated along the valley floor downstream of the inflow boundary and upstream of the outflow boundary, away from the mine areas. These ET areas correspond to areas of lower elevation in the simulated ground surface (based on STRM data). While these areas appear large, they only represent ET from one or two model cells. In reality the ET that would be lost would result from a variable ground surface elevation over these areas and the ET losses, if they occurred, would be over a wider area over the valley floor. The adopted cell size and sample of ground surface acts to concentrate simulated ET over smaller areas or single model cells.

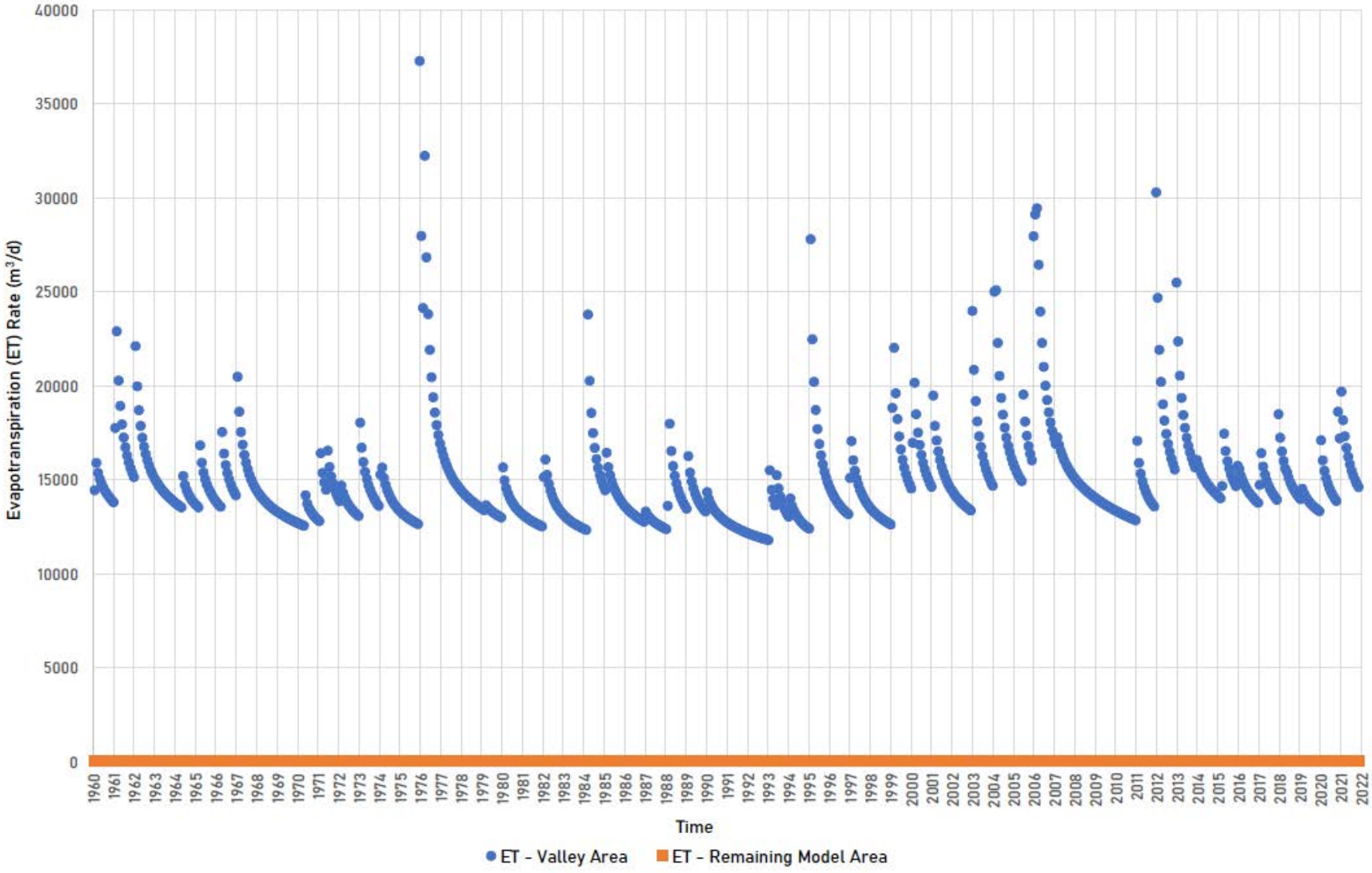

Figure 2.43 Predicted ET Rates in Valley Area vs Remaining Model Area

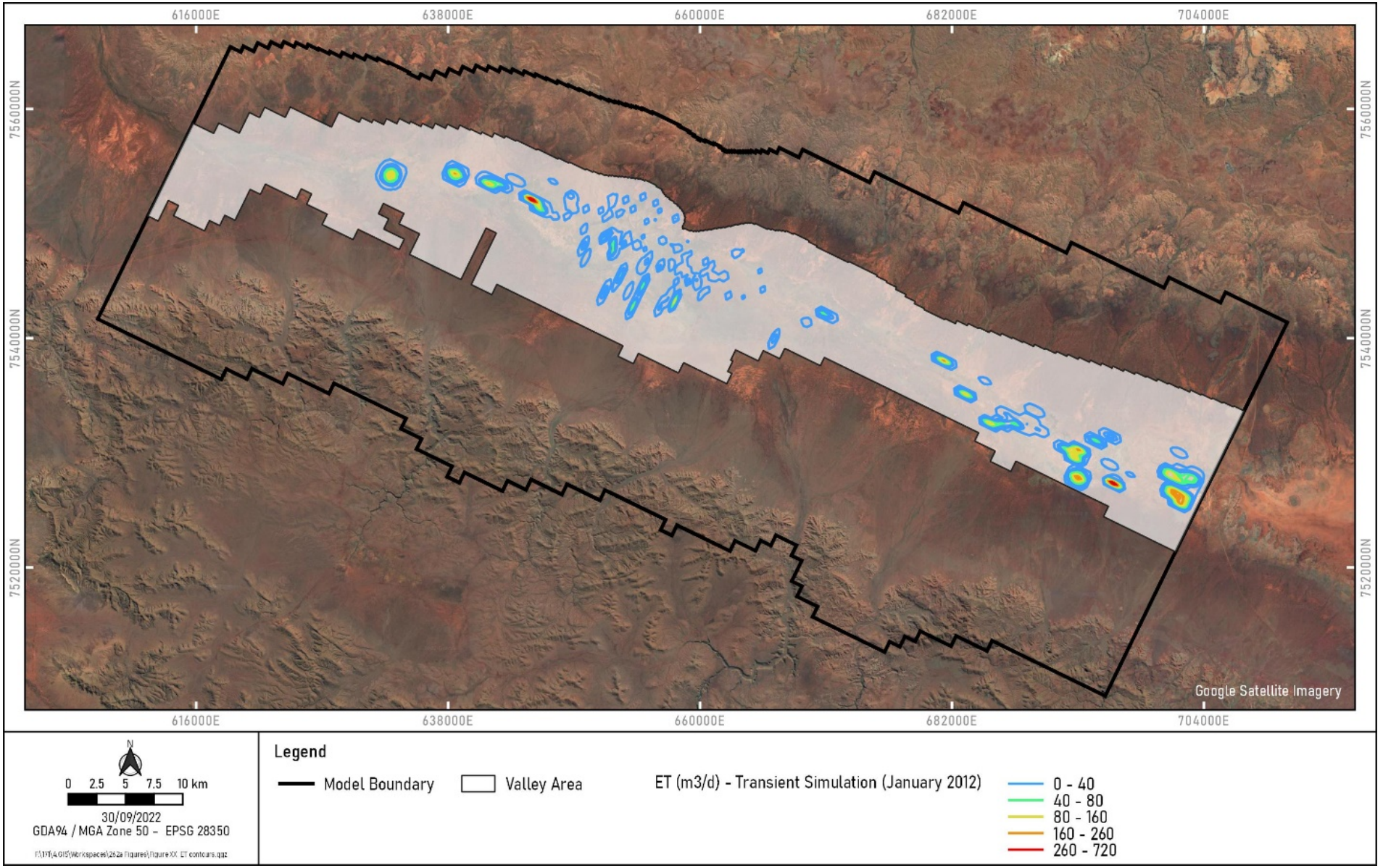

Figure 2.44 Simulated ET January 2012

2.5.7 Other Model Details

Other details of model setup are outlined below:

- Over the model calibration and prediction periods, stress periods were set at a monthly time increment.
- The Modflow SURFACT Automatic Time Stepping (ATO) package was used for model calibration and predictions with the following parameters:
  - An initial time length of 10 days was used.
  - A minimum time step of 1 x 10^{-6} and a maximum time step of 31 days.
  - A time multiplier of 1.2 and a reduction factor of 2.0.
- The model was run with Modflow SURFACT Block Centred Flow 4 (BCF4) package using the Variable Saturated Flow Option (Pseudo Soil Relations) to accommodate re-saturation.
- The model was run with the Pre-Conjugated Gradient 5 (PCG5) solver with the following parameters:
  - Number of outer iterations = 50.
  - Number of inner iterations = 20.
  - Maximum orthogonalizations = 10.
  - Head change criterion = 0.001.
  - Relative Convergence Criterion = 0.
  - Newton Raphson Linearisation (Backtracking Factor) = 0.9.
  - Newton Raphson Linearisation (Residual Reduction Factor) = 1.

3. MODEL PREDICTION SET UP

The Base Case (Scenario 1) calibrated groundwater flow model was used to:

- Simulate LOM dewatering to achieve dry mining conditions based on indicative dewatering bore locations and pumping rates for a number of mining scenarios or operational constraints to identify a feasible mining scenario with a viable groundwater management solution.
- Estimate the LOM surplus water disposal requirements (based on dewatering requirements and site water use).
- Assess the potential to dispose of excess water via MAR using bores within the current tenement boundaries.
- Predict the impacts of dewatering and MAR over the catchment (groundwater drawdown and mounding).
- Predict the development of water quality across the catchment, resulting from the interactions between dewatering and MAR, using integrated flow and transport modelling for the final or preferred mining scenario.
- Assess the impact of the preferred mine closure strategies (backfilled pits), including the time taken for water levels to reach pre-mining or long term equilibrium levels.

The model prediction set up is described in the following sections, with further detail on model prediction set up and prediction results provided in a separate report (GWC, 2024).

3.1 Prediction Setup

Details of the model predictions completed are outlined below. Further detail is provided in the accompanying model prediction report (GWC, 2024).

- Dewatering bores were simulated using the Fracture Well (FWL) package in Modflow SURFACT. Dewatering bores were assumed to pump from the base of modelled aquifers in / around pit areas and at a maximum rate of 4320 kL/d (50 L/s) with a minimum water level constraint of 2 m above the base of the modelled aquifer (i.e., pumping at dewatering locations ceased once predicted water levels at pumping locations reached 2 m above the base of the modelled aquifer). The maximum bore pumping rates were based on Source Reliable Output analysis of step test data (AQ2 2024).
- With respect to the locations of the dewatering bores:
    - Ex-pit bores are preferentially located on the southern side of pits, adjacent to the deepest parts of the pit where the aquifer is deepest (i.e. on the down-dip side of the pit) to ensure maximum duration of pumping (with up-dip locations becoming dewatered first). Bores were placed with a minimum spacing of 200 m in mineralised Marra Mamba and fractured / weathered Marra Mamba.
    - In-pit bores / sumps are located in the deepest parts of the pits if / when dewatering could not be achieved by ex-pit bores alone.
    - Simulated ex-pit and in-pit bore depth ranged from around 55 m to 90 m in total depth consistent with aquifer geometry and pit depth.
- Once mining at a particular location was completed, dewatering ceased and water levels were allowed to rebound (i.e. pits are not assumed to be kept open and dewatered over the entire life of mine nor are the impacts of pit voids simulated). The rebound of water levels was simulated assuming that pits were infilled with material with the same aquifer parameters as the dewatered in-situ aquifers (i.e. no long term evaporative losses from mine voids were simulated).

- MAR bores were also simulated using the FWL package with individual bore injection rates ranging between 864 kL/d (10 L/s) and 2592 kL/d (30 L/s), with MAR bores extending to the base of the Tertiary units, hardcap, or fractured bedrock.
- The process to determine the optimal re-injection rate and duration for each MAR bore was iterative and was based on a predicted water level constraint. The process of simulating MAR that satisfied the predicted water level constraints is described below.
    - An operational constraint was applied to MAR locations. GWC (2024) reports this water level constraint was set at 2.5 mbgl at MAR locations to prevent rise of groundwater levels to surface (0.5 m below where the ET package operates).
    - In early AQ2 predictions (not presented here), in addition to the operational constraint, a skin factor was calculated for each bore (external to the model) and varied across proposed MAR bore locations based on transmissivity and a 60% bore efficiency rate. The estimated skin factor (drawup) was added to the 3 m operational constraint to provide a total maximum modelled water level at each MAR bore.
    - The maximum modelled water level condition was simulated using the Drain (DRN) package in Modflow SURFACT at each MAR location.
    - Any water removed at MAR locations by the DRN constraint was assumed to be "rejected" from the aquifer. Based on the amount of rejected MAR simulated, individual MAR bore injection rates were adjusted. accordingly (i.e. reduced so that the predicted water level at MAR locations remained below the applied constraint). This process was also completed to allow optimal injection rates at MAR bore locations (i.e. sometimes there was capacity for additional re-injection).
    - The simulation of inflow (via injection bores) and outflow (via the DRN package) flow components at MAR locations, using Modflow SURFACT packages that were not used for any other parts of the modelled water balance allowed simple and transparent assessment and review of model simulated water balance components. As Modflow SURFACT does not allow constraints to be applied to fixed head cells, nor does it allow fixed head cells to be de-activated, a complicated water budgeting process would have been required to separate groundwater inflows and outflows at MAR locations.
- In response to MAR, water levels were predicted to increase across the proposed MAR borefield areas. The set up of the ET package, with an extinction depth set at 2 mbgl, was such that an increase in predicted ET was also predicted at some locations in the MAR borefield area. Similar to the constraint set at each bore, MAR injection rates were adjusted to result in no net increase in simulated evapotranspiration across the catchment.
- Predictions were simulated using a monthly time increment or stress period, with initial water levels for model predictions taken from the end of the calibration model (water levels predicted for the end of December 2021).
- Recharge assigned to model predictions was calculated using the approach outlined in Sections 2.3.2 and 2.5.5, using SILO rainfall data. The prediction used rainfall from the period 1960 to 1982. Over this period, the average rainfall was a good approximation to the long-term average annual rainfall, but also included variations in annual total rainfall.
- A No Development (i.e. no dewatering or MAR) scenario was also run to allow calculation of drawdown and comparison of model predicted water balances from simulation of dewatering and MAR associated with the proposed dewatering and MAR approach. The No Development scenario was run over the same time periods as the dewatering and MAR predictions. This simulation included the same aquifer properties, boundary and rainfall conditions but did not include dewatering or MAR.
- GWC (2024) has undertaken a sensitivity analysis on the modelled closure simulations to assess the potential impact of climate variability, namely rainfall variability.

3.2 Model Uncertainty

While the model has been calibrated to Base Case (most likely or Scenario 1) aquifer parameters and an alternative set of aquifer parameters (Scenario 2), there still remains uncertainty in the model calibration. In part, this uncertainty is related to the aquifer parameters assigned to key hydrogeological units, which may impact the prediction of long-term groundwater inflows and impacts.

The uncertainty relates to whether the derived transmissivity is representative of an entire unit (i.e. a bulk estimate for the unit) or results from combined "sub-units" (e.g. a fractured zone with high permeability and unfractured zone, likely more extensive, but with lower permeability). This uncertainty includes:

- Unmineralised / Fractured Marra Mamba: Derived aquifer parameters for the Unmineralised / Fractured Marra Mamba range between 2 and 174 m/d with a geometric mean of 10 m/d adopted for this unit (refer to the Baseline Assessment report (AQ2 2024) for the full list of hydraulic testing parameters). However, it could be that a lower hydraulic conductivity is more representative of the bulk aquifer unit with increased permeability (hydraulic conductivity values) along particular fault lines (the evidence for which are currently under review).
- Marra Mamba ore and Pisolite / CID: An apparent fracture-flow type response was observed at many bores in the orebody areas and yields during drilling were greatest within the Pisolite / CID unit and / or hardcap of the Marra Mamba Formation. It is possible these are associated with a specific and discrete high permeability horizon. When calibrating the model to the pumping test data, it became evident that two different model scenarios provided a good match to measured data; the base case scenario (which has been used for the model predictions outlined above) and a second scenario with:
    - a lower hydraulic conductivity for the Marra Mamba Ore and sub-mineralised halo (i.e. 13 m/d and 12 m/d respectively, compared to 25 m/d);
    - a high hydraulic conductivity for the CID / Pisolite (i.e. 60 m/d, compared to 14 m/d in the base case), with 60 m/d based on the derived permeability value from the pumping test at MDPB0017.

3.3 Model Limitations, Confidence, Assumptions and Recommendations

The regional groundwater model for Mulga Downs has been further developed as part of this study to provide a representation of the regional aquifer system. It includes the analysis of available data collected as part of hydrogeological investigations completed to date. As with all models there are limitations associated with the data availability, conceptualisation and representation of dynamic flow processes. There is also inherent uncertainty in all long-term hydrogeological modelling. To address this, in the absence of long-term or operational dewatering data, an alternative model calibration has been investigated. A Sensitivity Analysis has been completed (as part of model predictions) to predict outcomes under a range of aquifer conditions and assess the impact of aquifer parameter uncertainty. Results of the Sensitivity Analysis (presented in the accompanying report, GWC (2024)), suggest that the hydraulic conductivity of the Unmineralised / Fractured Marra Mamba Unit, over the range of values tested, has the greatest impact on predicted dewatering. The Sensitivity Analysis also showed an increase in predicted dewatering requirements of up to 30% when the specific yield of the Undifferentiated Tertiary Unit, located to the south of the proposed mining area was increased to 20 % (from the Base Case calibrated value of 2%).

More confidence in model predictions will only be achieved with longer term groundwater monitoring, or operational data that stresses the orebody aquifers and provides more information on the regional and orebody scale response to long-term dewatering.

The following list identifies areas where limitations in the model features and / or data availability have been identified. For some of these, the availability of data in the future may lead to improvements in future work programmes:

- The model was set up to simulate the regional aquifer system and predicted dewatering requirements. MAR capacity and regional drawdown and mounding impacts and mine closure. The model does not provide a representation of localised features. These features are not required for the simulation of dewatering requirements and regional drawdown impacts.
- The model is not suitable to predict the development of pit wall pressures in response to dewatering. The prediction of groundwater behaviour (pore pressures) relevant to geotechnical assessments would require the development of pit scale models that adequately represent the horizonal and vertical flow patterns that would develop close to an active pit.
- A number of key hydrogeological units have been delineated and uniform aquifer properties have been assigned to each unit across the model domain. The availability of hydrogeological data for key areas (for example orebody aquifers) may enable variations in aquifer parameters within hydrogeological units to be included in the groundwater model in the future.
- An area of enhanced aquifer hydraulic connection (i.e. the submineralised zone) has been included around the proposed mining areas. The extent of this zone has been inferred based on the extent of mineralisation and extends along strike across the mining area. Aquifer parameters for this zone have been estimated, based on derived parameters from limited drilling and testing.
- The model is calibrated to transient data, with long-term water level monitoring available over periods of several years. The longest monitoring record extends for a period of 7 years (bore MDPZ0818). The model predictions completed to date extend for a period of 22 years, which exceeds the longest groundwater monitoring records. Additionally, the aquifer stresses that are included in model predictions far exceed any measured seasonal water level variations. Long-term behaviour of the aquifer system in response to dewatering, may differ from that simulated and more confidence in model predictions can only be obtained if model performance is compared to longer term and larger scale operational stresses.
- Dewatering requirements are simulated using primarily ex-pit bores around each pit area to the base of permeable material. Appropriate conditions are applied to each pumping location (minimum water levels, locations based on aquifer extents and maximum individual bore pumping rates) with a view to producing a more consistent dewatering rate over the mine life that also aligns with site water demands and management (i.e. MAR capacity). In future work, dewatering predictions could also be run to include constraints on water quality if the advective transport approach outlined in the sections below is adopted.
- The available long term monitoring data suggests limited groundwater responses to rainfall recharge across the catchment (of the order of 1 to 2 m). This data has been used to calibrate the groundwater flow model. Ongoing review, as more data are collected, will allow assessment of requirements to provide an improved approximation of catchment recharge and simulated recharge to groundwater.
- The current modelling has been completed using Modflow SURFACT (a third party version of Modflow). The implementation of newer versions of Modflow (for example Modflow USG or Modflow 6) should be considered in the context of project requirements (timing and outcomes) as part of future groundwater modelling studies for the Project.
- The model currently uses fixed head model boundaries at the upstream and downstream ends of the valley. These boundaries were set sufficiently far away from the Mulga Downs mining area so as to have minimal impact on model predictions. The outcomes of the current work, suggest that very large areas, away from the immediate Mulga Downs mining areas and may be required to accommodate all of the proposed MAR. As part of future work programmes, it is recommended that the suitability of these model boundaries is considered in the context of future MAR (and potentially dewatering). General Head Boundaries could be implemented however, this will require the inclusion of additional model calibration parameters, which may or may not be supported by available data.

- No calibration to porosity has been completed to support particle tracking and solute transport modelling via testing of a range of porosity values or the use of measured porosity values. The porosity assigned in the flow only model calibration does not impact the flow solution or resolve any uncertainties around the assigned valued of porosity. By way of sensitivity or uncertainty assessment, it is recommended that future model predictions (particle tracking, if completed or integrated flow and transport predictions) assess the impact of a range of porosity values on flow path predictions and / or prediction of groundwater salinity which will allow assessment of the potential for variable travel times (as part of particle tracking predictions) and changes in groundwater salinity (integrated flow and transport predictions).

The following points summarise the assumptions included in the model set up and predictions:

- The elevation of the ground surface data was sourced from the SRTM 1 arc-second elevation data (NASA, 2021). This data was used as the available LiDAR data set, at the time of model set-up, did not cover the extent the groundwater model.
- Model predictions have been completed using historical rainfall sequences (from 1960 onwards). Predictions do not account for potential climate change and the subsequent impact on evaporation and rainfall conditions in the future.
- The model includes an approximation for groundwater recharge from rainfall based on a threshold or total amount of rainfall that must occur prior to the onset of recharge to groundwater. This approximation was derived for the current depth to water across the catchment. During model predictions, these recharge estimates were not updated to account for the temporary increase in depth to water, or depth of the soil column above the water table, that will occur as a result of dewatering of the mine area.
- The extent of dewatering required for each orebody area was based on pit shells provided by HPPL. It is likely that final pits will differ and may have some impact on dewatering requirements over the life of the mine.
- Dewatering predictions have been simulated using advanced dewatering (via mainly ex pit bores).
- Once mining at a particular location was completed, dewatering ceased and water levels were allowed to rebound (i.e. pits are not assumed to be kept open and dewatered over the entire life of mine nor are the impacts of pit voids simulated). The rebound of water levels was simulated assuming that pits were infilled with material with the same aquifer parameters as the dewatered in-situ aquifers (i.e. no long term evaporative losses from mine voids were simulated).
- MAR has been simulated for excess dewatering disposal within the tenement. In these areas, limited testing has been completed to assess practical aspect of aquifer re-injection (i.e. potential chemical and biological clogging risk factors).
- Mine closure predictions (GWC, 2024) have assumed that:
    - Mined out pits will be infilled to above pre-development groundwater levels such that no in pit lake level develops and the final landform will be engineered such that there is no net increase or decrease in recharged to the infilled pit voids.
    - The proposed infill material has the same aquifer parameters (hydraulic conductivity and specific yield) as the Undifferentiated Tertiary, to represent the likely waste characteristics.
- Integrated flow and transport modelling has been completed (using Modflow SURFACT) to predict the development of water quality across the modelled catchment over the life of mine. The approach uses an initial salinity (TDS) distribution across the modelled catchment that is based on available salinity measurements across the catchment. The model is not calibrated to any pre-development salinity changes with time.
- No density dependence is included in integrated flow and transport model predictions.

4. REFERENCES

AQ2, 2021. Mulga East – Preliminary Groundwater Management Assessment. Report for JBS&G / HPPL (Doc Ref: 171G_163c), April 2021.

AQ2 2024. Mulga Downs: Groundwater, Surface Water and Ecohydrological Studies. Baseline Assessment. Unpublished report for HanRoy (Doc Ref: 171X_492), October 2024.

Barnett et al, 2102. Australian groundwater modelling guidelines, Waterlines report, National Water Commission, Canberra. June 2012.

DWER, 2022. Water Information Reporting Online Tool. http://wir.water.wa.gov.au/Pages/Water-Information-Reporting.aspx

GWC, 2024. Mulga Downs Groundwater Modelling. Unpublished report for Darkwater Consulting Pty Ltd. October 2024.

Hydrogeologic Inc., 1996 MODHMS / Modflow SURFACT A Comprehensive MODFLOW-Based Hydrologic Modelling System.

Environmental Simulations Inc (2022), Groundwater Vistas Version 8.23 Build 32.

MWH, 2009. Murray's Hill Groundwater Investigation, Stage 2. Report for HPPL, March 2009.

MWH, 2012. Assessment of Fenceline Borefield Area (Mulga East). Report for HPPL, October 2012.

MWH, 2014. Conceptualisation Hydrogeology of the Mulga East Deposit. Report for HPPL, March 2014.

NASA, 2021. NASA Shuttle Radar Topography Mission (SRTM) Version 3.0 Global 1 arc second Data.

Sequent, 2022. Leapfrog Geo Version 2021.2.

SILO, 2022. SILO – Australian Climate Data from 1889 to Yesterday. *Queensland Government.* Evaporation data retrieved 16/03/2022 from https://www.longpaddock.qld.gov.au/silo/.

Skrzypek, G., Dogramaci, and Grierson, P.F. 2013. Geochemical and hydrological processes controlling groundwater salinity of a large inland wetland of northwest Australia. Chemical Geology 357 (2013) 164- 177.

Skrzypek, G., Dogramaci, S., Rouillard, A. and Grierson, P.F. 2016. Groundwater Seepage controls in a hydrologically terminal basin of semi-arid northwest Australia. Journal of Hydrology. 542 (2016) 627-636

Thorne, A.M., and Tyler, I.M., 1996. Roy Hill. W.A., Sheet SF 50-12 (2nd edition): Western Australia Geological Survey, 1:250,000 Geological Series.

Thorne, A.M., Tyler, I.M., Blockley, J.G. and Blight, D.F., 1996, Mount Bruce. W.A., Sheet SF50-11 (2nd edition): Western Australia Geological Survey, 1:250,000 Geological Series.

APPENDIX F
NUMERICAL GROUNDWATER MODEL PREDICTIONS
(GWC 2024)

Darkwater Consulting

Mulga Downs Groundwater Modelling

5 November 2024

Groundwater Consulting Pty Ltd

ABN: 25-651-401-446

Document history & status

Revision	Date issued	Issued by	Revision type
A	21/10/2022	M.Pavlovic	Draft
B	02/11/2022	M.Pavlovic	Interim Draft
C	03/11/2022	M.Pavlovic	Draft
D	17/12/2022	M.Pavlovic	Draft
E	20/04/2023	M.Pavlovic	Draft
F	28/04/2023	M.Pavlovic	Draft
G	21/08/2023	M.Pavlovic	Draft
H	07/10/2024	M.Pavlovic	Draft
I	10/10/2024	M.Pavlovic	Draft
J	11/10/2024	M.Pavlovic	Draft
K	05/11/2024	M.Pavlovic	Final

Distribution of copies

Version	Date issued	Quantity	Electronic	Issued to
Rev A	21/10/2022	1	1	Doug Brown
Rev B	02/11/2022	1	1	Doug Brown
Rev C	03/11/2022	1	1	Doug Brown
Rev D	17/12/2022	1	1	Doug Brown
Rev E	20/04/2023	1	1	Doug Brown
Rev F	28/04/2023	1	1	Doug Brown
Rev G	21/08/2023	1	1	Doug Brown
Rev H	07/10/2024	1	1	Doug Brown
Rev I	10/10/2024	1	1	Doug Brown, Bobak Willis Jones
Rev J	10/10/2024	1	1	Doug Brown, Bobak Willis Jones
Rev K	05/11/2024	1	1	Doug Brown, Bobak Willis Jones

Last Saved:	5 November 2024
File Name:	GWC-020-2022-Mulga Downs Groundwater Modelling Report - 05112024 - RevK.docx
Author:	Milos Pavlovic
Project Manager:	Milos Pavlovic
Client:	Darkwater Consulting
Document Title:	Mulga Downs Groundwater Modelling
Document Version:	Rev K
Project Number:	020-2022

Table of Contents

Figures

Tables

Appendices

Executive Summary

Groundwater Consulting Pty Ltd was commissioned to undertake groundwater modelling of the Mulga Downs mine. The main modelling objective was to assess the dewatering and MAR (Managed Aquifer Recharge) requirements as well as the impacts associated with the simulated dewatering activities. The study utilised the existing Mulga Downs groundwater model developed by AQ2.

The model simulates the MDE_LOM_20 Life of Mine plan (LoM). The LoM plan spans over a 15.5-year period, from January 2027 until June 2042. Results suggested that dewatering requirements over the LoM would be around 113 GL with a peak dewatering rate of 31.3 ML/d, which is a significant reduction compared to the previously simulated 20 MTPa plan where the total predicted dewatering over the LoM was 541 GL with a peak dewatering rate of 83 ML/d.

The projected water demand simulated in the current model was 2 ML/d (estimate provided by HanRoy). Results show that predicted dewatering, less the projected water demand, could be successfully re-injected back into the aquifer. At the time of this study, HanRoy considered Managed Aquifer Recharge (MAR) as the only option for surplus water disposal. The current model simulates MAR using injection bores located within the tenement boundary.

Impacts of simulated MAR on predicted mounding were monitored at 18 selected nominal tracking points across the site, selected based on environmental features of interest. Results show that predicted water levels would not go above the proposed buffer, assigned at 2.5m below ground level, at all tracking locations in the current model. Impacts of simulated MAR and dewatering were also checked against the No Development model by comparing predicted evapotranspiration between the Development and No-Development models. Predicted evapotranspiration in the model that simulates mining activities (Development model) was lower than evapotranspiration simulated in the No-Development model. This comparison shows that the balance between predicted mounding and drawdown would not result in predicted water levels being above the simulated extinction depth of evapotranspiration.

Results of uncertainty analyses suggested that the hydraulic conductivity and aquifer storage of the Unmineralised/Fractured Marra Mamba unit, Orebody aquifer, Undifferentiated Tertiary, Upper Calcrete, and CID Pisolite units play an important role and have the greatest control on predicted mounding and drawdown. Future field investigations of these units should be considered a priority.

Uncertainty analyses also suggested that MAR would raise the water table above predicted base case water levels for a range of aquifer parameters tested in this assessment. Out of 18 tracking locations, mounding above the buffer was predicted only at two of them. The probability that predicted water levels would exceed the proposed buffer level was 13% and 40% at those two locations.

In terms of water quality, the model predicted an increase in salinity at Murray Hill, Fridge West, and Fridge Hill mining areas due to MAR and their proximity to the high-salinity areas in the valley. Horseshoe West and Horseshoe Hill mining areas are predicted to become fresher due to their proximity to lower-salinity areas on the northeastern end of the tenement. In the base case model, the maximum predicted salinity was in the Murray Hill mining area. The initial salinity at Murray Hill was around 2,000 mg/L. The maximum TDS in this area was predicted to reach around 5,000 mg/L. In the case of lower simulated porosity values, TDS in this area was predicted to reach 7,000 mg/L.

At selected tracking points across the site, areas where the initial measured TDS was above 5,000 mg/L were predicted to become fresher over the LoM. Areas where the initial TDS was below 5,000 mg/L were predicted to become more saline, but TDS in those areas was not predicted to go above 5,000 mg/L.

Areas where the initial measured TDS was below 4,000 mg/L, and if they were near injection areas, were predicted to become more saline. In most cases, increases in predicted TDS could be described as temporary, and as soon as the injection ceases, TDS was predicted to decline.

The results of the particle tracking assessment for MAR bores suggested that injected solutes will not migrate beyond the tenement boundary, aside from 2 MAR bores located along the southern tenement boundary in the east, and 1 MAR bore located on the western tenement boundary. At these three bores, particles were predicted to travel at a maximum distance of 1.2 km beyond the tenement boundary (eastern MAR bores), and 400m beyond the tenement

boundary (western MAR bore). Particle tracks associated with MAR bores were not predicted to extend beyond the 'Mungurrdu Ethnographic Area Boundary ('MEA Boundary' hereafter).

Particle tracks associated with dewatering were not predicted to extend beyond the tenement boundary, meaning that potential solutes removed by the simulated dewatering system would originate within the tenement. Due to the proximity to the MEA Boundary, particles associated with dewatering at MH4 were predicted to extend 700m to the south and come close to the Fortescue Valley. The longest simulated dewatering in the model was the dewatering of the Fridge West deposit. It was simulated to start in January 2031 and continue until the end of mining (June 2042). Therefore, particle tracks associated with this deposit were predicted to extend further compared to particle tracks at other deposits. Particle tracks associated with dewatering at FW5 and FW6 pits were predicted to extend in the east, west, and south directions, reaching a distance of 1.6km and coming close to the MEA boundary at the end of mining.

Section 1 Introduction

1.1 Background

HanRoy plans to expand its iron ore mining operations in the Pilbara region. The proposed Mulga Downs mine is located within the Chichester Range, on the northern flanks of the Fortescue Valley, approximately 200 kilometres south of Port Hedland and 180 kilometres northwest of Newman, Western Australia (Figure 1-1).

Groundwater Consulting Pty Ltd (GWC) has been engaged, under direct contract to Darkwater Consulting, to undertake groundwater modelling for the proposed mine to support both State and Commonwealth approvals. Previous predictive modelling, completed by GWC in 2023 (GWC, 2023), considered a 20 million tonnes per annum (MTPA) mine plan for the project. This report outlines the modelling results for the revised mine plan, MDE_LOM_20 which provides an output of around 10 MTPA.

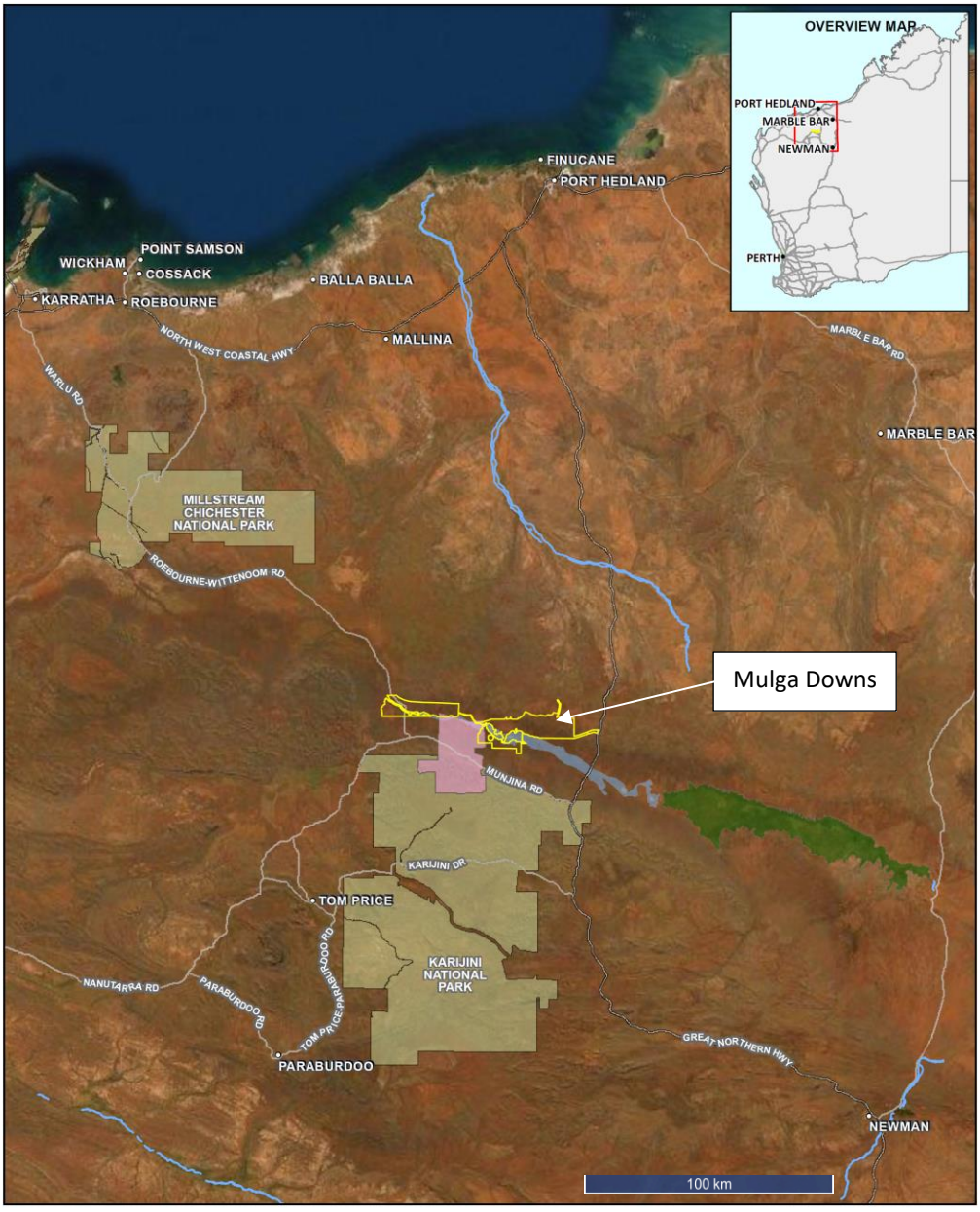

Figure 1-1 Site Location

1.2 Project objectives and scope

The original groundwater model was developed by AQ2 in July 2022 (AQ2, 2022). No further changes have been made to the original model setup and calibration. The model was primarily used to trial various mine planning options and provide estimates for dewatering and water disposal strategies.

The model was used as a predictive tool to assess the following:

- **Mine Dewatering Feasibility** – The model simulated the MDE_LOM_20 mine plan over the life of the mine (LoM) to estimate dewatering requirements and assess the impacts of the proposed development. The results presented in this report provide estimates of the dewatering volumes required to maintain dry mining conditions throughout the LoM, along with indicative dewatering borefield locations and individual bore rates.
- **Disposal Assessment**—The model estimated the water balance for the LoM and assessed the potential range of water surpluses. At the time of this study, HanRoy only considered a simulated water disposal option via Managed Aquifer Recharge (MAR), using reinjection bores located within the tenement boundary.
- **Potential Impacts of Mine Dewatering** - The model assessed the potential magnitude of groundwater level drawdown and mounding resulting from simulated dewatering and MAR at Mulga Downs.
- **Water Quality Assessment -** The model was also used to assess water quality changes, as it is anticipated that dewatering will result in higher salinity water migration towards the dewatering bores and that the MAR water quality may differ from baseline water quality.
- **Mine Closure -** The model was also used to assess aspects of mine closure for two backfilling scenarios and to estimate the time required for the aquifer(s) to return to pre-mining levels.

Section 2 Model Predictions

2.1 Approach

The calibrated model, developed by AQ2 (AQ2, 2022), was used to complete dewatering and MAR predictions over the LoM for the proposed Mulga Downs project. The LoM plan involved simulating pit progressions across seven main mining areas, each comprising multiple pits. These mining areas are presented in Figure A1 and listed in Table 2-1.

Table 2-1 Simulated pits at Mulga Downs

	Mining Areas						
	Murray Hill	Anticline Hill	Fridge West	Fridge Central	Fridge Hill	Horseshoe West	Horseshoe Hill
Pits	MH1	AH1	FW1	FC1	FH1	HW1	HH1
	MH2	AH2	FW2	FC2	FH2	HW2	HH2
	MH3	AH3	FW3	FC3	FH3	HW3	
	MH4	AH4	FW4		FH4	HW4	
	MH5	AH5	FW5			HW5	
	MH6	AH6	FW6				
		AH7					
		AH8					
		AH9					
		AH10					

Numbers in orange represent pits above the water table.

As outlined in Section 1 of this report, the primary objective of this modelling study was to estimate the dewatering rates required to maintain dry mining conditions at Mulga Downs and the potential impacts of the proposed development. The current plan involves excess water disposal only via Managed Aquifer Recharge (MAR). Discharge to the environment or any alternative water disposal methods was not considered at the time of this study.

2.2 Prediction Setup

Details of the model prediction are summarised below:

- Initial conditions were taken from the end of the transient calibration run.
- Dewatering bores were simulated using the Fracture Well (FWL) package in MODFLOW-SURFACT. It was assumed that these bores would pump below the pit base in and around pit areas, with a maximum abstraction rate of 4,320 kL/d (50 L/s). Once mining at a specific location was completed, dewatering was simulated to cease, allowing water levels to rebound. In this case, pits were not assumed to remain dewatered over the entire life of mine, nor were the impacts of pit voids included in the simulation.
- MAR bores were also simulated using the FWL package, with individual bore injection rates ranging from 464 kL/day (5.4 L/s) to 2,959 kL/day (34.2 L/s). These bores extend to the base of the aquifer units, injecting surplus water at depth. The optimal re-injection rate and duration for each MAR bore were determined based on a predicted water level constraint. As water levels at MAR locations were expected to raise, an operational constraint was applied to prevent groundwater levels from breaching the 2.5 mBGL (meters below ground level) buffer. This constraint was simulated in the model by applying a drain cell, 2.5 mBGL at each MAR bore location. Drains were assigned using the Drain (DRN) package in MODFLOW-SURFACT. In this case, if any water was removed at MAR by the DRN, it would be considered "rejected" MAR. In such cases, individual MAR injection rates would be adjusted accordingly (i.e., reduced to ensure that the predicted water levels at MAR locations remained below the applied constraint).
- Mining was simulated using monthly time increments or stress periods.
- Rainfall recharge over the LoM was calculated using the SILO rainfall data. The prediction was based on rainfall data from the period 1960 to 1982. This period was selected because the average rainfall was a good approximation of the long-term annual average while also reflecting natural variations in yearly rainfall totals.
- A "No Development" case (i.e., no dewatering or MAR) was developed to calculate predicted drawdown and mounding and compare predicted water balances with and without mining. This case was run over the same period as the development/mining case. It included the same aquifer properties, boundary conditions, evapotranspiration, and rainfall conditions but didn’t simulate dewatering or MAR. Predicted drawdown and mounding were calculated by subtracting the predicted water levels of the development case from those of the no-development case.
- HanRoy provided 2 ML/day water demand estimates for the project. These estimates were incorporated into the model by subtracting 2 ML/day from the predicted dewatering rates before assigning them to MAR bores.

2.3 Results

Predicted dewatering is presented in Figure 2-1.

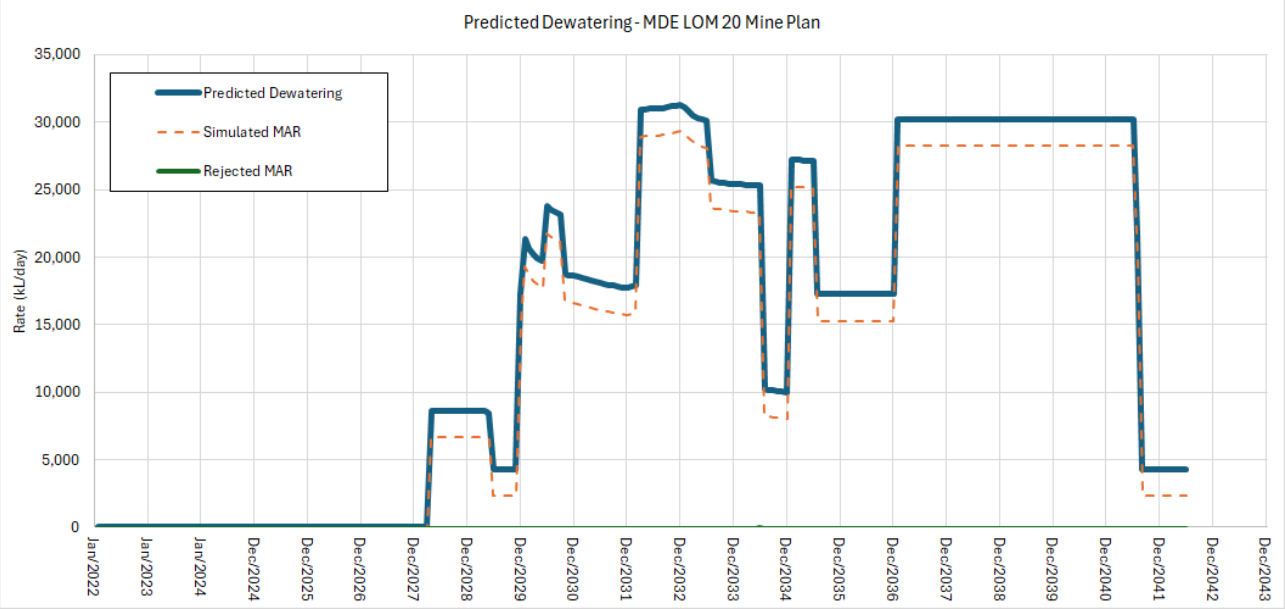

Figure 2-1 Predicted dewatering

Dewatering was predicted to peak at 31.3 ML/day (11.4 GL/year) in 2032, coinciding with the commencement of mining and dewatering at HW5. Another contributing factor to this peak was the start of aquifer injection in the "REJ East" MAR area. The total predicted dewatering over the life of the mine (LoM) was approximately 113 GL. As presented in Figure 2 -1, predicted dewatering was successfully reinjected back into the aquifer using MAR bores without any shortfalls reported as “rejected MAR”.

Pit hydrographs are presented in Figures A2-A15. These hydrographs demonstrate that, with the adopted dewatering setup, the model was successful in lowering water levels below the pit benches at all times. In some cases, pits will be mined to the water table, and then mining will be halted for a period of time before recommencing below the water table (e.g. FW6). This is to manage ore moisture content and grade factors. Where there is a discrepancy between actual and simulated water levels, the actual water level will be used to inform the RL for the above water table (AWT) mining elevation. The AWT mining elevation RL will be continually updated and refined with additional data to inform the mine plan as the project progresses.

Predicted evapotranspiration (EVT) is presented in Figure 2-2. To assess the effects of dewatering and MAR across the model domain, predicted EVT in the development model was compared to predicted EVT in the No-Development model. The results indicate that, from July 2028 until December 2030 and from January 2036 until June 2042, simulated dewatering would lower the water table across the site, reducing predicted EVT below the No-Development EVT level. From January 2031 until December 2035, simulated MAR is predicted to raise the water table across the site, increasing predicted EVT compared to the No-Development case by a maximum of 4 ML/d. The results show that the EVT peak of 7.5 ML/d in December 2037, predicted in the No Development case, is lower in the development/mining case. The total predicted EVT over the life of the mine is 1.6 GL lower in the mining case compared to the "No Development" case. The EVT comparisons between the "No Development" and development/mining cases are presented in Table 2-2.

Table 2-2 Predicted dewatering over the Life of Mine

Scenario	Total Predicted EVT
No Development	110.1 GL
Development	108.5 GL

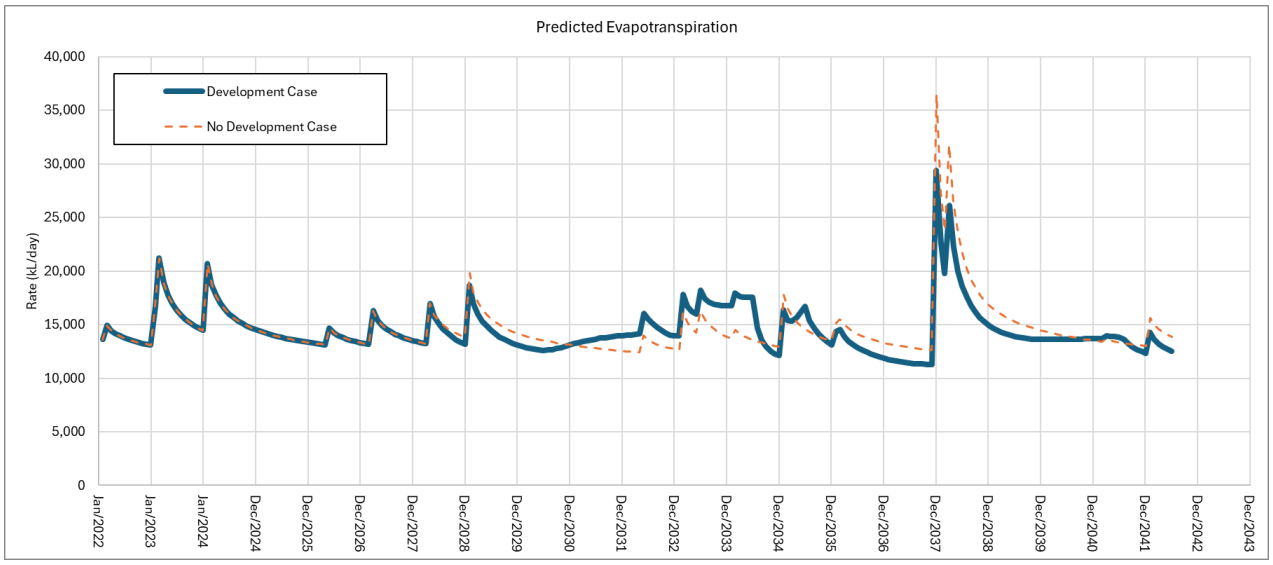

Figure 2-2 Predicted evapotranspiration (EVT)

Mine dewatering was simulated using 23 abstraction bores. Bore locations are presented in Figure A16. After dewatering at specific locations was completed, 9 of these bores were simulated as MAR bores. In total, MAR was simulated using 28 injection bores located within the tenement boundaries (Figure A16). The actual number of bores may differ from simulated due to a number of factors, including local scale heterogeneity of aquifers, operational utilisation rates and other site-specific factors.

Monitoring bores in the model were divided into two categories:

- Pit Monitoring Bores, which track in-pit water levels to ensure dewatering has been achieved, and
- Environmental Monitoring Bores, which monitor predicted drawdown and mounding at key locations across the site. For simplicity, they are labelled as T1-T18. Their actual locations and the areas they are intended to monitor are summarised in Table 2-3. Environmental tracking points were provided by AQ2

All monitoring bores are presented in Figure A17.

Table 2-3 Selected Enviro Tracking Points

ID	Area
T1	Murray West MAR
T2	Valley Between Murray West & Koodjeepindarranna Claypan
T3	Koodjeepindarranna Claypan
T4	Valley Near Murray Hill
T5	Valley Between Murray Hill & Gnalka Gnoona Claypan

ID	Area
T6	Gnalka Gnoona Claypan
T7	Restricted Stygo 1 West
T8	Valley Far West
T9	Restricted Stygo 2 Southwest
T10	Restricted Stygo 3 South
T11	Valley Fridge West
T12	Valley Fridge Central
T13	Valley Central
T14	Between Valley & Horseshoe
T15	Valley Fridge Hill
T16	Valley Horseshoe
T17	Valley Far Southeast
T18	Wirrilimarra

Figures A18 to A28 present predicted drawdown and mounding contours. Unlike typical mining projects in the Pilbara, where the maximum predicted drawdown and mounding usually occur at the end of mining, the predicted drawdown at Mulga Downs is highly transient. This also applies to the simulated dewatering and MAR, which are dynamic processes. While some areas undergo depressurisation and dewatering, mounding occurs in others. The selected periods shown in Figures A18 to A28 correspond to predicted peaks in dewatering and MAR.

West of Mulga Downs, the drawdown was predicted to extend 6 km northeast of the Murray Hill deposit by January 2032 (Figure A19), coinciding with dewatering at Murray Hill and Anticline Hill.

Simulated MAR was predicted to reduce and truncate the extent of the predicted drawdown to the east and west, preventing further propagation. In July 2035, the maximum extent of the predicted drawdown to the east was 2 km southeast of the Horseshoe West deposit, as shown in Figure A23.

To the south, the maximum predicted drawdown was predicted to extend across the valley, reaching approximately 7.5 km south of the Fridge West deposit from 2038 (Figures A24 to A28).

West of Mulga Downs, mounding was predicted to extend 6 km northeast of the most western MAR area (MW) by July 2034 (Figure A22). The maximum extent of predicted mounding to the east was 8 km southeast of the Far East MAR area between 2032 and 2033 (Figures A19-A21) and between 2039 and 2042 (Figures A26-A28). During those two periods, the “Far East” area was used to dispose of most dewatering volumes.

To the south, the maximum predicted mounding was predicted to extend across the valley, reaching approximately 10 km south of the Far East MAR area in 2032 (Figures A19 and A20).

At nominal tracking points, T1-T18, maximum predicted drawdown and mounding are summarised in Table 2-4:

Table 2-4 Predicted Drawdown and Mounding at Tracking Points

ID	Location	Predicted Max Drawdown (m)	Predicted Max Mounding (m)
T1	Murray West MAR	6.8	-2.1
T2	Valley Between Murray West & Koodjeepindarranna Claypan	2.9	-1.8
T3	Koodjeepindarranna Claypan	1.3	-1.0

ID	Location	Predicted Max Drawdown (m)	Predicted Max Mounding (m)
T4	Valley Near Murray Hill	3.0	-8.7
T5	Valley Between Murray Hill & Gnalka Gnoona Claypan	0.6	-4.3
T6	Gnalka Gnoona Claypan	0.2	-2.7
T7	Restricted Stygo 1 West	1.5	-0.6
T8	Valley Far West	0.8	-0.5
T9	Restricted Stygo 2 Southwest	0.3	-1.2
T10	Restricted Stygo 3 South	-	-2.2
T11	Valley Fridge West	-	-7.7
T12	Valley Fridge Central	2.2	-4.3
T13	Valley Central	0.0	-2.8
T14	Between Valley & Horseshoe	6.3	-3.6
T15	Valley Fridge Hill	2.6	-2.5
T16	Valley Horseshoe	2.9	-1.9
T17	Valley Far Southeast	1.3	-0.3
T18	Wirrilimarra	0.6	-

Figures A29-A33 show predicted water levels at the T1 to T18 locations, plotted against the buffer. The results suggest that simulated dewatering and MAR at Mulga Downs will not raise the water table above the buffer at those locations. In some cases, predicted water level peaks came close to the buffer, but these can be described as short-term or temporary.

The predicted average water balance is presented in Table 2-5. As shown in Table 2-5, the development model predicts that simulated dewatering and MAR account for 35% and 31% of the overall water balance, respectively.

In the Development case, average predicted inflows from aquifer storage (aquifer depletion) were estimated to be around 10 ML/d higher than in the No-Development case because of dewatering. Average predicted outflows into aquifer storage (aquifer recovery) were estimated to be around 9 ML/d higher than the No-Development case because of MAR. On average, over the LoM, the model predicts that the development of the Mulga Downs project would result in around 1.5 ML/d of aquifer storage depletion. In general, the results suggest that the objective to conserve water by injecting it back into the aquifers was achieved. The predicted average aquifer depletion is around 7.5% of the average predicted dewatering (estimated at 19.9 ML/d).

Inflows and outflows from the Constant Head Boundaries (CHB) contribute 14% and 6% of the overall water balance, respectively. Compared to the water balance results of the No-Development case, predicted inflows from the CHBs in the development case were, on average, 12 kL/d lower, while predicted CHB outflows were only 2 kL/d higher. In

summary, the differences between boundary inflows and outflows in the mining and no-mining scenarios were minimal, at 0.15% and 0.06%, respectively.

The average predicted evapotranspiration in the development case was 1.85% lower than in the No-Development case due to the water level drawdown associated with simulated dewatering. Inflows from aquifer storage (or storage depletion) were predicted to be 50% higher than in the No-Development case, representing the depletion of aquifer storage in the pit areas by the simulated dewatering system.

Table 2-5 Development and No Development Water Balance – Average Over the Prediction Period (Jan 2027-June2042)

Water Balance Component	Inflow (kL/day)	Outflow (kL/day)
Aquifer Storage	21,359 (10,774)	19,822 (10,820)
North Catchment Inflow	1,158 (1,158)	- (-)
South Catchment Inflow	119 (119)	- (-)
Fortescue Valley East Inflow/Outflow	6,810 (6,822)	- (-)
Fortescue Valley West Outflow	- (-)	3,608 (3,606)
Rainfall Recharge	10,229 (10,229)	- (-)
Evapotranspiration	- (-)	14,405 (14,676)
Dewatering	- (-)	19,920 (-)
Managed Aquifer Recharge	18,080 (-)	- (-)
TOTAL	**57,755 (29,102)**	**57,755 (29,102)**

Values in parentheses represent the No Development case

Section 3 Closure Assessment

3.1 Approach

The base case prediction model, described in the previous section of this report, was used to complete post-mining closure predictions for Mulga Downs. Closure predictions were completed from the end of mining until predicted groundwater levels across the site recovered to a final/equilibrium level. The current closure plan, provided by HanRoy, involves backfilling all mined-out pits with waste to above water table, nominally 402 mRL. The exact backfilling sequence and timing will be defined at a later date.

The recharge assigned to the base case closure model represents monthly rainfall data from the prediction period, repeated during the closure period to simulate variable monthly recharge for the base case closure predictions. Recharge zones, rates, and percentages in the base case closure model are identical to those used in the base case prediction model.

To investigate the impact of climate change, namely rainfall variability, the "Climate Change in Australia Technical Report", developed by CSIRO and Bureau of Meteorology in 2015, was used. In the report, Mulga Downs falls within the Rangelands North projection area. It should be noted that the report suggests that changes to rainfall within this region are possible but unclear. The report also indicates that the change direction cannot be confidently projected given the spread of model results. Therefore, the report suggests that impact assessment in this region should consider the risk of a drier and wetter climate. The projected range between wet and dry periods was +/- 27% compared to the long-term average rainfall. Therefore, two closure sensitivity simulations investigated the impact of future rainfall projections on predicted aquifer recovery. The "High Rainfall" case investigated aquifer recovery in case future rainfall is 27% higher compared to the base case. The "Low Rainfall" case investigated aquifer recovery in case future rainfall is 27% lower compared to the base case. A corresponding No Development model was developed for each closure scenario to calculate predicted drawdown and aquifer recovery.

3.2 Base Case Closure Predictions

Once mining is complete and dewatering ceases, groundwater levels in the Mulga Downs area will keep recovering until a balance between groundwater inflows and groundwater outflows is reached. If pit voids are infilled above the pre-development water table, groundwater levels will eventually recover to predevelopment levels. The hydrogeology of the Mulga Downs area (i.e. a system highly connected to the regional aquifer) means this recovery may occur over a relatively short period. In addition, simulated MAR conserves water that the dewatering system removes during mining, enhancing aquifer recovery times.

The base case prediction model was used to predict groundwater behaviour for two cases once mining and dewatering were complete. Details of mine closure setup are outlined below:

- Initial conditions for closure predictions were taken from the end of dewatering at Mulga Downs (June 2042).
- Closure predictions do not include any further pumping within the model domain.
- The hydraulic parameters for backfill material were implemented at the end of the full mining sequence before the closure simulation period commences.
- Parameters of the infill material will be the same as parameters assigned to the Tertiary unit since waste material will mostly be comprised of the Tertiary unit. The hydraulic conductivity of this unit is 8 m/d which is significantly lower compared to the orebody conductivity of 25 m/d. The specific yield of the Tertiary material of 1% is also lower compared to orebody Sy of 3%.
- The mined-out voids will be infilled to above the pre-development water table, nominally at 402 mRL.
- Climate change scenarios were completed on the base case model, simulating 27% higher ("High Rainfall Case") and 27% lower rainfall ("Low Rainfall Case") compared to the base case.

- For each simulated closure case, the Base Case, High Rainfall case and Low Rainfall case, a corresponding No Development model was developed to provide drawdown calculations. Drawdown was calculated by subtracting predicted water levels of the development run from the corresponding No Development model run.

3.3 Base Case Closure Results

Figures B1 to B23 show predicted in-pit water level recovery relative to the proposed backfill level across all pits. The results suggest that predicted in-pit water levels will not raise above the proposed backfill level of 402 mRL.

Aquifer recovery is presented in Figures B24 to B64. Aquifer recovery is straightforward at most of the monitoring locations, represented by reductions of predicted drawdown from dewatered conditions back to zero or to the pre-development level. At some locations, namely the environmental ones, aquifer recovery is represented by reductions of predicted mounding. At some of them, mounding becomes a drawdown before recovery takes place. In most cases, drawdown is predicted to be less than 0.1m, taking tens of years to recover to the pre-development level (refer to figures B-47, B-53, B-54 and others). Therefore, the closure summary assumes that aquifer recovery is achieved once the predicted drawdown becomes less than 0.1m. With this assumption, groundwater levels are predicted to recover at all monitoring locations within 10 years. Mining areas, such as parts of Anticline Hill (pits AH4,5,6,7,8,9 and 10), Fridge Central, Fridge Hill, Fridge West, Murray Hill and most of the Horseshoe West pits (except northern parts of HW1) are predicted to recover within 5 years.

Enviro locations, labelled T1-T18, are also predicted to recover within 10 years. The longest recovery is predicted at the T18 location (far east area). The unmineralised Marra Mamba unit, simulated at 0.05 m/d, is predicted to slow down the recovery at this location.

Aquifer recovery is also summarised in Figure 3-1 below.

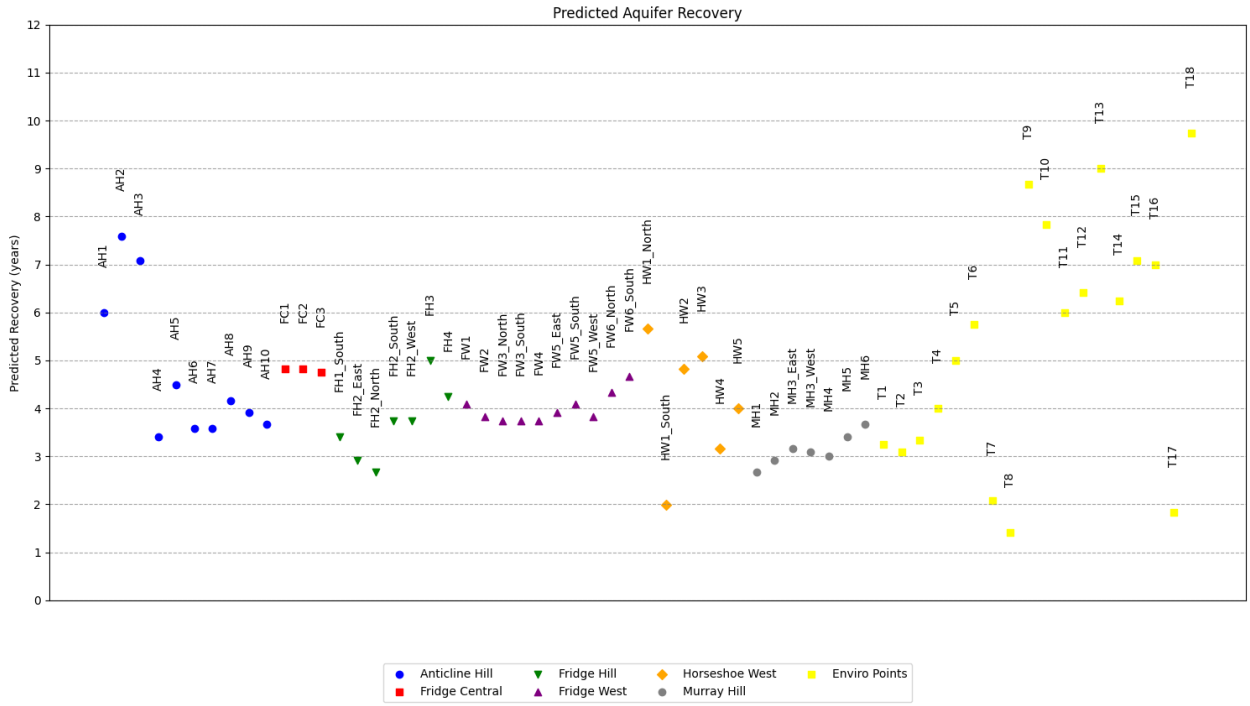

Figure 3-1 Predicted aquifer recovery (summary)

3.4 Closure Sensitivity Results

Figures B1 to B23 also show predicted groundwater levels across the Mulga Downs mine area for two sensitivity runs. The results show that even if post-mining rainfall becomes 27% higher compared to the base case, in-pit water levels will not raise above the proposed level of backfill.

A simulated dry climate scenario, where rainfall recharge was reduced by 27% compared to the base case closure model, resulted in a slightly slower aquifer recovery (Figure 3-2, blue dots). Predicted aquifer recovery in this case was up to 37% slower than the base case closure model (T3 monitoring point). Although the percentage-wise difference in recovery times may seem high, at the T3 monitoring point, the base case predicted recovery was ~3.3 years, and with this recharge setup, it is ~5.3 years (Figure 3-2). Only at monitoring points T2, T3, T4 and T10 the difference between the Base Case predicted recovery and the recovery predicted in the "Low Recharge" case was greater than 1 year (1.24 and 1.58 years, respectively). At all other locations, this difference was less than 1 year and at 52 out of 61 this difference was less than 0.5 years.

A simulated wet climate scenario, where rainfall recharge was increased by 27% compared to the base case closure model, resulted in a slightly faster aquifer recovery (Figure 3-2, orange dots). Predicted aquifer recovery in this case was up to 40% faster than the base case closure model (T1, T2 and T3 monitoring points). Again, although the percentage-wise difference in recovery times may seem high, at the T3 monitoring point, the base case predicted recovery was ~3.3 years, and with this recharge setup, it is ~2 years (Figure 3-2). Only at monitoring points T1, T2, T3, T9 and T10 the difference between the Base Case predicted recovery and the recovery predicted in the "High Recharge" case was greater than 1 year (1.16, 1.17, 1.33, 1.58 and 1.17 years, respectively). At all other locations, this difference was less than 0.5 years.

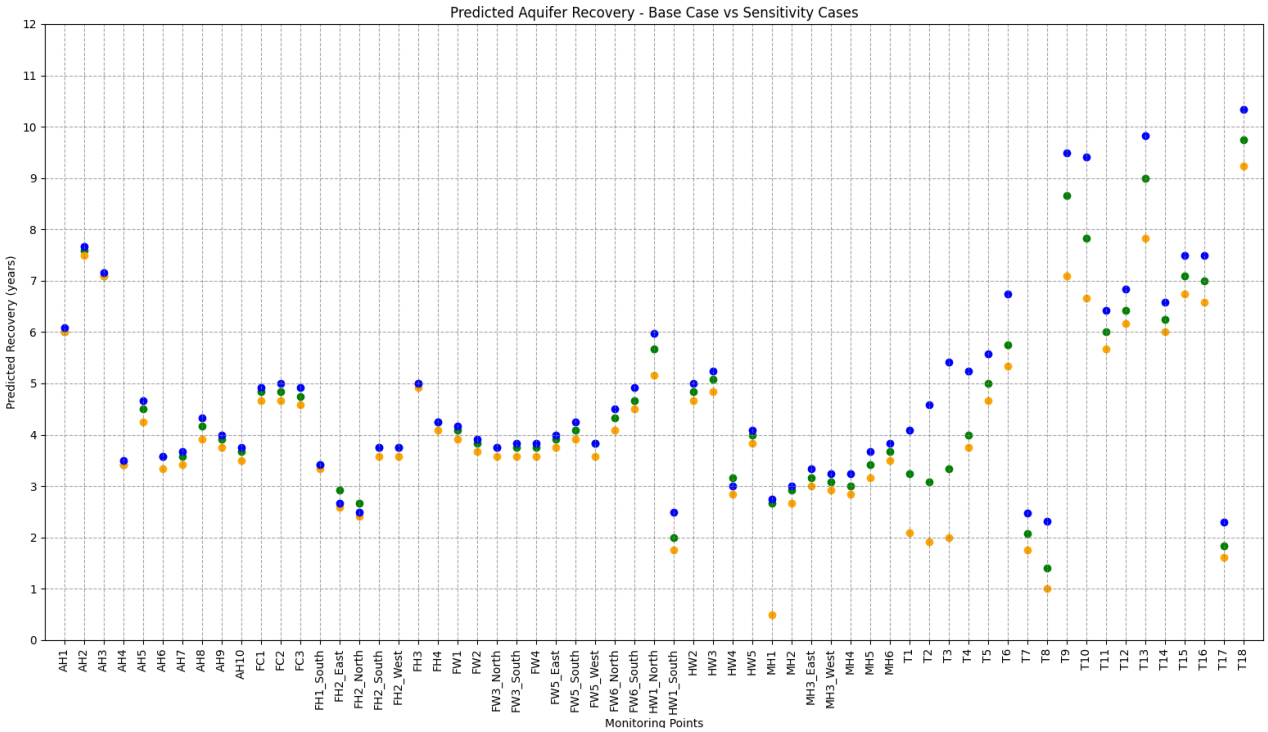

Figure 3-2 Predicted aquifer recovery – comparison between the Base Case and Sensitivity Cases (green dots=Base Case, blue dots=Low Recharge case and orange dots=High Recharge case)

3.5 Alternative Backfilling Case

The 20 MTPa model, completed in 2023, simulated the parameters of backfill material were the same as those of the mined-out material. That is, after mining and dewatering ceased, no further changes to the model properties were adopted in the 2023 model. The mined-out material (orebody) generally has higher conductivity properties and storage. The alternative backfilling case was developed to compare the effect of backfilling pits with the less permeable material, which was simulated in the Base Case model, and the material that would be more conductive and more porous. Consistent with the 2023 model, in this closure run, no further changes were made to the material and aquifer properties. The same units and parameters that were simulated in the calibration and prediction runs were simulated in this closure run. This model run is referred to as “In-situ” hereafter.

The results of this model run are presented in Figures B65 to B128. The base case results are labelled as “Backfill_Waste” on charts, where waste represents the low k material simulated in the Base Case closure model.

Figures B65 to B87 present predicted in-pit water levels. Comparisons between the two model runs show negligible differences in predicted in-pit water levels. They also show that predicted in-pit water levels will not raise above the proposed level of backfill. The same goes for predicted aquifer recovery. As shown in figures B88 to B128, comparisons between the two model runs show negligible differences in predicted aquifer recovery. This could be expected since predicted water levels in both cases are not too much different from one another.

Section 4 Groundwater Salinity Assessment

4.1 Modelling Objectives

This assessment aimed to assess the potential for increased groundwater salinity across the site resulting from simulated dewatering and MAR at Mulga Downs.

The groundwater quality across the project area ranges from fresh to saline. Concentrations of Total Dissolved Solids (TDS) and Electrical Conductivity (EC) range from 180 mg/L TDS (EC 300 µS/cm) in the upper reaches of the groundwater system to 17,000 mg/L TDS (EC 23,000 µS/cm) in the Fortescue Valley area and around the Claypans.

The salinity profiles for the shallower and/or higher elevation bores along the northern boundary of the project area (i.e., single monitoring bores MDPZ7459 (5 to 28 mg), MDPZ7454 (27 to 58 mg), and MDPZ7455 (32 to 60 mg)) show no change in salinity with depth and are fresh throughout the profiles.

Changes in salinity with depth are evident, and the salinity generally increases with depth (AQ2, 2022)

Therefore, upon the commencement of dewatering, it is anticipated that the TDS of dewatering (and therefore surplus water) will likely be below 5,000 mg/L and that dewatering throughout the LoM will become increasingly more saline as drawdowns propagate northwards towards the valley.

This assessment was designed to assess changes to water quality over the LoM.

4.2 Model Setup

The model setup is consistent with the base case dewatering model described in Section 2. It should be noted that the calibrated model is not calibrated to aquifer porosity values since there is no data to provide constraints on porosity. As described in AQ, 2023 report, Section 2.5.4 – Appendix I, “Assigned porosity values are not calibrated or constrained by the model calibration completed to date”. No calibration to porosity has been completed to support particle tracking and solute transport modelling. Therefore, sensitivity assessment was designed to test a range of porosity values, assessing the impacts of higher or lower adopted porosity on predicted salinity. Porosity values for the Base Case, as well as Sensitivity cases 1 and 2, were provided by AQ2. The simulated porosity values are summarised in Table 4-1.

Table 4-1 Assigned porosity values

Unit	Unconfined Storage Sy (%)	Base Case Porosity (%)	Sensitivity Case 1 Porosity (%)	Sensitivity Case 2 Porosity (%)
Upper Calcrete	1	10	1	25
Undifferentiated Tertiary	2	25	2	35
Pisolite / CID	5	15	5	35
Basal Crete	1	10	1	35
Fresh Dolomite of Wittenoom Formation	0.1	5	0.1	10
Weathered West Angela Member	1	20	1	20
West Angela Hardcap	5	20	5	35

Unit	Unconfined Storage Sy (%)	Base Case Porosity (%)	Sensitivity Case 1 Porosity (%)	Sensitivity Case 2 Porosity (%)
West Angela Hardcap (at BoreMDPB0020)	5	20	5	35
Marra Mamba / West Angela Ore (includes sub-mineralised halo)	3	15	3	25
Unmineralised / Fractured Marra Mamba (Mulga East)	1	8	1	10
Unmineralised Marra Mamba (Regional)	0.5	5	0.5	10
Fresh Marra Mamba / Jeerinah	0.1	1	0.1	1

Further work should also focus on gathering porosity data and the model should be refined further when more field data become available.

The Modflow-Surfact Transport module was used to simulate water quality changes. All boundary conditions simulated in the base case model remain unchanged.

Salinity assessment was conducted by incorporating measured TDS values in the model as initial conditions. The monitoring database comprises 61 monitoring bores with measured TDS. Unfortunately, long-term monitoring records were not available at the time of this study. Therefore, the model was not calibrated to measured TDS. To account for this, initial conditions were generated from the available monitoring records by gridding data within the model domain. To replicate the 3D profile of measured TDS, the gridding process was depth-based, and initial conditions were generated for each model layer. Generated grids were translated back into the model as initial conditions. Initial concentrations for each layer are presented in Appendix C (Figures C1 to C11).

The model setup simulates the constant head boundaries as steady-state boundary conditions. Therefore, the concentration assigned to the constant head boundaries was also simulated as a steady state. Zero concentration was assigned to all simulated constant head boundaries. The reason for that is there are no available TDS measurements close to the simulated boundaries. Also, since some boundaries are long, such as the northern and southern boundaries, gridded data provides a range of gridded TDS along those boundaries. To replicate that in the model, boundaries would have to be heterogeneous, which wasn't part of the original model setup. Since we understand this might be a limitation of the current model, water quality changes over the prediction run were monitored to make sure that the current setup does not result in either boundaries bringing too much fresh water into the model or that the boundaries do not take excessive amounts of saline water out of the model. Eight nominal bores were scattered along the boundaries as reference points to monitor these changes. Bore locations are presented in Figure C12.

4.3 Results

The results for all three salinity cases (Base Case, Sensitivity Case 1 and Sensitivity Case 2) are presented in Figures C13 – C38. Predicted TDS removed by the simulated dewatering system is monitored at dewatering bore locations. Since dewatering bores are spatially distributed in x, y and z directions, predicted TDS represents a range of estimated TDS values across the profile. The results were used to calculate the weighted average TDS resulting from pit dewatering Figure C38). Weighted average TDS concentration was calculated as a sum of individual predicted bore rates multiplied by the predicted TDS for that particular bore for all dewatering bores, divided by the total predicted dewatering. It was calculated for every time step in the model and represents a time-varying value). The weighted average predicted TDS is predicted to range between 1,830 to 3,030 mg/L in the Base Case assessment. The predicted

weighted average TDS concentrations were assigned back to the MAR bores as time-varying values to estimate changes in water quality in the re-injection areas.

In Sensitivity Case 1, TDS associated with dewatering is predicted to range between 2,220 and 4,170 mg/L. The main reason for the higher predicted TDS in this case is that simulated porosity values were lower compared to the Base Case.

In Sensitivity Case 2, TDS associated with dewatering is predicted to range between 1,670 and 2,930 mg/L, which is slightly lower than the Base Case. The main reason for the lower predicted TDS in this case is that simulated porosity values were higher than in the Base Case.

Predicted TDS at individual pit locations is presented in Figures C13-C19 and summarised in Table 4-2.

The model predicts an increase in salinity at Murray Hill, Fridge West, and Fridge Hill mining areas due to managed aquifer recharge and their proximity to the high-salinity areas in the valley. Horseshoe West and Horseshoe Hill mining areas are predicted to become fresher due to their proximity to lower-salinity areas on the northeastern end.

Table 4-2 Range of Predicted TDS (Mining Areas) – Base Case

Pit	Minimum TDS Range (mg/L)	Average TDS Range (mg/L)	Maximum TDS Range (mg/L)
Murray Hill	1,900 – 2,135	2,230 – 2,720	2,480 – 4,955
Anticline Hill	1,640 – 1,710	2,380 – 2,720	3,050 – 3,560
Fridge West	1,700 – 1,960	2,040 – 2,440	2,340 – 3,200
Fridge Central	1,610 – 1,750	1,810 – 1,900	2,050 – 2,125
Fridge Hill	1,170 – 1,650	1,480 – 1,890	1,630 – 2,330
Horseshoe West	580 – 1,730	1,380 – 1,850	1,690 – 1,950
Horseshoe Hill	1,670 – 1,790	1,700 – 1,810	1,720 – 1,830

Predicted TDS at selected tracking points (T1-T18) is presented in Figures C20 – C37. Predicted TDS is presented as a weighted average. The weighting is performed based on the thickness of each layer. In general, areas where the initial measured TDS was above 5,000 mg/L were predicted to become fresher over the LoM, and areas where the measured TDS was below 5,000 mg/L were not predicted to go above 5,000 mg/L. Also, areas where the initial measured TDS was below 4,000 mg/L and if they were near injection areas, they were predicted to become more saline. In most cases, increases in predicted TDS could be described as temporary, and as soon as the injection ceases, TDS was predicted to decline.

Sensitivity Case 1, which simulates porosity values lower than the Base Case, produced the greatest difference between Base Case TDS and predicted TDS in this case. TDS is predicted to be higher in areas closer to MAR compared to the Base Case. TDS is predicted to be lower than the Base Case in areas close to the mine.

The difference between the Base Case predicted TDS and TDS predicted in Sensitivity Case 2 was not as high. In this case, TDS is predicted to be lower in areas closer to MAR and higher in areas close to the mine compared to the Base Case.

To monitor the impacts of the simulated constant head and on predicted TDS, nominal bores close to the simulated boundaries were added to the model as described in Section 4.1. Results are summarised in Table 4-3. They suggest that simulated constant head and concentration boundaries had negligible impact on predicted water quality across

the catchment. Differences between starting concentrations at the beginning of the model run and predicted concentrations at the end of the model run were up to 37 mg/L.

Table 4-3 Predicted TDS near the boundaries

Location	Starting TDS (mg/L)	Predicted TDS (mg/L) at the end of mining	Difference (mg/L)
Western Boundary	1,993	1,956	37
Eastern Boundary	5,001	4,974	27
Northern Boundary 1	4,128	4,119	9
Northern Boundary 2	2,884	2,879	5
Northern Boundary 3	2,161	2,159	2
Southern Boundary 1	7,375	7,375	0
Southern Boundary 2	5,586	5,586	0
Southern Boundary 3	4,164	4,164	0

Section 5 Particle Tracking Assessment

5.1 Modelling Objectives

The base case dewatering model, combined with the porosity values of the base case salinity model, was used to assess the likely flow paths associated with dewatering and managed aquifer recharge. Since the original model was developed using the Modflow-Surfact code, the ModPATH, version 3, code was used for this assessment. ModPATH is a particle tracking code for calculating the three-dimensional flow pathlines and travel times of solute particles. ModPATH simulation of particle tracking was set to track particles in the "Backward Tracking" mode. This is an alternative way of mapping the capture area for the well, from the well cell, plotting the final locations of the particles. The Backward Tracking option often allows capture areas to be delineated with fewer particles than would be required for an equivalent Forward Tracking analysis. In this assessment, particles were placed at dewatering and MAR bore locations, across the entire profile of the well. That is, if, for example, a MAR bore was set to inject water in Layer 10, 10 particles were placed at this bore location, from Layer 1 to Layer 10. Particle release times correspond to the simulated operational time of dewatering and MAR bores.

5.2 Results

Particle tracking results are presented in Appendix D. Particle tracking for MAR bores suggested that injected solutes will not migrate beyond the tenement boundary, aside from 2 MAR bores located along the southern tenement boundary in the east, and 1 MAR bore located on the western tenement boundary. At these three bores, particles were predicted to travel at a maximum distance of 1.2km beyond the tenement boundary at the eastern MAR bores, and 400m beyond the tenement boundary at the western MAR bore. Particle tracks associated with MAR bores were not predicted to extend beyond the MEA Boundary.

Particle tracking for dewatering bores suggests that solutes drawn by the bores were from within the tenement boundary. Due to the proximity to the MEA Boundary, particles associated with dewatering at MH4 were predicted to originate 700m to the south of the tenement boundary and come close to the valley. The longest simulated dewatering in the model was the dewatering of the Fridge West deposit. It was simulated to start in January 2031 and continue until the end of mining (June 2042). Therefore, predicted particle tracks associated with this deposit were predicted to originate from further away compared to particle tracks at other deposits. Particle tracks associated with dewatering at FW5 and FW6 pits were predicted to originate in east, west and south direction, from a distance of 1.6km, originating close to the MEA Boundary.

Section 6 Uncertainty Analysis

6.1 Setup

As mentioned in the previous chapters of this report, the original model was designed in Groundwater Vistas using the Modflow-Surfact code. The model was originally designed to provide deterministic outputs and comprise 156 rows, 301 columns, and 11 layers. The total active cell count in the model is 445,753. The reason for this setup is that the original model was designed to assess salinity in addition to dewatering and drawdown predictions. When combined, calibration and prediction models exceed one hour in terms of the model run time. The original model was calibrated without using PEST or any other automated calibration utilities that could provide parameter ranges. Therefore, using the non-linear, stochastic, approach to address model uncertainties would require a significant model rebuild and simplifications to bring the cell count and the model run times down.

Uncertainty analyses were performed in accordance with the Groundwater Modelling Guidelines (Barnett et al., 2012) and the IESC Guidelines (IESC, 2024).

The main objective of this assessment was to assess predictive uncertainty related to predicted drawdown and mounding at selected environmental locations across the model domain (referred to as the Quantities of Interest (QoI) hereafter). A linear error propagation approach, also known as First Order Second momentum or linear uncertainty analyses, was adopted for this assessment. Linear error propagation is a technique in which the effect of the parameters on the outcomes is approximated by a linear function such as the Jacobian matrix, which is the matrix of all first-order partial derivatives of model outputs to parameters. The partial derivatives are numerically approximated by the slope of changes in output by perturbing each parameter of the model by a small amount. In general, if the variability in parameters can be fully described by standard deviation and covariance matrix and the model output is a linear function of the parameters, the uncertainty in model outcomes is obtained by combining the Jacobian matrix and the covariance matrix. The main drawback of this approach is that the estimates of uncertainty can be biased (i.e. overestimated or underestimated) if the parameters are not normally distributed or the model outputs are not a linear function of the parameters (Doherty, 2015, IESC, 2024 and Bernett et al, 2012).

The selected QoI are presented in Table 2-3 of this report. They comprise 18 selected locations across the model domain, where uncertainty analyses aimed to provide a range of predicted drawdown and mounding associated with the proposed development at Mulga Downs.

The ranges of model predictions are presented through summary statistics, using the mean, and the range spanned between the 1st and 99th percentiles. An exceedance probability of predicted mounding was assessed against the buffer level, while exceedance criteria related to predicted drawdown weren't defined at the time of this study.

First, linear uncertainty analyses were performed on the history-matching dataset to demonstrate that the observations can constrain the parameters that are relevant to the QoI. The history matching model was combined with the base case prediction model to provide predictive analyses related to the QoI.

Selected locations and parameter ranges for this assessment were provided by AQ2. Parameter ranges are presented in Table 6-1 below. The provided ranges are mostly based on tested parameter values across the site. In the absence of tested values for hydrostratigraphic units in the Mulga Downs area, parameter ranges for these units were adopted from other iron ore mining projects either close to Mulga Downs or within the Pilbara region.

Table 6-1 Simulated range of parameters

Unit		Horizontal Hydraulic Conductivity, Kh (m/d)		Specific Yield, Sy (%)		Specific Storage, Ss (1/m)	
		Min	Max	Min	Max	Min	Max
Tertiary Cover	Upper Calcrete	1	20	1	10	1E-7	1E-5
	Undifferentiated Tertiary	1	15	1	5		
	Pisolite / CID	5	25	1	10		
	Basal Crete	0.5	15	1	5		
Bedrock	Brockman Formation	0.0001	0.01	0.1	0.5		
	Fresh Dolomite of Wittenoom Formation	0.001	0.1	0.1	1		
	Weathered West Angela Member	0.01	5	0.1	1		
	West Angela Hardcap	5	40	1	10		
	West Angela Hardcap (in the vicinity of bore MDPB0020)	20	150	1	10		
	Marra Mamba / West Angela Ore	10	50	0.1	10		
	Unmineralised / Fractured Marra Mamba (Mulga East)	1	20	0.1	2		
	Fresh Marra Mamba / Jeerinah (Mulga East)	0.01	0.1	0.1	1		
	Unmineralised Marra Mamba / Jeerinah (Regional)	0.0001	0.1	0.1	1		

By tying these two parameters together, the ratio between horizontal and vertical hydraulic conductivity was maintained consistent with the base case model.

6.2 Results

The results of the uncertainty analyses are presented in Appendix E. They are also summarised in Table 6-2 below. Since predicted drawdowns and mounding were subject to this assessment rather than the absolute water levels, the proposed buffer level of 2.5 mBGL was converted back into a level above the water table at each selected tracking location, as shown in Table 6-2. In Table 6-2, the fifth column relates to the probability of exceedance. The 60th and 87th percentiles mean that there is a 40% and 13% probability that the outcome will be above the buffer level.

Table 6-2 Exceedance probability at selected nominal enviro tracking points

ID	Area	Maximum predicted mounding 99th percentile (m)	Buffer Level (m)	Exceedance Probability (%)	Maximum predicted drawdown 1st percentile (m)
T1	Murray West MAR	-12.1	-7.8	40	4.4
T2	Valley Between Murray West & Koodjeepindarranna Claypan	-4.14	-7	0	3.8
T3	Koodjeepindarranna Claypan	-1.9	-4	0	2.6
T4	Valley Near Murray Hill	-6.1	-4.8	13	12.5
T5	Valley Between Murray Hill & Gnalka Gnoona Claypan	-2.4	-3	0	6.2

ID	Area	Maximum predicted mounding 99th percentile (m)	Buffer Level (m)	Exceedance Probability (%)	Maximum predicted drawdown 1st percentile (m)
T6	Gnalka Gnoona Claypan	-1.3	-4.3	0	4.2
T7	Restricted Stygo 1 West	-3	-10.1	0	2.3
T8	Valley Far West	-1.9	-2.1	0	2
T9	Restricted Stygo 2 Southwest	-1	-4	0	2.6
T10	Restricted Stygo 3 South	-0.2	-3.4	0	3.6
T11	Valley Fridge West	-0.6	-2.6	0	11.9
T12	Valley Fridge Central	-3.7	-3.9	0	6.9
T13	Valley Central	-0.19	-0.8	0	3.8
T14	Between Valley & Horseshoe	-8.7	-10.2	0	7.3
T15	Valley Fridge Hill	-3.2	-4.2	0	5.5
T16	Valley Horseshoe	-3.3	-5.2	0	5
T17	Valley Far Southeast	-2	-5	0	1.5
T18	Wirrilimarra	-1.1	-38.6	0	0.4

The results show that the buffer level of 2.5 mBGL could potentially be exceeded at locations T1 and T4. Maximum estimated mounding at those two locations is presented further in Table 6-3:

Table 6-3 Predicted mounding - Probability estimates at T1 and T4 nominal enviro monitoring points

ID	Area	Buffer Level (m)	Maximum predicted mounding (m) Percentiles				Exceedance Probability (%)
			50th	68th	95th	99th	
T1	Murray West MAR	-7.8	-6.8	-8.6	-10.4	-12.1	40
T4	Valley Near Murray Hill	-4.8	-3	-4.05	-5.1	-6.1	13

The numbers in red represent predicted mounding that exceeds the buffer level.

The IESC Guidelines were used to describe the likelihood of exceedance for tracking points T1 and T4. Table 6-4 was copied from the guidelines and the results for all tracking points were added to the table.

Table 6-4 Likelihood of exceedance

Tracking Point	Probability	Percentile (outcomes ranked from small to large)	Description (in terms of likelihood of exceedance)
None		<10%	It is **very likely** that the predicted mounding would exceed the proposed buffer level
None		10–33%	It is **likely** that the predicted mounding would exceed the proposed buffer level
T1	P60	33–67%	It is **as likely as not** that the predicted mounding would exceed the proposed buffer level
T4	P87	67–90%	It is **unlikely** that the predicted mounding would exceed the proposed buffer level
None		>90%	It is **very unlikely** that the predicted mounding would exceed the proposed buffer level

For T2, T3 and T5-T18, tracking points, results suggested that the predicted mounding will always remain below the proposed buffer, suggesting that for the simulated parameter ranges, the possibility of exceeding the proposed buffer is none.

Contributions to predictive uncertainty variance at tracking point T1 are presented in Figure 6-1. The results suggest that the T1 tracking point is most sensitive to hydraulic conductivity values of the Unmineralised / Fractured Marra Mamba Formation in the Mulga East area, Undifferentiated Tertiary unit, CID Pisolite unit, Orebody and Upper Calcrete. Those are the units located between the T1 and the simulated dewatering system, and if they are more or less conductive compared to the base case, that will produce either more or less drawdown at T1 compared to the base case prediction.

The results also show that the T1 is sensitive to hydraulic conductivity values related to the Jeerinah Formation. This is because this unit in the model hosts a constant head inflow boundary on the northern edge of the model. If this unit is more conductive, it will provide more inflow, and vice versa. This does not mean that the hydraulic conductivity of this unit needs to be investigated further; instead, it is a water balance aspect of how much inflow could be expected from the north.

The results indicate that the T1 tracking point is highly sensitive to the specific yield values of the Upper Calcrete, as it is located within this hydrostratigraphic unit in the model. It is also influenced by the specific yields of the Orebody, Undifferentiated Tertiary, and CID Pisolite units, which connect the target area to the orebody. Given their significant impact on both predicted dewatering and drawdown, prioritizing the investigation of the specific yields in these units should be a key focus in the next round of field investigations.

The results indicate that the T1 tracking point is highly sensitive to the specific storage values of the Upper Calcrete. It is also because this target is located within this hydrostratigraphic unit in the model. It should be noted that Figure 6-1 presents normalised values for predicted sensitivities. Real sensitivities T1 to specific storage are minor compared to the influence of hydraulic conductivity and specific yield.

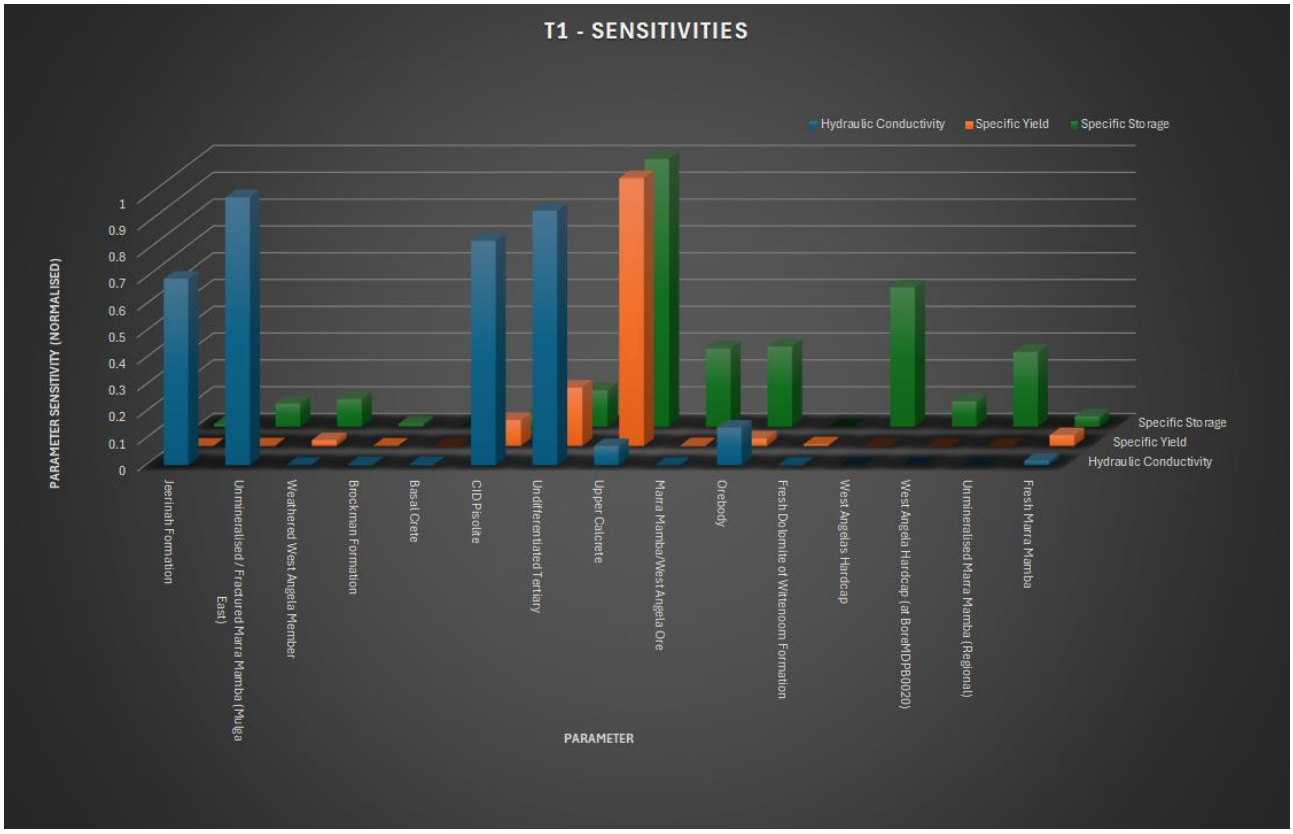

Figure 6-1 Nominal T1 tracking point (parameter sensitivity)

Contributions to predictive uncertainty variance at tracking point T4 are presented in Figure 6-2. Same as the T1 tracking point, the T4 tracking point is also most sensitive to hydraulic conductivity values of the Unmineralised / Fractured Marra Mamba Formation in the Mulga East area, Orebody, Undifferentiated Tertiary unit, CID Pisolite unit and Upper Calcrete. Those are the units located between the T4 and the simulated dewatering system, and if they are more or less conductive compared to the base case, that will produce either more or less drawdown at T4 compared to the base case prediction.

The results also show that the T4 is sensitive to hydraulic conductivity values related to the Jeerinah Formation. This is because this unit in the model hosts a constant head inflow boundary on the northern edge of the model.

The results indicate that the T4 tracking point is highly sensitive to the specific yield values of the Orebody as it is located closer to the mine compared to the T1.

The results also indicate that the T4 tracking point is highly sensitive to the specific storage values of the Orebody aquifer as well as the Unmineralised Marra Mamba unit due to its proximity to the mine and the impact that parameters assigned to these two units has on predicted dewatering and drawdown.

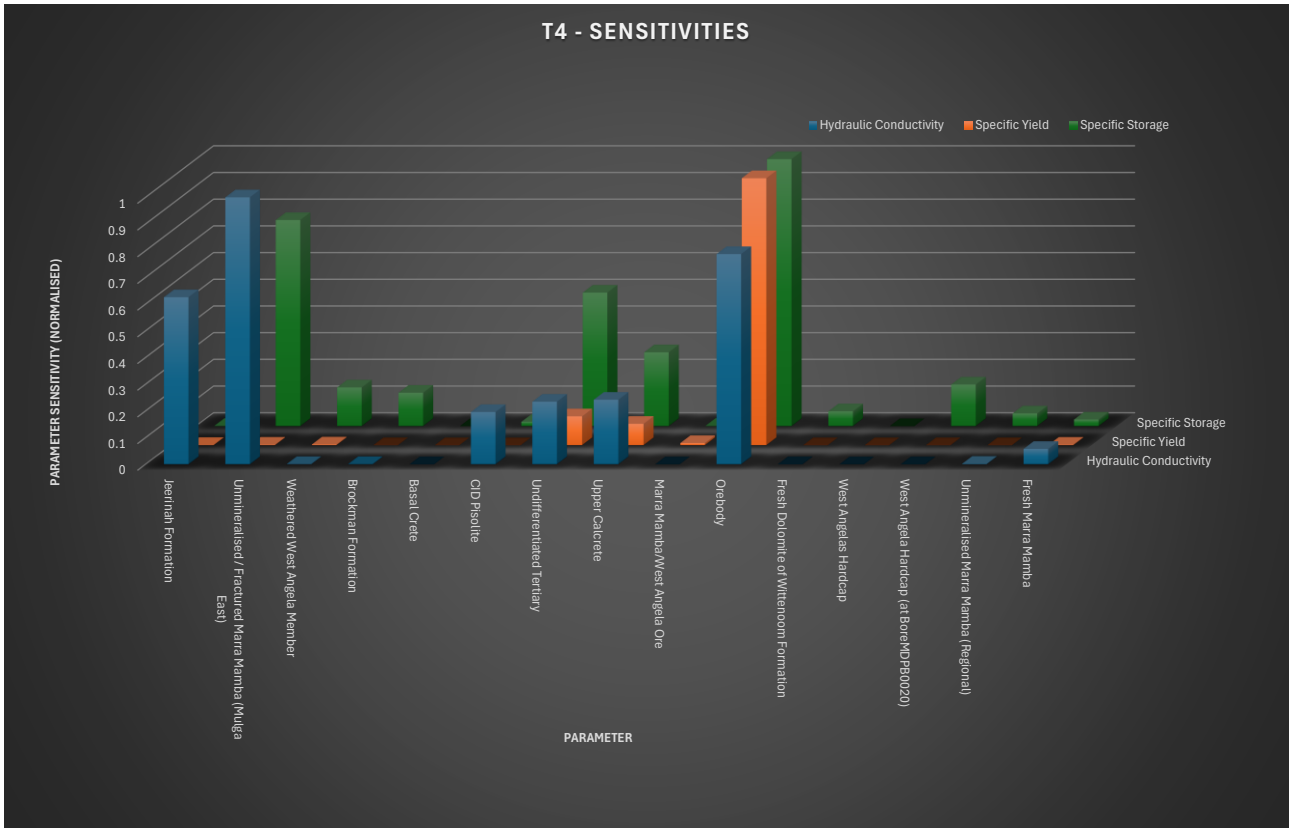

Figure 6-2 Nominal T4 tracking point (parameter sensitivity)

Section 7 Conclusions and Recommendations

7.1 Dewatering and MAR

Using the recently developed mine plan for the Mulga Downs mine (MDE_LOM_20), model predictions suggest that dewatering requirements over the LoM would be around 113 GL, which is a significant reduction compared to the previously simulated 20 MTPa plan where the total predicted dewatering over the LoM was 541 GL. Peak dewatering was predicted in 2032 at 31.3 ML/d. In the previously simulated 20 MTPa plan, peak dewatering was predicted at 83 ML/d.

The simulated dewatering and MAR system comprises:

- 23 dewatering bores.
- 9 dewatering bores were also used as MAR bores once dewatering ceases at that particular location/pit.
- 28 MAR bores (including 9 bores mentioned in the previous bullet point).

The actual number of bores may differ from simulated due to a number of factors, including local scale heterogeneity of aquifers, operational utilisation rates and other site-specific factors.

The simulated dewatering system was predicted to be sufficient to enable dry mining conditions throughout the LoM.

Managed aquifer recharge was predicted to successfully re-inject surplus water back into the aquifer without raising the water table above the buffer. This aspect was monitored at 18 selected tracking points and by comparing development and no-development predicted EVT.

7.2 Simulated Drawdowns

Unlike typical mining projects in the Pilbara, where the maximum predicted drawdown and mounding usually occur at the end of mining, the predicted drawdown at Mulga Downs is highly transient. This also applies to the simulated dewatering and MAR, which are dynamic processes. While some areas undergo depressurisation and dewatering, mounding occurs in others.

West of Mulga Downs, the drawdown was predicted to extend 6 km northeast of the Murray Hill deposit by January 2032 (Figure A19), coinciding with dewatering at Murray Hill and Anticline Hill.

Simulated MAR was predicted to reduce and truncate the extent of the predicted drawdown to the east and west, preventing further propagation. The maximum extent of predicted drawdown to the east was 2 km southeast of the Horseshoe West deposit in July 2035.

To the south, the maximum predicted drawdown was predicted to extend across the valley, reaching approximately 7.5 km south of the Fridge West deposit from 2038 to 2042.

West of Mulga Downs, mounding was predicted to extend 6 km northeast of the most western MAR area (MW) by July 2034. The maximum extent of predicted mounding to the east was 8 km southeast of the Far East MAR area between 2032 and 2033 and between 2039 and 2042. During those two periods, the “Far East” area was used to dispose of most dewatering volumes.

To the south, the maximum predicted mounding was predicted to extend across the valley, reaching approximately 10 km south of the Far East MAR area in 2032.

At selected tracking points, T1-T18, the maximum predicted drawdown was 6.8m at T1. The maximum predicted mounding was 8.7m at T4.

7.3 Simulated Post-mining (Closure) Requirements

HanRoy is committed to backfilling the pits with waste at the cessation of mining. The closure scenarios assume the backfilling of all pits above the water table, nominally at 402 mRL. The current closure plan involves backfilling all mined-out pits with waste. The waste material will mainly comprise the Tertiary unit located above the orebody. Therefore, the parameters assigned to backfill were consistent with the parameters of the Tertiary unit in the model. Backfill material is implemented at the end of the full mining sequence prior to the closure period commences.

In addition to the base case closure run, two additional climate scenarios were simulated in the closure assessment. The "High Rainfall" scenario simulates 27% higher post-mining rainfall compared to the base case, and the "Low Rainfall" scenario simulates 27% lower post-mining rainfall compared to the base case. In all three cases, aquifers were predicted to recover to pre-mining levels within 10.5 years. The base case results suggest that in-pit water levels will recover to pre-mining levels within 2 to 7.5 years from the end of mining. Water levels at tracking points were predicted to recover within 1.4 to 9.8 years from the end of mining.

7.4 Simulated Water Quality (TDS)

In addition to the base case, two additional water quality simulations were completed for the project, simulating higher and lower porosity values than the base case. Higher porosity values result in lower velocities in the model and slower movement of simulated TDS, and vice versa; lower porosity values result in higher velocities in the model, enabling simulated TDS to move faster through the porous medium.

The model predicts an increase in salinity at Murray Hill, Fridge West, and Fridge Hill mining areas due to managed aquifer recharge and their proximity to the high-salinity areas in the valley. Horseshoe West and Horseshoe Hill mining areas are predicted to become fresher due to their proximity to lower-salinity areas on the northeastern end. In the base case model, the maximum predicted salinity was in the Murray Hill mining area, where TDS was predicted to reach 4,020 mg/L. In the case of lower simulated porosity values, TDS in this area was predicted to reach 7,000 mg/L.

At nominal tracking points (T1-T18), areas where the initial measured TDS was above 5,000 mg/L were predicted to become fresher over the LoM. Areas where the measured TDS was below 5,000 mg/L were predicted to become more saline, but TDS in those areas was not predicted to go above 5,000 mg/L.

Areas where the initial measured TDS was below 4,000 mg/L, and if they were near injection areas, were predicted to become more saline. In most cases, increases in predicted TDS could be described as temporary, and as soon as the injection ceases, TDS was predicted to decline. The base case model predicted the largest TDS increase at the T1 tracking point, located in the "West MAR" area. TDS at this location was predicted to increase from 1,200 mg/L (initial TDS) to 3,900 mg/L in 2034. Also, at the end of the injection period at "West MAR", TDS at this location was predicted to decline, reaching 2,900 mg/L at the end of mining at Mulga Downs (June 2042).

7.5 Simulated Particle Tracking

The results of the particle tracking assessment suggested that particle tracks will not extend beyond the tenement boundary, aside from 2 MAR bores located along the southern tenement boundary in the east, and 1 MAR bore located on the western tenement boundary. At these three bores, particles were predicted to extend at a maximum distance of 1.2km at the eastern MAR bores, and 400m at the western MAR bore. Particle tracks associated with MAR bores were not predicted to extend beyond the MEA Boundary. That means that any solutes injected into MAR bores would largely remain within the tenement boundary aside from those three locations.

Particle tracks associated with dewatering were not predicted to extend beyond the tenement boundary either. This means that solutes removed by the simulated dewatering system would come from areas within the tenement. Due to the proximity to the MEA Boundary, particles associated with dewatering at MH4 were predicted to extend 700m to the south and come close to the valley. The longest simulated dewatering in the model was the dewatering of the Fridge West deposit. It was simulated to start in January 2031 and continue until the end of mining (June 2042).

Therefore, predicted particle tracks associated with this deposit were predicted to extend further compared to particle tracks at other deposits. Particle tracks associated with dewatering at FW5 and FW6 pits were predicted to extend in the east, west, and south directions, reaching a distance of 1.6 km and coming close to the MEA boundary at the end of mining.

7.6 Model Uncertainties

Uncertainty analyses suggested that simulated MAR could potentially result in higher predicted mounding across the site. Uncertainty analyses were performed using the Linear Error Propagation approach for a range of aquifer parameters. The results suggested that at two tracking points (T1 and T4), predicted mounding could potentially raise above the buffer.

In terms of parameters adopted to describe the hydrogeology of the Mulga Downs area, the results suggested that the hydraulic conductivity and aquifer storage of the Unmineralised/Fractured Marra Mamba, Orebody aquifer, Undifferentiated Tertiary, Upper Calcrete and CID Pisolite units play an important role and have the greatest control on predicted mounding and drawdown. Further field investigations of these units should be considered as a priority.

The results also suggested that parameters associated with the Jeerinah Formation have an important role in the model. This is because the unit in the model hosts a constant head inflow boundary in the north. This doesn't mean that future field investigations of this unit should be considered a priority; it is rather a water balance aspect and would involve adjusting the parameters of this boundary if required.

In terms of risk and likelihood, the results suggested that it is very unlikely that the proposed buffer would be exceeded at tracking points T2, T3 and T5-T18. At tracking point T1, it is as likely as not that the outcome would exceed the proposed buffer. At tracking point T4, it is unlikely that the outcome would exceed the proposed buffer.

Section 8 References

AQ2, 2022: Mulga Downs Site Water Management (Hydrology & Hydrogeology) Pre-Feasibility Study, July 2022.

AQ2, 2023: Numerical Groundwater Modelling – Appendix I, Rev B, Report 347a, April 2023.

Barnett et al, 2012: Australian groundwater modelling guidelines, Waterlines report, National Water Commission, Canberra. June 2012

CSIRO, 2015: CSIRO and Bureau of Meteorology 2015, Climate Change in Australia Information for Australia's Natural Resource Management Regions: Technical Report, CSIRO and Bureau of Meteorology, Australia

Doherty, 2015 Calibration and Uncertainty Analysis for Complex Environmental Models, PEST: complete theory and what it means for modelling the real world. John Doherty, Watermark Numerical Computing, 2015.

GWC, 2023 Mulga Downs Groundwater Modelling, August 2023, Report revision G

IESC, 2024 Information guidelines for proponents preparing coal seam gas and large coal mining development proposals, February 2024

Appendix A Model Predictions

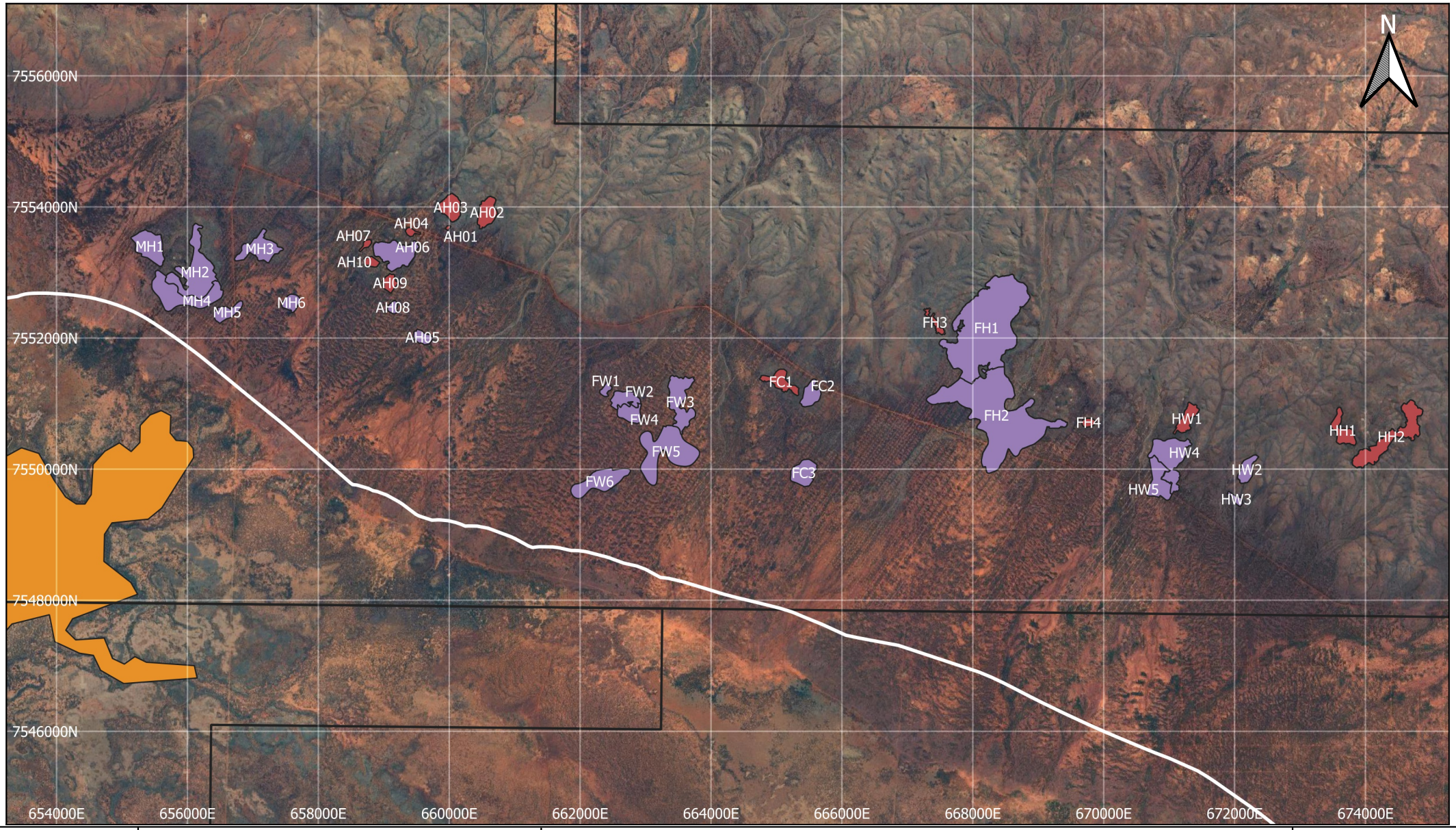

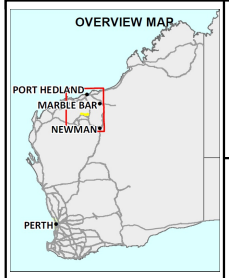

0 2.5 5 km

Legend

- Pits Above Water Table
- Pits Below Water Table
- MEA Boundary
- Gnalka Gnoona Claypan
- Tenement Boundary

AUTHOR: MP

DRAWN: MP

DATE: 28/09/2024

Report NO: GWC-020-2022

REVISION: H

JOB No: 020-2022

NOTES & DATA SOURCES:

Not for construction

ESPG:28350 (GDA94/MGA zone 50)

Figure A1

Simulated pits at Mulga Downs

FIGURE A2 - MDE LOM 20 - PREDICTED INPIT WATER LEVELS AT MURRAY HILL

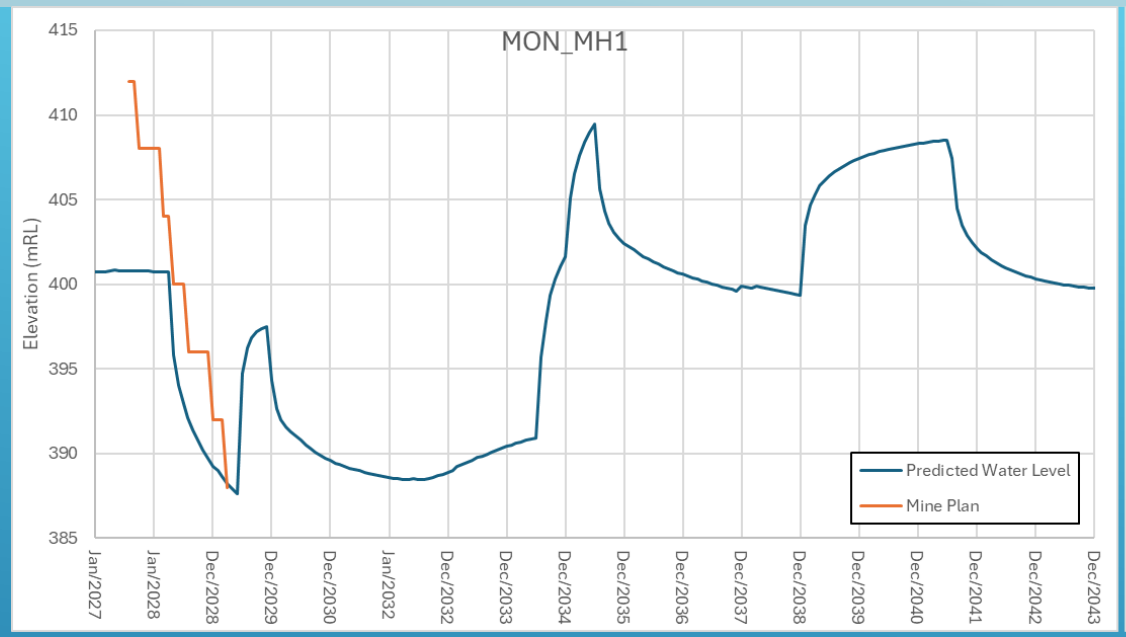

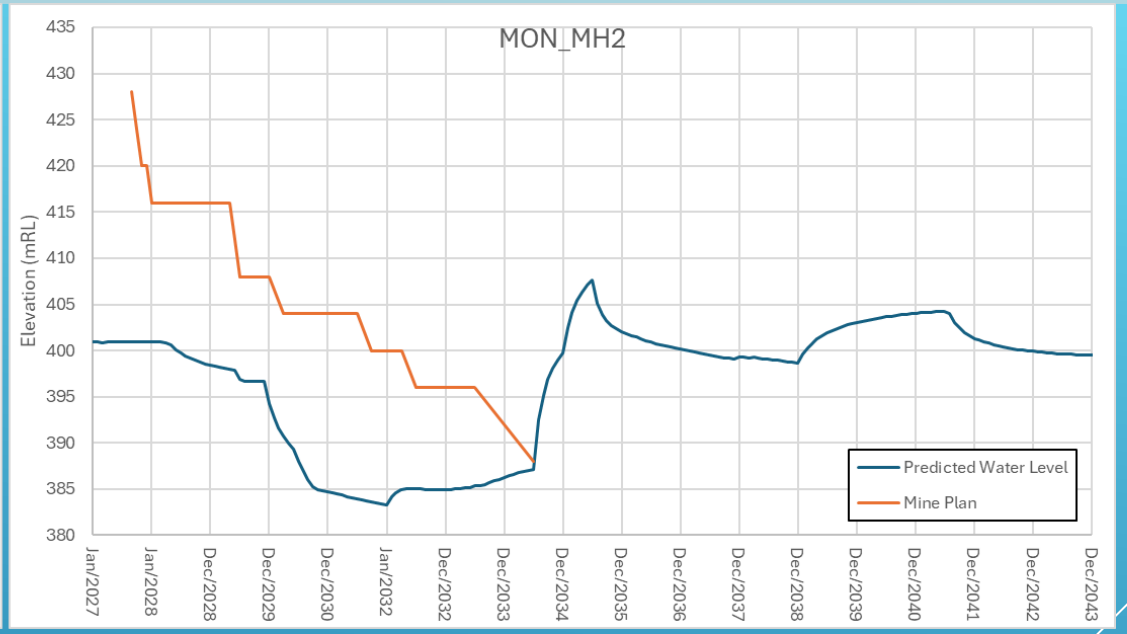

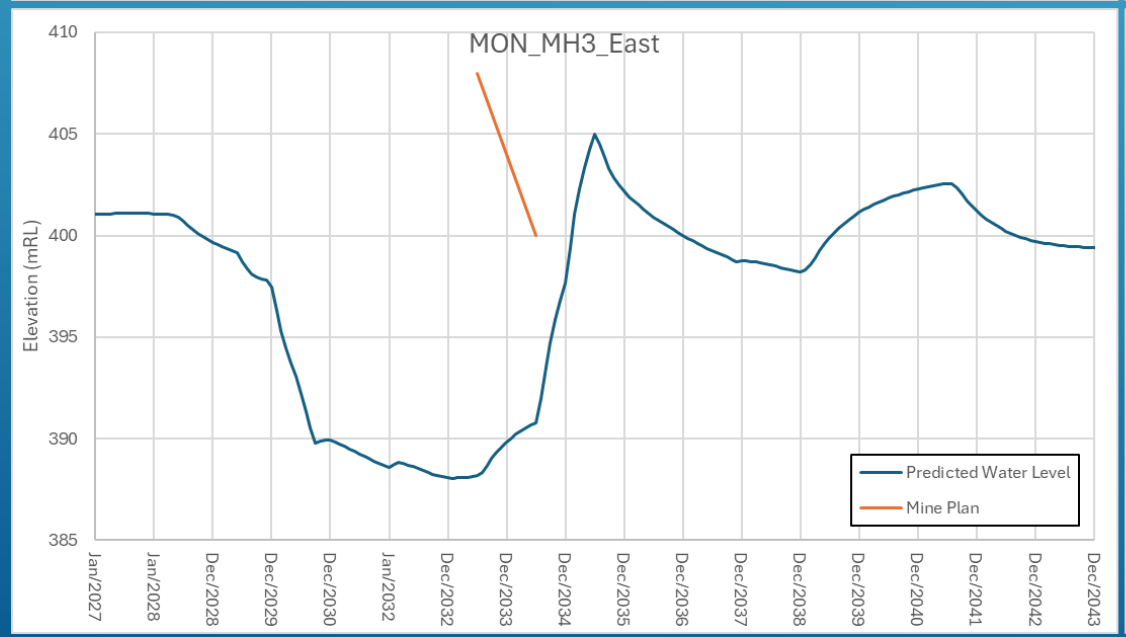

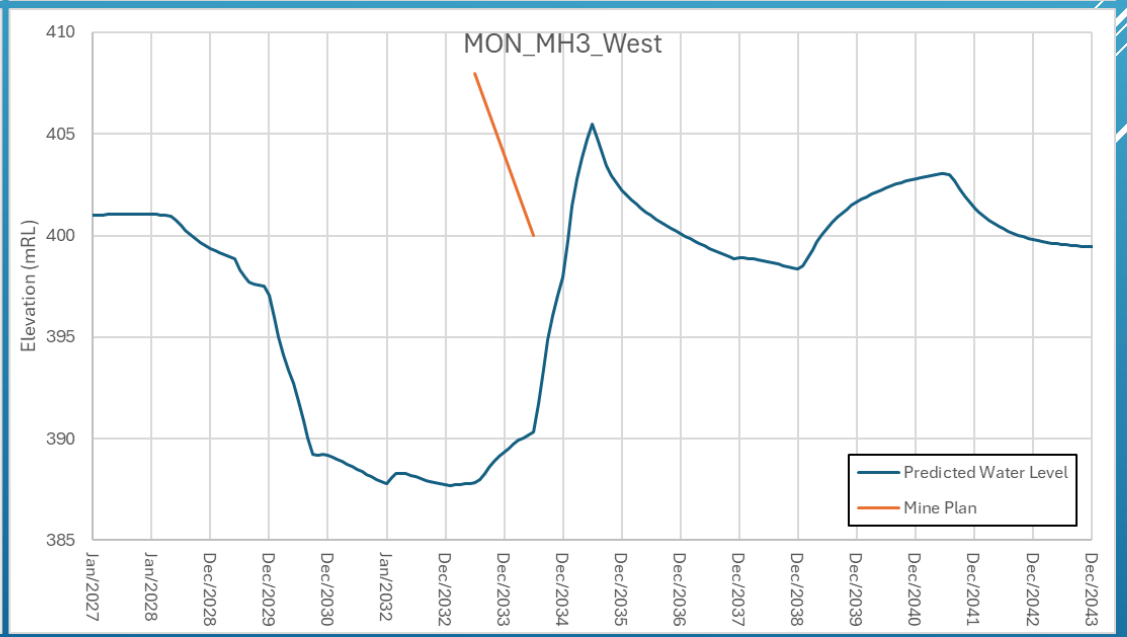

FIGURE A3 - MDE LOM 20 - PREDICTED INPIT WATER LEVELS AT MURRAY HILL

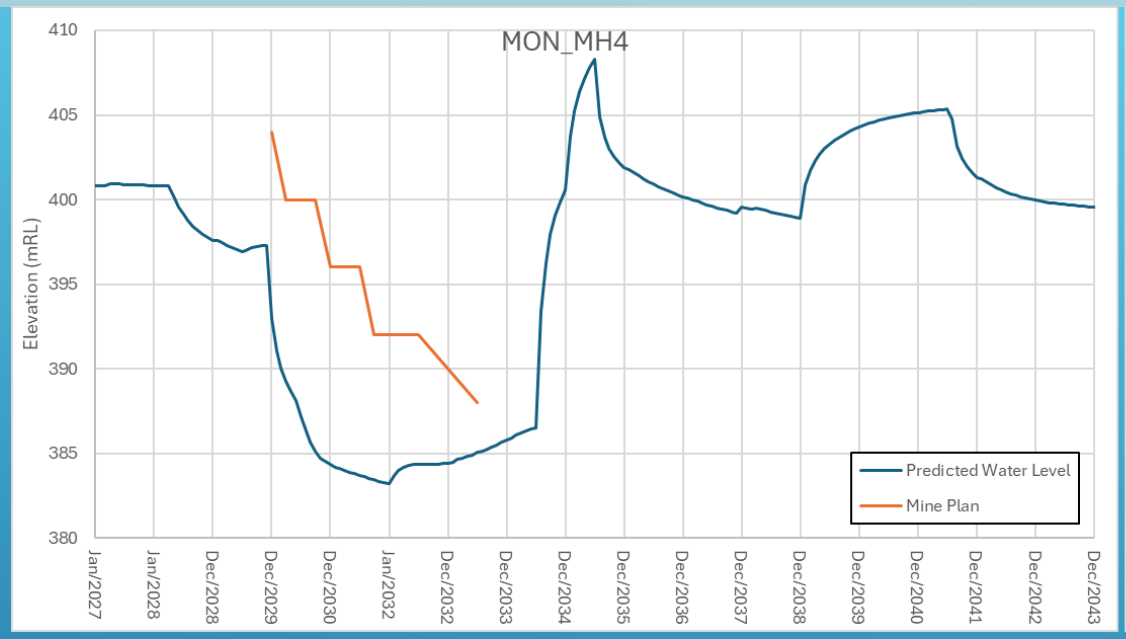

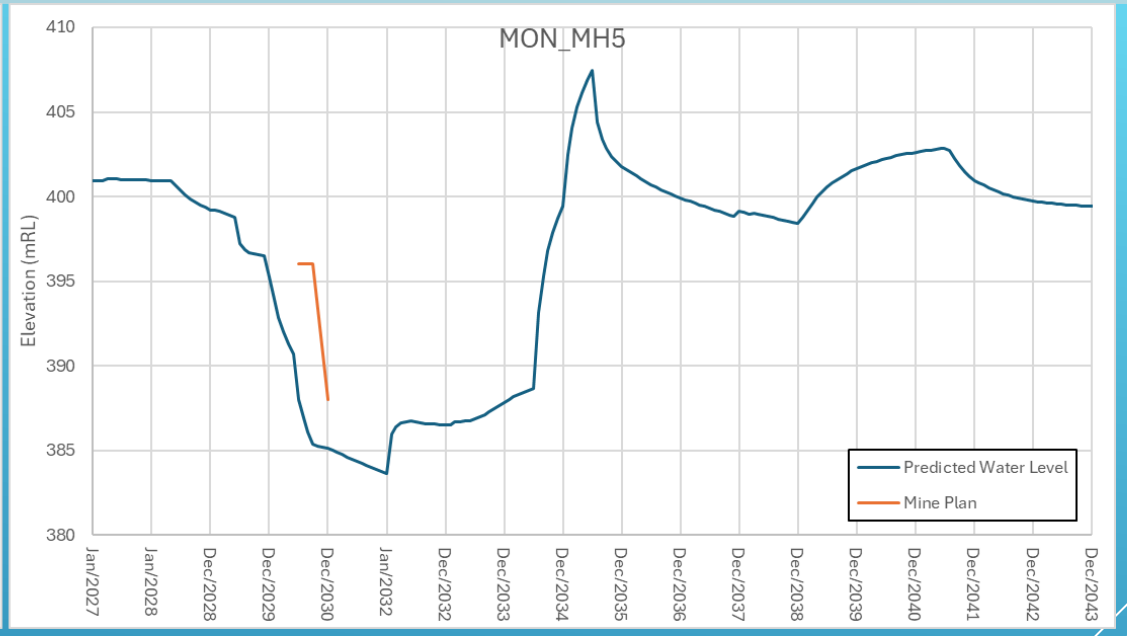

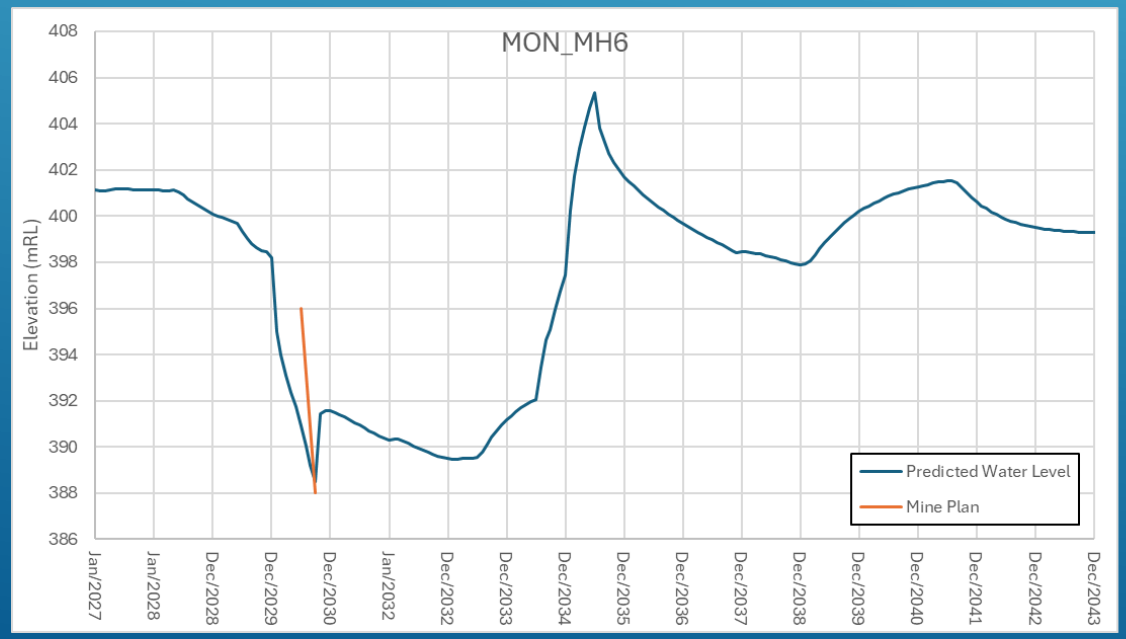

FIGURE A4 - MDE LOM 20 - PREDICTED INPIT WATER LEVELS AT ANTICLINE HILL

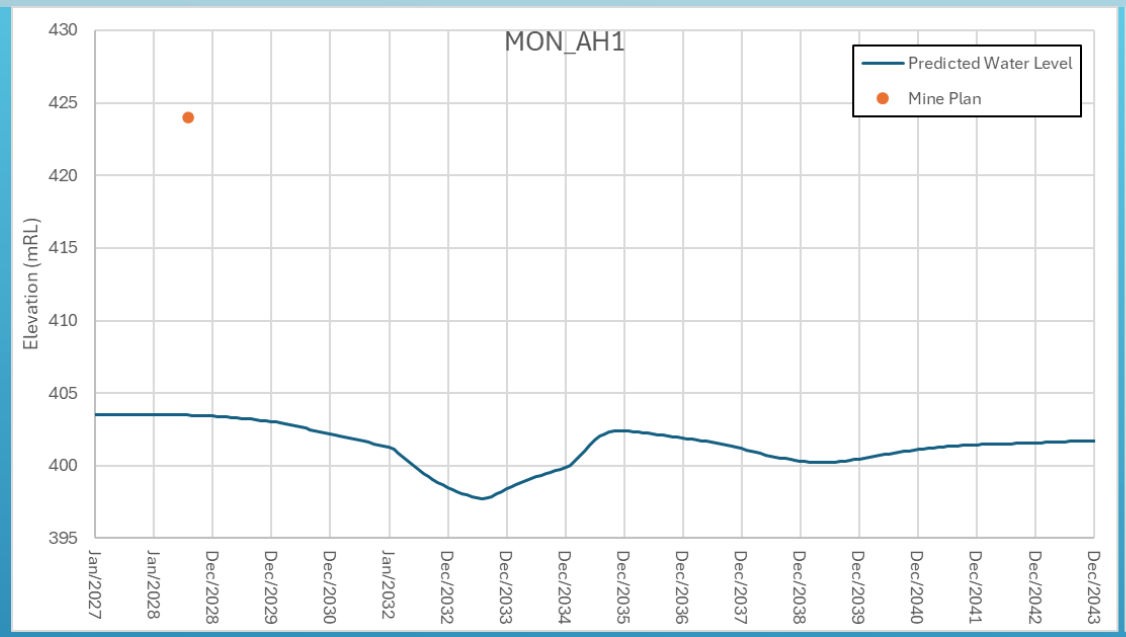

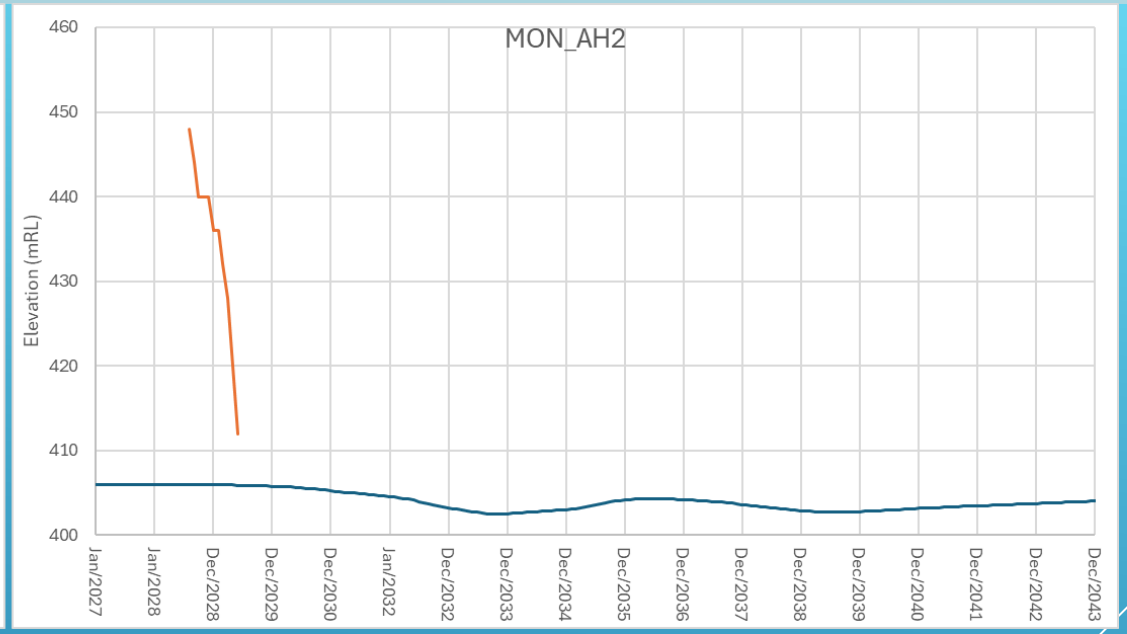

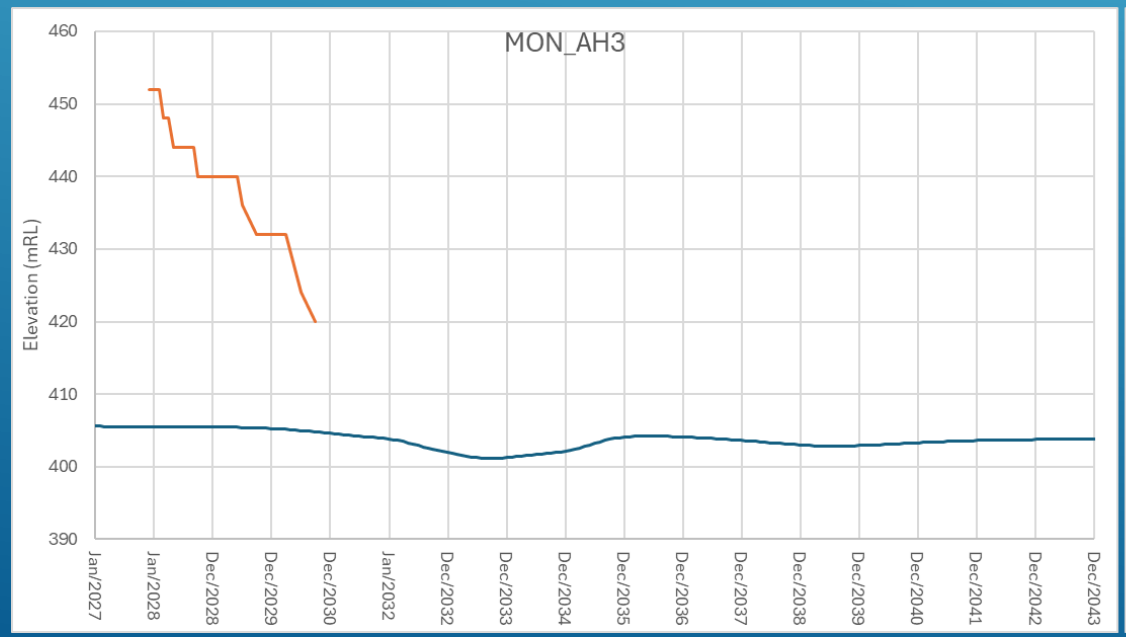

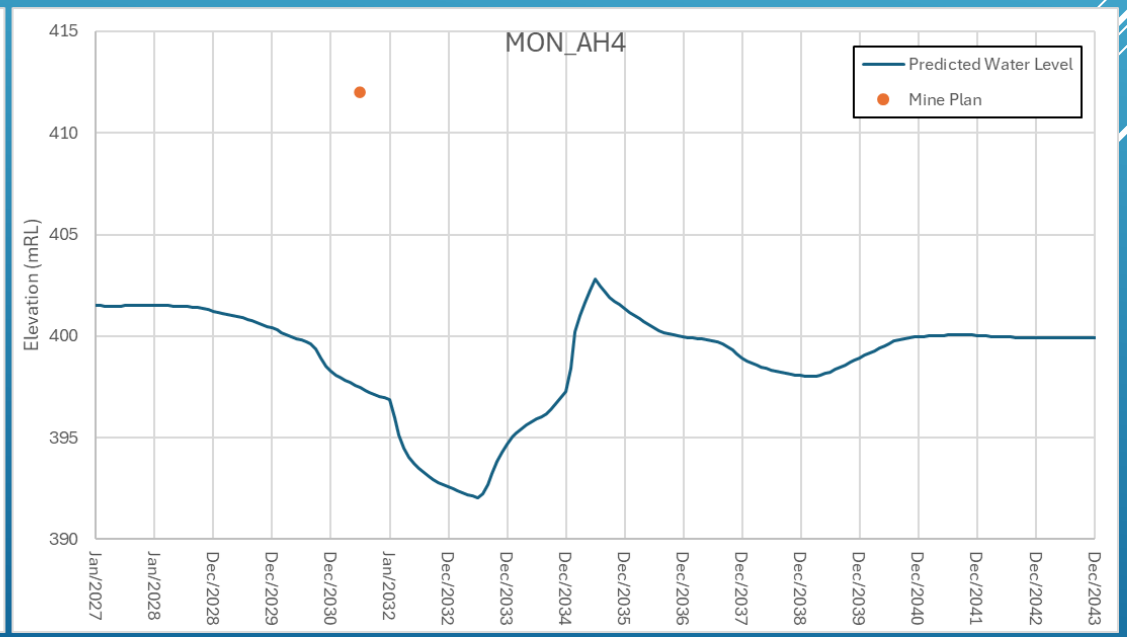

FIGURE A5 - MDE LOM 20 - PREDICTED INPIT WATER LEVELS AT ANTICLINE HILL

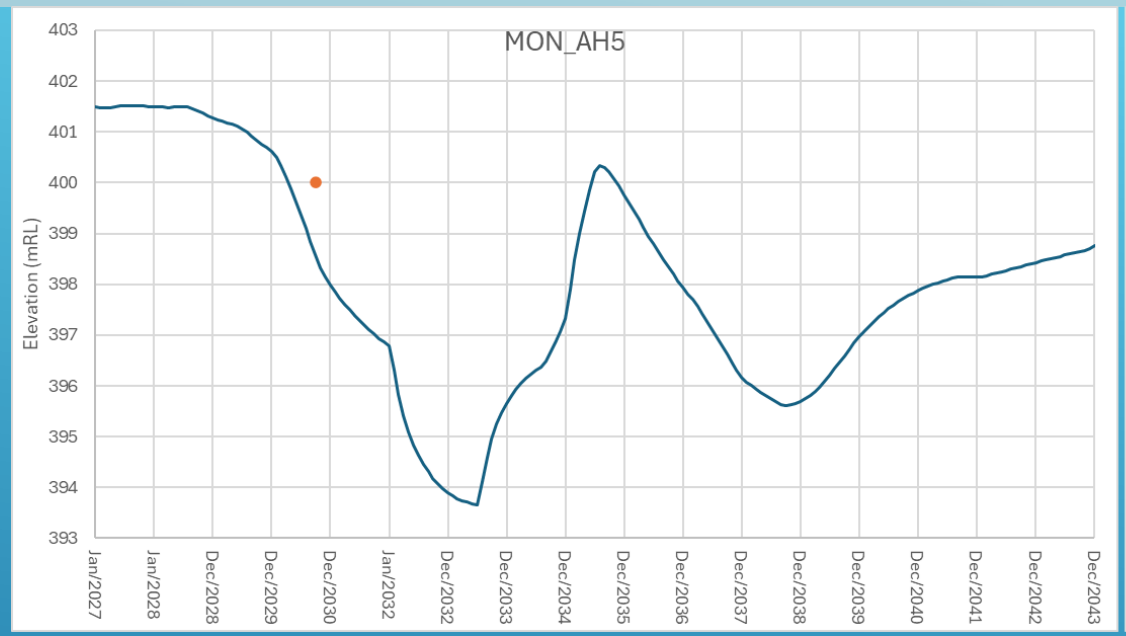

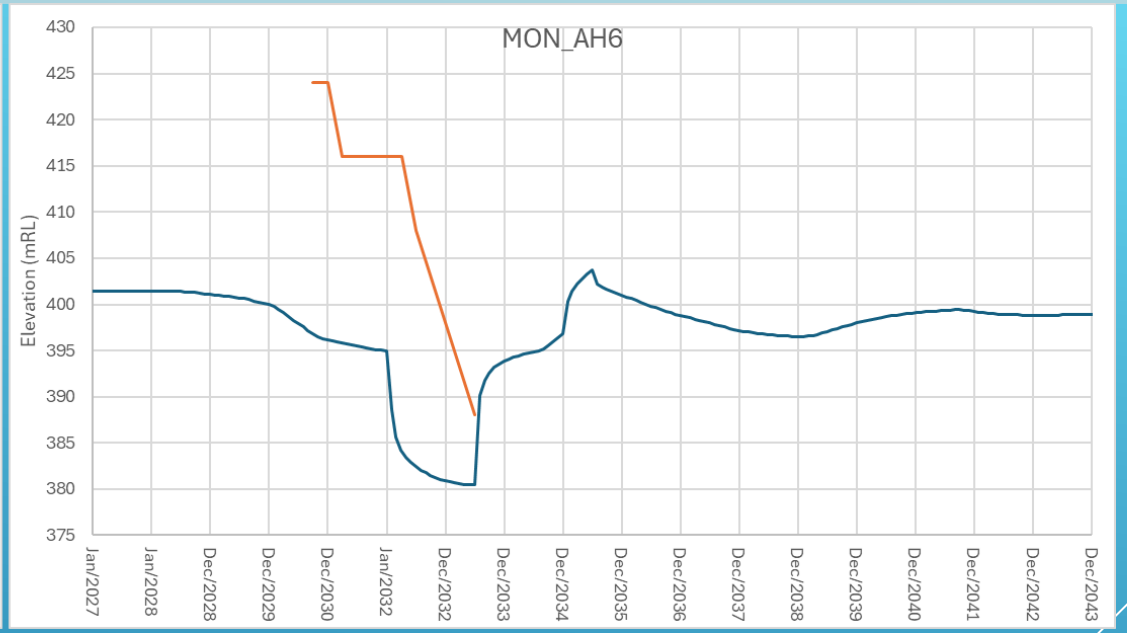

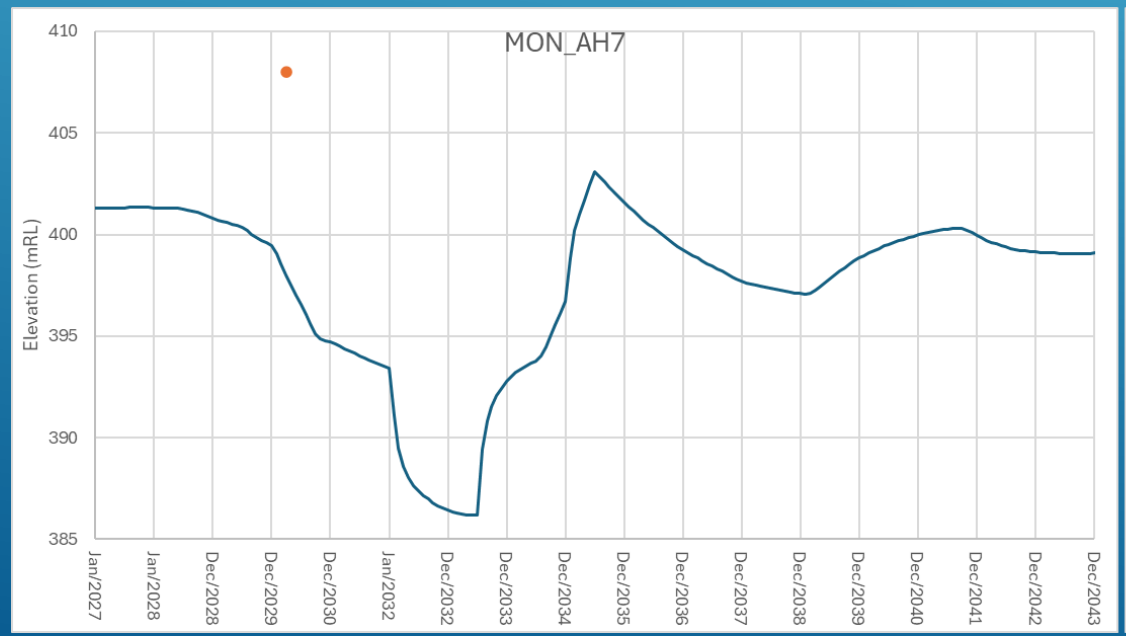

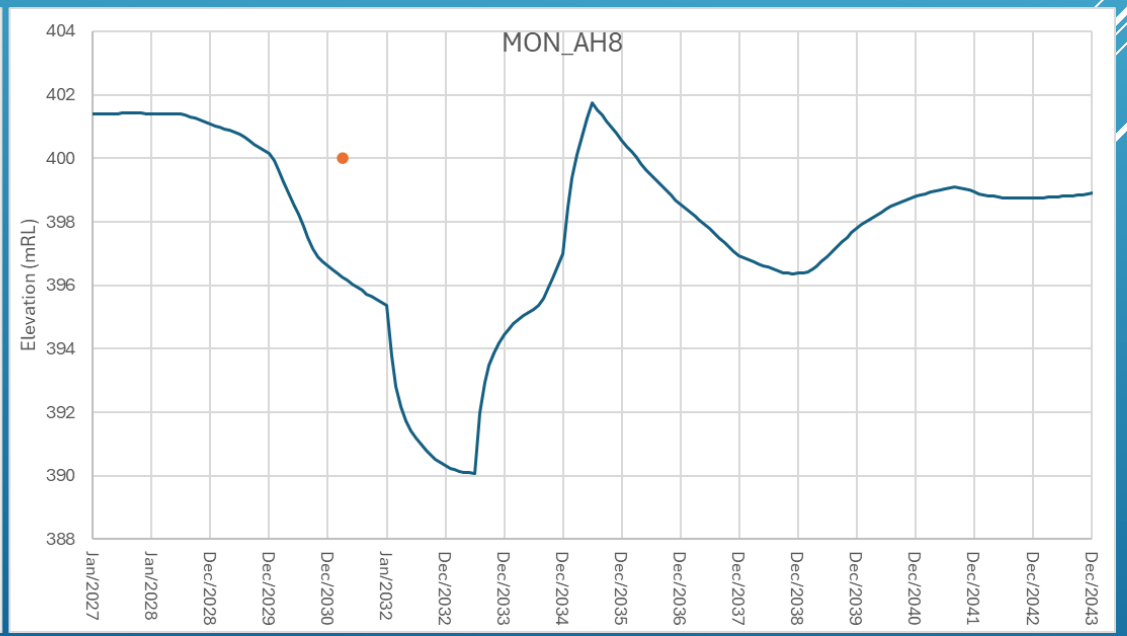

FIGURE A6 - MDE LOM 20 - PREDICTED INPIT WATER LEVELS AT ANTICLINE HILL

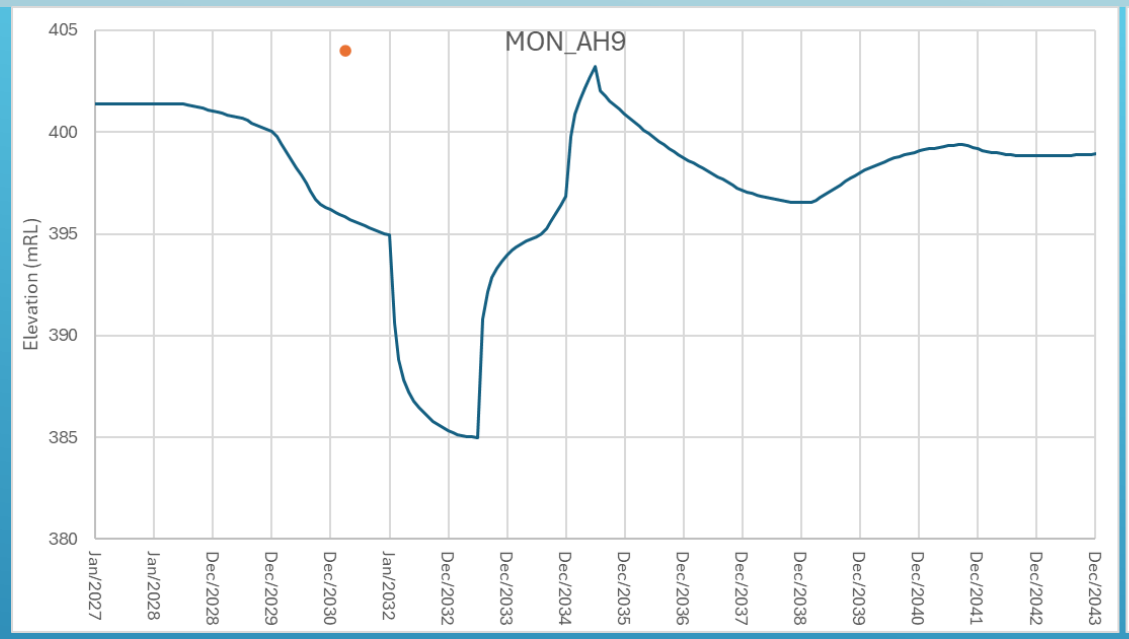

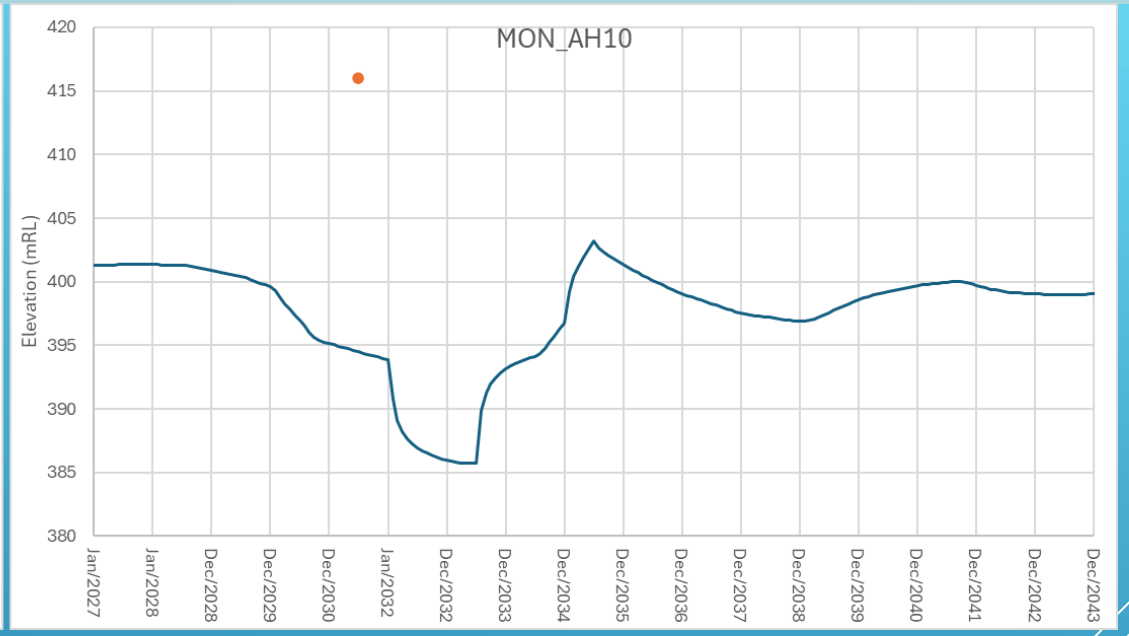

FIGURE A7 - MDE LOM 20 - PREDICTED INPIT WATER LEVELS AT FRIDGE WEST

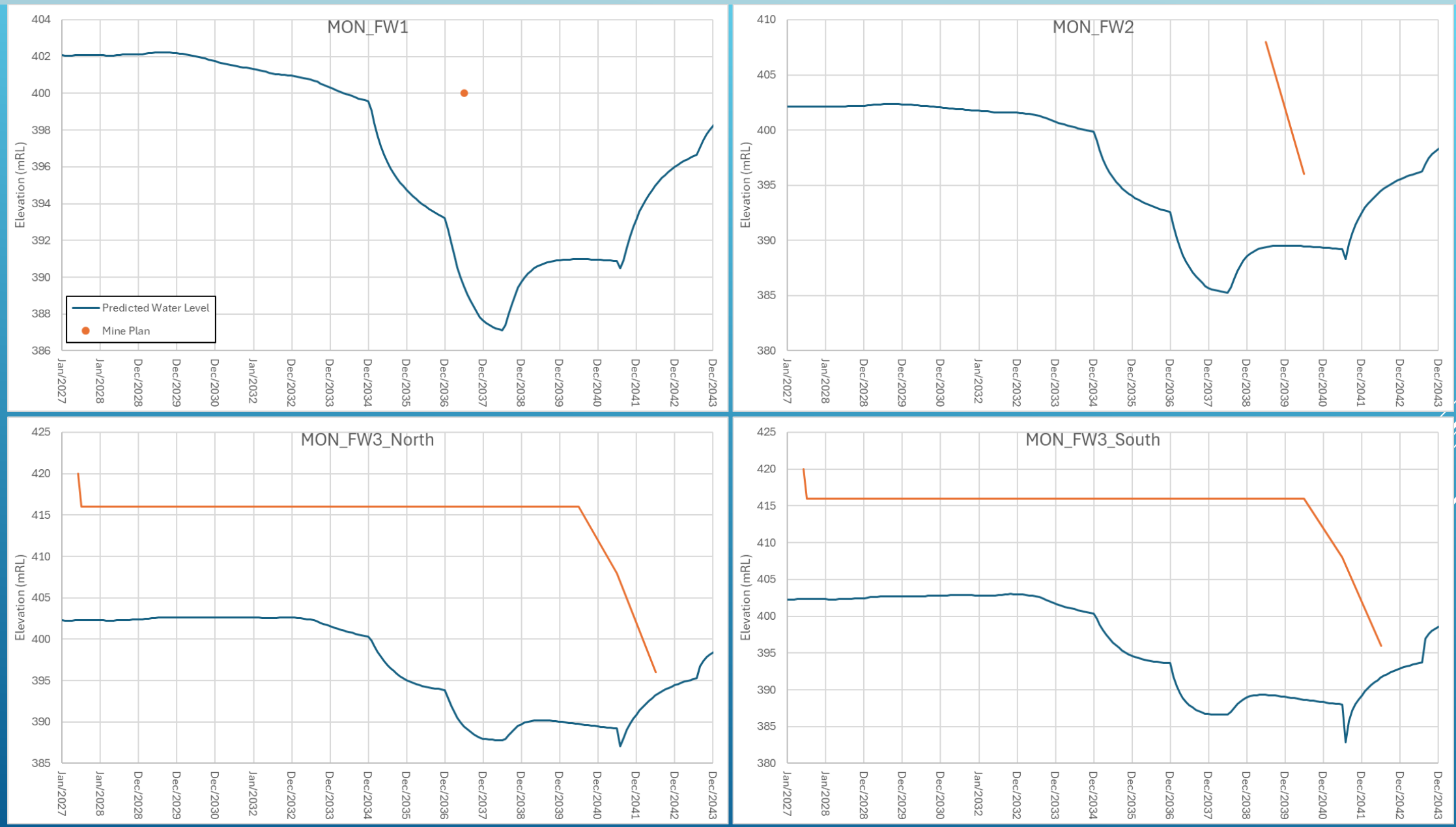

FIGURE A8 - MDE LOM 20 - PREDICTED INPIT WATER LEVELS AT FRIDGE WEST

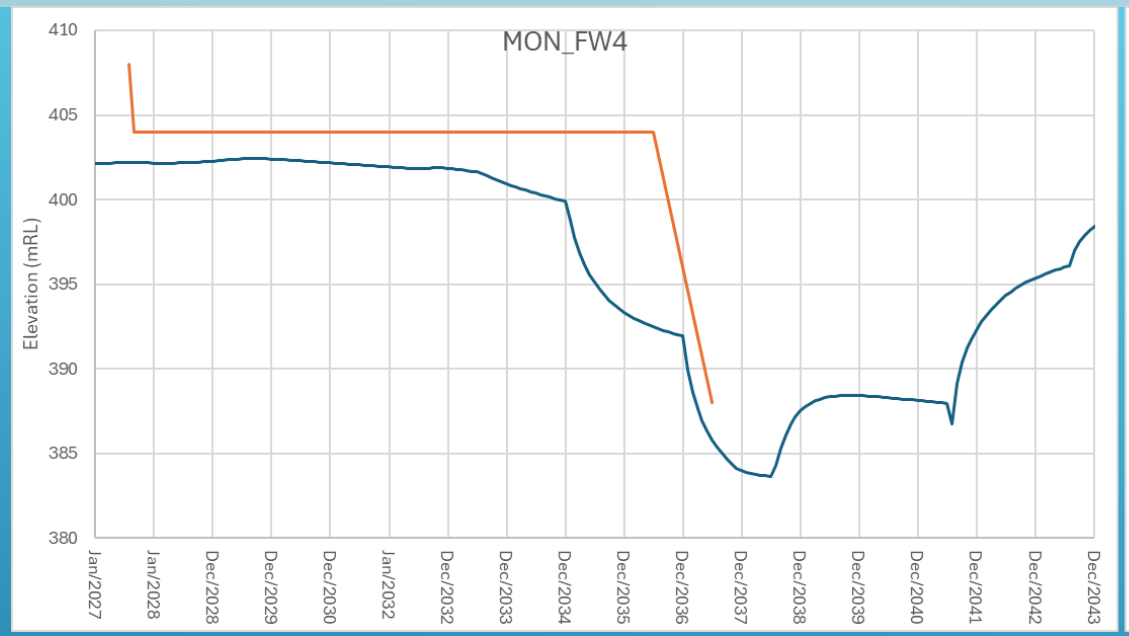

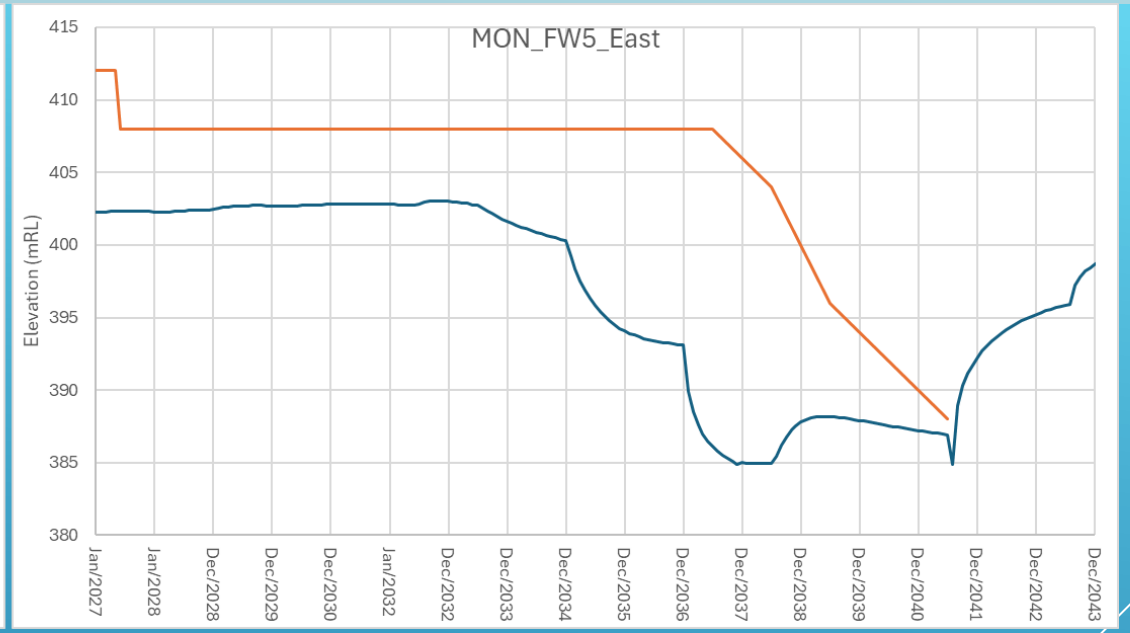

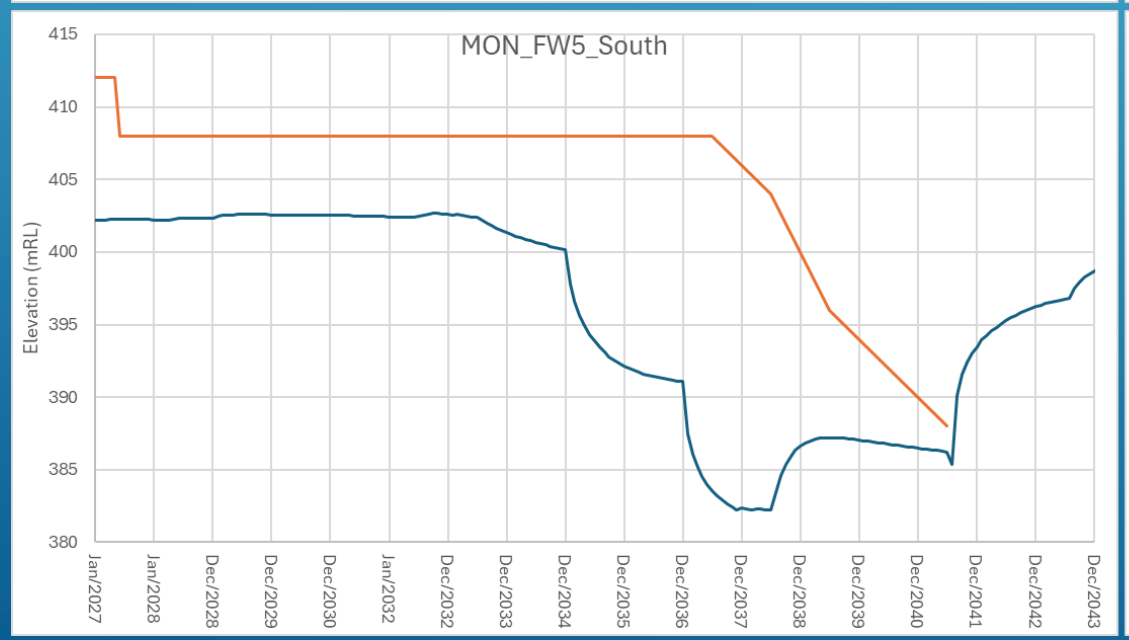

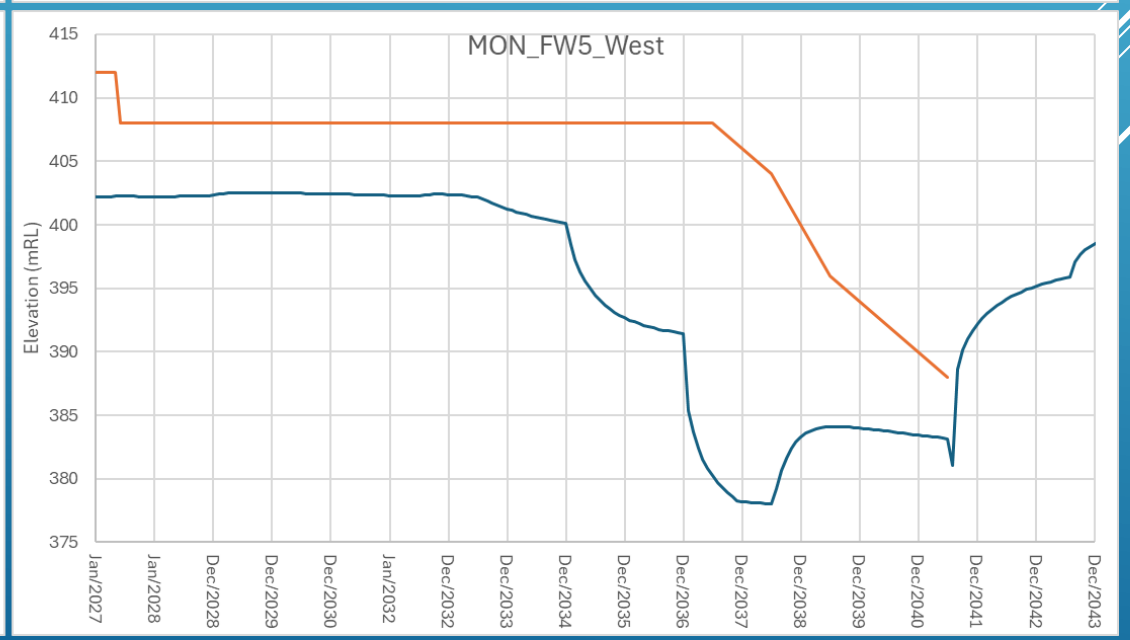

FIGURE A9 - MDE LOM 20 - PREDICTED INPIT WATER LEVELS AT FRIDGE WEST

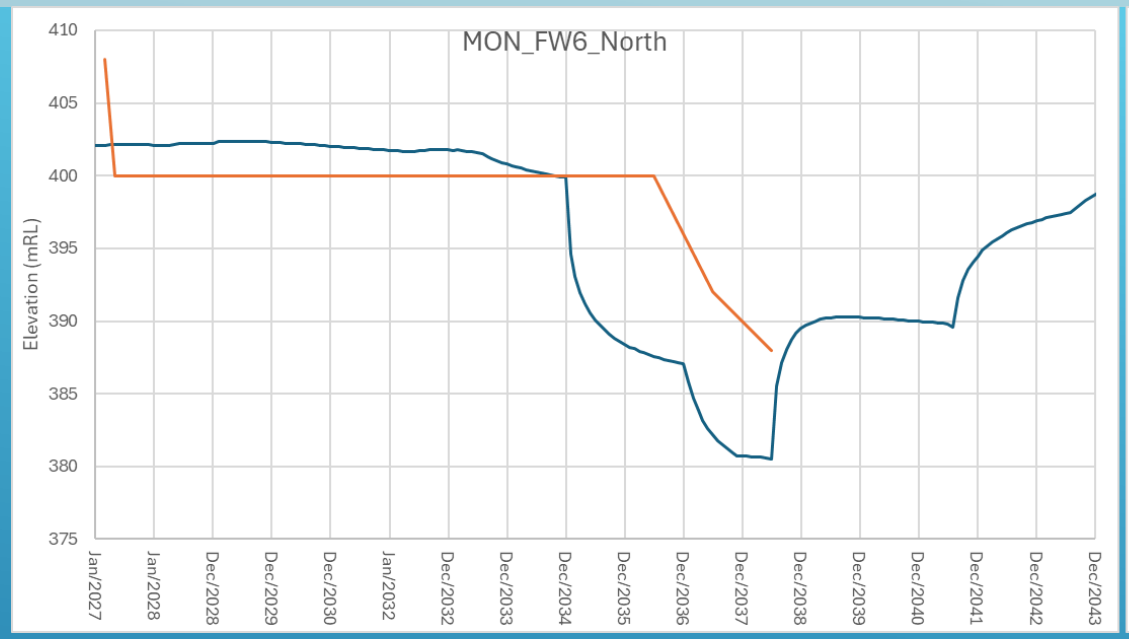

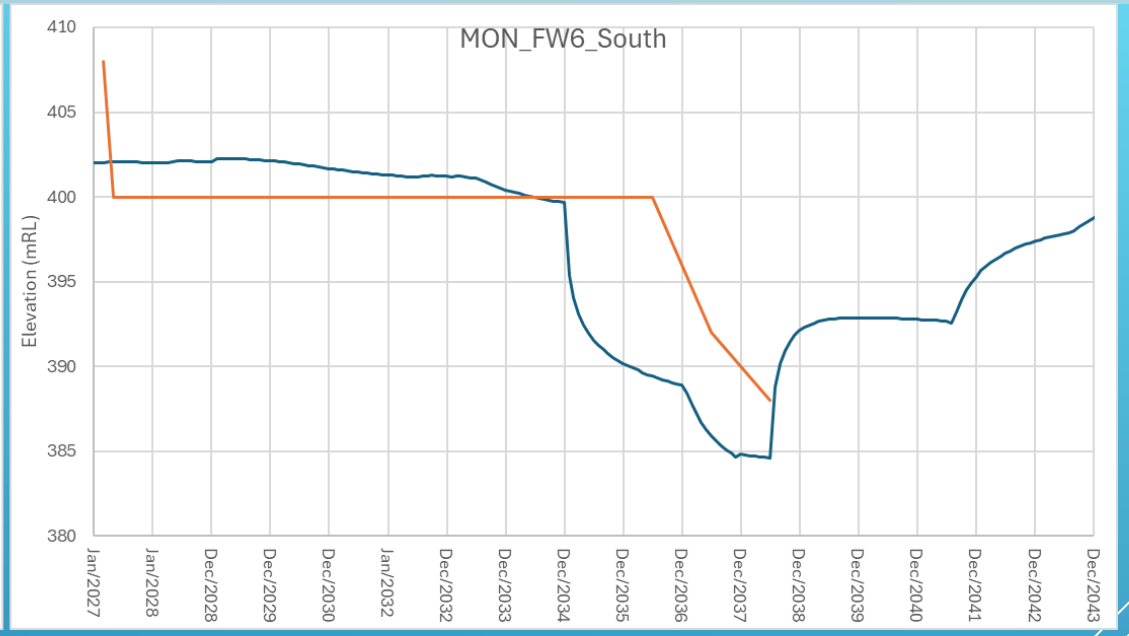

FIGURE A10 - MDE LOM 20 - PREDICTED INPIT WATER LEVELS AT FRIDGE CENTRAL

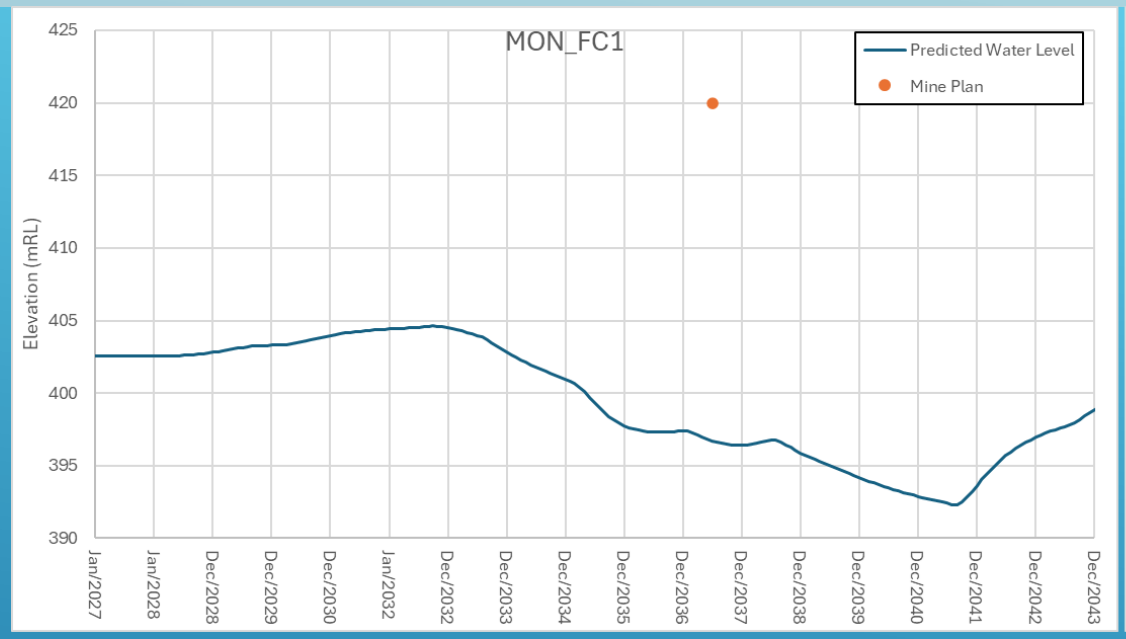

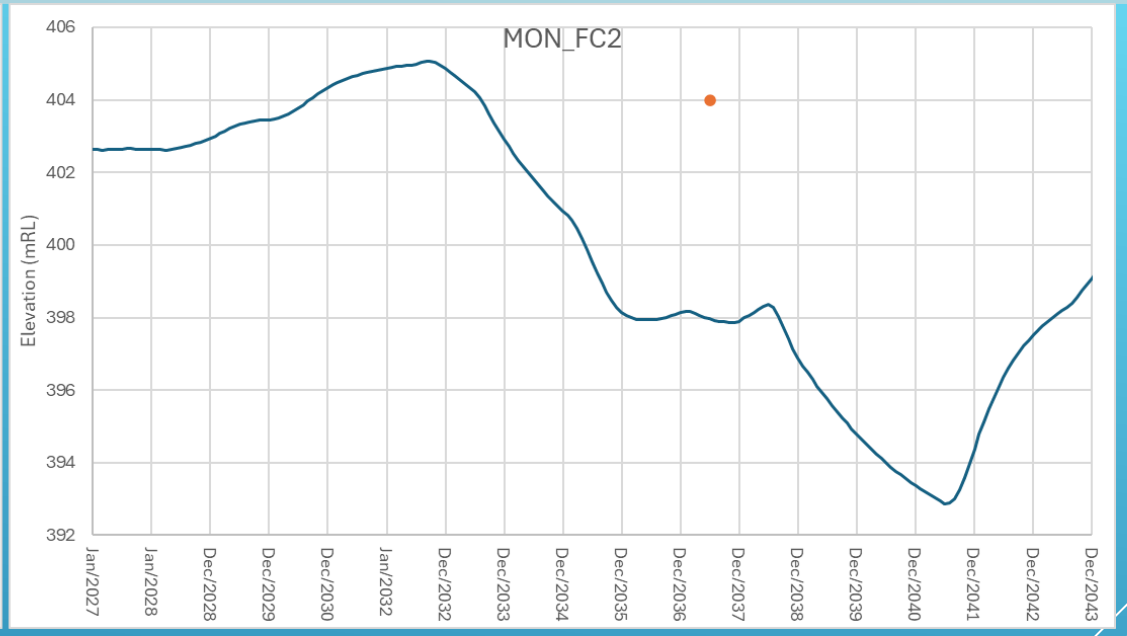

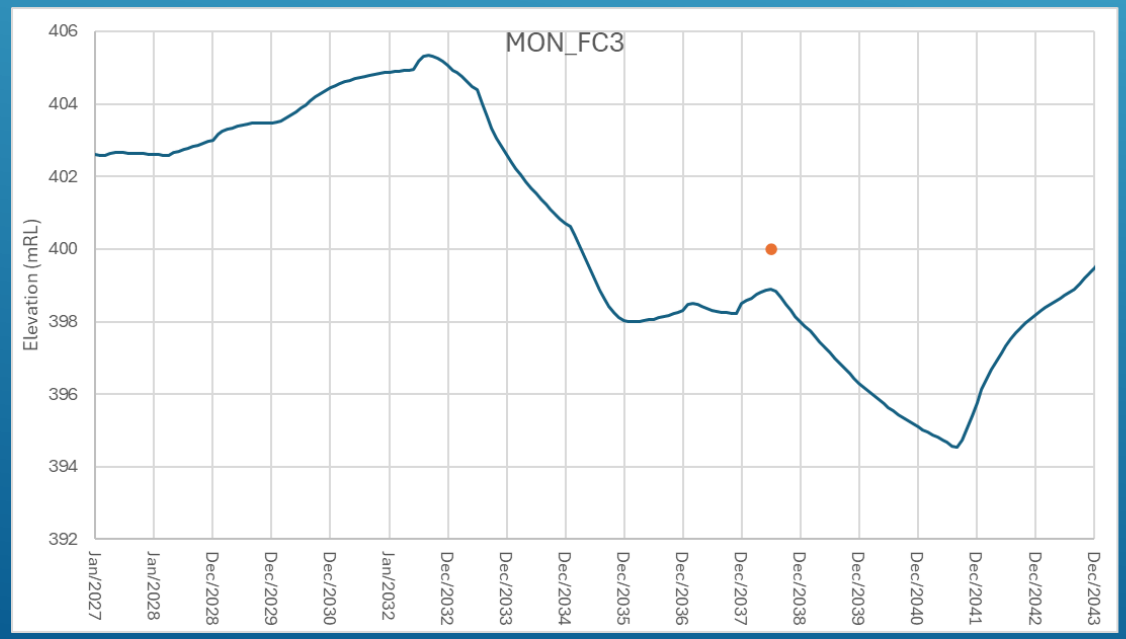

FIGURE A11 - MDE LOM 20 - PREDICTED INPIT WATER LEVELS AT FRIDGE HILL

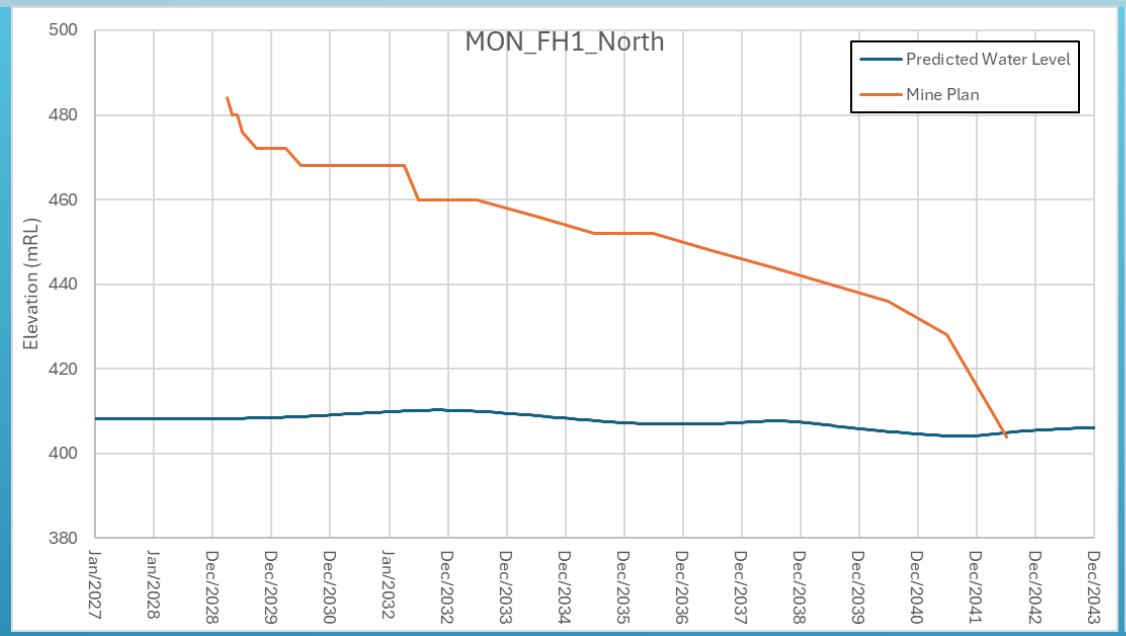

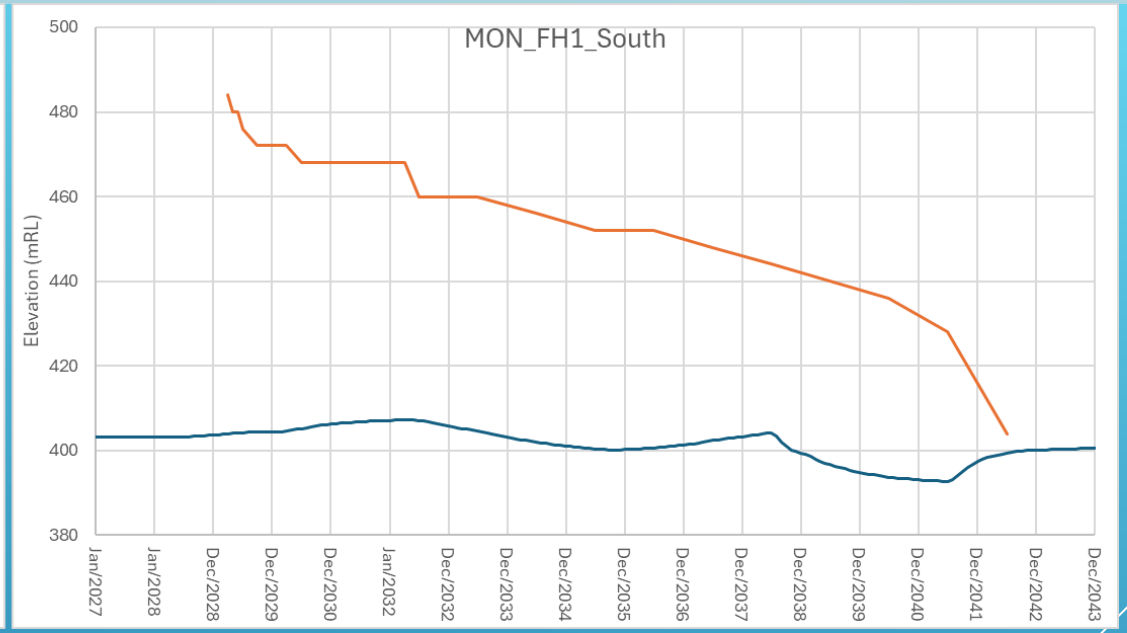

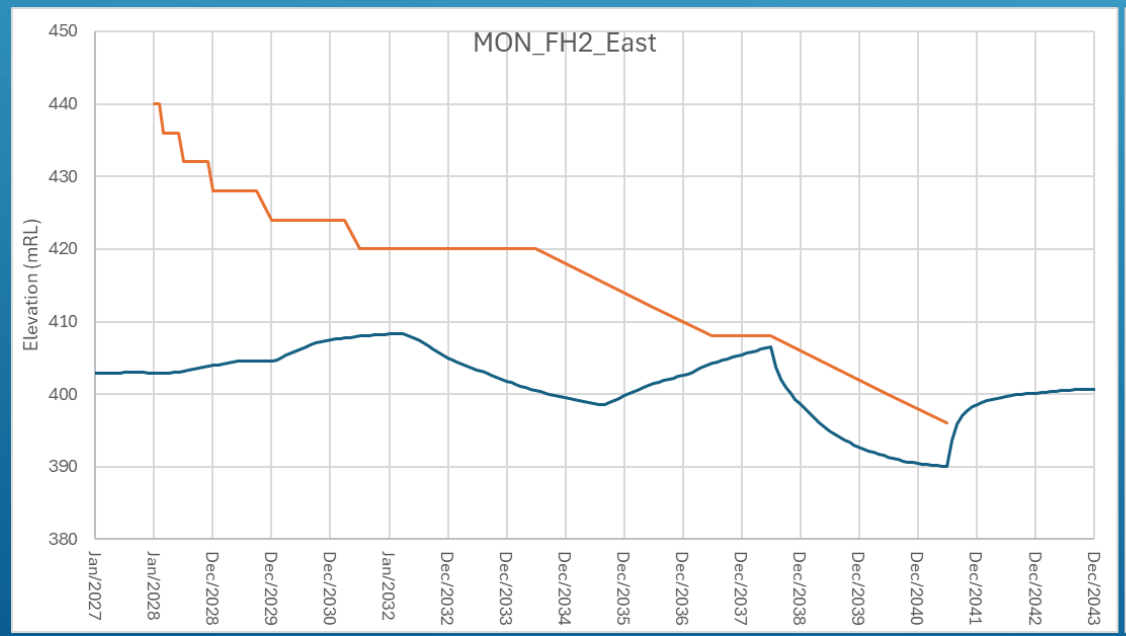

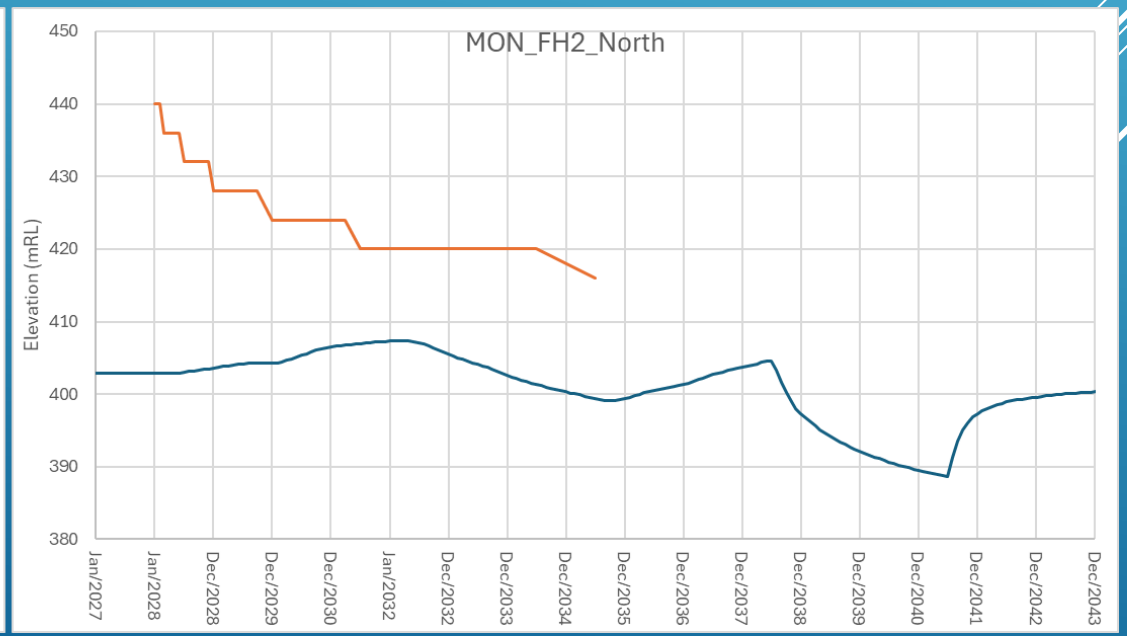

FIGURE A12 - MDE LOM 20 - PREDICTED INPIT WATER LEVELS AT FRIDGE HILL

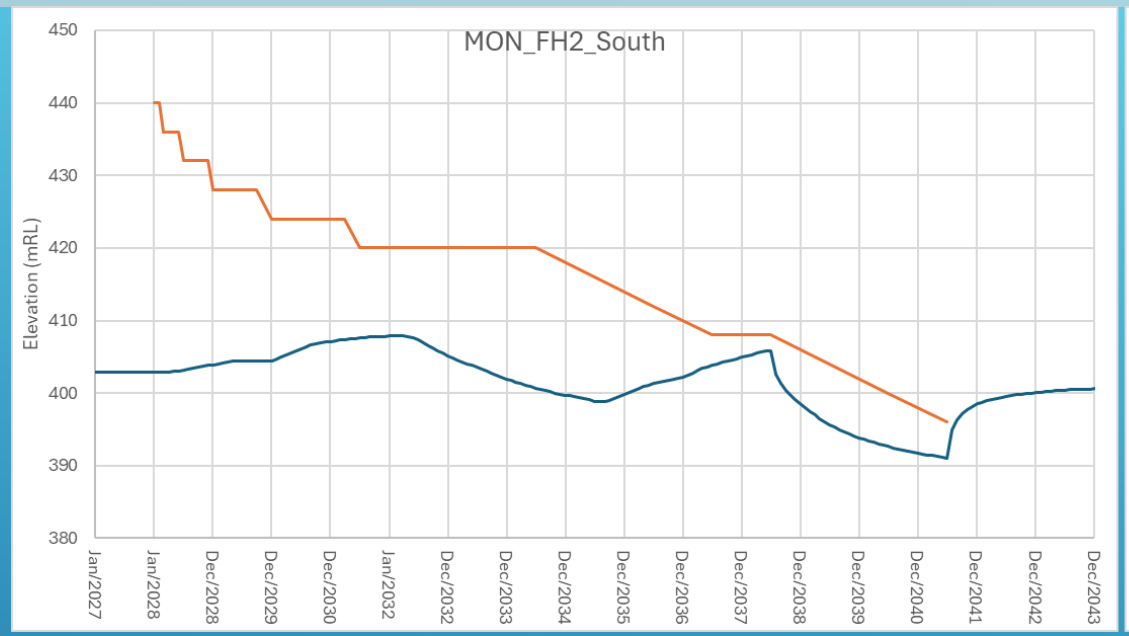

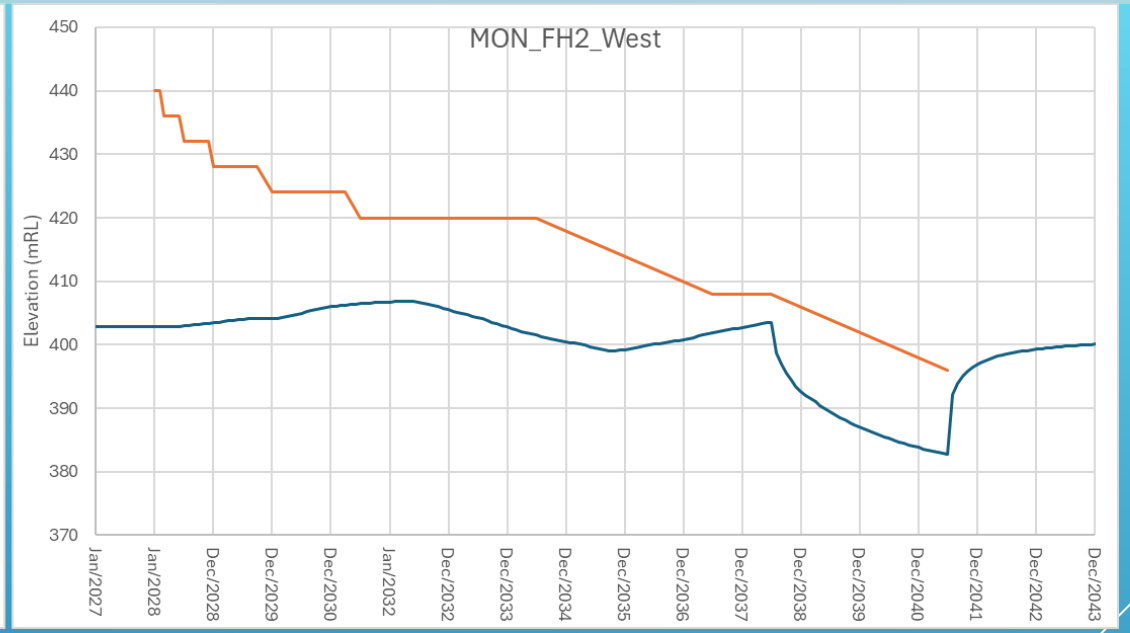

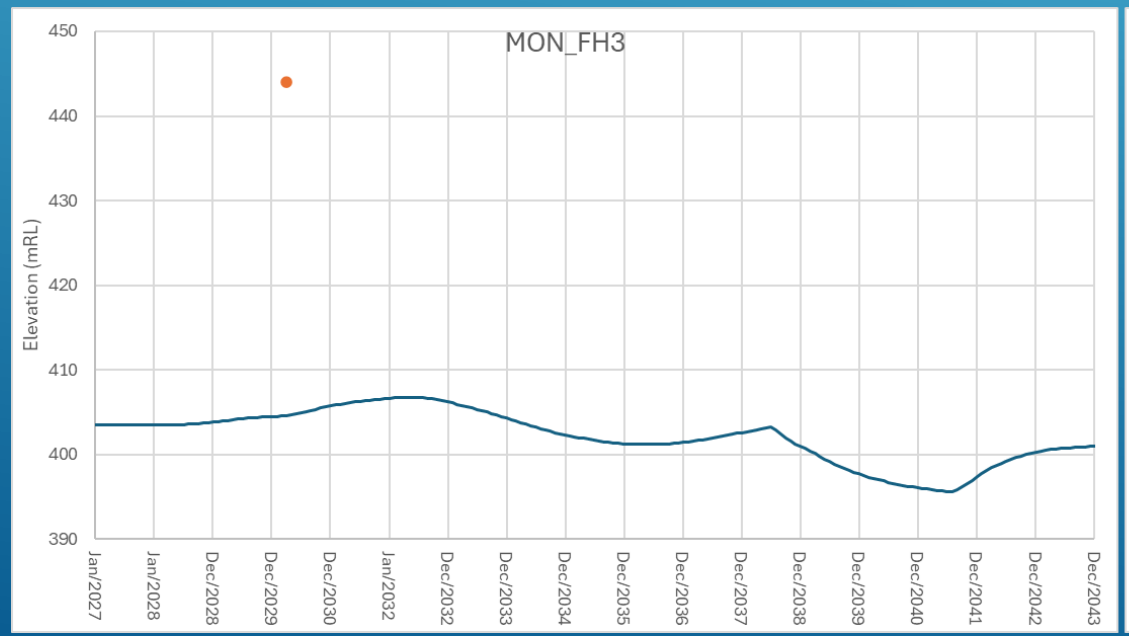

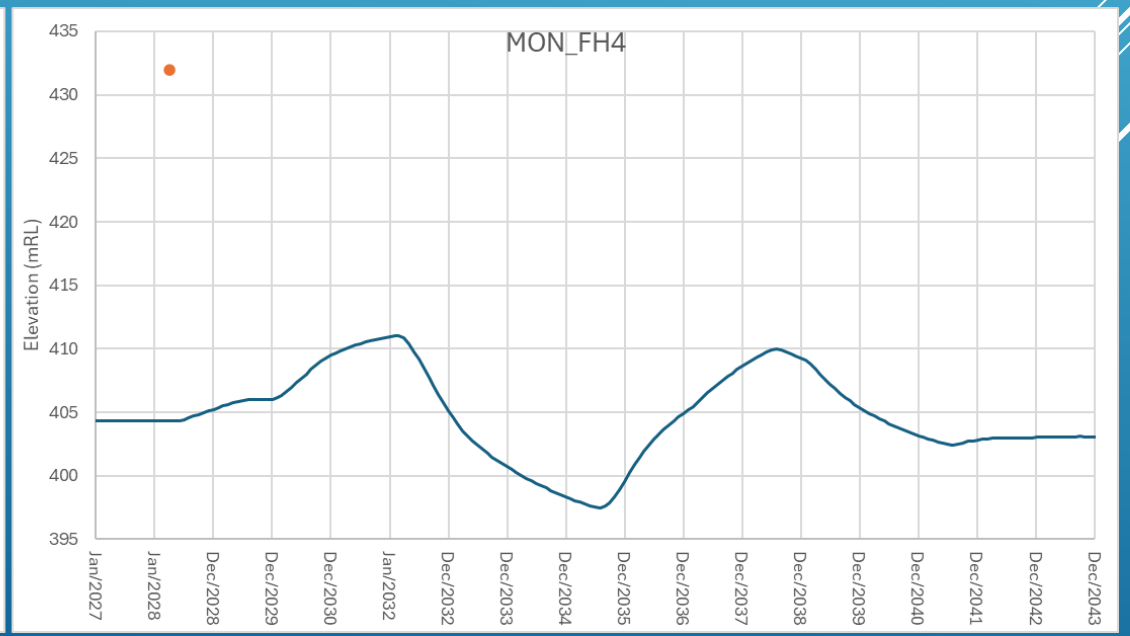

FIGURE A13 - MDE LOM 20 - PREDICTED INPIT WATER LEVELS AT HORSESHOE WEST

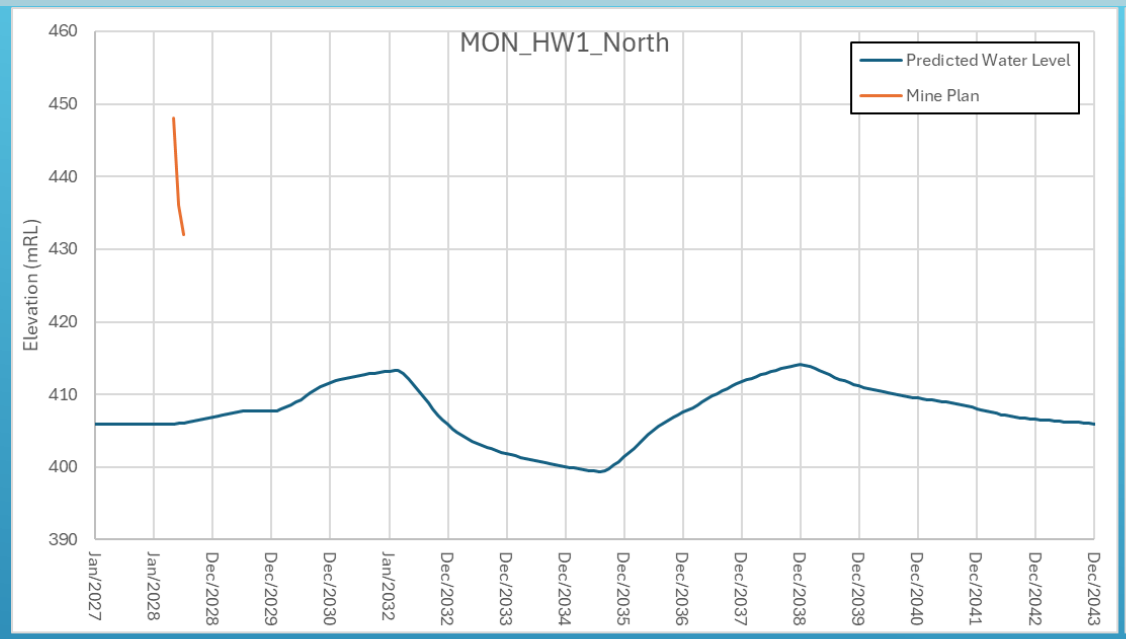

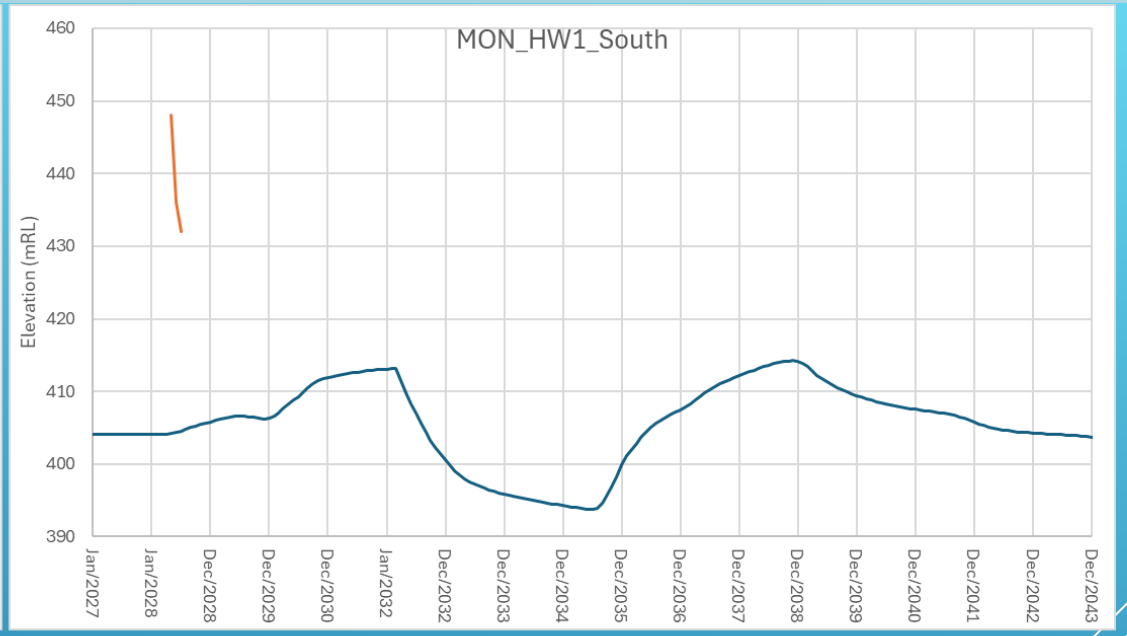

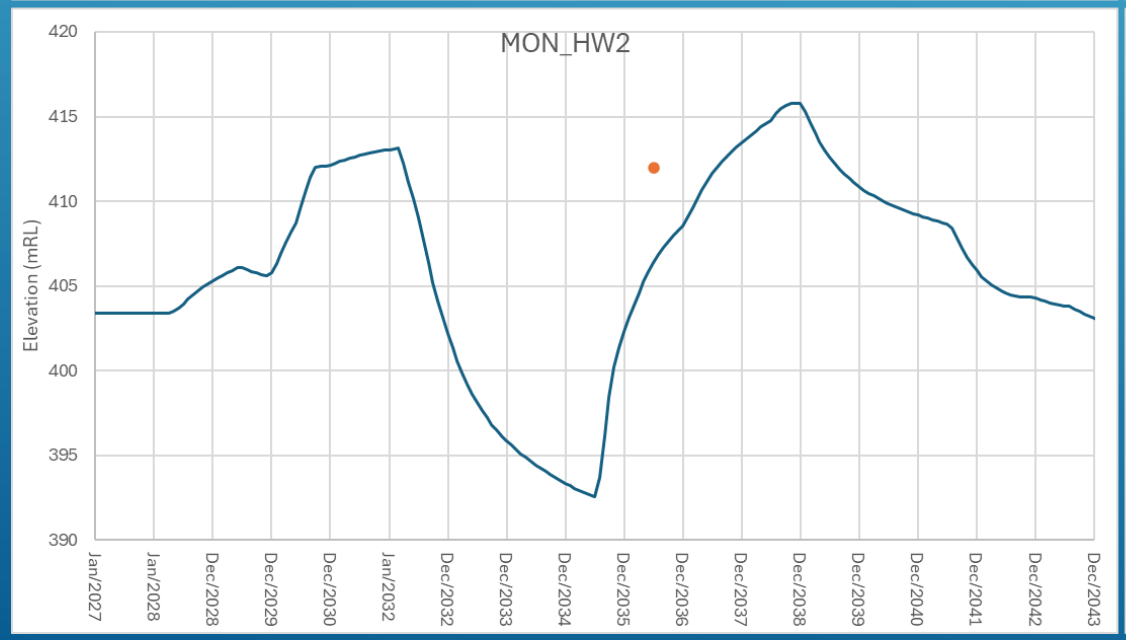

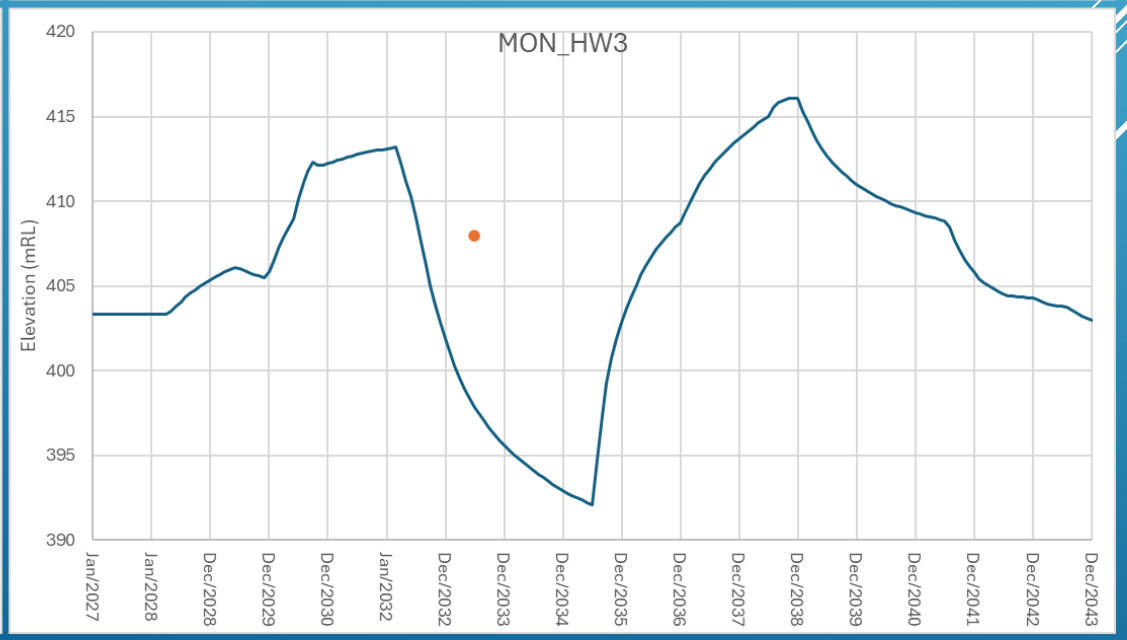

FIGURE A14 - MDE LOM 20 - PREDICTED INPIT WATER LEVELS AT HORSESHOE WEST

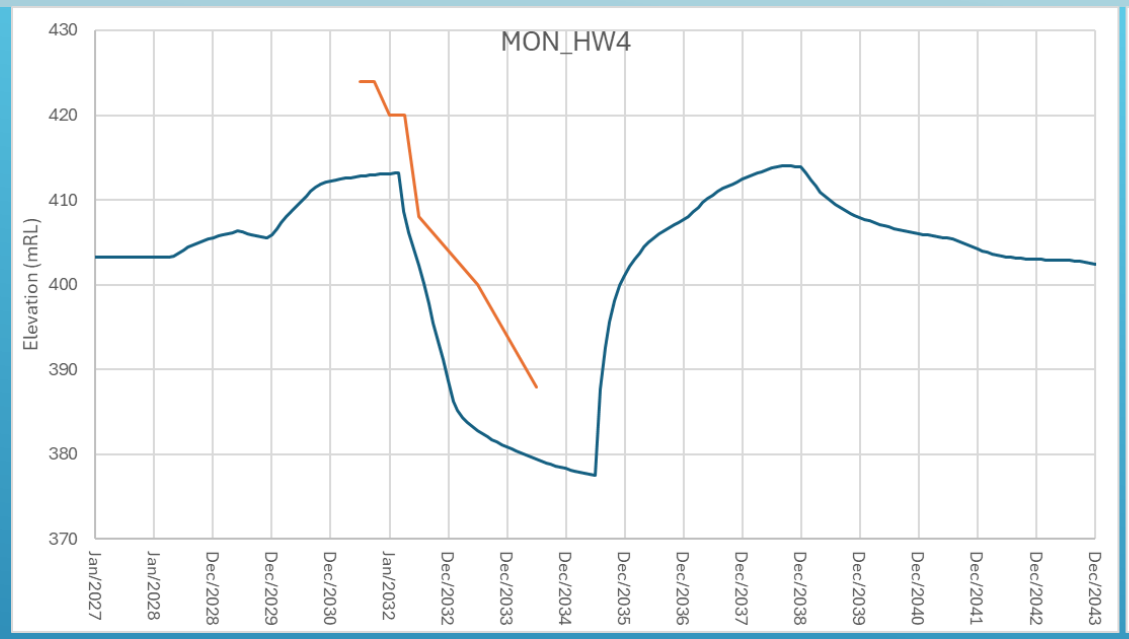

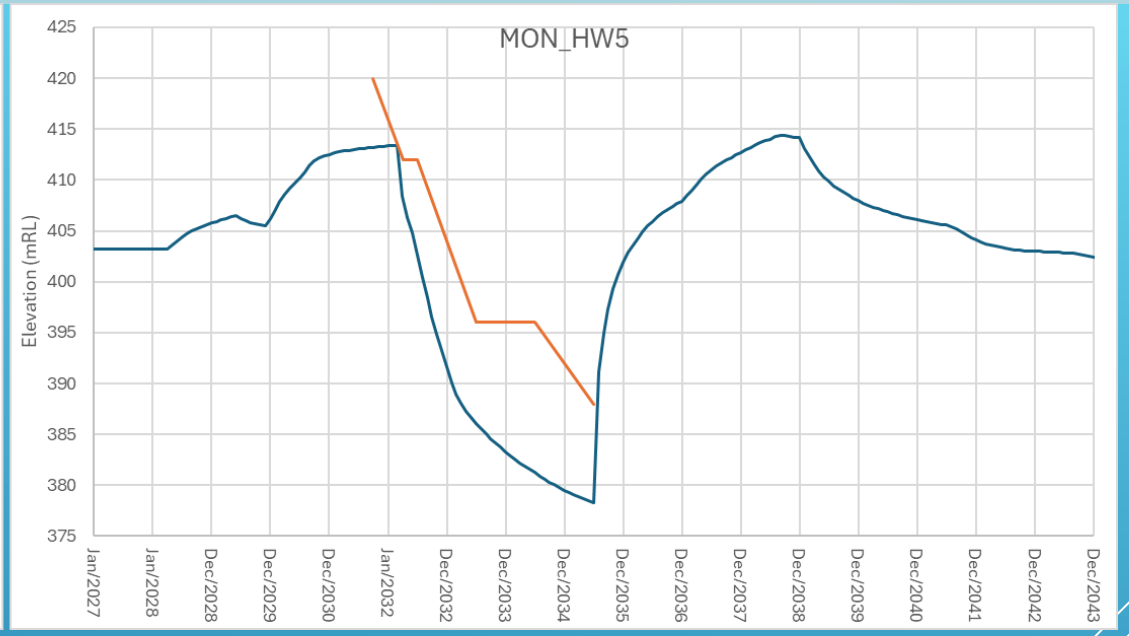

FIGURE A15 - MDE LOM 20 - PREDICTED INPIT WATER LEVELS AT HORSESHOE HILL

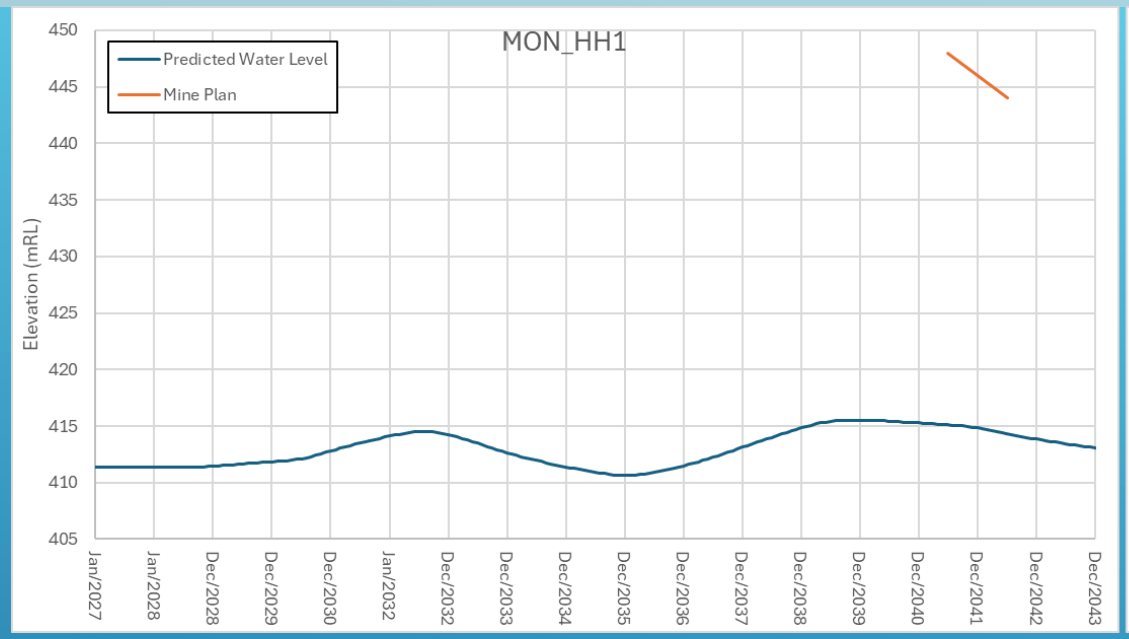

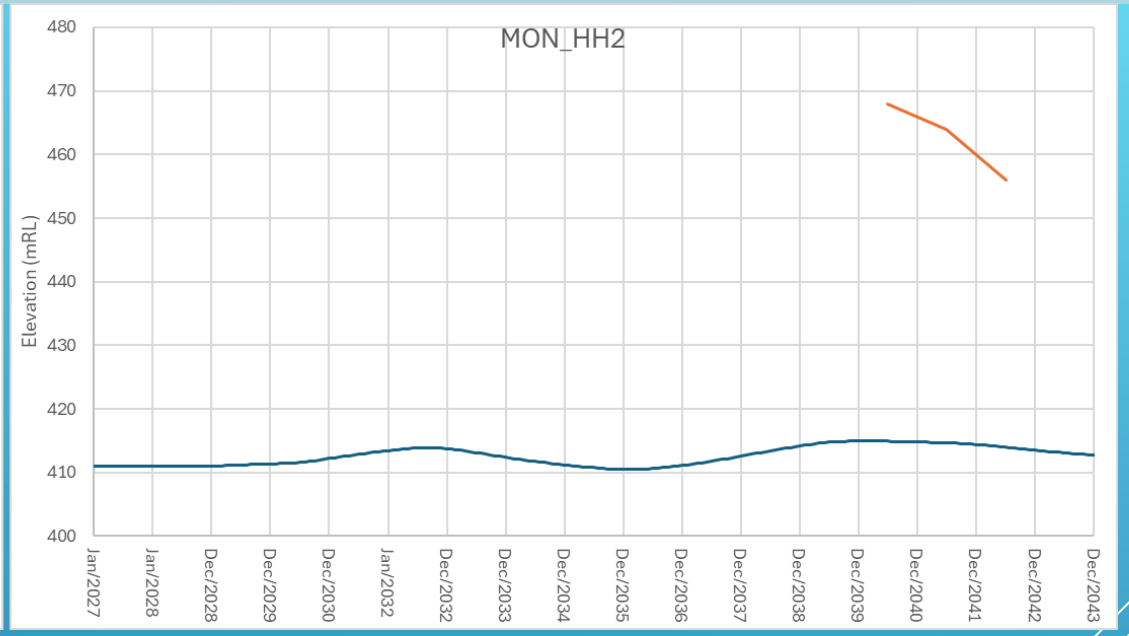

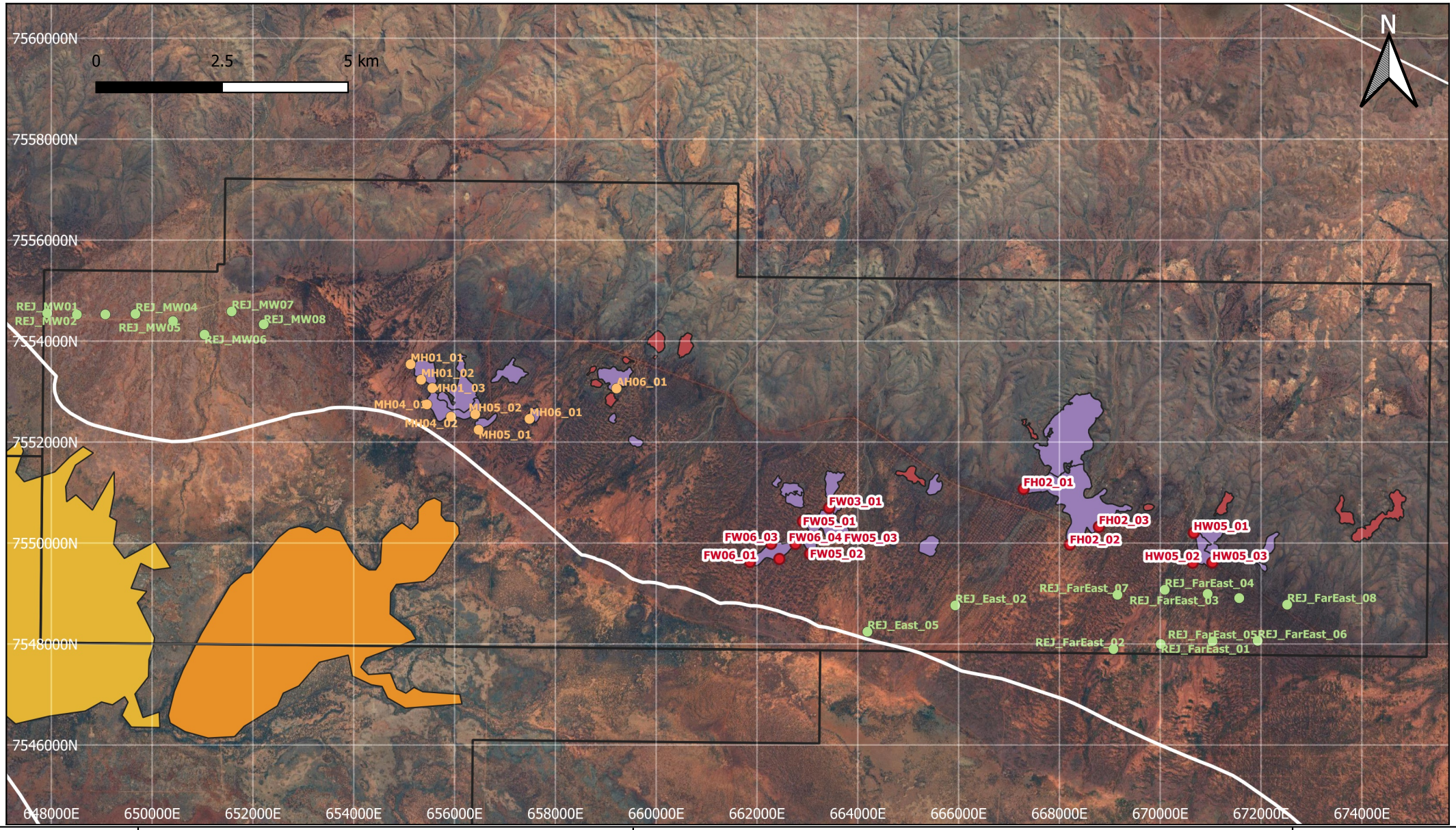

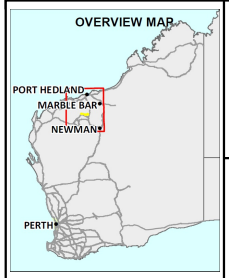

NOTES & DATA SOURCES:
Not for construction
ESPG:28350 (GDA94/MGA zone 50)

AUTHOR: MP
DRAWN: MP
DATE: 29/09/2024

Report NO: GWC-020-2022
REVISION: H
JOB No: 020-2022

Legend

- Pits Above Water Table Pits
- Below Water Table
- MEA Boundary
- Gnalka Gnoona Claypan
- Koodjeepindarranna Claypan
- Tenement Boundary
- Dewatering Bore
- Dewatering Bore Converted to MAR Bore
- MAR Bore

Figure A16

Simulated Dewatering and MAR Bores

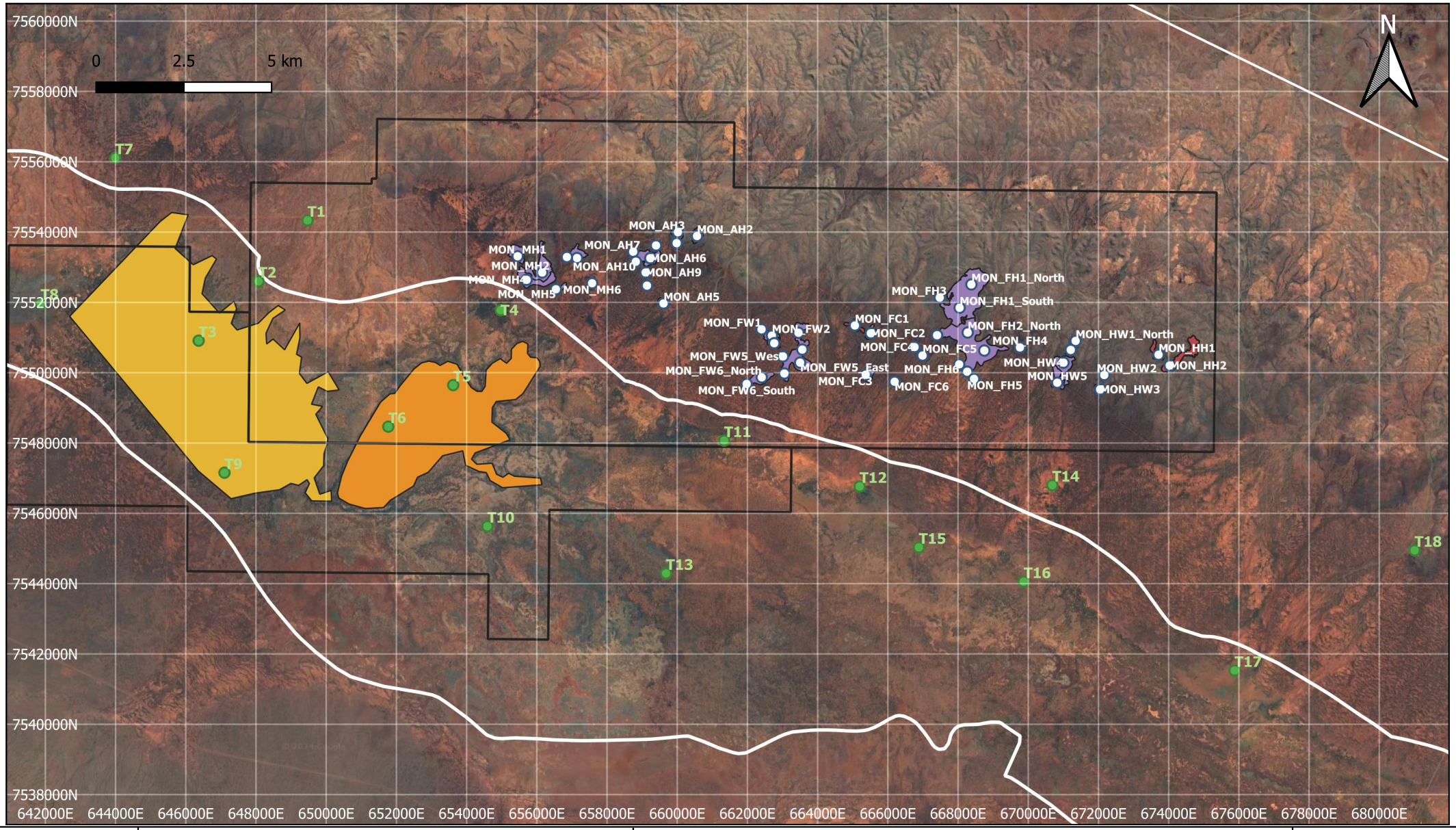

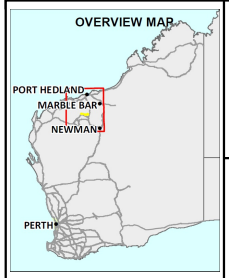

NOTES & DATA SOURCES:
Not for construction
ESPG:28350 (GDA94/MGA zone 50)

AUTHOR: MP
DRAWN: MP
DATE: 29/09/2024

Report NO: GWC-020-2022
REVISION: H
JOB No: 020-2022

Legend

- Pits Above Water Table
- Pits Below Water Table
- MEA Boundary
- Gnalka Gnoona Claypan
- Koodjeepindarranna Claypan
- Tenement Boundary
- Nominal Monitoring Enviro Point
- Nominal Pit Monitoring Bore

Figure A17

Simulated Monitoring Bores

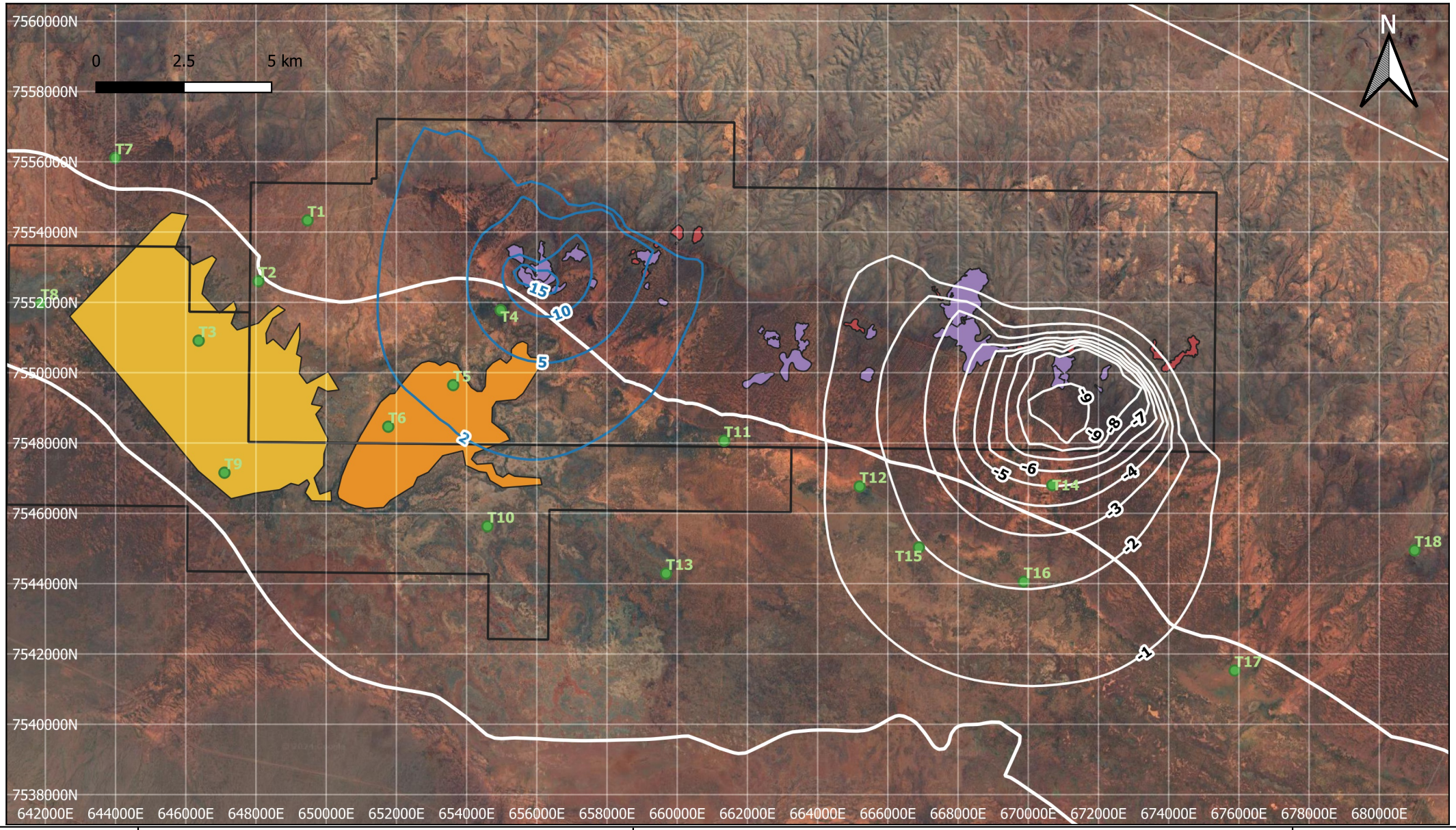

OVERVIEW MAP

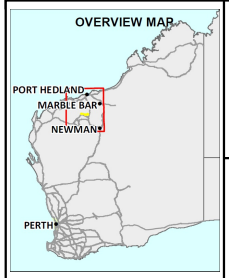

NOTES & DATA SOURCES:
Not for construction
ESPG:28350 (GDA94/MGA zone 50)

AUTHOR: MP
DRAWN: MP
DATE: 29/09/2024

Report NO: GWC-020-2022
REVISION: H
JOB No: 020-2022

Legend

- Pits Above Water Table
- Pits Below Water Table
- MEA Boundary
- Gnalka Gnoona Claypan
- Koodjeepindarranna Claypan
- Tenement Boundary
- Nominal Monitoring Enviro Point
- Predicted Drawdown (m)
- Predicted Mounding (m)

Figure A18

Predicted Drawdown in October 2030

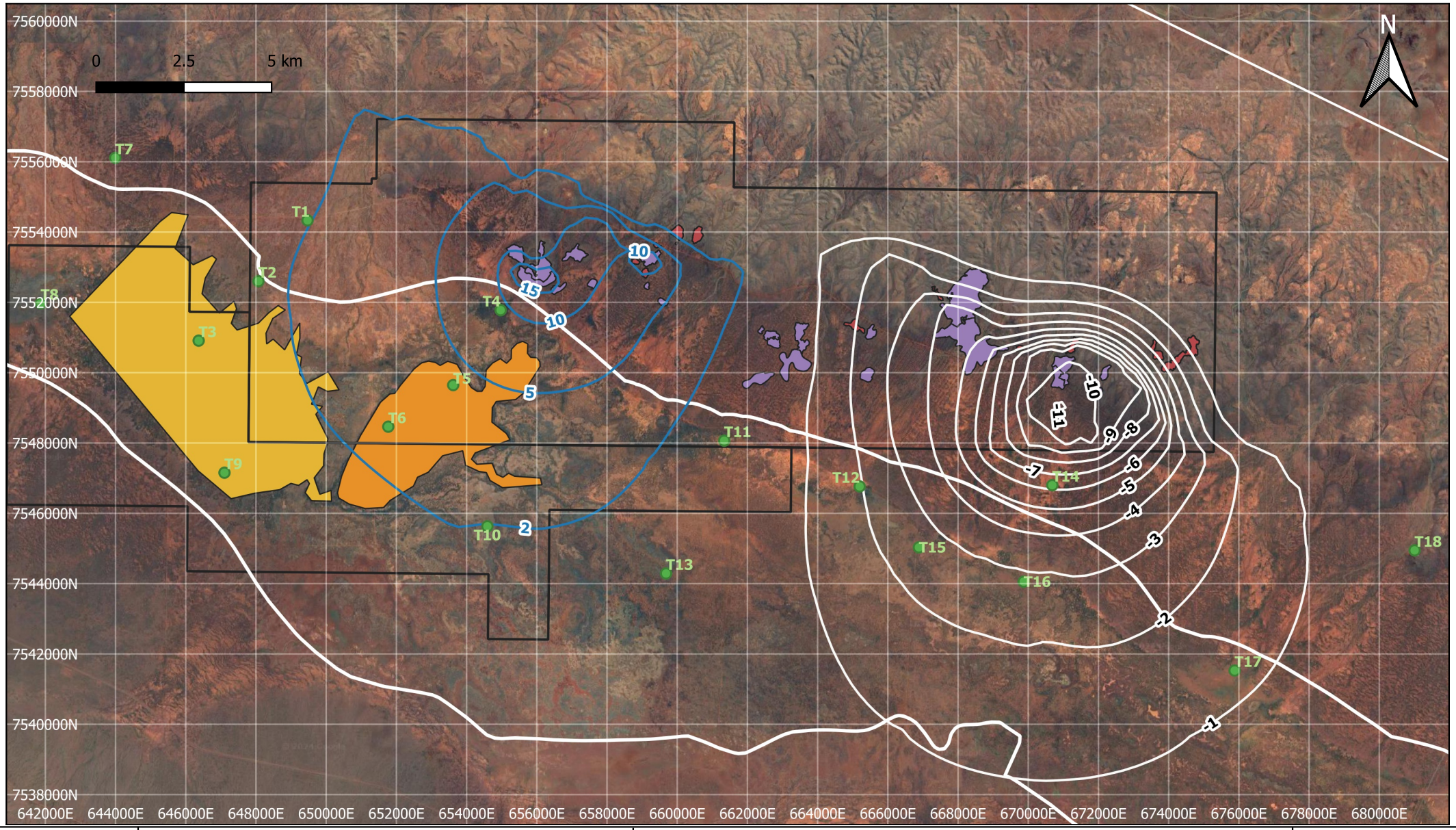

OVERVIEW MAP

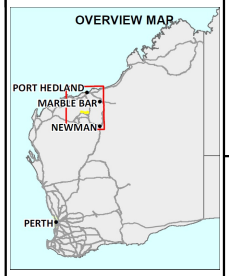

NOTES & DATA SOURCES:
Not for construction
ESPG:28350 (GDA94/MGA zone 50)

AUTHOR: MP
DRAWN: MP
DATE: 29/09/2024

Report NO: GWC-020-2022
REVISION: H
JOB No: 020-2022

Legend

- Pits Above Water Table
- Pits Below Water Table
- MEA Boundary
- Gnalka Gnoona Claypan
- Koodjeepindarranna Claypan
- Tenement Boundary
- Nominal Monitoring Enviro Point
- Predicted Drawdown (m)
- Predicted Mounding (m)

Figure A19

Predicted Drawdown in January 2032

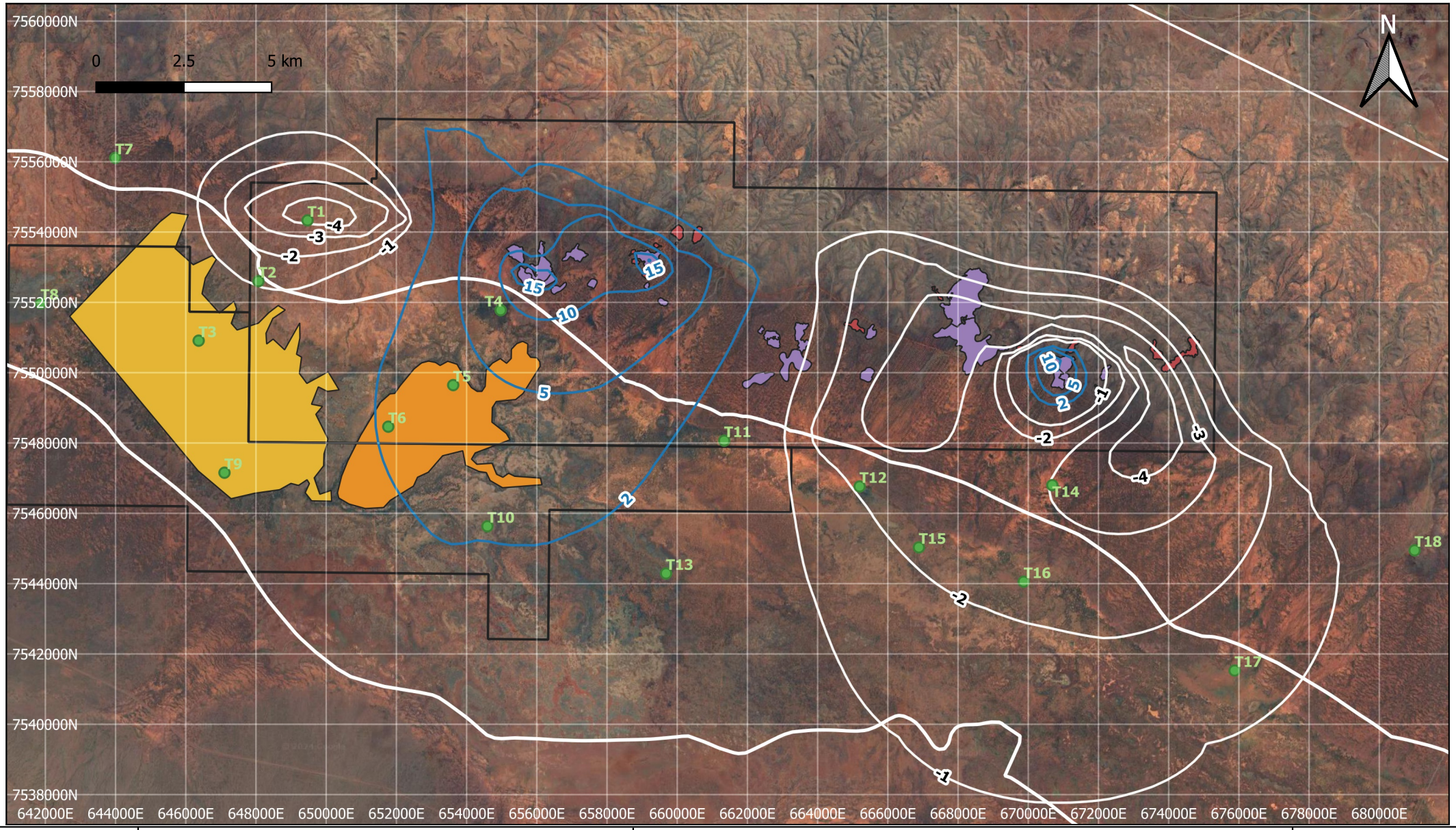

OVERVIEW MAP

PORT HEDLAND
MARBLE BAR
NEWMAN
PERTH

NOTES & DATA SOURCES:
Not for construction
ESPG:28350 (GDA94/MGA zone 50)

AUTHOR: MP
DRAWN: MP
DATE: 29/09/2024

Report NO: GWC-020-2022
REVISION: H
JOB No: 020-2022

Legend

- Pits Above Water Table
- Pits Below Water Table
- MEA Boundary
- Gnalka Gnoona Claypan
- Koodjeepindarranna Claypan
- Tenement Boundary
- Nominal Monitoring Enviro Point
- Predicted Drawdown (m)
- Predicted Mounding (m)

Figure A20

Predicted Drawdown in October 2032

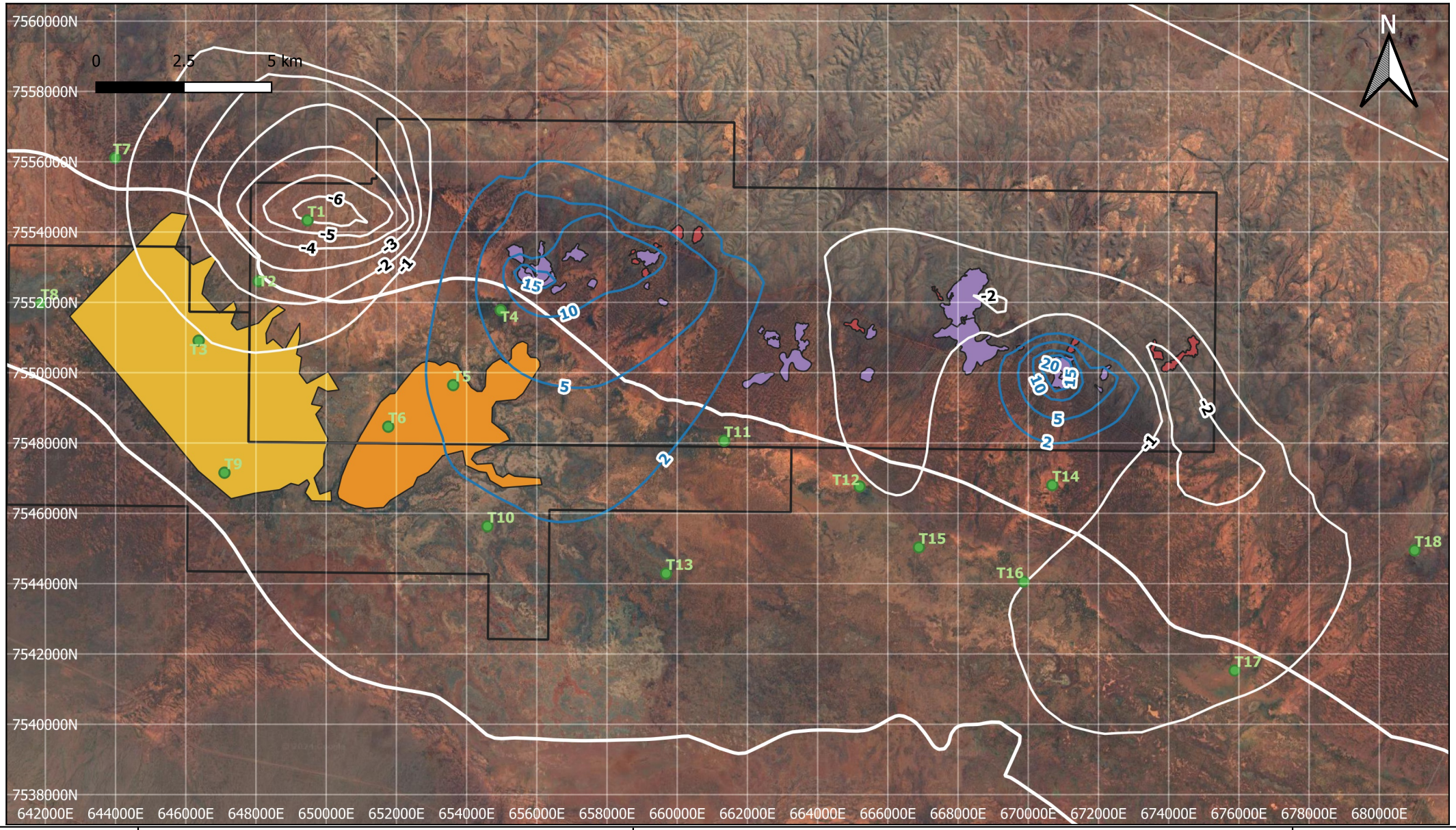

NOTES & DATA SOURCES:
Not for construction
ESPG:28350 (GDA94/MGA zone 50)

AUTHOR: MP
DRAWN: MP
DATE: 29/09/2024

Report NO: GWC-020-2022
REVISION: H
JOB No: 020-2022

Legend

- Pits Above Water Table
- Pits Below Water Table
- MEA Boundary
- Gnalka Gnoona Claypan
- Koodjeepindarranna Claypan
- Tenement Boundary
- Nominal Monitoring Enviro Point
- Predicted Drawdown (m)
- Predicted Mounding (m)

Figure A21

Predicted Drawdown in July 2033

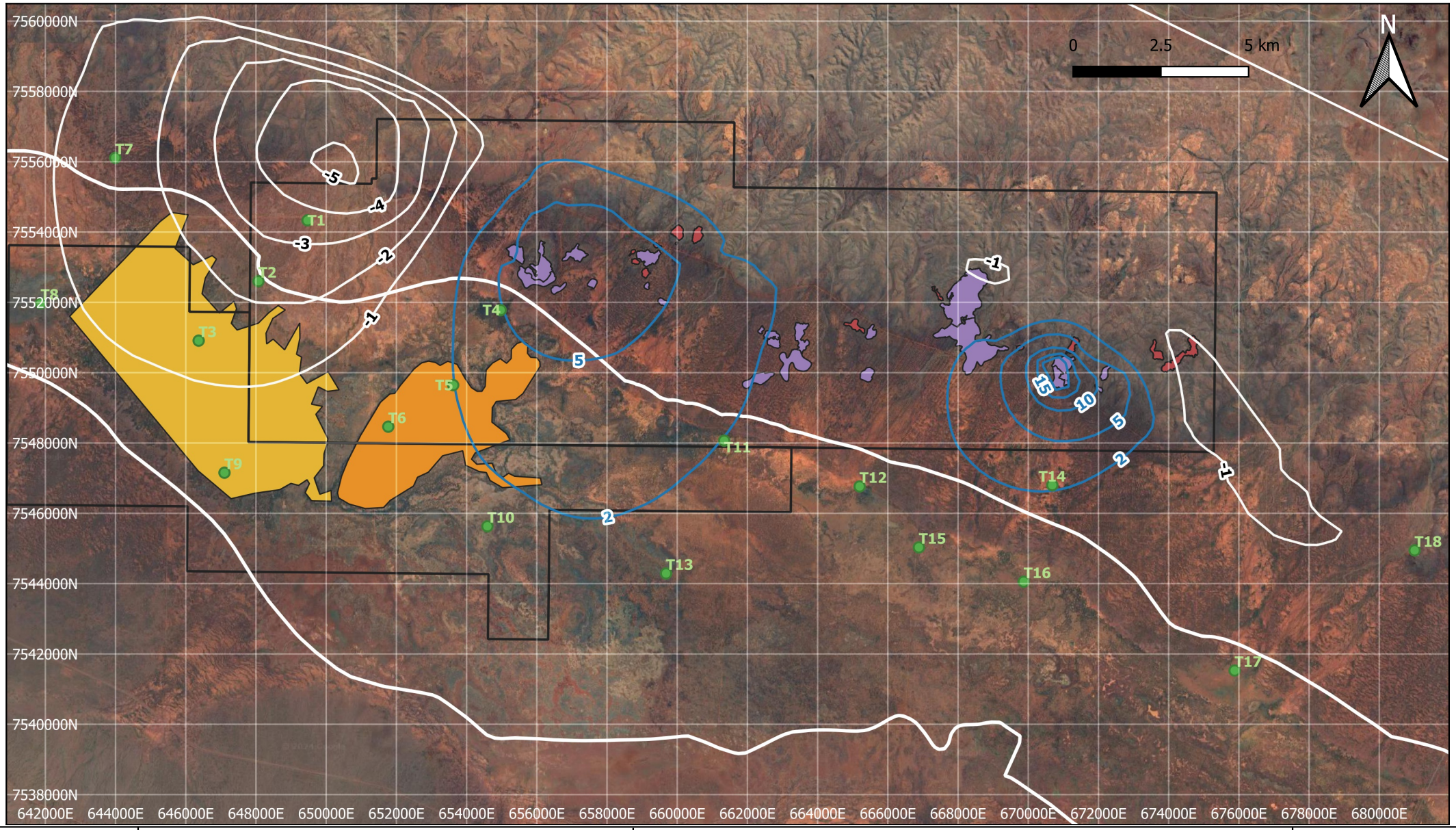

OVERVIEW MAP

PORT HEDLAND
MARBLE BAR
NEWMAN
PERTH

NOTES & DATA SOURCES:

Not for construction
ESPG:28350 (GDA94/MGA zone 50)

AUTHOR: MP
DRAWN: MP
DATE: 29/09/2024

Report NO: GWC-020-2022
REVISION: H
JOB No: 020-2022

Legend

- Pits Above Water Table
- Pits Below Water Table
- MEA Boundary
- Gnalka Gnoona Claypan
- Koodjeepindarranna Claypan
- Tenement Boundary
- Nominal Monitoring Enviro Point
- Predicted Drawdown (m)
- Predicted Mounding (m)

Figure A22

Predicted Drawdown in July 2034

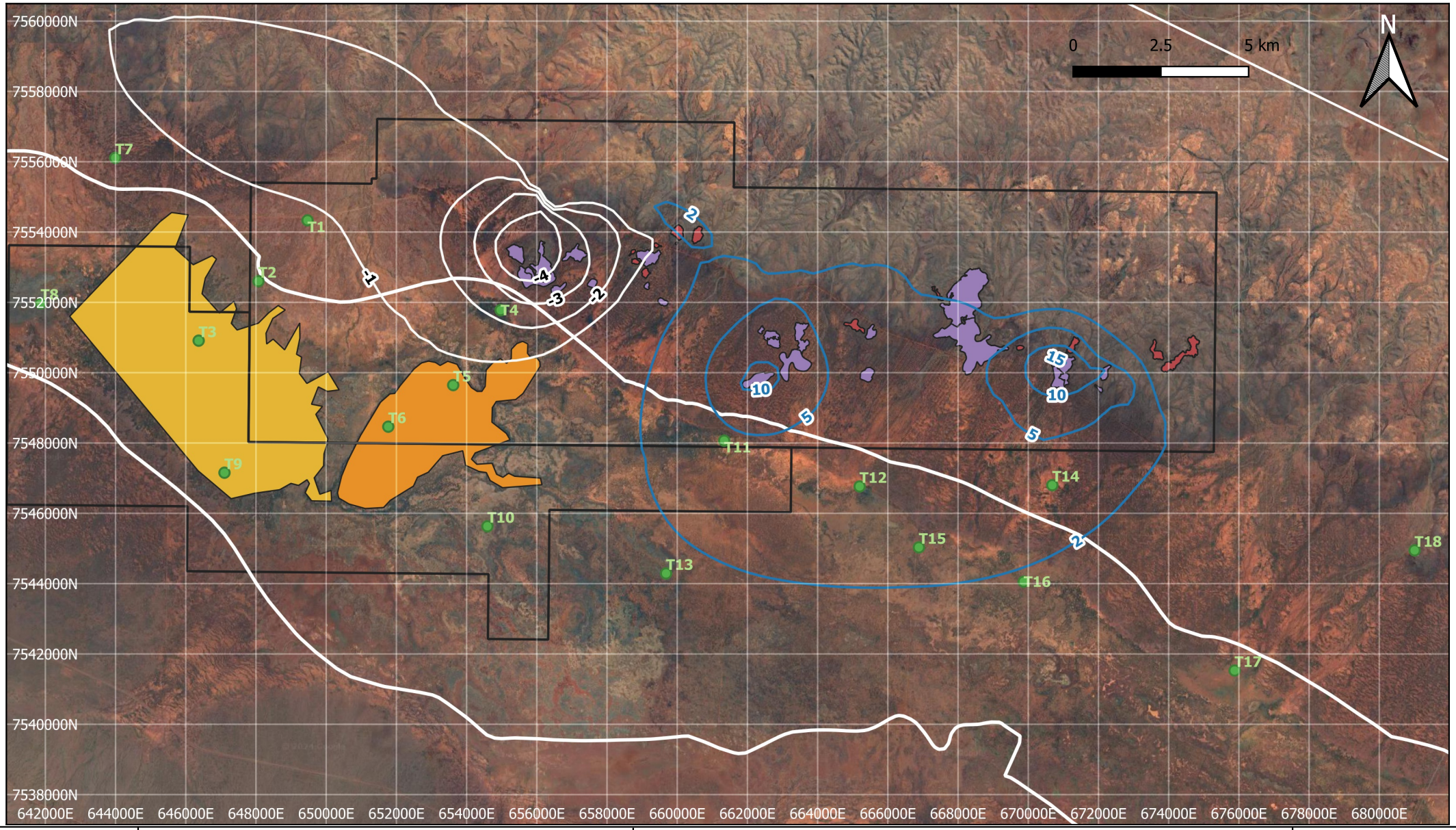

OVERVIEW MAP

PORT HEDLAND
MARBLE BAR
NEWMAN
PERTH

NOTES & DATA SOURCES:

Not for construction

ESPG:28350 (GDA94/MGA zone 50)

AUTHOR: MP

DRAWN: MP

DATE: 29/09/2024

Report NO: GWC-020-2022

REVISION: H

JOB No: 020-2022

Legend

- Pits Above Water Table
- Pits Below Water Table
- MEA Boundary
- Gnalka Gnoona Claypan
- Koodjeepindarranna Claypan
- Tenement Boundary
- Nominal Monitoring Enviro Point
- Predicted Drawdown (m)
- Predicted Mounding (m)

Figure A23

Predicted Drawdown in July 2035

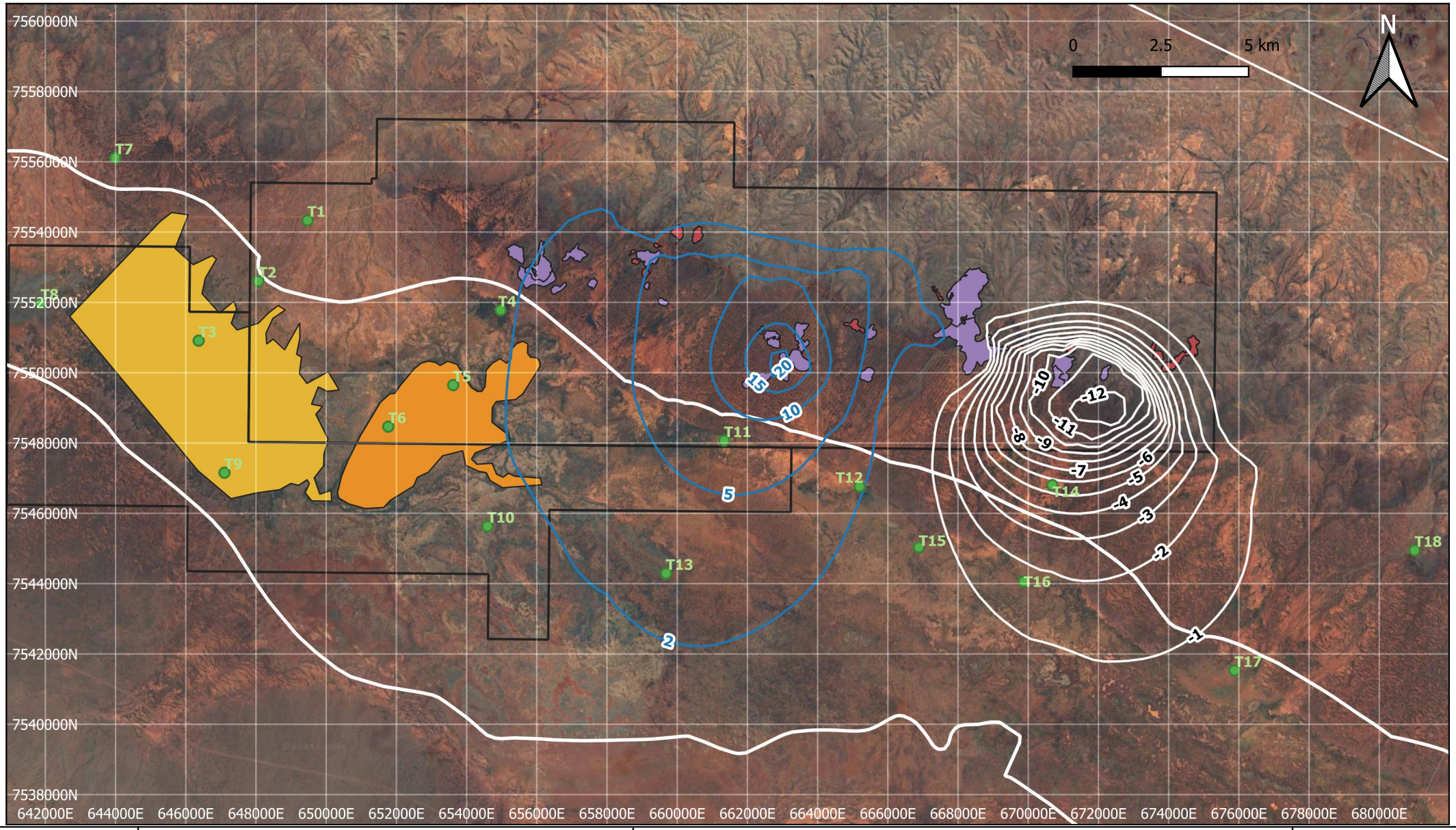

NOTES & DATA SOURCES:
Not for construction
ESPG:28350 (GDA94/MGA zone 50)

AUTHOR: MP
DRAWN: MP
DATE: 29/09/2024

Report NO: GWC-020-2022
REVISION: H
JOB No: 020-2022

Legend

- Pits Above Water Table
- Pits Below Water Table
- MEA Boundary
- Gnalka Gnoona Claypan
- Koodjeepindarranna Claypan
- Tenement Boundary
- Nominal Monitoring Enviro Point
- Predicted Drawdown (m)
- Predicted Mounding (m)

Figure A24

Predicted Drawdown in July 2038

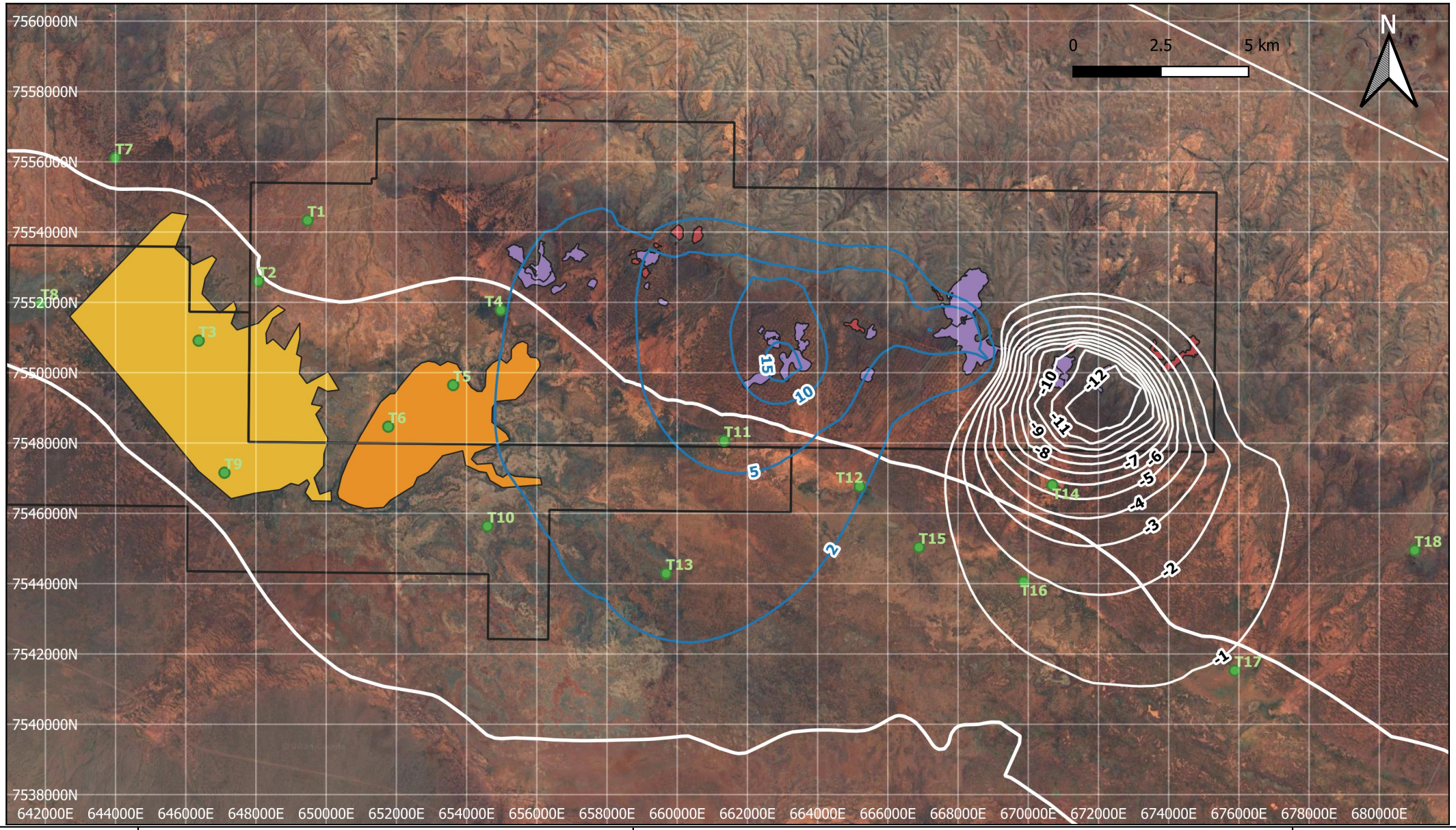

OVERVIEW MAP

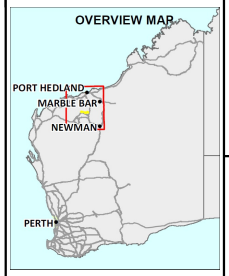

NOTES & DATA SOURCES:

Not for construction

ESPG:28350 (GDA94/MGA zone 50)

AUTHOR: MP

DRAWN: MP

DATE: 29/09/2024

Report NO: GWC-020-2022

REVISION: H

JOB No: 020-2022

Legend

- Pits Above Water Table
- Pits Below Water Table
- MEA Boundary
- Gnalka Gnoona Claypan
- Koodjeepindarranna Claypan
- Tenement Boundary
- Nominal Monitoring Enviro Point
- Predicted Drawdown (m)
- Predicted Mounding (m)

Figure A25

Predicted Drawdown in December 2038

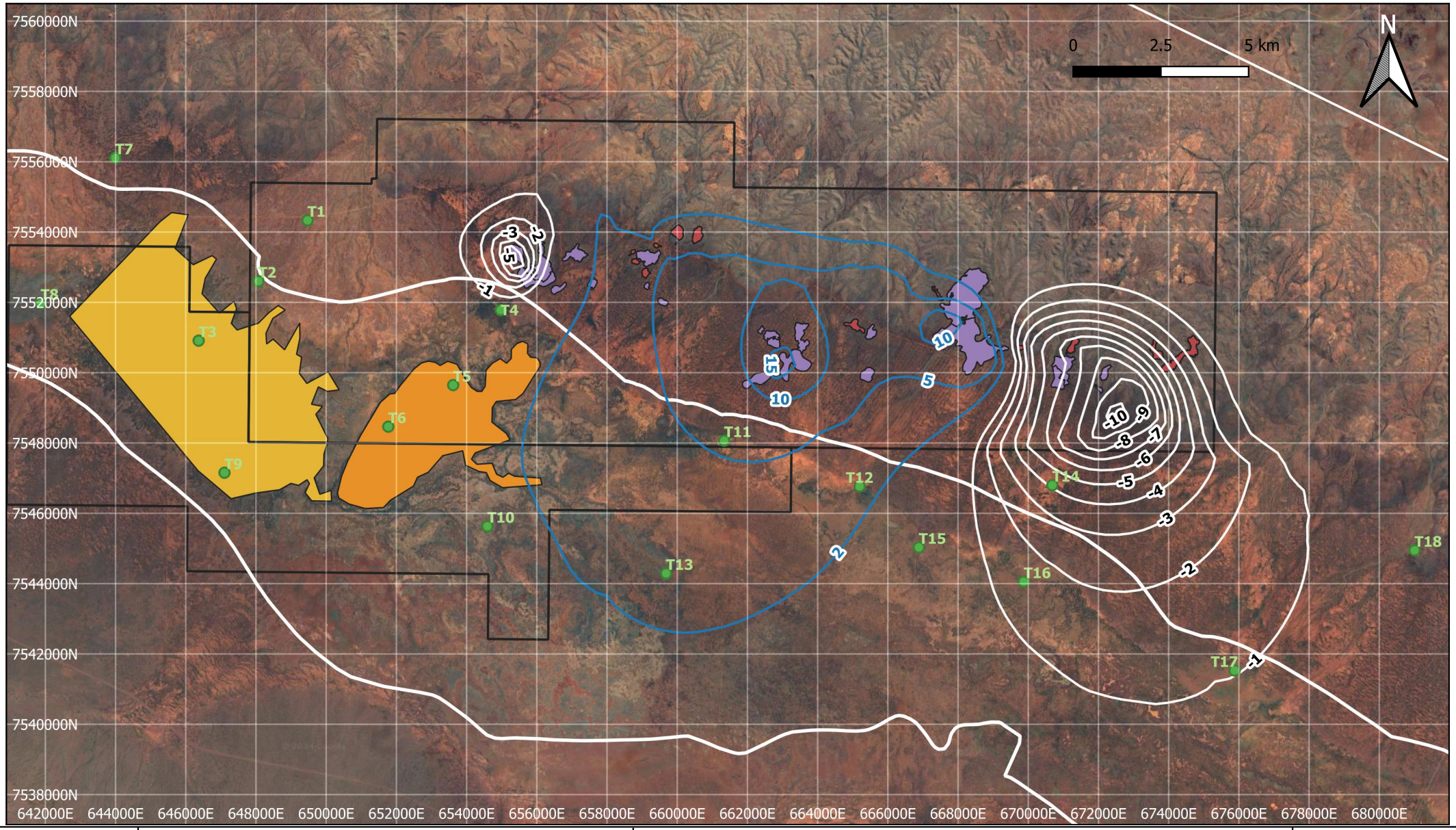

OVERVIEW MAP

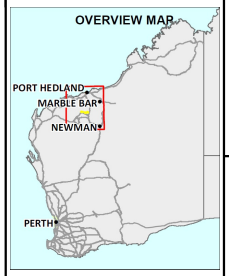

NOTES & DATA SOURCES:

Not for construction

ESPG:28350 (GDA94/MGA zone 50)

AUTHOR: MP

DRAWN: MP

DATE: 29/09/2024

Report NO: GWC-020-2022

REVISION: H

JOB No: 020-2022

Legend

- Pits Above Water Table
- Pits Below Water Table
- MEA Boundary
- Gnalka Gnoona Claypan
- Koodjeepindarranna Claypan
- Tenement Boundary
- Nominal Monitoring Enviro Point
- Predicted Drawdown (m)
- Predicted Mounding (m)

Figure A26

Predicted Drawdown in July 2039

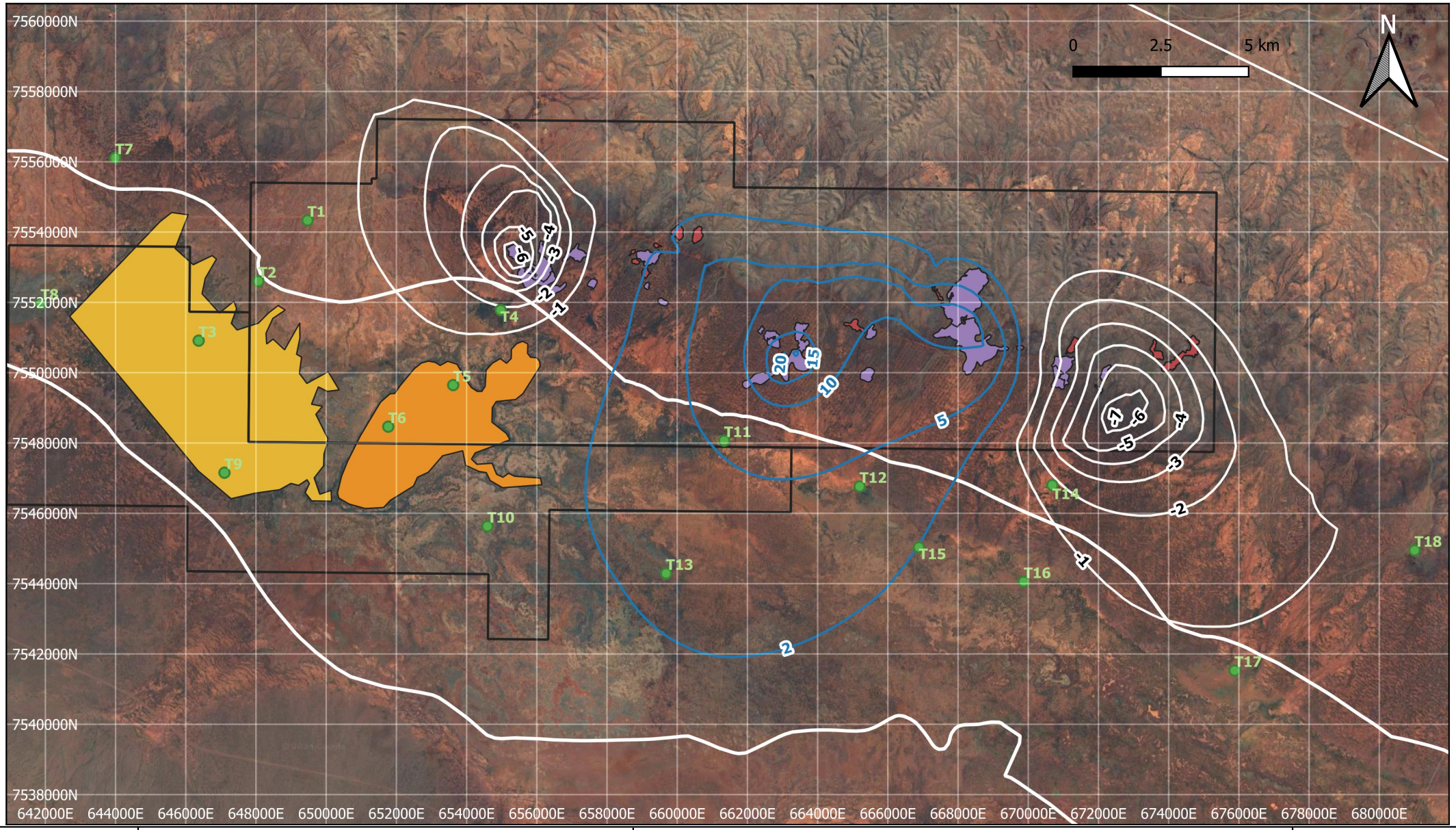

OVERVIEW MAP

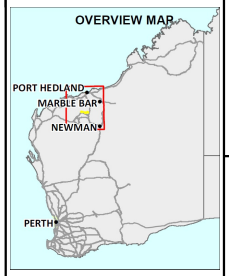

NOTES & DATA SOURCES:

Not for construction

ESPG:28350 (GDA94/MGA zone 50)

AUTHOR: MP

DRAWN: MP

DATE: 29/09/2024

Report NO: GWC-020-2022

REVISION: H

JOB No: 020-2022

Legend

- Pits Above Water Table
- Pits Below Water Table
- MEA Boundary
- Gnalka Gnoona Claypan
- Koodjeepindarranna Claypan
- Tenement Boundary
- Nominal Monitoring Enviro Point
- Predicted Drawdown (m)
- Predicted Mounding (m)

Figure A27

Predicted Drawdown in July 2041

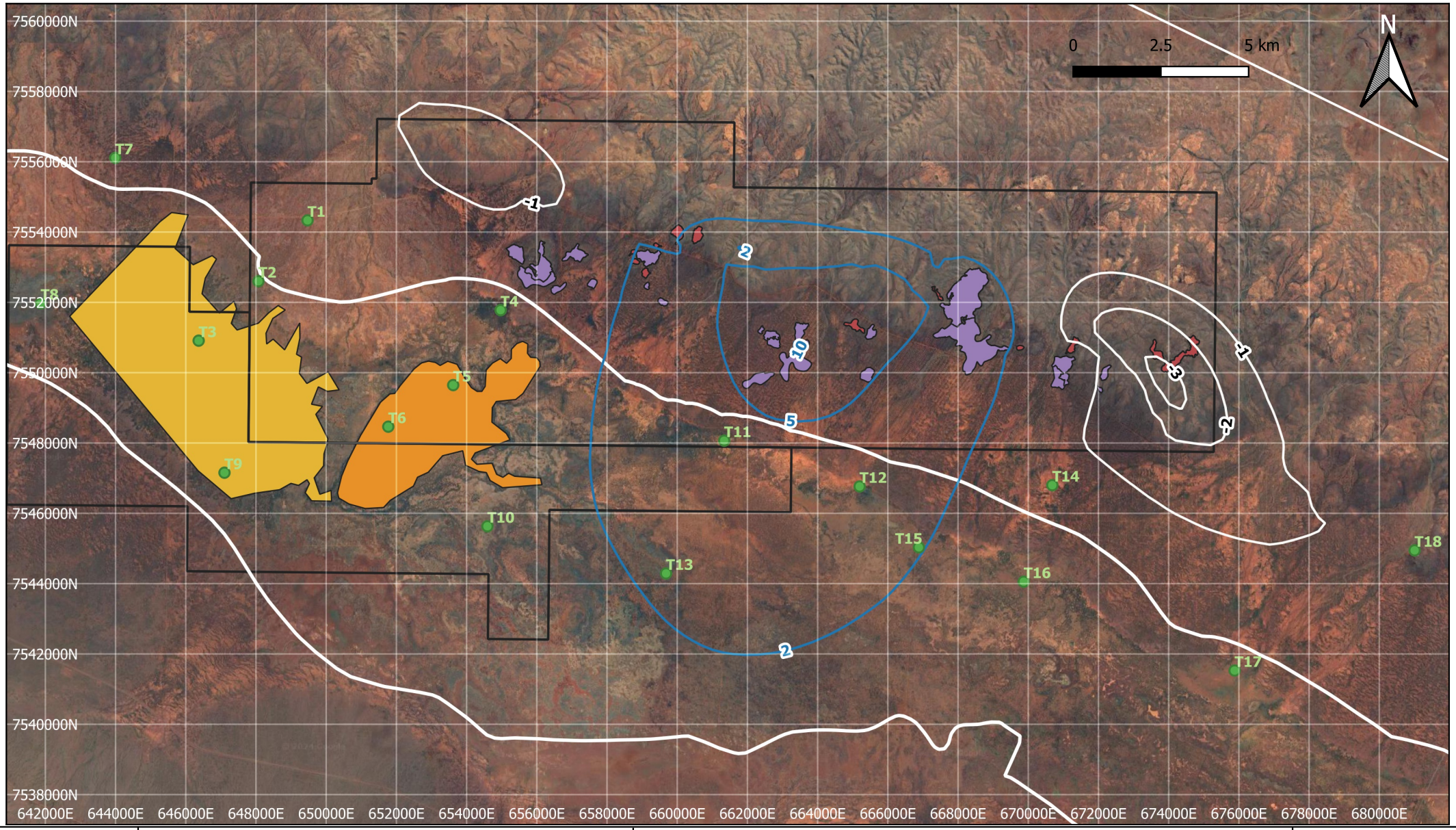

OVERVIEW MAP

PORT HEDLAND
MARBLE BAR
NEWMAN
PERTH

NOTES & DATA SOURCES:
Not for construction
ESPG:28350 (GDA94/MGA zone 50)

AUTHOR: MP
DRAWN: MP
DATE: 29/09/2024

Report NO: GWC-020-2022
REVISION: H
JOB No: 020-2022

Legend

- Pits Above Water Table
- Pits Below Water Table
- MEA Boundary
- Gnalka Gnoona Claypan
- Koodjeepindarranna Claypan
- Tenement Boundary
- Nominal Monitoring Enviro Point
- Predicted Drawdown (m)
- Predicted Mounding (m)

Figure A28

Predicted Drawdown in June 2042 (End of Mining)

FIGURE A29 - PREDICTED WATER LEVELS AT ENVIRO LOCATIONS

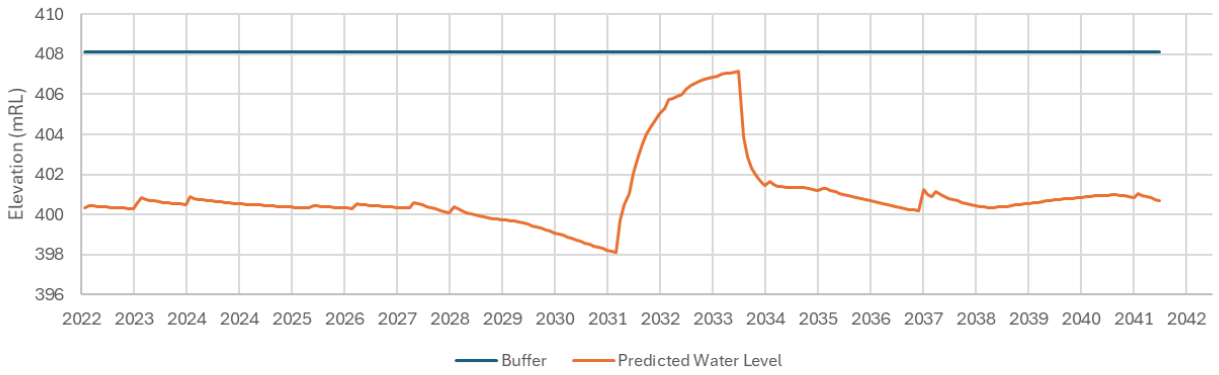

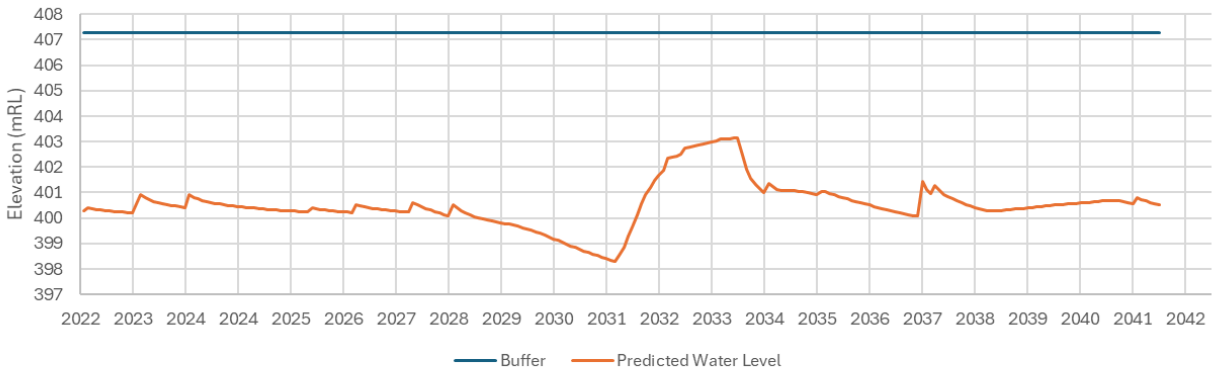

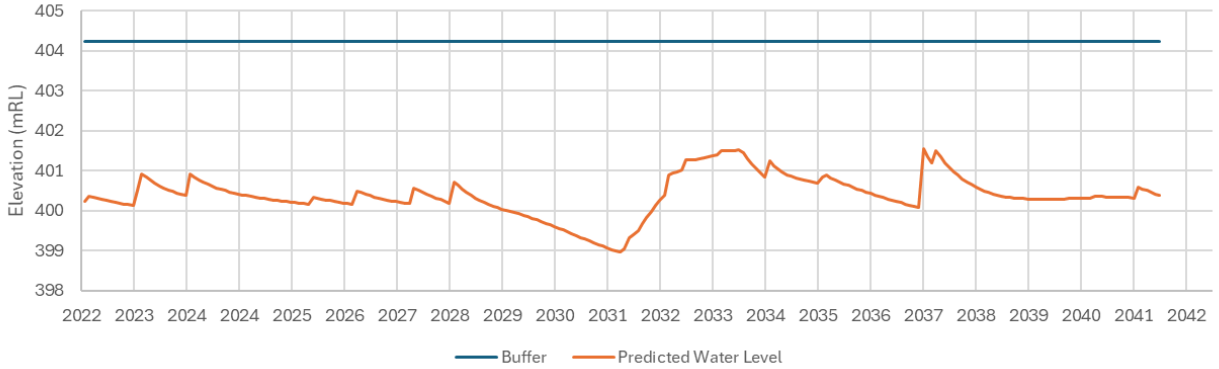

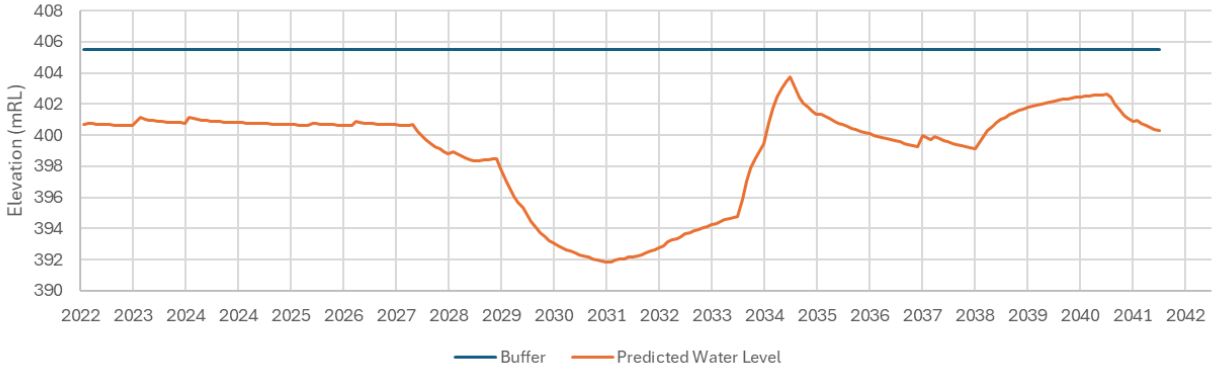

FIGURE A30 - PREDICTED WATER LEVELS AT ENVIRO LOCATIONS

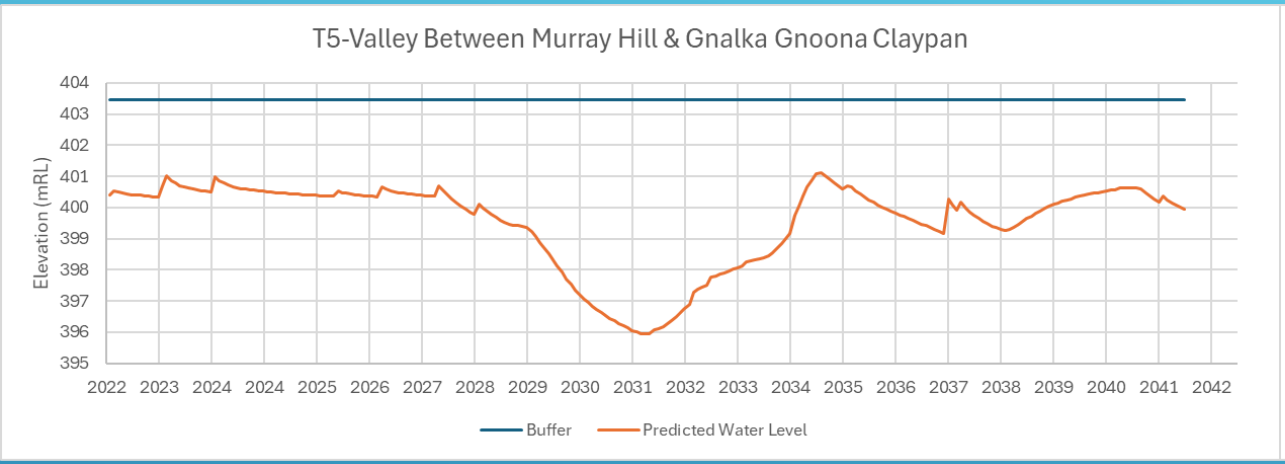

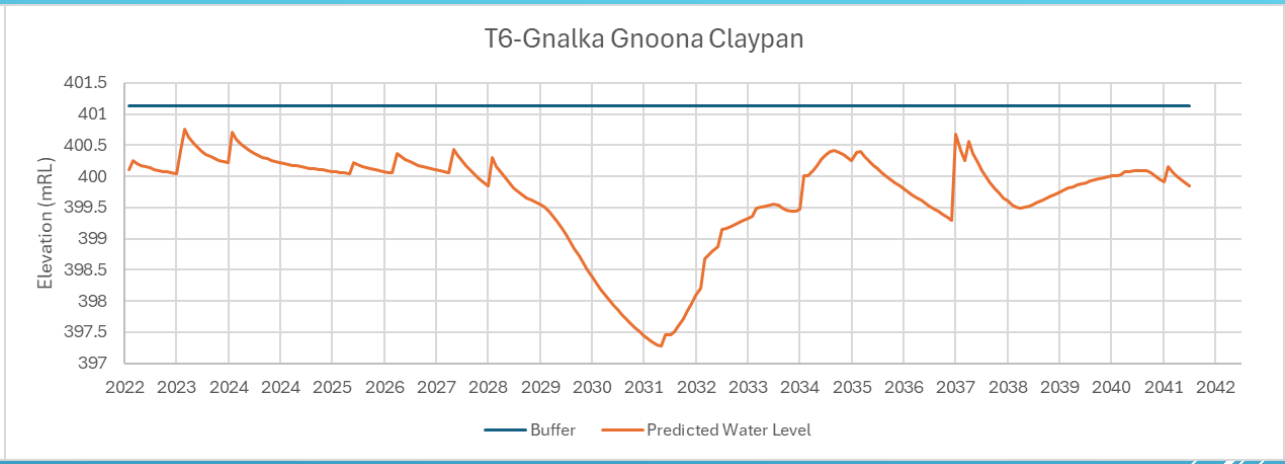

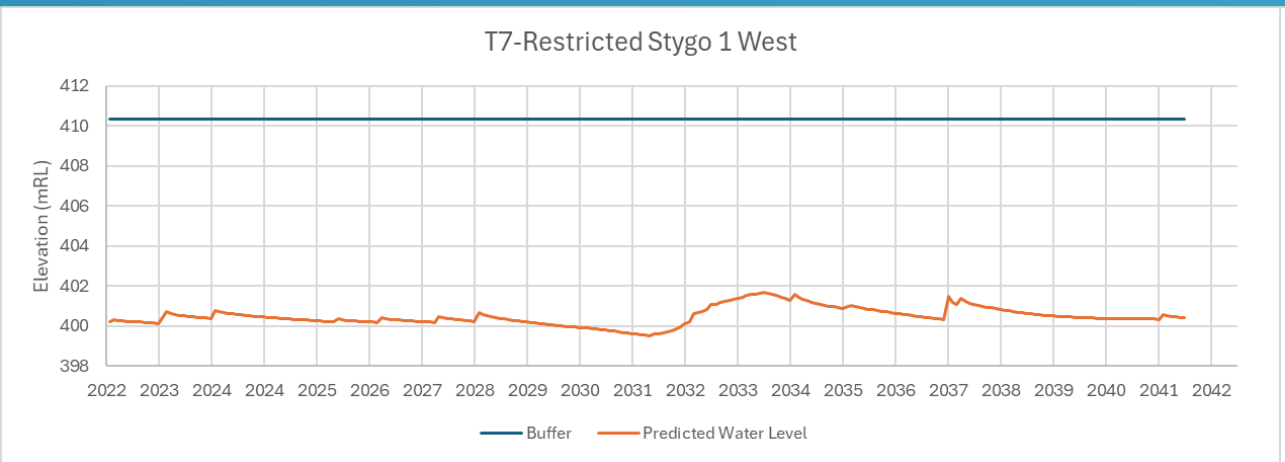

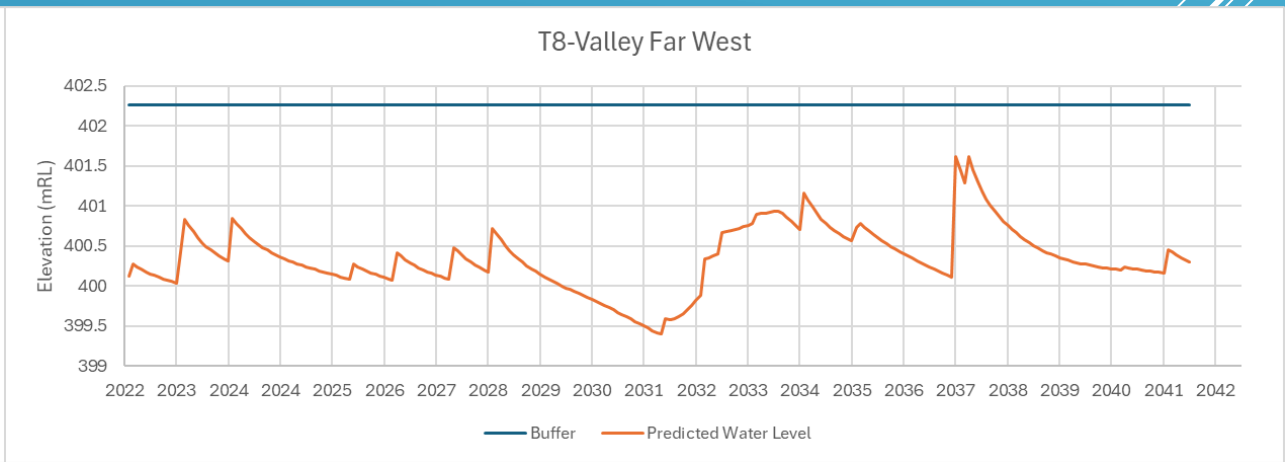

FIGURE A31 - PREDICTED WATER LEVELS AT ENVIRO LOCATIONS

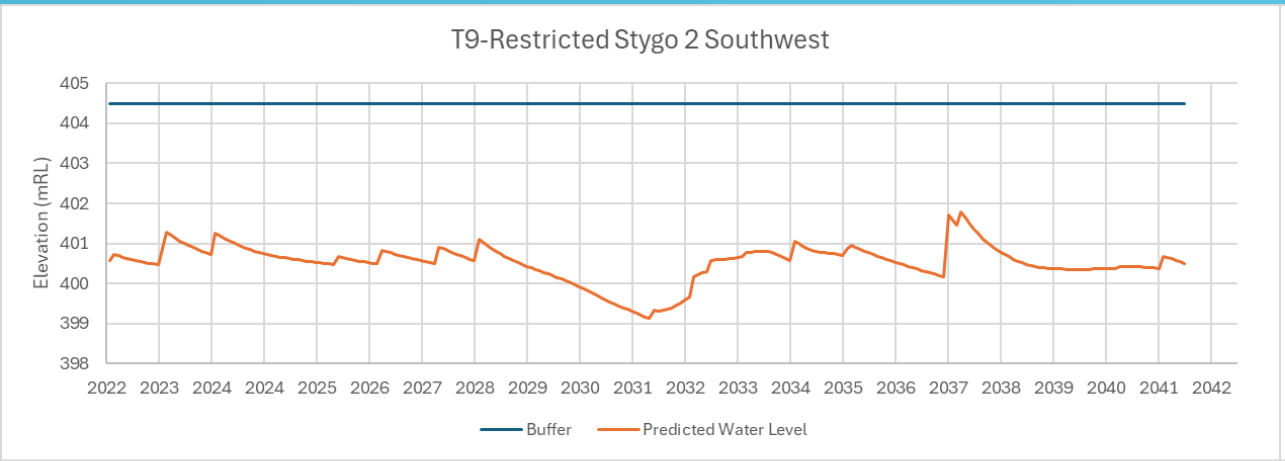

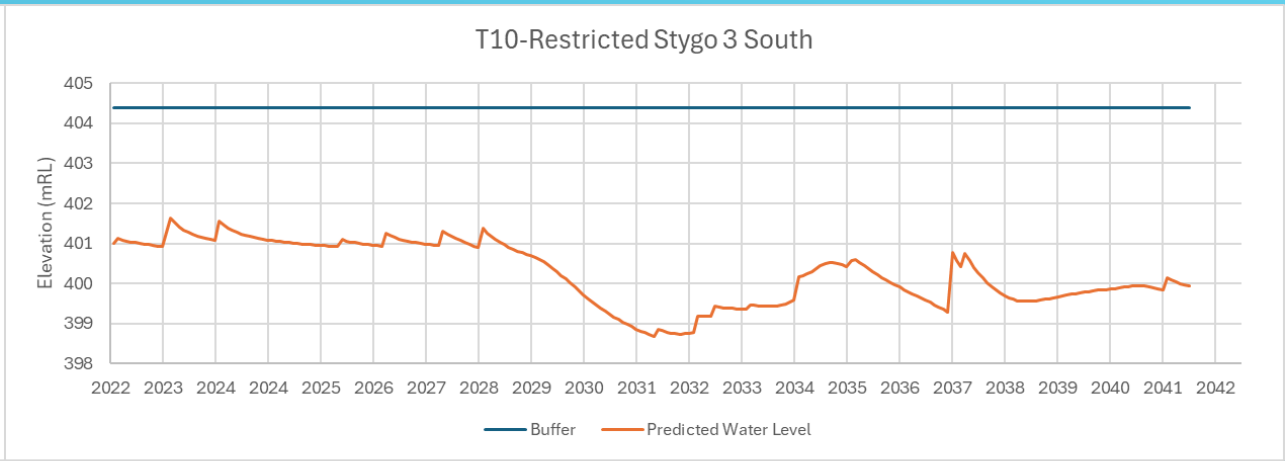

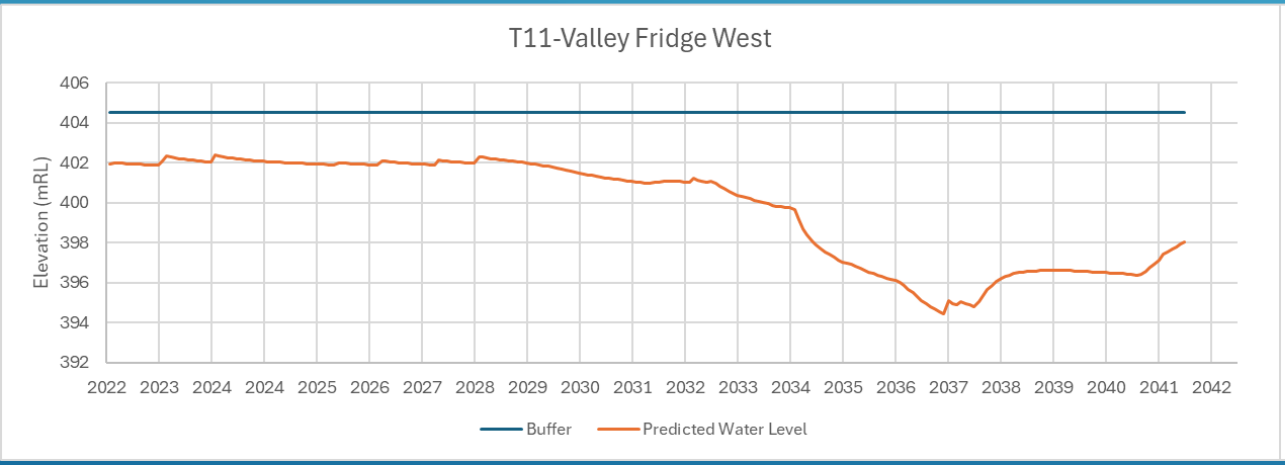

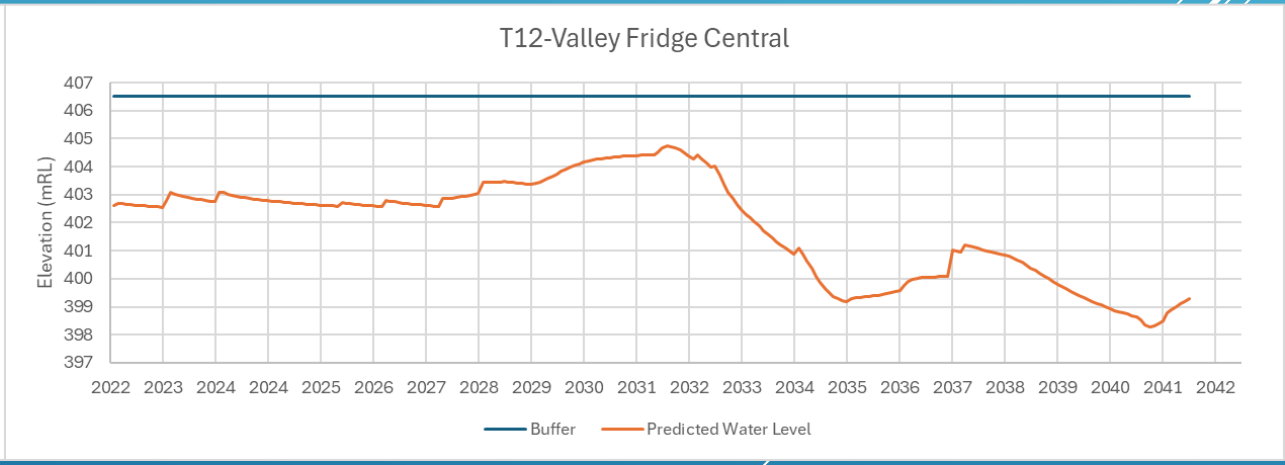

FIGURE A32 - PREDICTED WATER LEVELS AT ENVIRO LOCATIONS

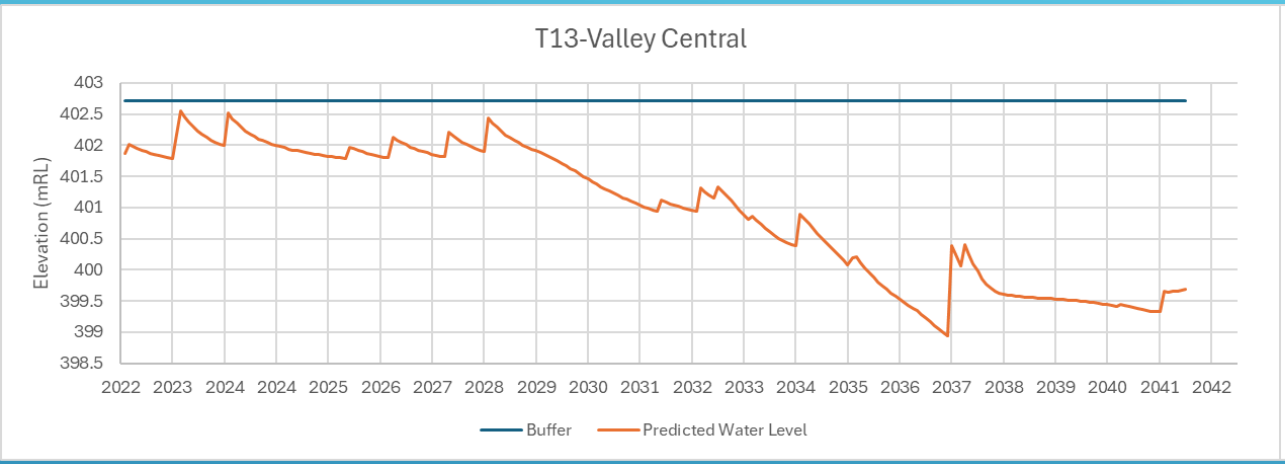

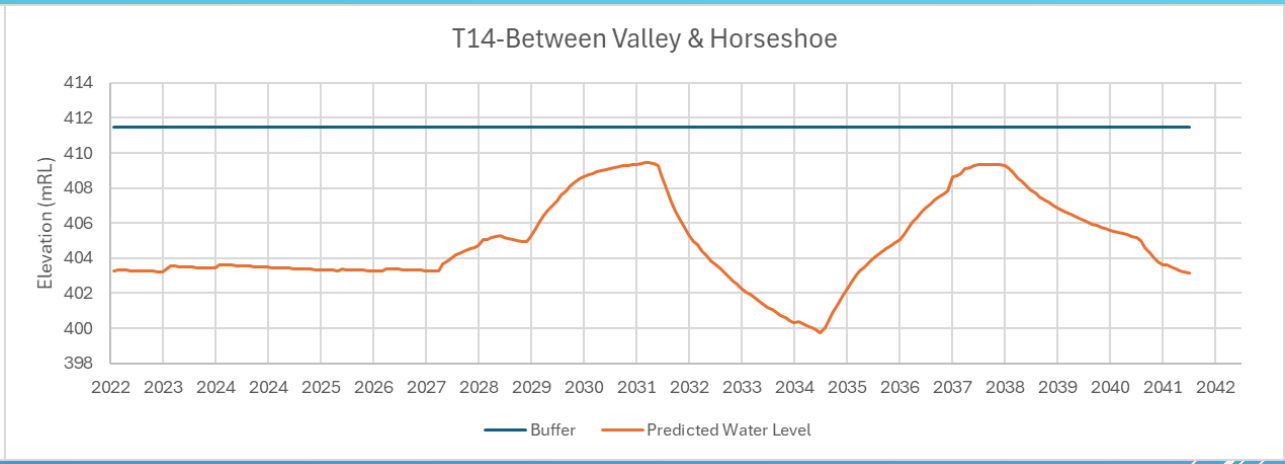

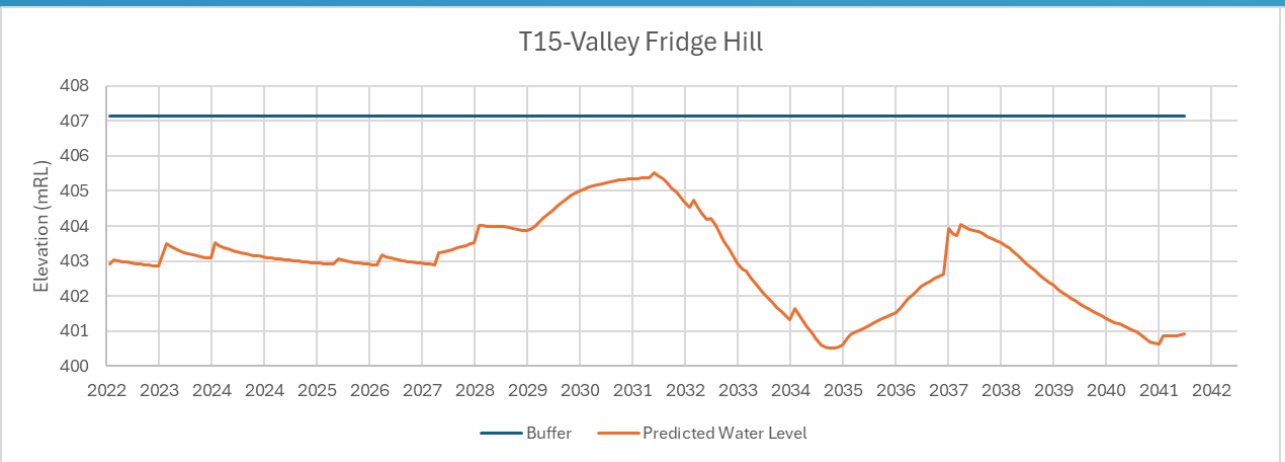

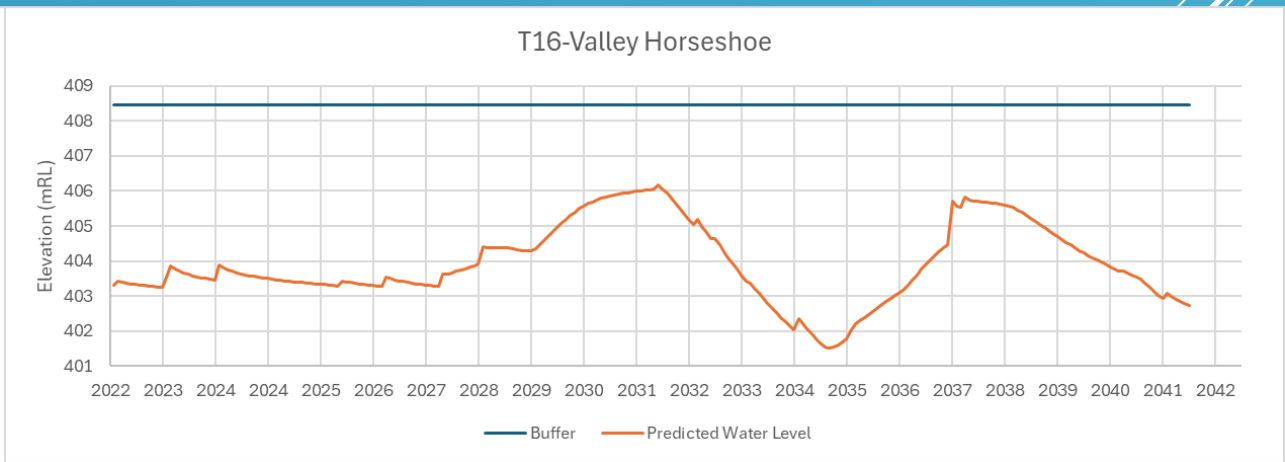

FIGURE A33 - PREDICTED WATER LEVELS AT ENVIRO LOCATIONS

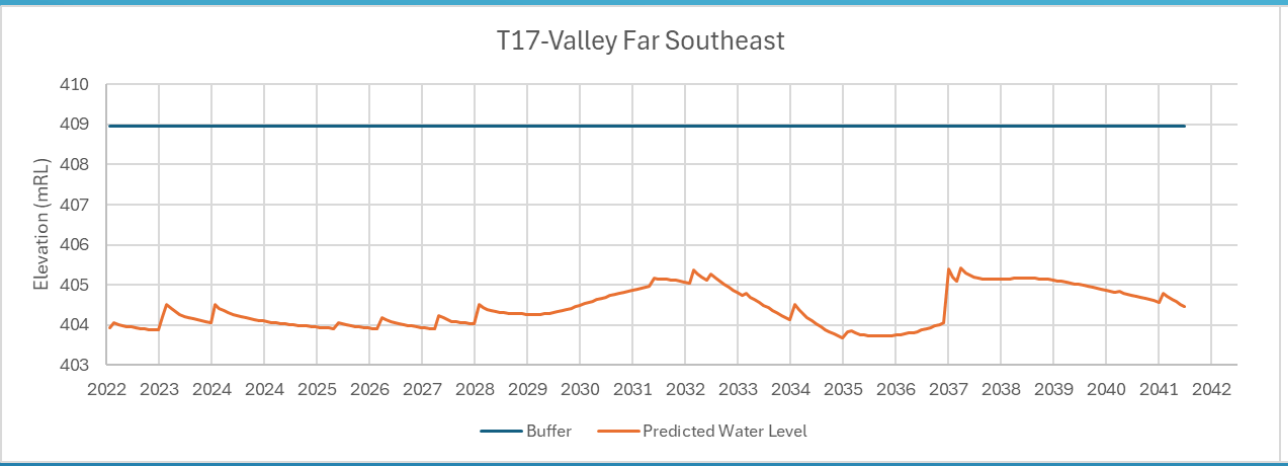

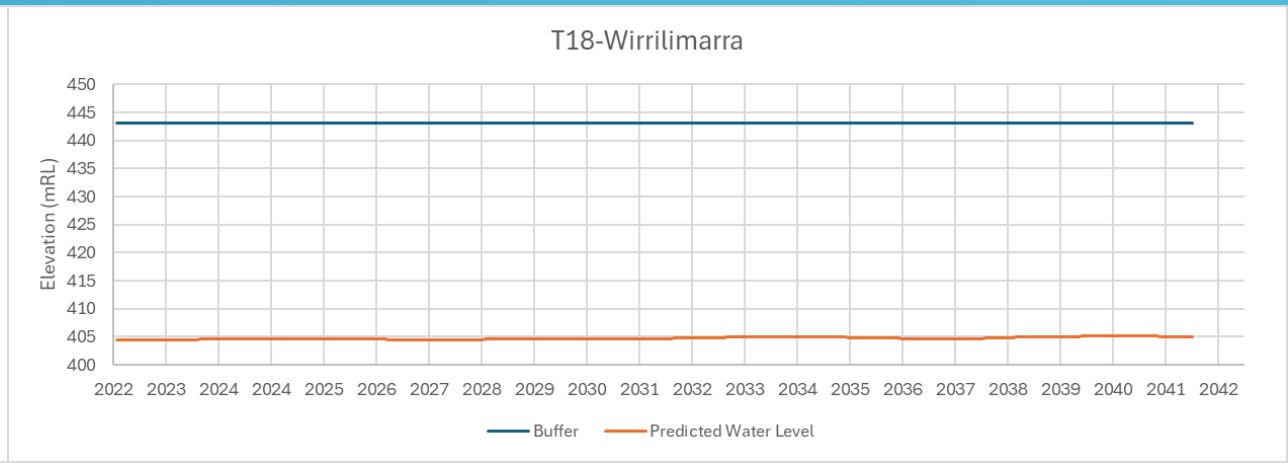

Appendix B Closure Results

Note: The elapsed time on charts is calculated from the end of mining

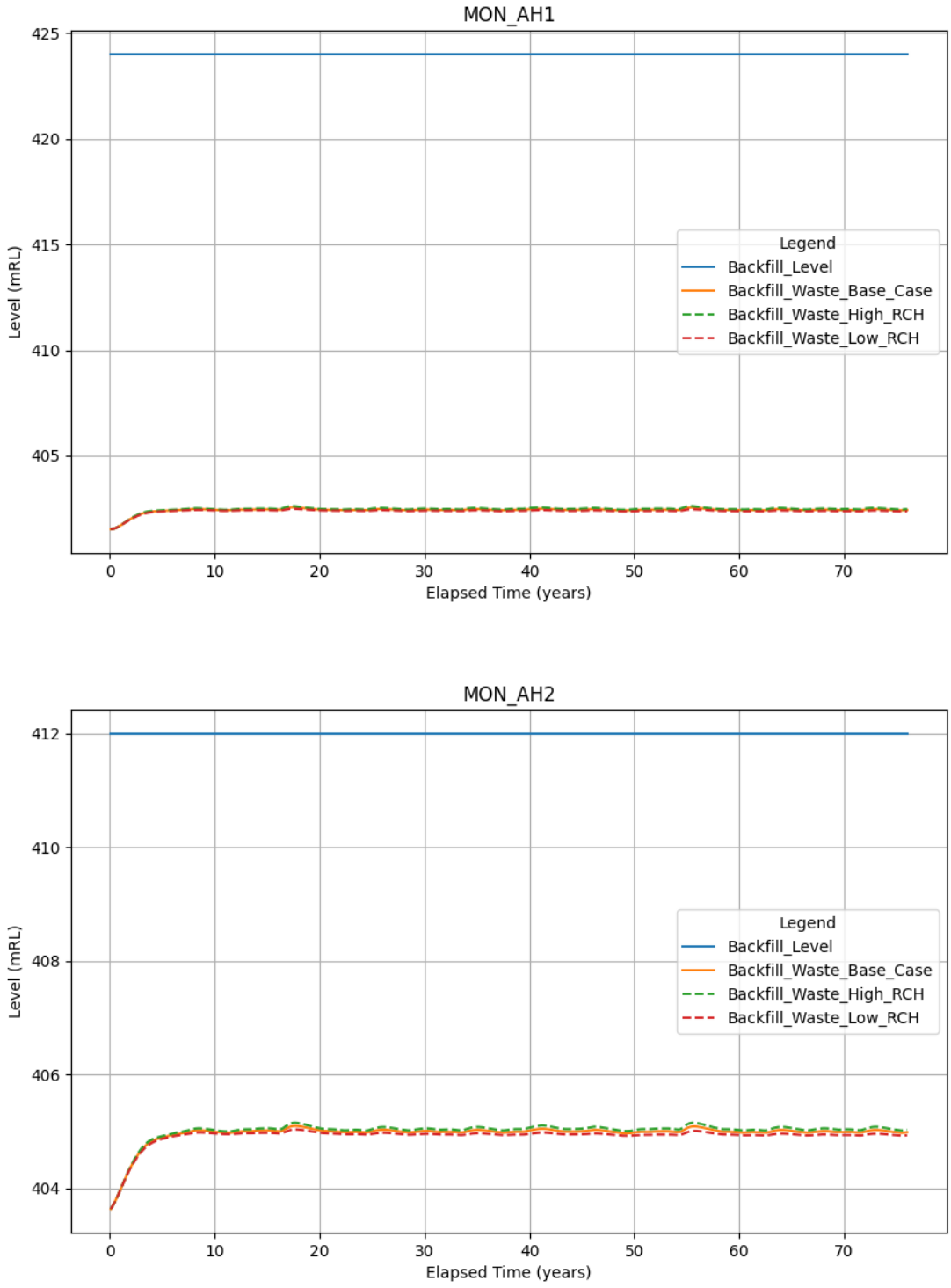

Figure B-1 Predicted pit water level recovery at Anticline Hill

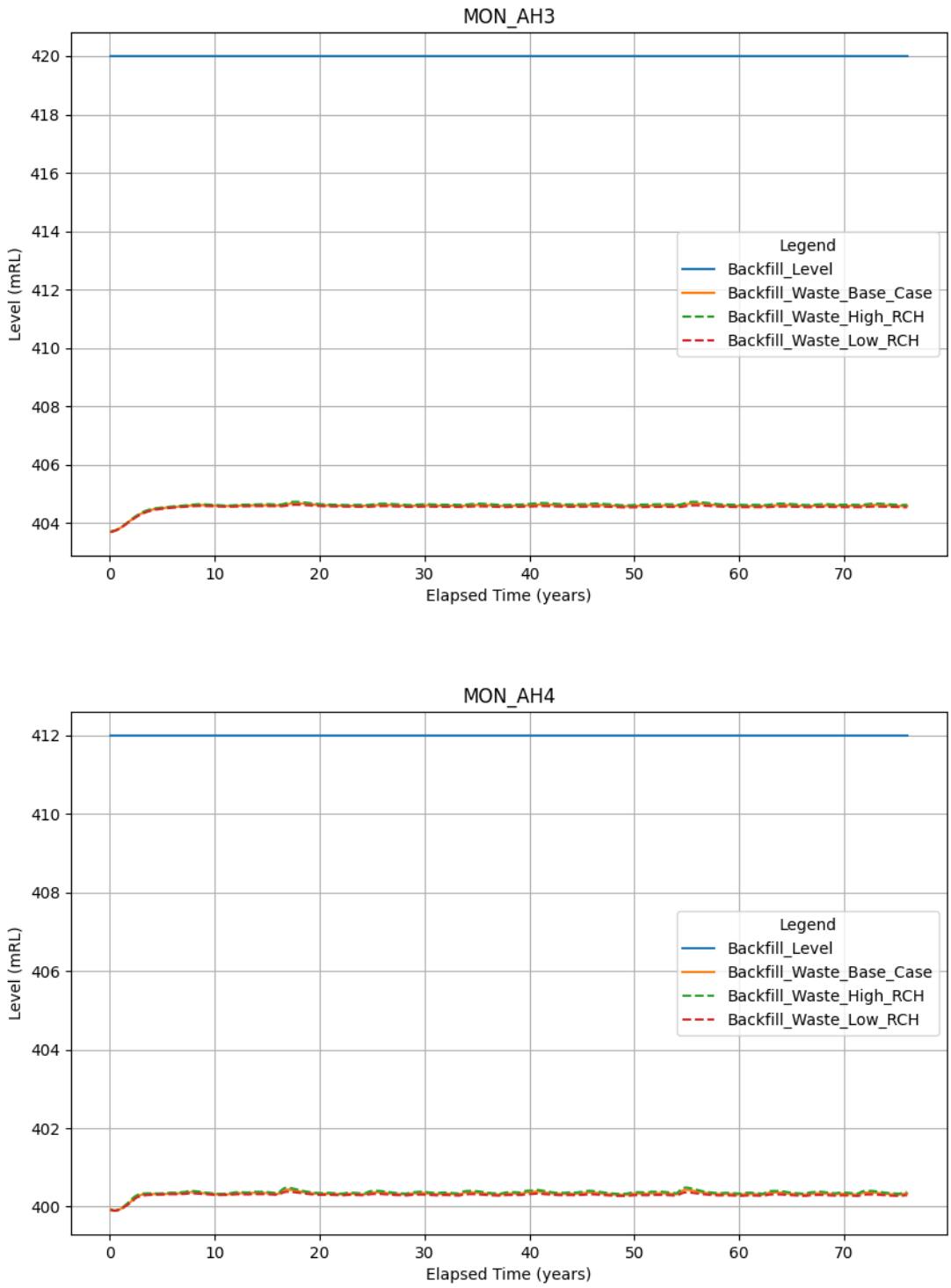

Figure B-2 Predicted pit water level recovery at Anticline Hill

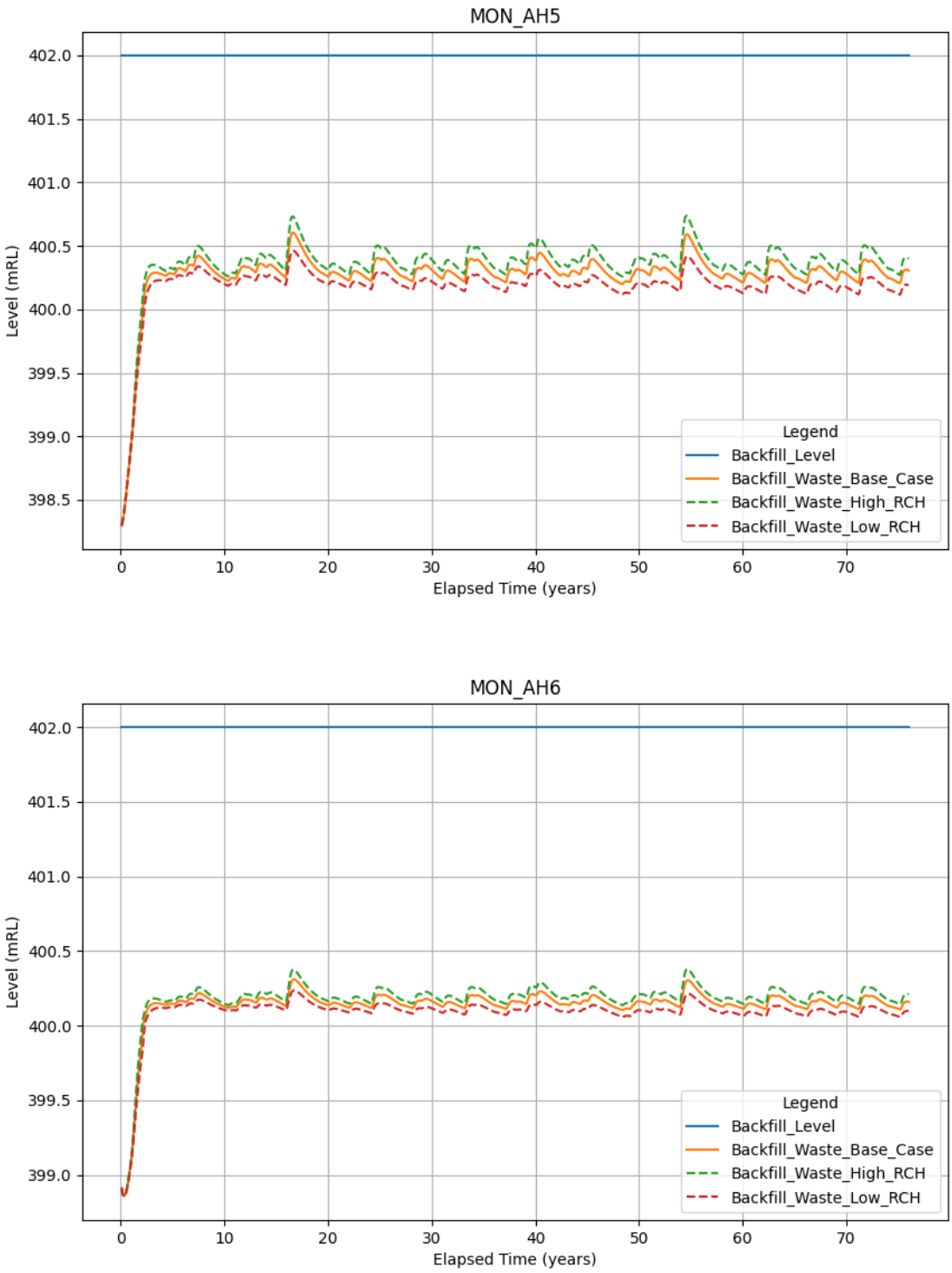

Figure B-3 Predicted pit water level recovery at Anticline Hill

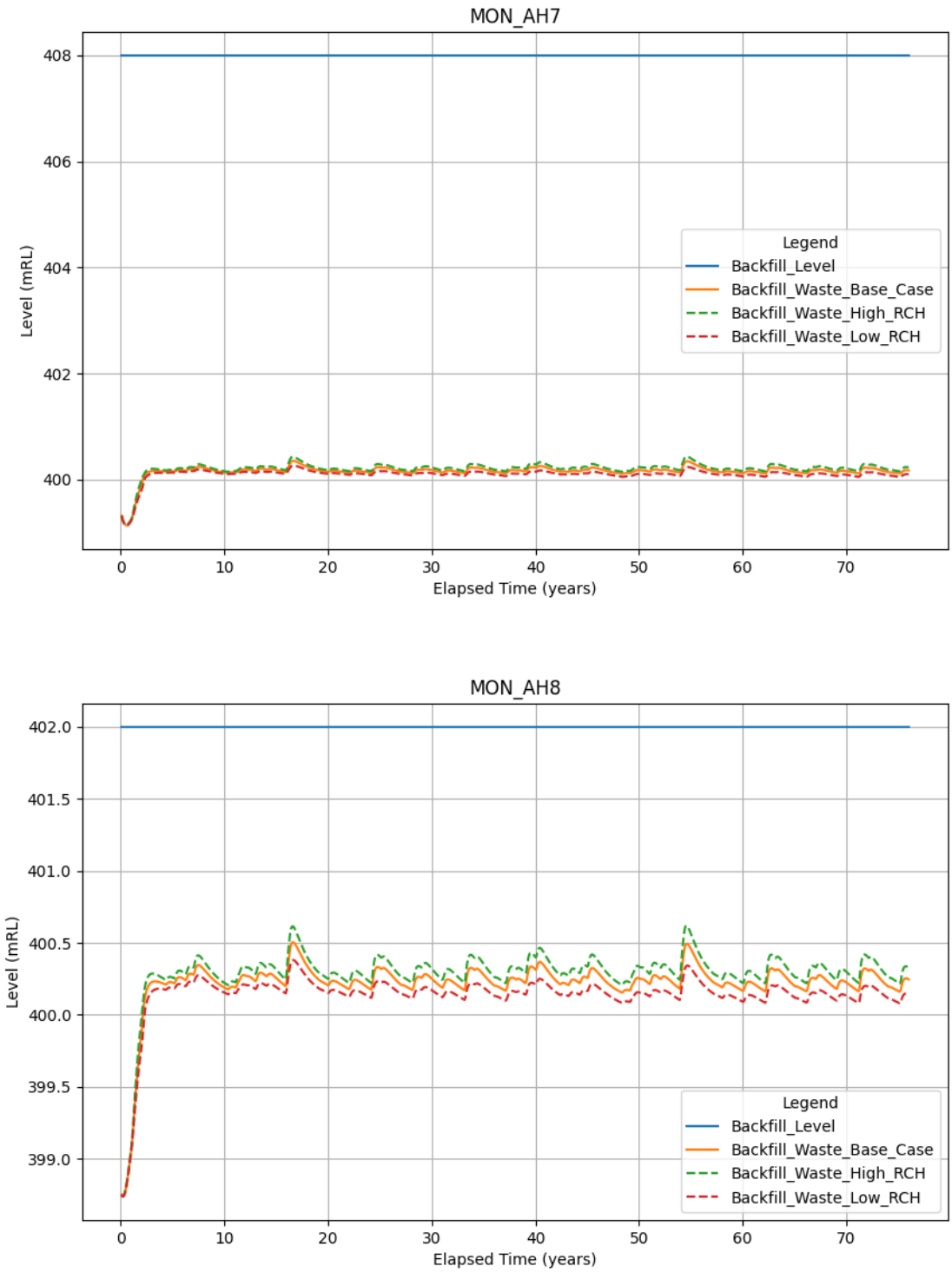

Figure B-4 Predicted pit water level recovery at Anticline Hill

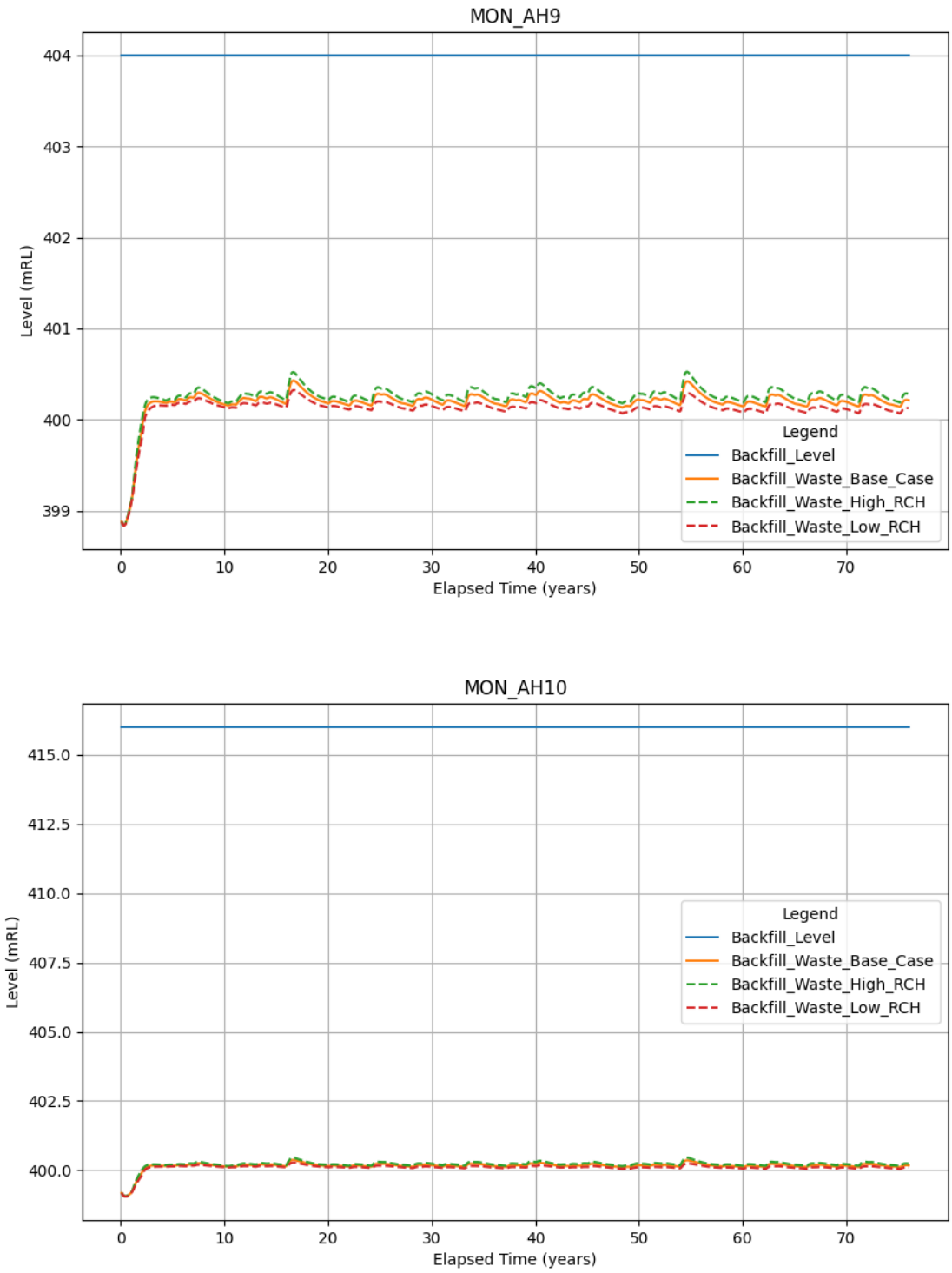

Figure B-5 Predicted pit water level recovery at Anticline Hill

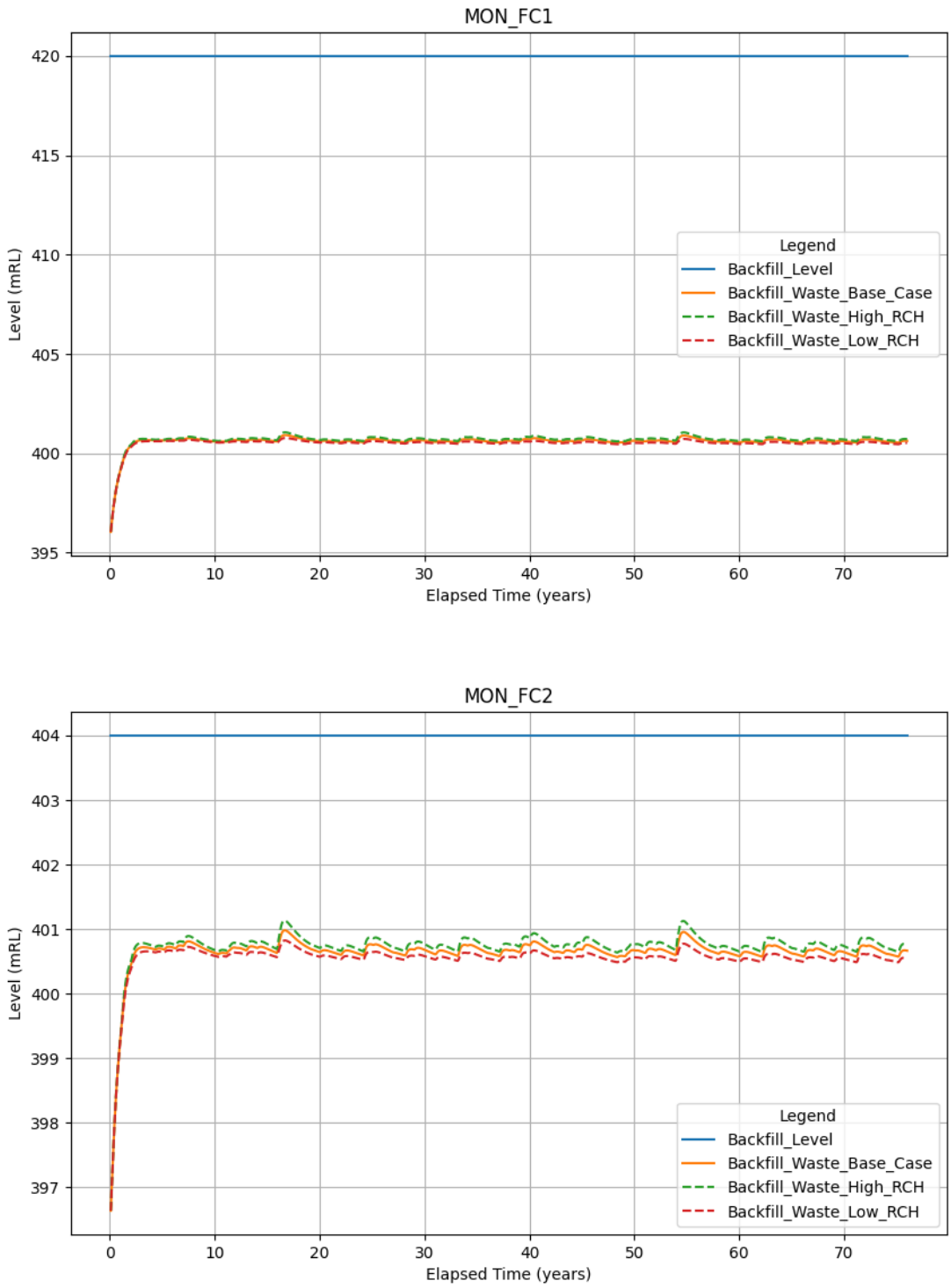

Figure B-6 Predicted pit water level recovery at Fridge Central

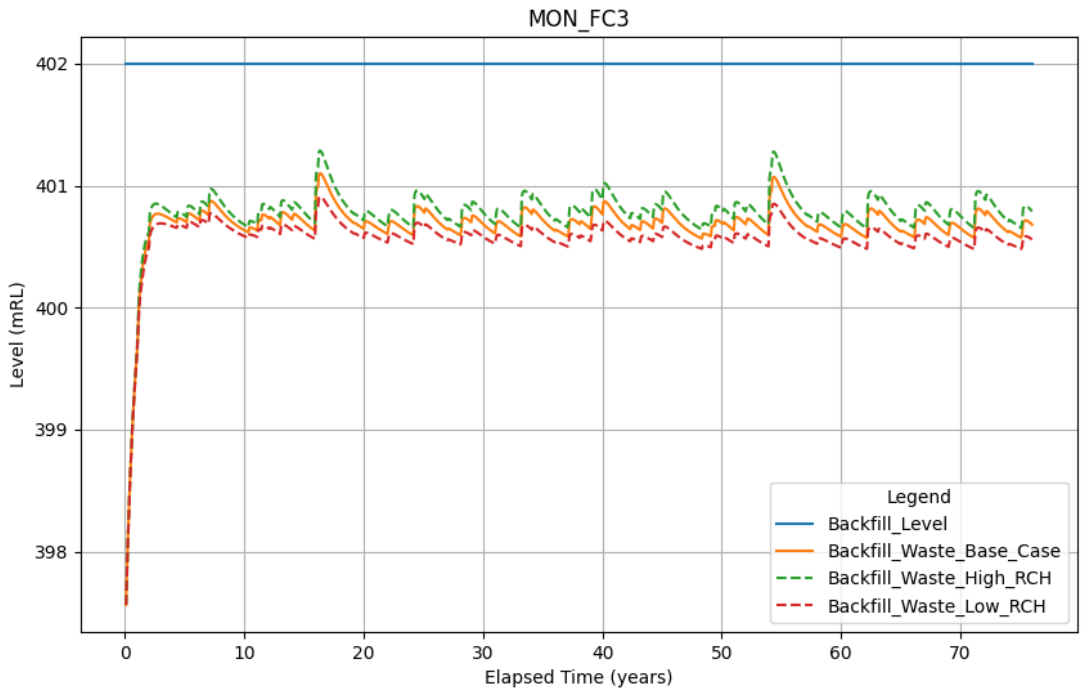

Figure B-7 Predicted pit water level recovery at Fridge Central

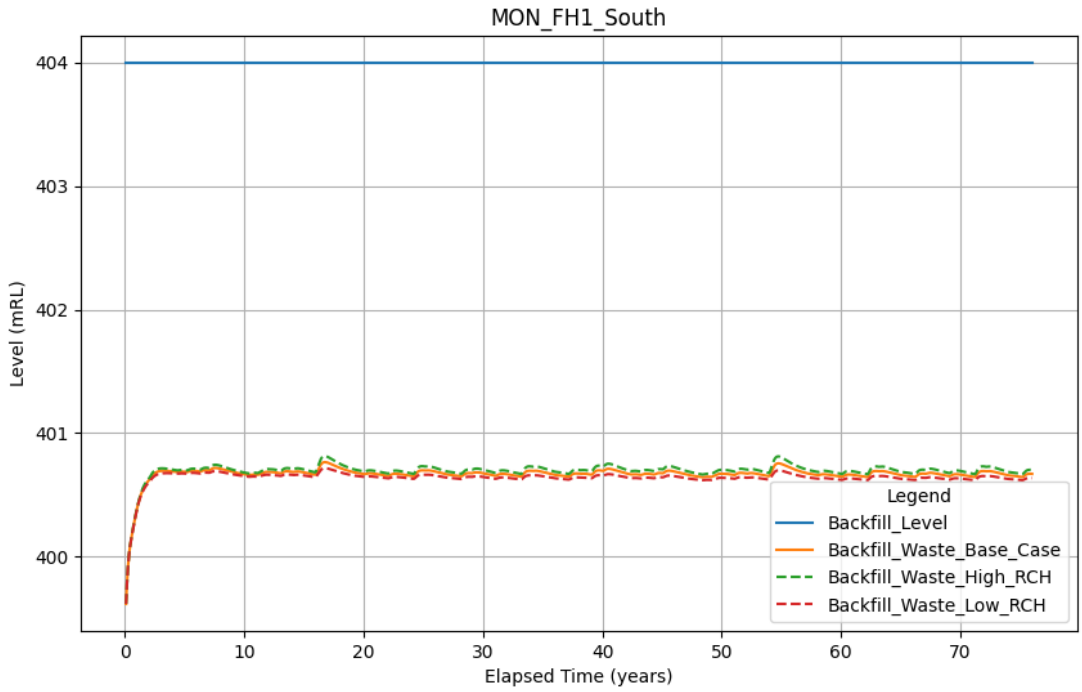

Figure B-8 Predicted pit water level recovery at Fridge Hill

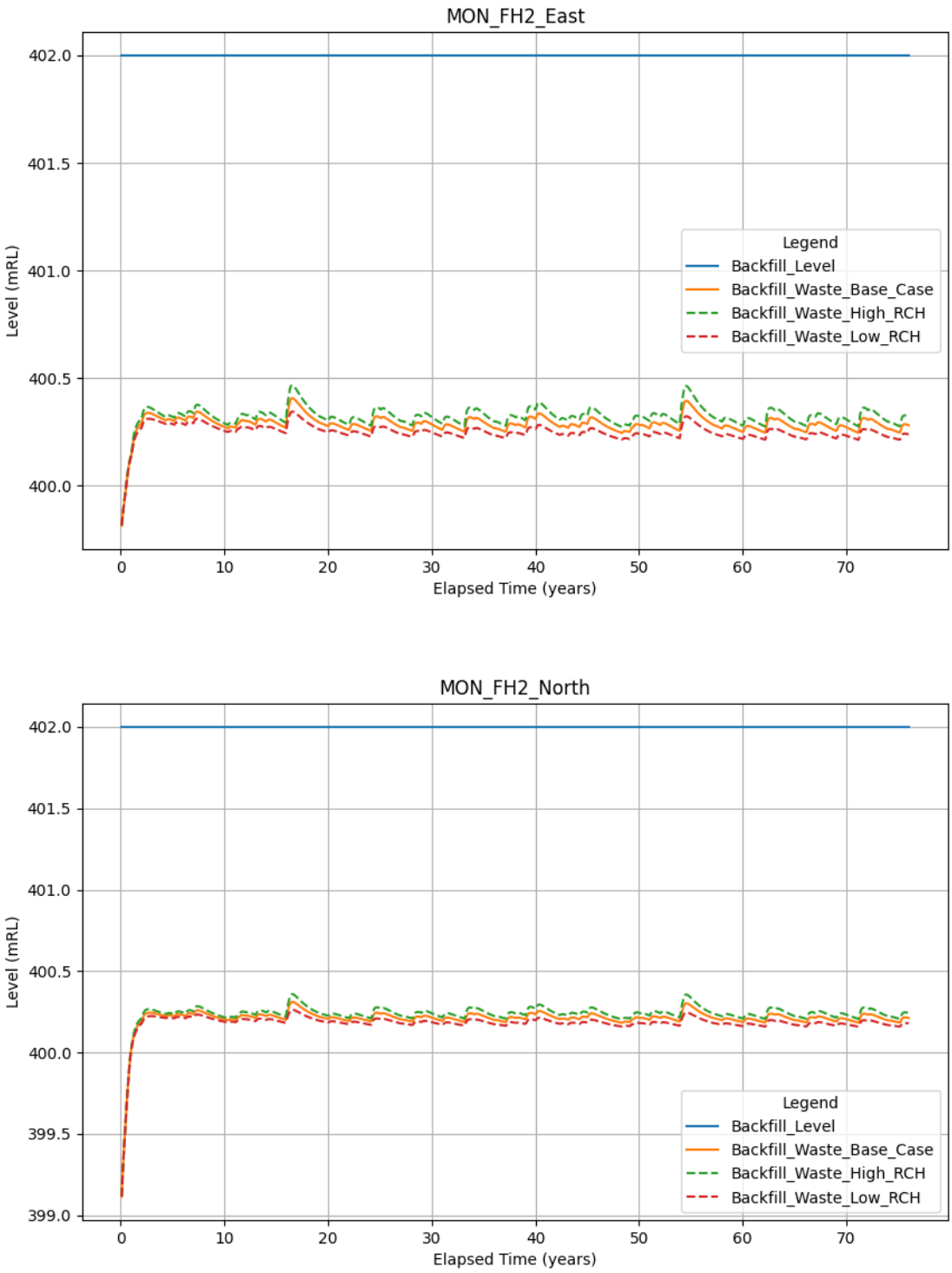

Figure B-9 Predicted pit water level recovery at Fridge Hill

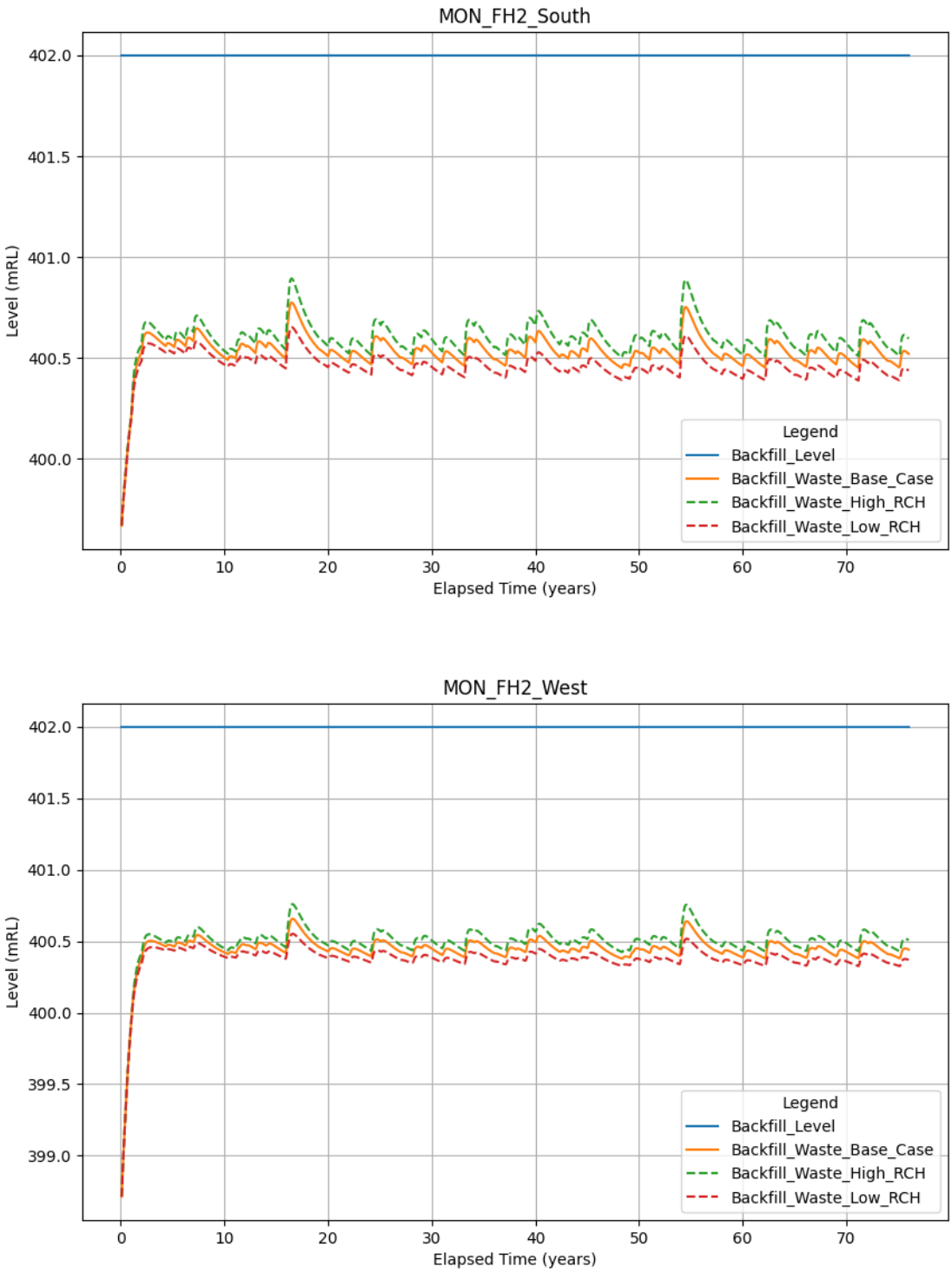

Figure B-10 Predicted pit water level recovery at Fridge Hill

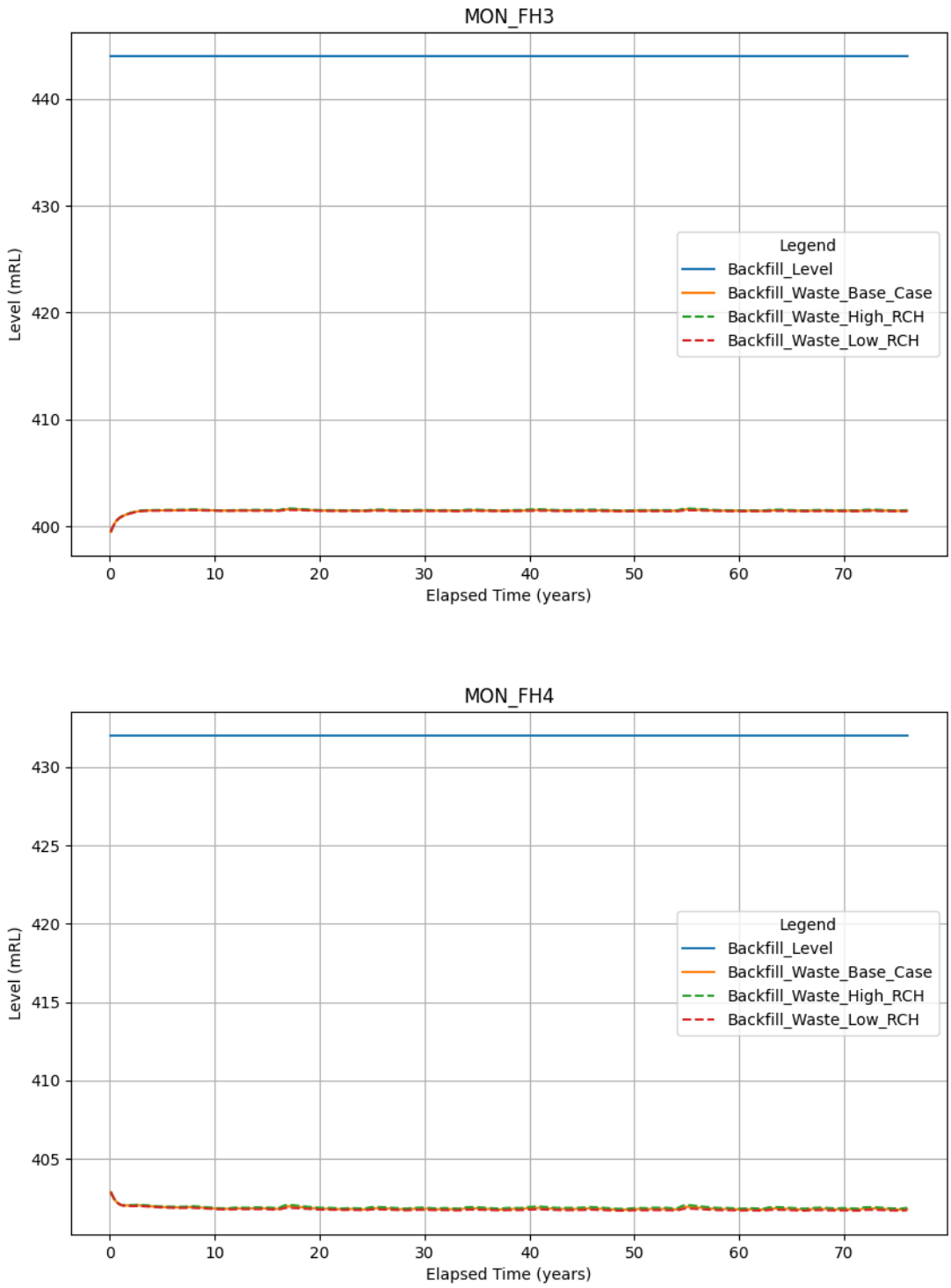

Figure B-11 Predicted pit water level recovery at Fridge Hill

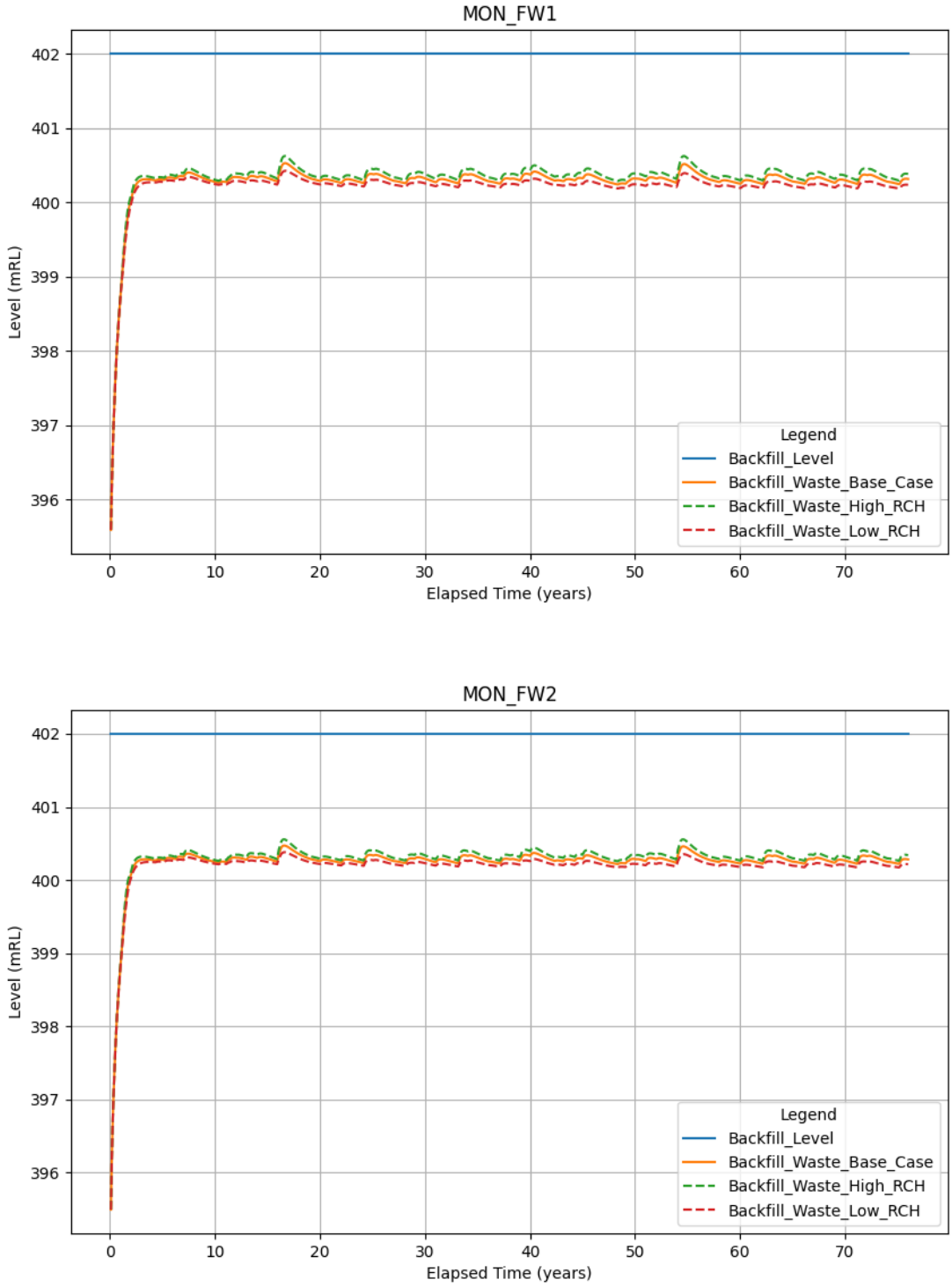

Figure B-12 Predicted pit water level recovery at Fridge West

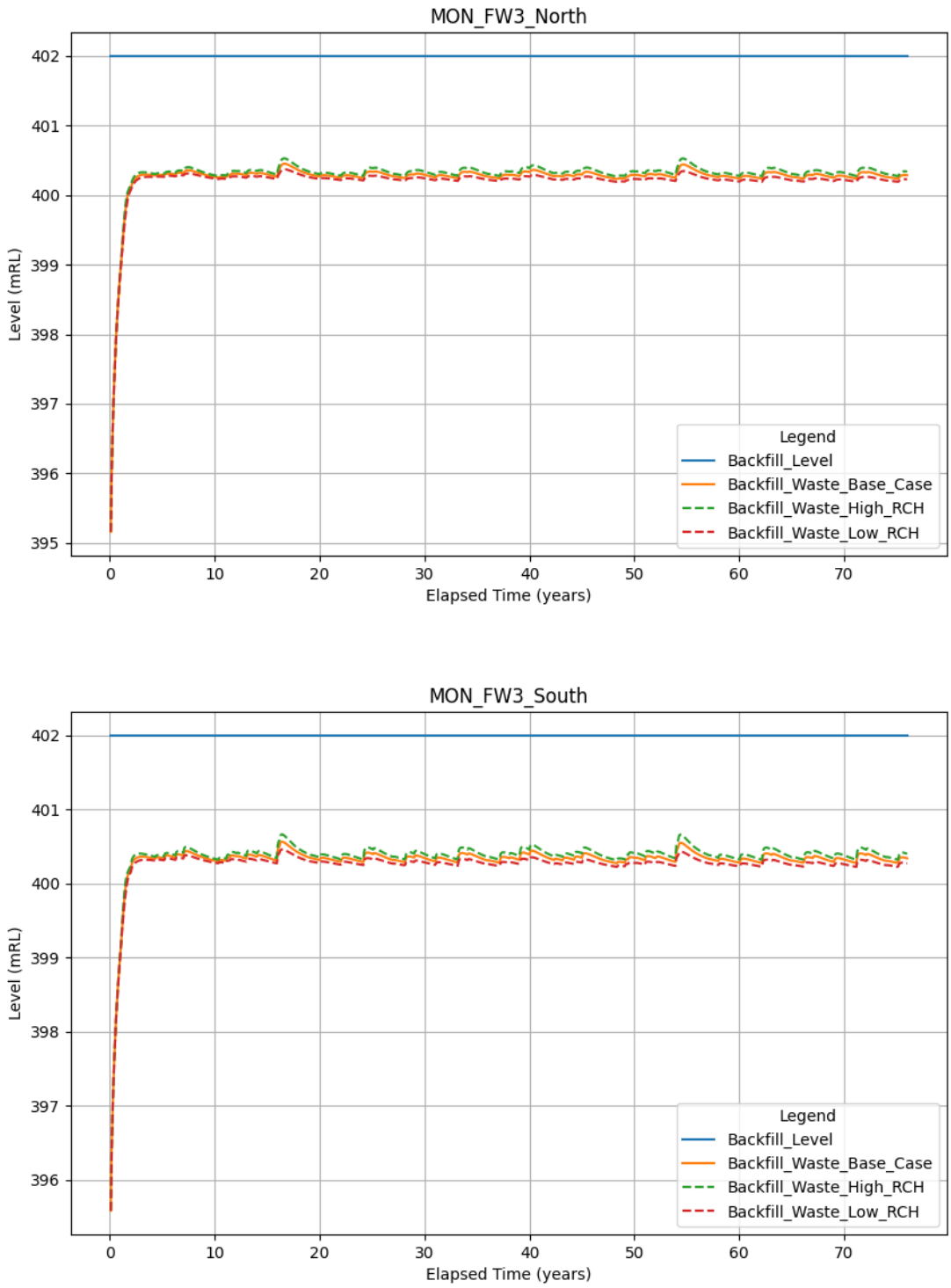

Figure B-13 Predicted pit water level recovery at Fridge West

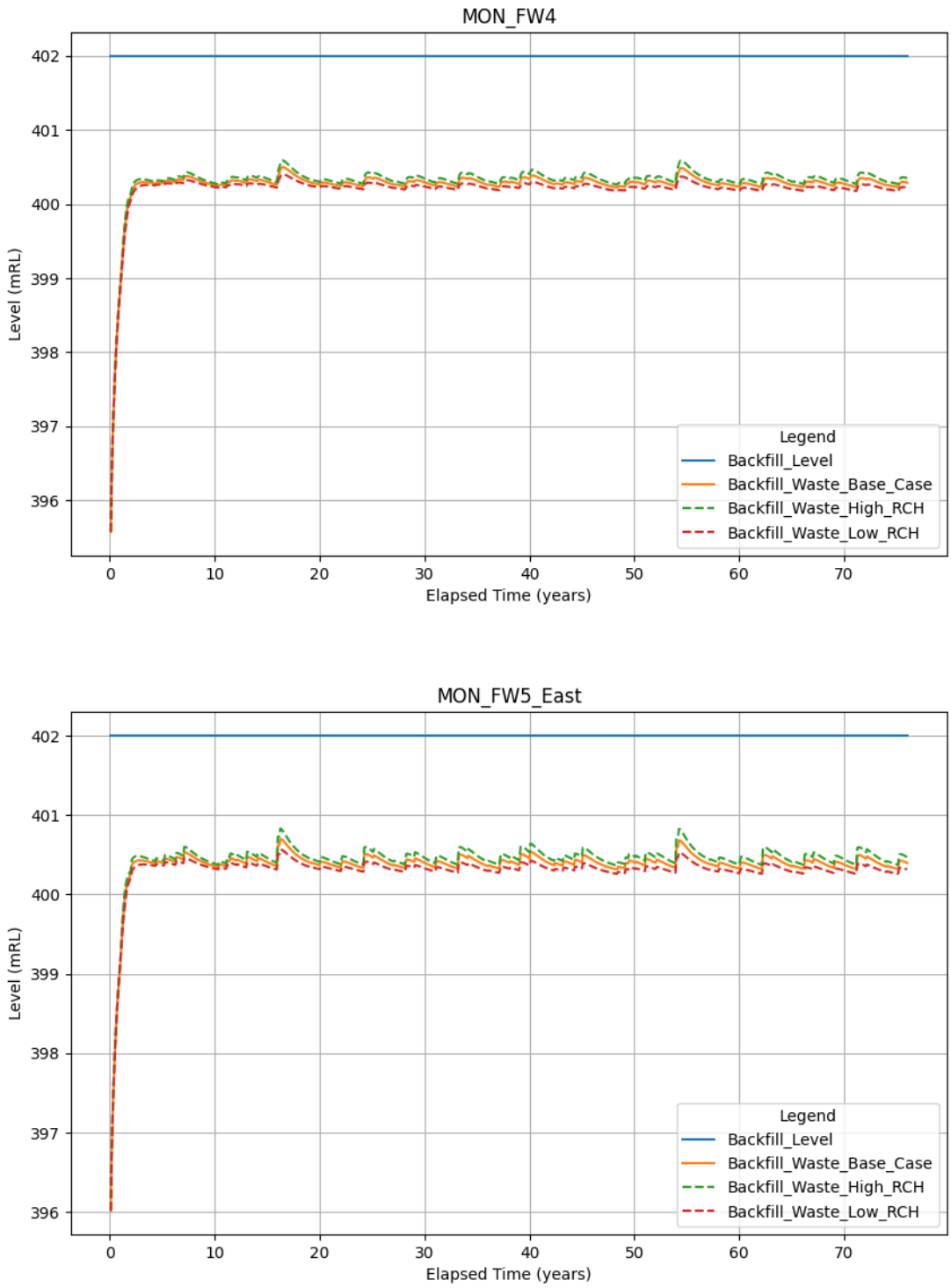

Figure B-14 Predicted pit water level recovery at Fridge West

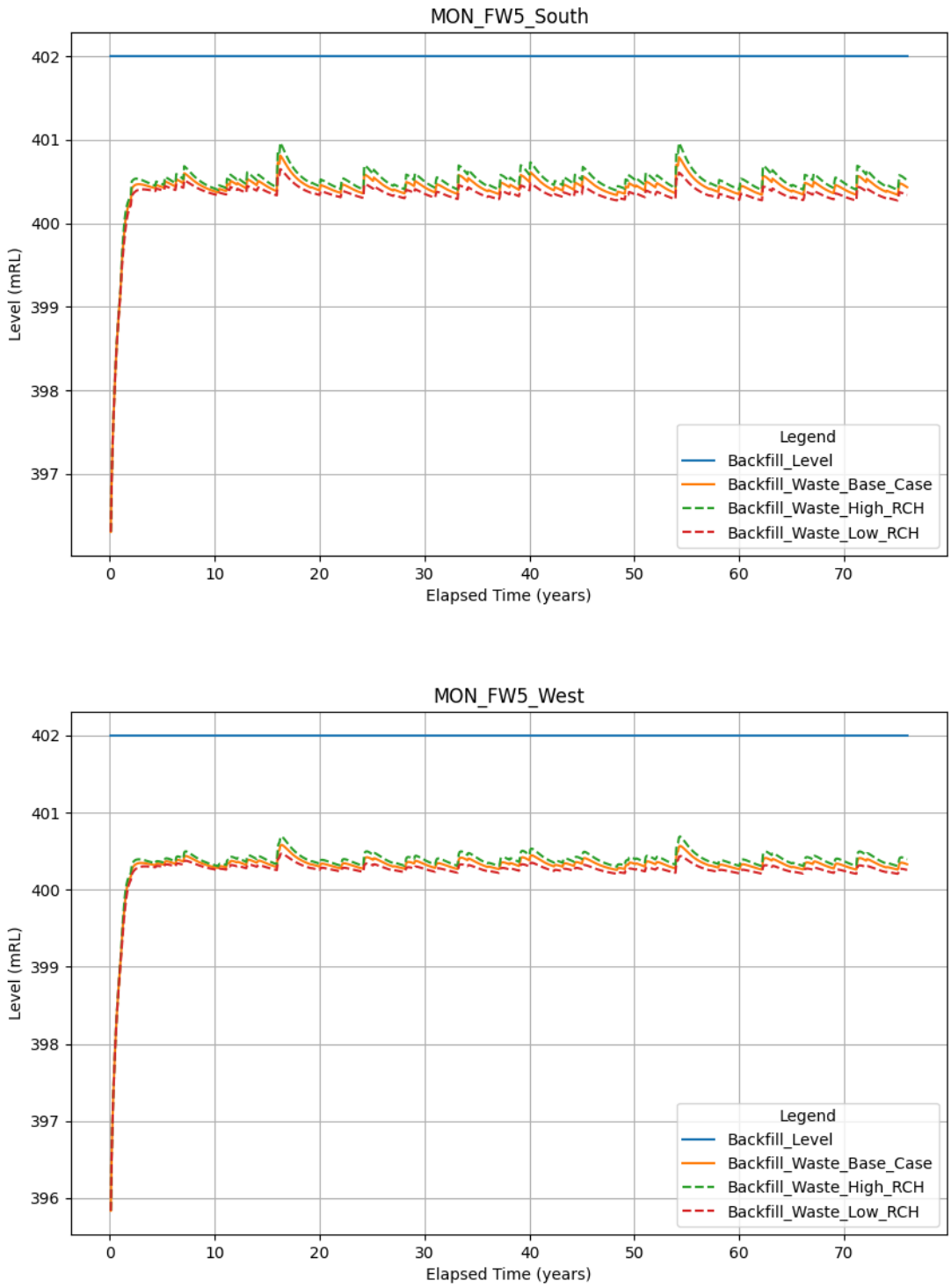

Figure B-15 Predicted pit water level recovery at Fridge West

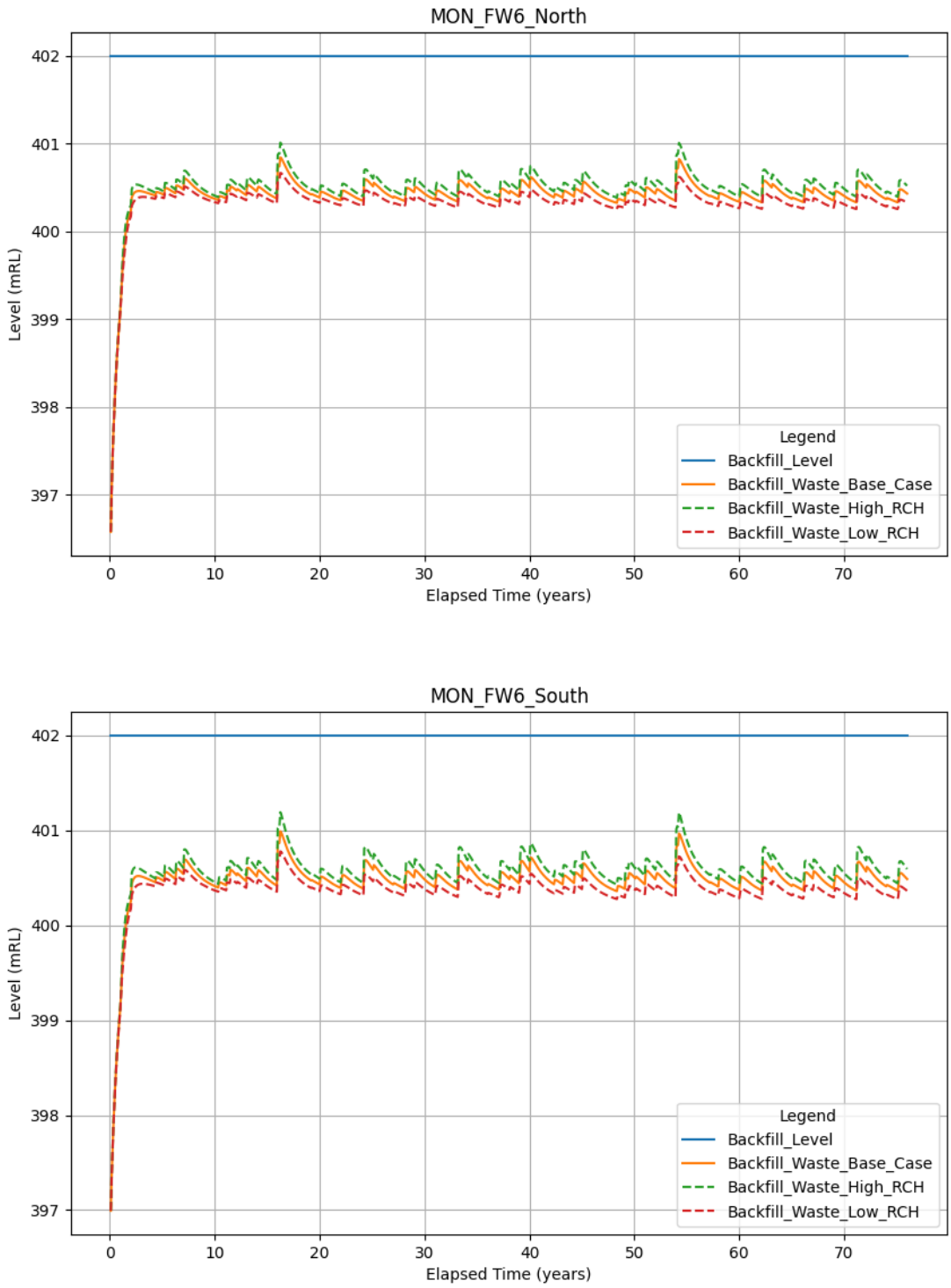

Figure B-16 Predicted pit water level recovery at Fridge West

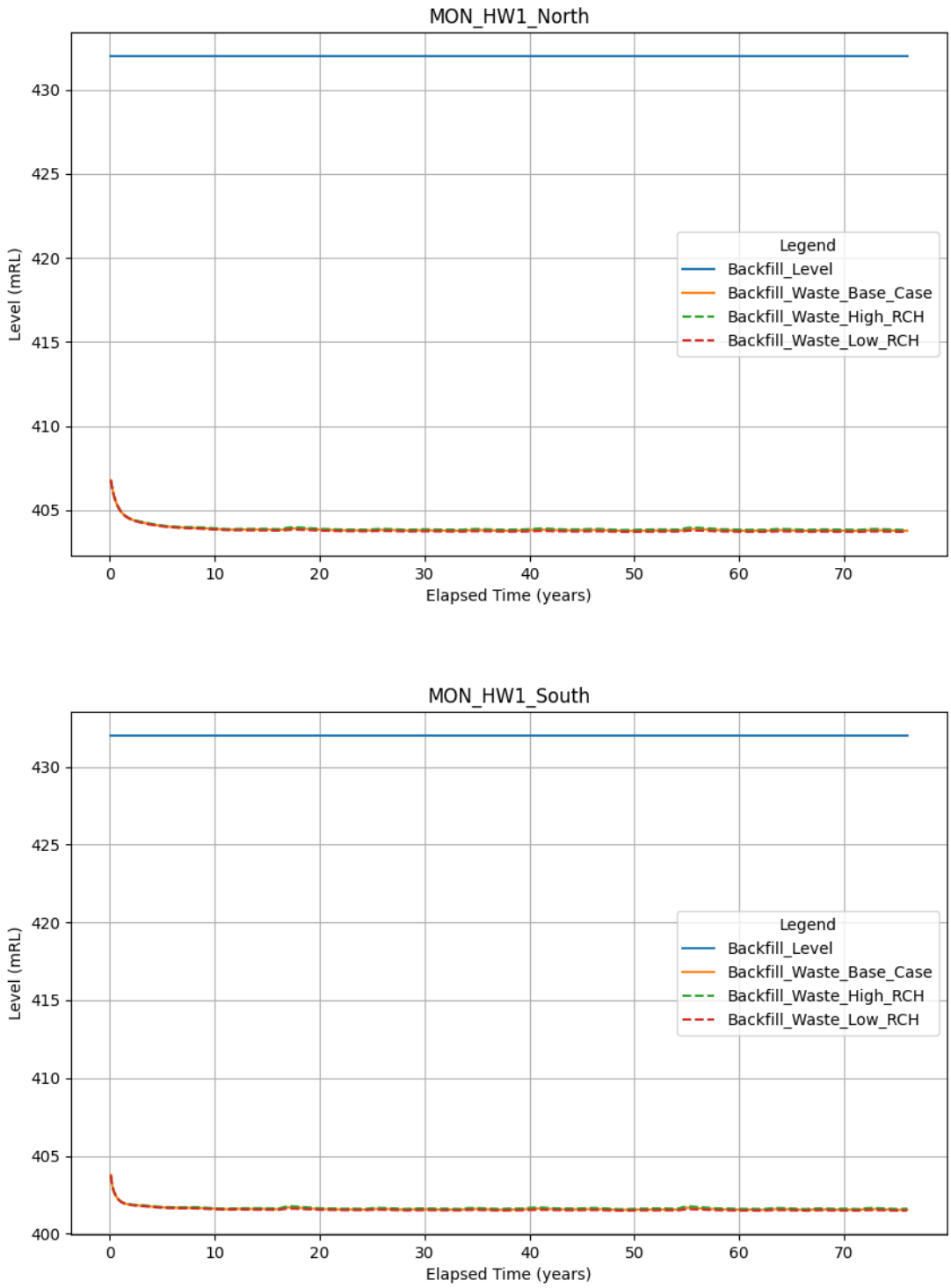

Figure B-17 Predicted pit water level recovery at Horseshoe West

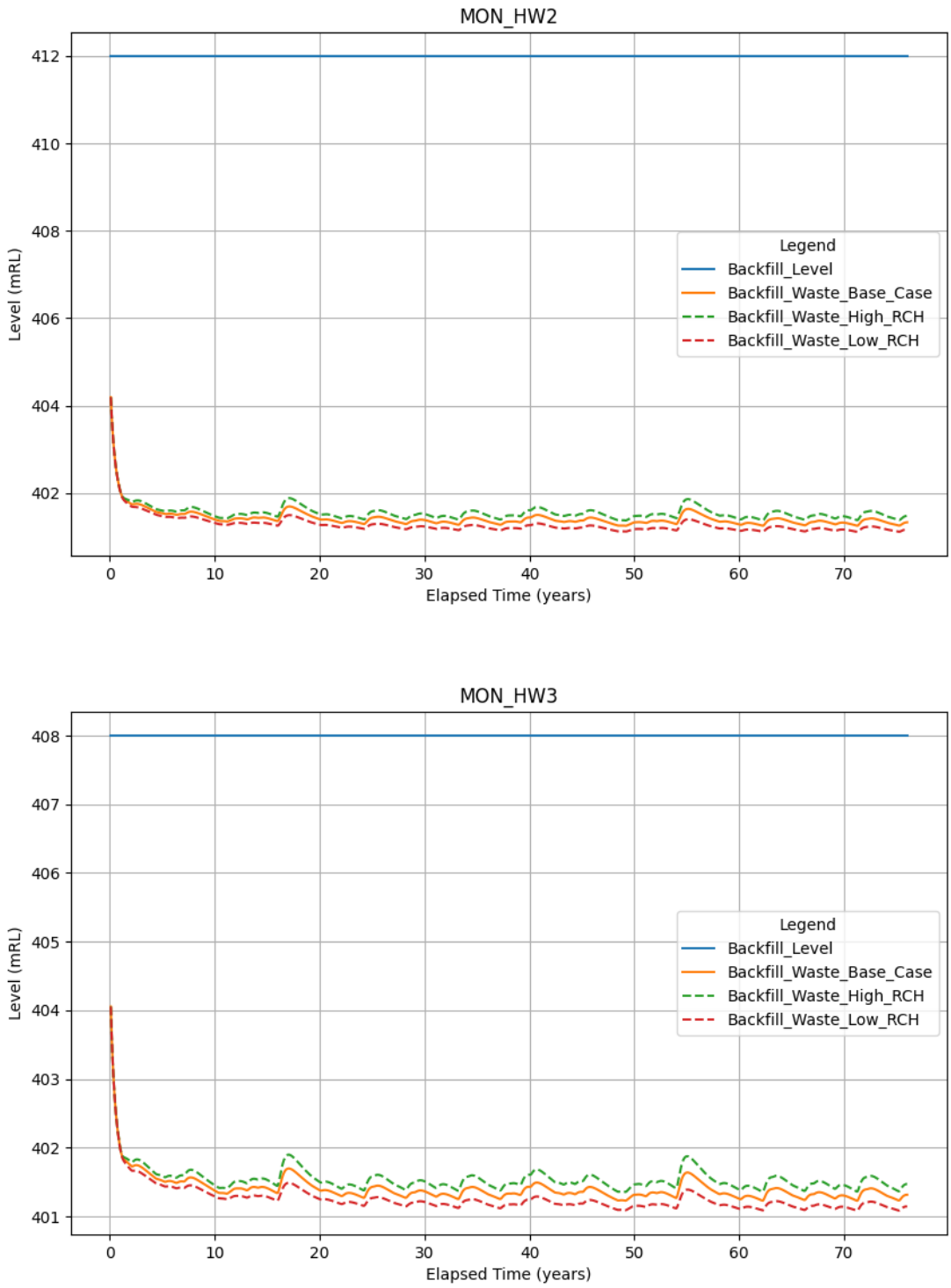

Figure B-18 Predicted pit water level recovery at Horseshoe West

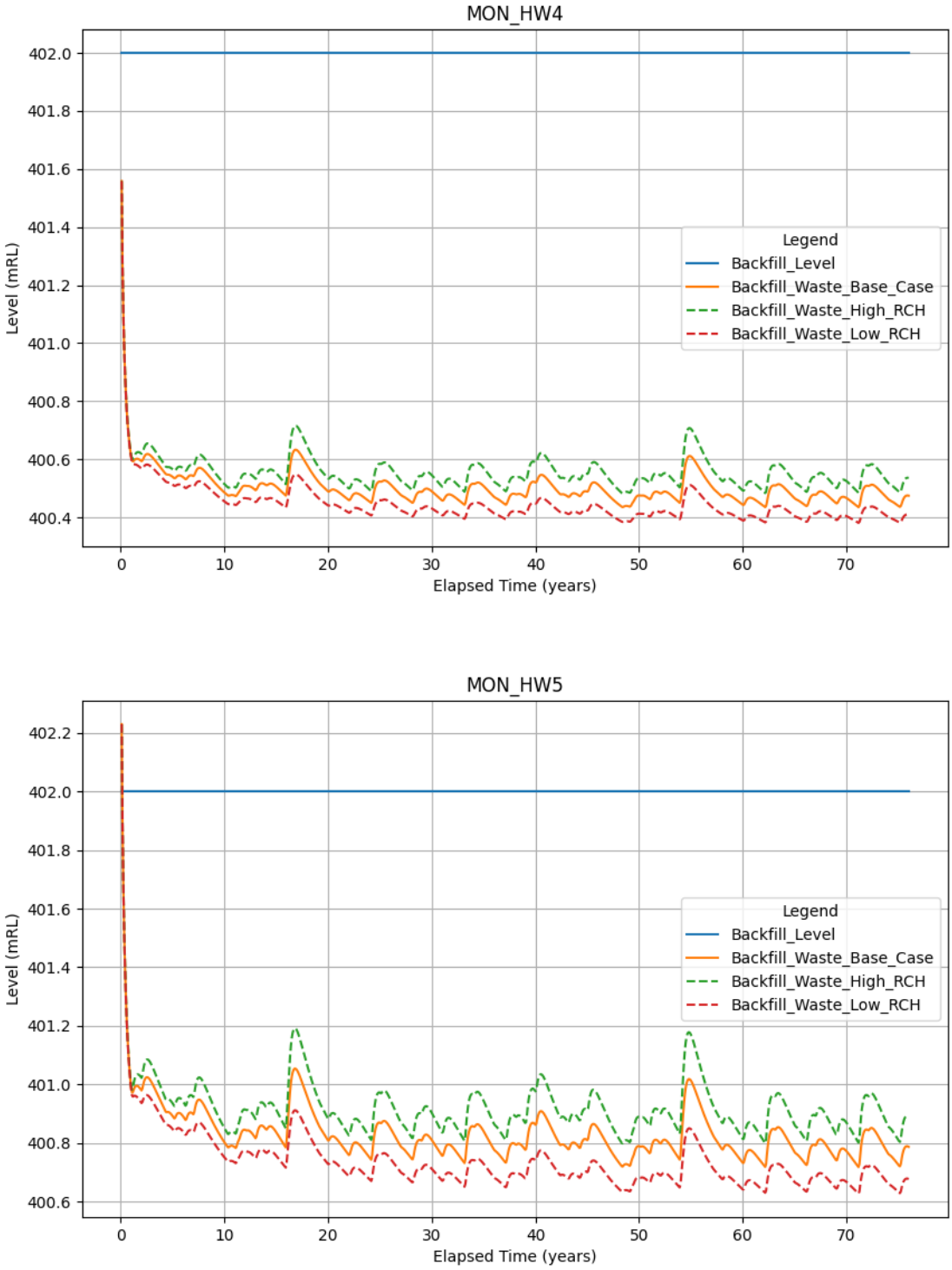

Figure B-19 Predicted pit water level recovery at Horseshoe West

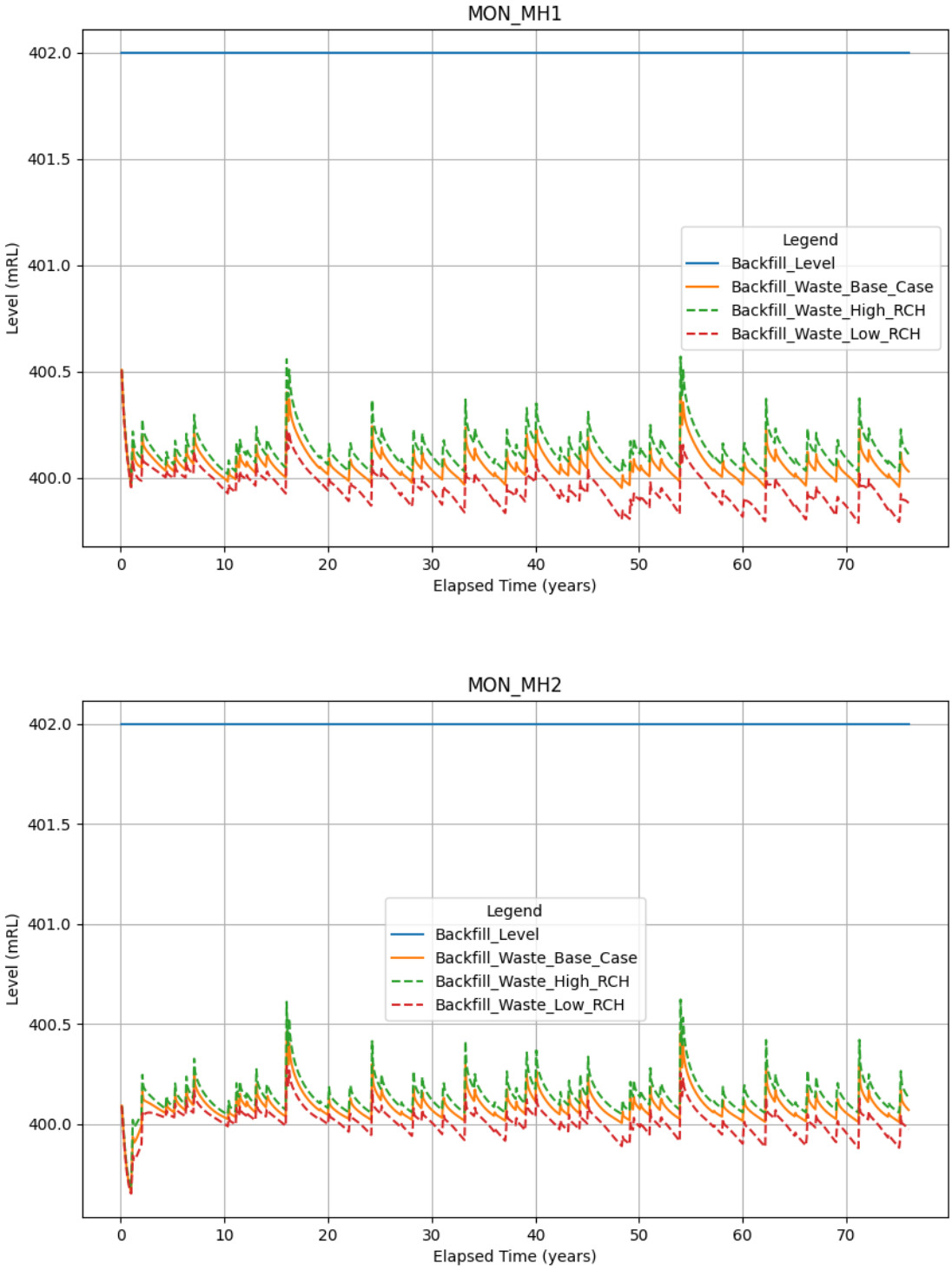

Figure B-20 Predicted pit water level recovery at Murray Hill

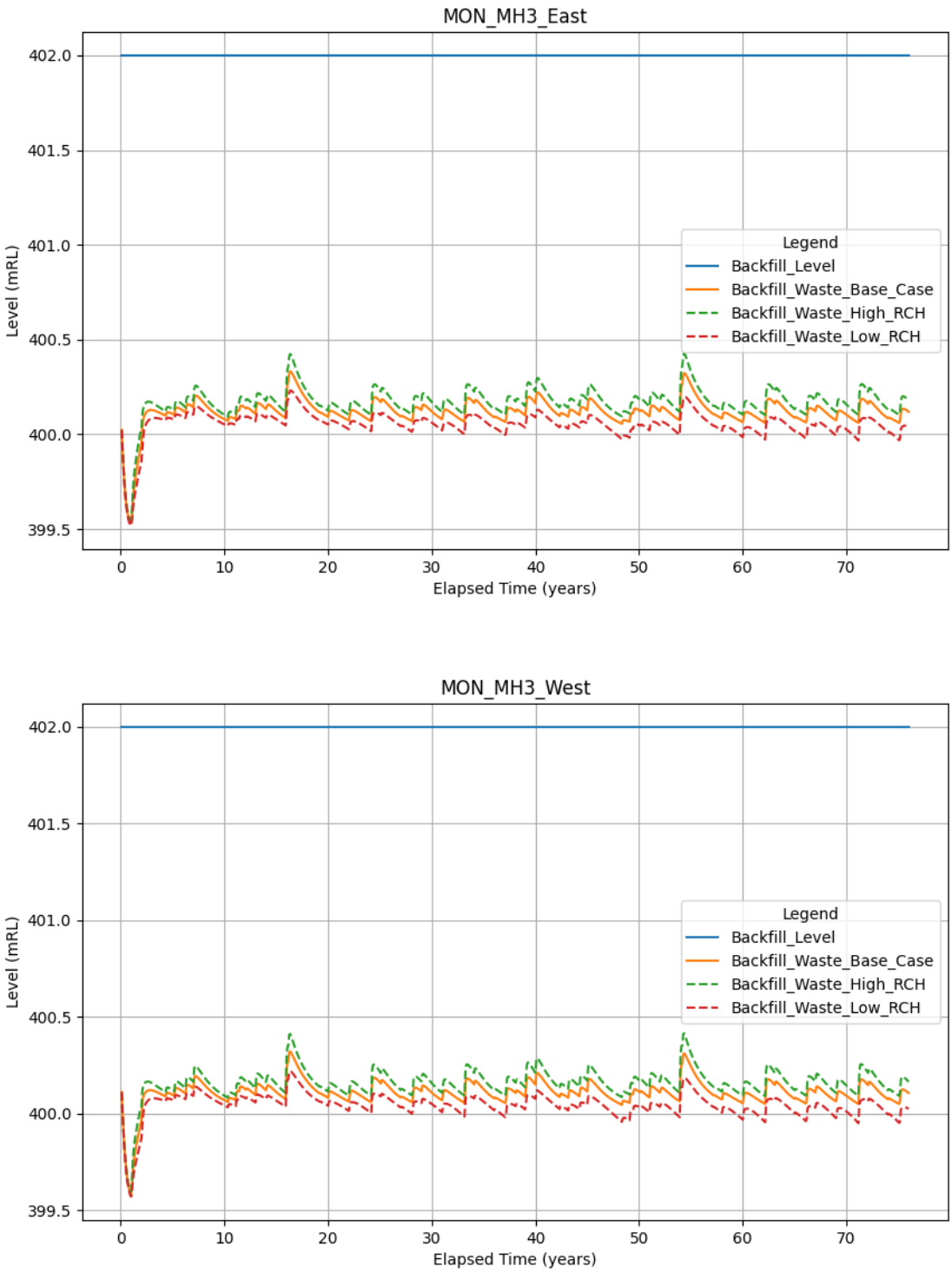

Figure B-21 Predicted pit water level recovery at Murray Hill

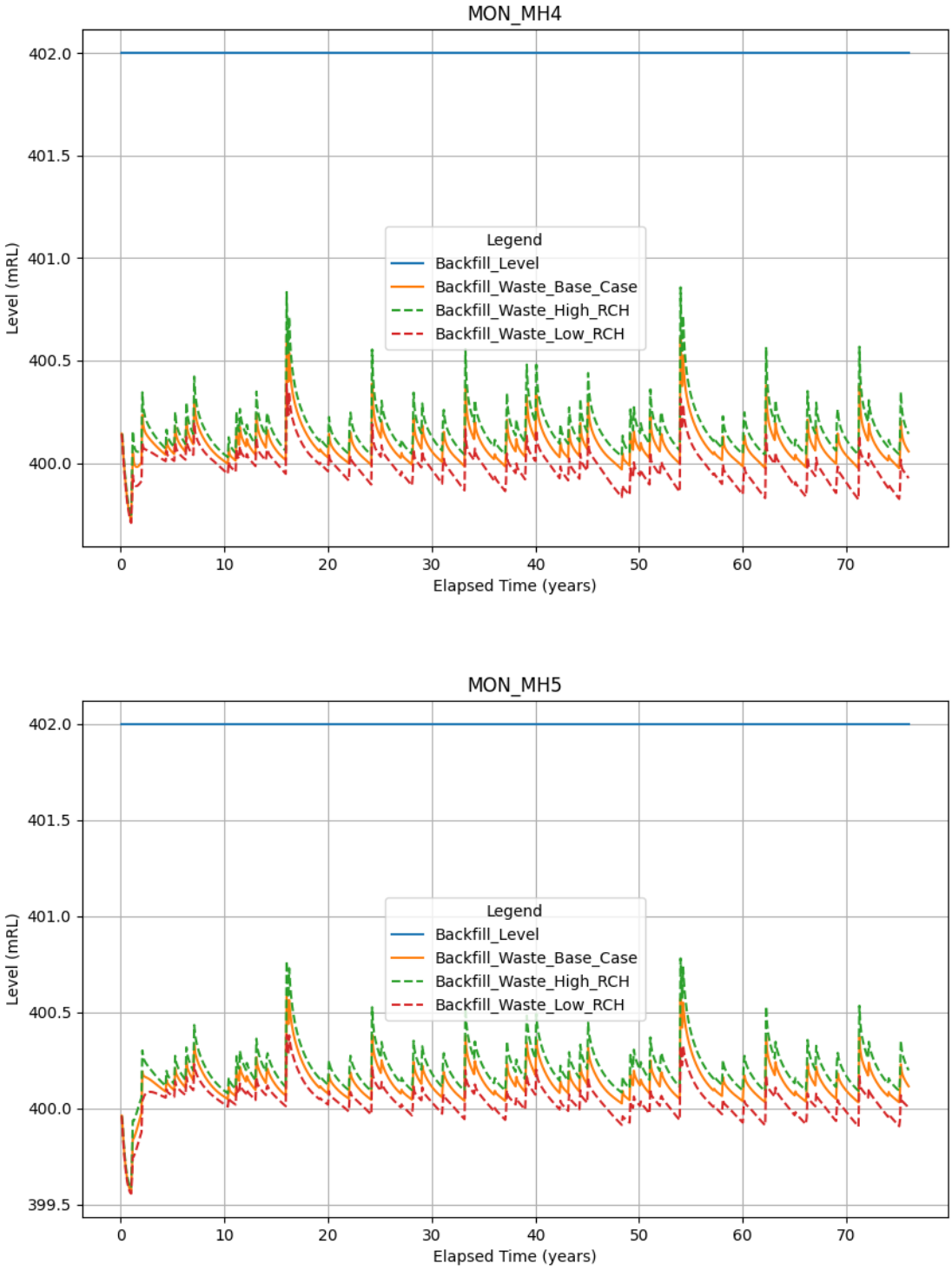

Figure B-22 Predicted pit water level recovery at Murray Hill

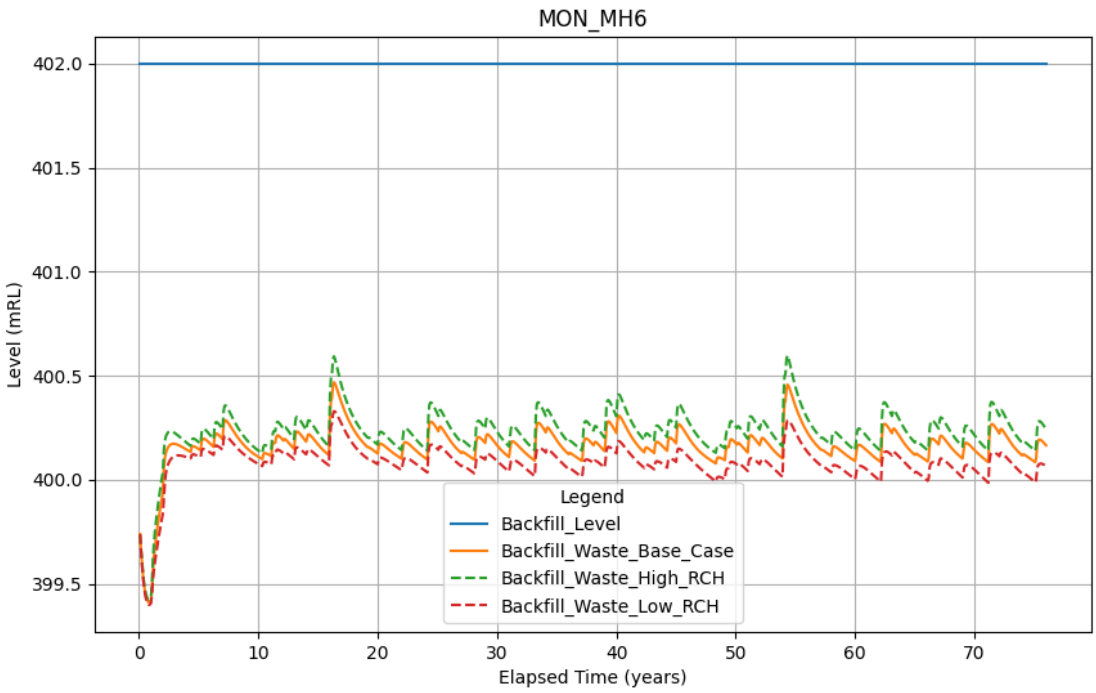

Figure B-23 Predicted pit water level recovery at Murray Hill

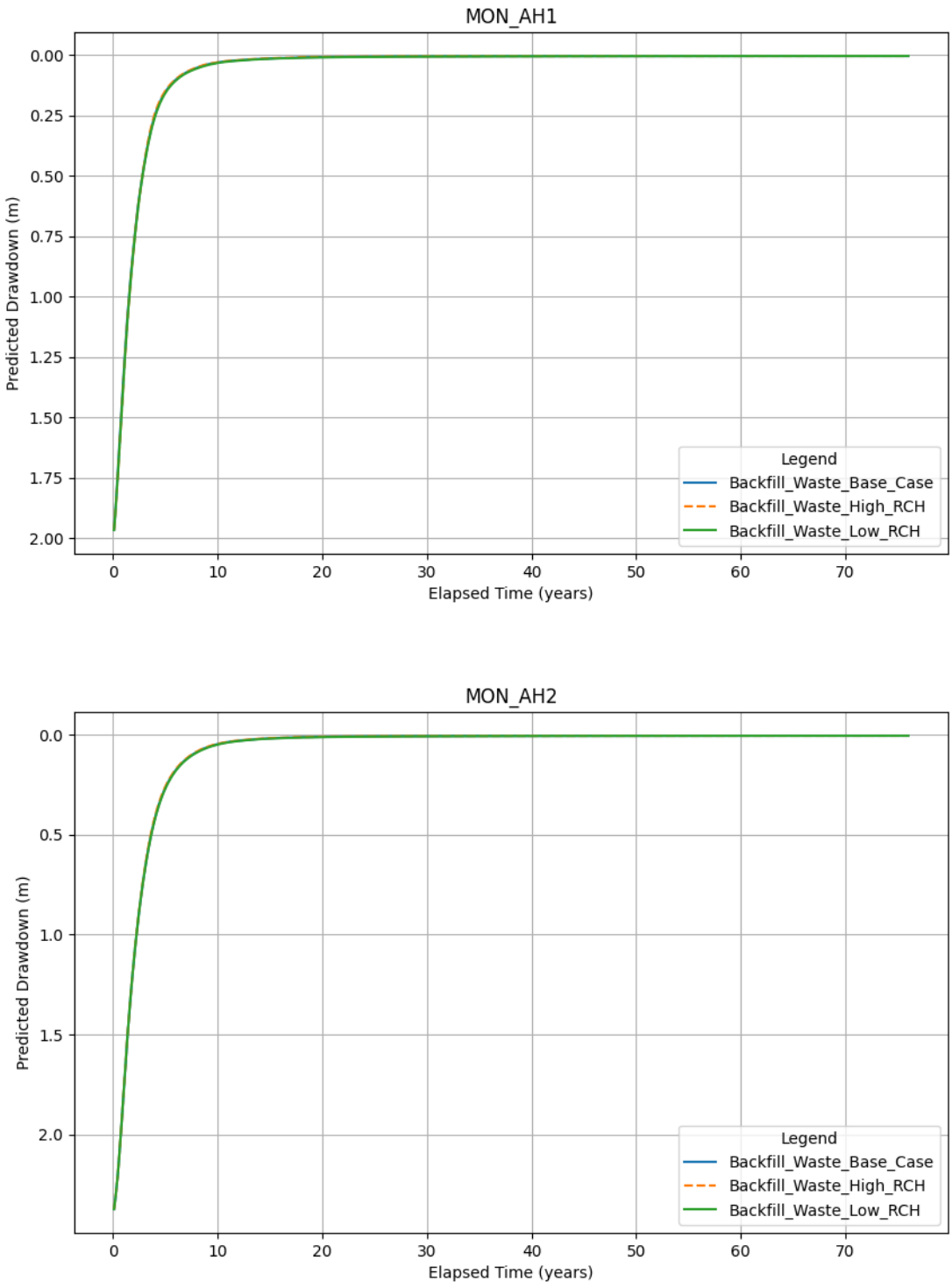

Figure B-24 Predicted aquifer recovery at Anticline Hill

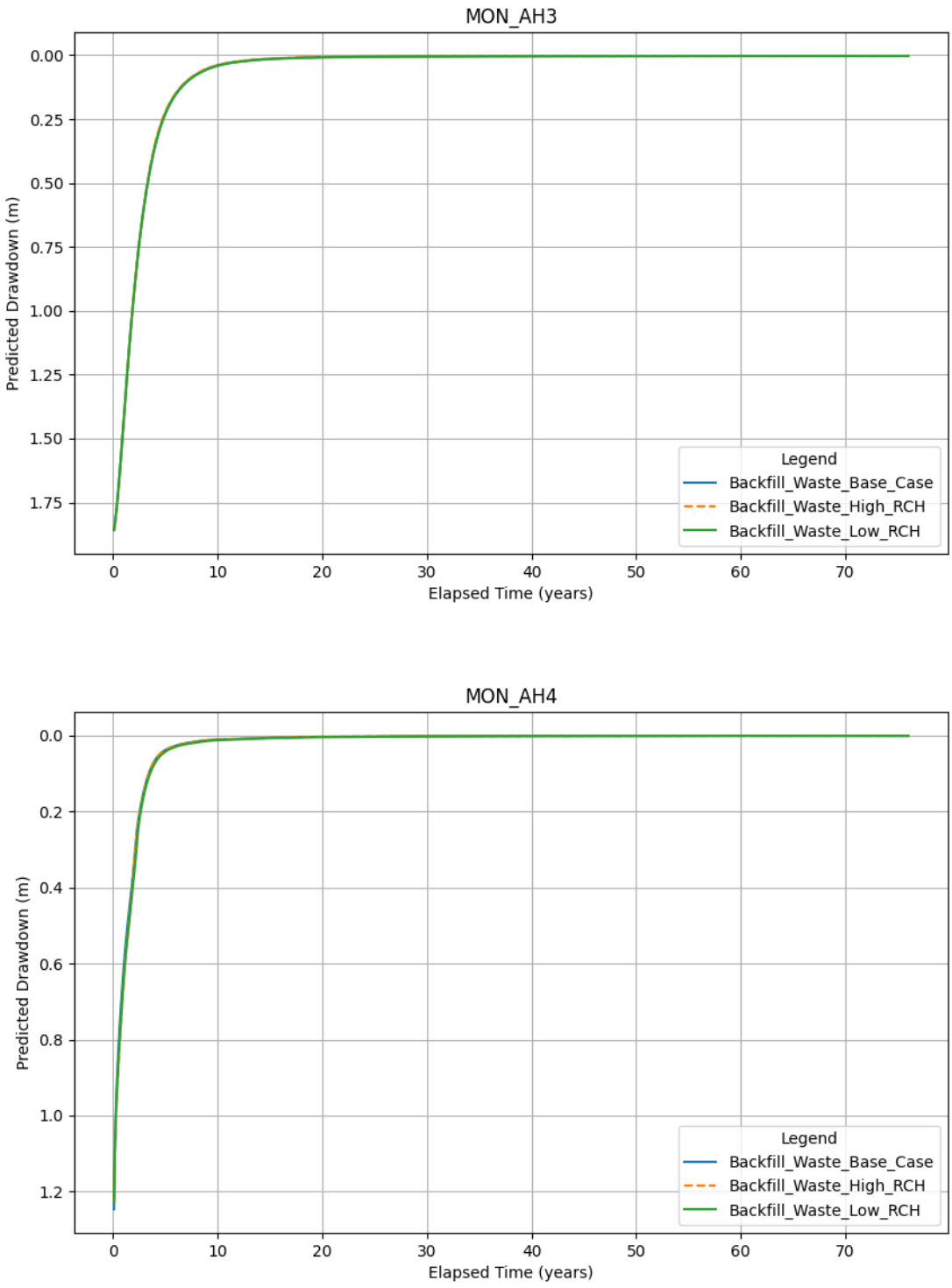

Figure B-25 Predicted aquifer recovery at Anticline Hill

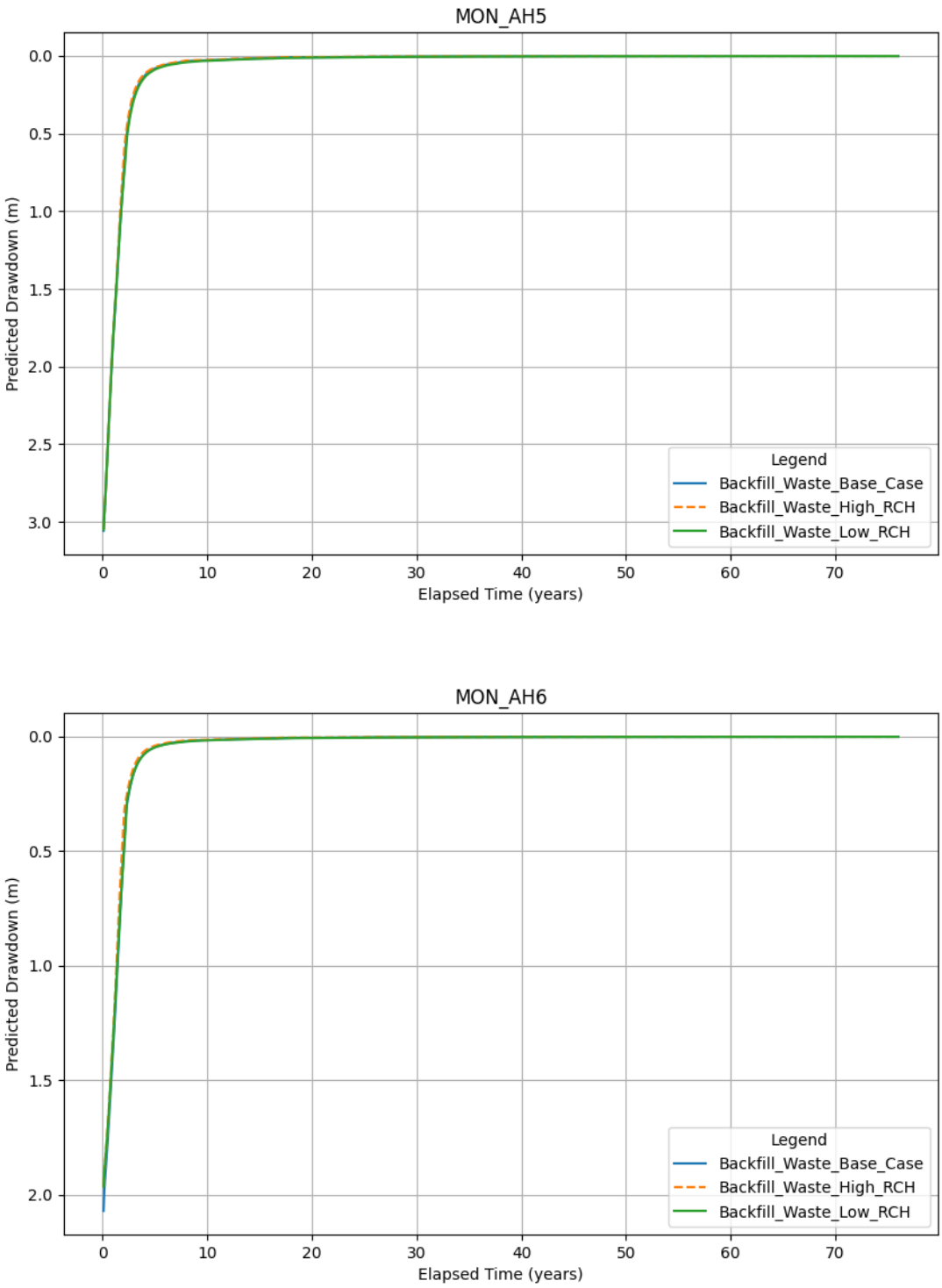

Figure B-26 Predicted aquifer recovery at Anticline Hill

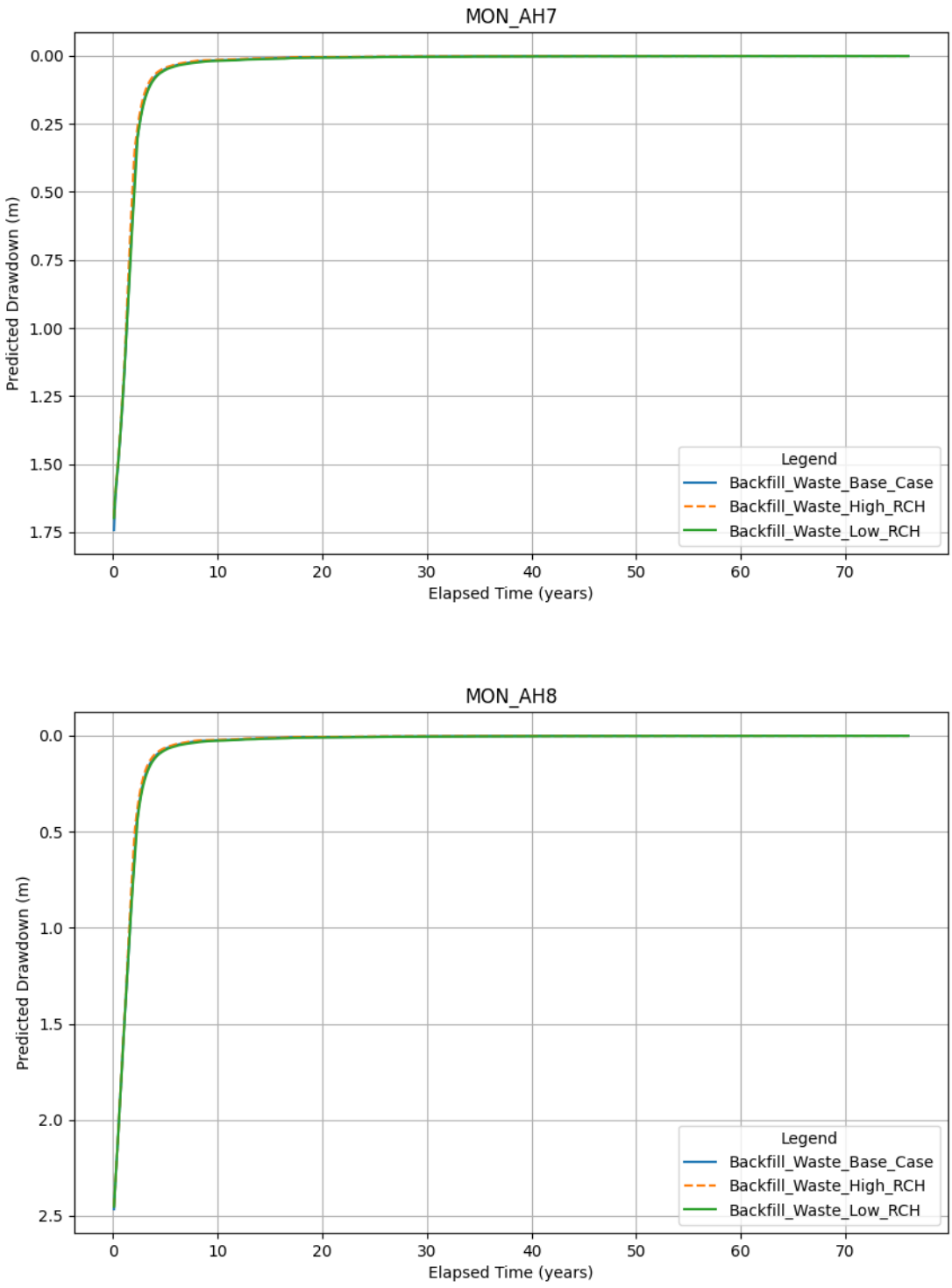

Figure B-27 Predicted aquifer recovery at Anticline Hill

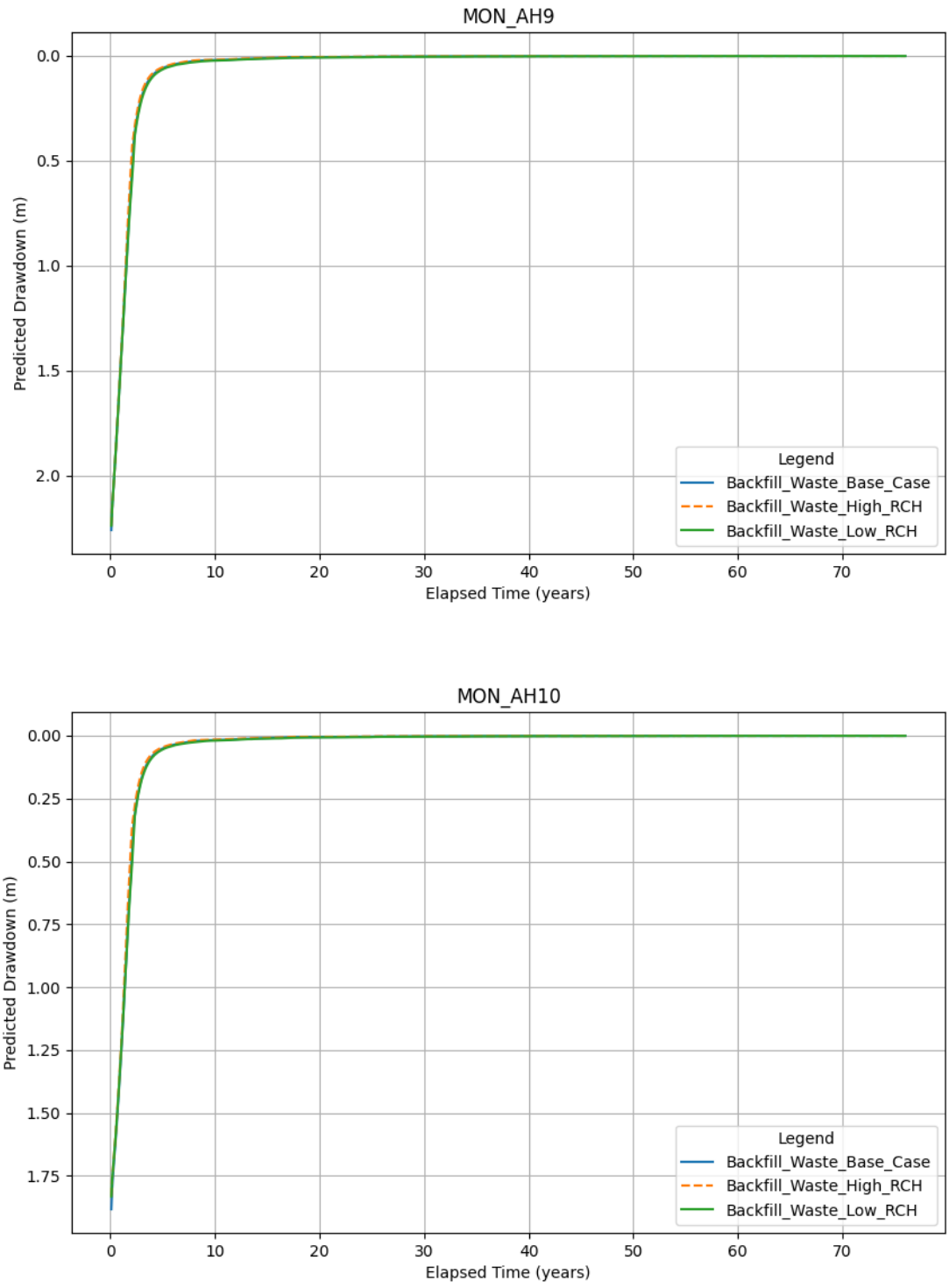

Figure B-28 Predicted aquifer recovery at Anticline Hill

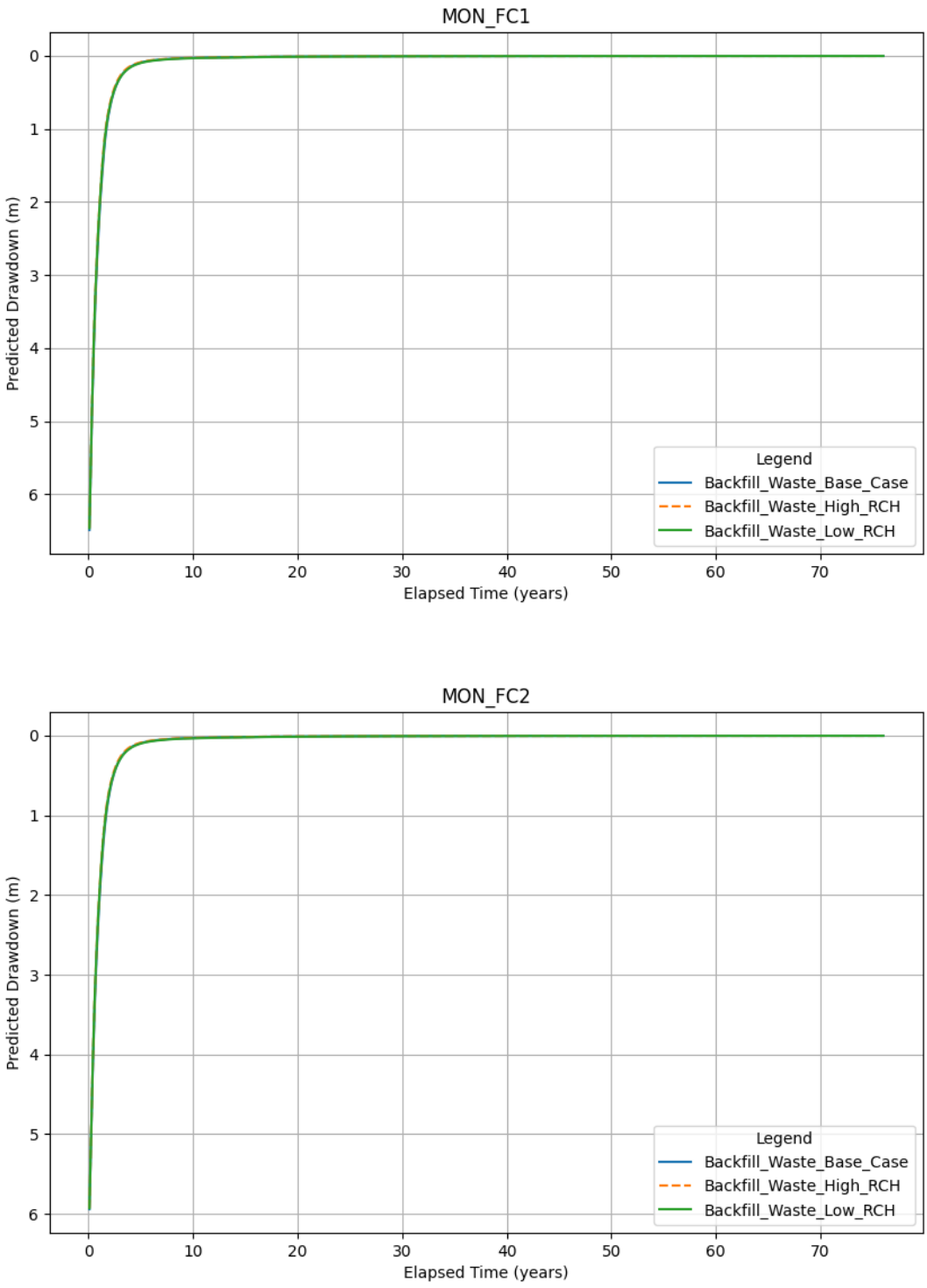

Figure B-29 Predicted aquifer recovery at Fridge Central

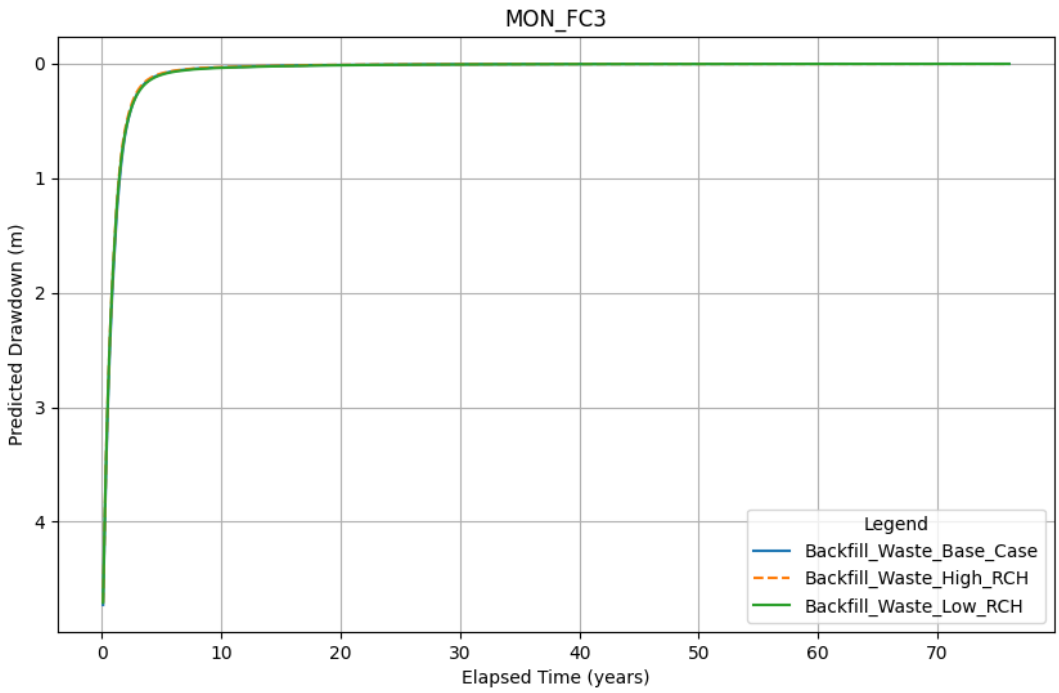

Figure B-30 Predicted aquifer recovery at Fridge Central

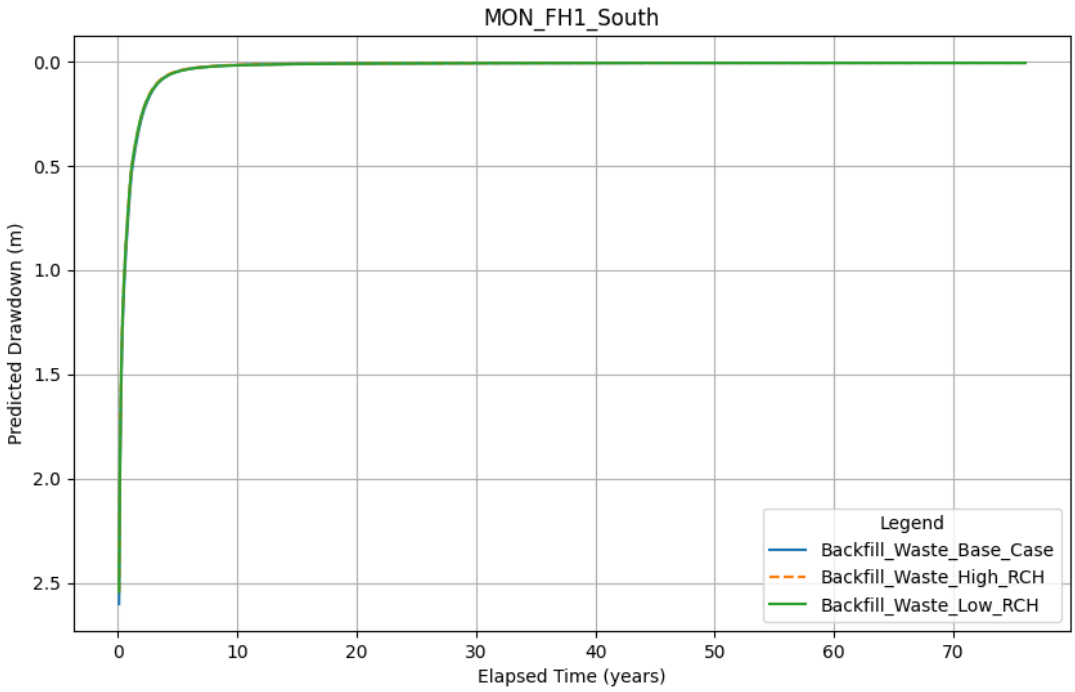

Figure B-31 Predicted aquifer recovery at Fridge Hill

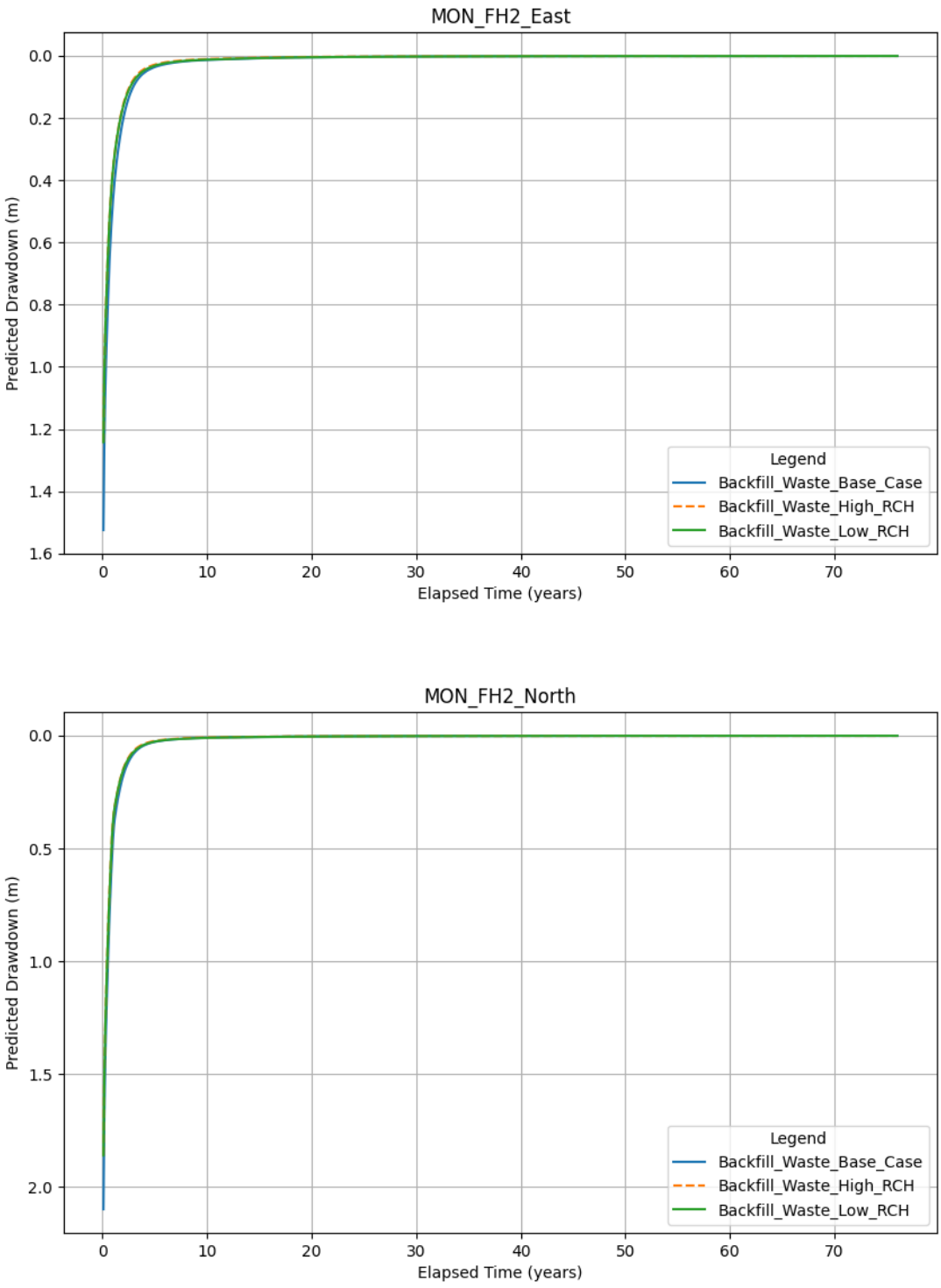

Figure B-32 Predicted aquifer recovery at Fridge Hill

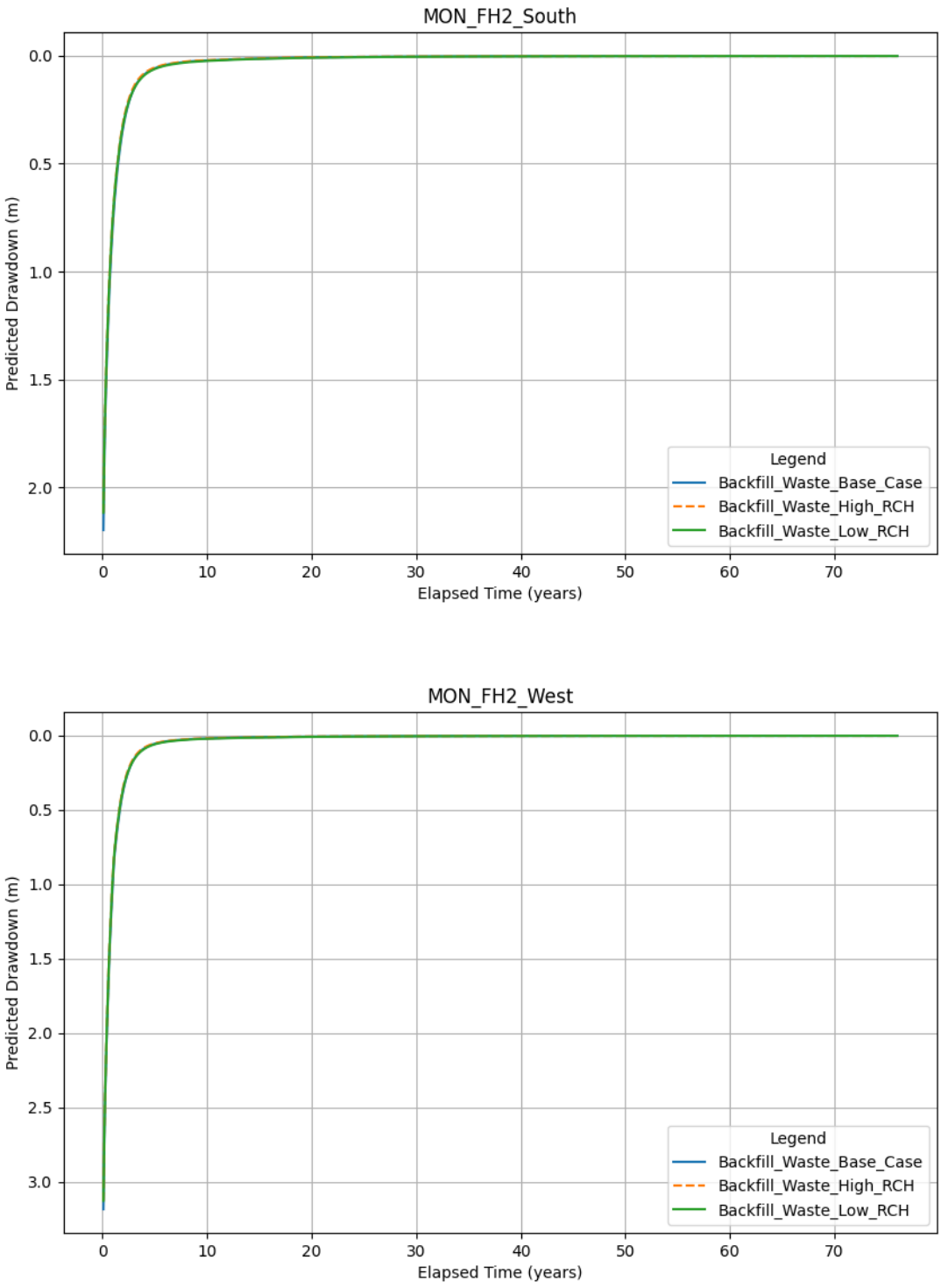

Figure B-33 Predicted aquifer recovery at Fridge Hill

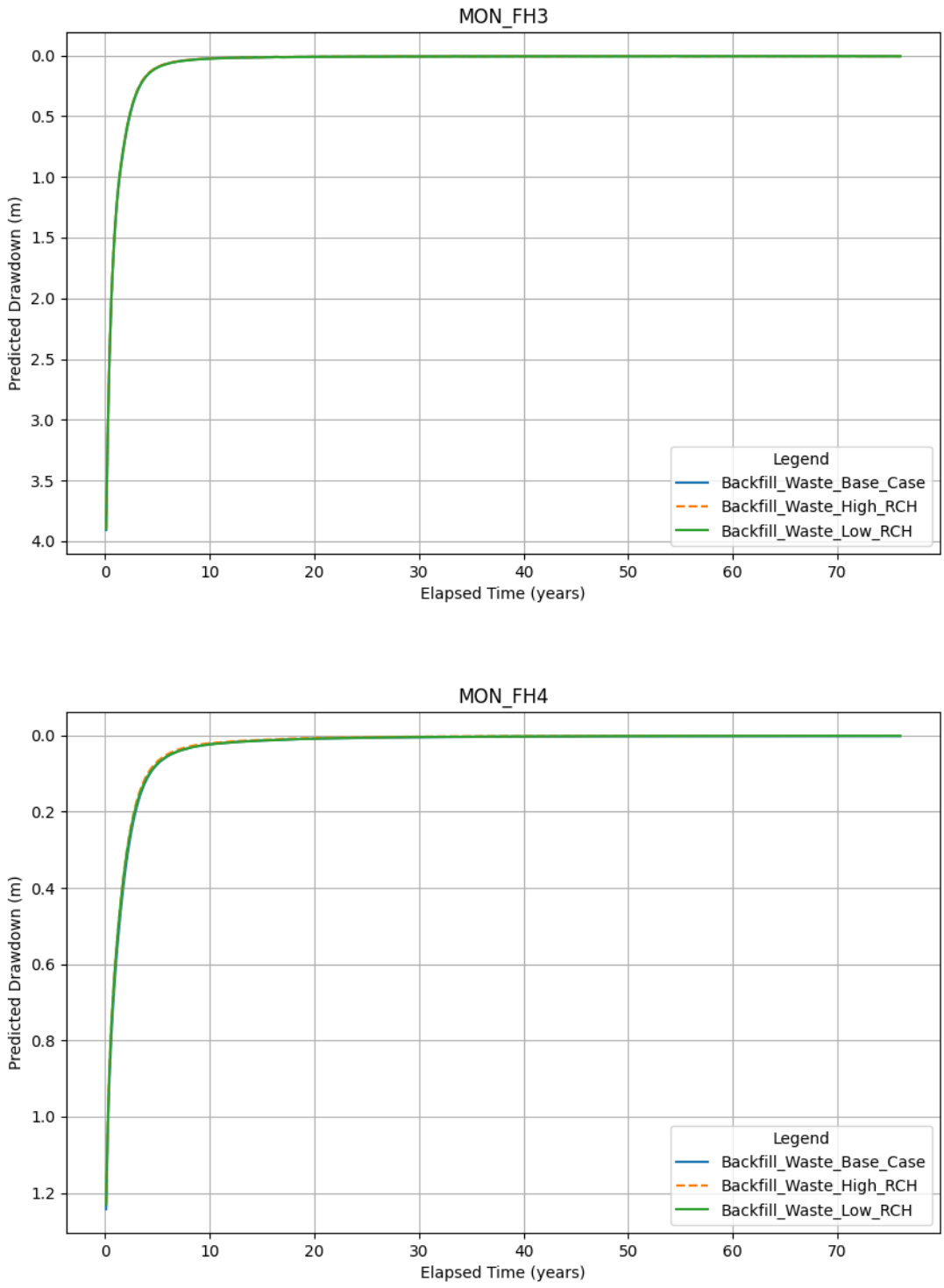

Figure B-34 Predicted aquifer recovery at Fridge Hill

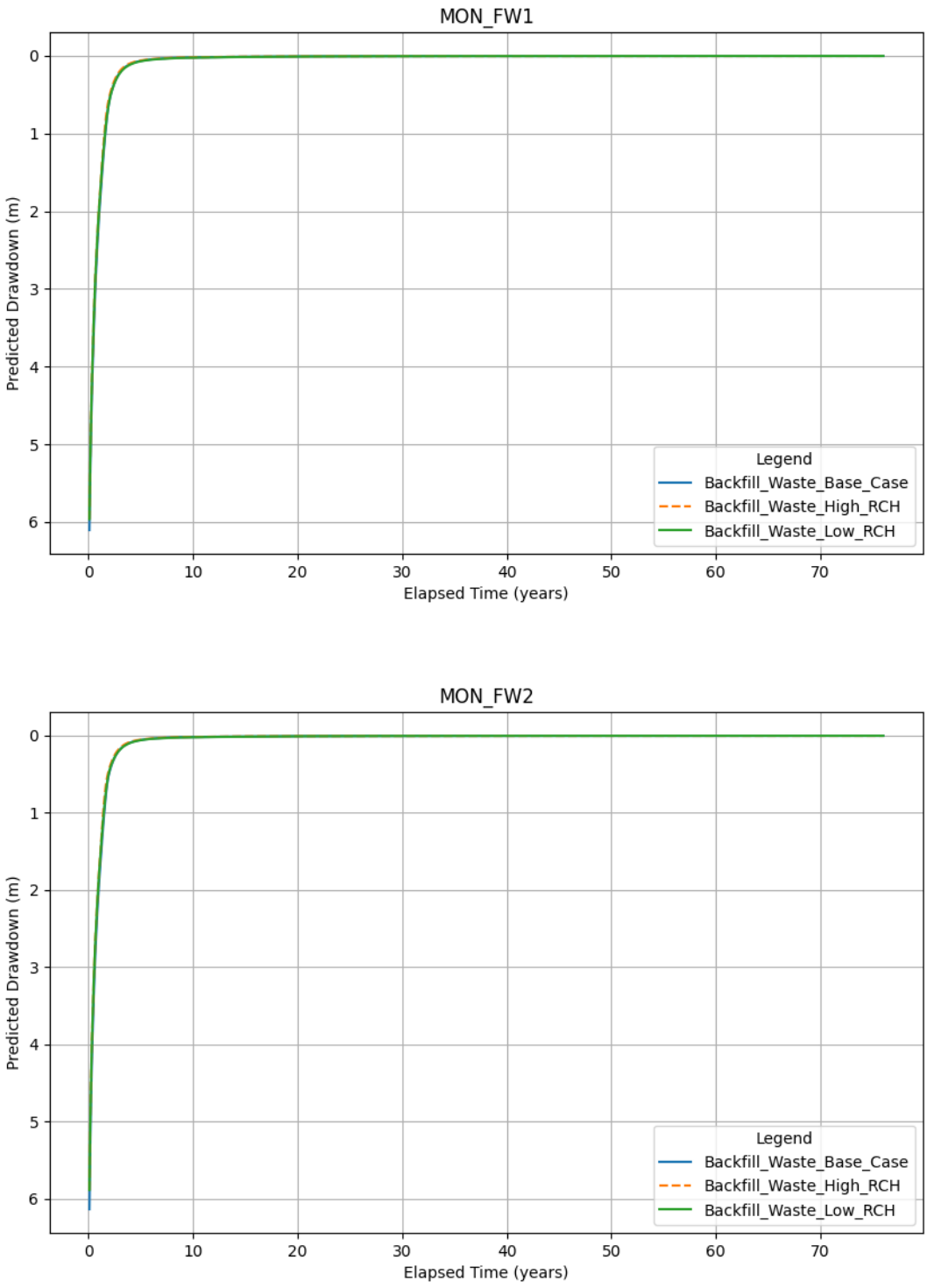

Figure B-35 Predicted aquifer recovery at Fridge West

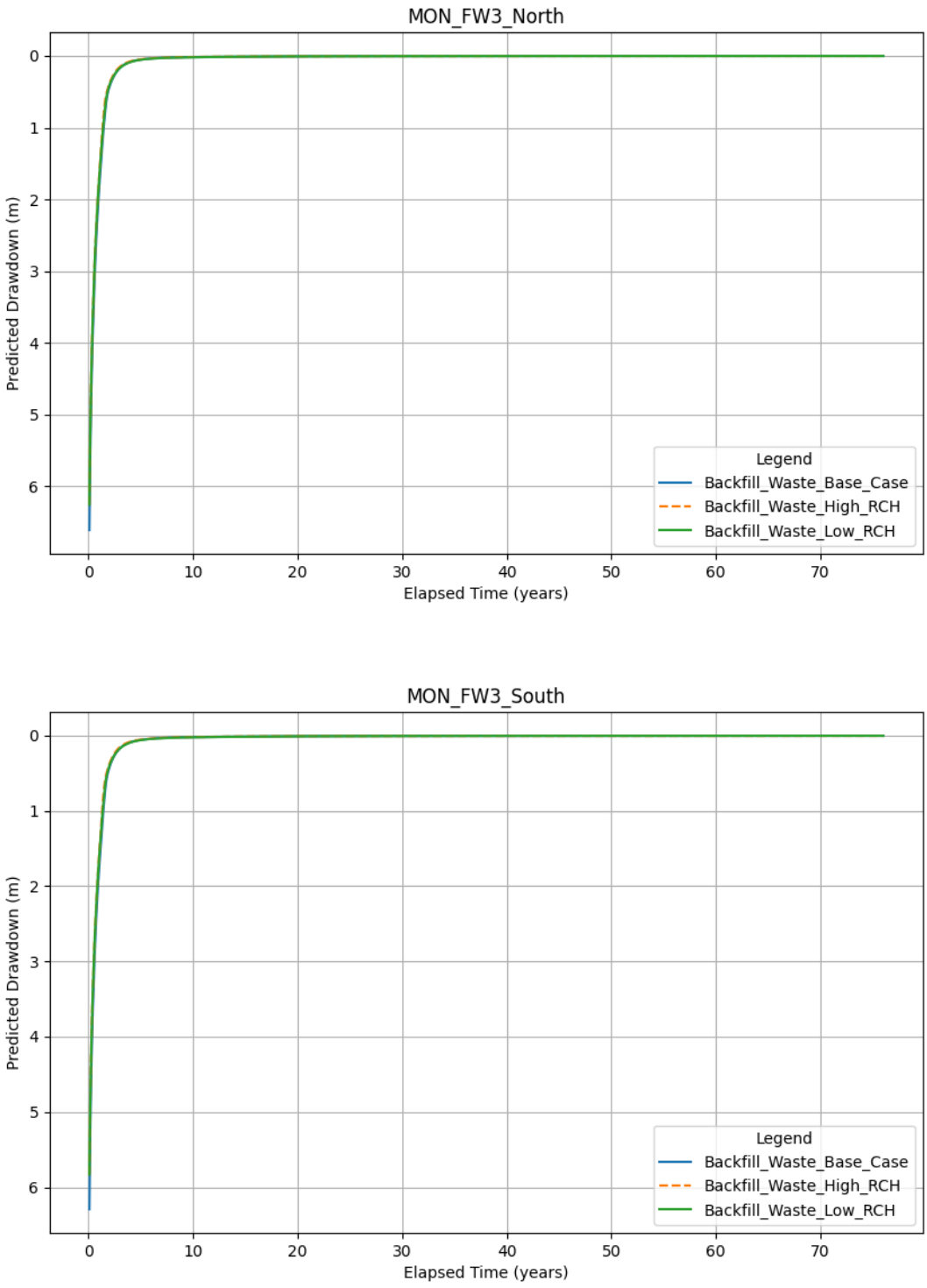

Figure B-36 Predicted aquifer recovery at Fridge West

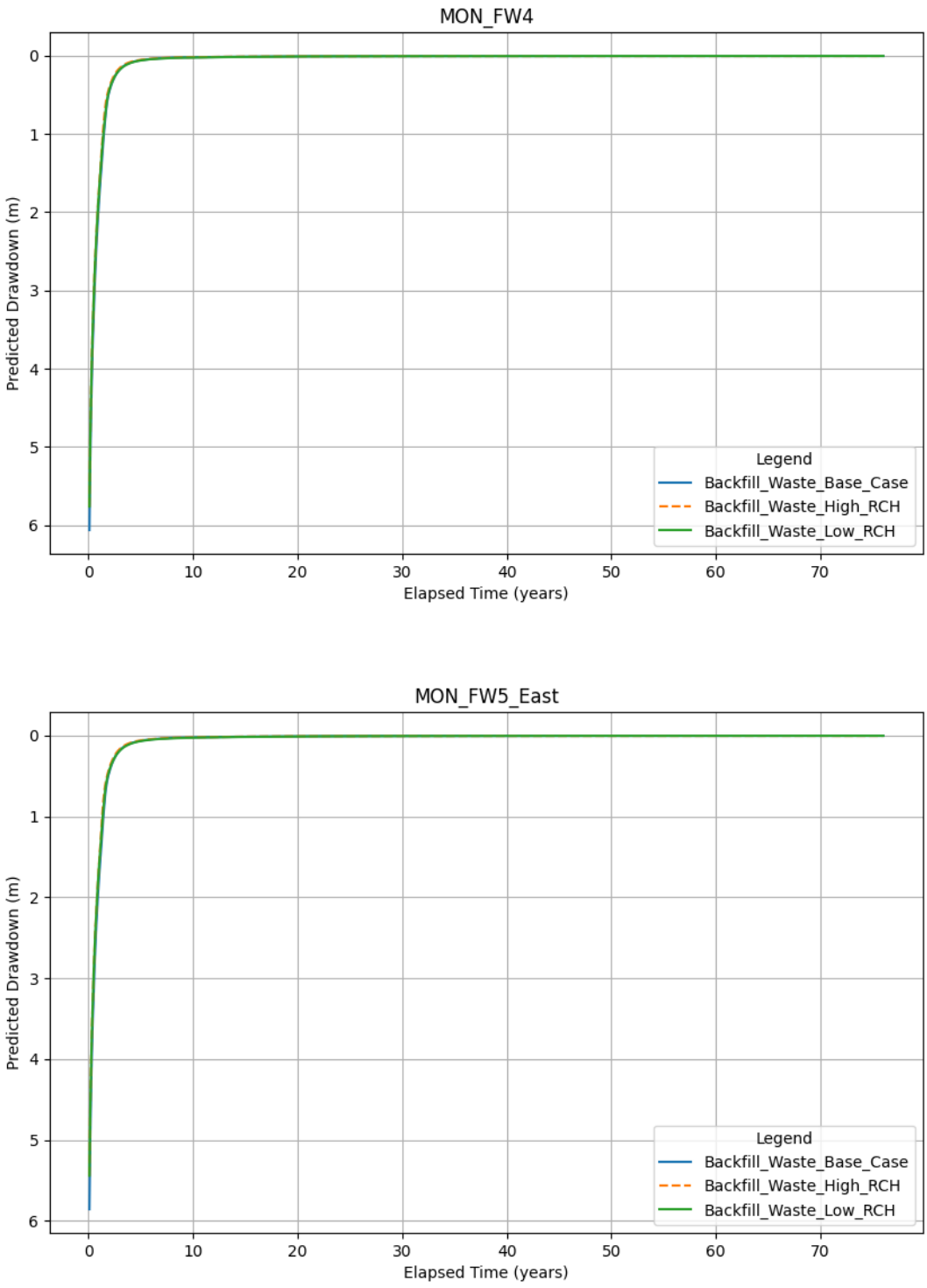

Figure B-37 Predicted aquifer recovery at Fridge West

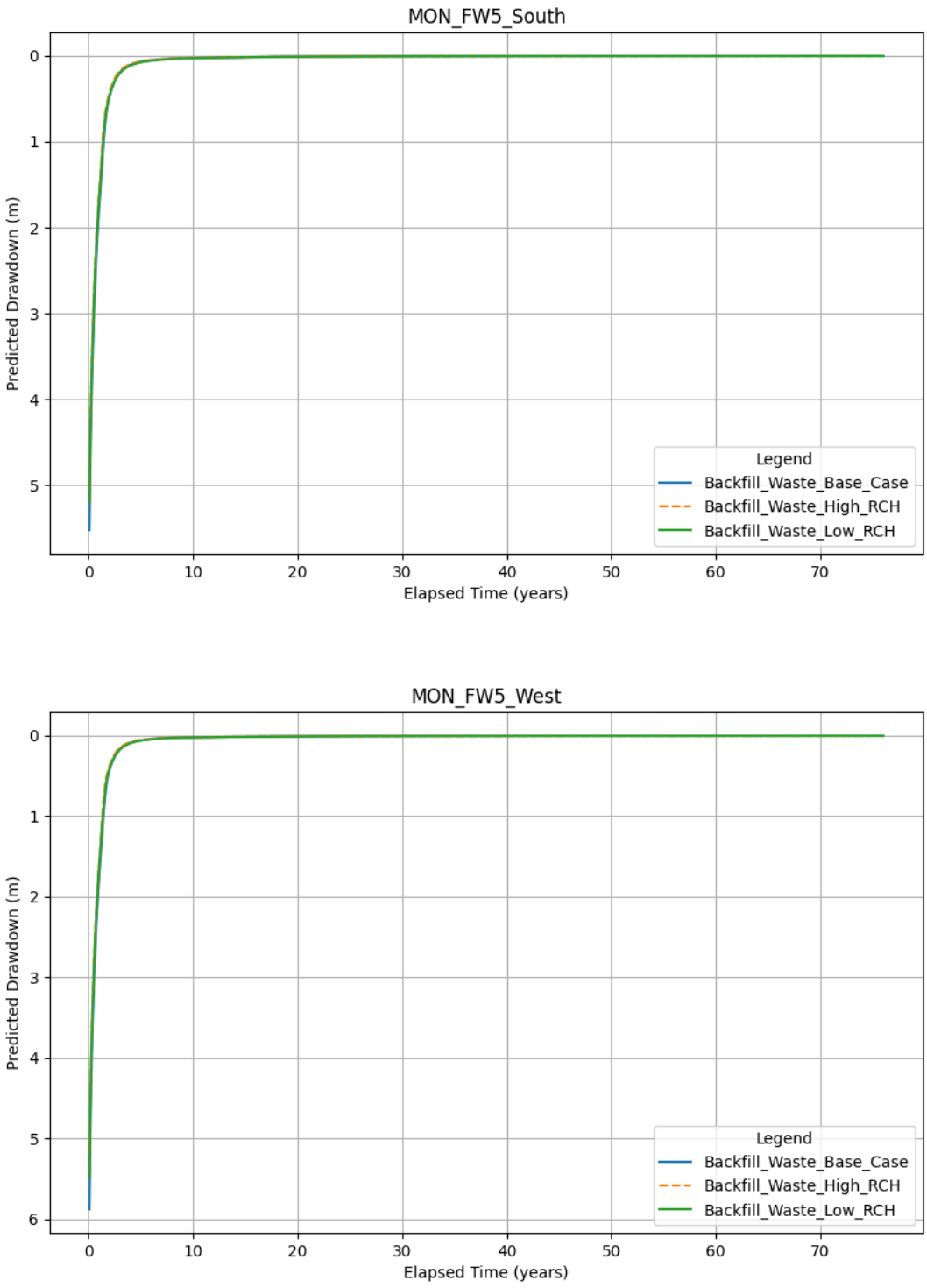

Figure B-38 Predicted aquifer recovery at Fridge West

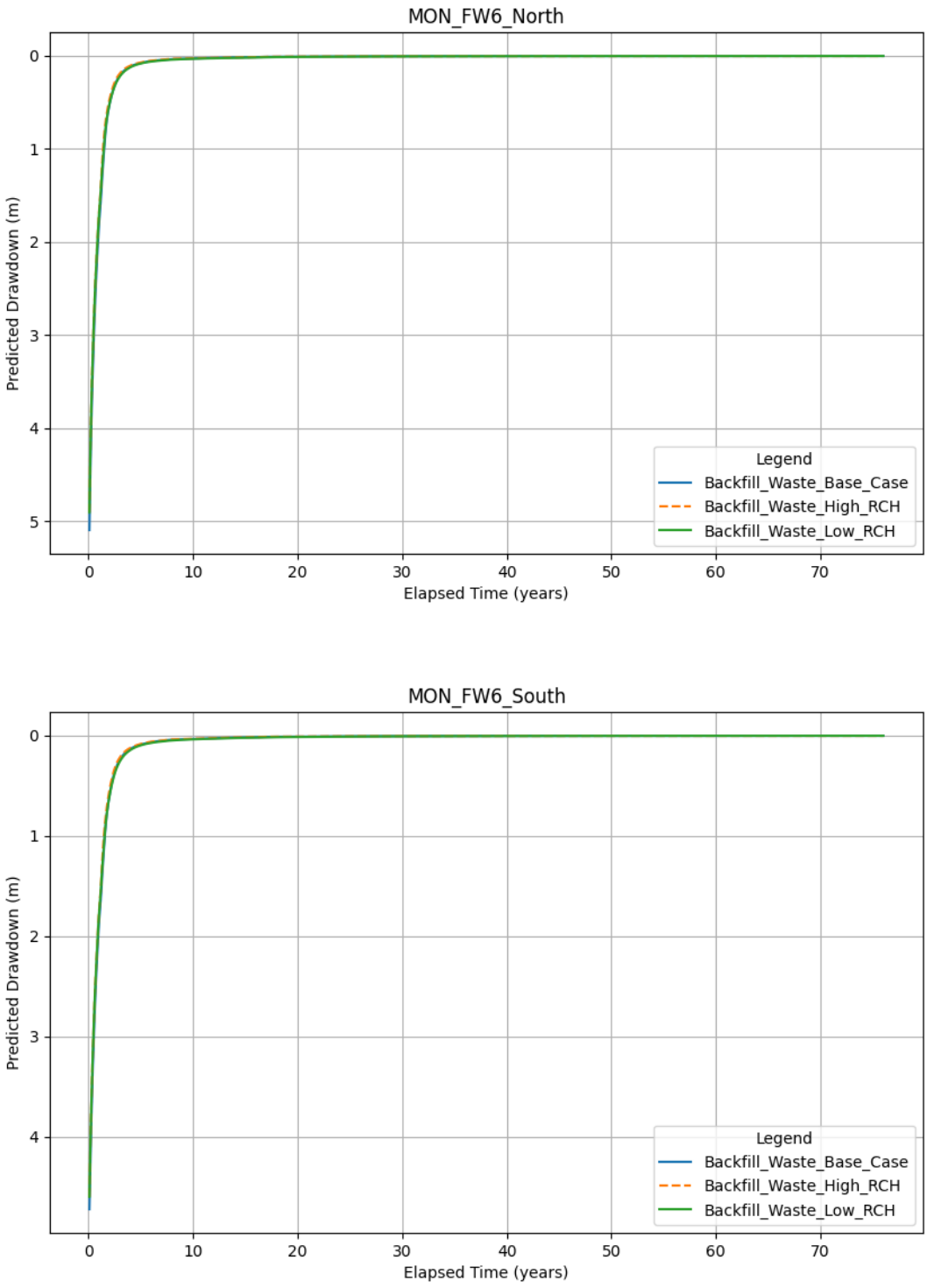

Figure B-39 Predicted aquifer recovery at Fridge West

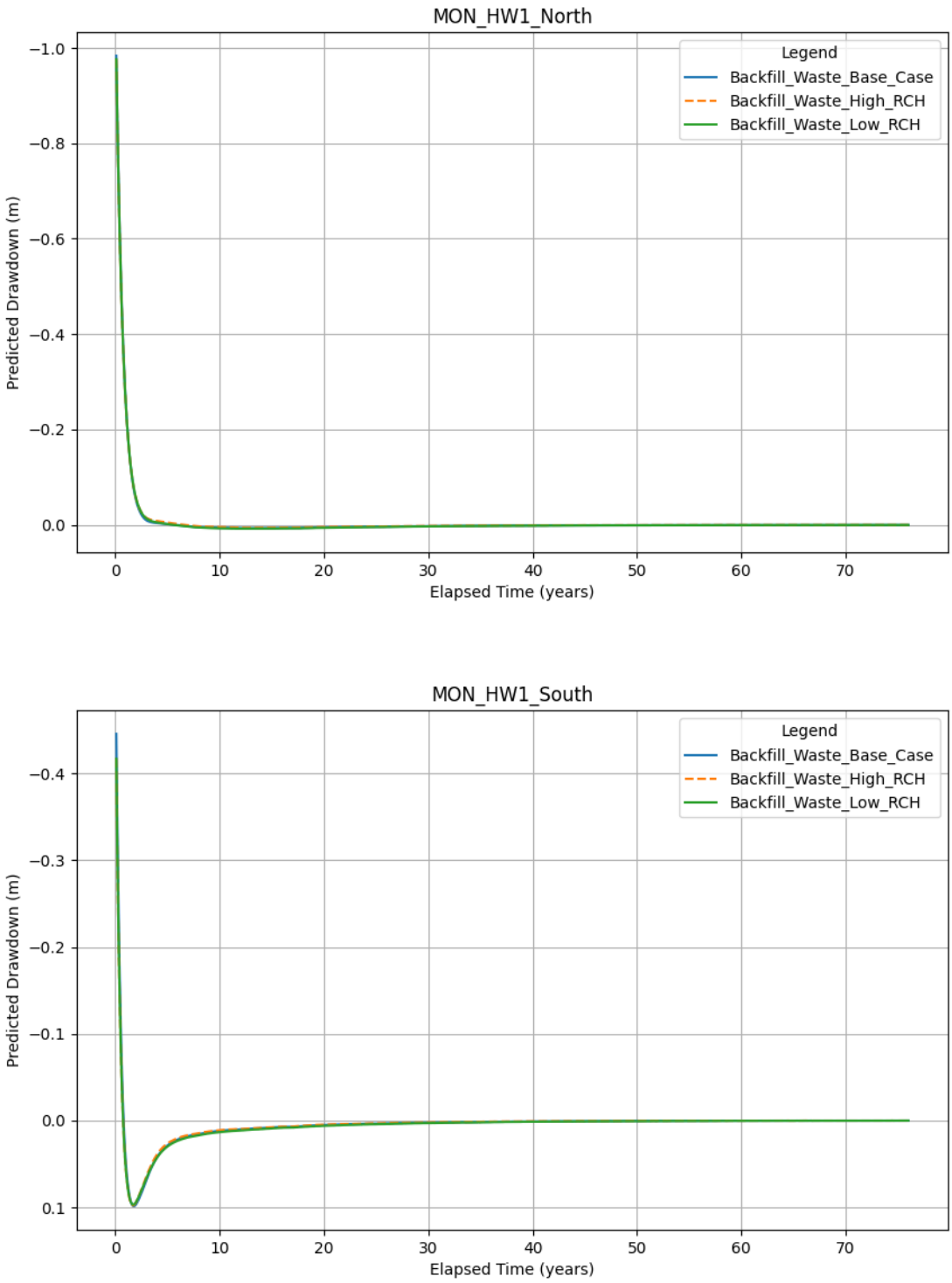

Figure B-40 Predicted aquifer recovery at Horseshoe West

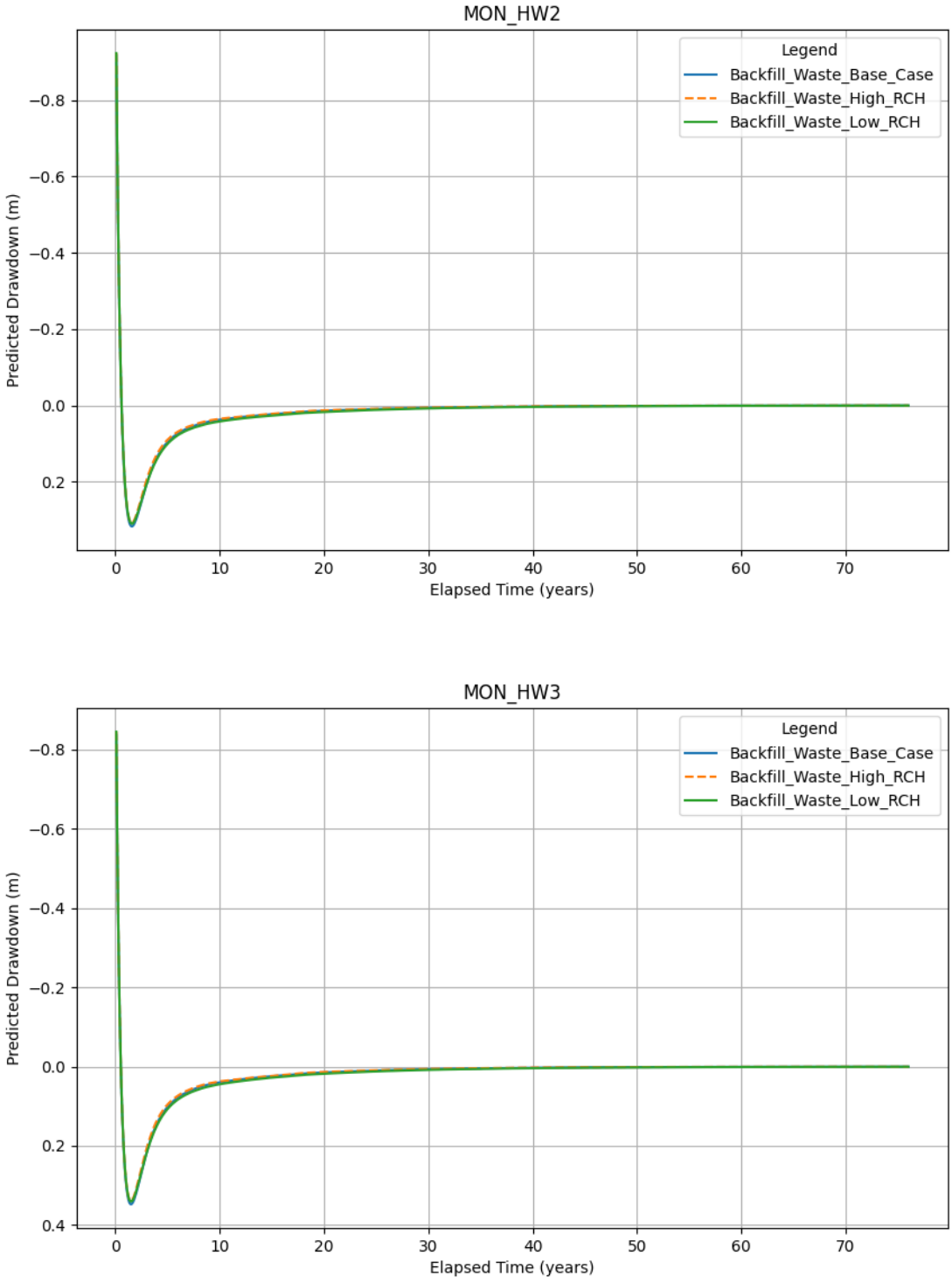

Figure B-41 Predicted aquifer recovery at Horseshoe West

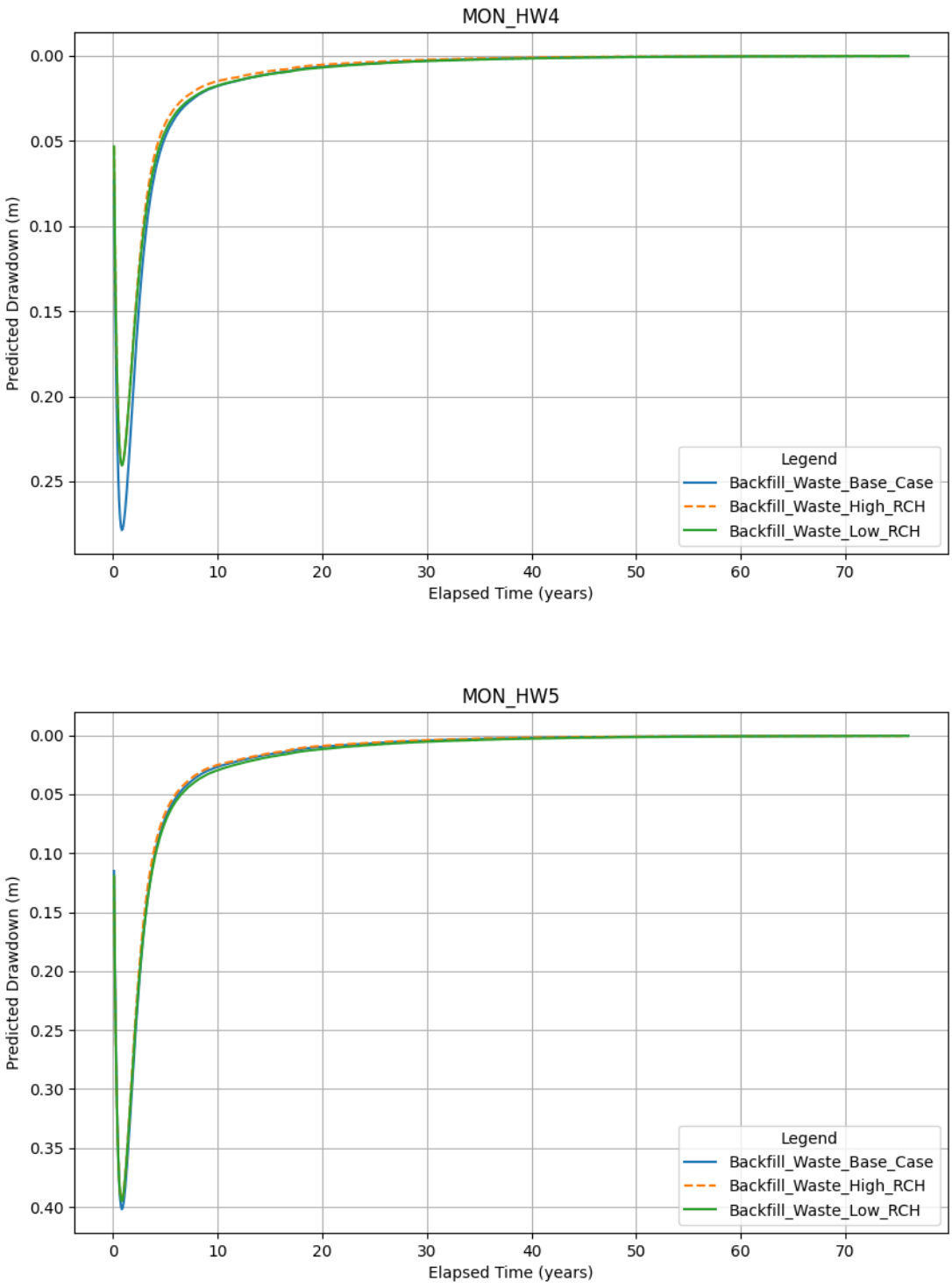

Figure B-42 Predicted aquifer recovery at Horseshoe West

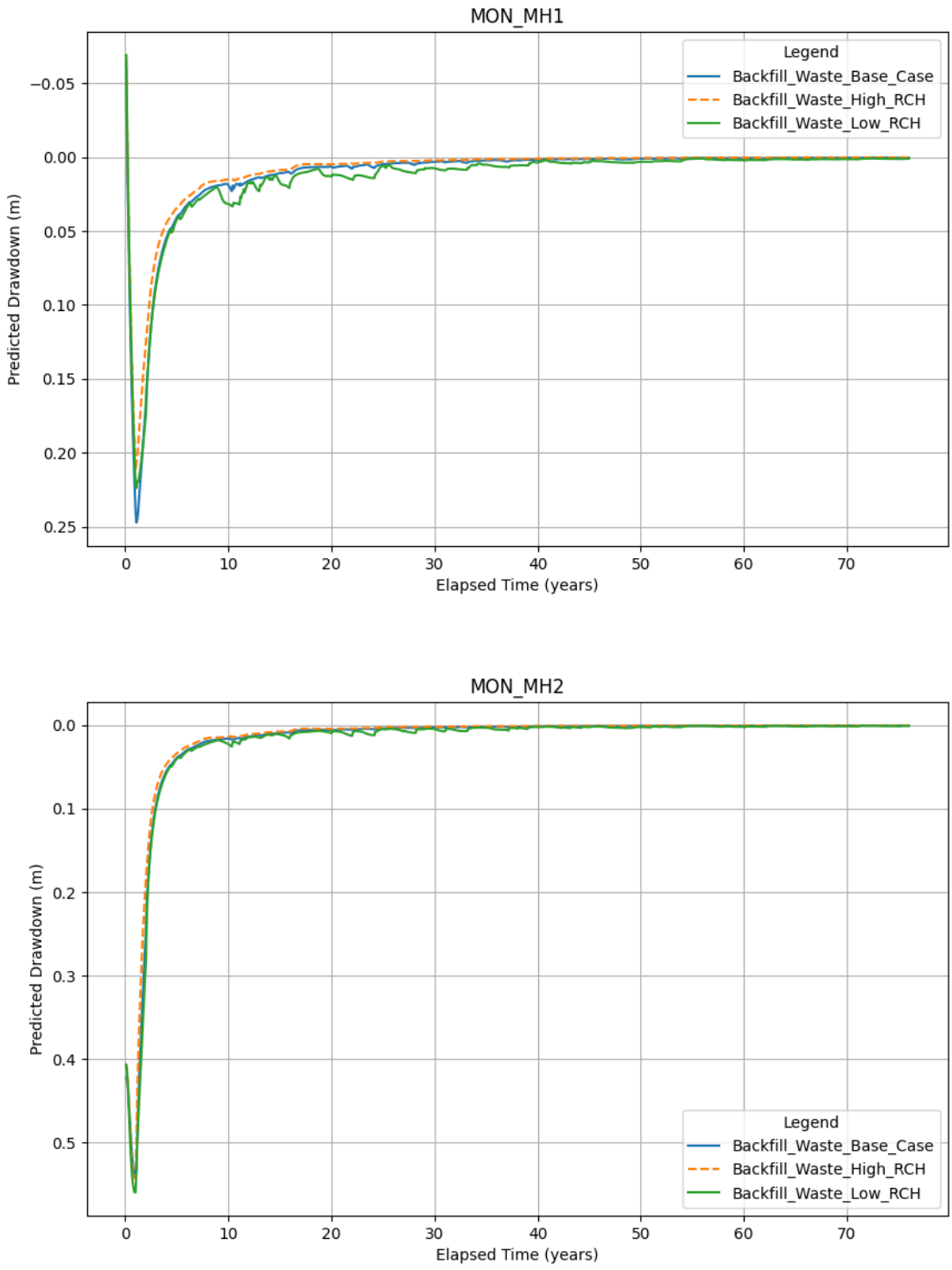

Figure B-43 Predicted aquifer recovery at Murray Hill

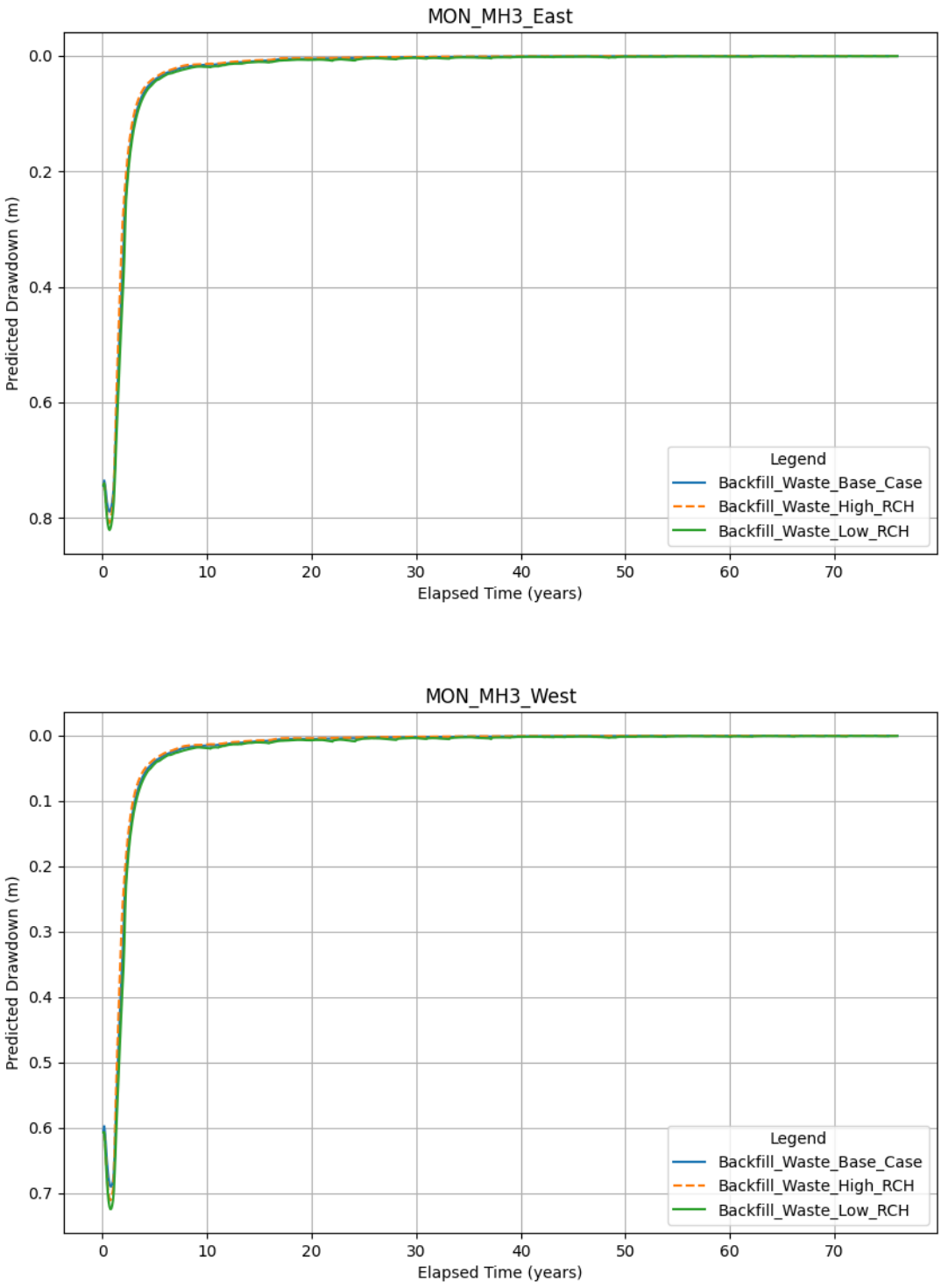

Figure B-44 Predicted aquifer recovery at Murray Hill

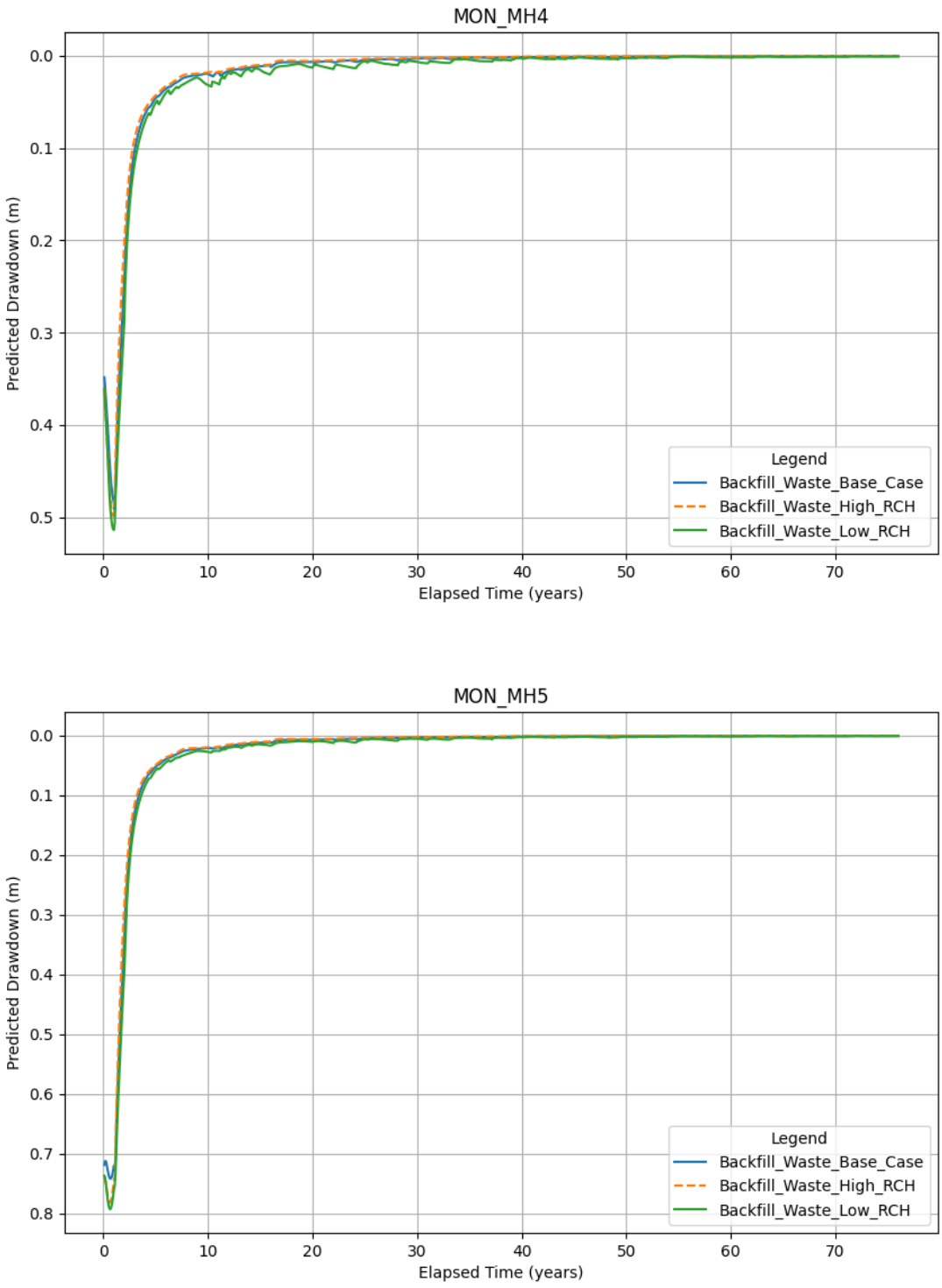

Figure B-45 Predicted aquifer recovery at Murray Hill

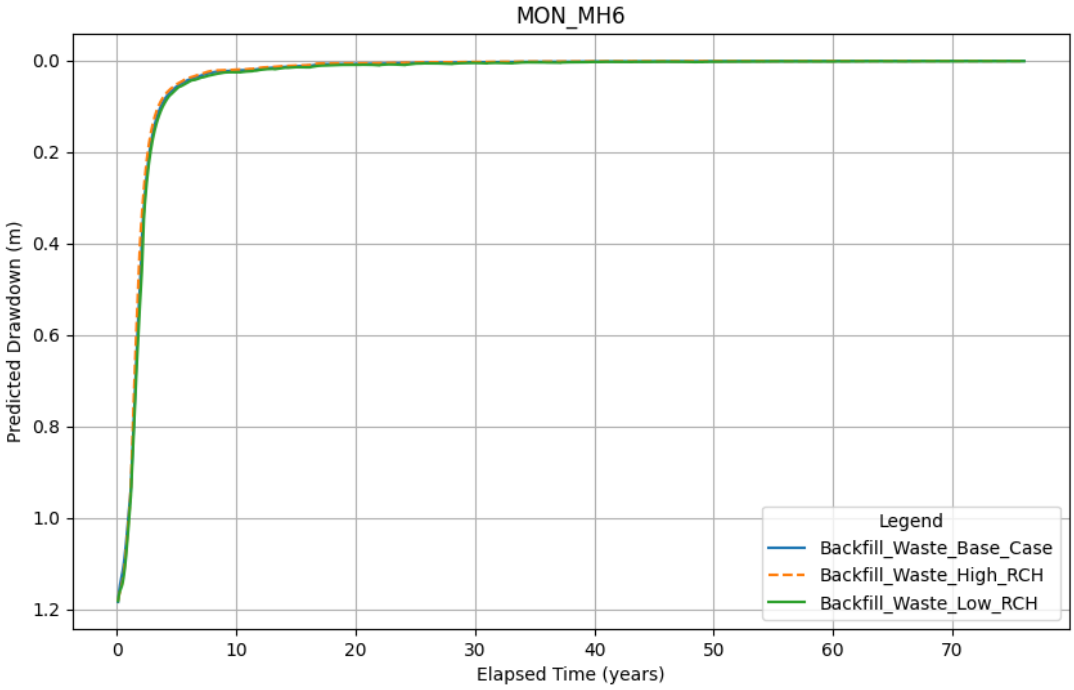

Figure B-46 Predicted aquifer recovery at Murray Hill

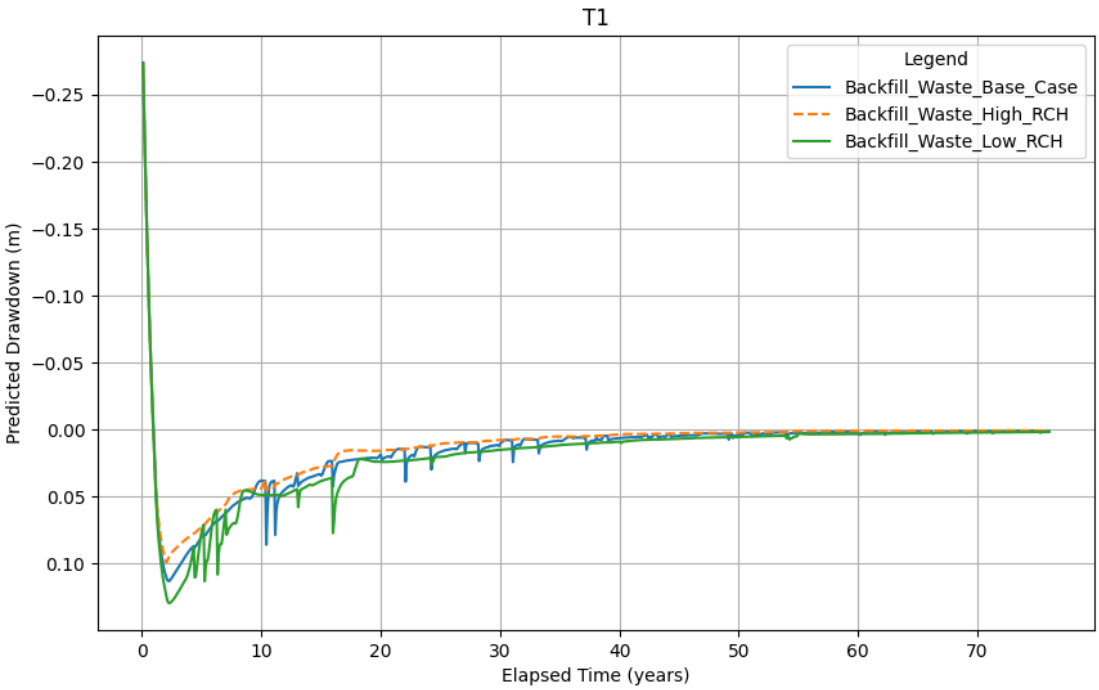

Figure B-47 Predicted aquifer recovery at T1 (Murray West MAR area)

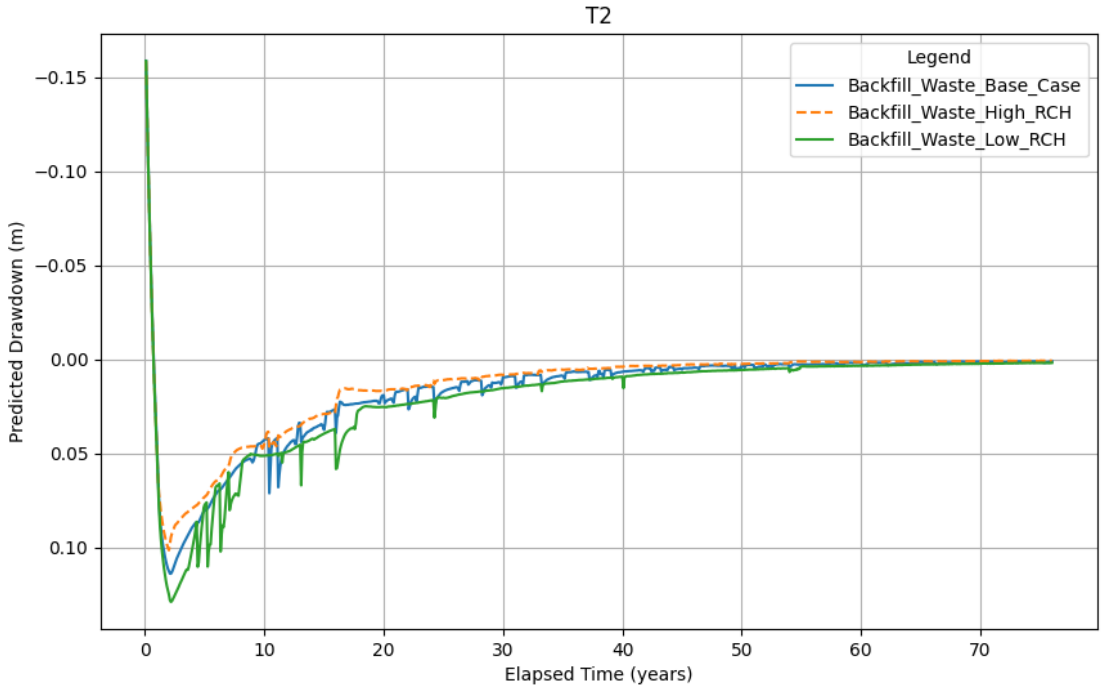

Figure B-48 Predicted aquifer recovery at T2 (valley between Murray West & Koodjeepindarranna claypan)

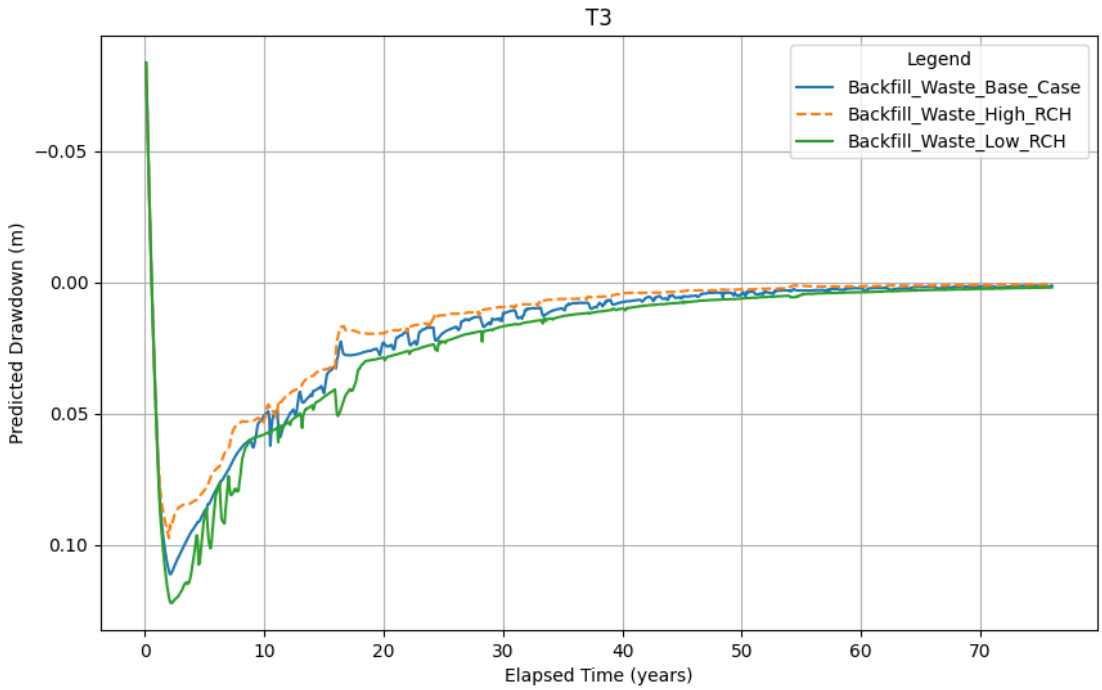

Figure B-49 Predicted aquifer recovery at T3 (Koodjeepindarranna claypan)

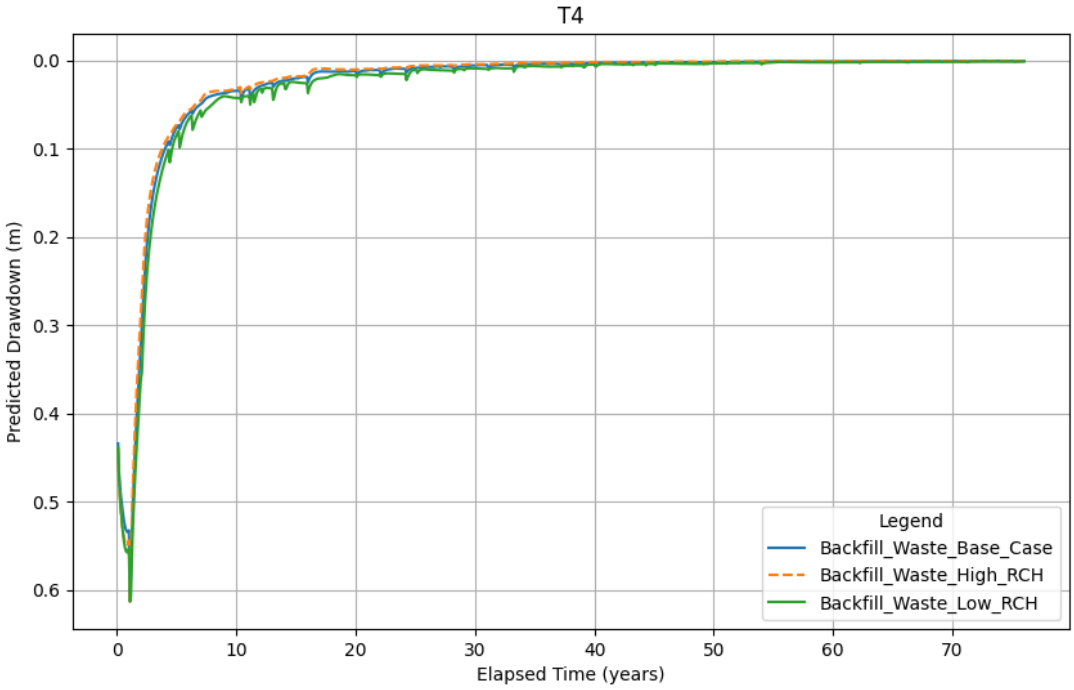

Figure B-50 Predicted aquifer recovery at T4 (valley near Murray Hill)

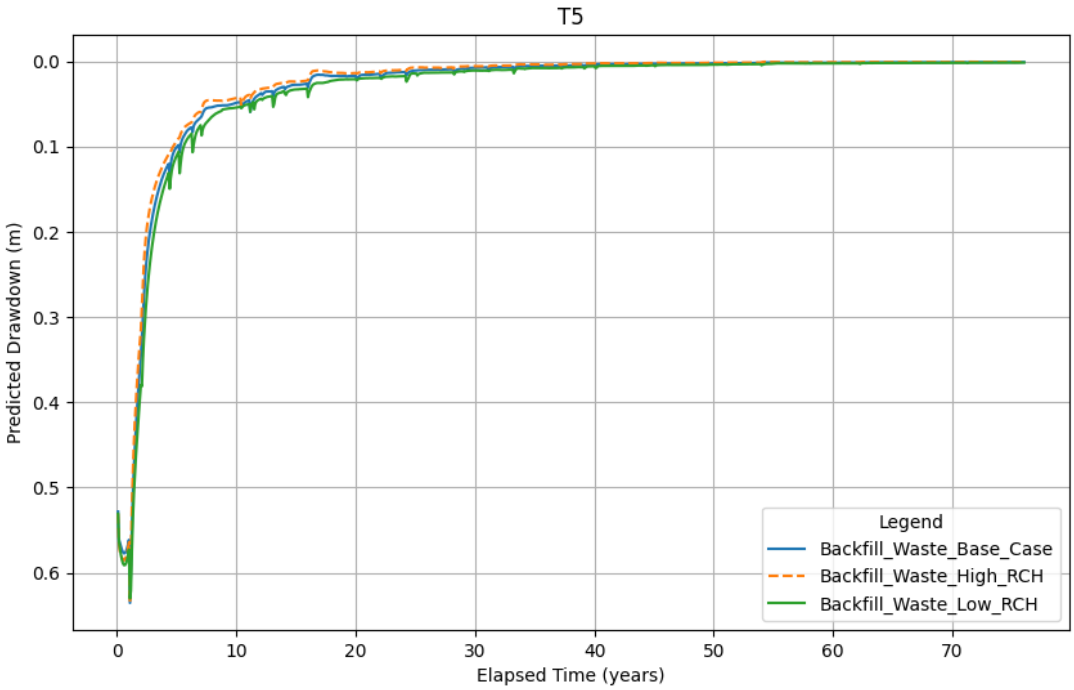

Figure B-51 Predicted aquifer recovery at T5 (valley between Murray Hill & Gnalka Gnoona claypan)

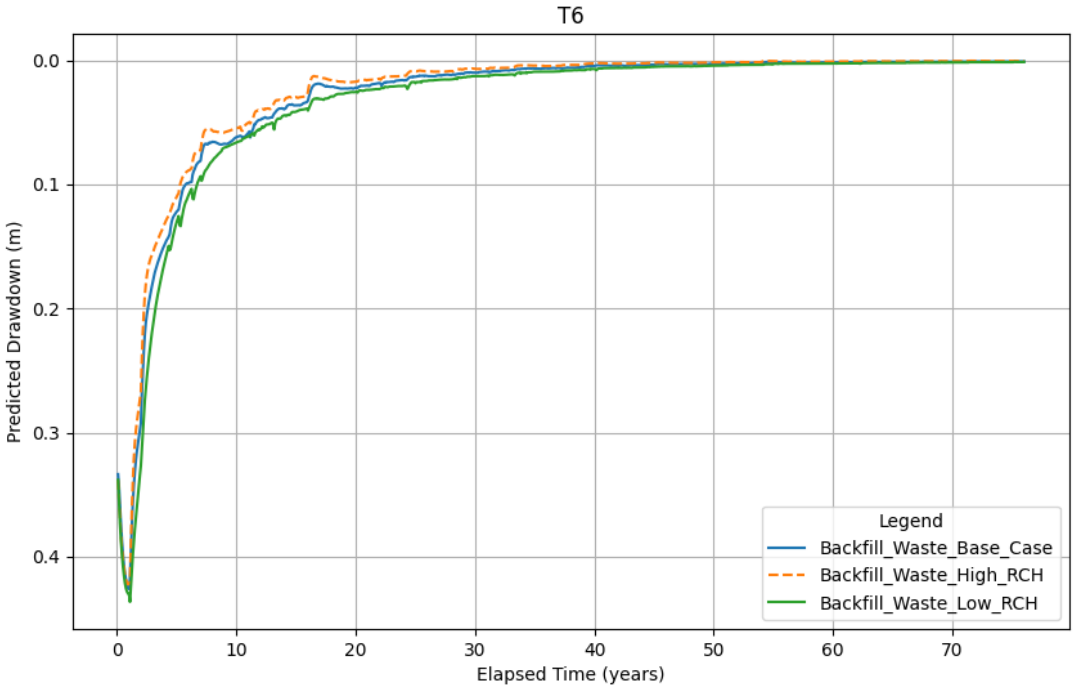

Figure B-52 Predicted aquifer recovery at T6 (Gnalka Gnoona claypan)

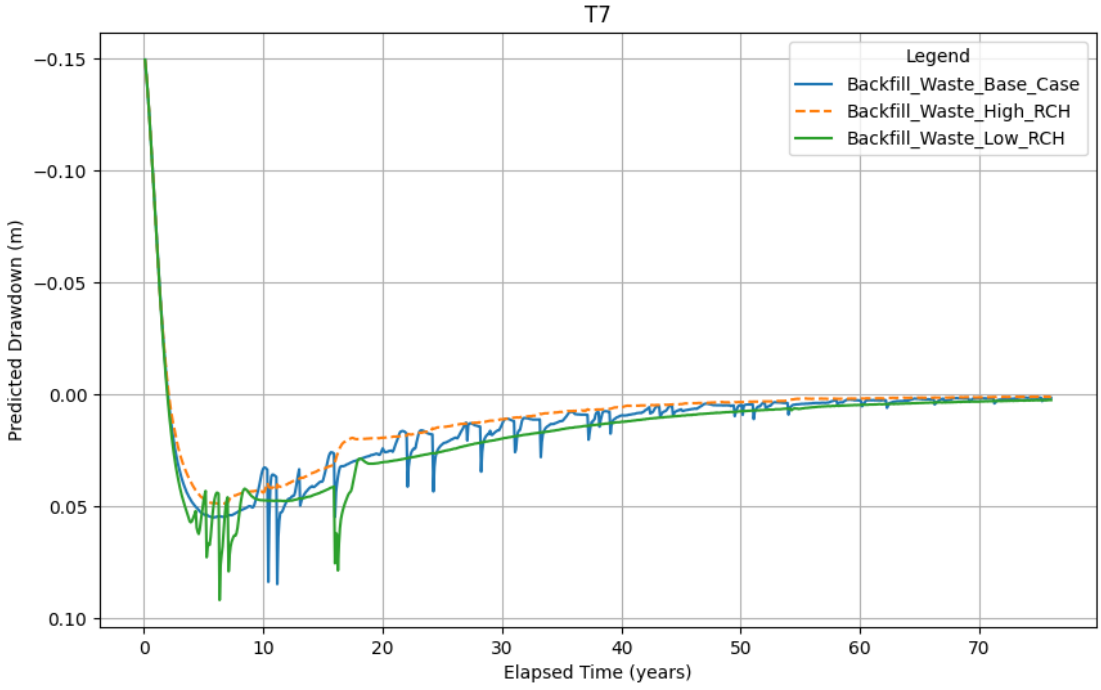

Figure B-53 Predicted aquifer recovery at T7 (restricted stygo 1 west)

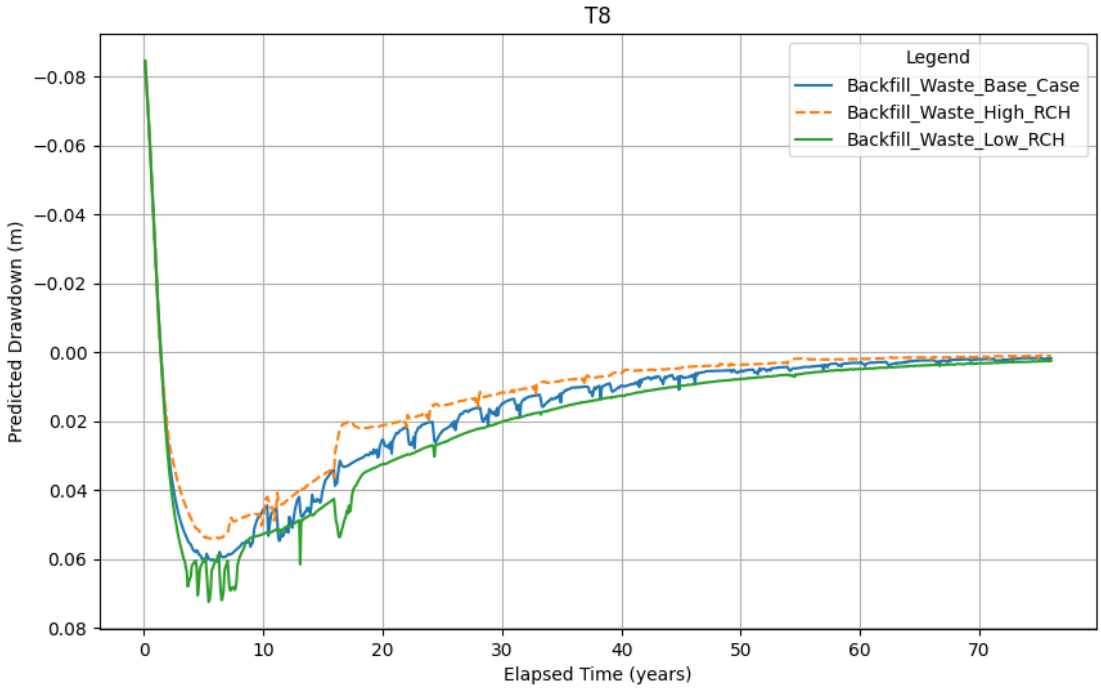

Figure B-54 Predicted aquifer recovery at T8 (valley Far West)

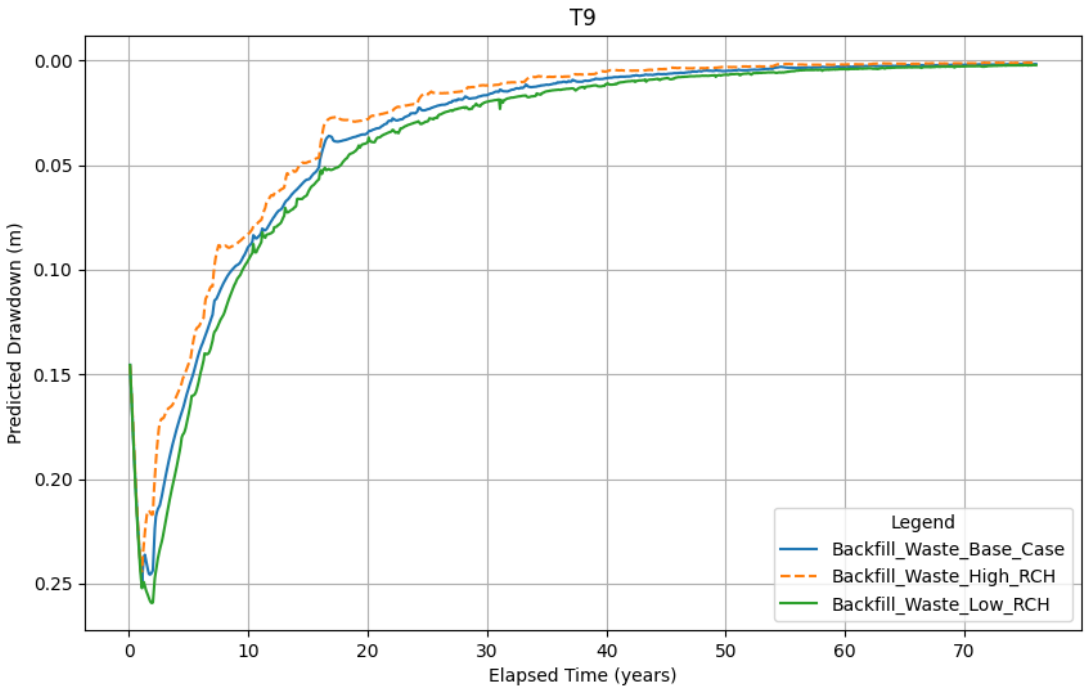

Figure B-55 Predicted aquifer recovery at T9 (restricted stygo 2 southwest)

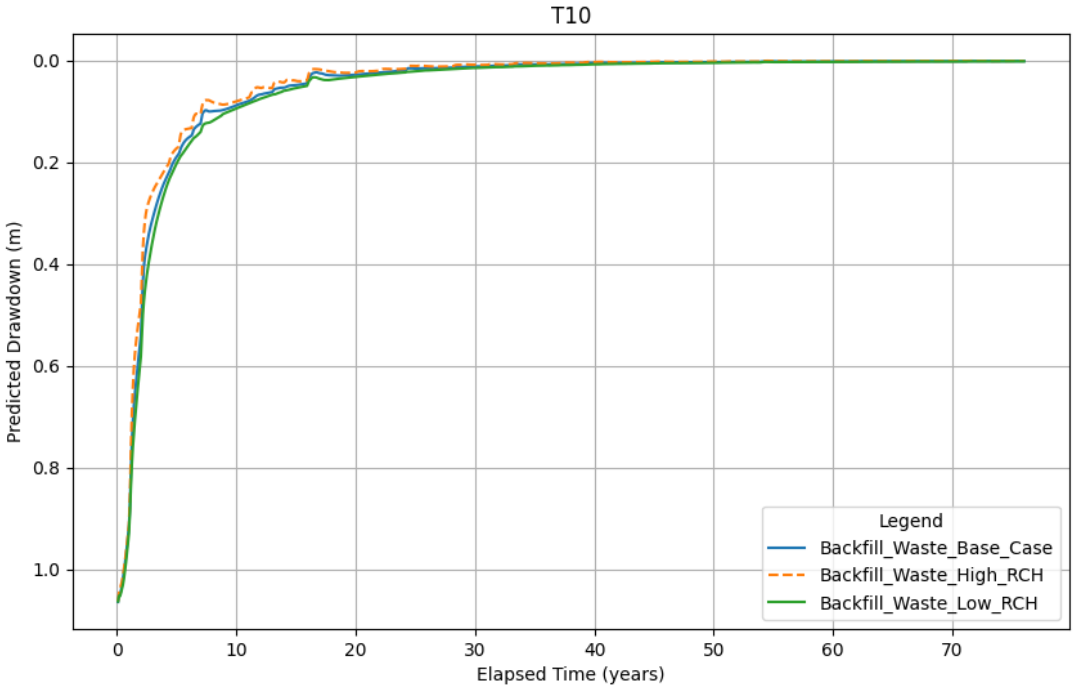

Figure B-56 Predicted aquifer recovery at T10 (restricted stygo 3 south)

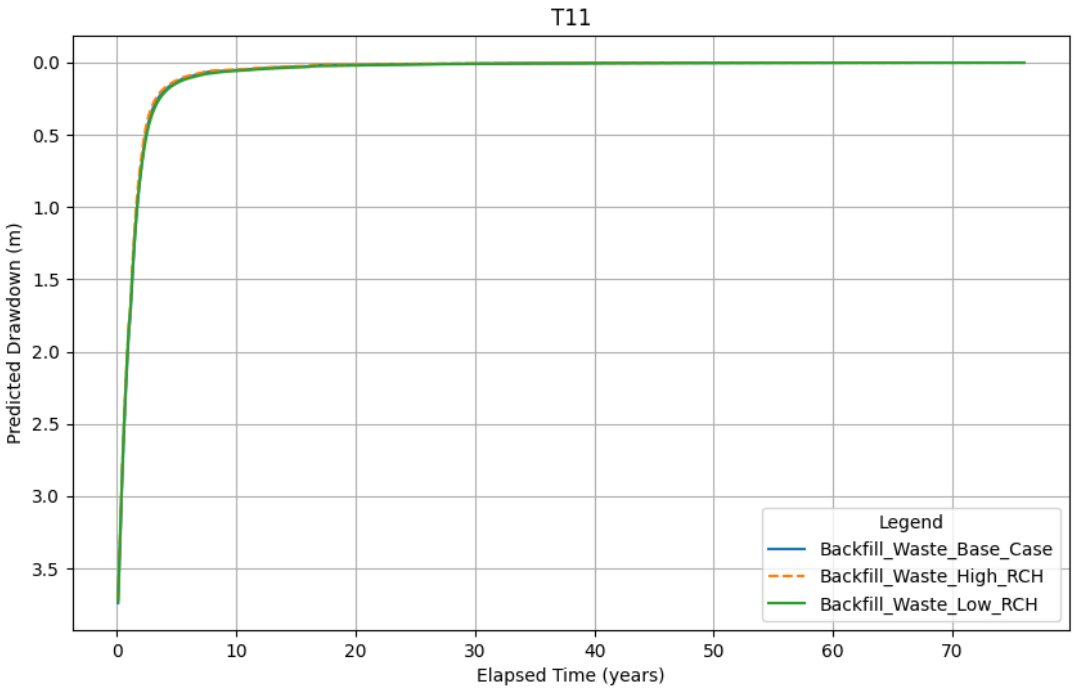

Figure B-57 Predicted aquifer recovery at T11 (valley Fridge West)

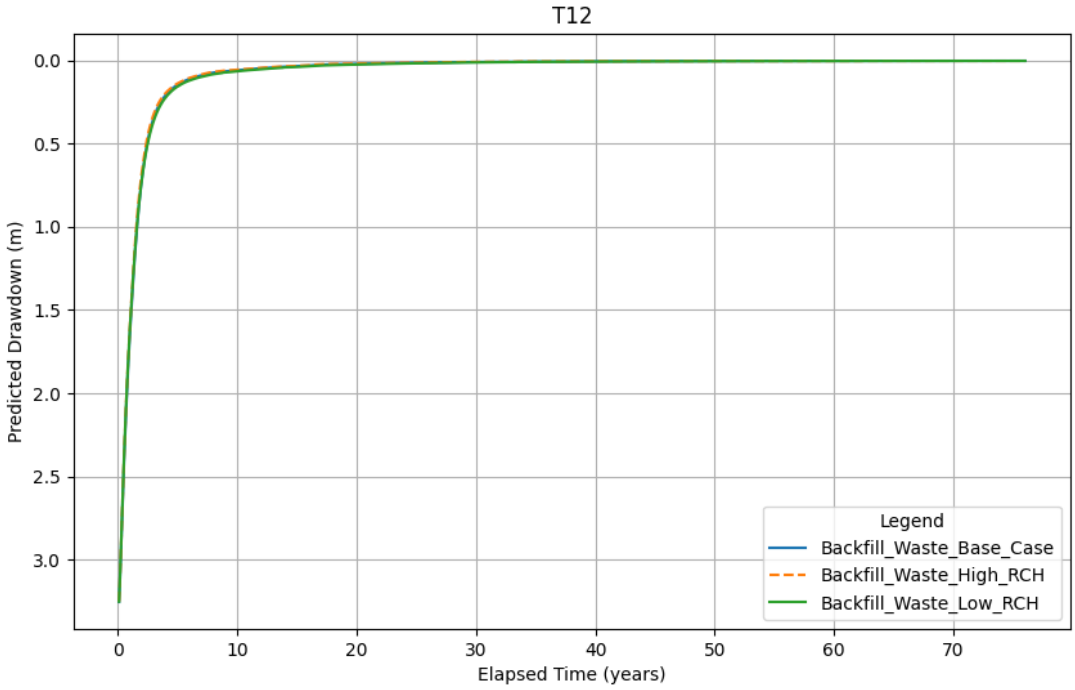

Figure B-58 Predicted aquifer recovery at T12 (valley Fridge Central)

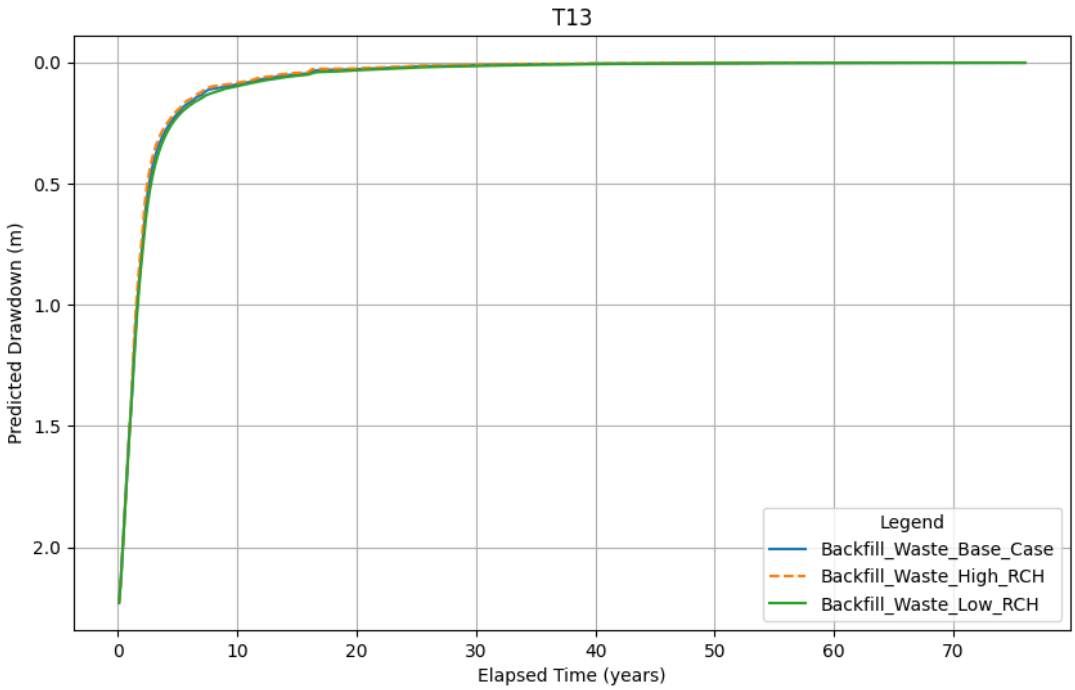

Figure B-59 Predicted aquifer recovery at T13 (valley Central)

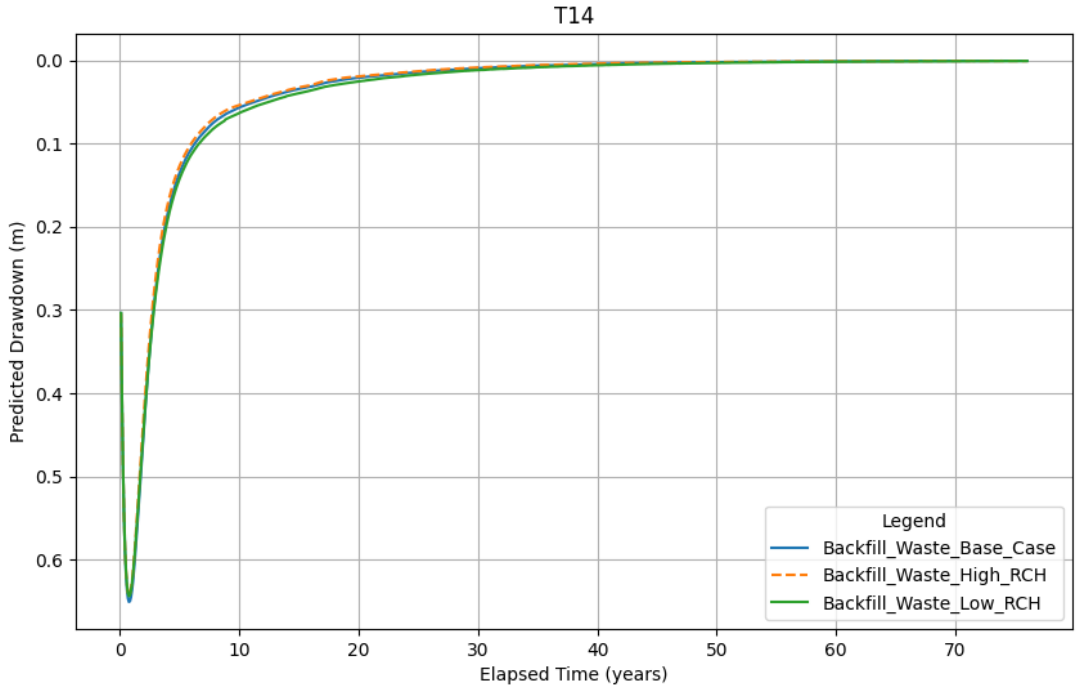

Figure B-60 Predicted aquifer recovery at T14 (area between valley & Horseshoe)

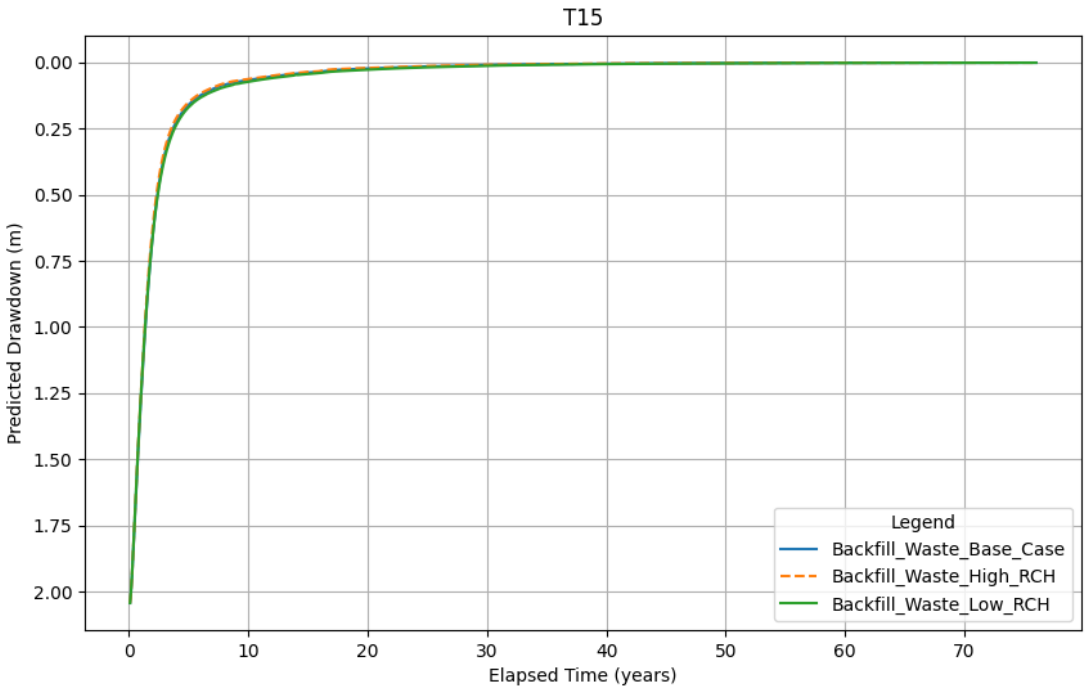

Figure B-61 Predicted aquifer recovery at T15 (valley Fridge Hill)

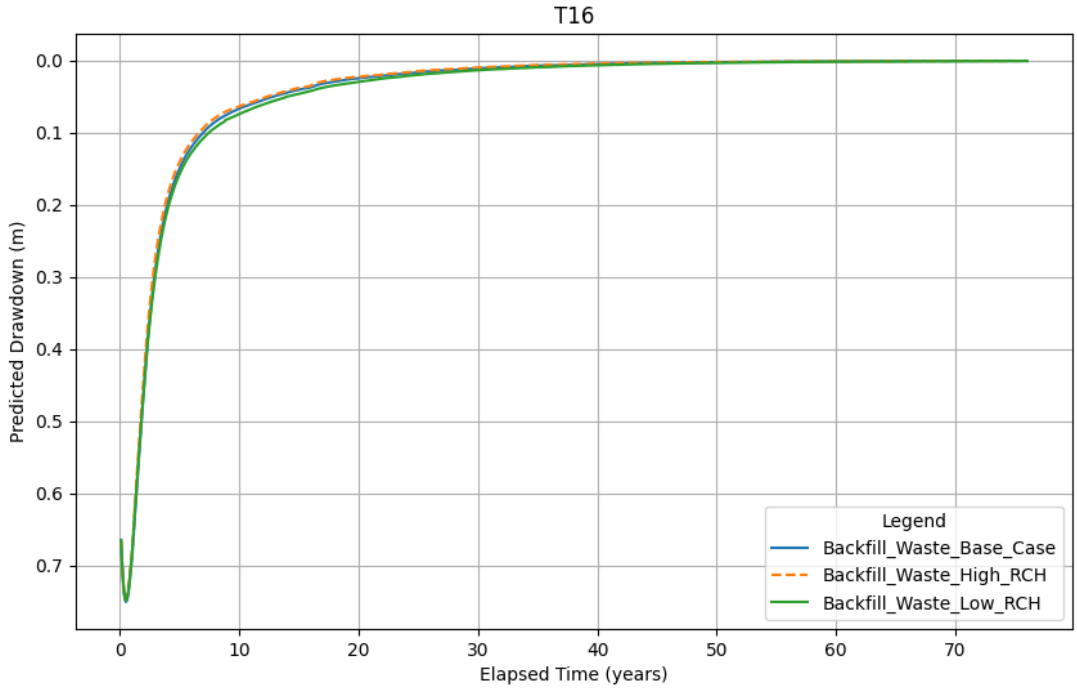

Figure B-62 Predicted aquifer recovery at T16 (valley Horseshoe)

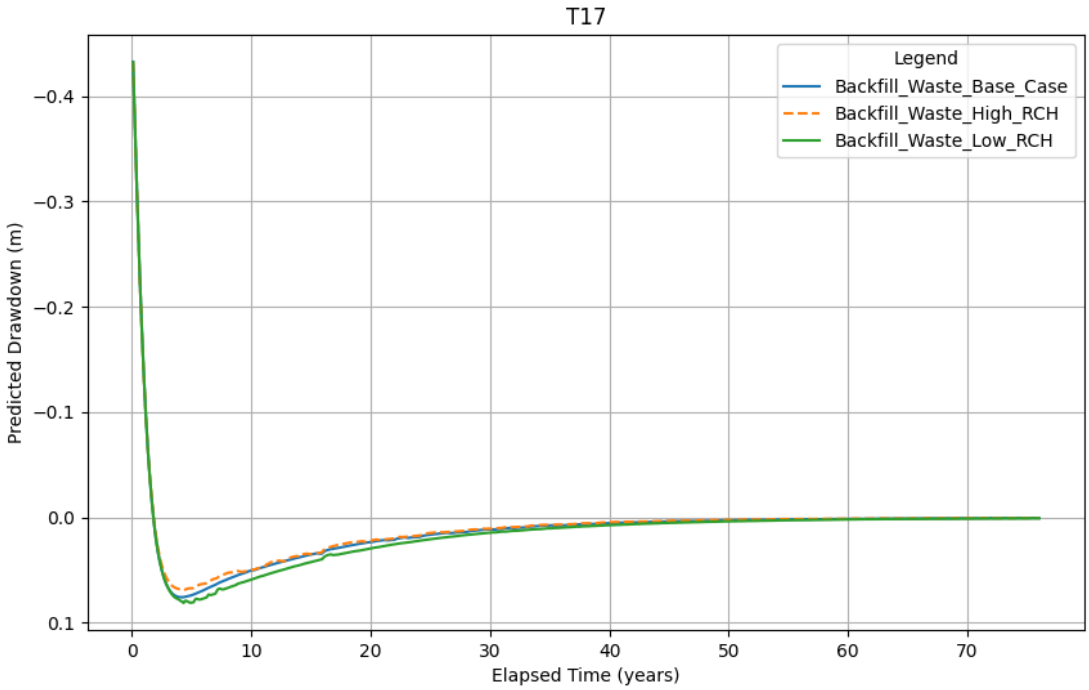

Figure B-63 Predicted aquifer recovery at T17 (valley Far Southeast)

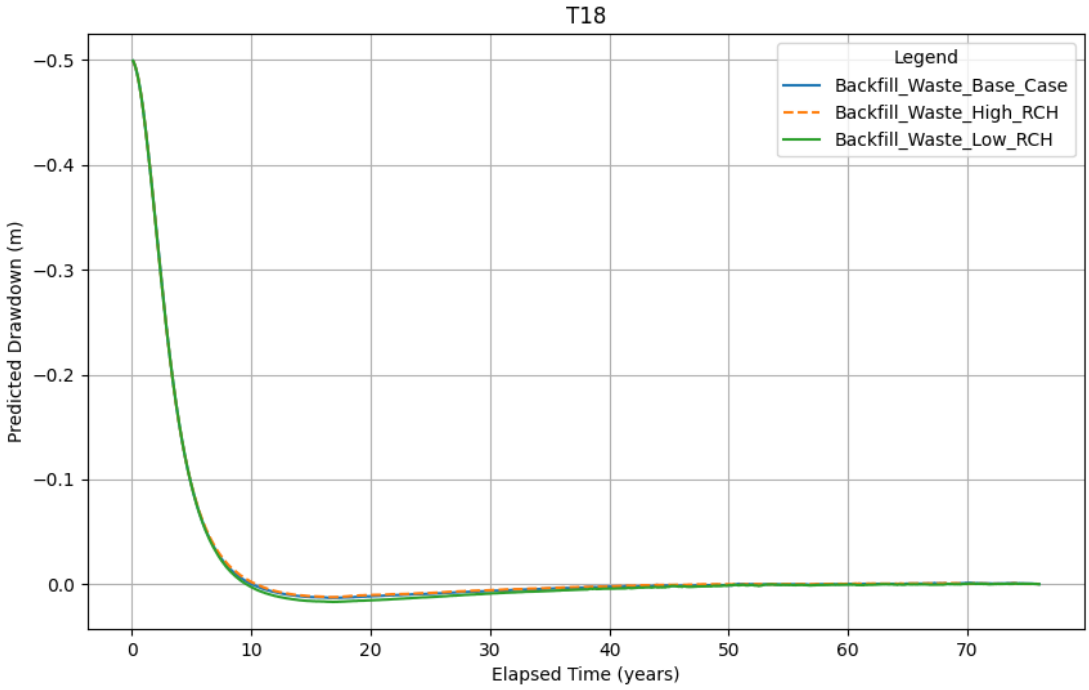

Figure B-64 Predicted aquifer recovery at T18 (Wirrilimarra area)

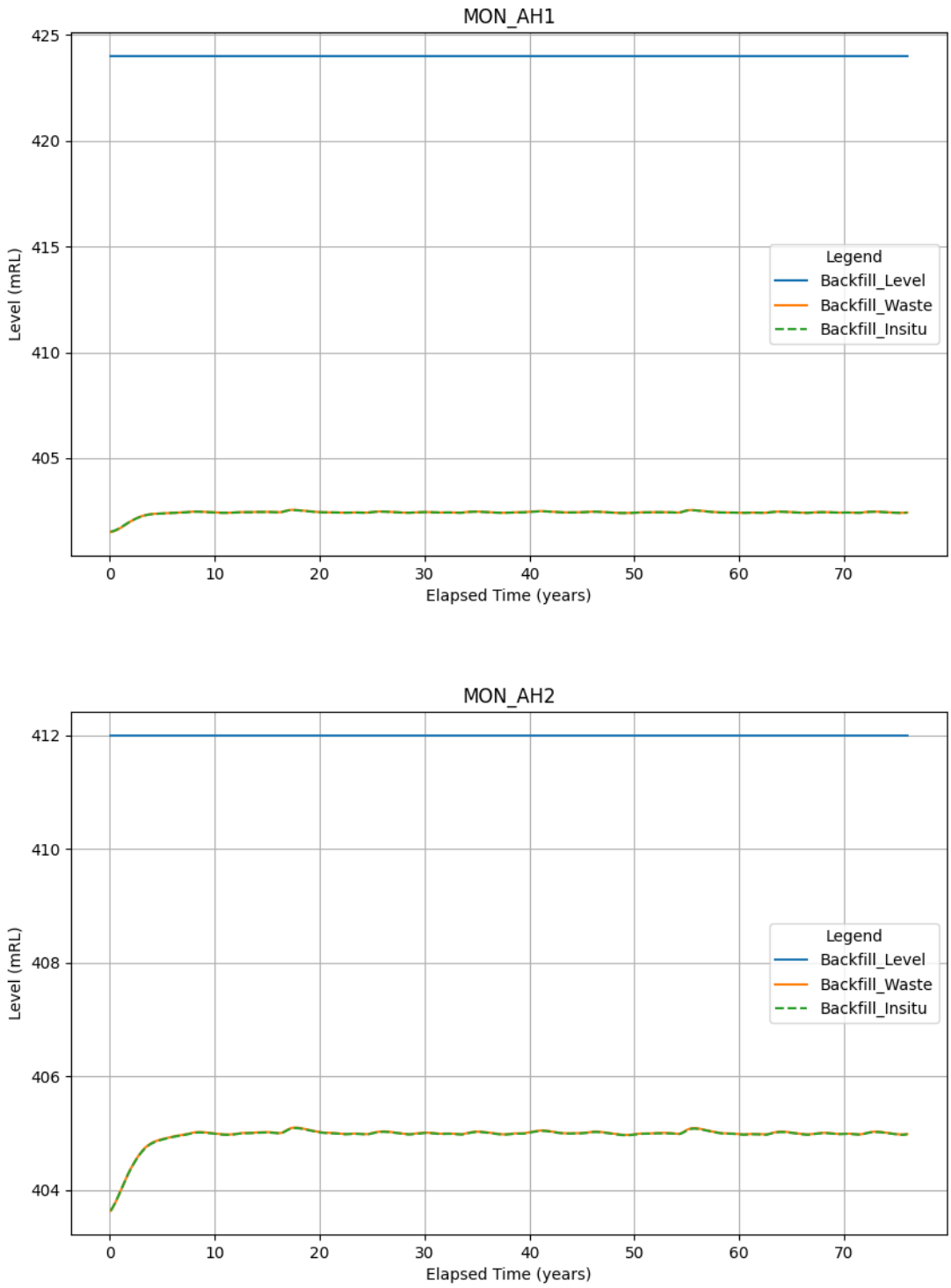

Figure B-65 Predicted pit water level recovery at Anticline Hill

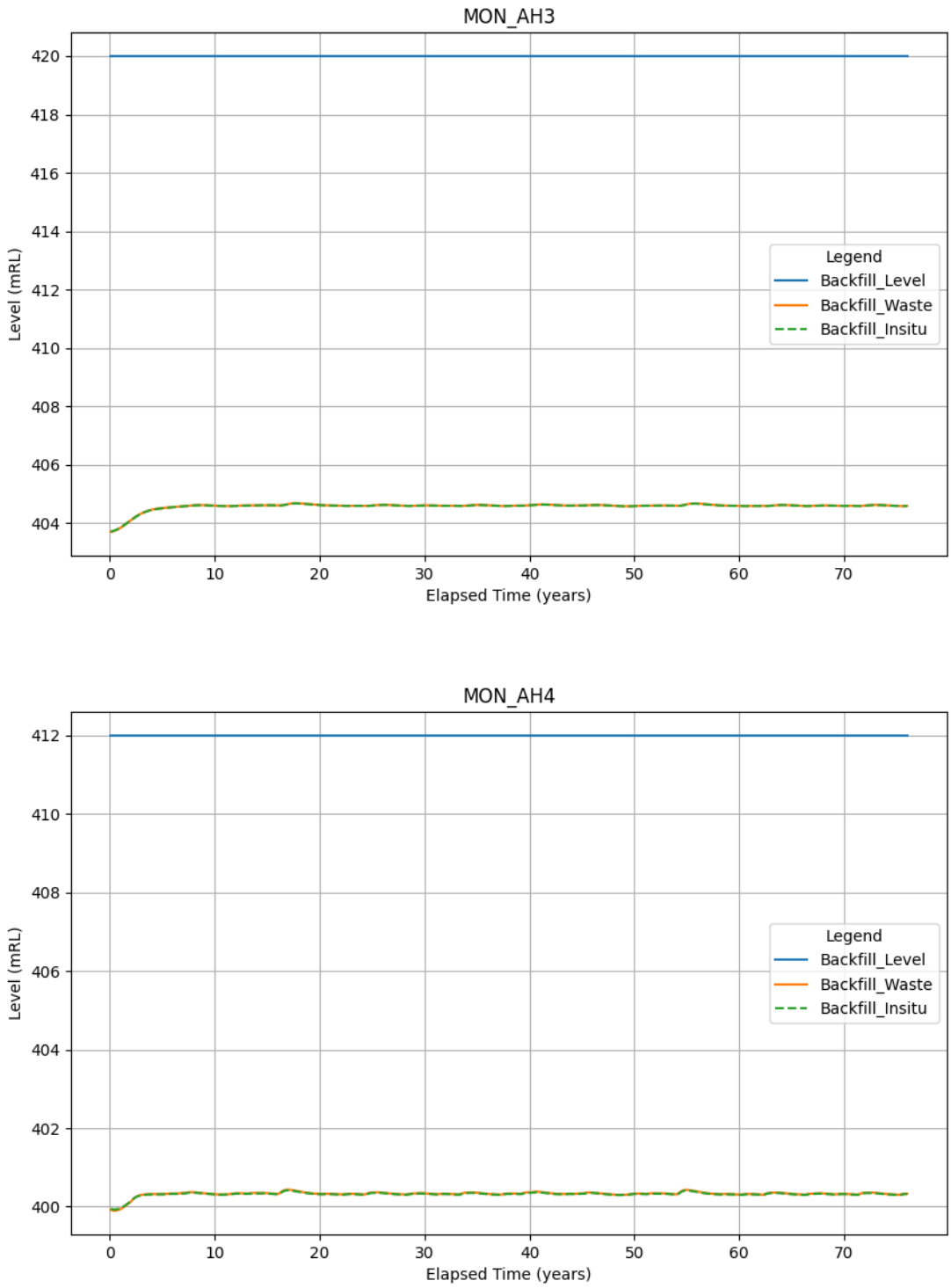

Figure B-66 Predicted pit water level recovery at Anticline Hill

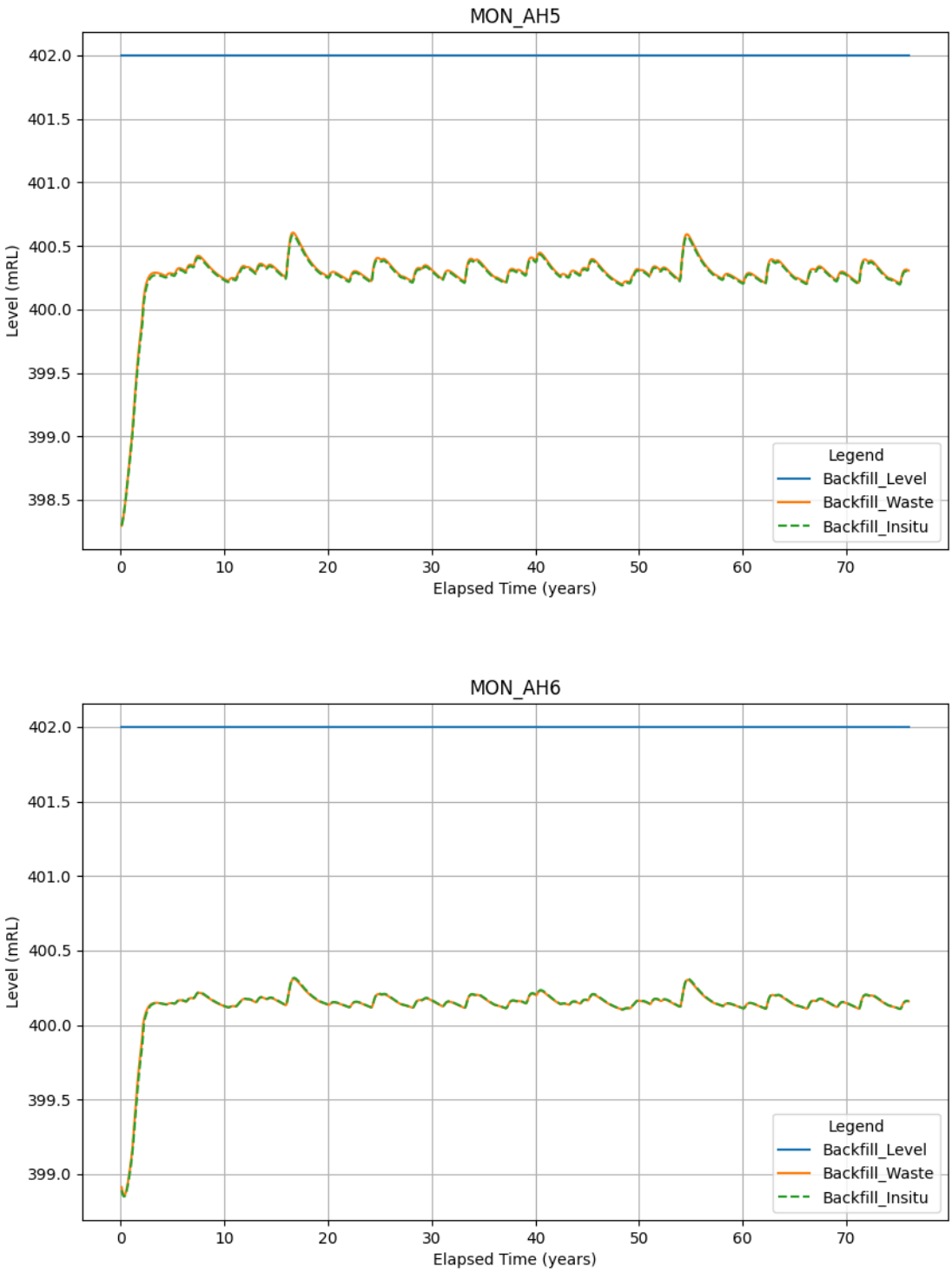

Figure B-67 Predicted pit water level recovery at Anticline Hill

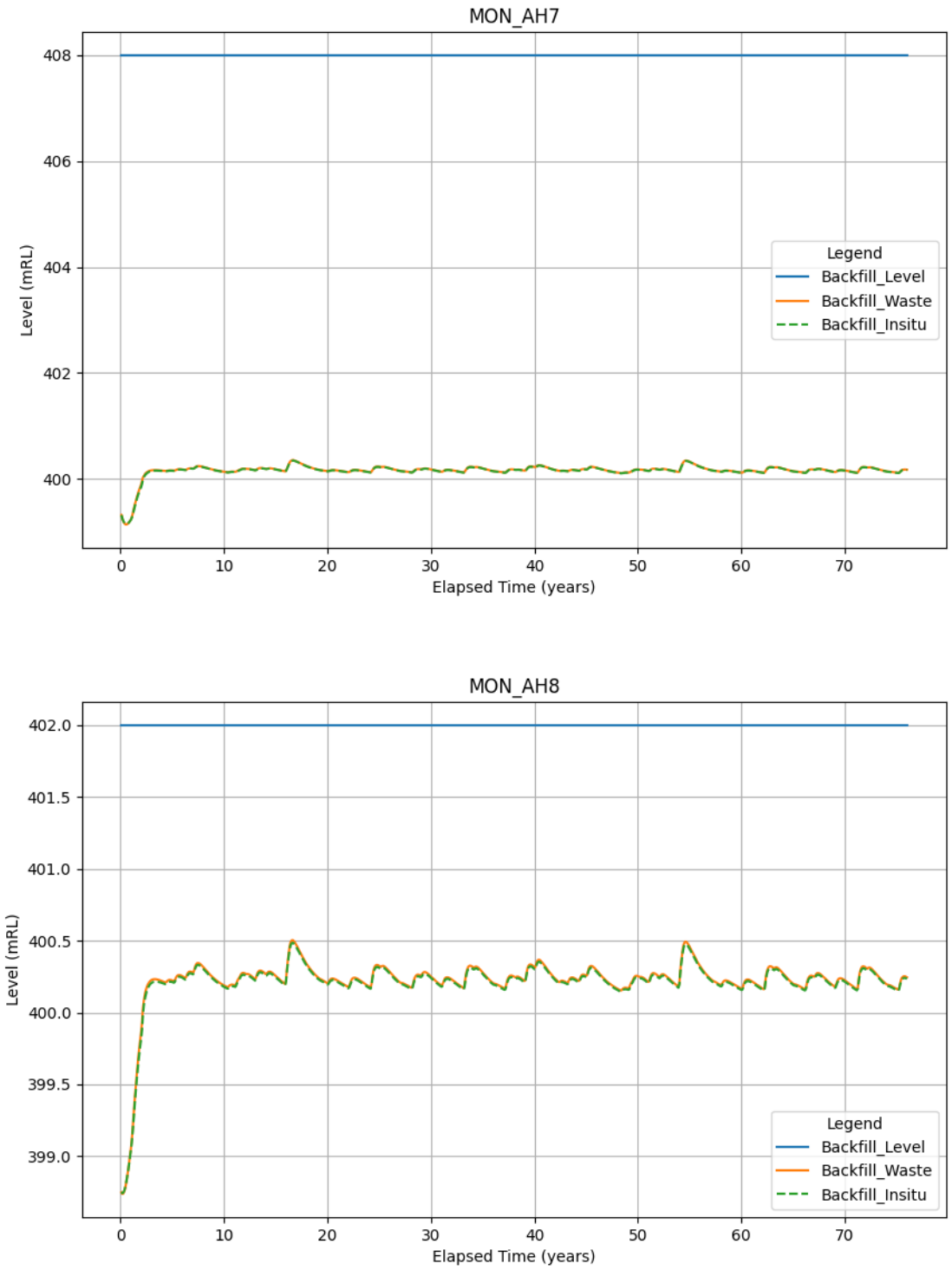

Figure B-68 Predicted pit water level recovery at Anticline Hill

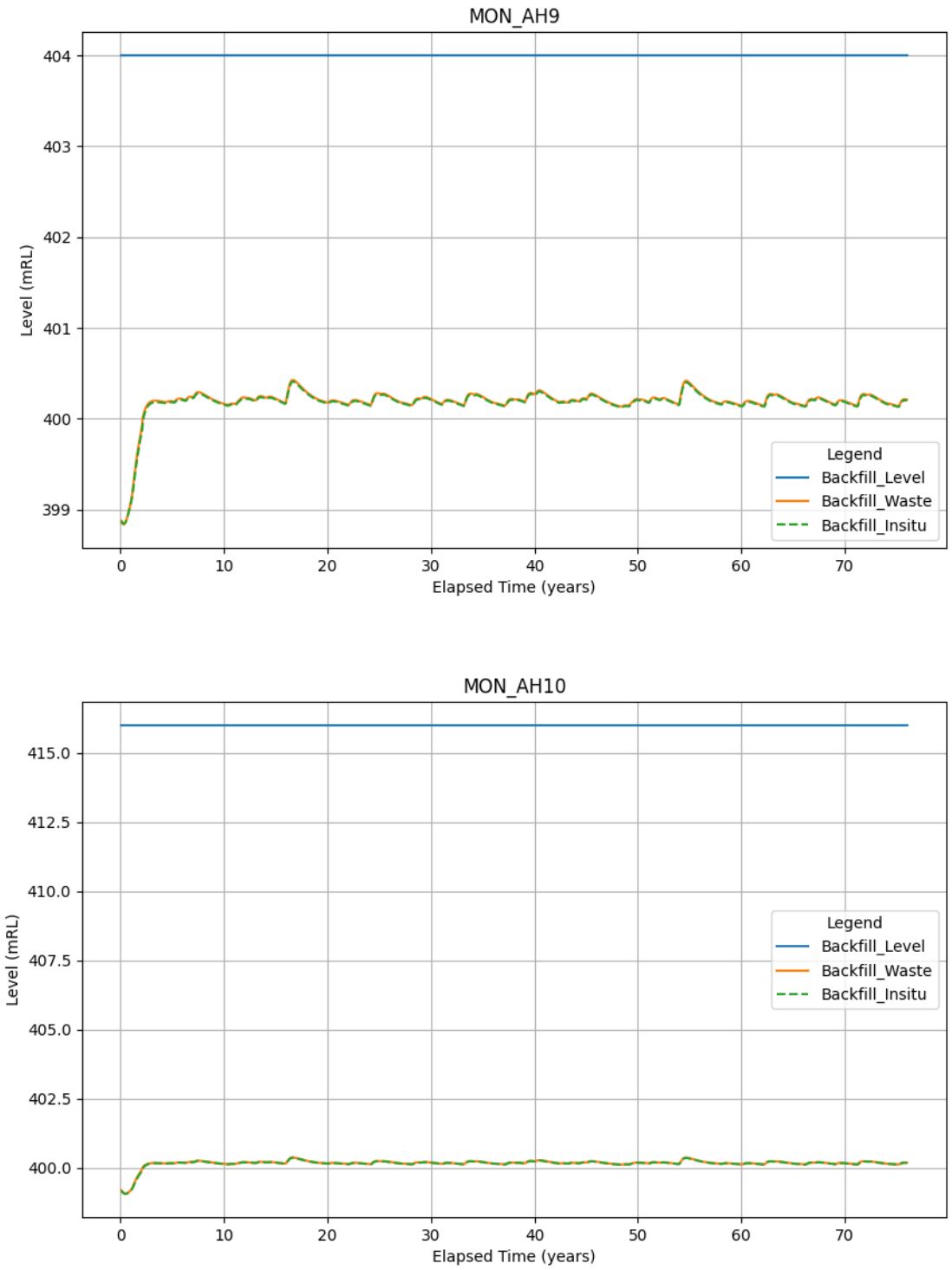

Figure B-69 Predicted pit water level recovery at Anticline Hill

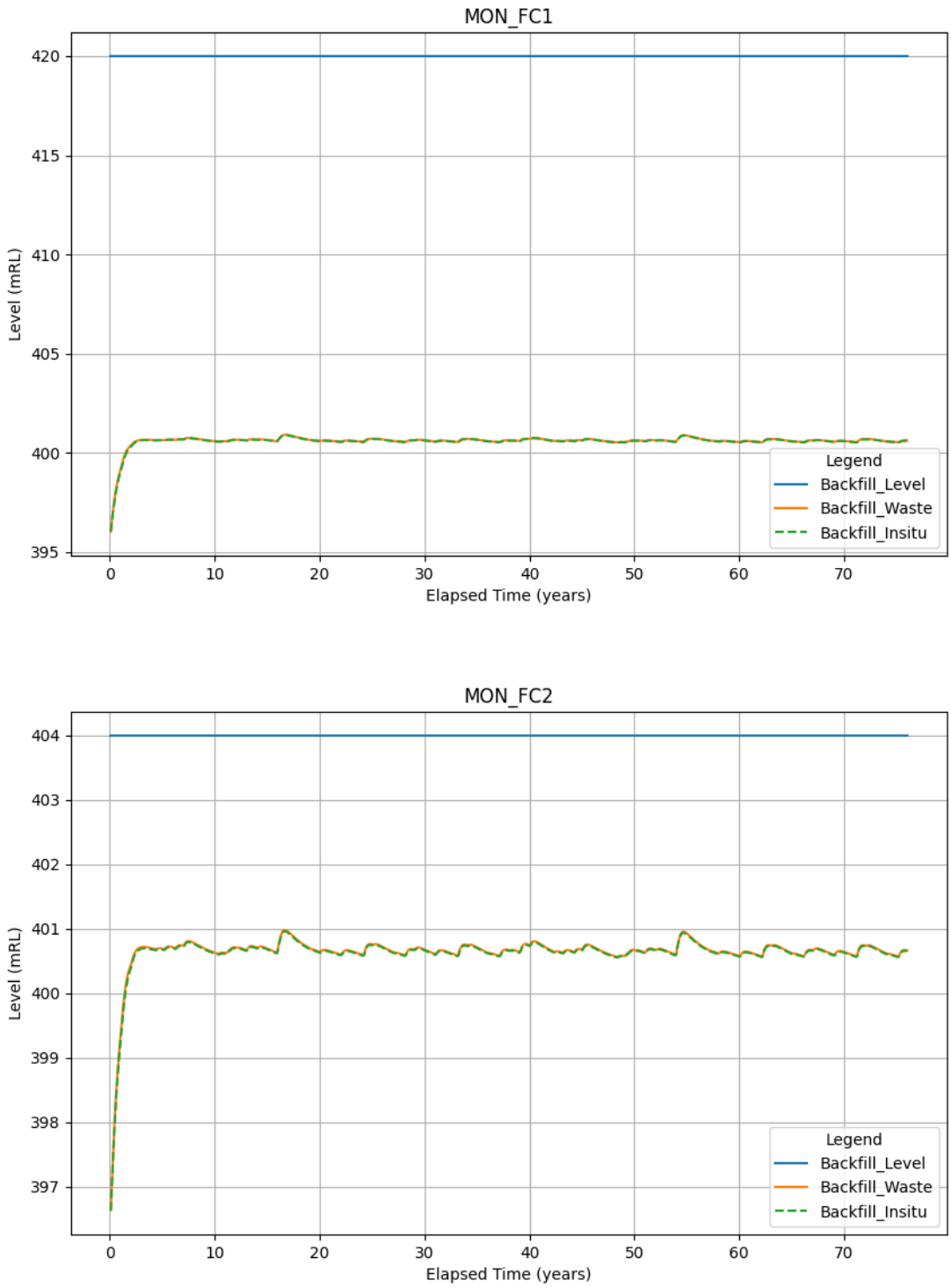

Figure B-70 Predicted pit water level recovery at Fridge Central

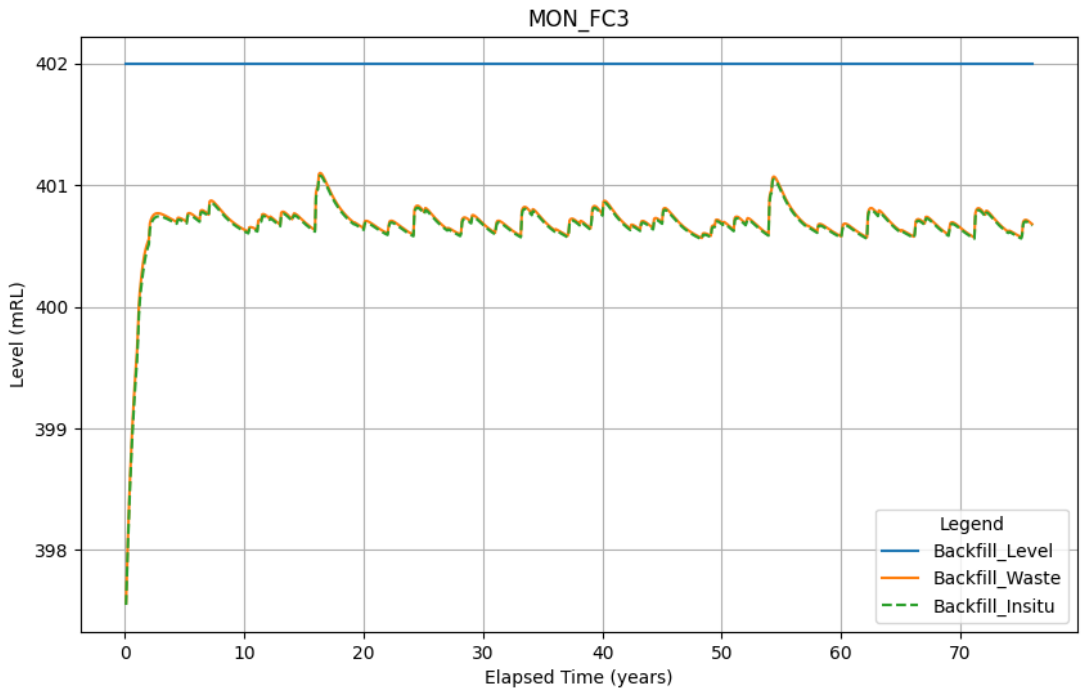

Figure B-71 Predicted pit water level recovery at Fridge Central

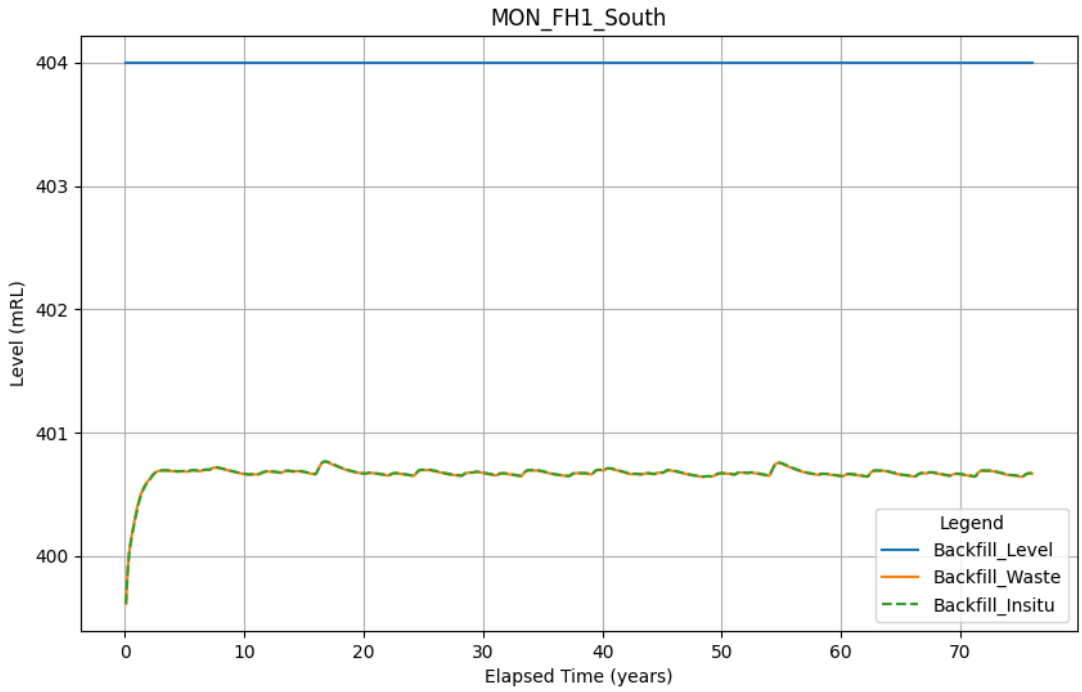

Figure B-72 Predicted pit water level recovery at Fridge Hill

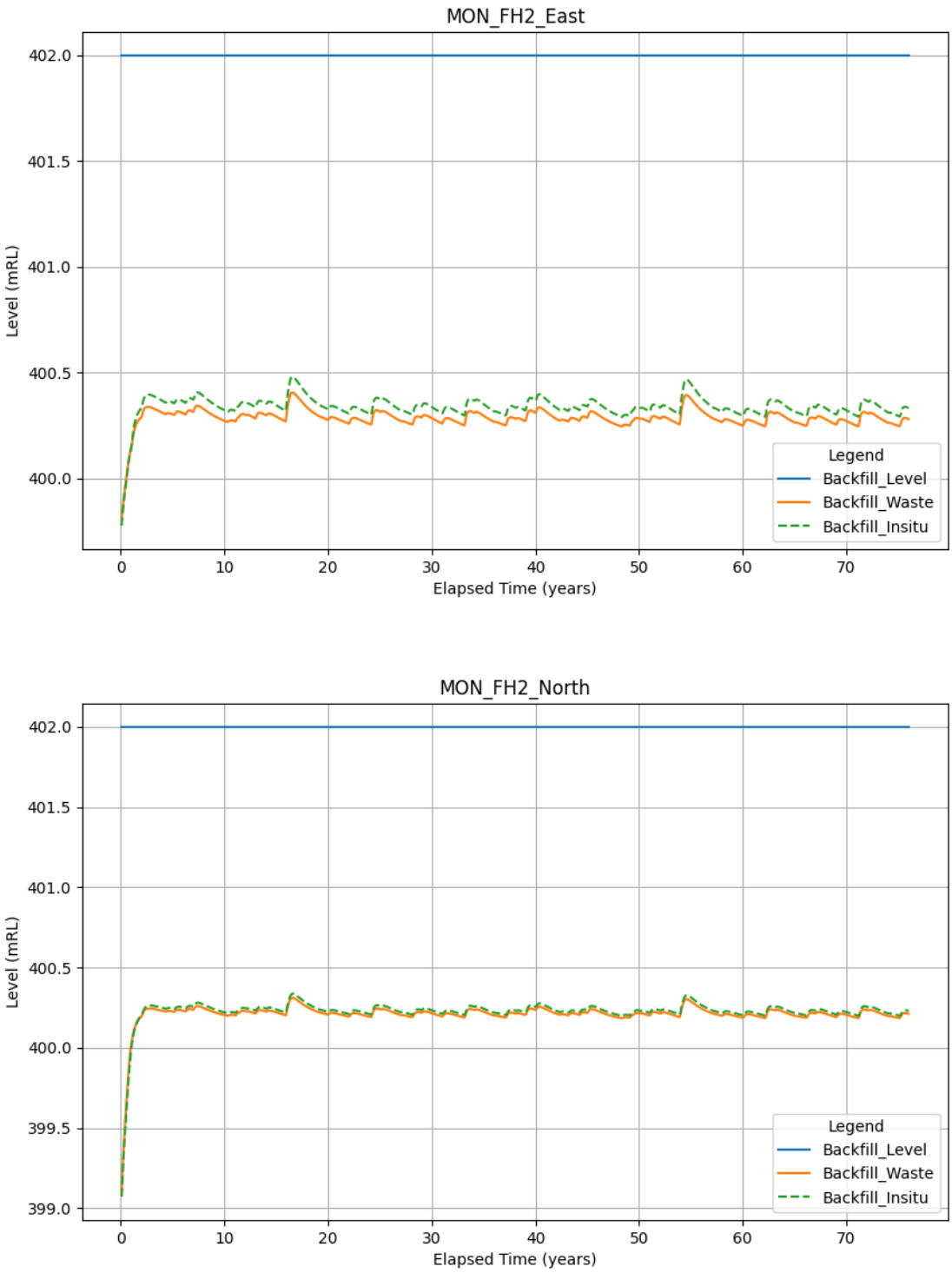

Figure B-73 Predicted pit water level recovery at Fridge Hill

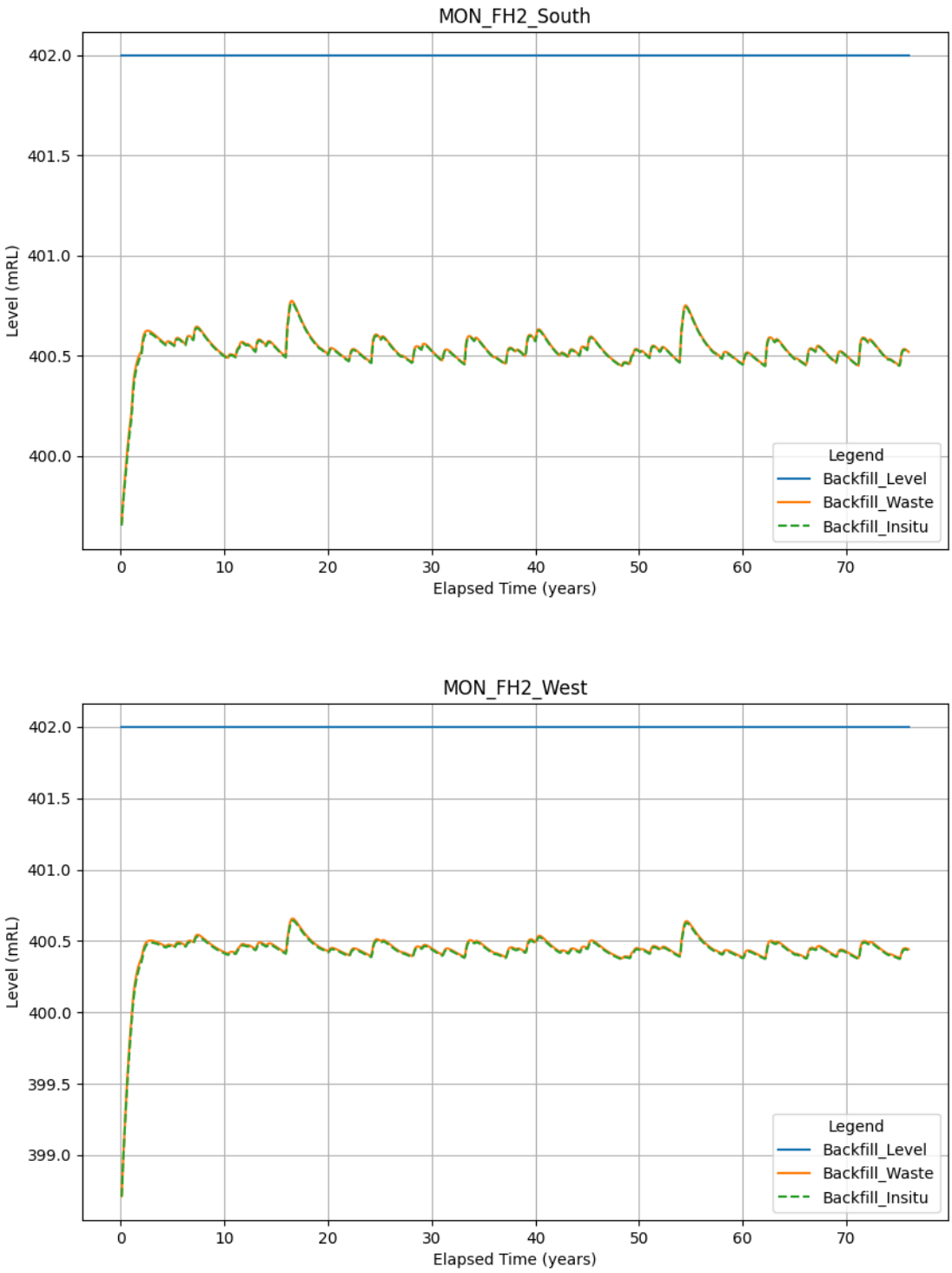

Figure B-74 Predicted pit water level recovery at Fridge Hill

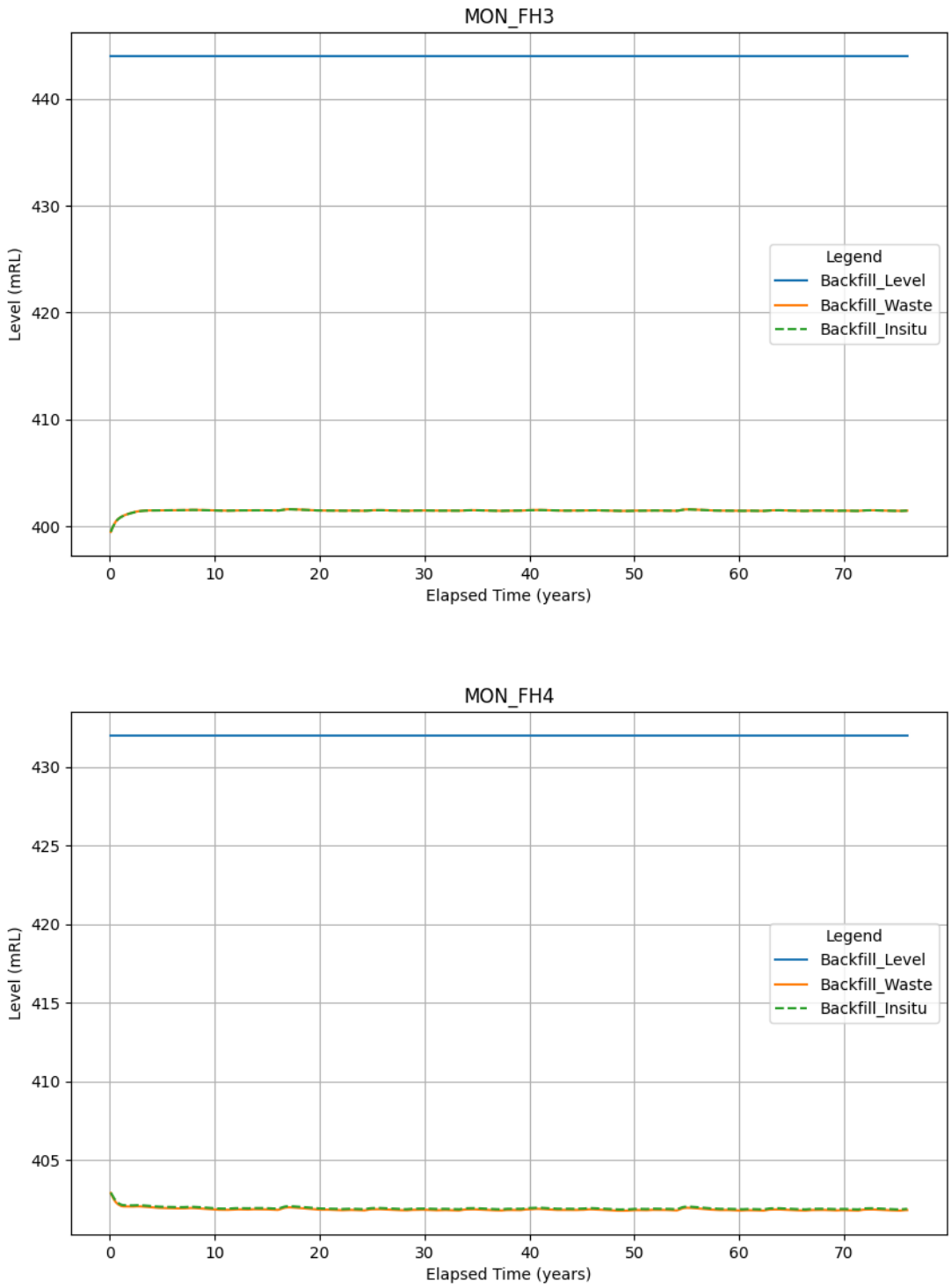

Figure B-75 Predicted pit water level recovery at Fridge Hill

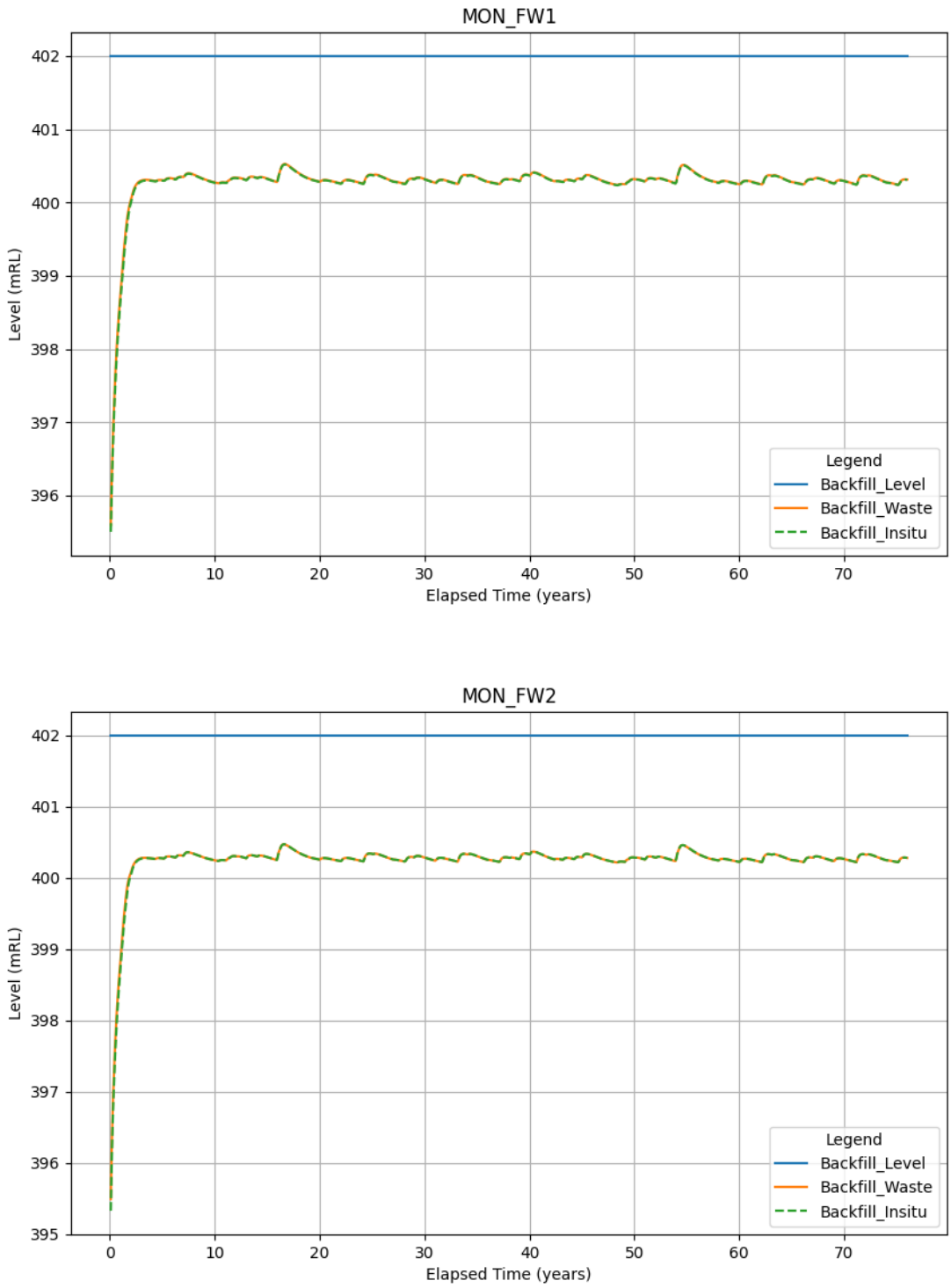

Figure B-76 Predicted pit water level recovery at Fridge West

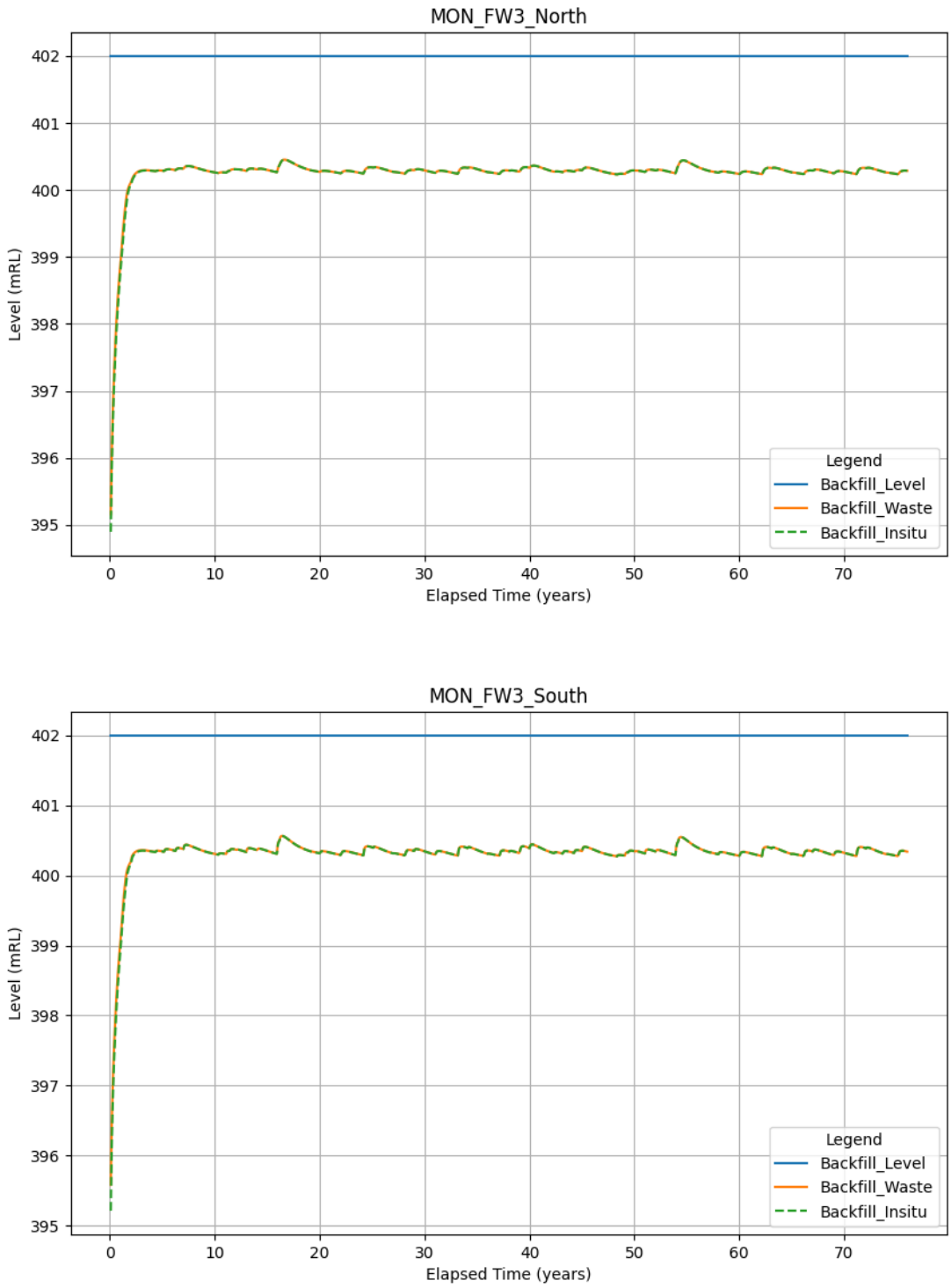

Figure B-77 Predicted pit water level recovery at Fridge West

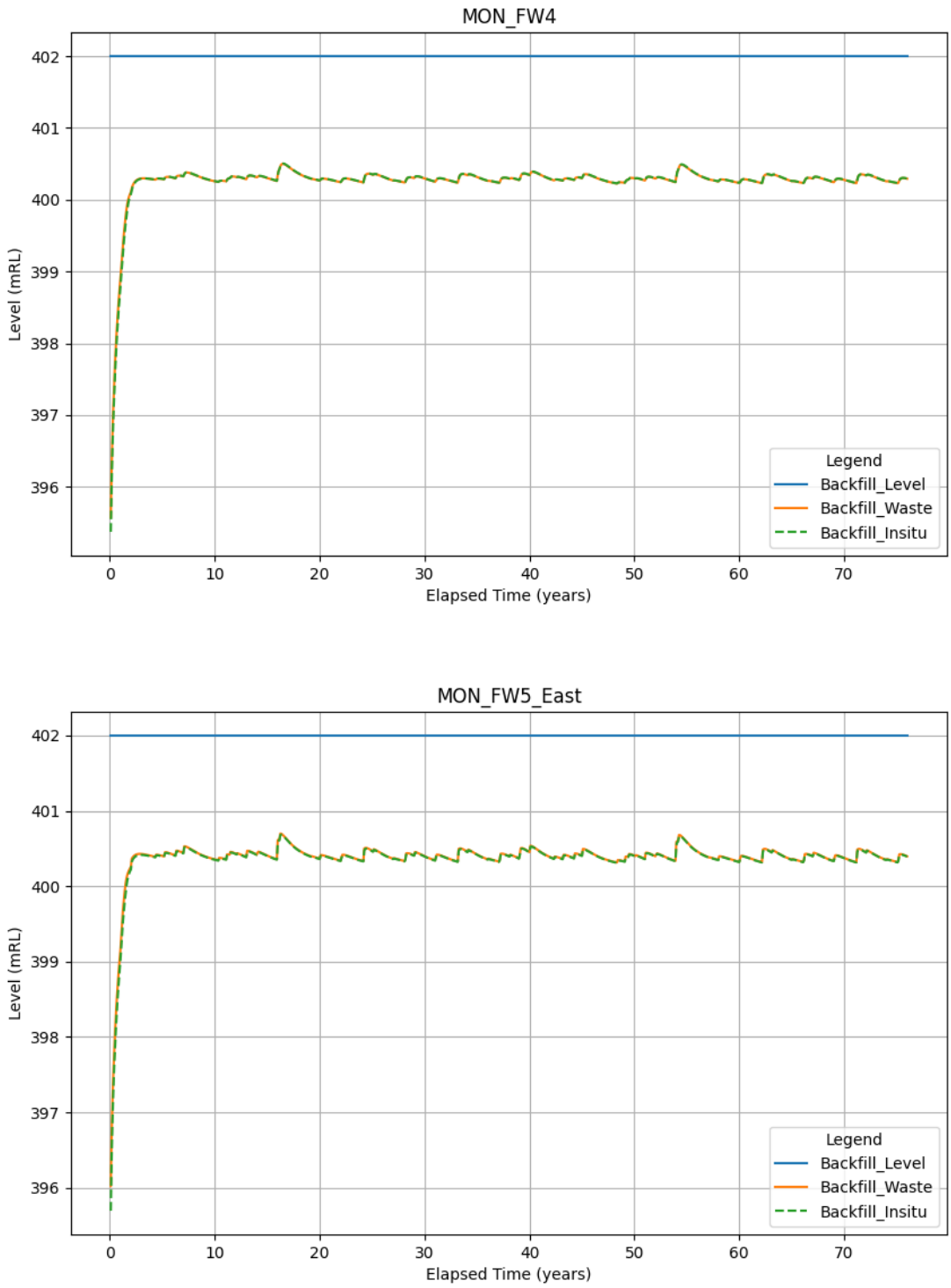

Figure B-78 Predicted pit water level recovery at Fridge West

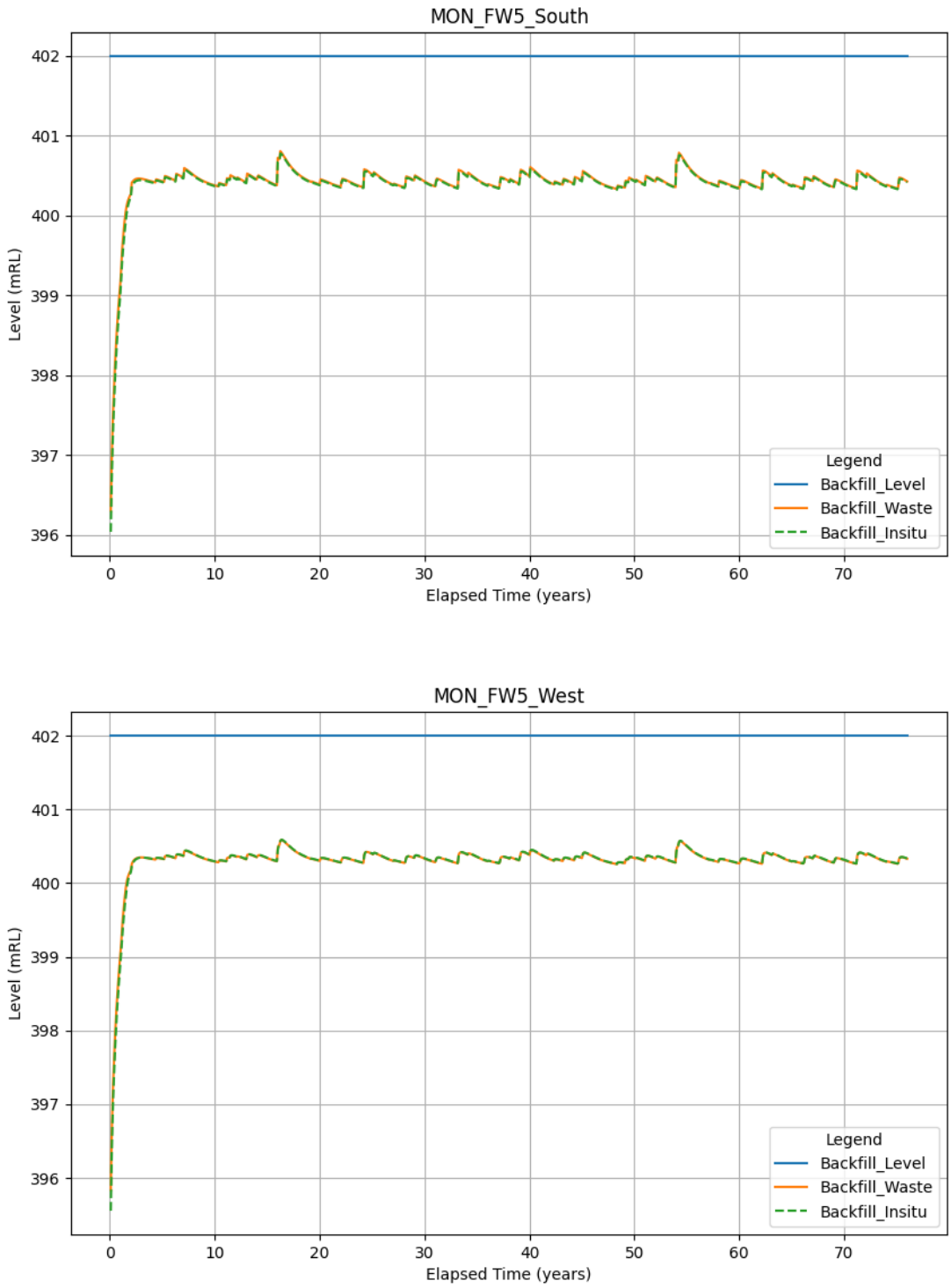

Figure B-79 Predicted pit water level recovery at Fridge West

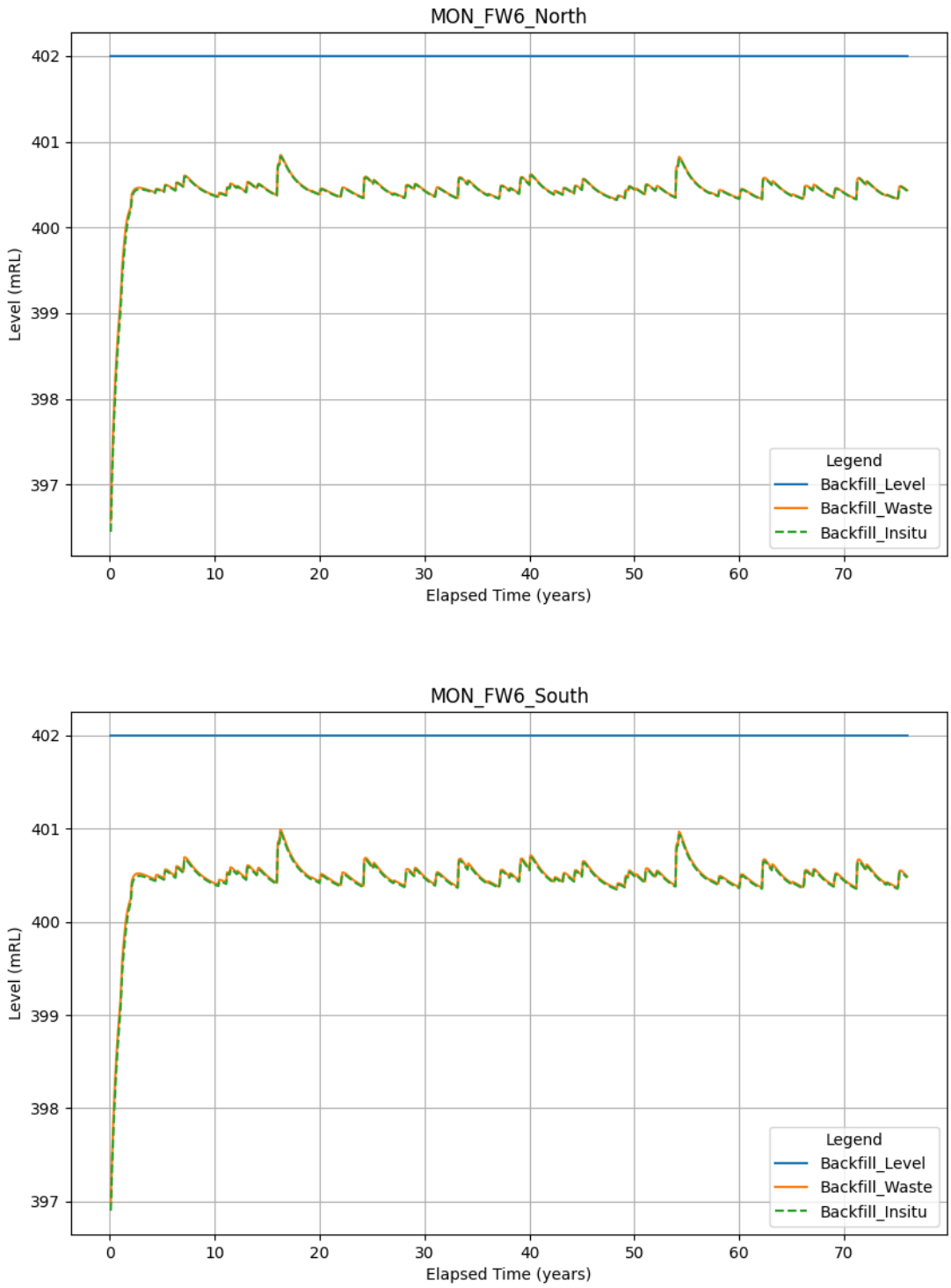

Figure B-80 Predicted pit water level recovery at Fridge West

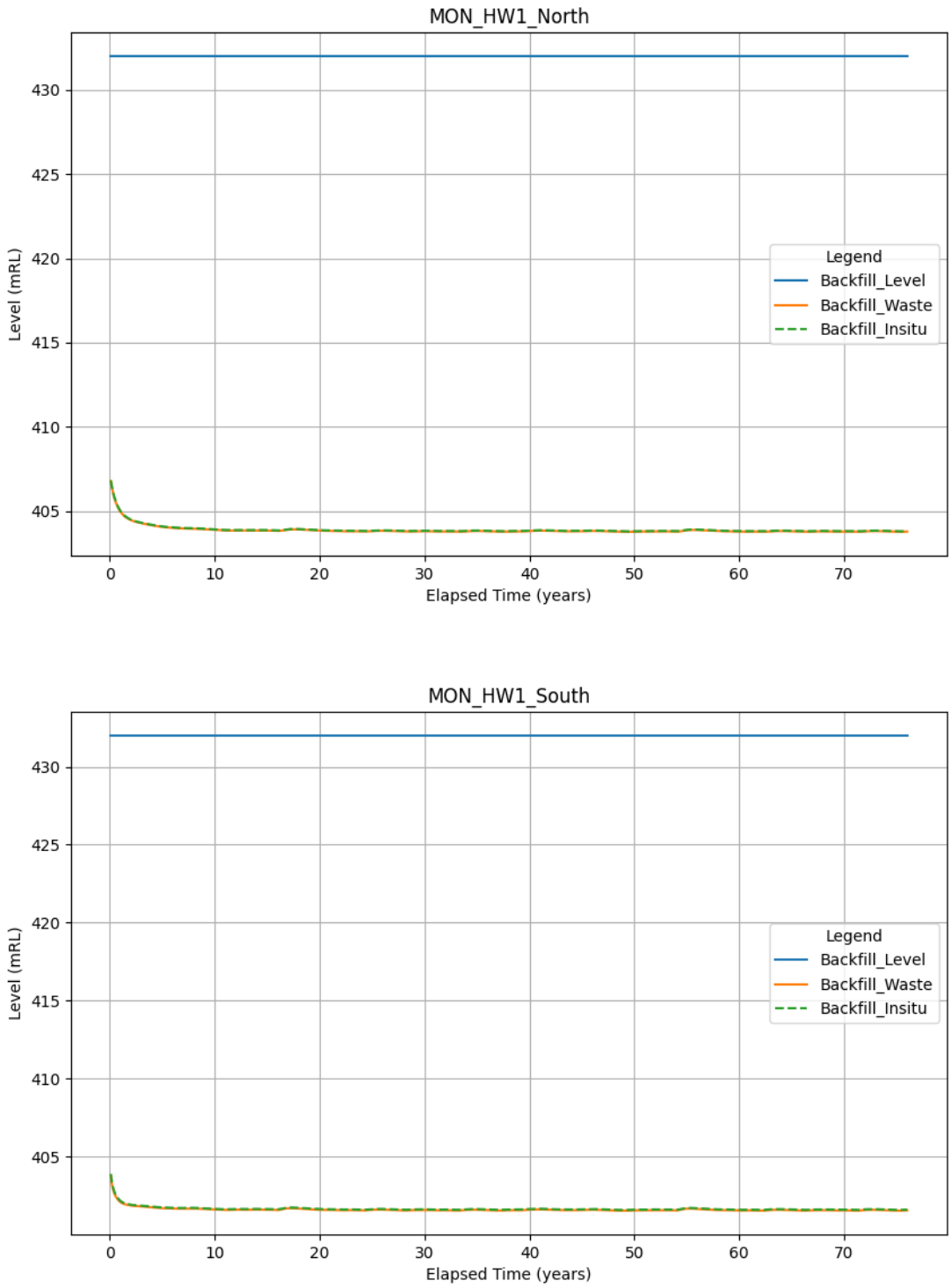

Figure B-81 Predicted pit water level recovery at Horseshoe West

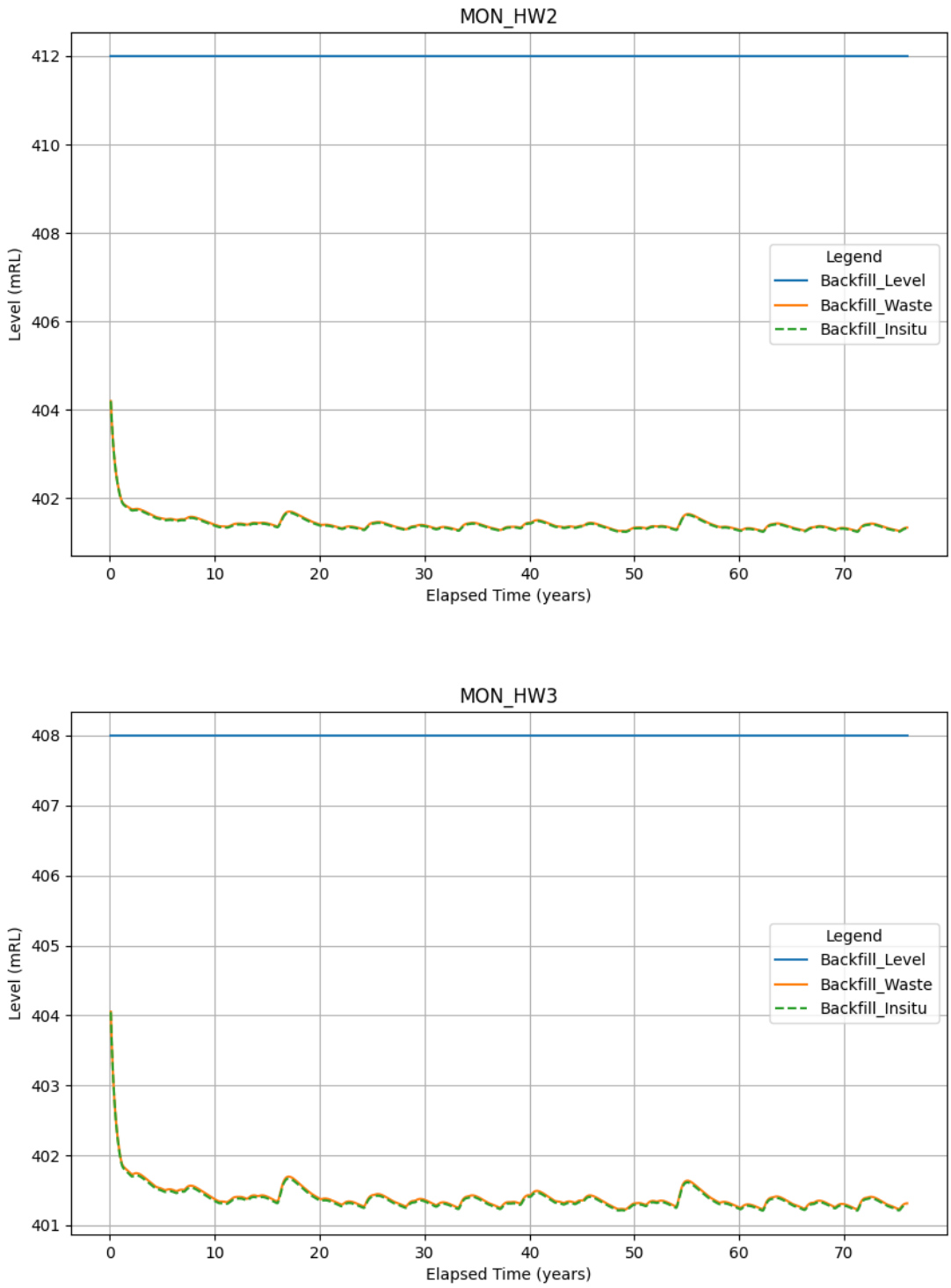

Figure B-82 Predicted pit water level recovery at Horseshoe West

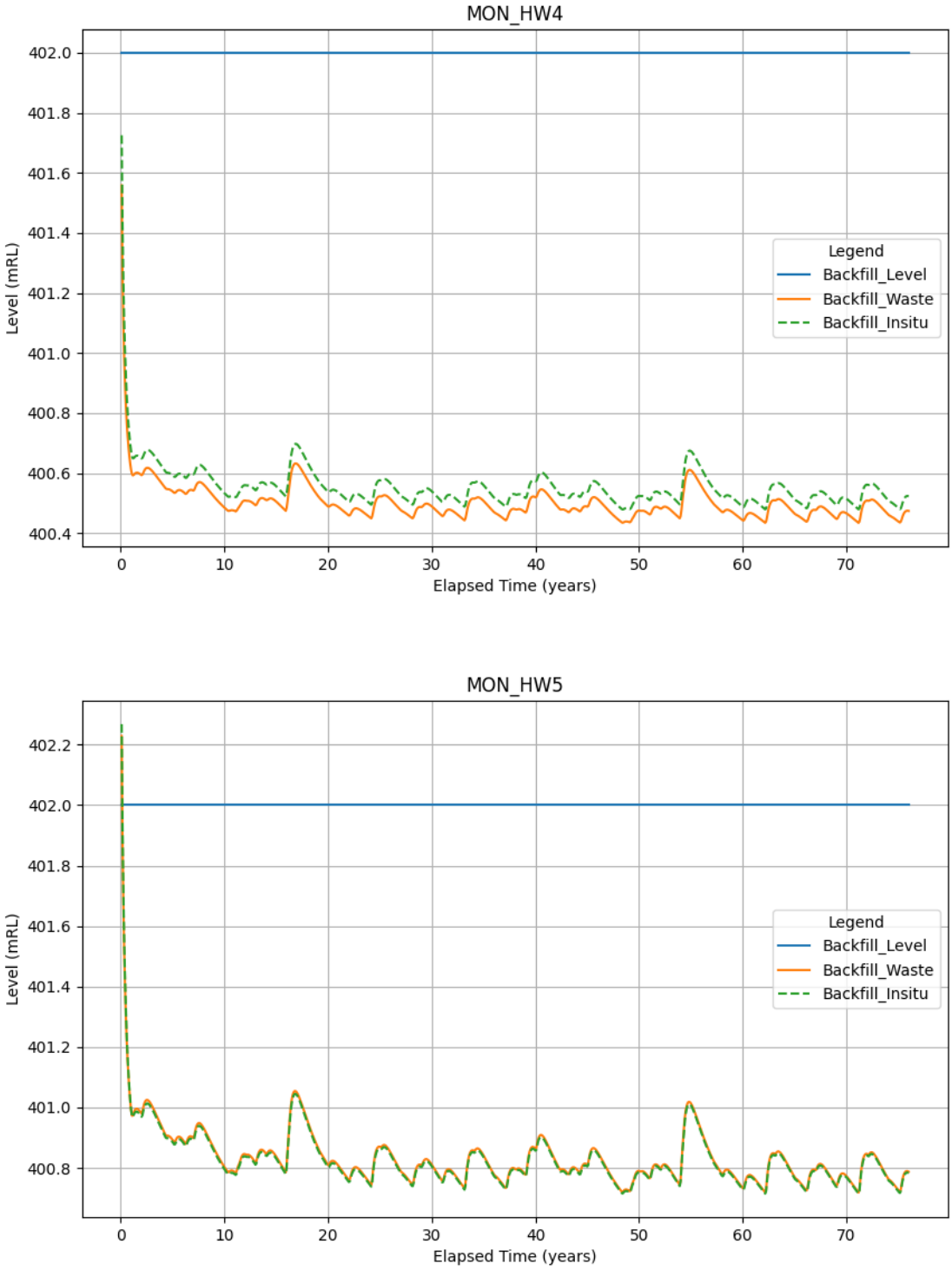

Figure B-83 Predicted pit water level recovery at Horseshoe West

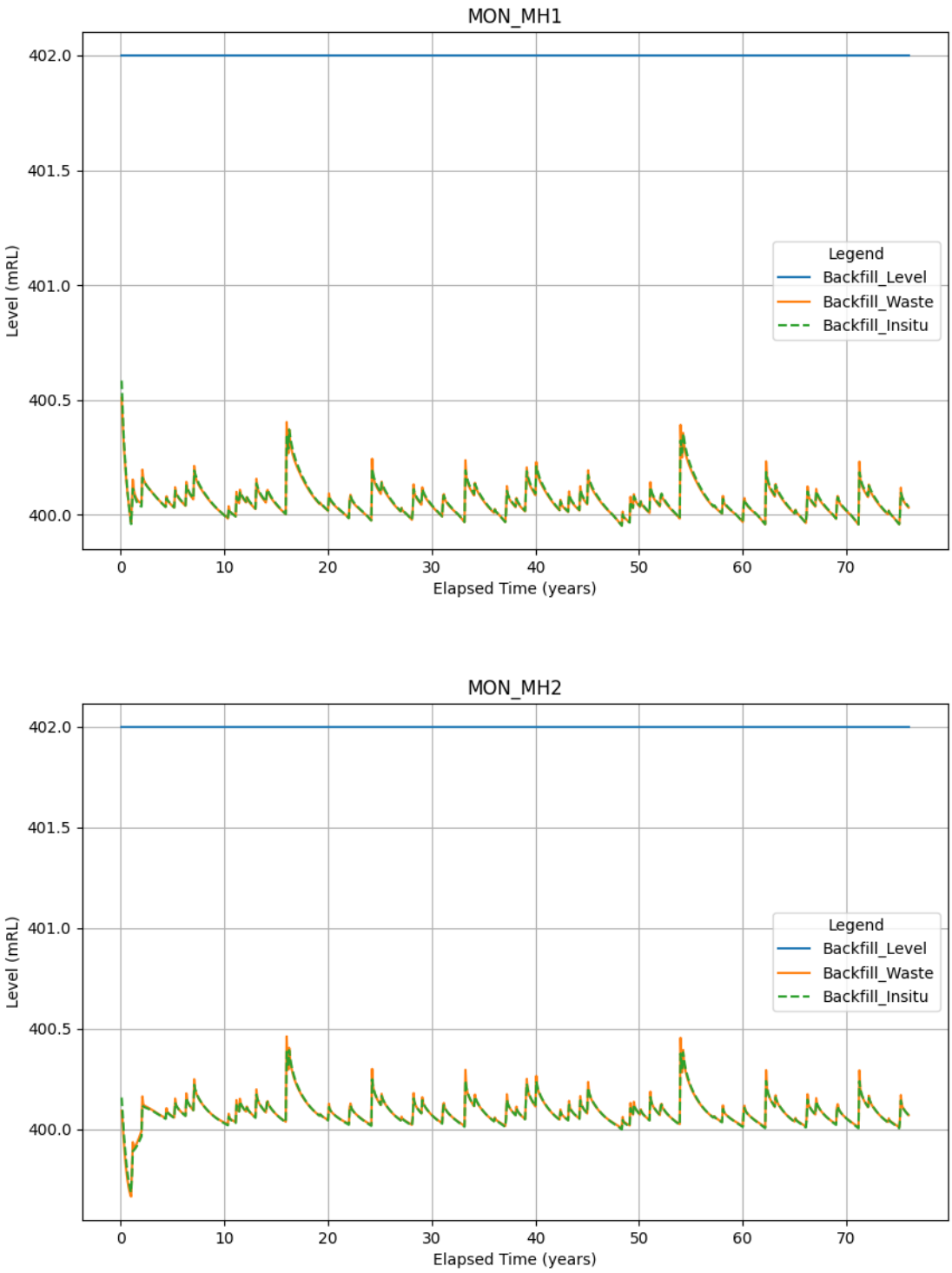

Figure B-84 Predicted pit water level recovery at Murray West

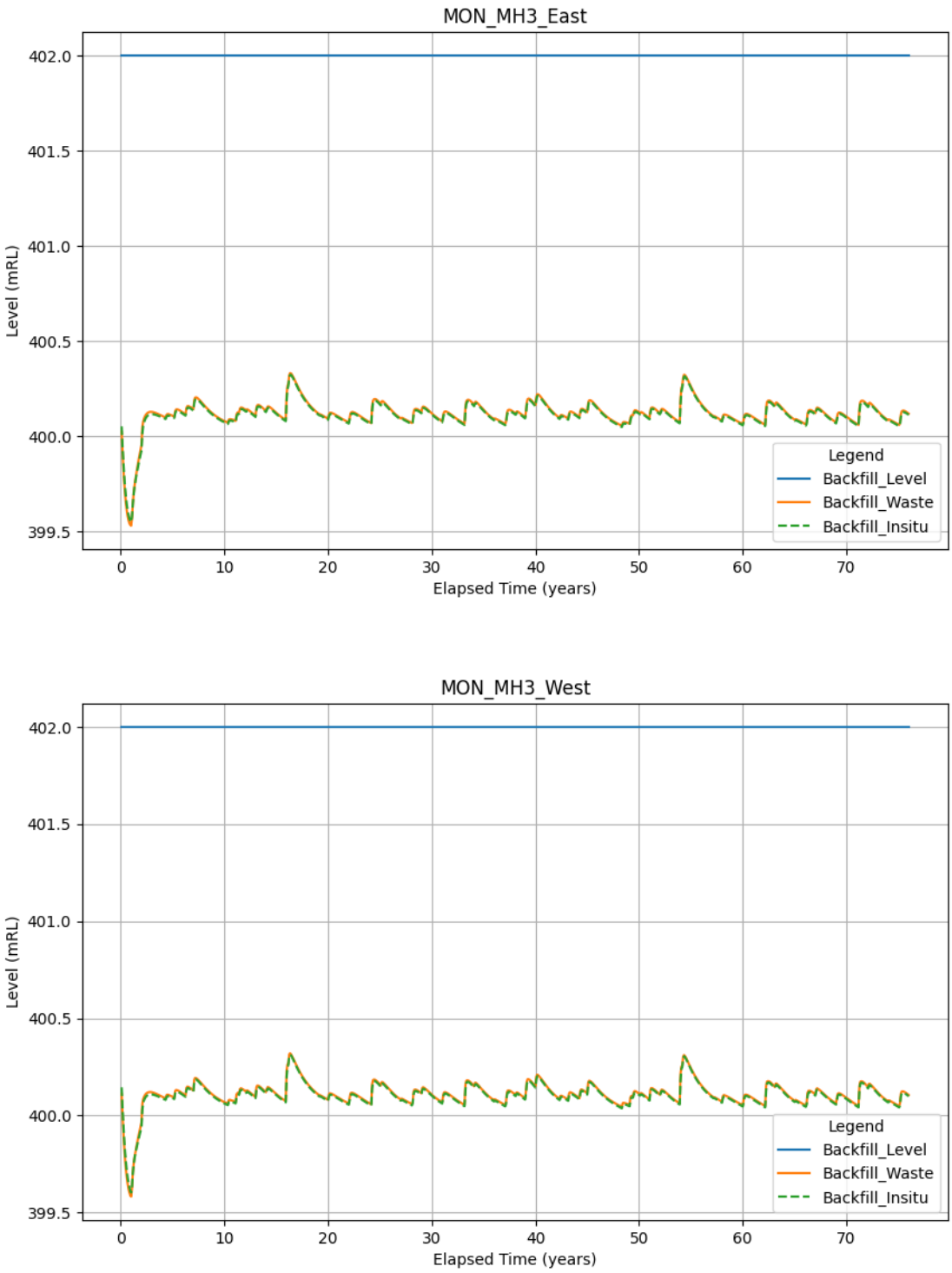

Figure B-85 Predicted pit water level recovery at Murray West

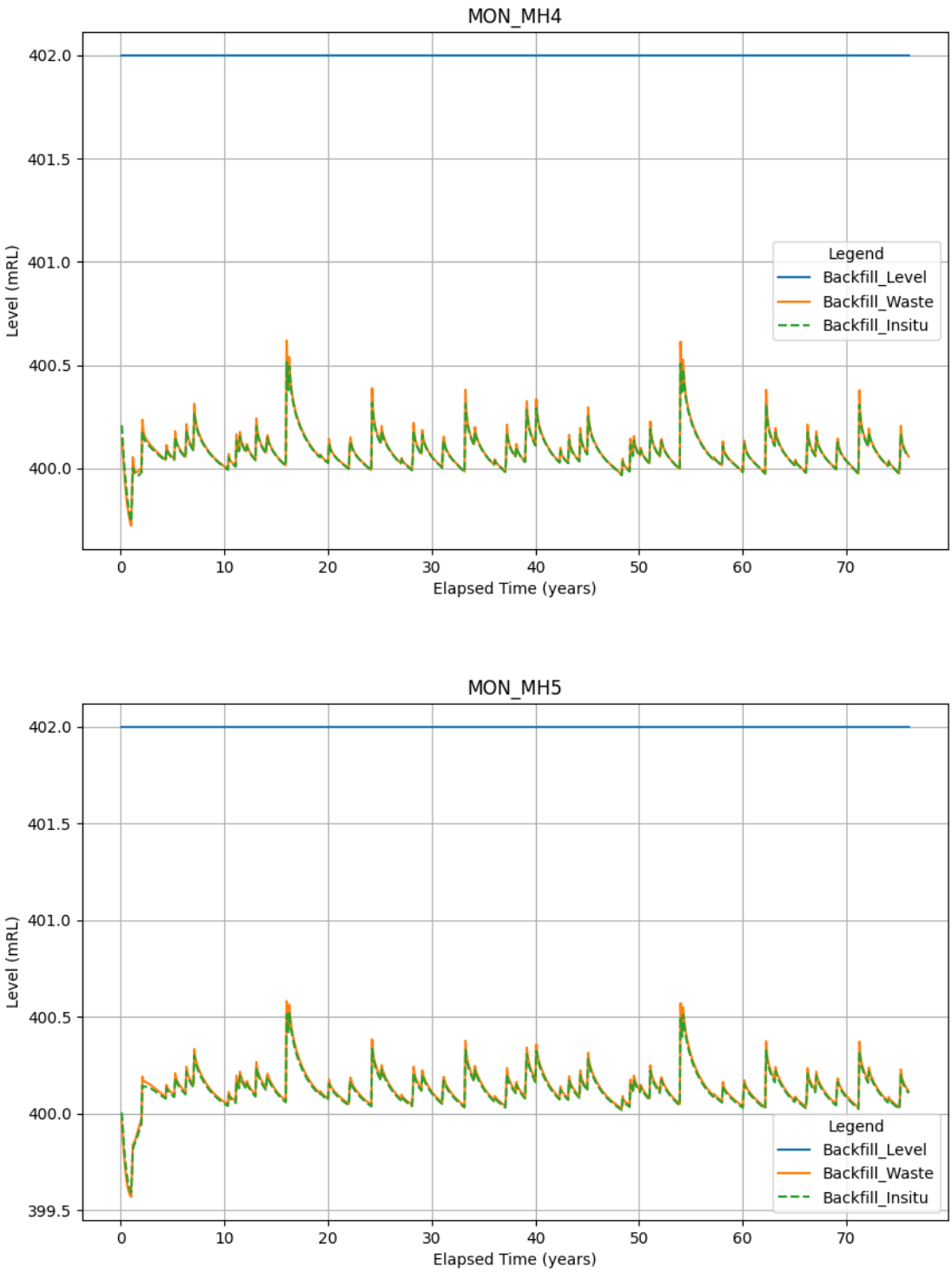

Figure B-86 Predicted pit water level recovery at Murray West

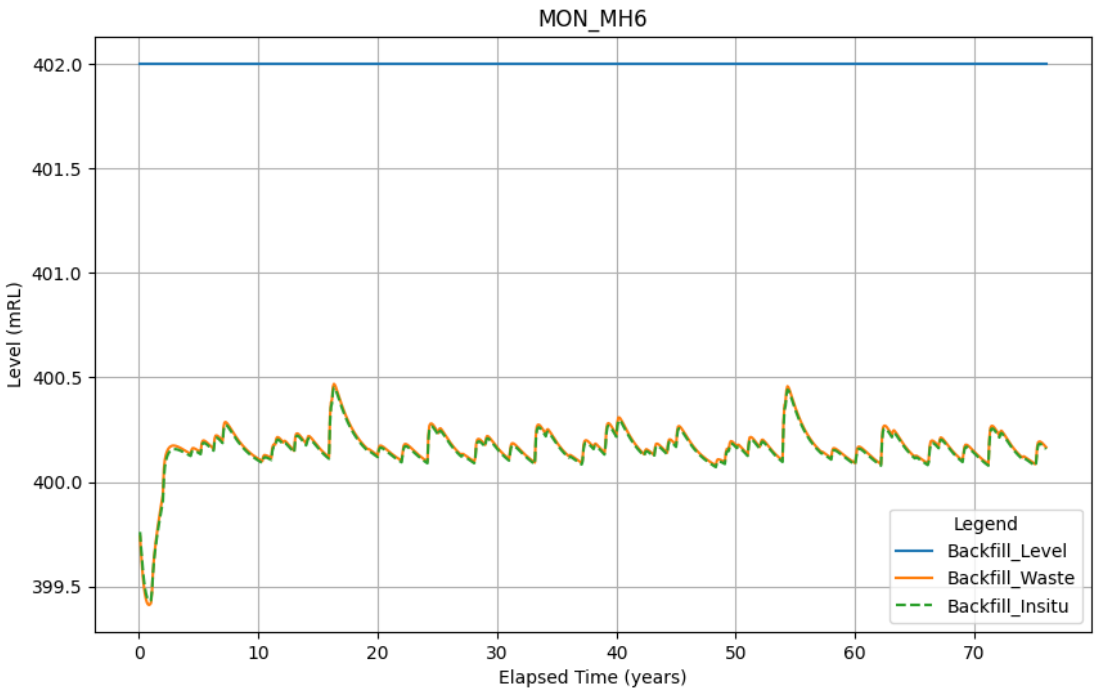

Figure B-87 Predicted pit water level recovery at Murray West

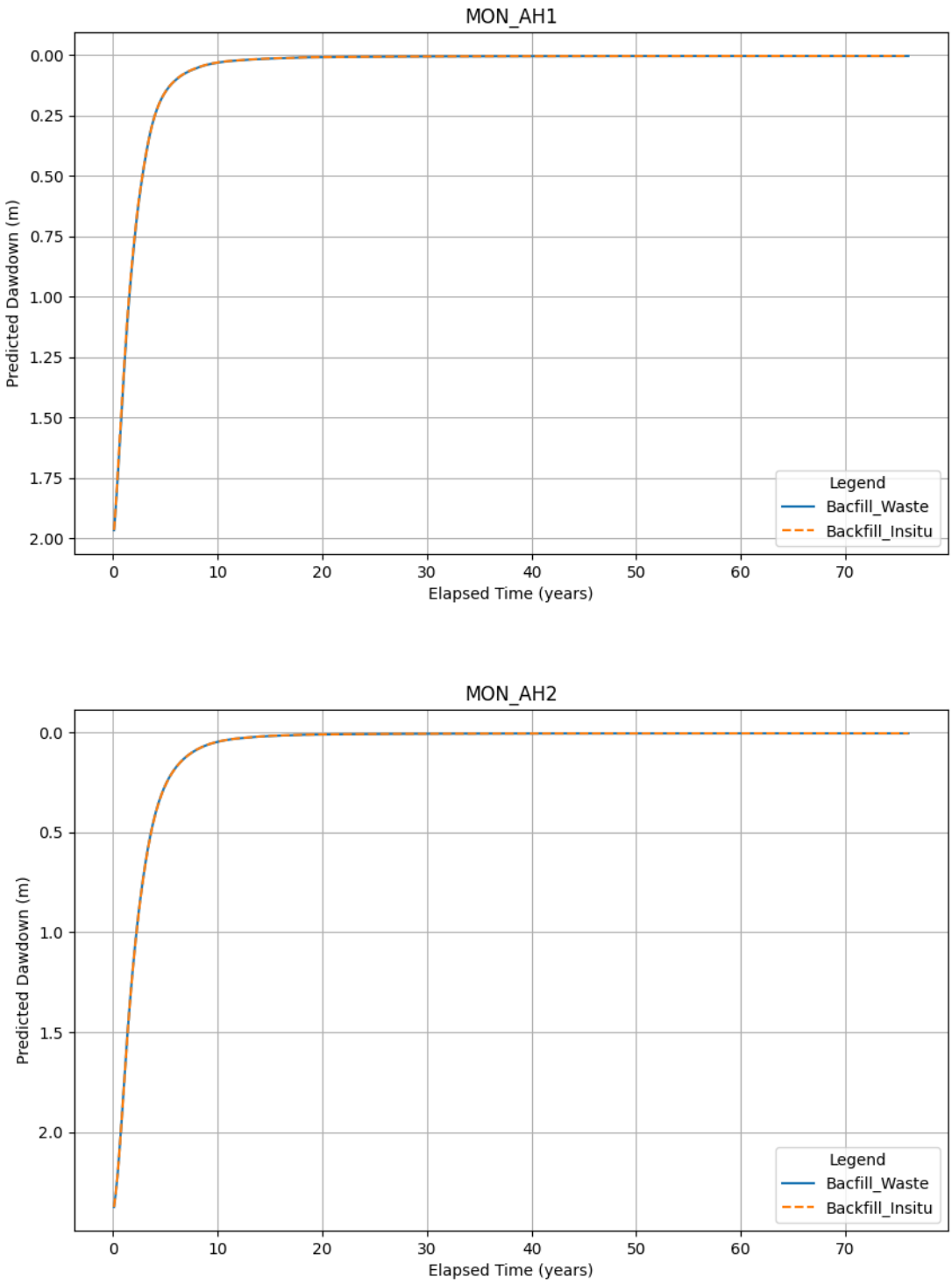

Figure B-88 Predicted aquifer recovery at Anticline Hill

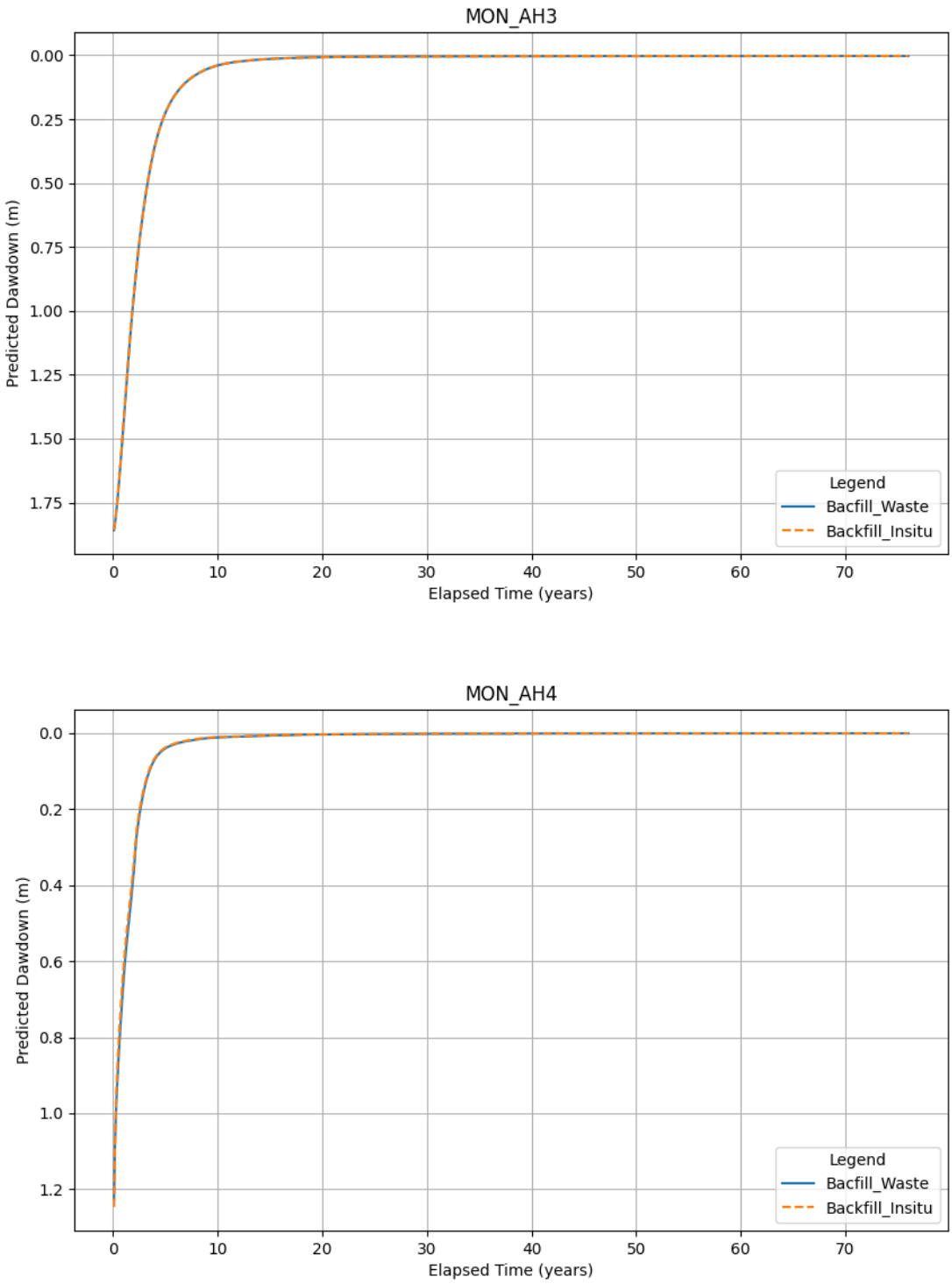

Figure B-89 Predicted aquifer recovery at Anticline Hill

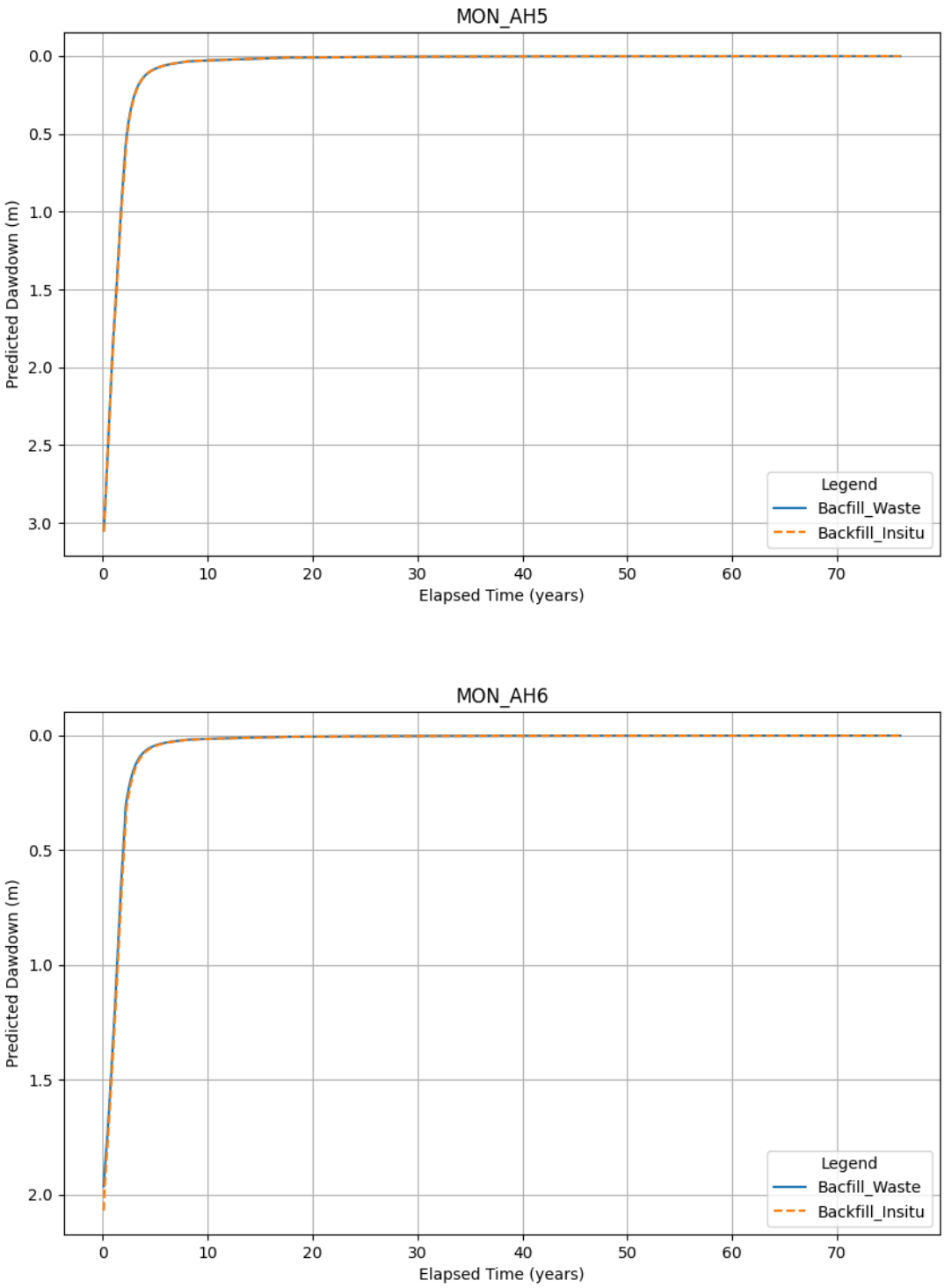

Figure B-90 Predicted aquifer recovery at Anticline Hill

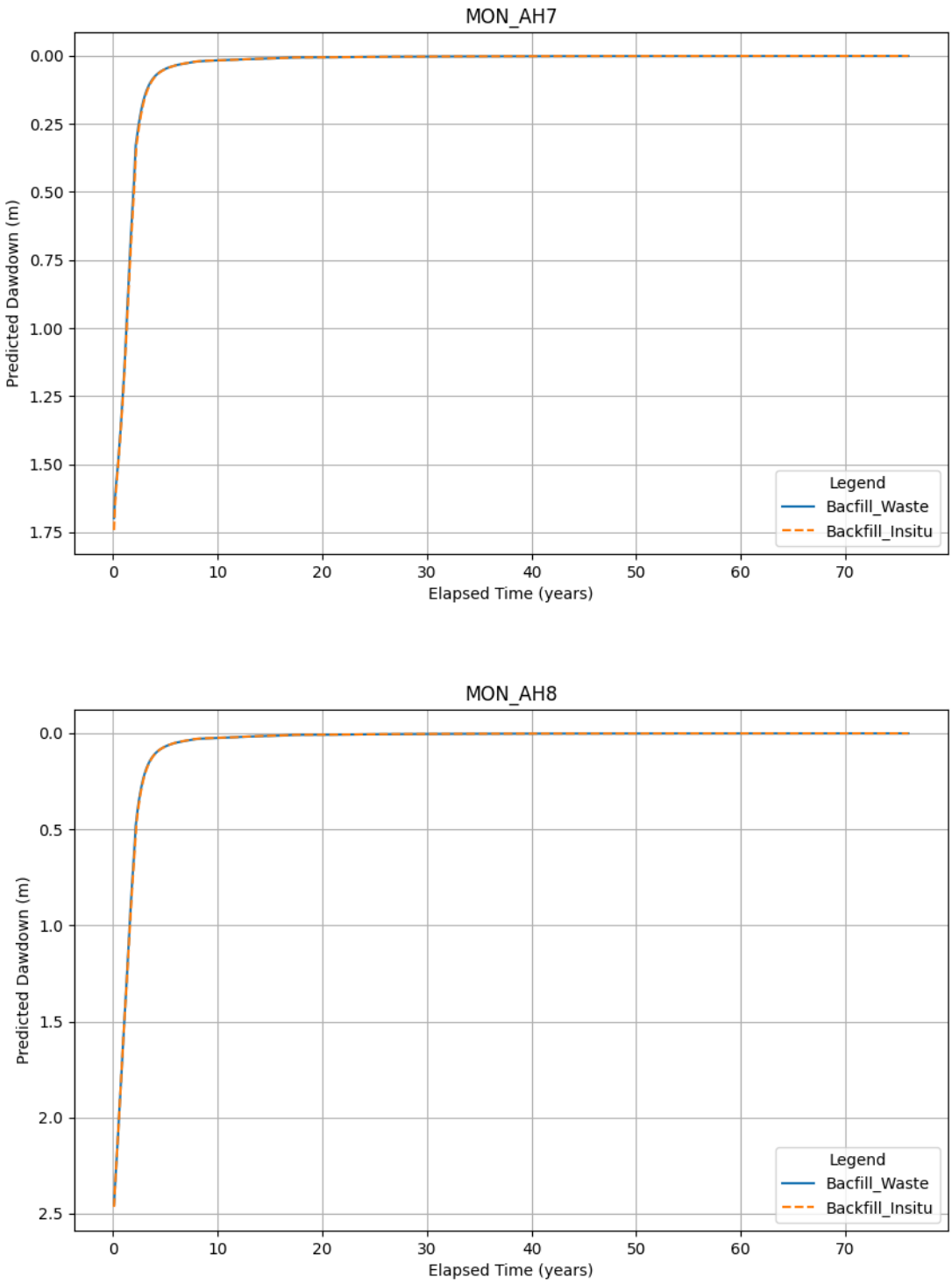

Figure B-91 Predicted aquifer recovery at Anticline Hill

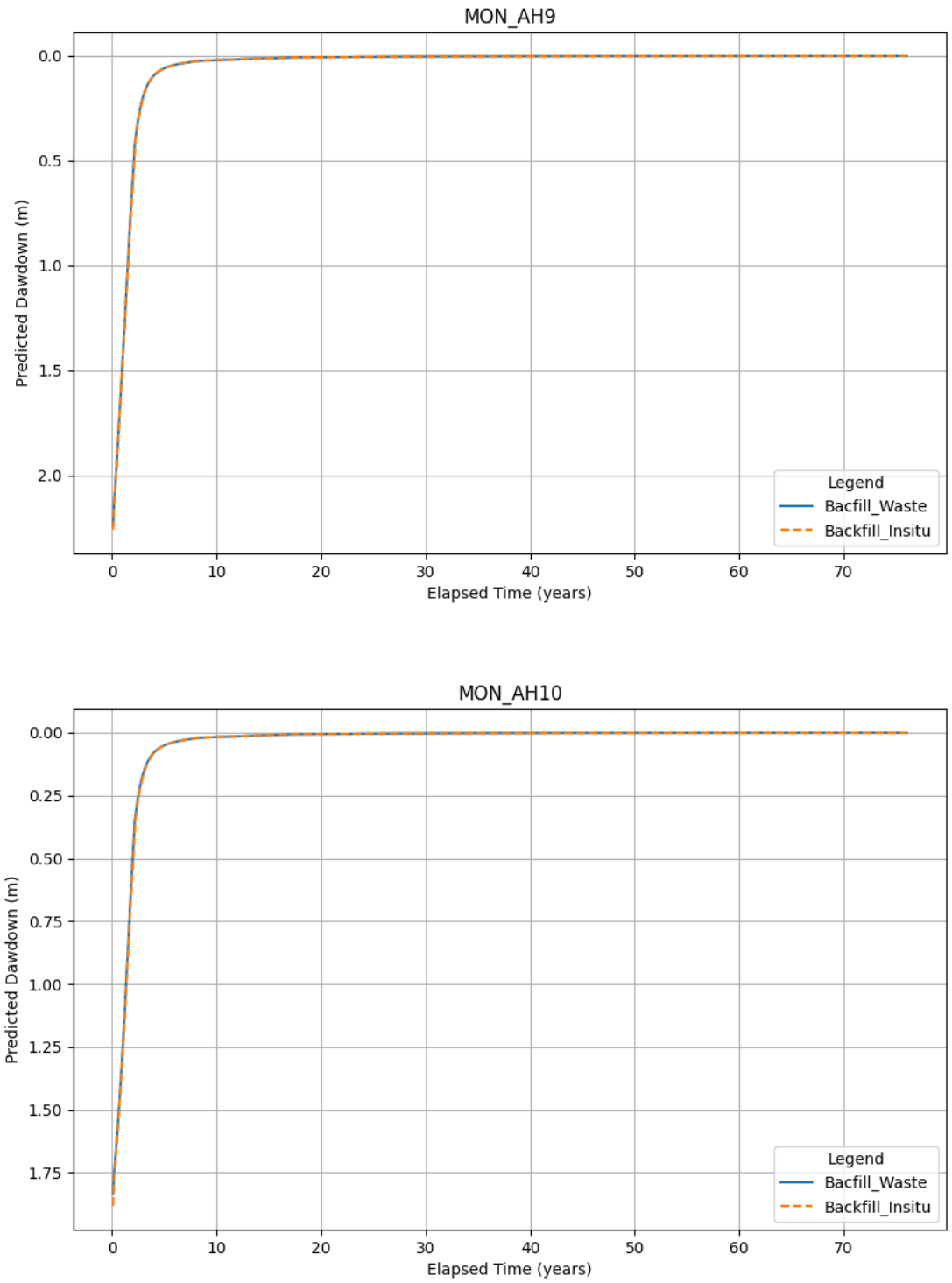

Figure B-92 Predicted aquifer recovery at Anticline Hill

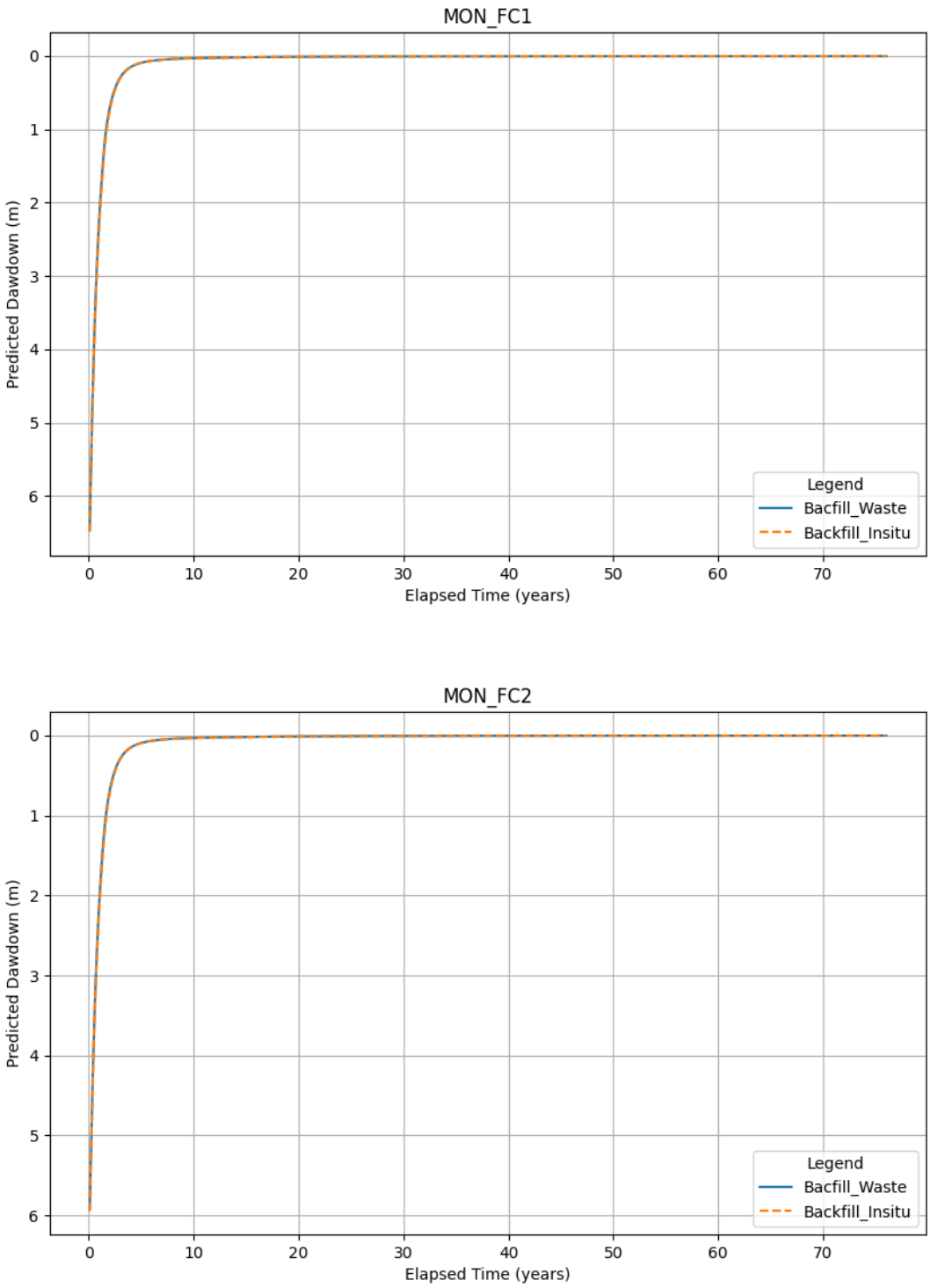

Figure B-93 Predicted aquifer recovery at Fridge Central

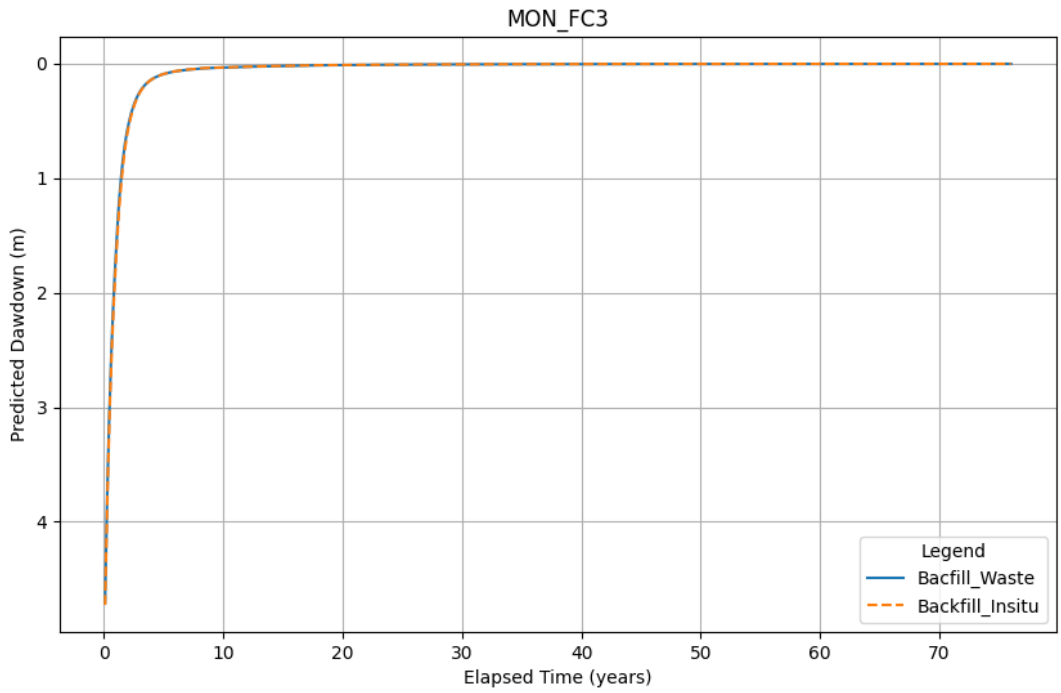

Figure B-94 Predicted aquifer recovery at Fridge Central

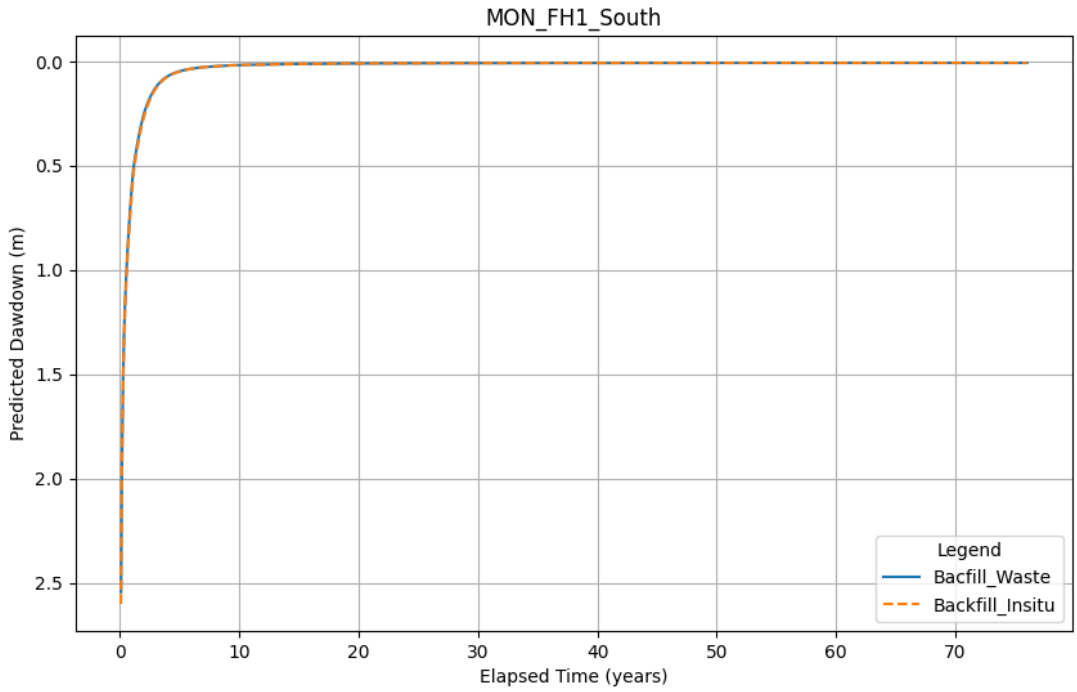

Figure B-95 Predicted aquifer recovery at Fridge Hill

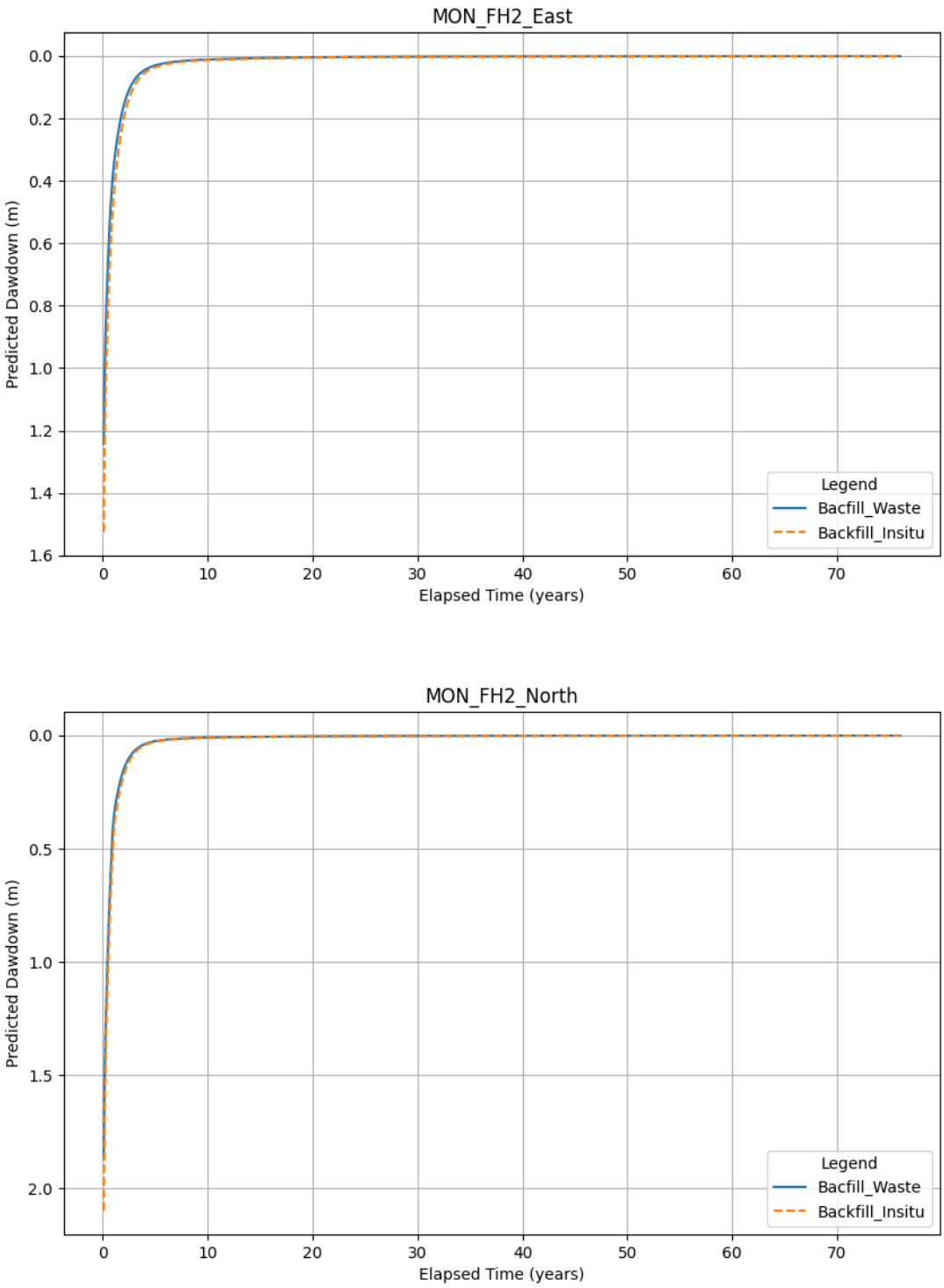

Figure B-96 Predicted aquifer recovery at Fridge Hill

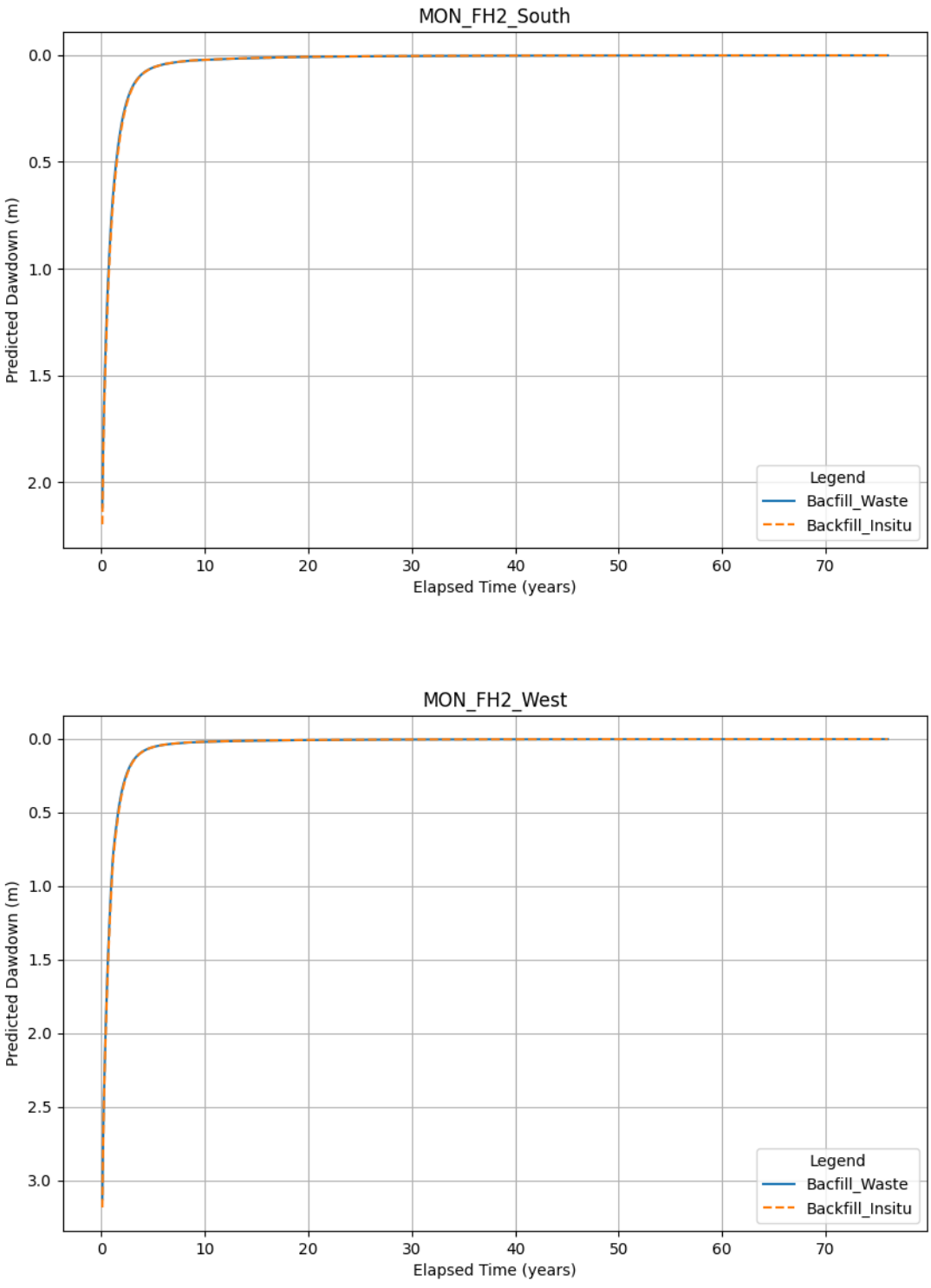

Figure B-97 Predicted aquifer recovery at Fridge Hill

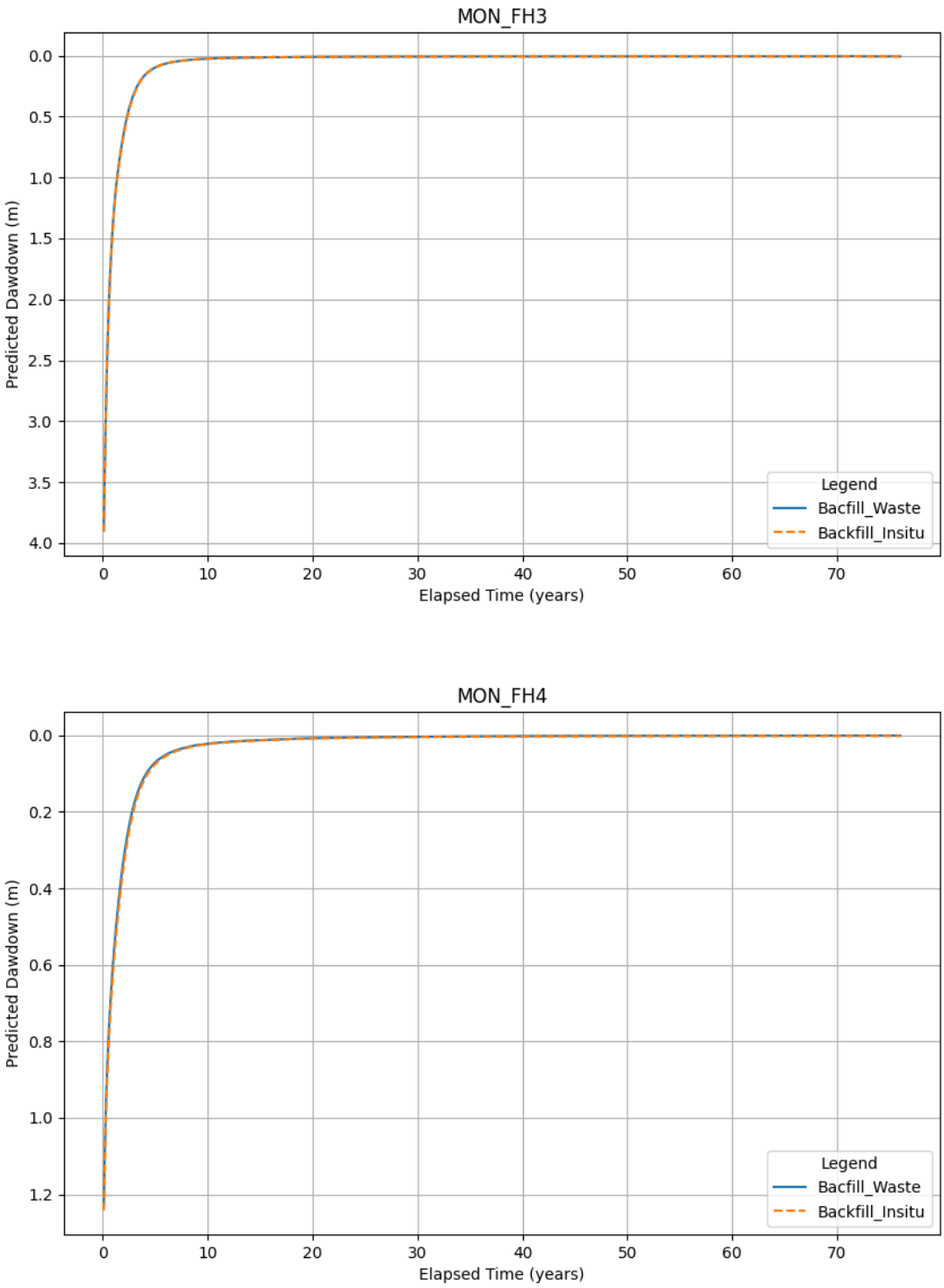

Figure B-98 Predicted aquifer recovery at Fridge Hill

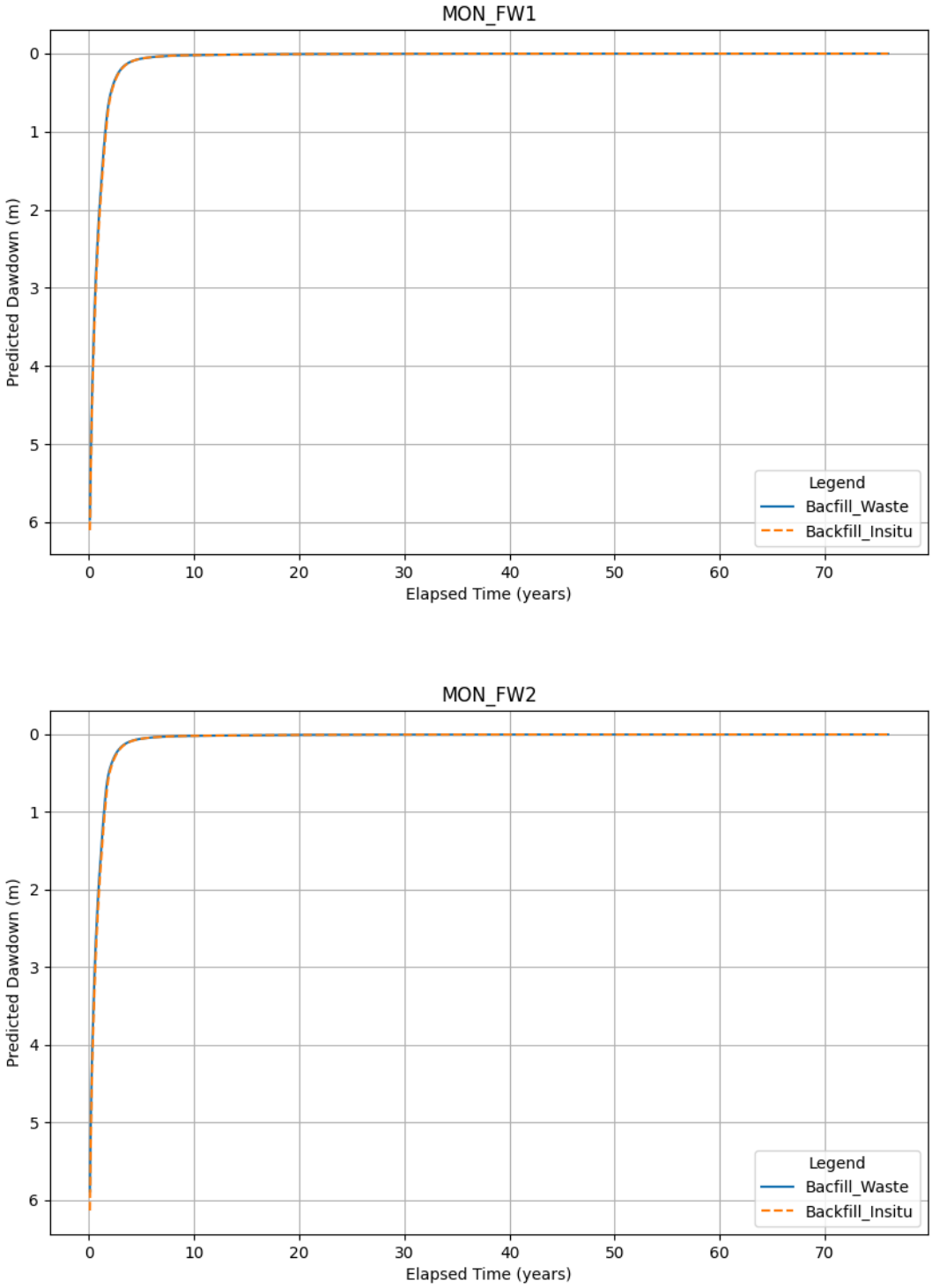

Figure B-99 Predicted aquifer recovery at Fridge West

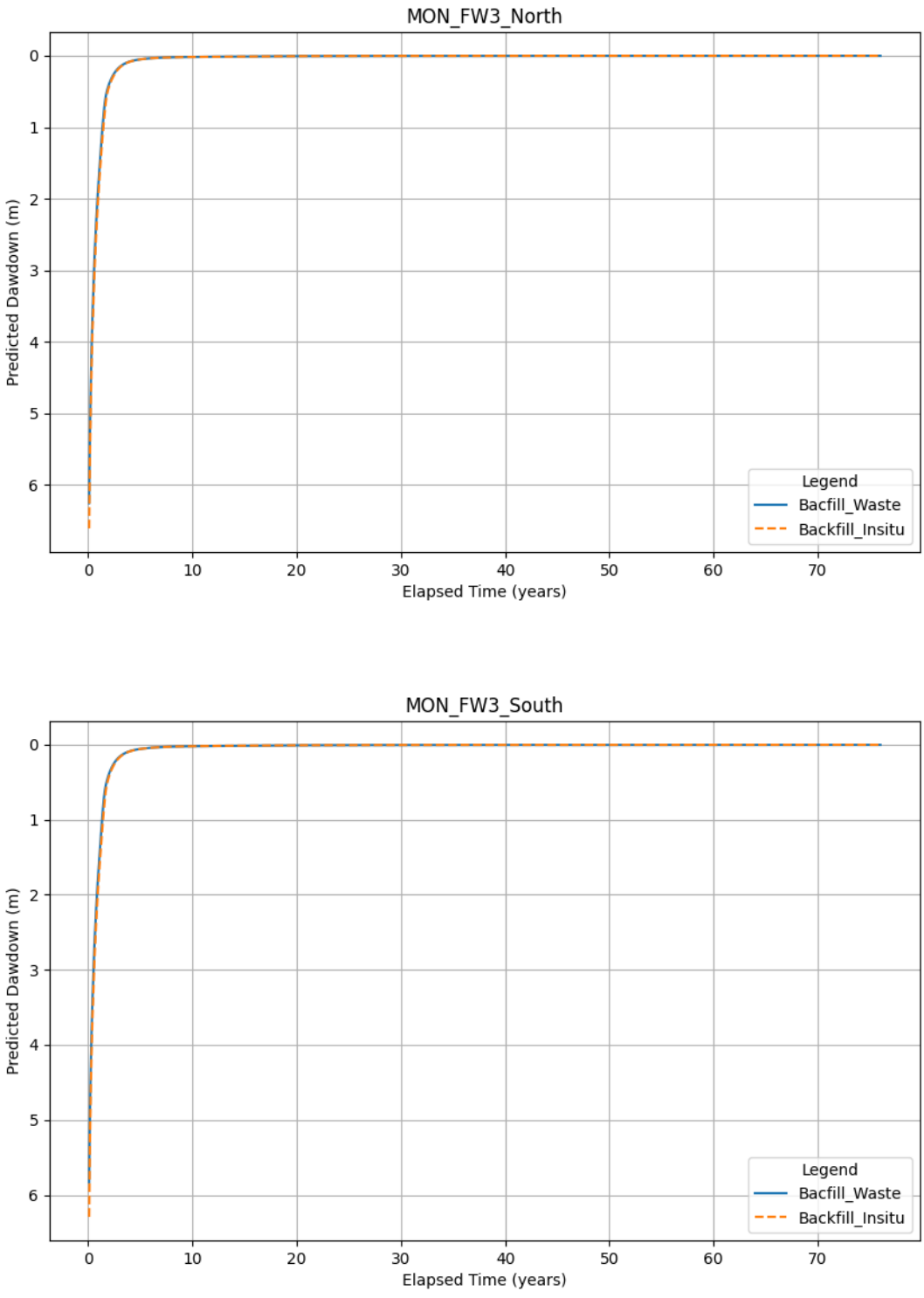

Figure B-100 Predicted aquifer recovery at Fridge West

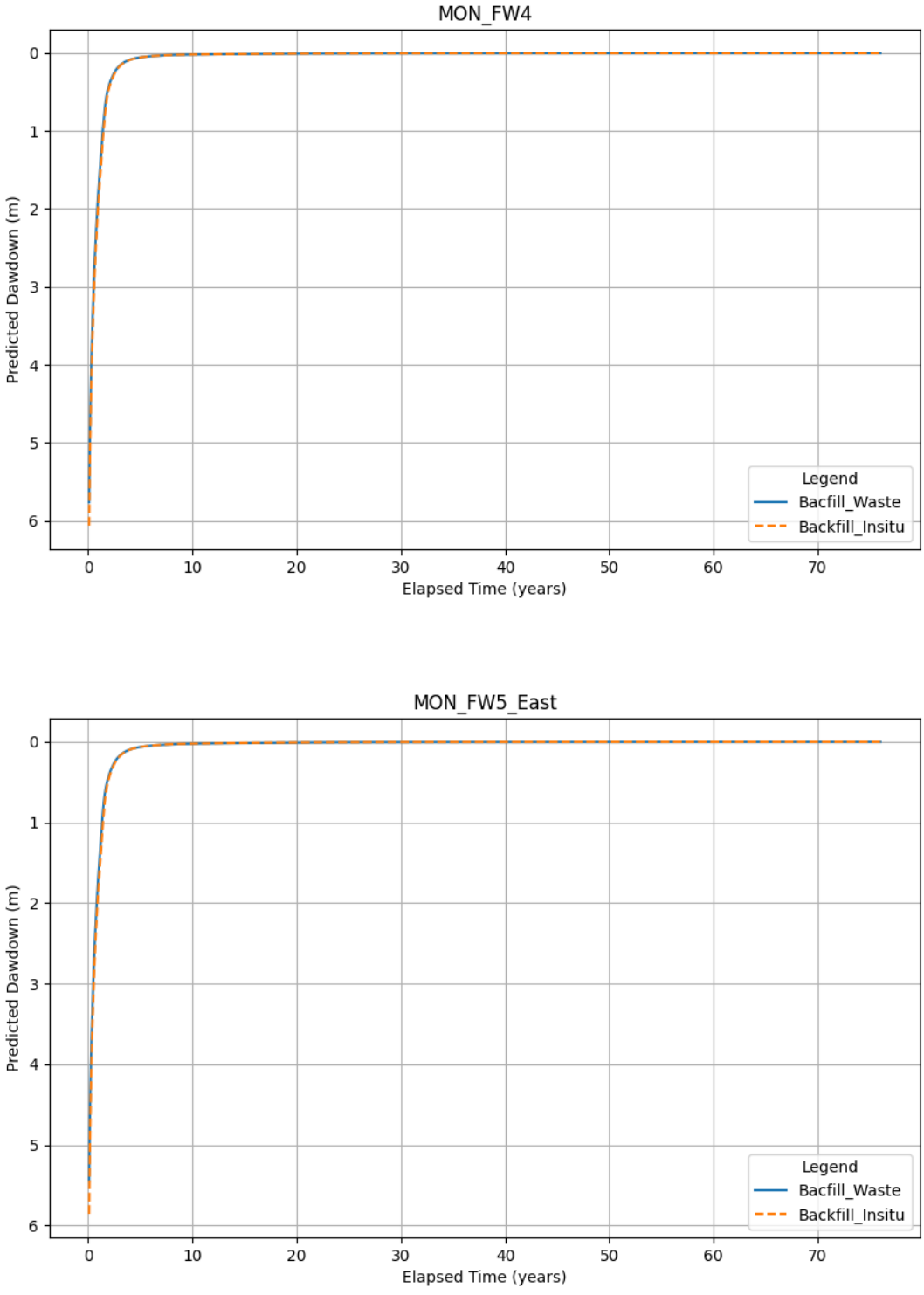

Figure B-101 Predicted aquifer recovery at Fridge West

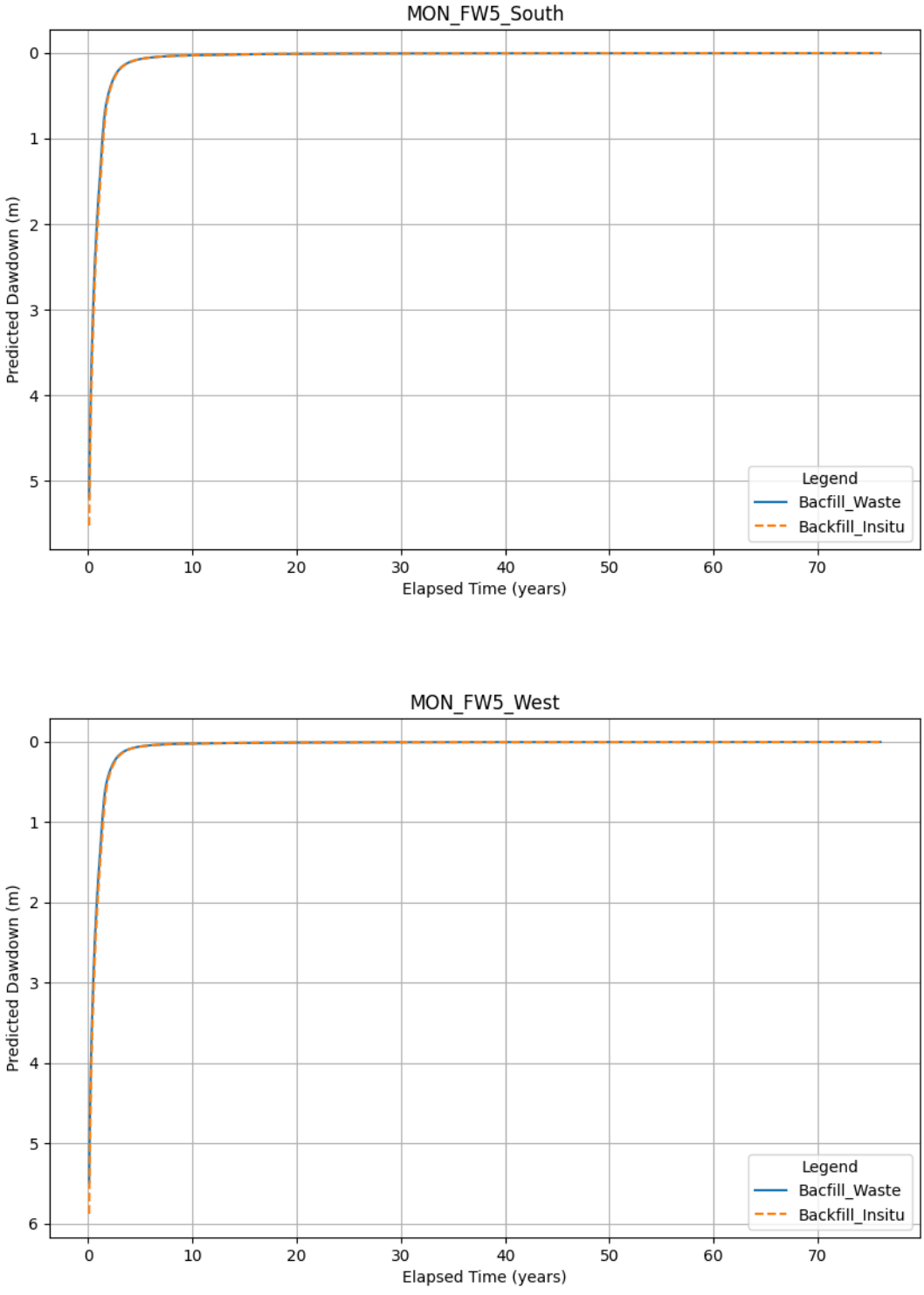

Figure B-102 Predicted aquifer recovery at Fridge West

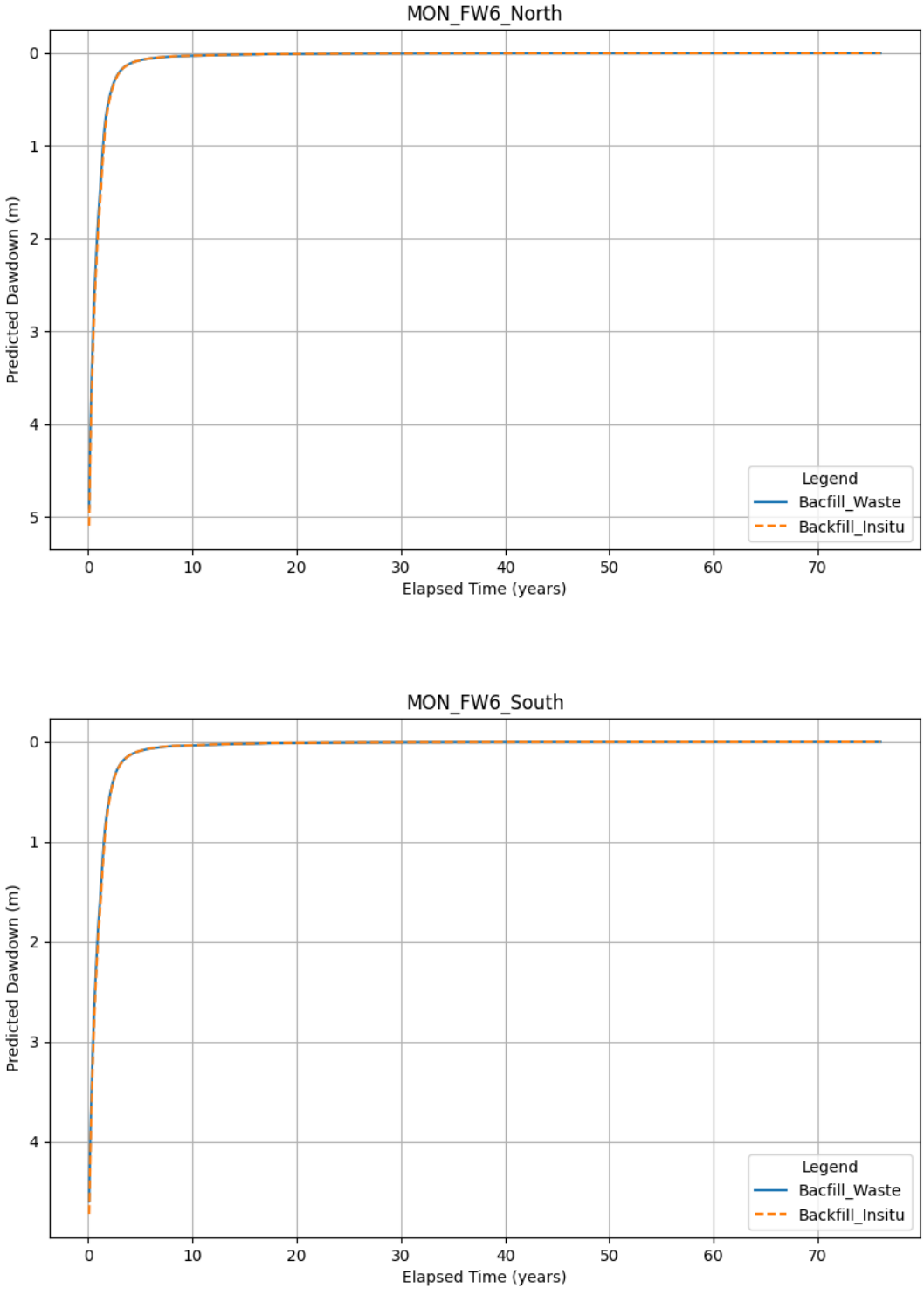

Figure B-103 Predicted aquifer recovery at Fridge West

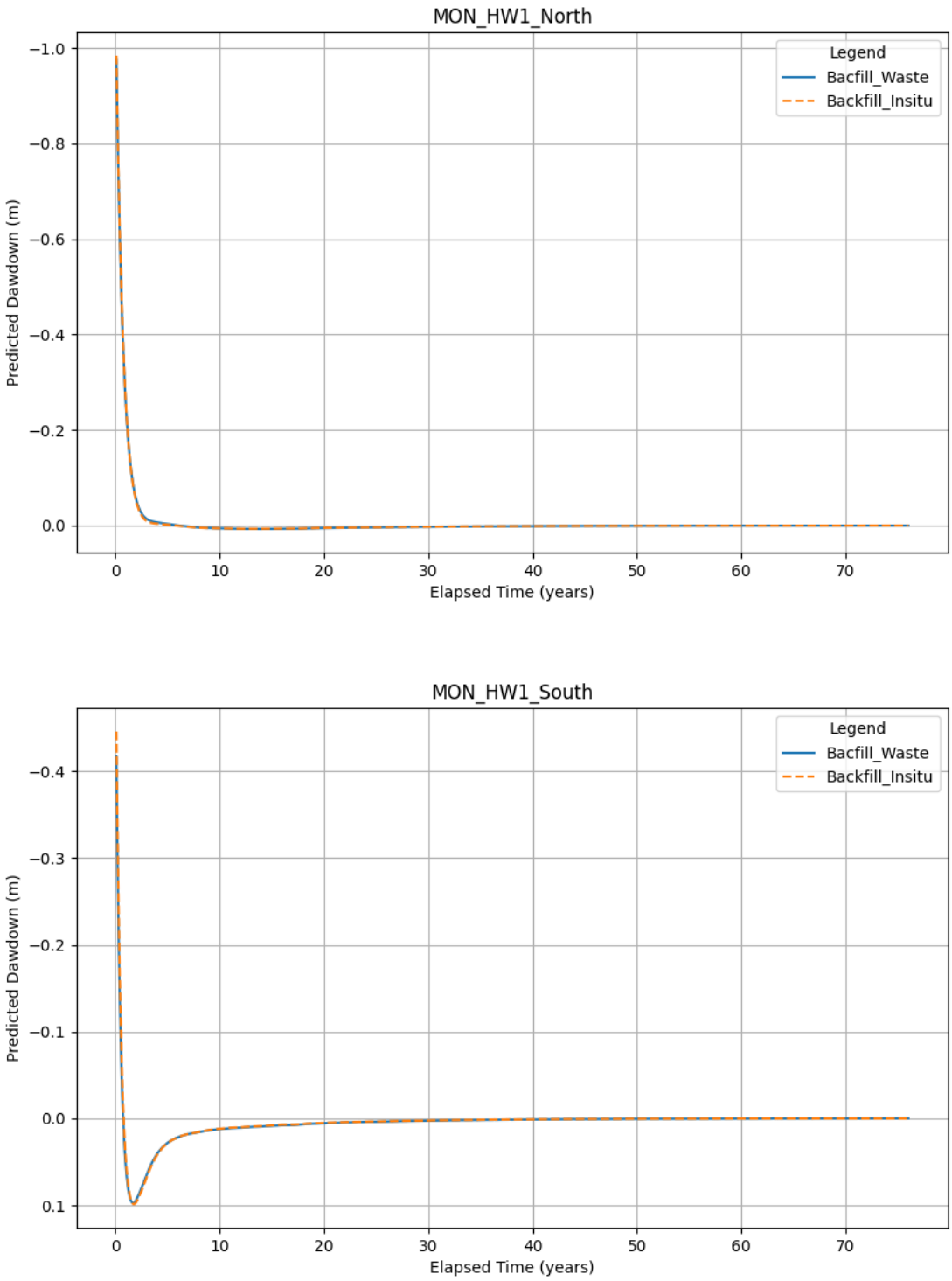

Figure B-104 Predicted aquifer recovery at Horseshoe West

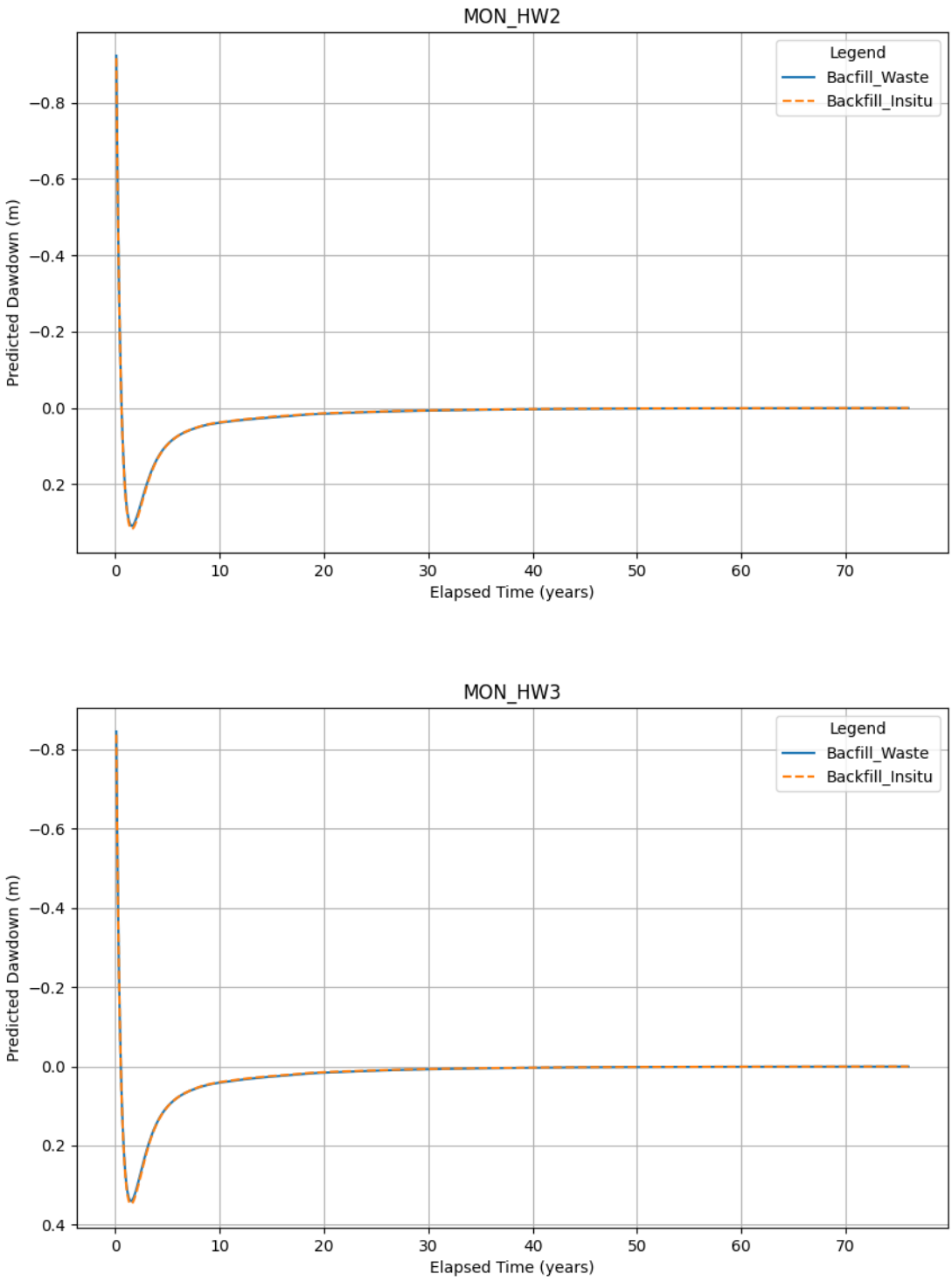

Figure B-105 Predicted aquifer recovery at Horseshoe West

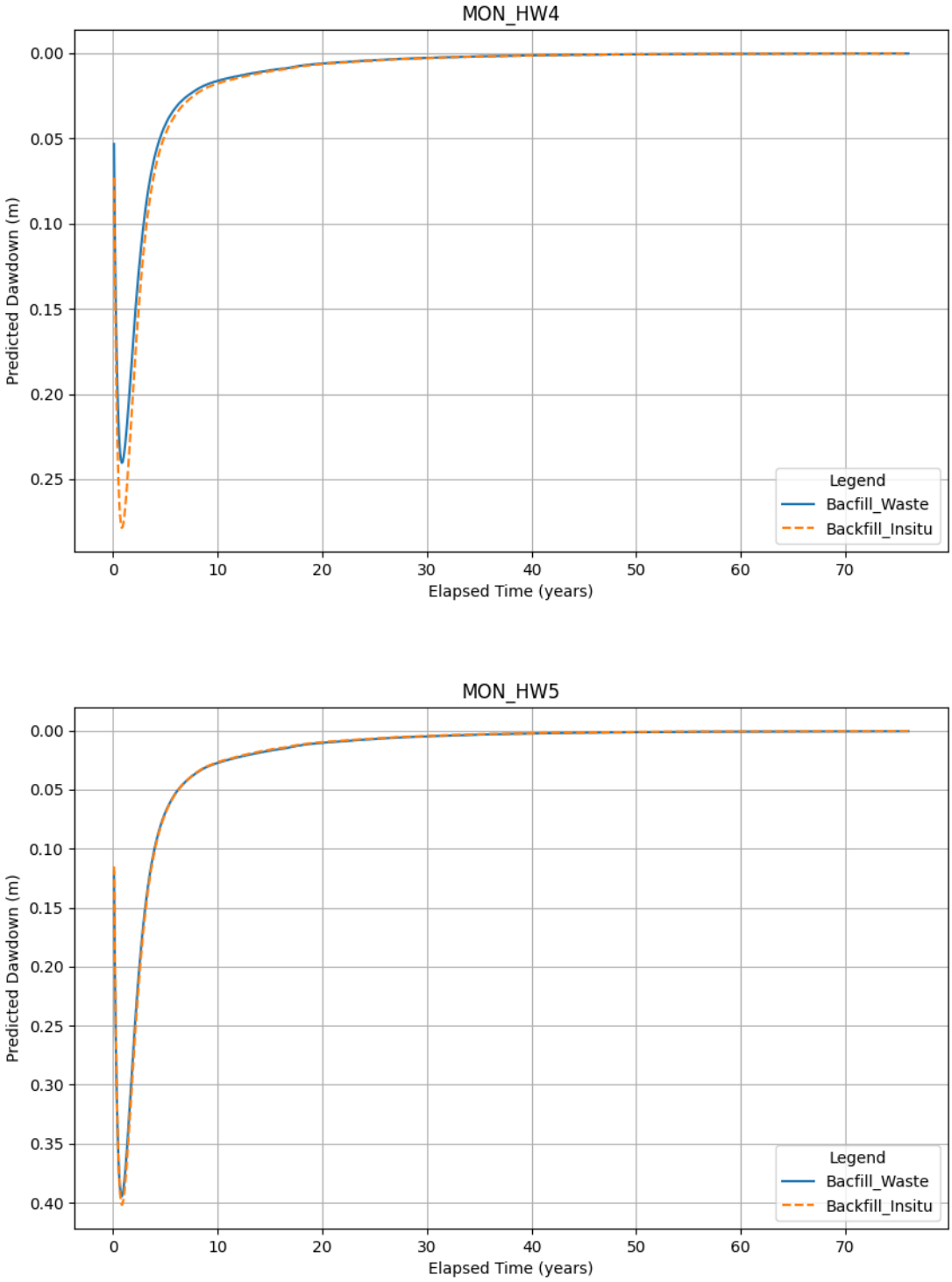

Figure B-106 Predicted aquifer recovery at Horseshoe West

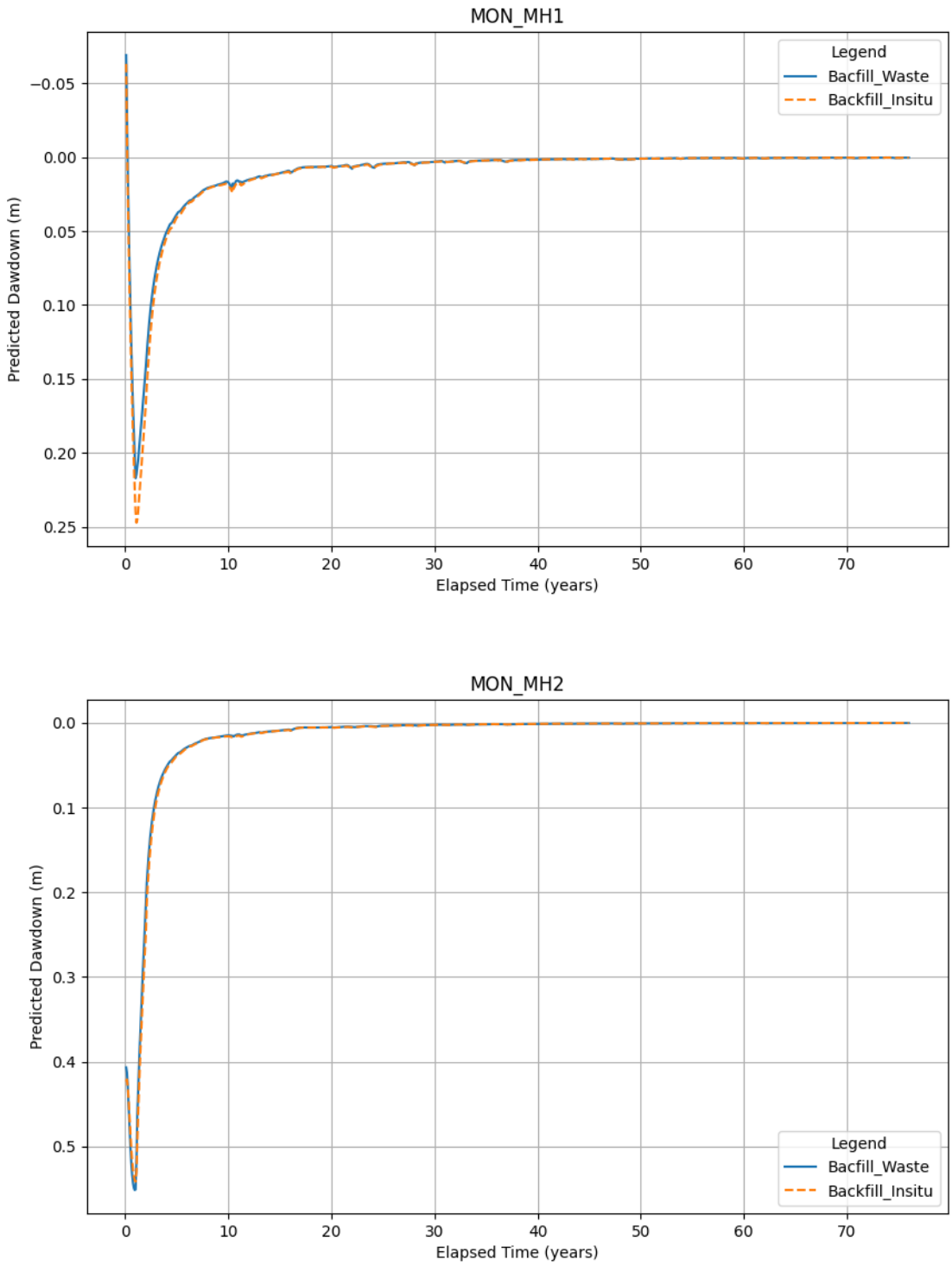

Figure B-107 Predicted aquifer recovery at Murray Hill

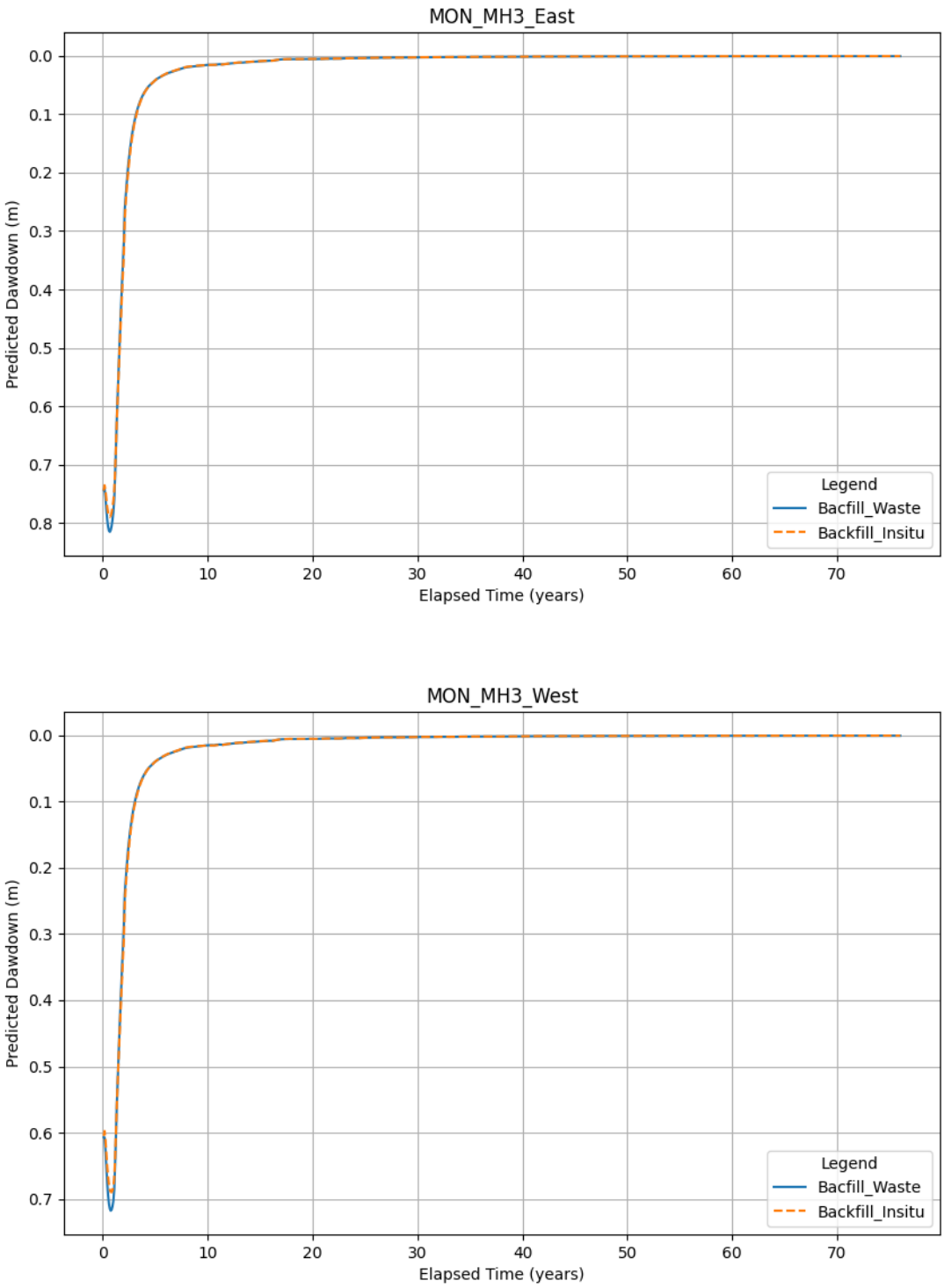

Figure B-108 Predicted aquifer recovery at Murray Hill

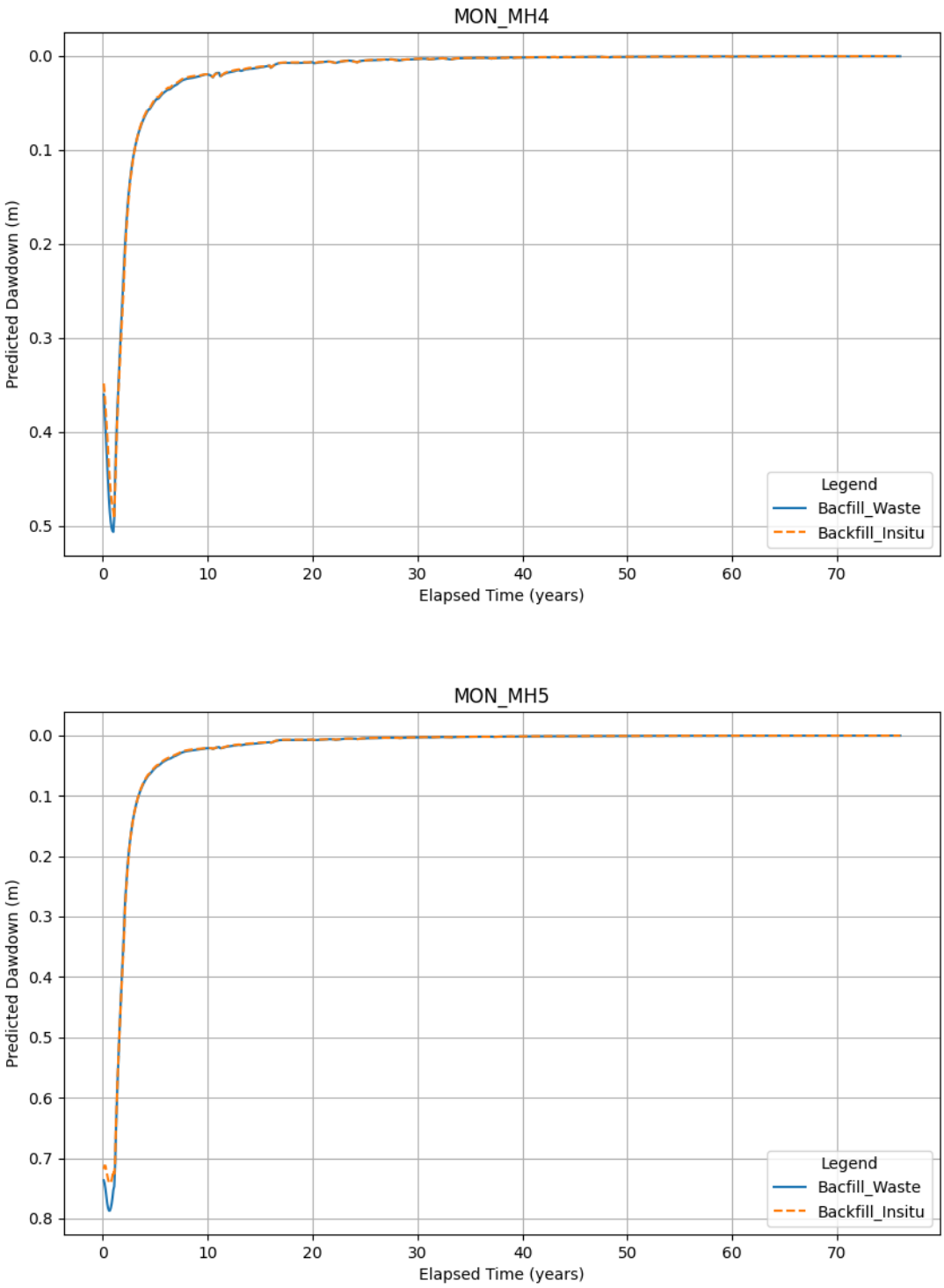

Figure B-109 Predicted aquifer recovery at Murray Hill

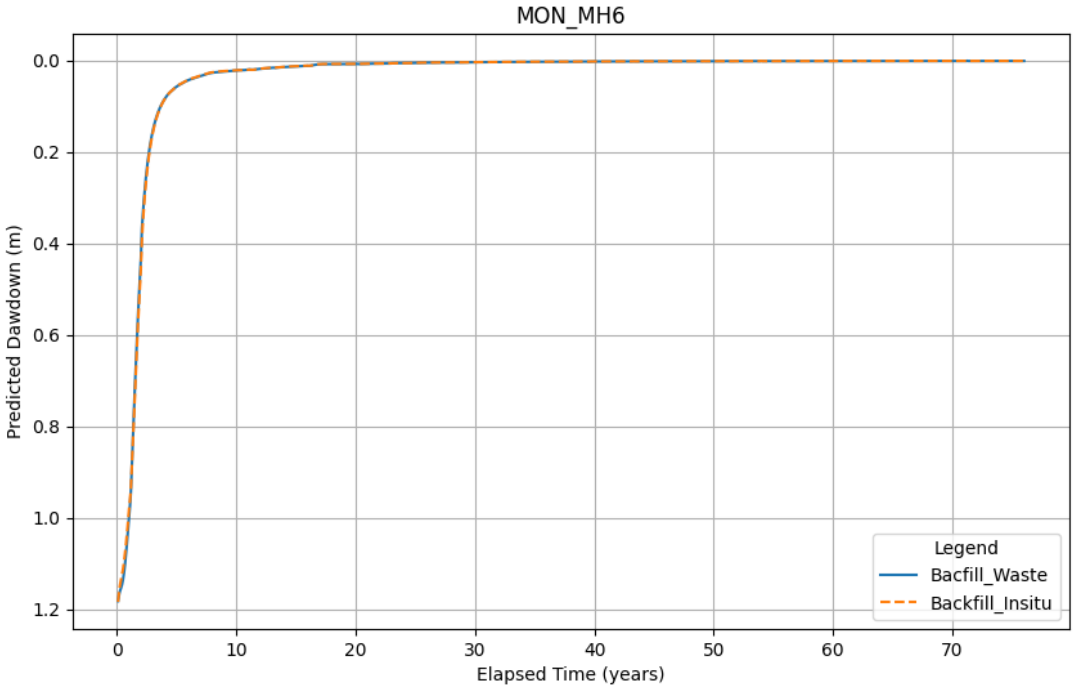

Figure B-110 Predicted aquifer recovery at Murray Hill

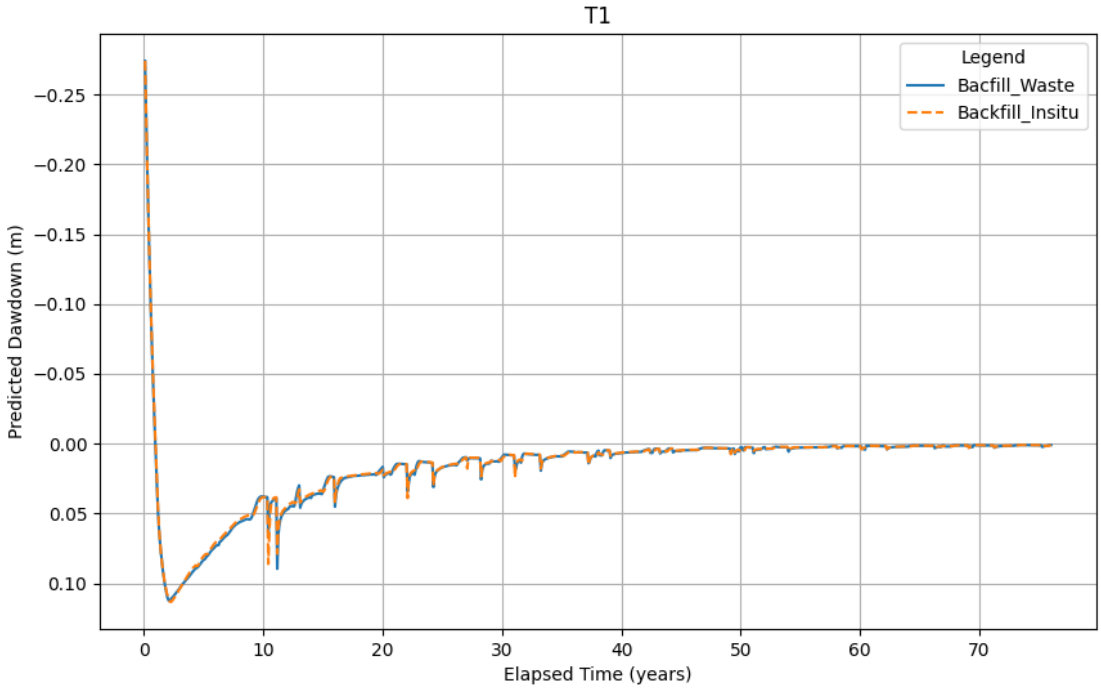

Figure B-111 Predicted aquifer recovery at T1 (Murray West MAR area)

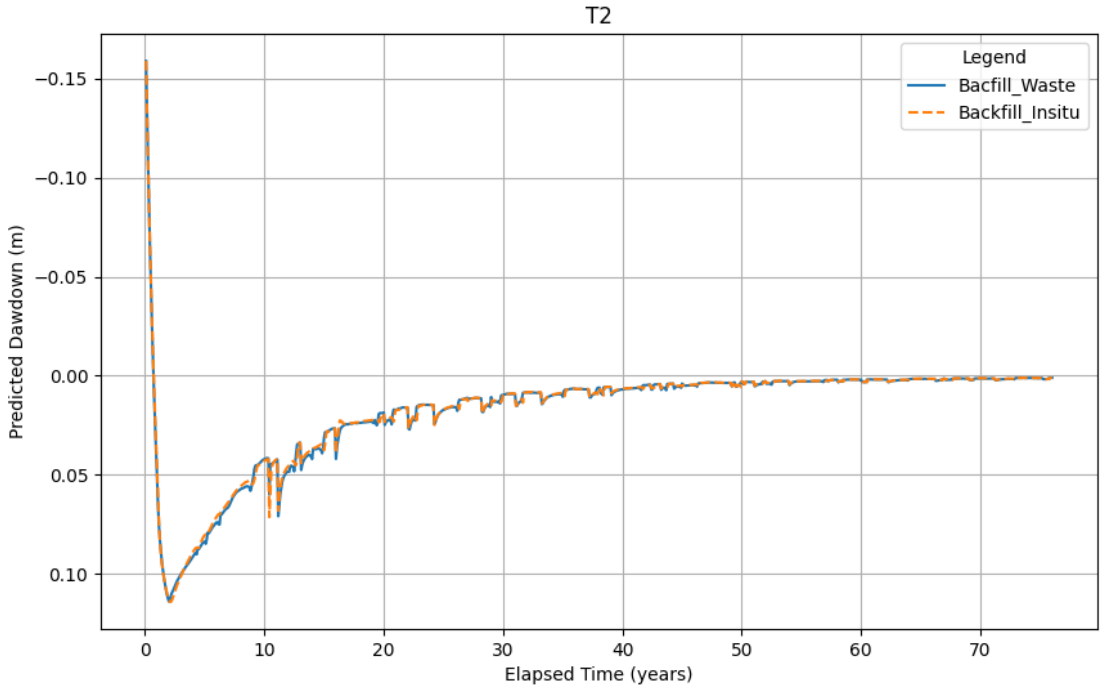

Figure B-112 Predicted aquifer recovery at T2 (valley between Murray West & Koodjeepindarranna claypan)

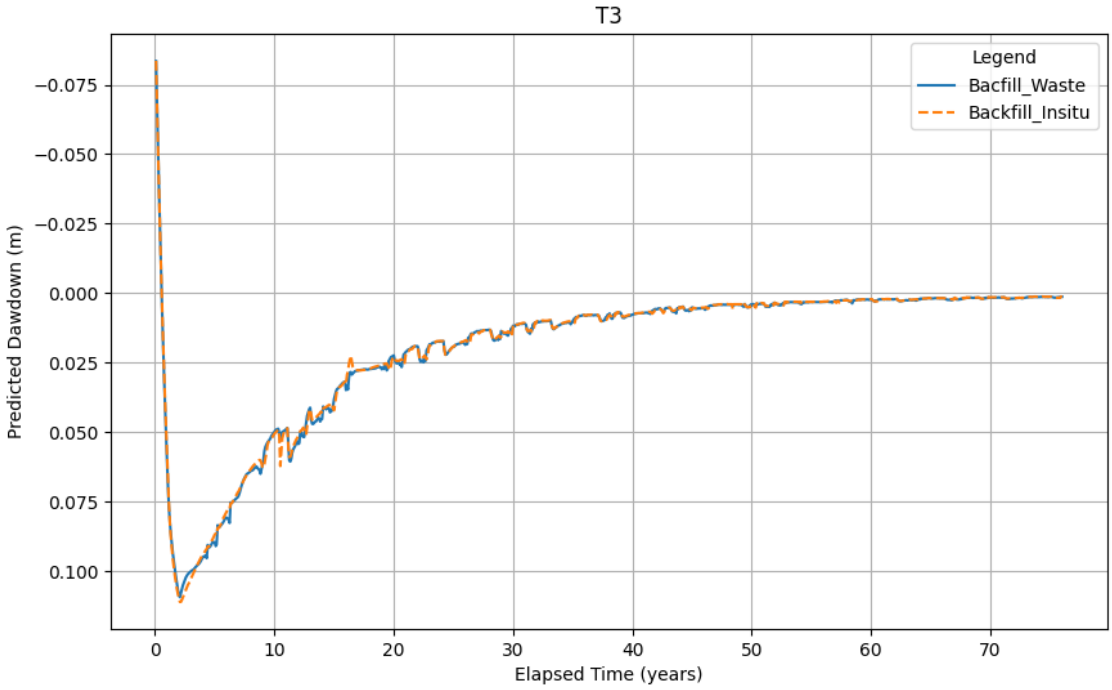

Figure B-113 Predicted aquifer recovery at T3 (Koodjeepindarranna claypan)

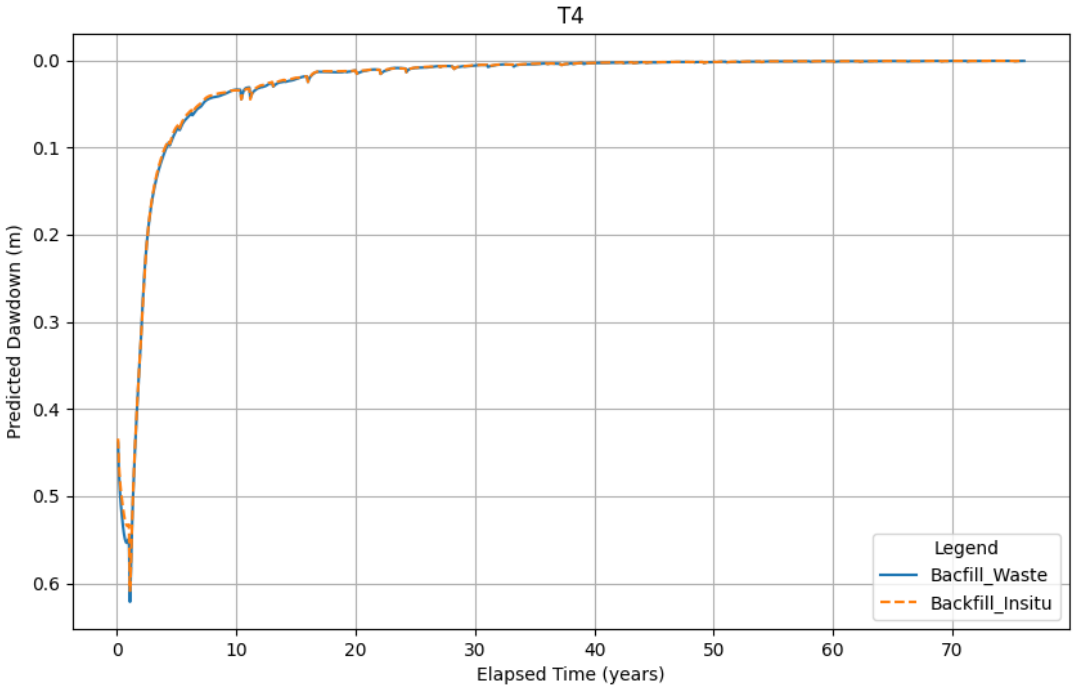

Figure B-114 Predicted aquifer recovery at T4 (valley near Murray Hill)

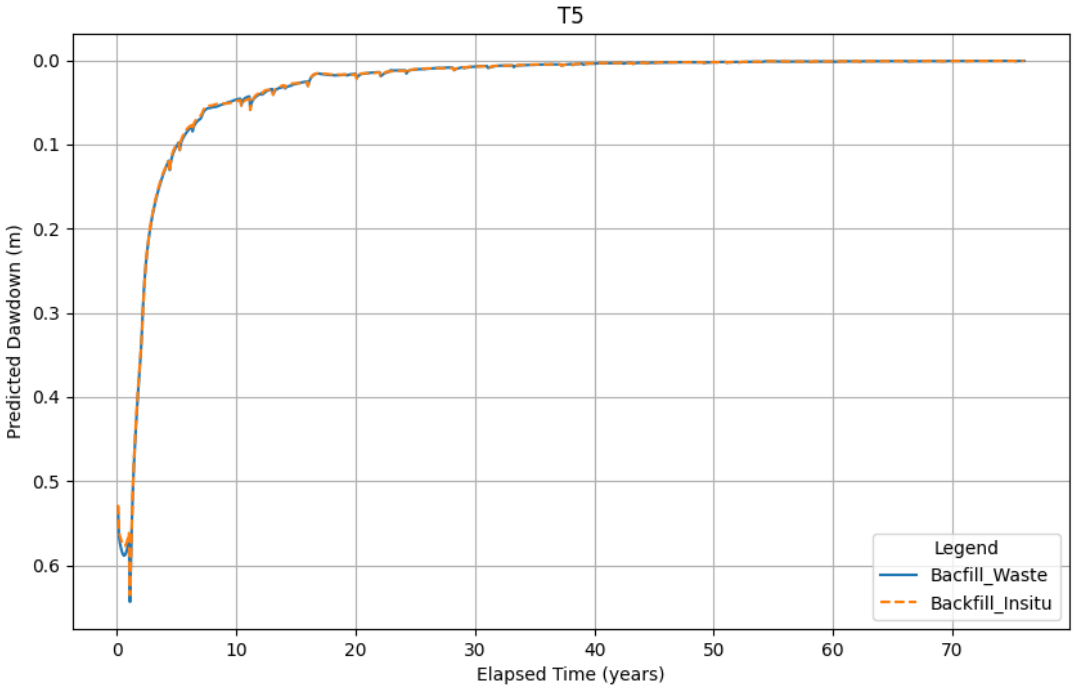

Figure B-115 Predicted aquifer recovery at T5 (valley between Murray Hill & Gnalka Gnoona claypan)

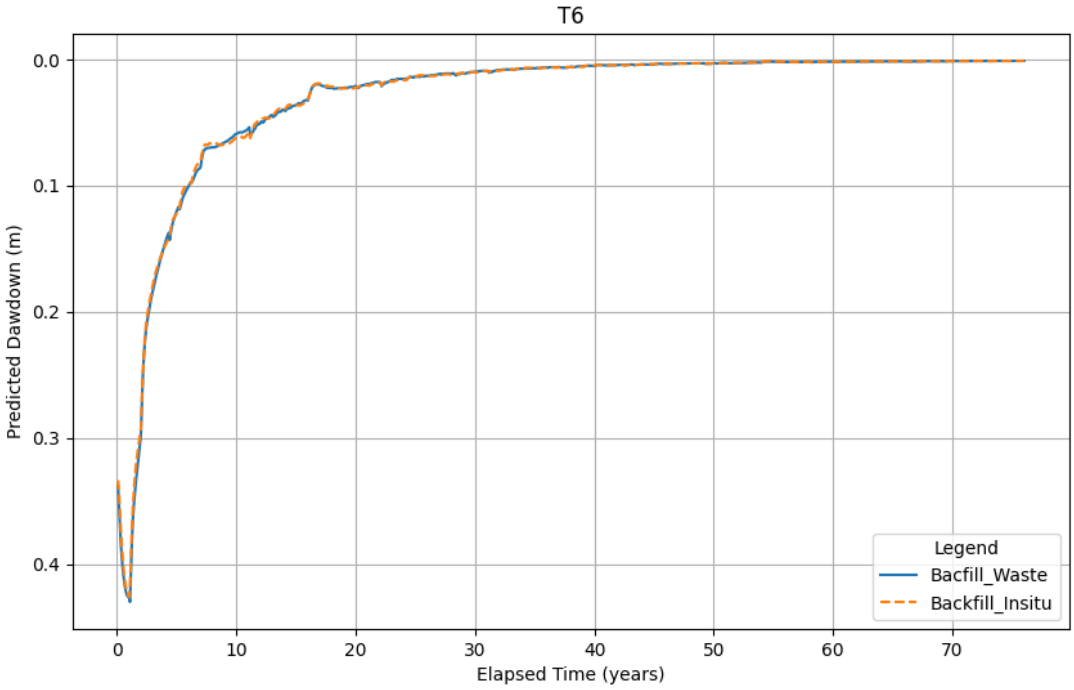

Figure B-116 Predicted aquifer recovery at T6 (Gnalka Gnoona claypan)

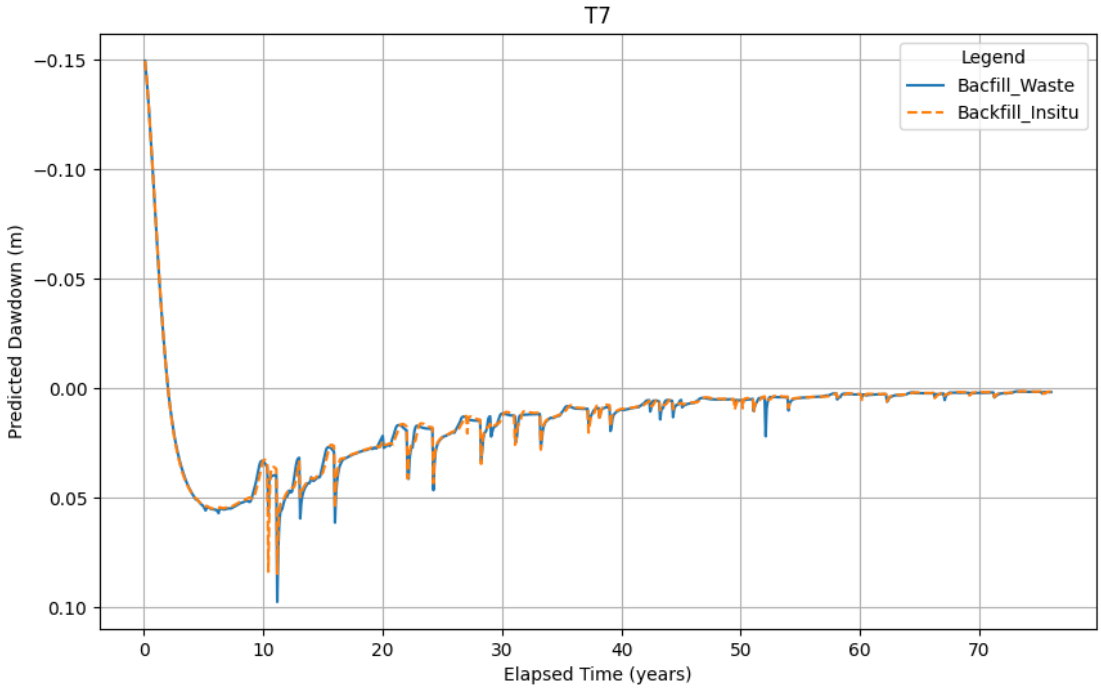

Figure B-117 Predicted aquifer recovery at T7 (restricted stygo 1 west)

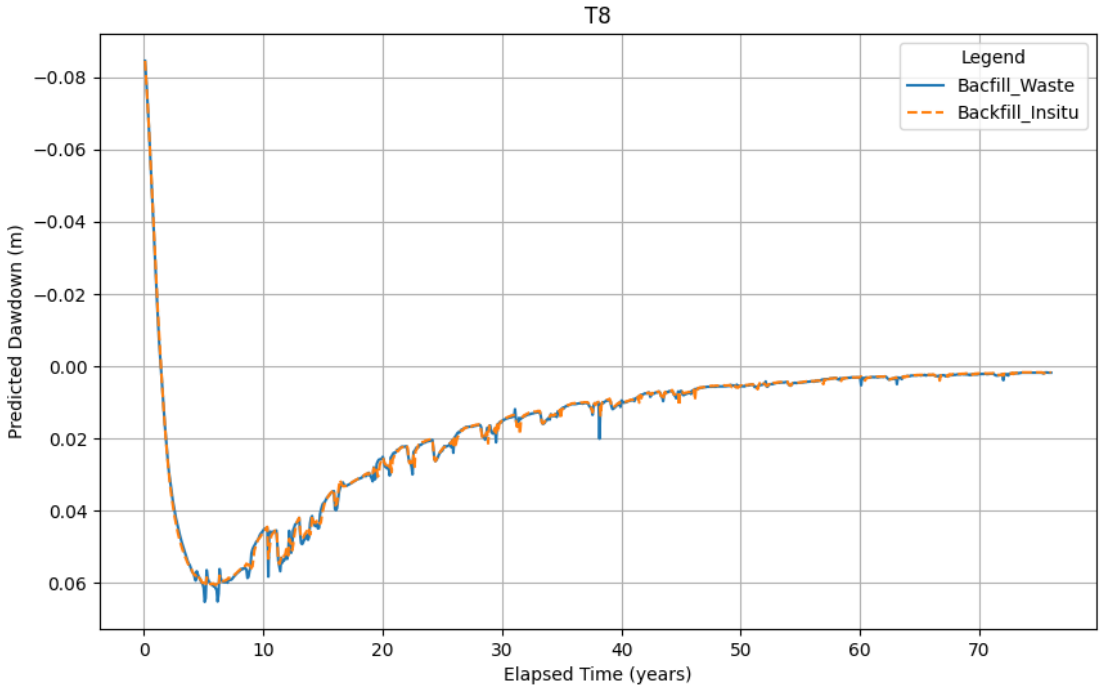

Figure B-118 Predicted aquifer recovery at T8 (valley Far West)

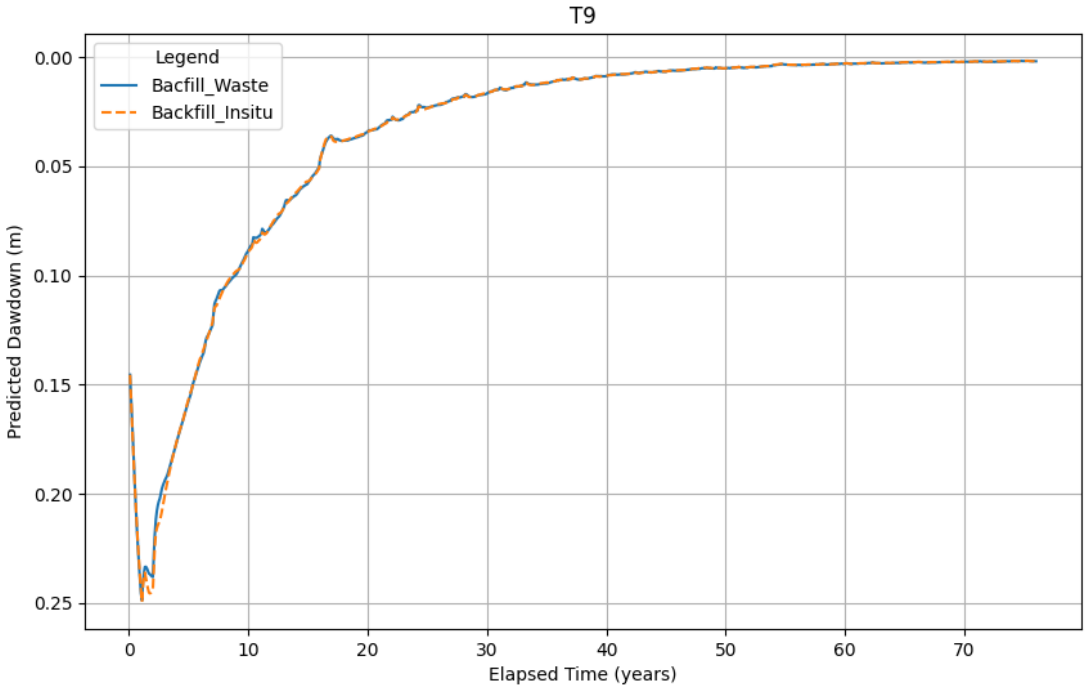

Figure B-119 Predicted aquifer recovery at T9 (restricted stygo 2 southwest)

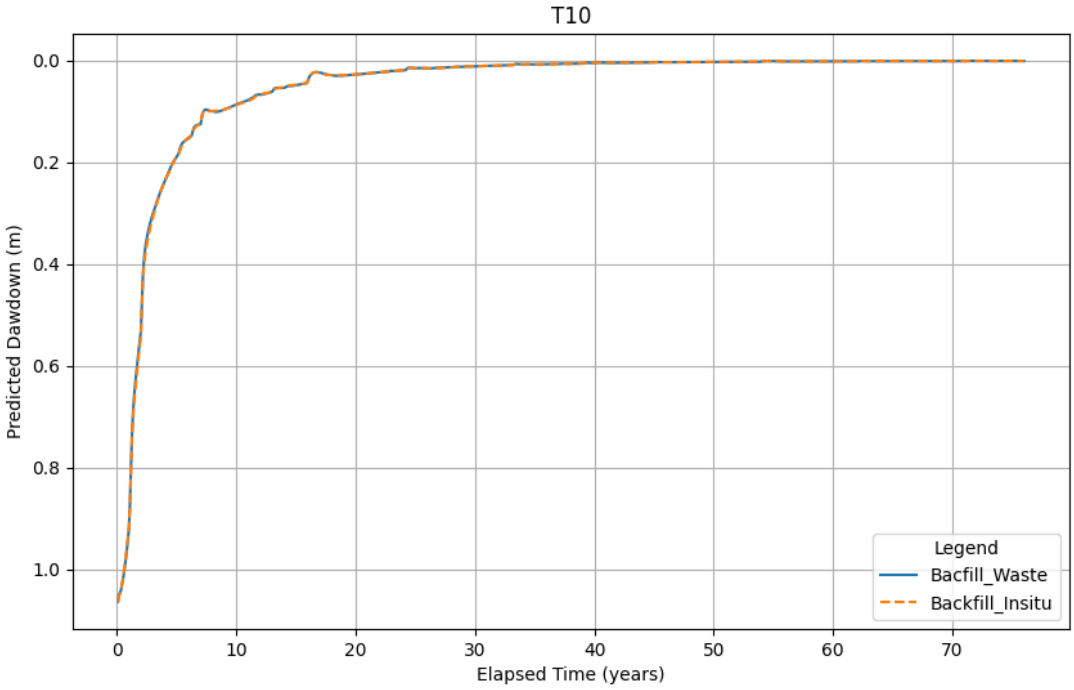

Figure B-120 Predicted aquifer recovery at T10 (restricted stygo 3 south)

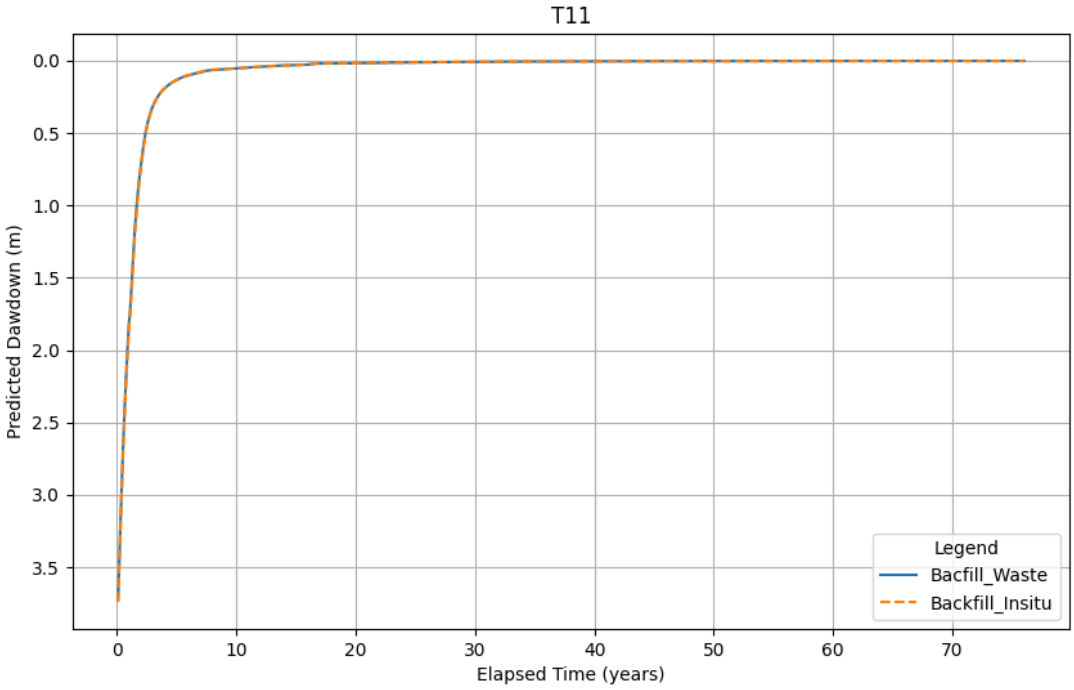

Figure B-121 Predicted aquifer recovery at T11 (valley Fridge West)

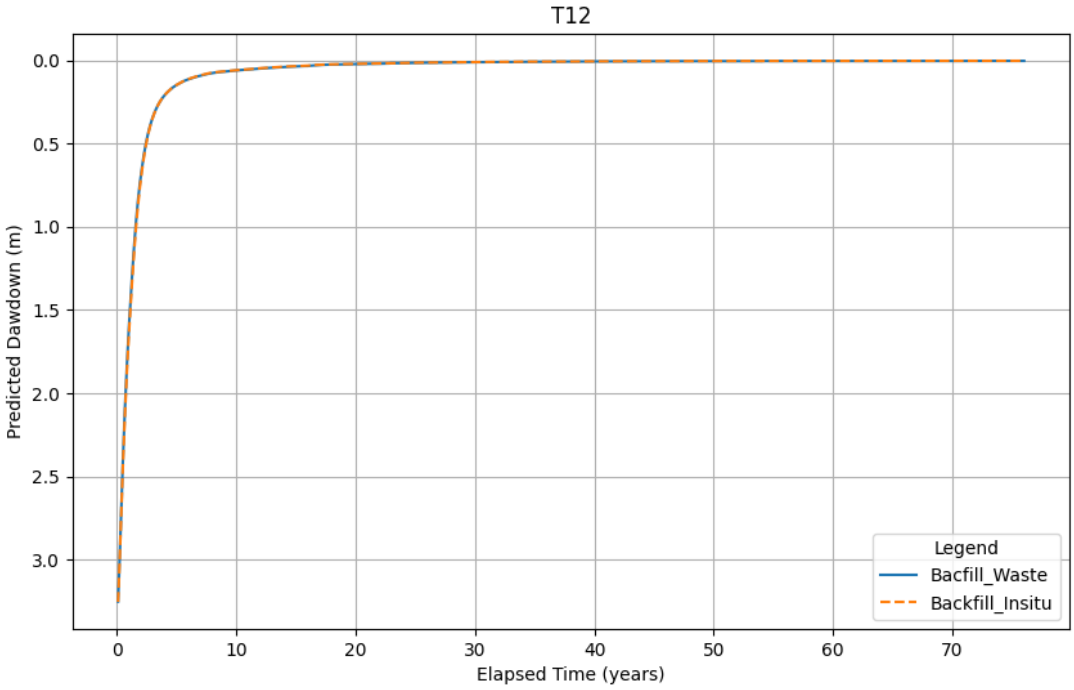

Figure B-122 Predicted aquifer recovery at T12 (valley Fridge Central)

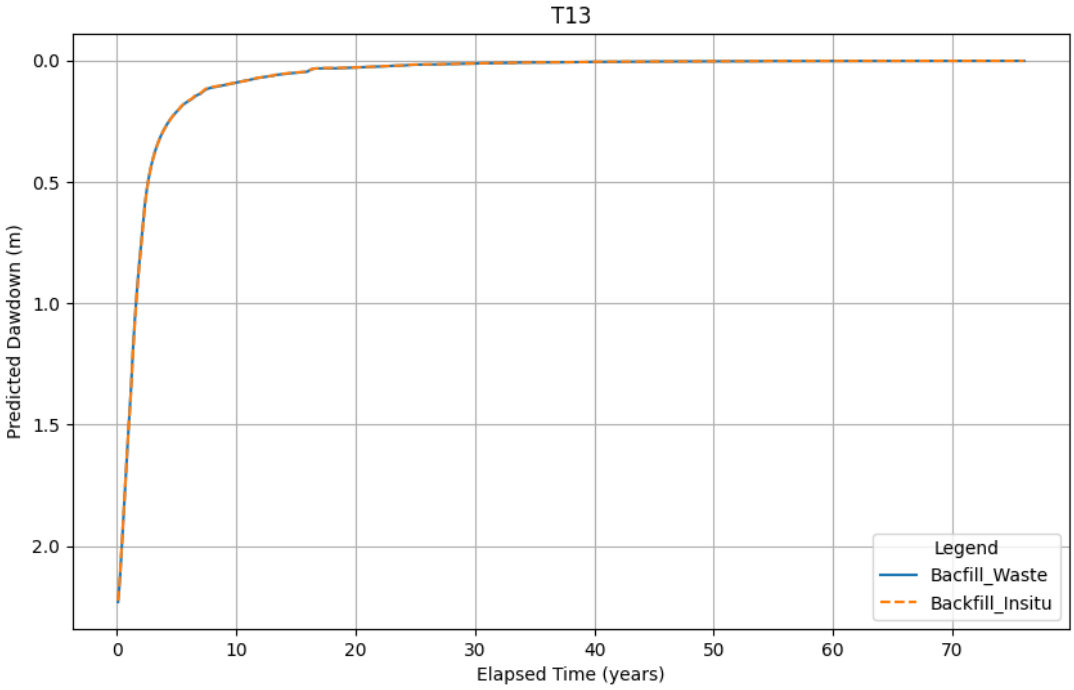

Figure B-123 Predicted aquifer recovery at T13 (valley Central)

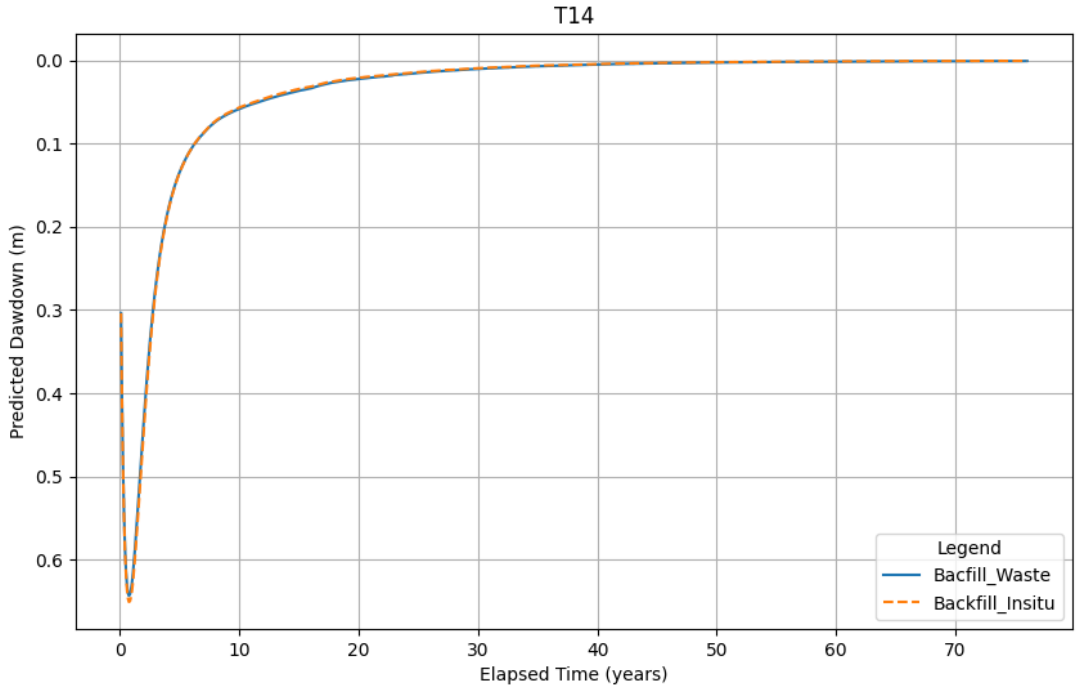

Figure B-124 Predicted aquifer recovery at T14 (area between valley & Horseshoe)

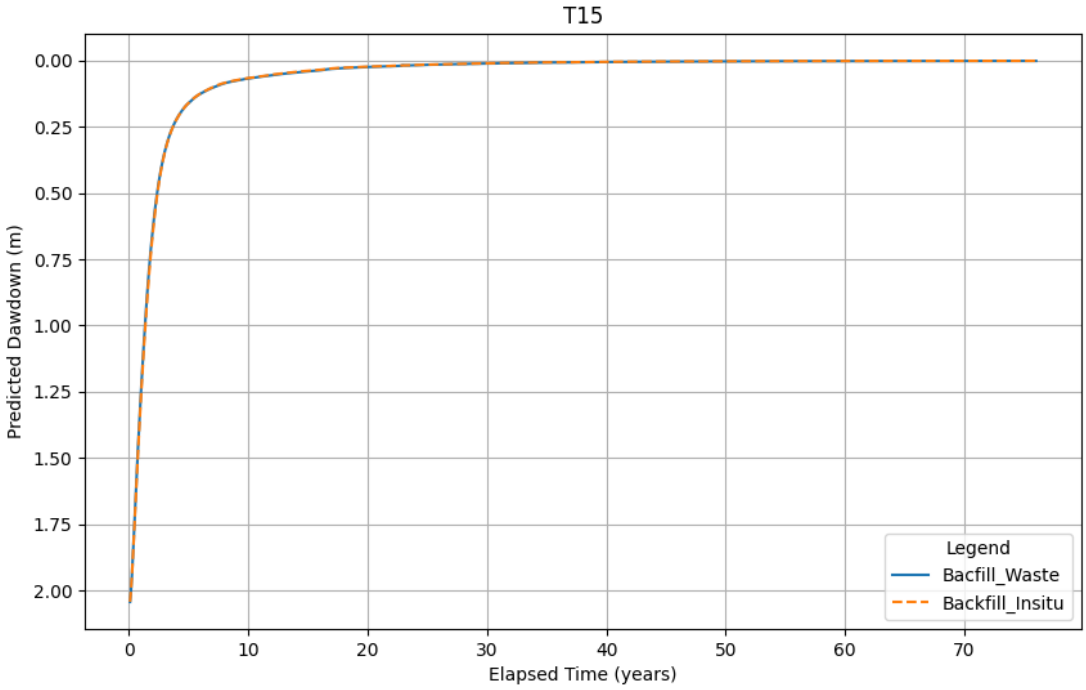

Figure B-125 Predicted aquifer recovery at T15 (valley Fridge Hill)

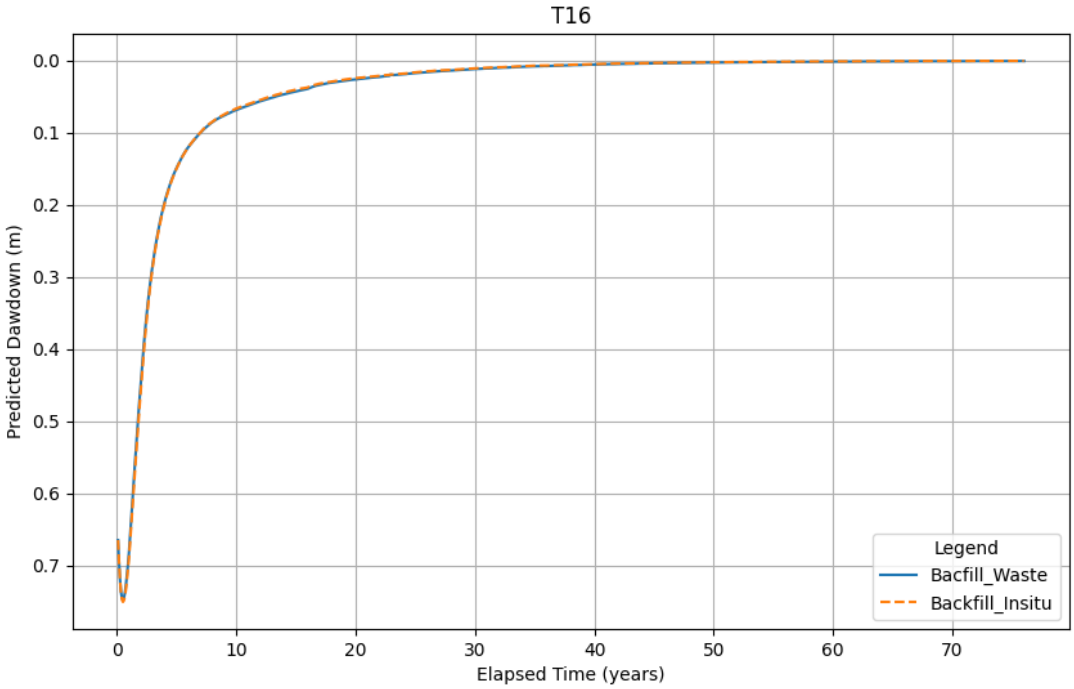

Figure B-126 Predicted aquifer recovery at T16 (valley Horseshoe)

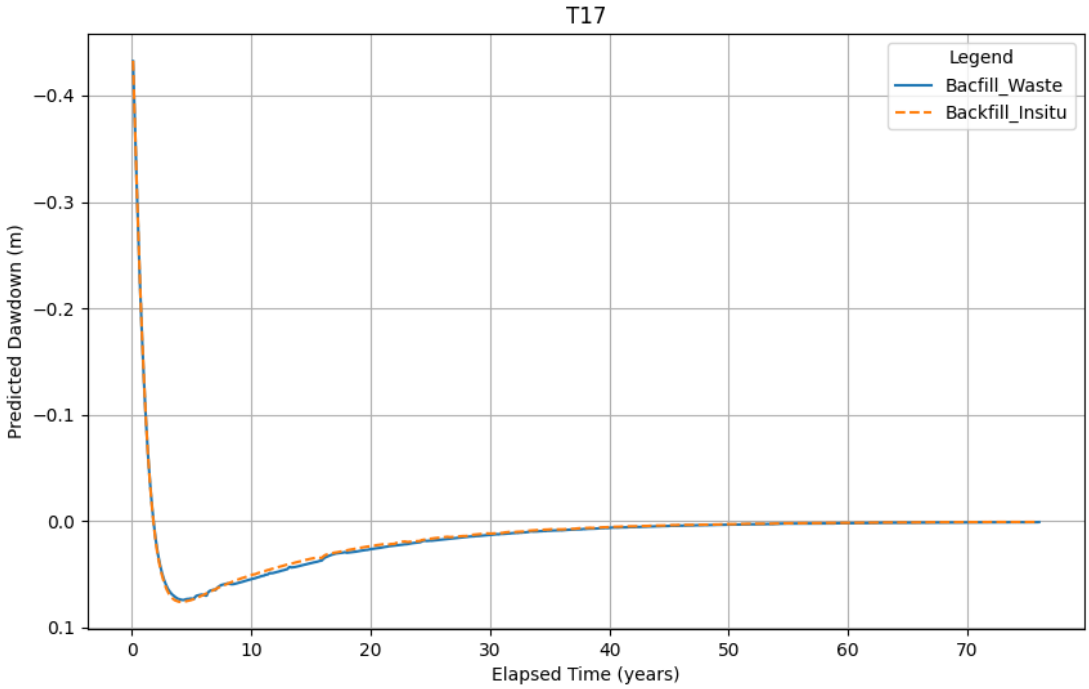

Figure B-127 Predicted aquifer recovery at T17 (valley Far Southeast)

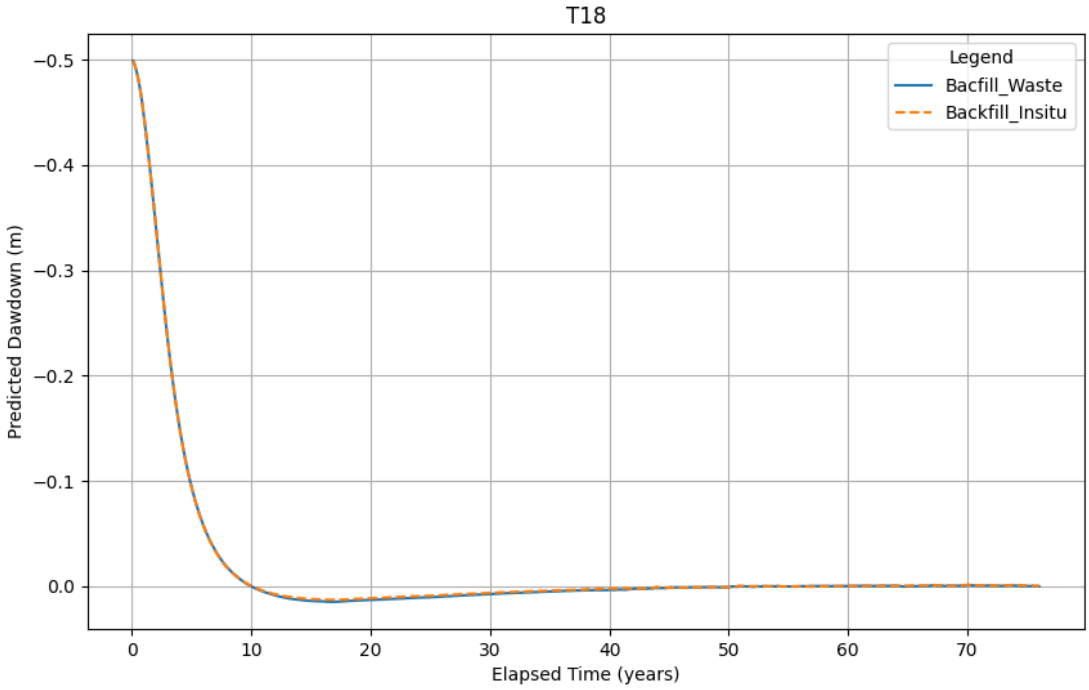

Figure B-128 Predicted aquifer recovery at T18 (Wirrilimarra area)

Appendix C TDS Results

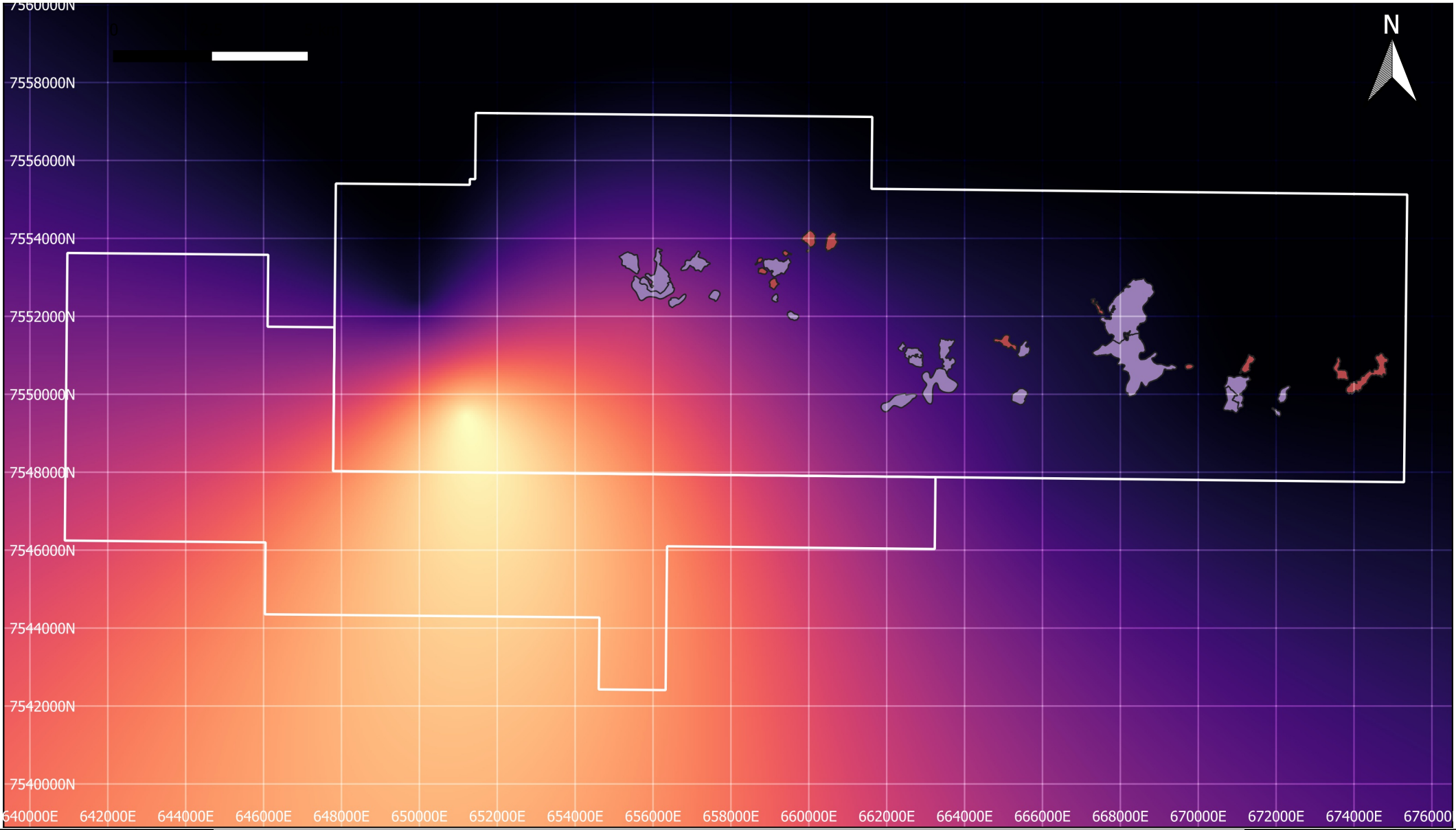

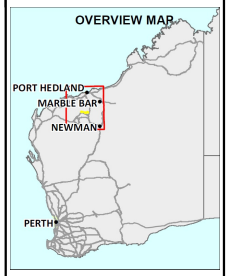

TDS (mg/L)										
213	1098	1320	1541	1762	1984	2205	2426	2647	2869	3090
435	3311	3532	3754	3975	4196	4418	4639	4860	5081	5303
656	5524	5745	5967	6188	6409	6630	6852	7073	7294	7515
877	7737	7958	8179	8401	8622	8843	9064	9286	9507	9728
	9950	10171	10392	10613	10835	11056	11277	11498		

Figure C1

Initial TDS assigned in model Layer 1

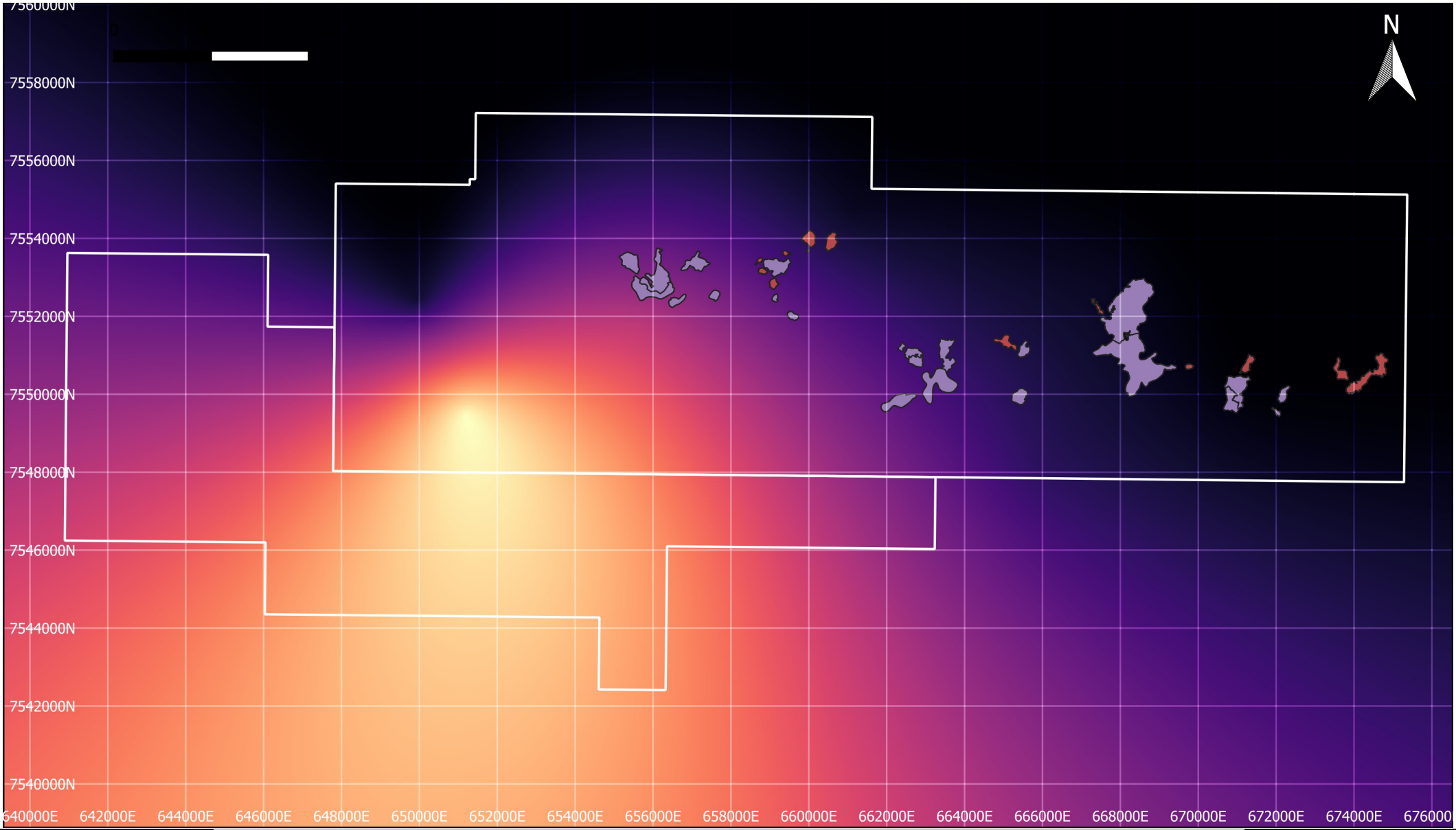

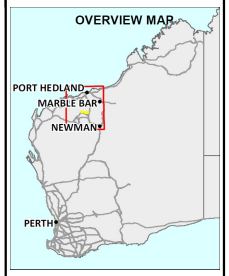

TDS (mg/L)											
213	1098	1320	1541	1762	1984	2205	2426	2647	2869	3090	3311
435	1541	1762	1984	2205	2426	2647	2869	3090	3311	3532	3754
656	1762	1984	2205	2426	2647	2869	3090	3311	3532	3754	3975
877	1984	2205	2426	2647	2869	3090	3311	3532	3754	3975	4196

3311	4418	4639	4860	5081	5303	5524	5745	5967	6188	6409	6630
3532	4639	4860	5081	5303	5524	5745	5967	6188	6409	6630	6852
3754	4860	5081	5303	5524	5745	5967	6188	6409	6630	6852	7073
3975	5081	5303	5524	5745	5967	6188	6409	6630	6852	7073	7294
4196	5303	5524	5745	5967	6188	6409	6630	6852	7073	7294	7515

6630	7737	8843	9950	11056							
6852	7958	9064	10171	11277							
7073	8179	9286	10392	11498							
7294	8401	9507	10613								
7515	8622	9728	10835								

Figure C2

Initial TDS assigned in model Layer 2

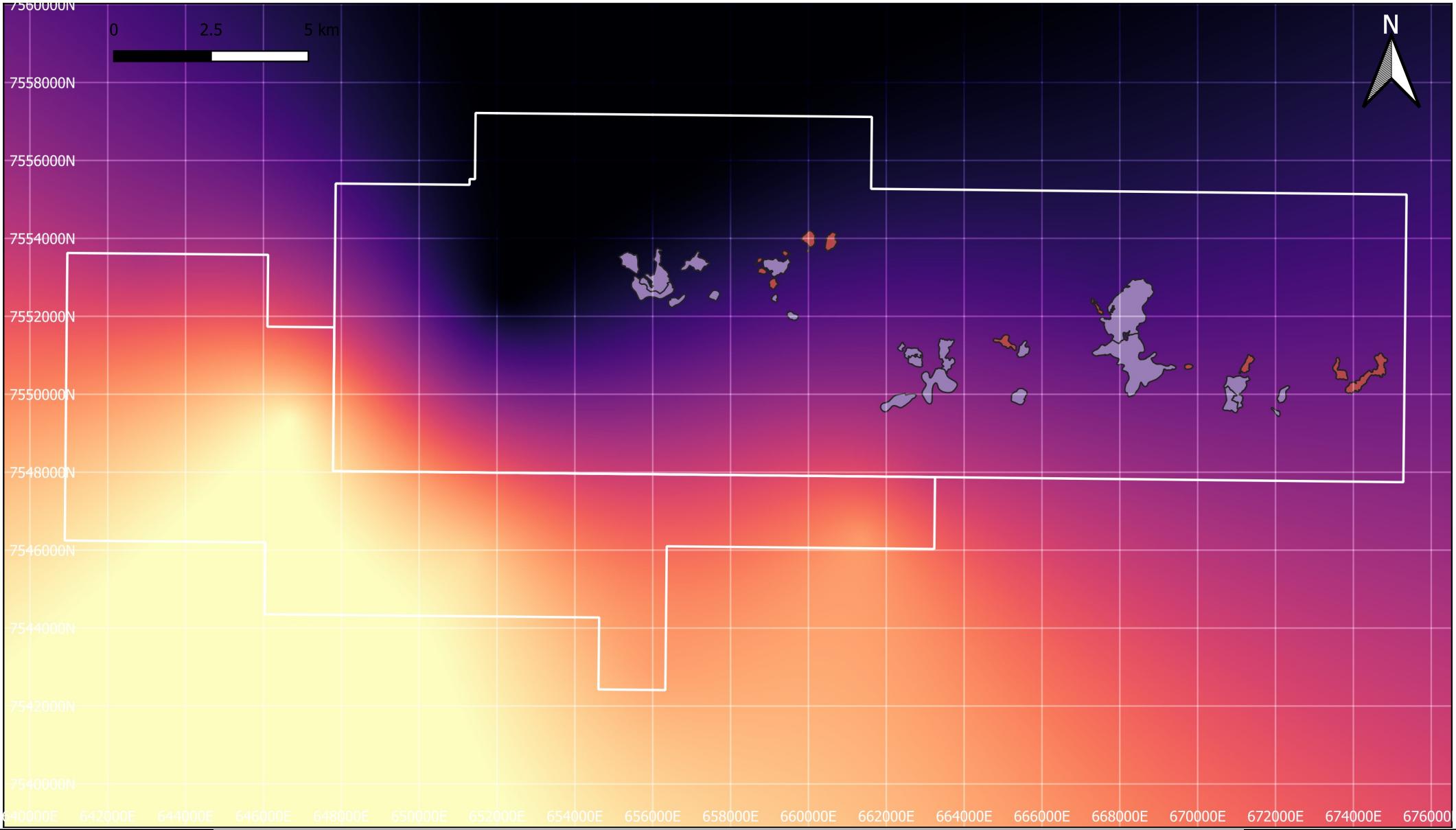

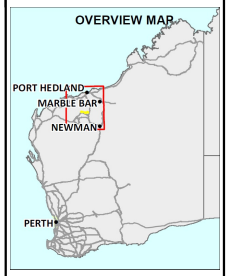

TDS (mg/L)

213	1098	2205	3311	4418	5524	6630	7737	8843	9950	11056
435	1320	2426	3532	4639	5745	6852	7958	9064	10171	11277
656	1541	2647	3754	4860	5967	7073	8179	9286	10392	11498
877	1762	2869	3975	5081	6188	7294	8401	9507	10613	
	1984	3090	4196	5303	6409	7515	8622	9728	10835	

Figure C3

Initial TDS assigned in model Layer 3

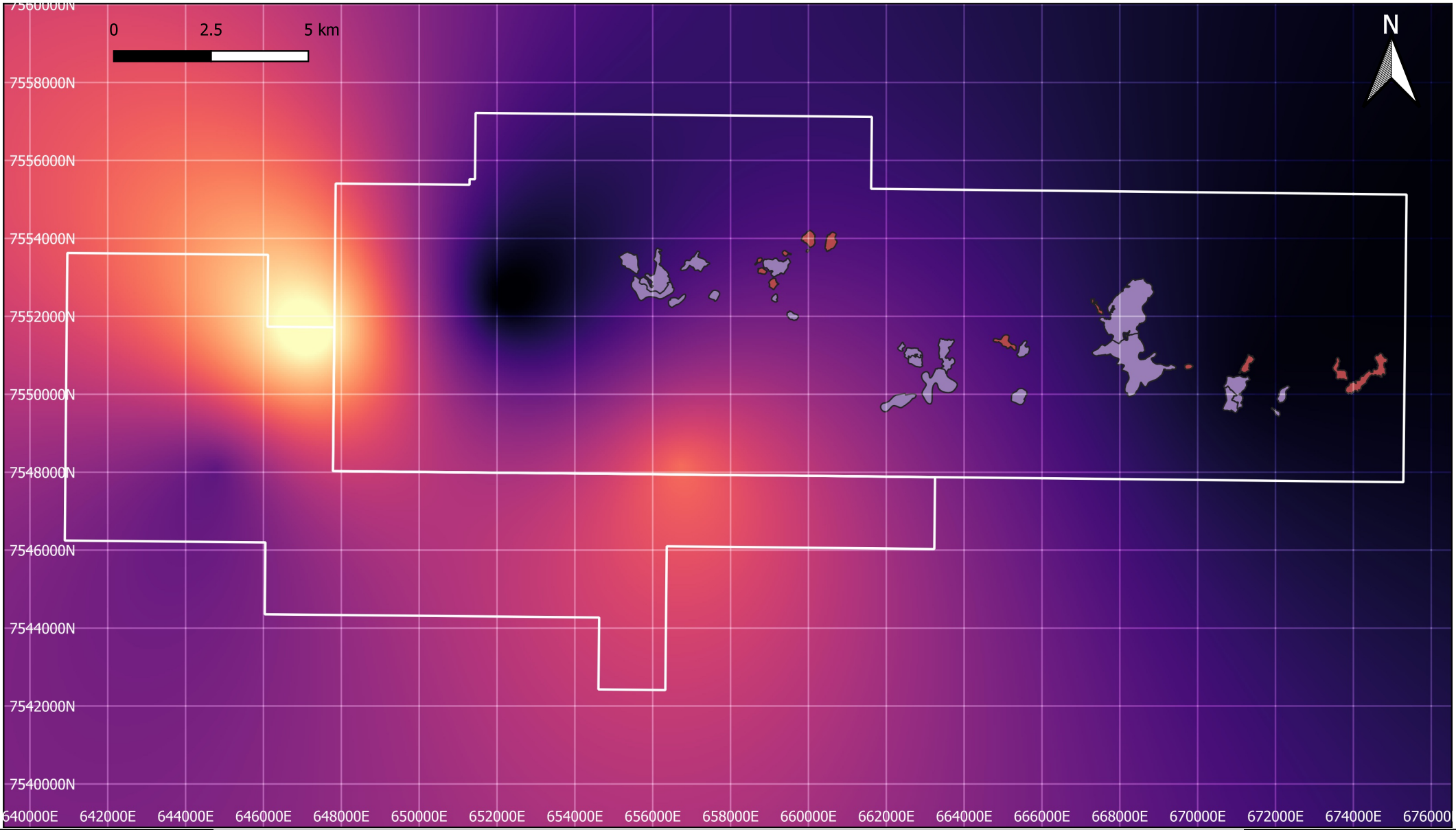

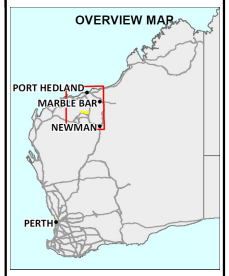

TDS (mg/L)

213	1098	2205	3311	4418	5524	6630	7737	8843	9950	11056
435	1320	2426	3532	4639	5745	6852	7958	9064	10171	11277
656	1541	2647	3754	4860	5967	7073	8179	9286	10392	11498
877	1762	2869	3975	5081	6188	7294	8401	9507	10613	
	1984	3090	4196	5303	6409	7515	8622	9728	10835	

Figure C4

Initial TDS assigned in model Layer 4

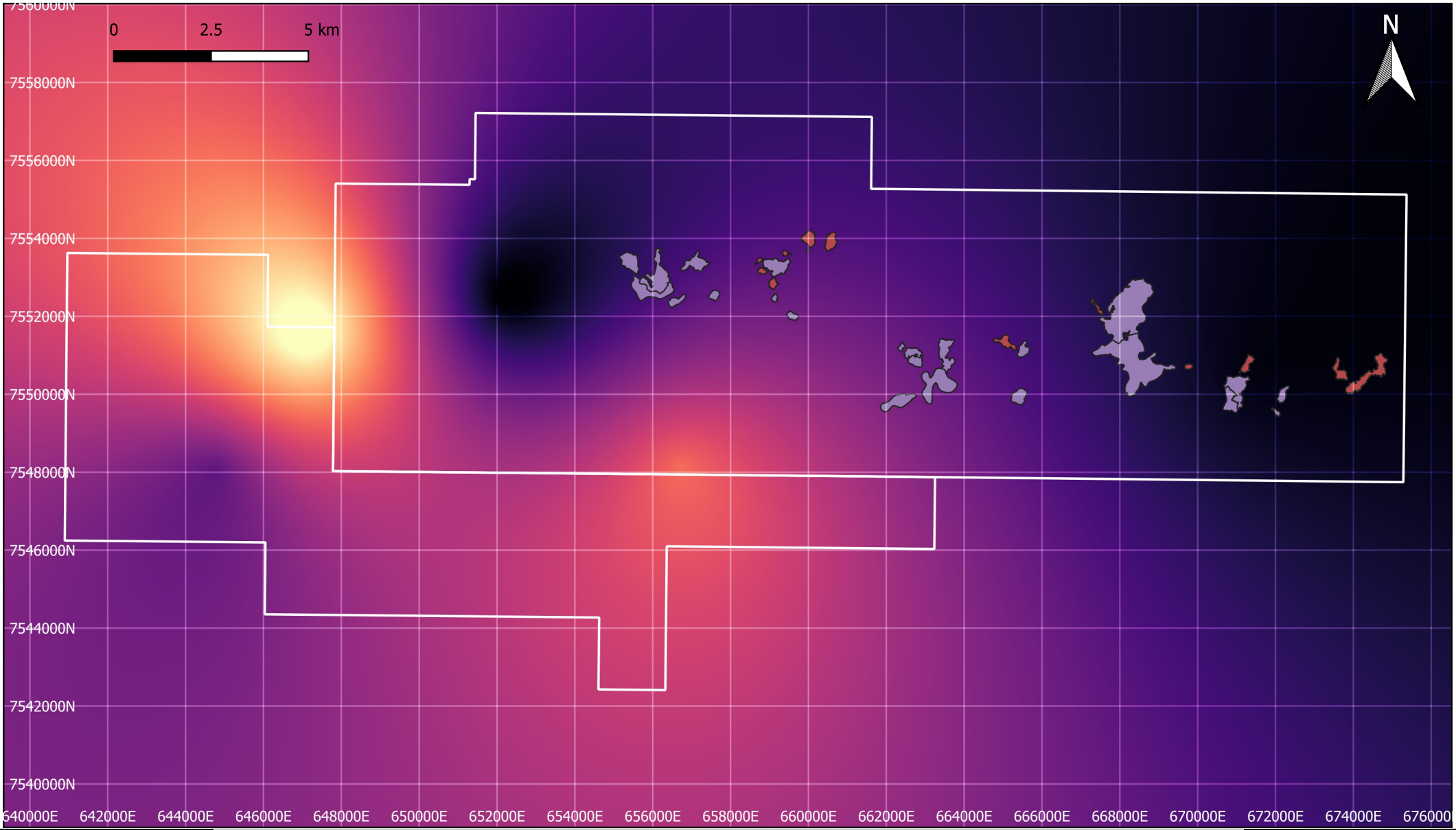

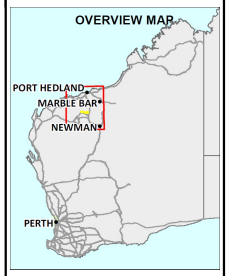

TDS (mg/L)

213	1098	1320	1541	1762	1984	2205	2426	2647	2869	3090	3311
435	1541	1762	1984	2205	2426	2647	2869	3090	3311	3532	3754
656	1762	1984	2205	2426	2647	2869	3090	3311	3532	3754	3975
877	1984	2205	2426	2647	2869	3090	3311	3532	3754	3975	4196

3311	4418	4639	4860	5081	5303	5524	5745	5967	6188	6409	6630
3532	4639	4860	5081	5303	5524	5745	5967	6188	6409	6630	6852
3754	4860	5081	5303	5524	5745	5967	6188	6409	6630	6852	7073
3975	5081	5303	5524	5745	5967	6188	6409	6630	6852	7073	7294
4196	5303	5524	5745	5967	6188	6409	6630	6852	7073	7294	7515

6630	7737	8843	9950	11056							
6852	7958	9064	10171	11277							
7073	8179	9286	10392	11498							
7294	8401	9507	10613								
7515	8622	9728	10835								

Figure C5

Initial TDS assigned in model Layer 5

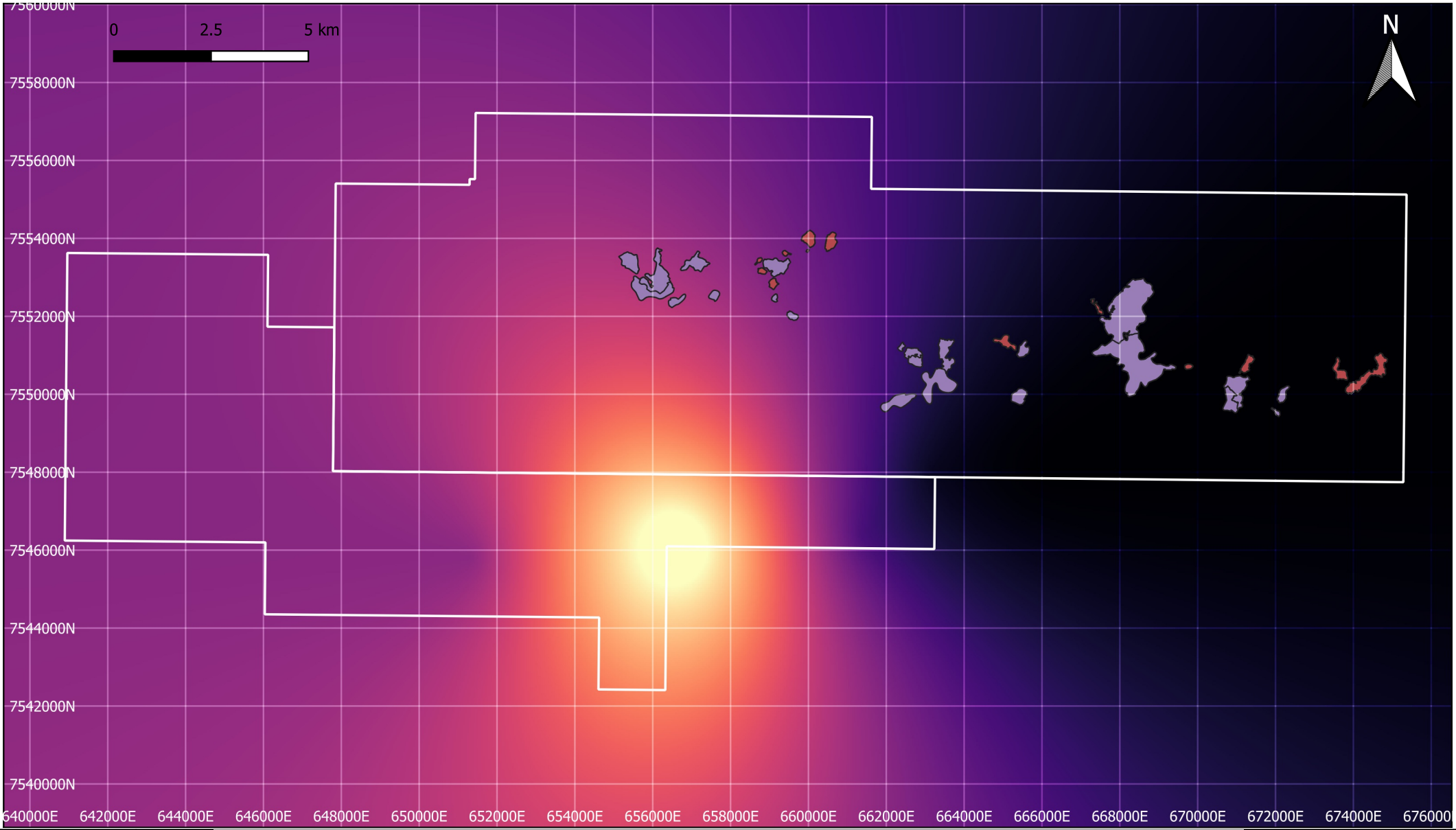

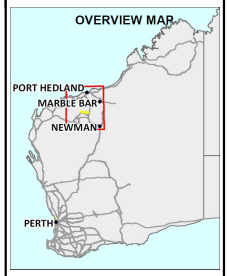

TDS (mg/L)											
213	1098	1320	1541	1762	1984	2205	2426	2647	2869	3090	3311
435	1541	1762	1984	2205	2426	2647	2869	3090	3311	3532	3754
656	1762	1984	2205	2426	2647	2869	3090	3311	3532	3754	3975
877	1984	2205	2426	2647	2869	3090	3311	3532	3754	3975	4196

3311	4418	4639	4860	5081	5303	5524	5745	5967	6188	6409	6630
3532	4639	4860	5081	5303	5524	5745	5967	6188	6409	6630	6852
3754	4860	5081	5303	5524	5745	5967	6188	6409	6630	6852	7073
3975	5081	5303	5524	5745	5967	6188	6409	6630	6852	7073	7294
4196	5303	5524	5745	5967	6188	6409	6630	6852	7073	7294	7515

6630	7737	8843	9950	11056							
6852	7958	9064	10171	11277							
7073	8179	9286	10392	11498							
7294	8401	9507	10613								
7515	8622	9728	10835								

Figure C6

Initial TDS assigned in model Layer 6

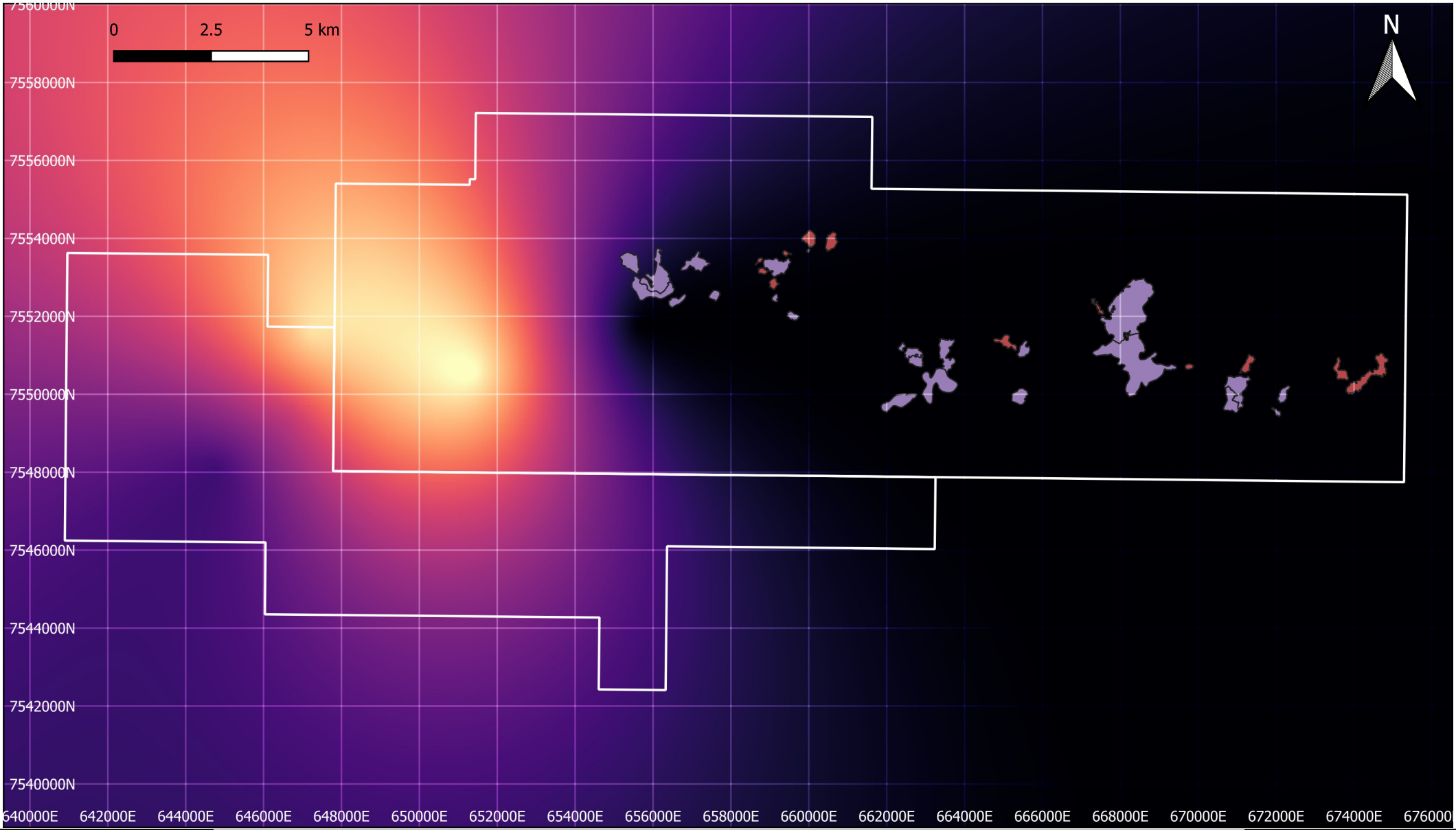

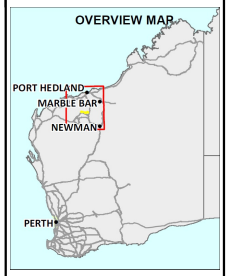

TDS (mg/L)

213	1098	1320	1541	1762	1984	2205	2426	2647	2869	3090
435	1541	1762	1984	2205	2426	2647	2869	3090	3311	3532
656	1984	2205	2426	2647	2869	3090	3311	3532	3754	3975
877	2426	2647	2869	3090	3311	3532	3754	3975	4196	4418
1098	2869	3090	3311	3532	3754	3975	4196	4418	4639	4860
1320	3311	3532	3754	3975	4196	4418	4639	4860	5081	5303
1541	3754	3975	4196	4418	4639	4860	5081	5303	5524	5745
1762	4196	4418	4639	4860	5081	5303	5524	5745	5967	6188
1984	4639	4860	5081	5303	5524	5745	5967	6188	6409	6630
2205	5081	5303	5524	5745	5967	6188	6409	6630	6852	7073
2426	5524	5745	5967	6188	6409	6630	6852	7073	7294	7515
2647	5967	6188	6409	6630	6852	7073	7294	7515	7737	7958
2869	6409	6630	6852	7073	7294	7515	7737	7958	8179	8401
3090	6852	7073	7294	7515	7737	7958	8179	8401	8622	8843
3311	7294	7515	7737	7958	8179	8401	8622	8843	9064	9286
3532	7737	7958	8179	8401	8622	8843	9064	9286	9507	9728
3754	8179	8401	8622	8843	9064	9286	9507	9728	9950	10171
3975	8622	8843	9064	9286	9507	9728	9950	10171	10392	10613
4196	9064	9286	9507	9728	9950	10171	10392	10613	10835	11056
4418	9507	9728	9950	10171	10392	10613	10835	11056	11277	11498

Figure C7

Initial TDS assigned in model Layer 7

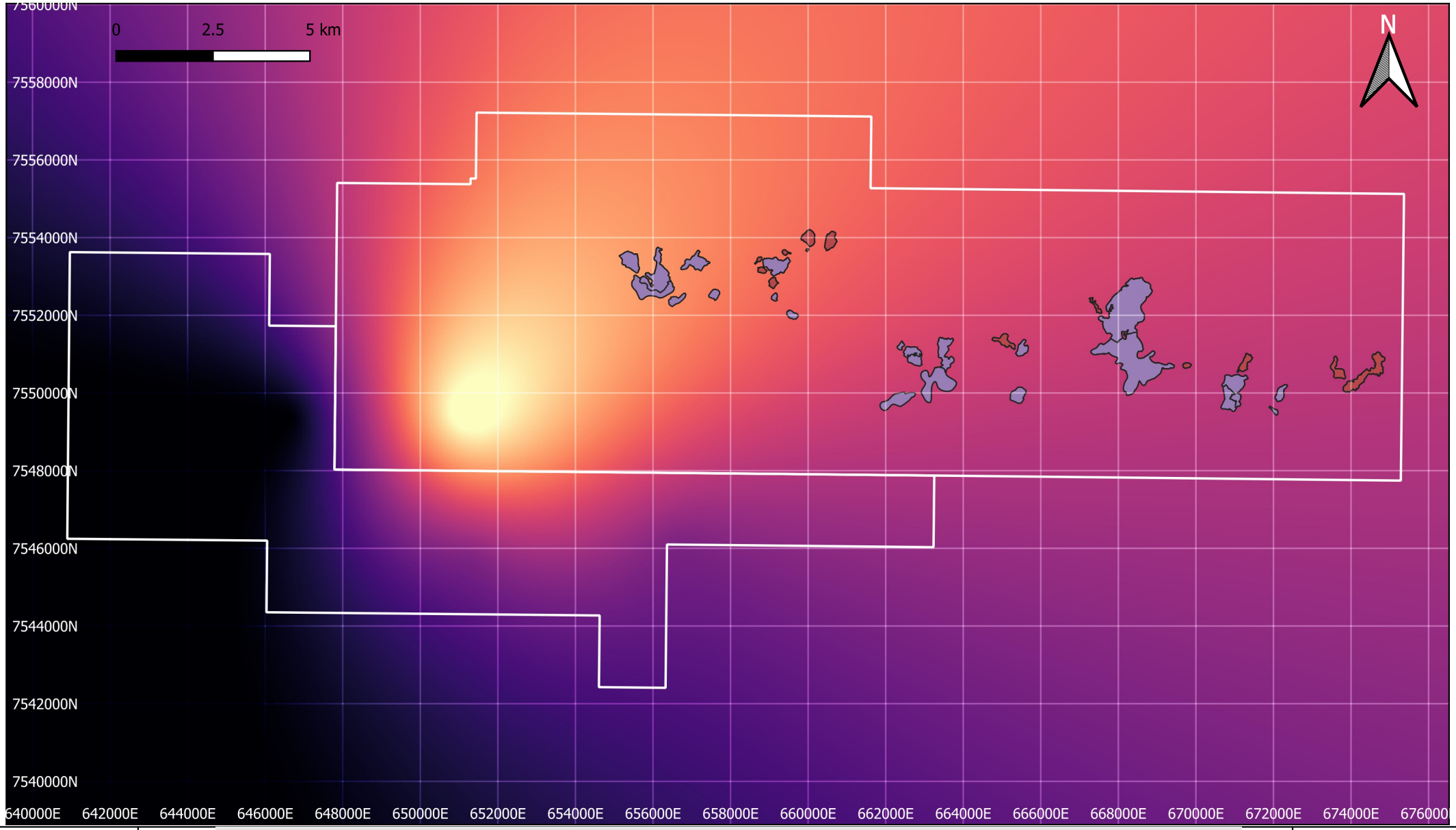

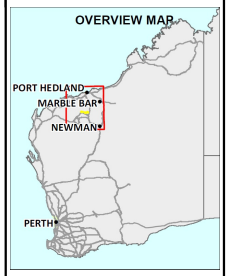

TDS (mg/L)

213	1098	2205	3311	4418	5524	6630	7737	8843	9950	11056
435	1320	2426	3532	4639	5745	6852	7958	9064	10171	11277
656	1541	2647	3754	4860	5967	7073	8179	9286	10392	11498
877	1762	2869	3975	5081	6188	7294	8401	9507	10613	
	1984	3090	4196	5303	6409	7515	8622	9728	10835	

Figure C8

Initial TDS assigned in model Layer 8

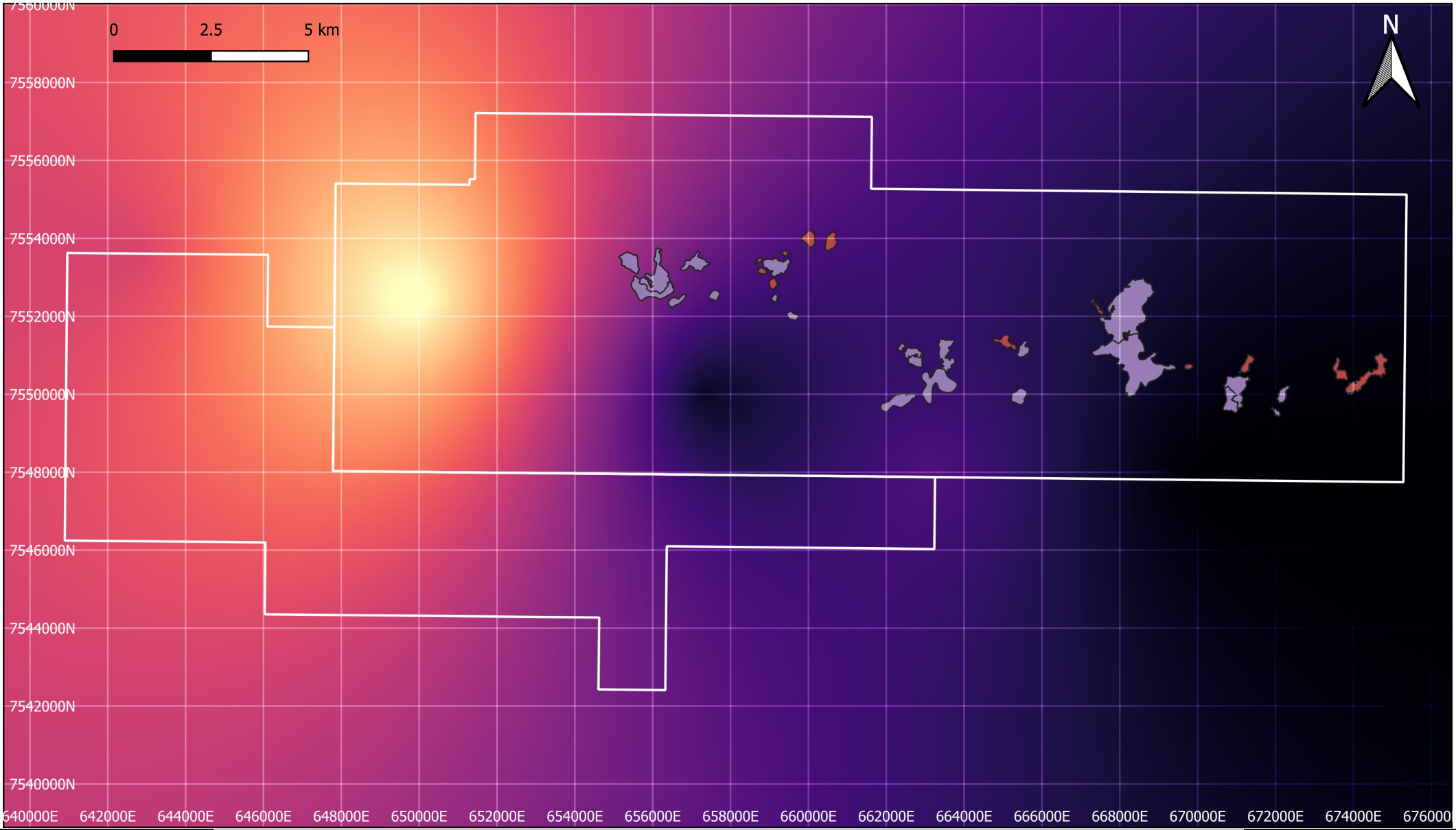

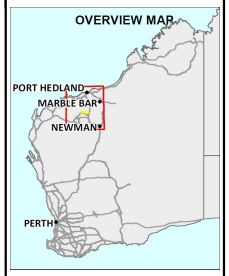

TDS (mg/L)											
213	1098	1320	1541	1762	1984	2205	2426	2647	2869	3090	3311
435	1541	1762	1984	2205	2426	2647	2869	3090	3311	3532	3754
656	1762	1984	2205	2426	2647	2869	3090	3311	3532	3754	3975
877	1984	2205	2426	2647	2869	3090	3311	3532	3754	3975	4196

4418	4639	4860	5081	5303	5524	5745	5967	6188	6409	6630	6852
4639	4860	5081	5303	5524	5745	5967	6188	6409	6630	6852	7073
4860	5081	5303	5524	5745	5967	6188	6409	6630	6852	7073	7294
4196	4418	4639	4860	5081	5303	5524	5745	5967	6188	6409	6630

7737	7958	8179	8401	8622	8843	9064	9286	9507	9728	9950	10171
7958	8179	8401	8622	8843	9064	9286	9507	9728	9950	10171	10392
7515	7737	7958	8179	8401	8622	8843	9064	9286	9507	9728	9950
6852	7073	7294	7515	7737	7958	8179	8401	8622	8843	9064	9286

11056				
11277				
11498				
10613				
10835				

Figure C9

Initial TDS assigned in model Layer 9

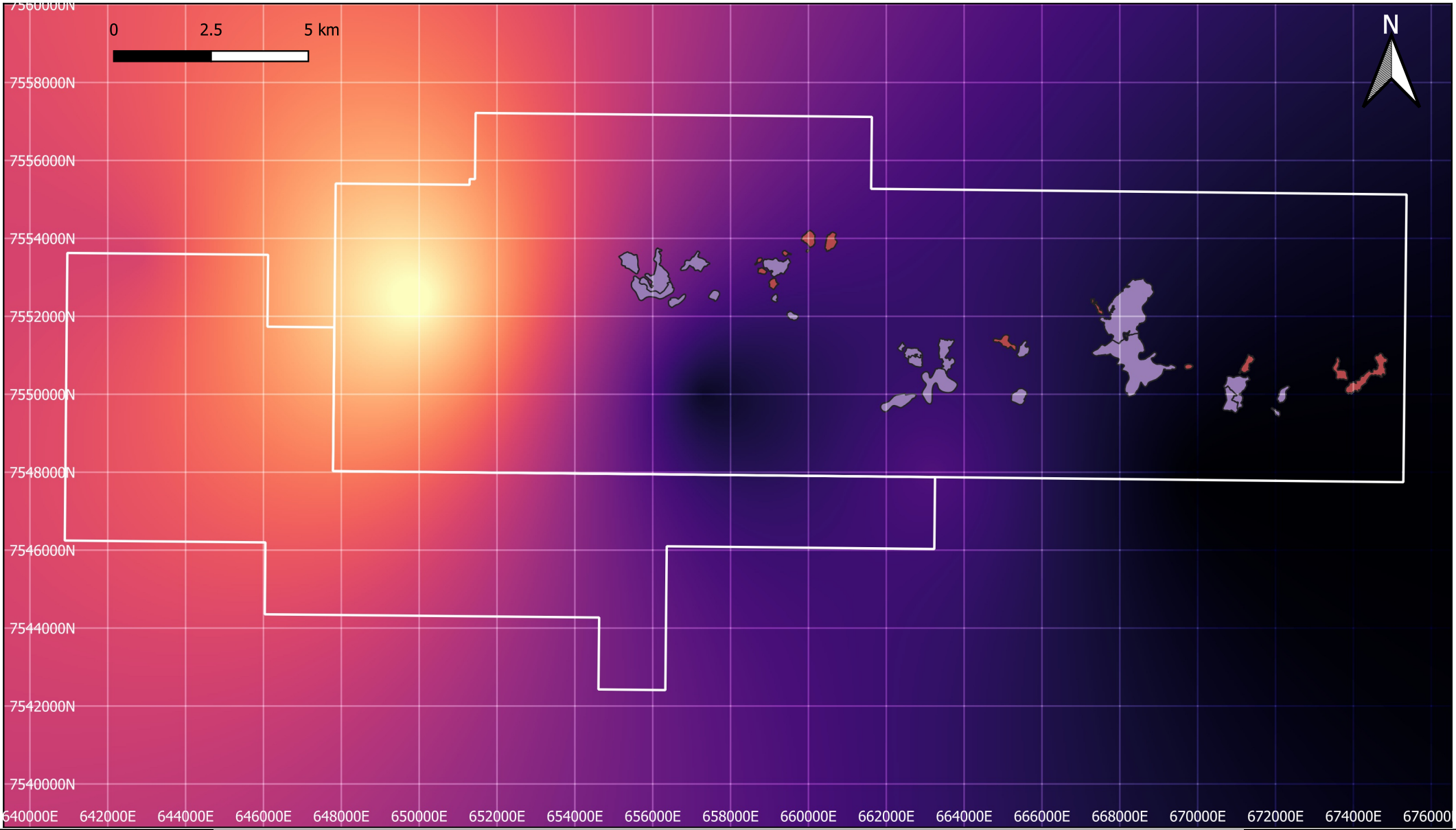

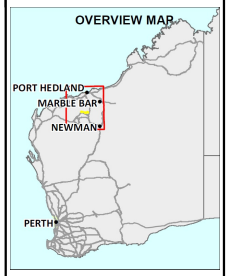

TDS (mg/L)

213	1098	1320	2205	2426	3311	3532	4418	4639	5524	5745	6630	6852	7737	7958	8843	9064	9950	10171	11056	11277
435	1541	1762	2647	2869	3754	3975	4860	5081	5967	6188	7073	7294	8179	8401	9286	9507	10392	10613	11498	
656	1984	3090	4196	5303	6409	7515	8622	9728	10835											
877																				

Figure C10

Initial TDS assigned in model Layer 10

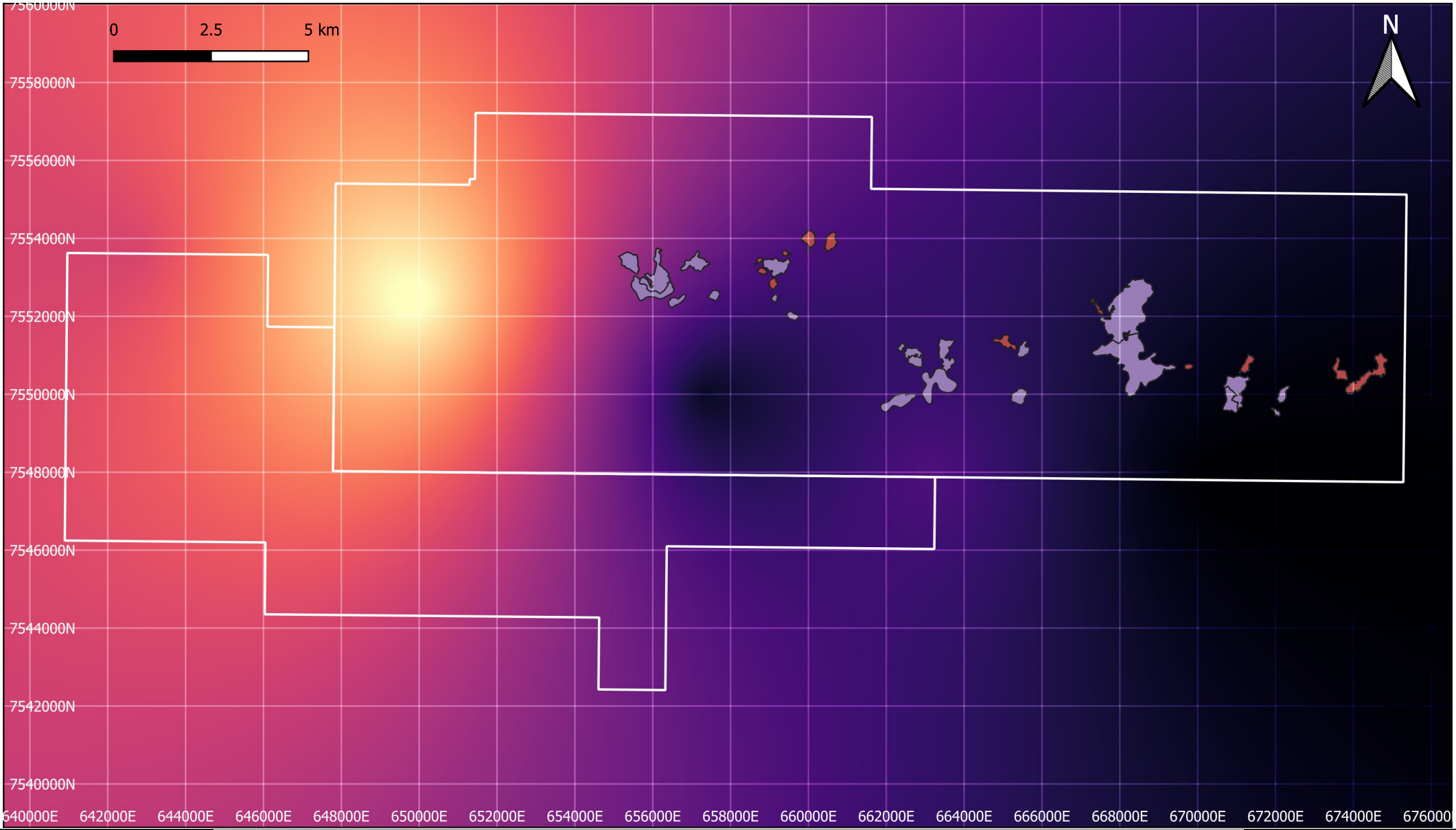

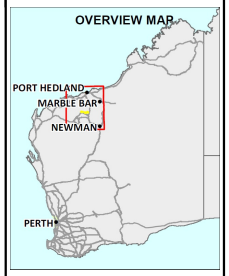

TDS (mg/L)

213	1098	1320	1541	1762	1984	2205	2426	2647	2869	3090	3311
435	1541	1762	1984	2205	2426	2647	2869	3090	3311	3532	3754
656	1762	1984	2205	2426	2647	2869	3090	3311	3532	3754	3975
877	1984	2205	2426	2647	2869	3090	3311	3532	3754	3975	4196

3311	4418	4639	4860	5081	5303	5524	5745	5967	6188	6409	6630
3532	4639	4860	5081	5303	5524	5745	5967	6188	6409	6630	6852
3754	4860	5081	5303	5524	5745	5967	6188	6409	6630	6852	7073
3975	5081	5303	5524	5745	5967	6188	6409	6630	6852	7073	7294
4196	5303	5524	5745	5967	6188	6409	6630	6852	7073	7294	7515

6630	7737	8843	9950	11056							
6852	7958	9064	10171	11277							
7073	8179	9286	10392	11498							
7294	8401	9507	10613								
7515	8622	9728	10835								

Figure C11

Initial TDS assigned in model Layer 11

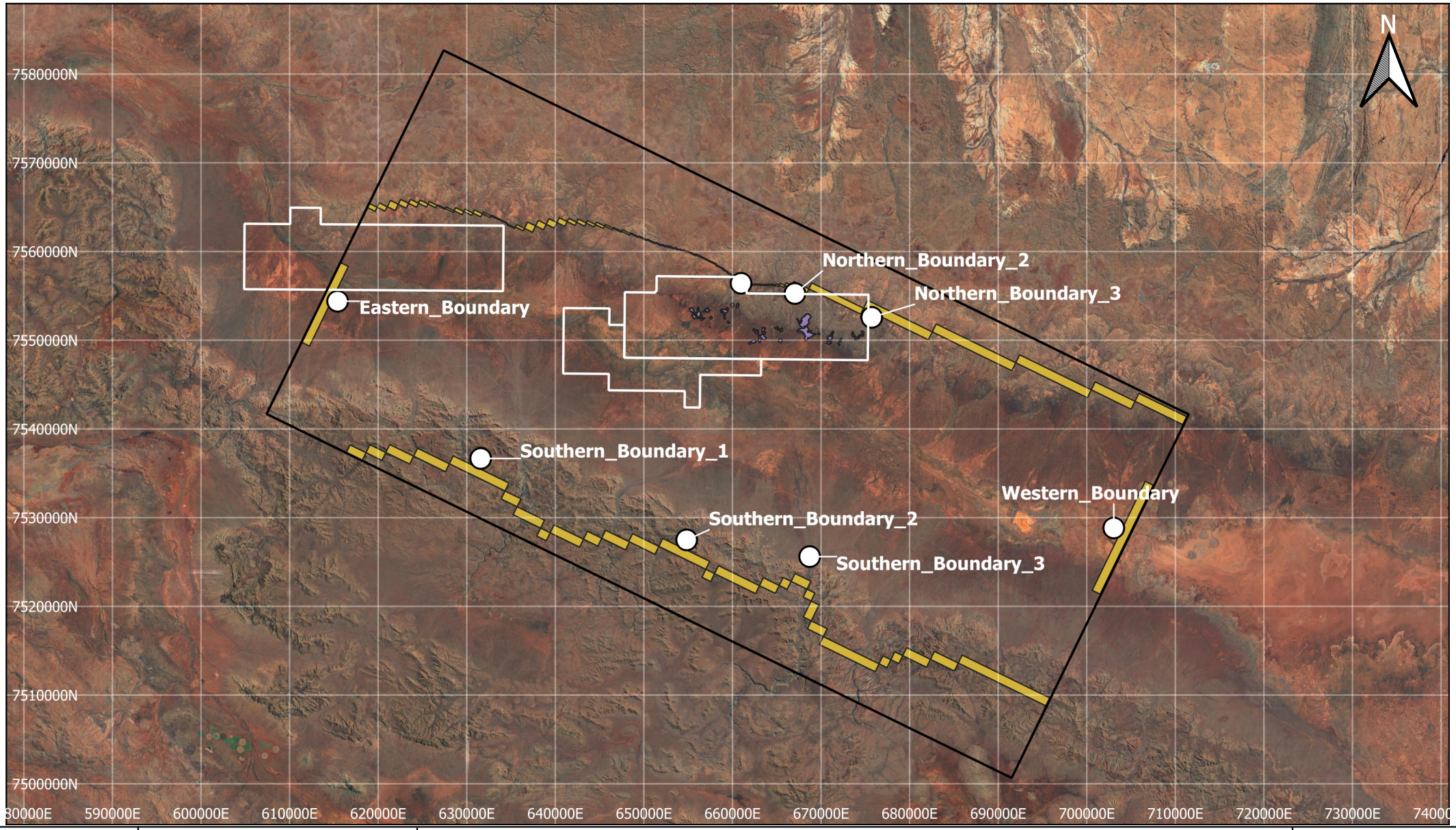

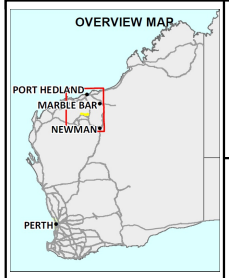

0 12.5 25 km

Legend

- Pits Above Water Table
- Pits Below Water Table
- Tenement Boundary
- Simulated Constant Head Boundary
- Model Domain

AUTHOR: MP

DRAWN: MP

DATE: 10/10/2024

Report NO: GWC-020-2022

REVISION: I

JOB No: 020-2022

NOTES & DATA SOURCES:

Not for construction

ESPG:28350 (GDA94/MGA zone 50)

Figure C12

Location of control points used to monitor TDS near the simulated constant head boudaries

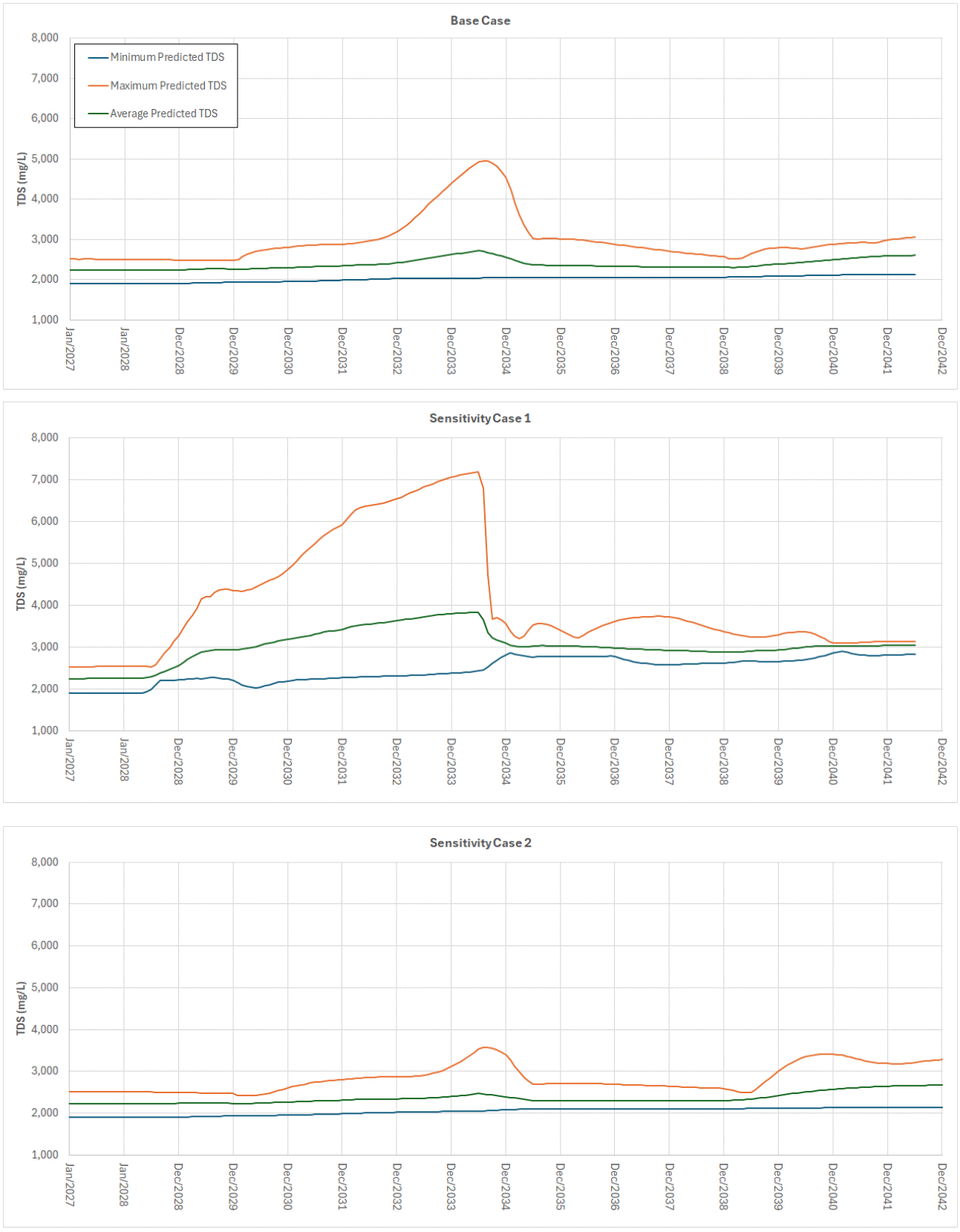

Figure C-13 Predicted TDS at Murray Hill

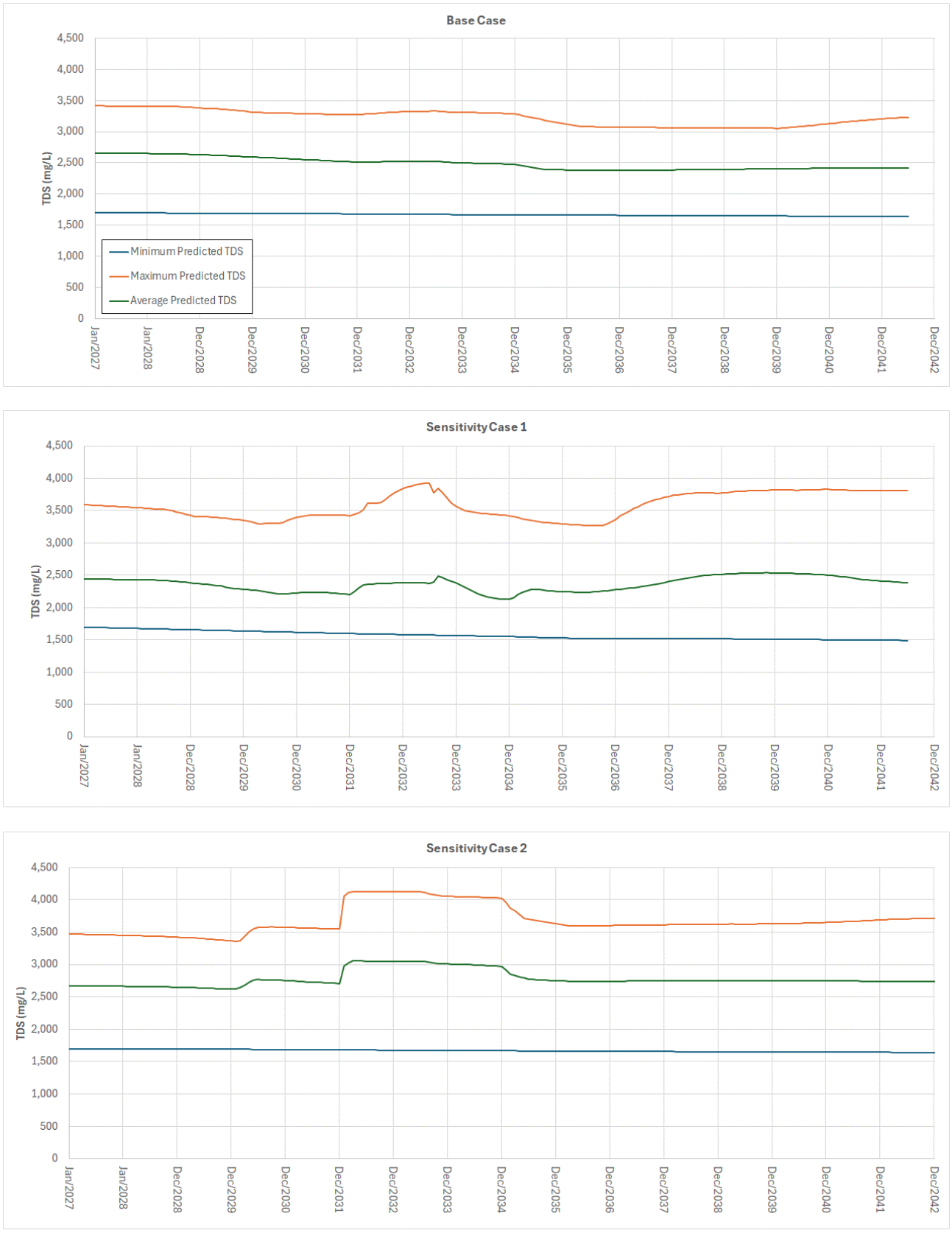

Figure C-14 Predicted TDS at Anticline Hill

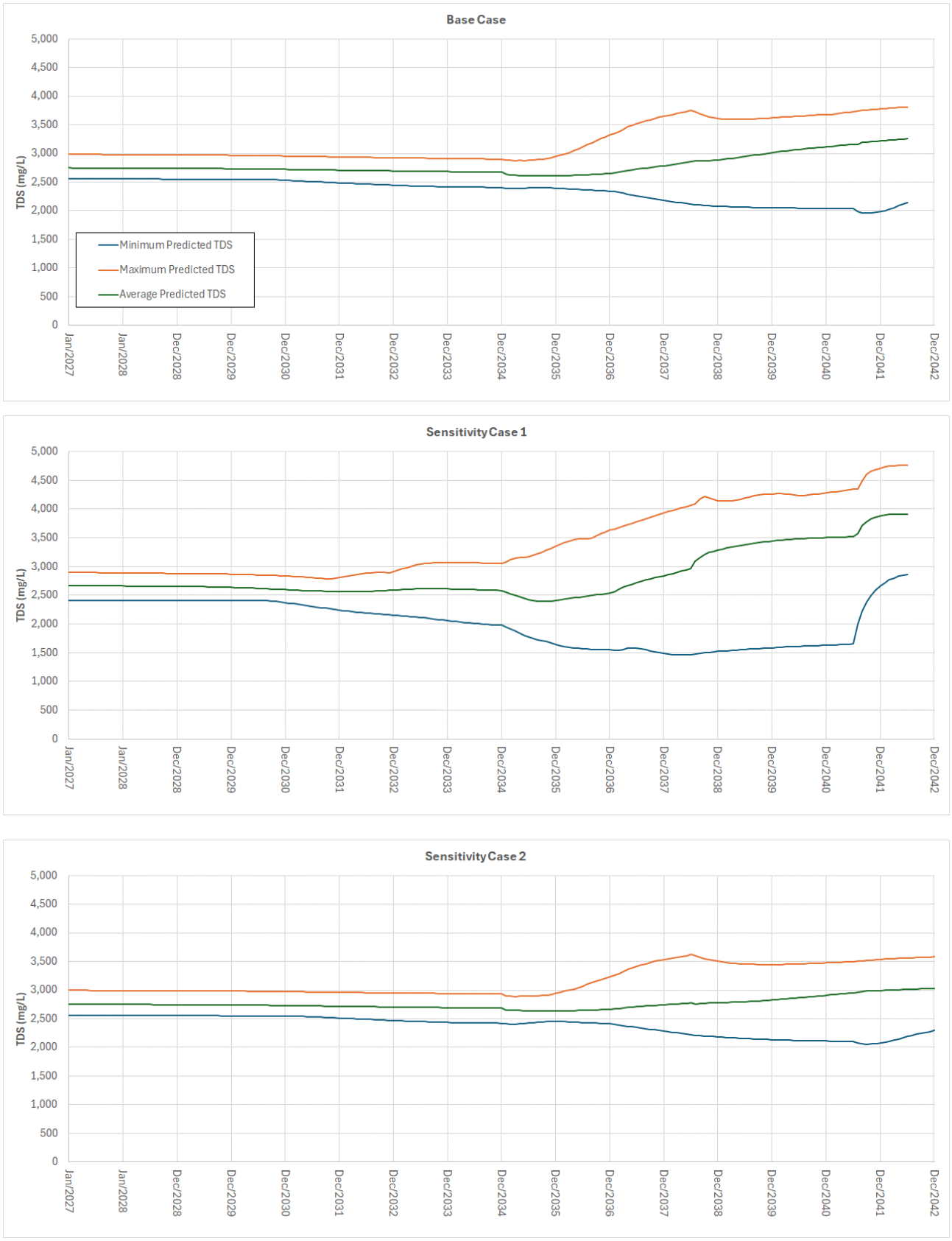

Figure C-15 Predicted TDS at Fridge West

Figure C-16 Predicted TDS at Fridge Central

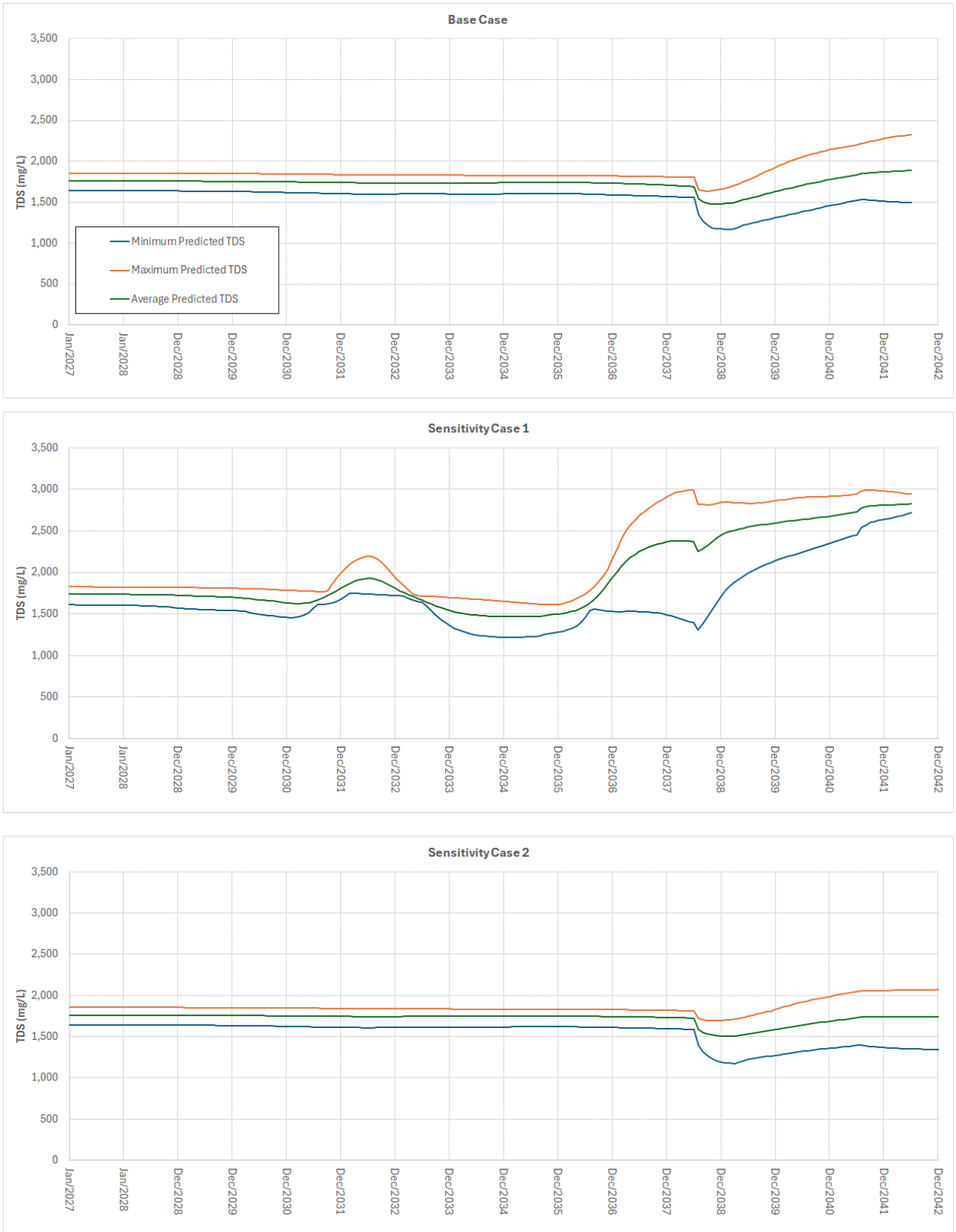

Figure C-17 Predicted TDS at Fridge Hill

Figure C-18 Predicted TDS at Horseshoe West

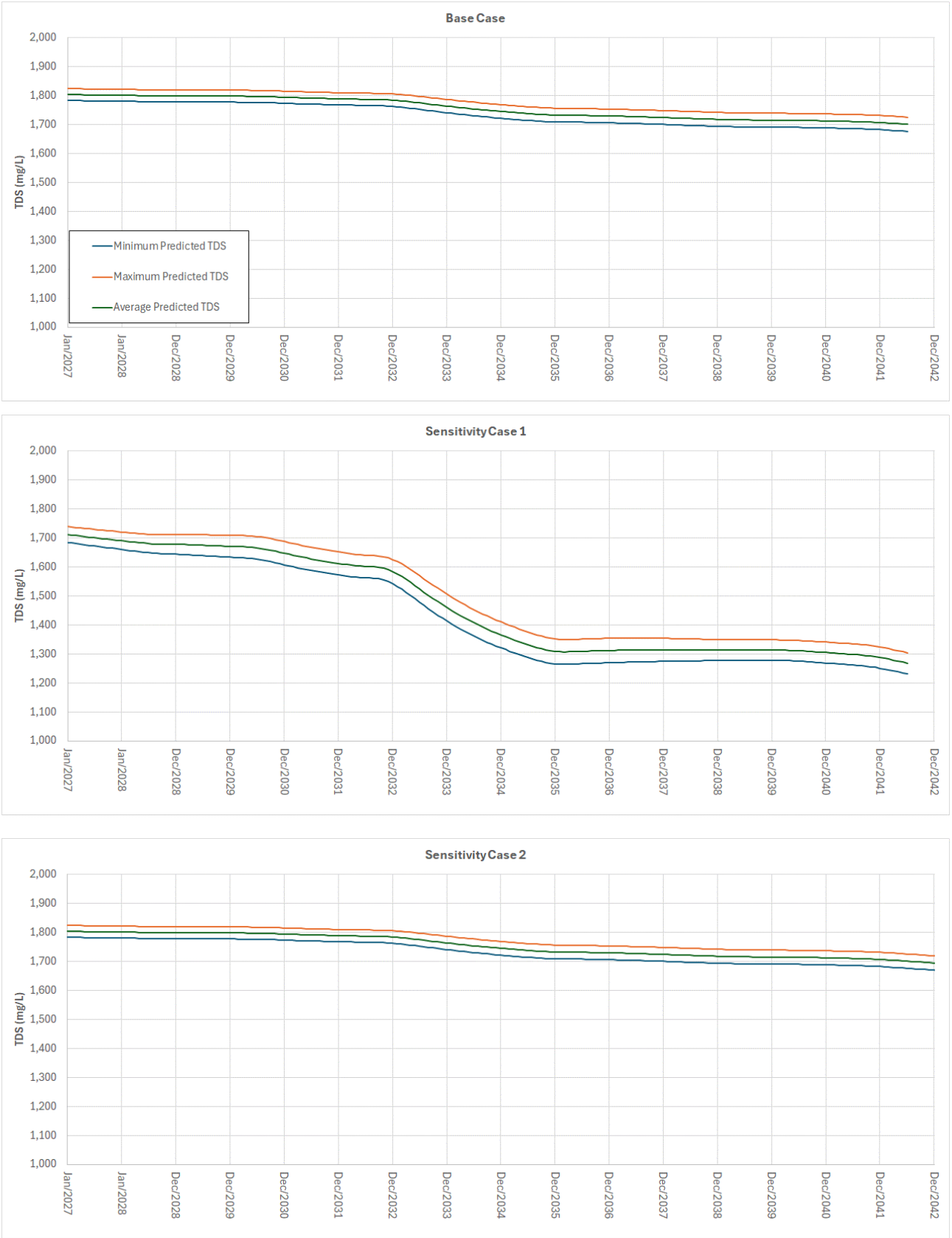

Figure C-19 Predicted TDS at Horseshoe Hill

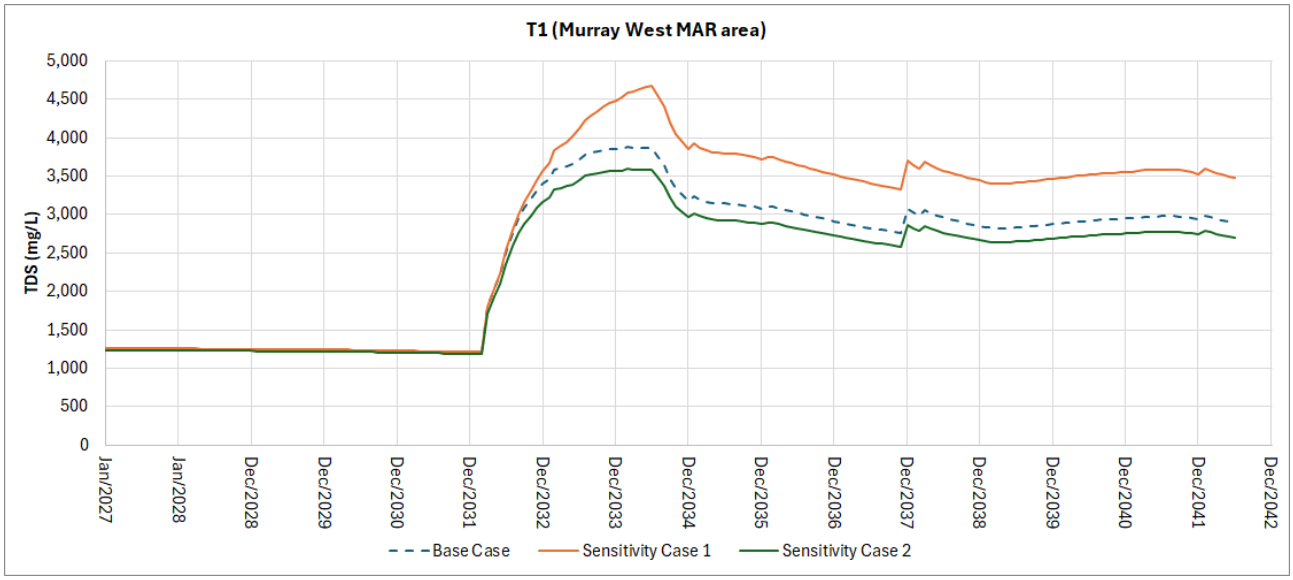

Figure C-20 Predicted TDS at T1 (Murray West MAR area)

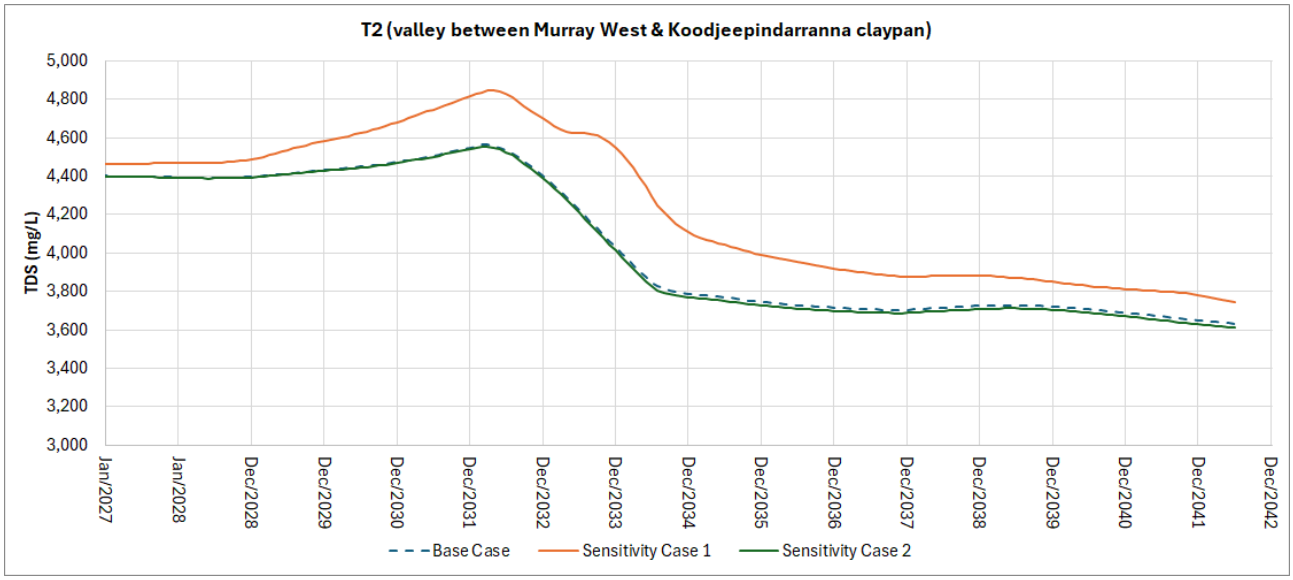

Figure C-21 Predicted TDS at T2 (valley between Murray West & Koodjeepindarranna claypan)

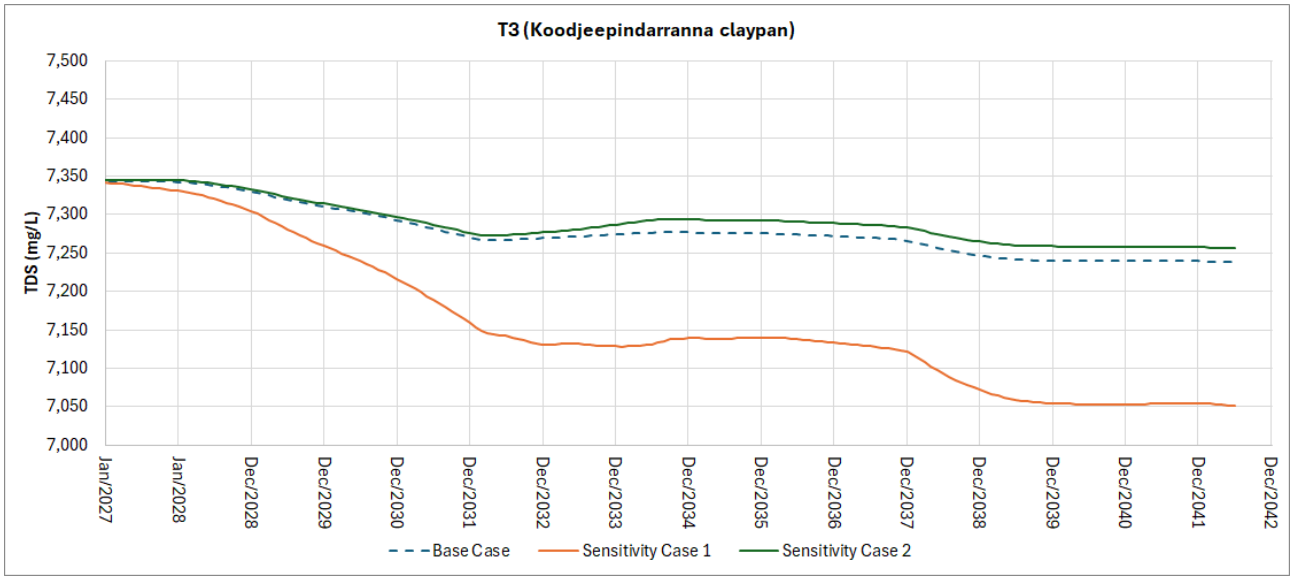

Figure C-22 Predicted TDS at T3 (Koodjeepindarranna claypan)

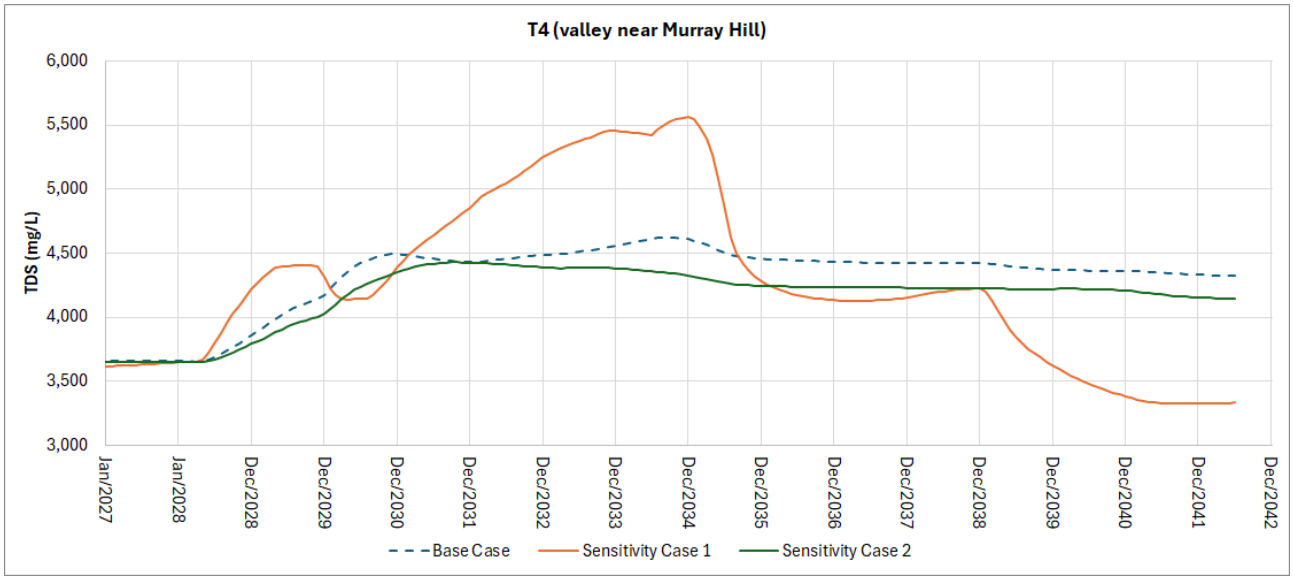

Figure C-23 Predicted TDS at T4 (valley near Murray Hill)

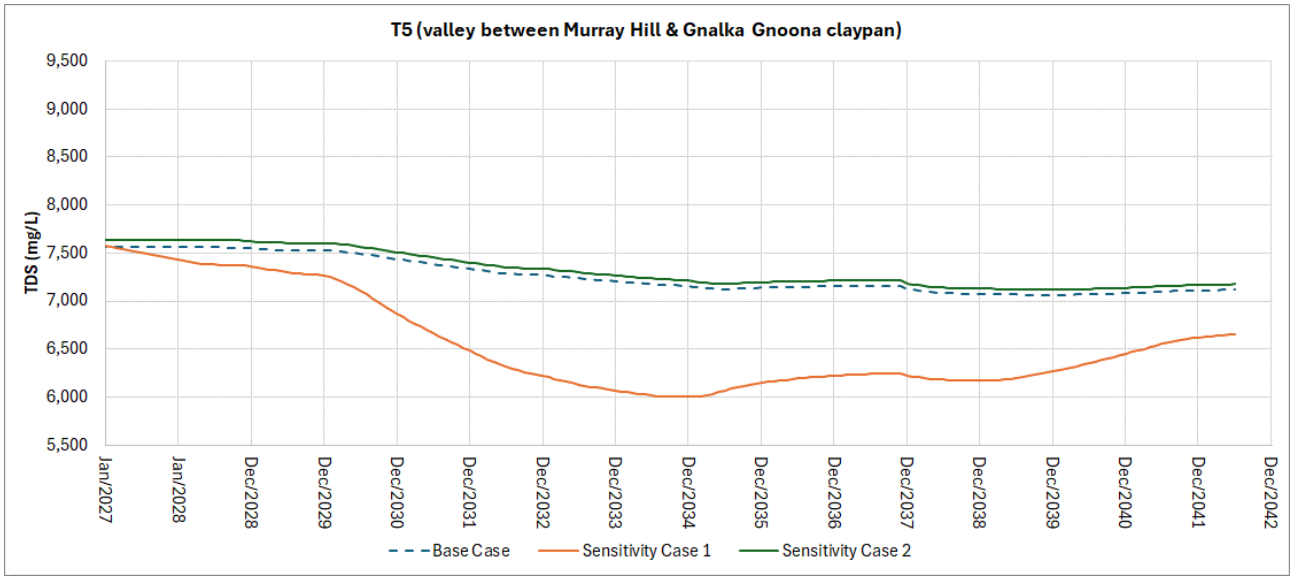

Figure C-24 Predicted TDS at T5 (valley between Murray Hill & Gnalka Gnoona claypan)

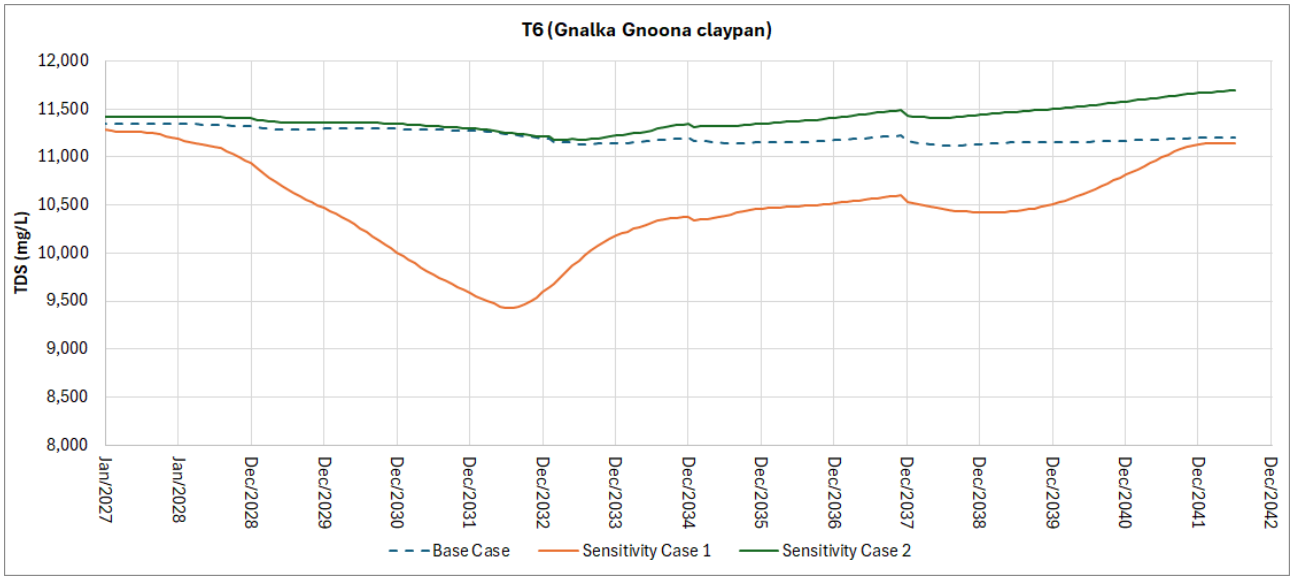

Figure C-25 Predicted TDS at T6 (Gnalka Gnoona claypan)

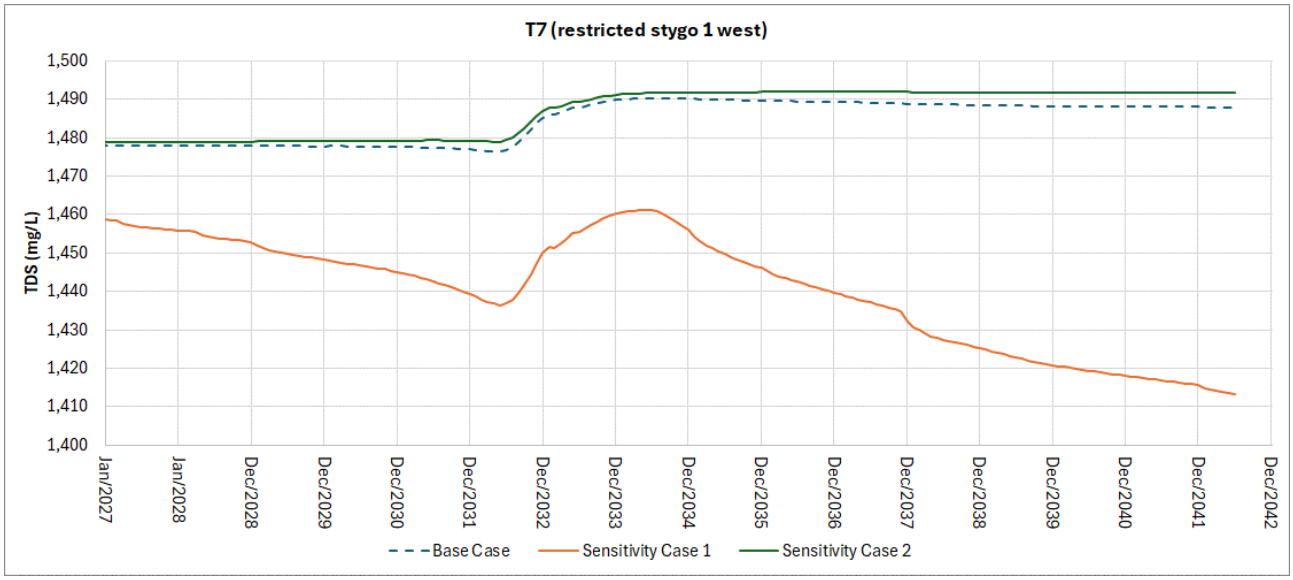

Figure C-26 Predicted TDS at T7 (restricted stygo 1 west)

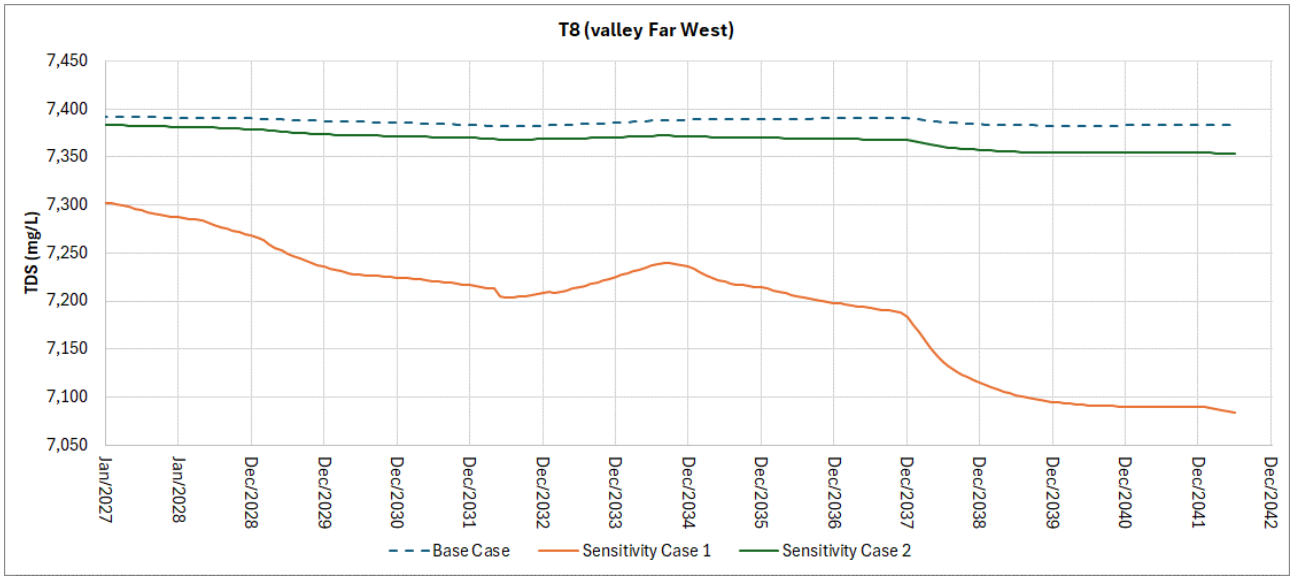

Figure C-27 Predicted TDS at T8 (valley Far West)

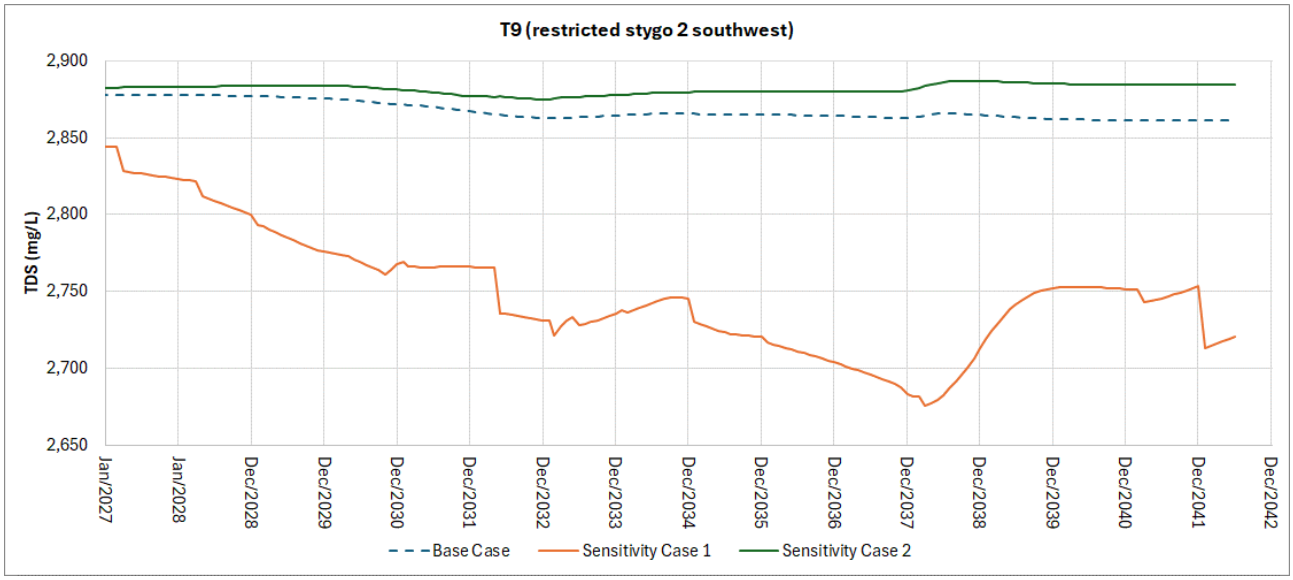

Figure C-28 Predicted TDS at T9 (restricted stygo 2 southwest)

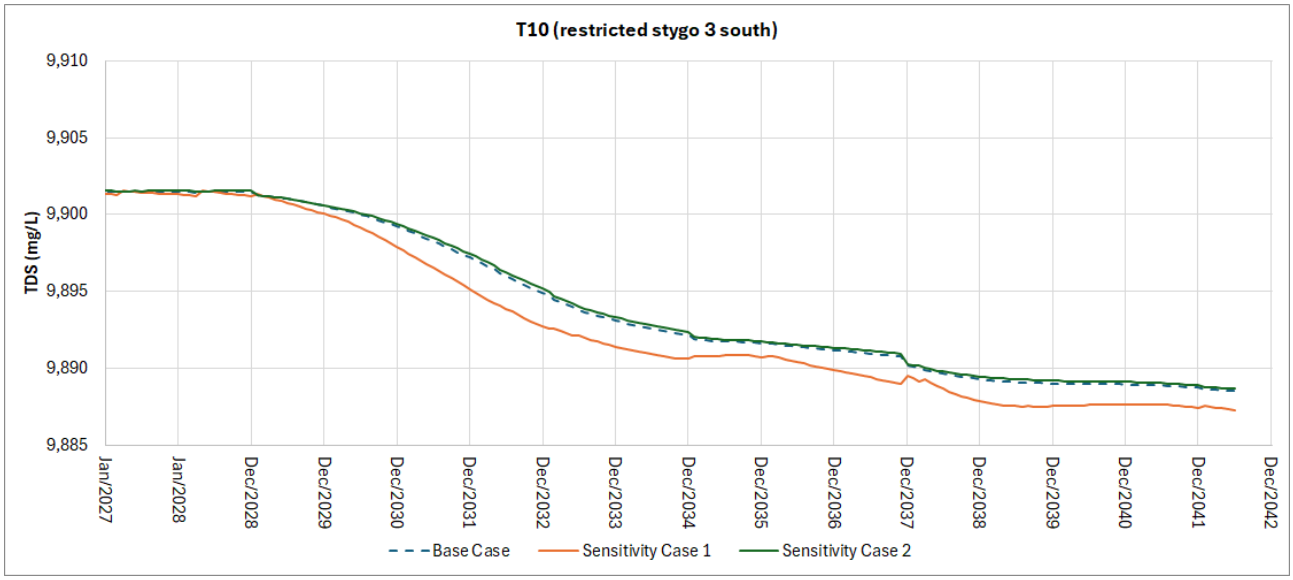

Figure C-29 Predicted TDS at T10 (restricted stygo 3 south)

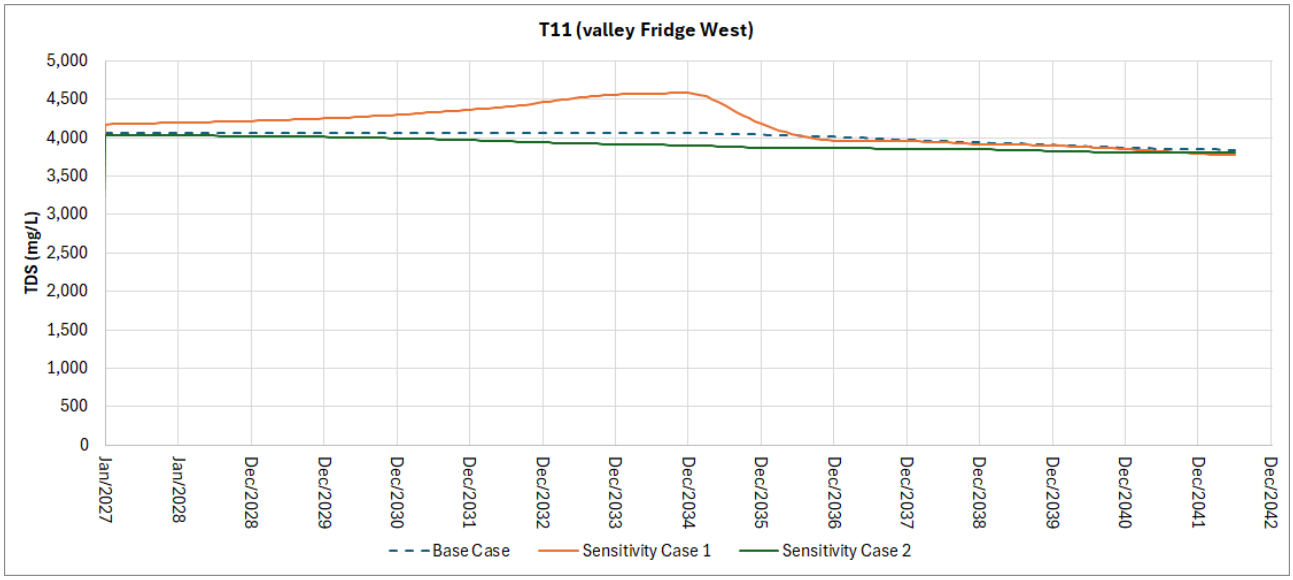

Figure C-30 Predicted TDS at T11 (valley Fridge West)

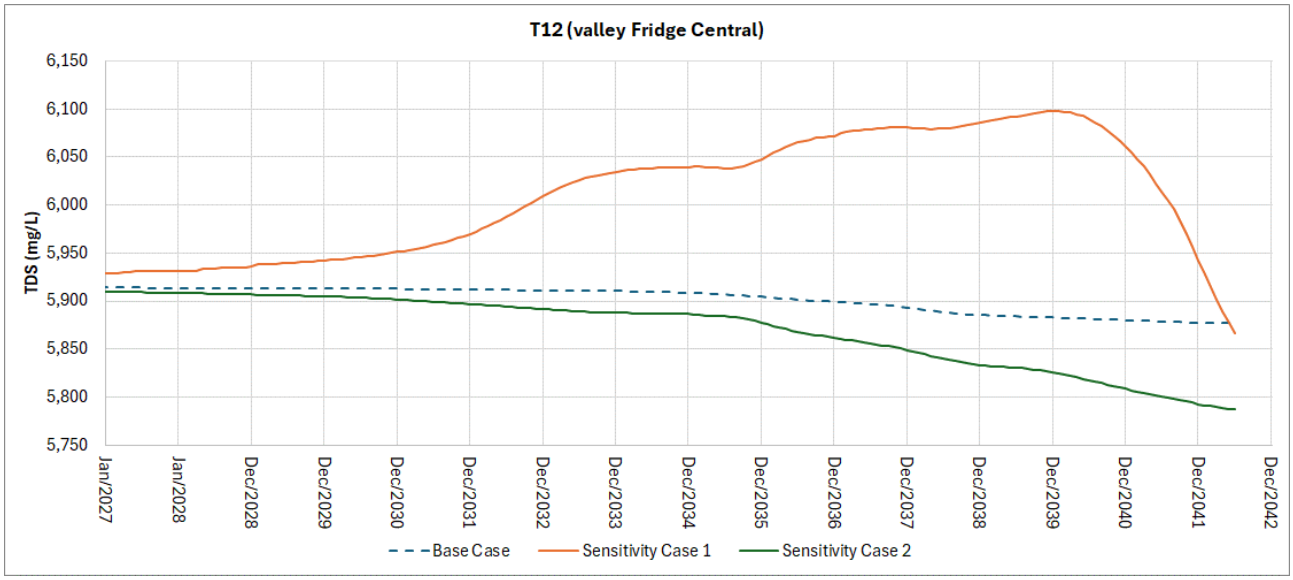

Figure C-31 Predicted TDS at T12 (valley Fridge Central)

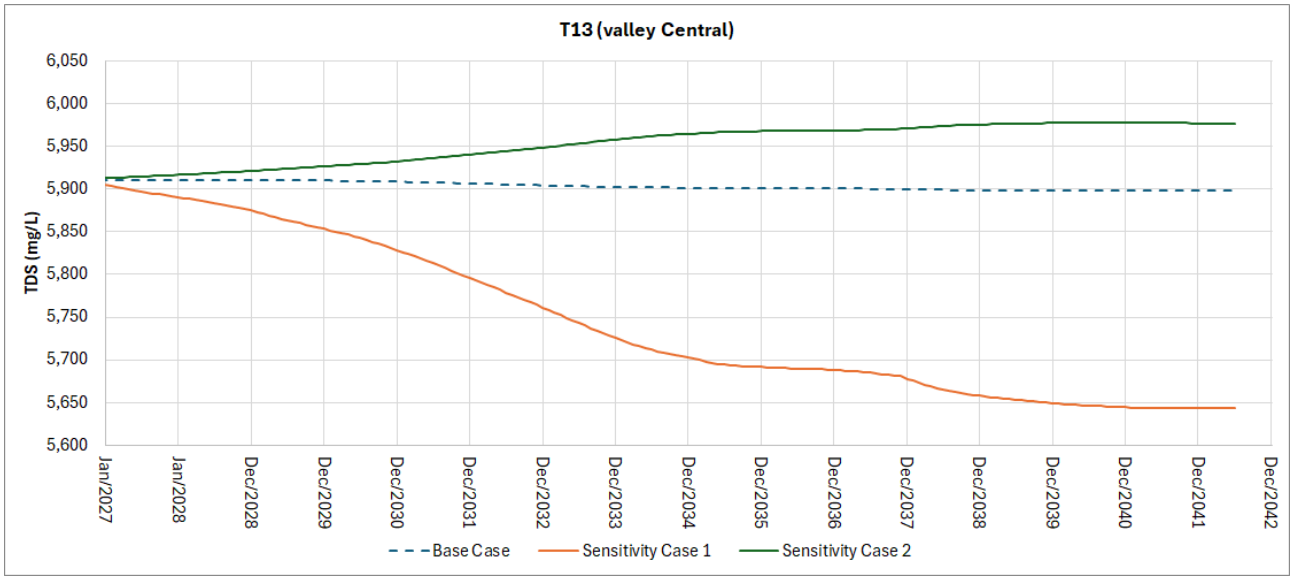

Figure C-32 Predicted TDS at T13 (valley Central)

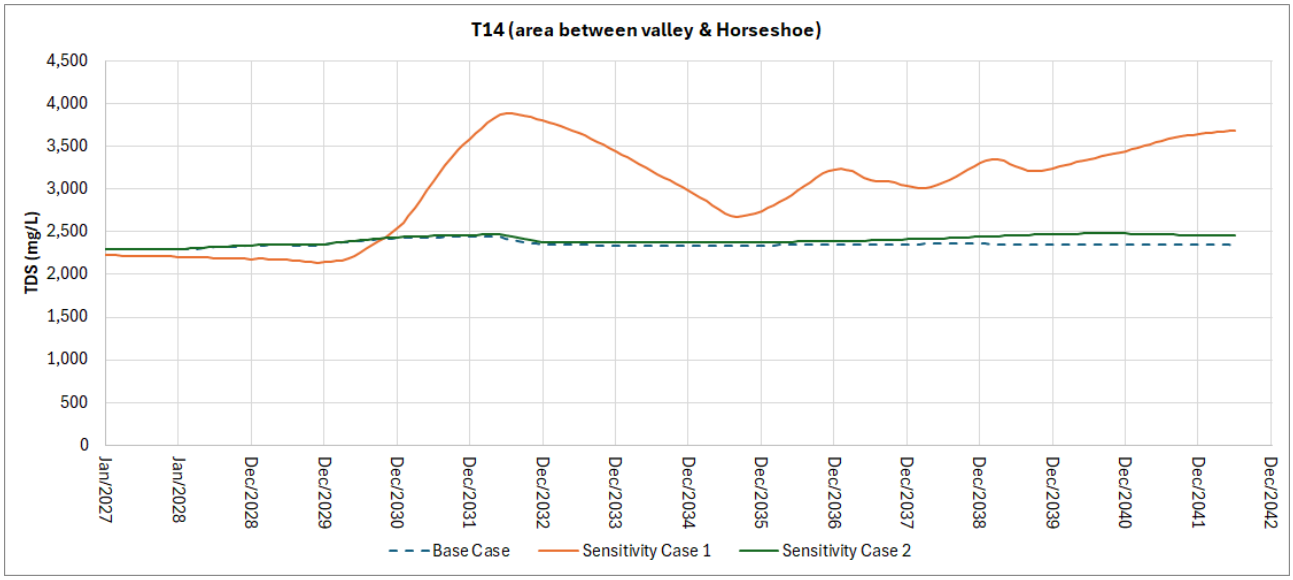

Figure C-33 Predicted TDS at T14 (area between valley & Horseshoe)

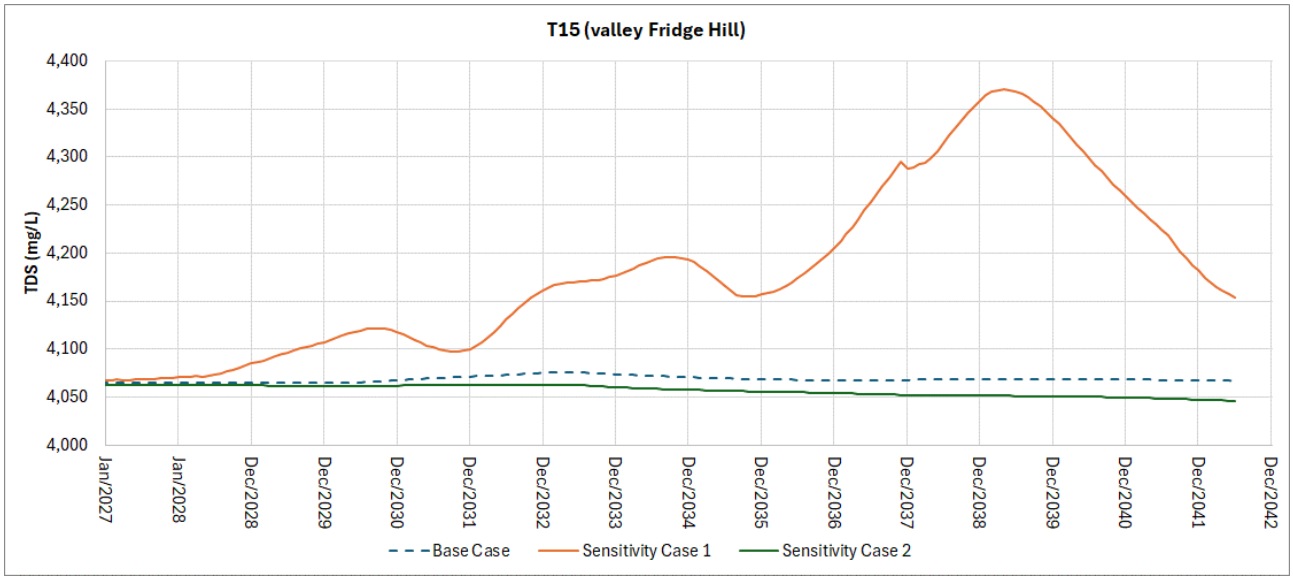

Figure C-34 Predicted TDS at T15 (valley Fridge Hill)

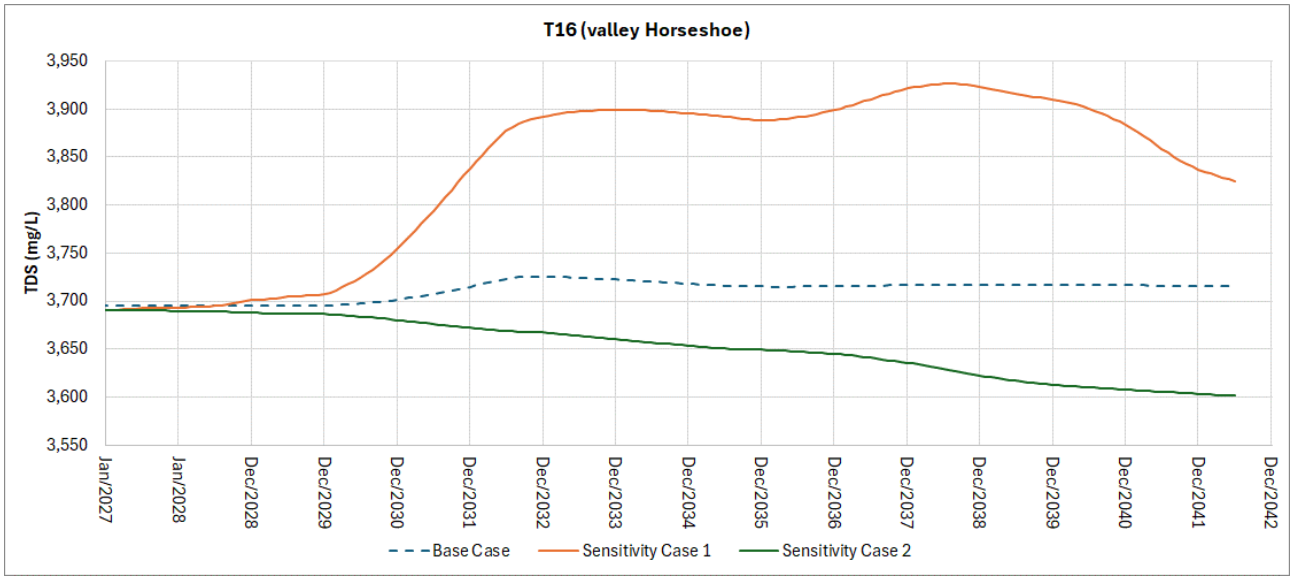

Figure C-35 Predicted TDS at T16 (valley Horseshoe)

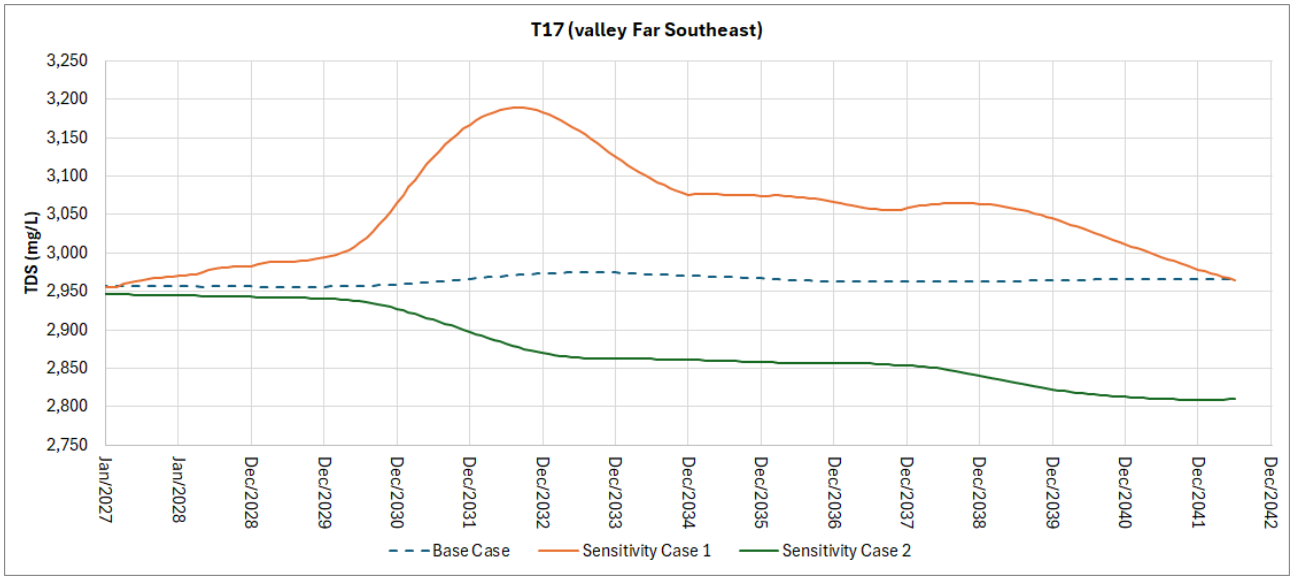

Figure C-36 Predicted TDS at T17 (valley Far Southeast)

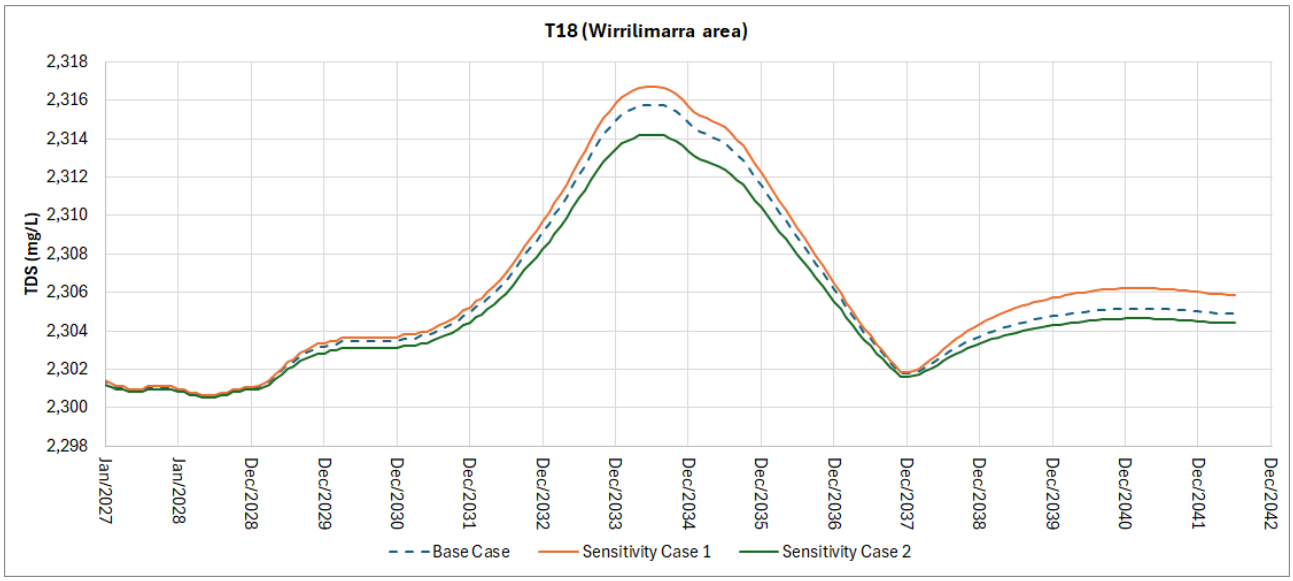

Figure C-37 Predicted TDS at T18 (Wirrilimarra area)

Appendix D Particle Tracking

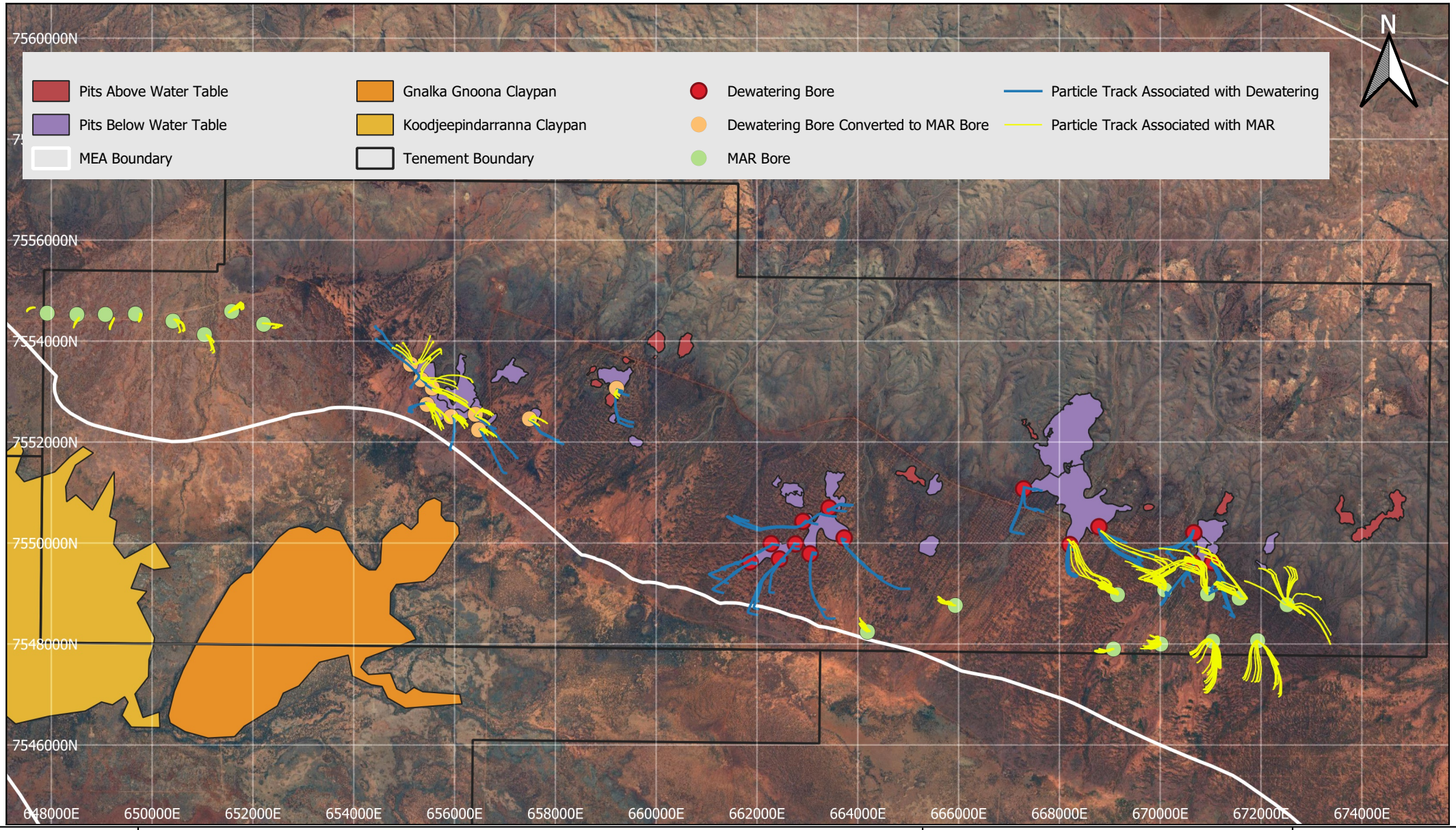

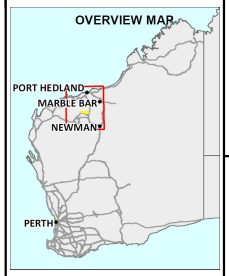

NOTES & DATA SOURCES:
Not for construction
ESPG:28350 (GDA94/MGA zone 50)

0 2.5 5 km

AUTHOR: MP
DRAWN: MP
DATE: 3/10/2024

Report NO: GWC-020-2022
REVISION: H
JOB No: 020-2022

Figure D1

Predicted particle tracks

Appendix E Uncertainty Results

NOTE: Positive values on charts represent predicted drawdown. Negative values on charts represent predicted mounding.

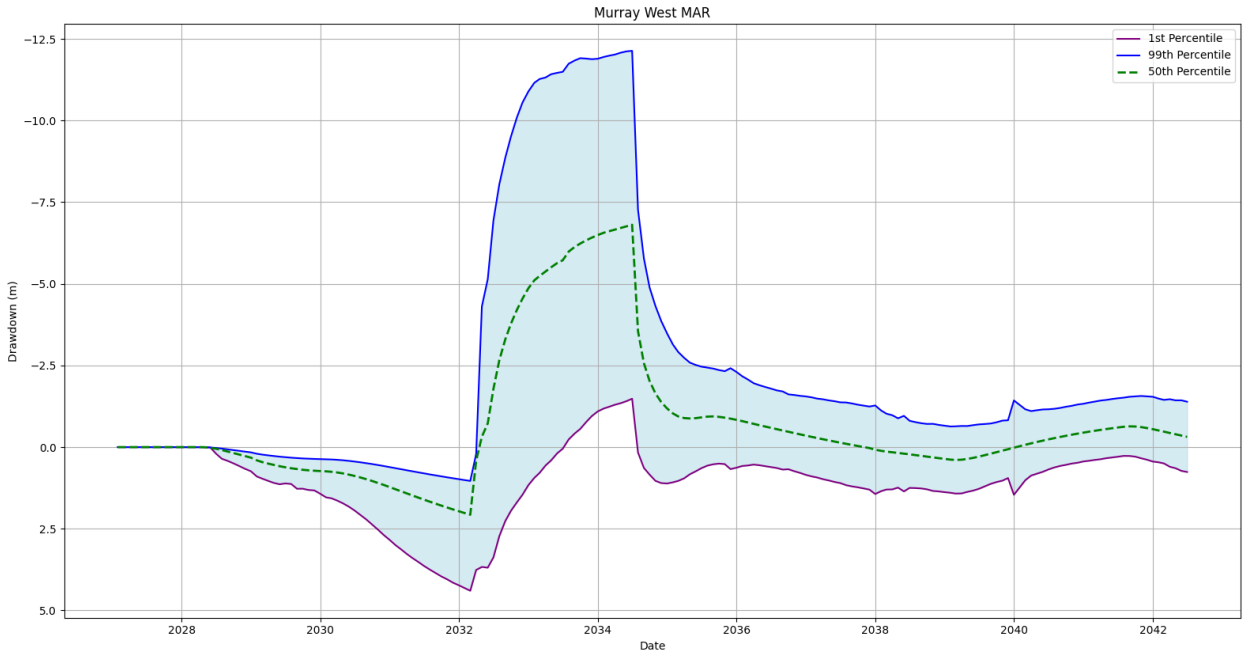

Figure E-1 Predicted aquifer recovery at T1 (Murray West MAR area)

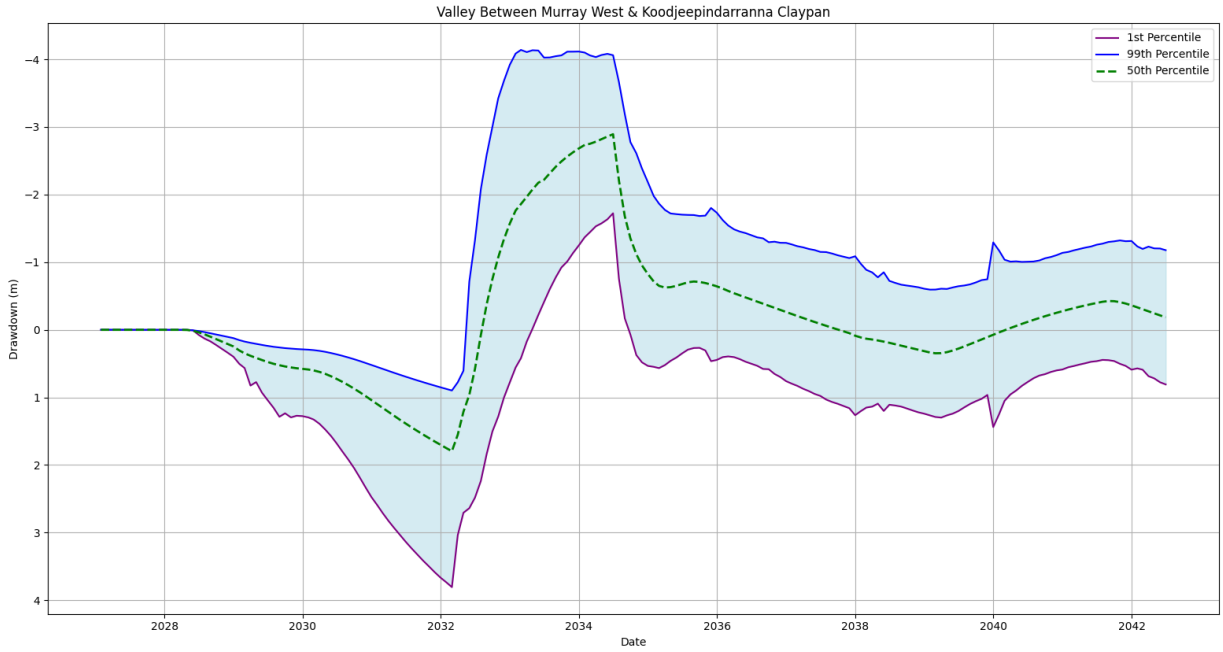

Figure E-2 Predicted aquifer recovery at T2 (valley between Murray West & Koodjeepindarranna claypan)

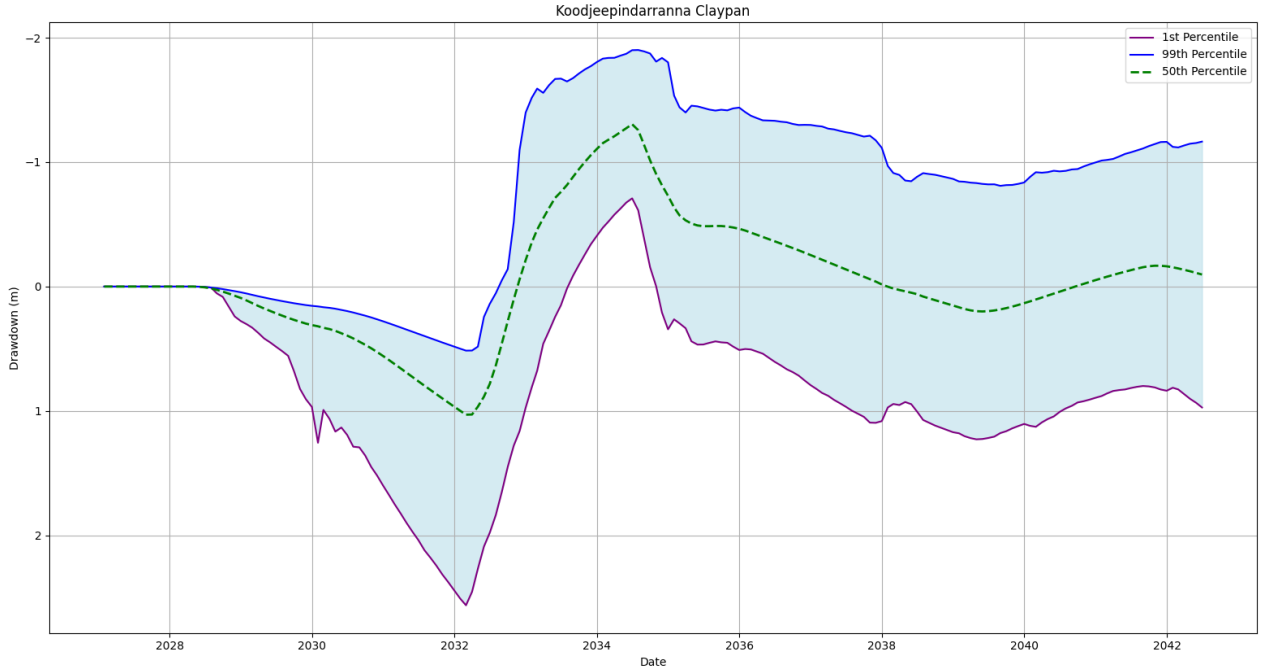

Figure E-3 Predicted aquifer recovery at T3 (Koodjeepindarranna claypan)

Figure E-4 Predicted aquifer recovery at T4 (valley near Murray Hill)

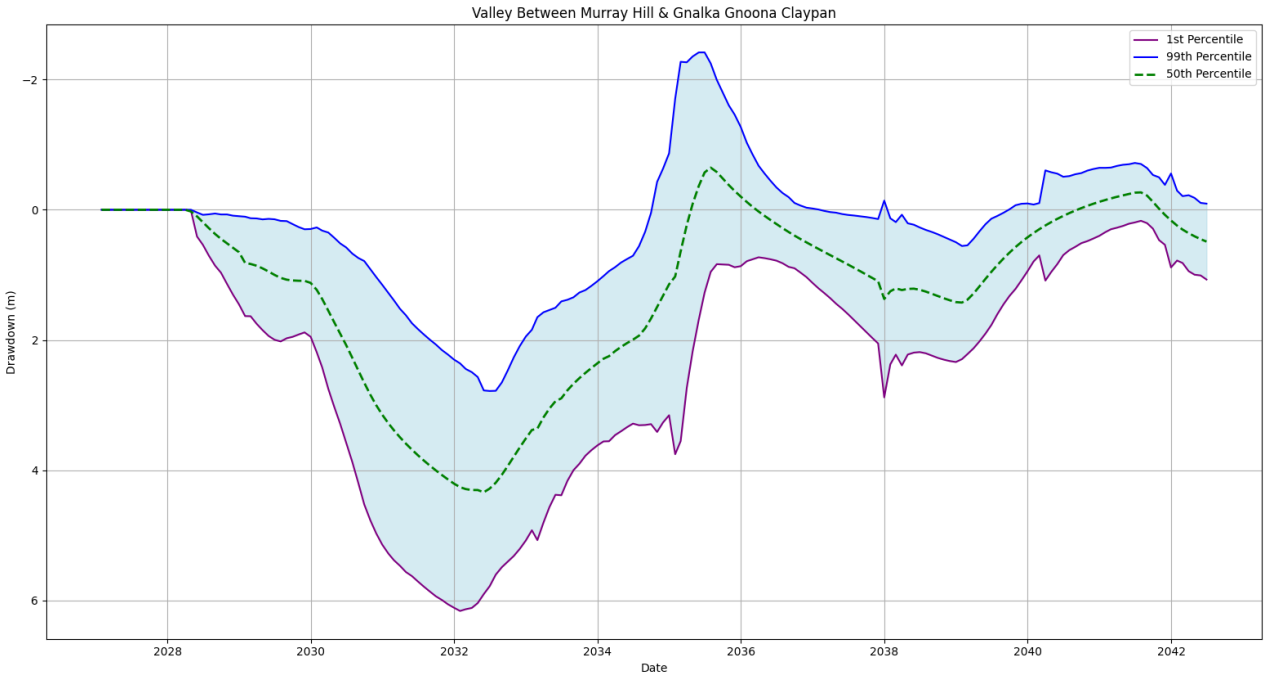

Figure E-5 Predicted aquifer recovery at T5 (valley between Murray Hill & Gnalka Gnoona claypan)

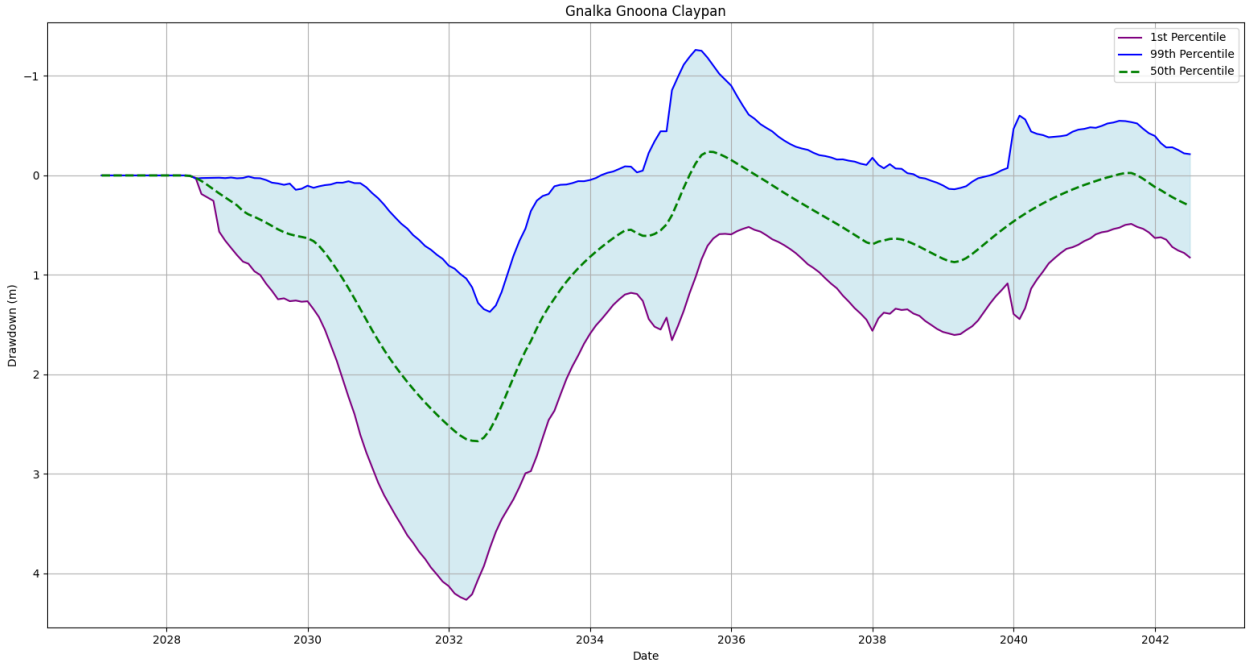

Figure E-6 Predicted aquifer recovery at T6 (Gnalka Gnoona claypan)

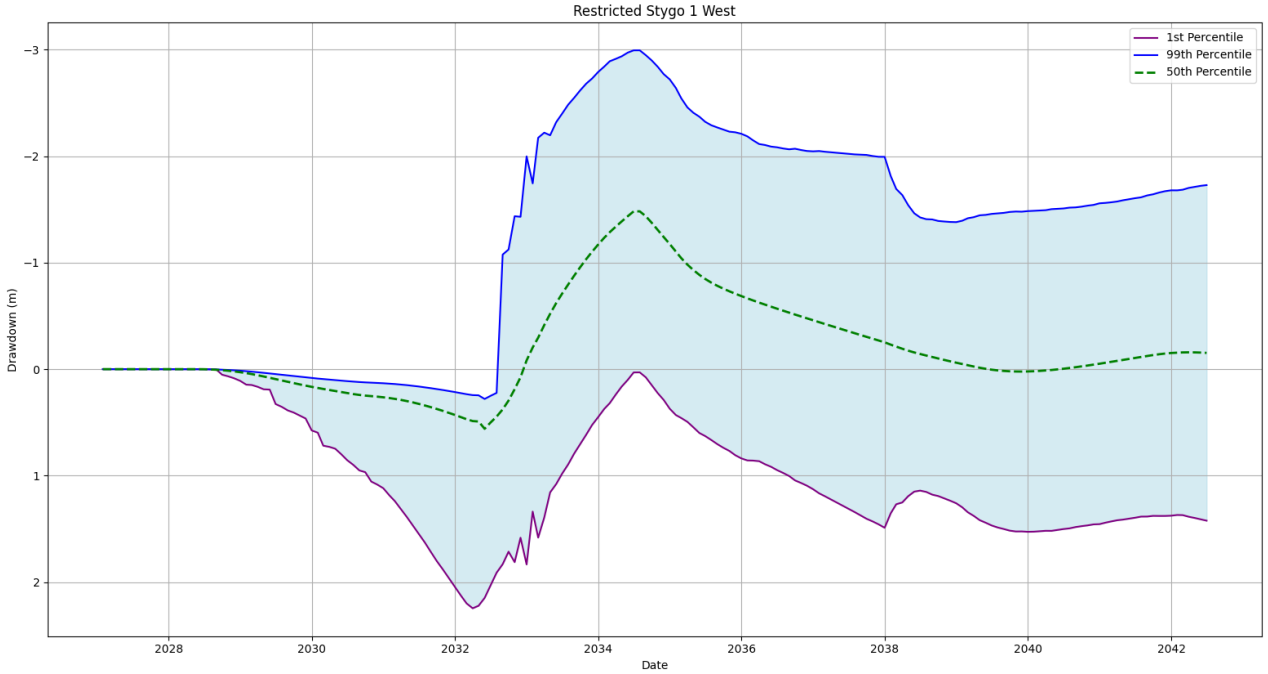

Figure E-7 Predicted aquifer recovery at T7 (restricted stygo 1 west)

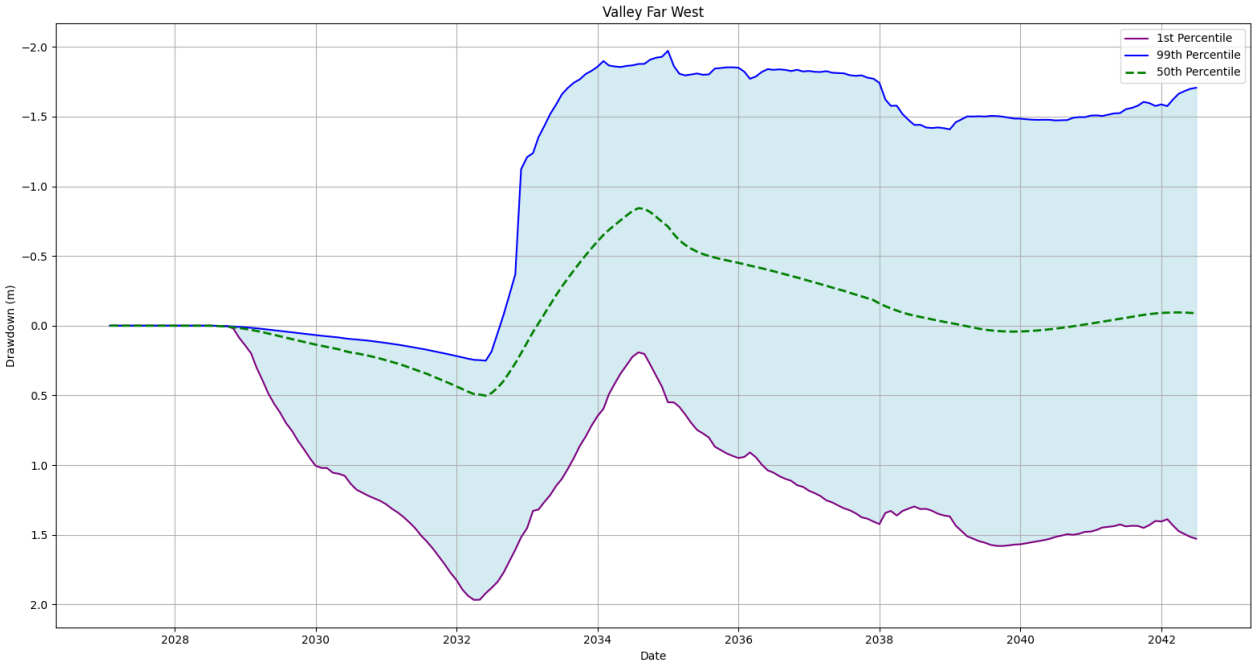

Figure E-8 Predicted aquifer recovery at T8 (valley Far West)

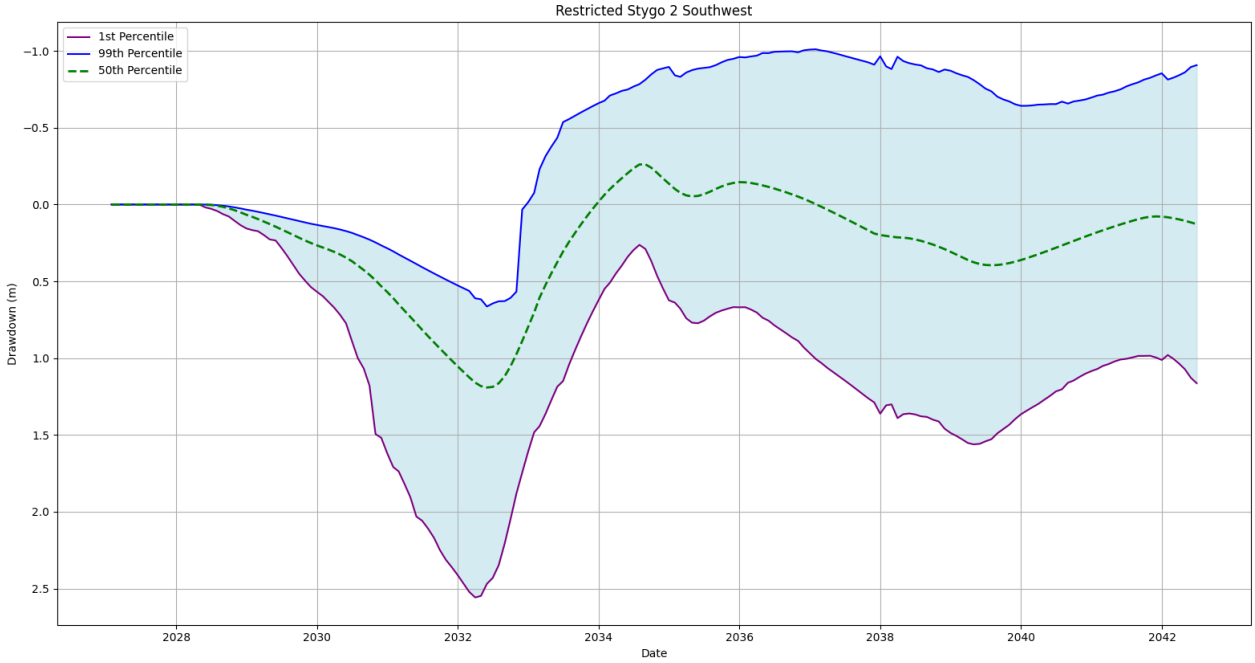

Figure E-9 Predicted aquifer recovery at T9 (restricted stygo 2 southwest)

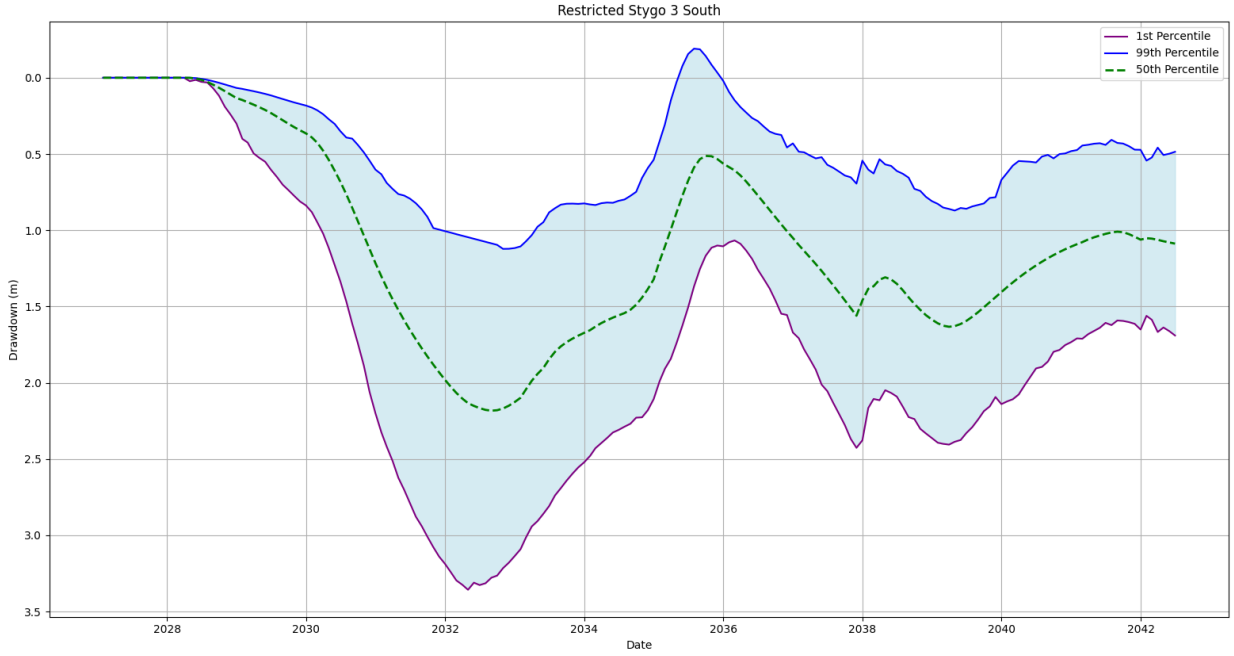

Figure E-10 Predicted aquifer recovery at T10 (restricted stygo 3 south)

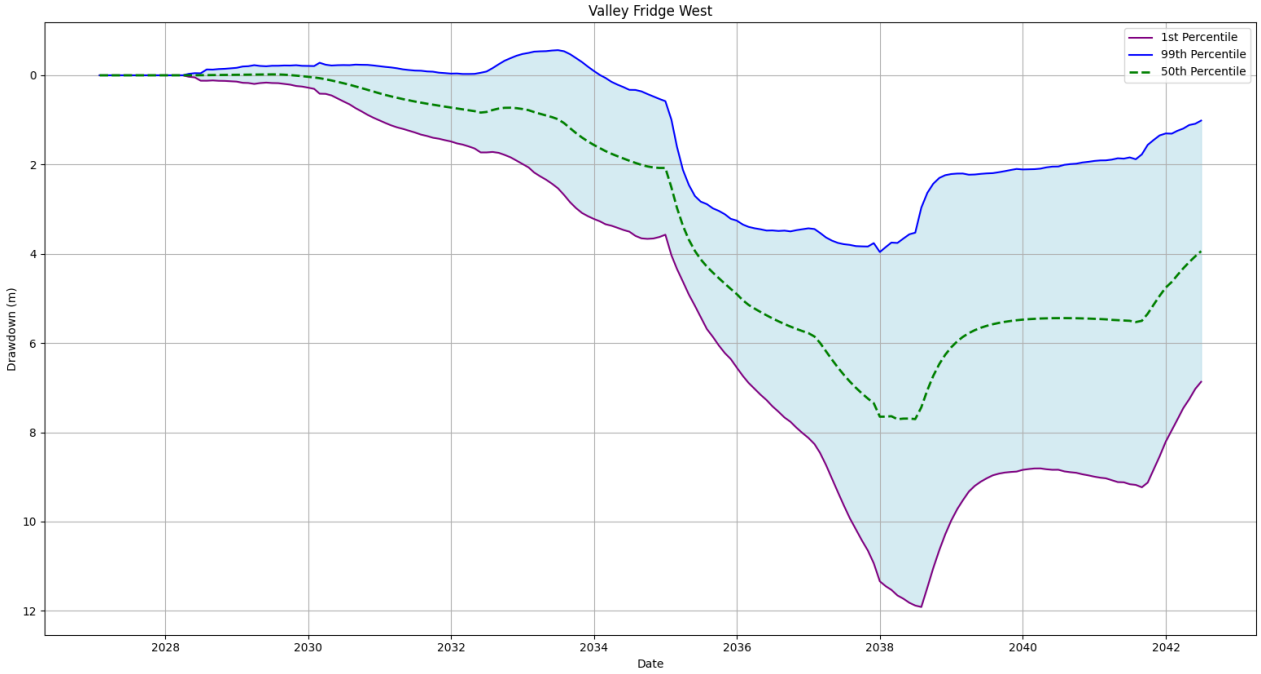

Figure E-11 Predicted aquifer recovery at T11 (valley Fridge West)

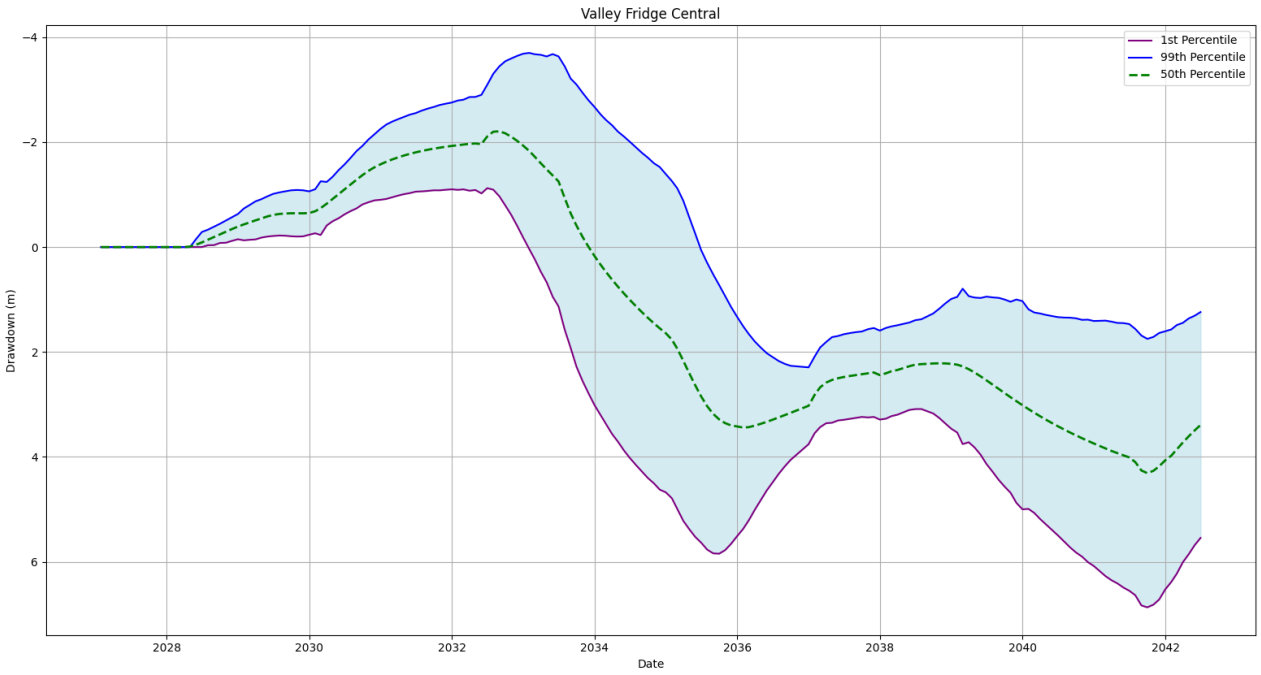

Figure E-12 Predicted aquifer recovery at T12 (valley Fridge Central)

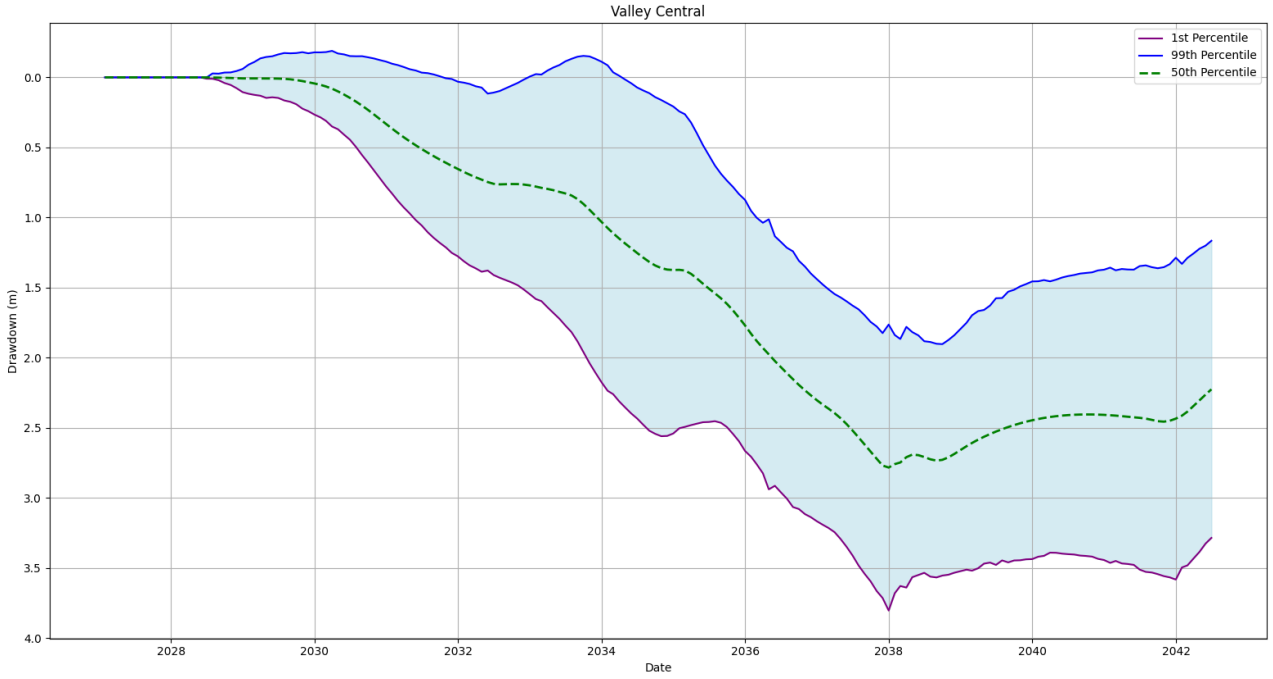

Figure E-13 Predicted aquifer recovery at T13 (valley Central)

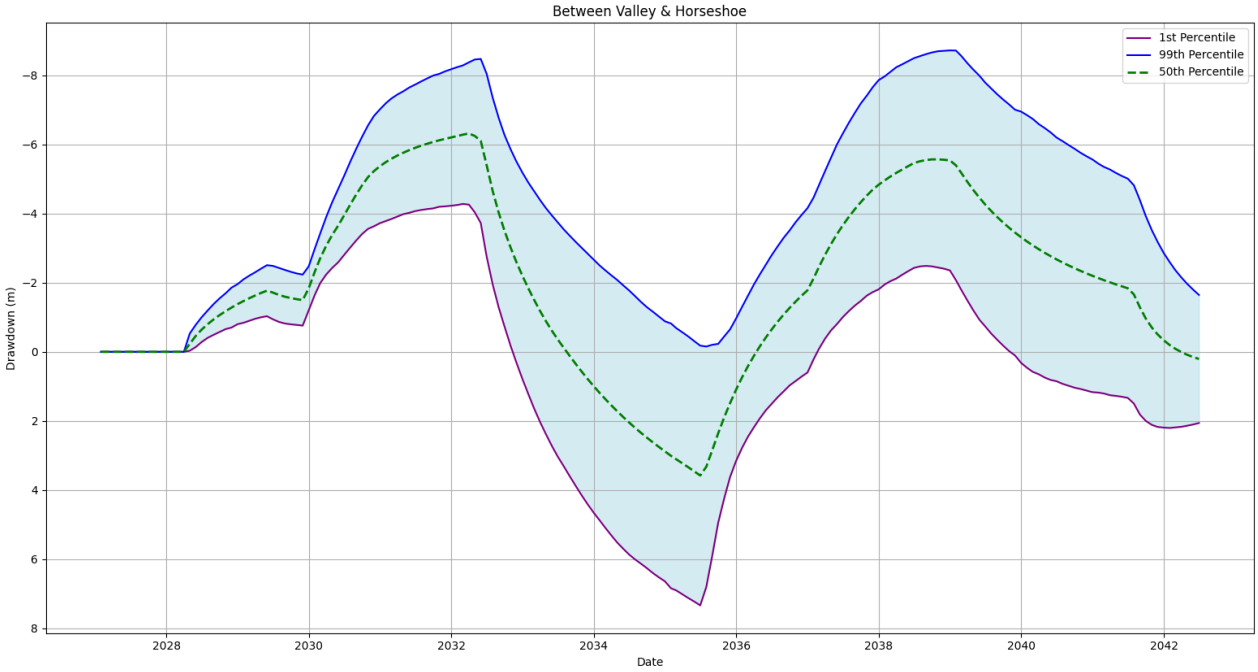

Figure E-14 Predicted aquifer recovery at T14 (area between valley & Horseshoe)

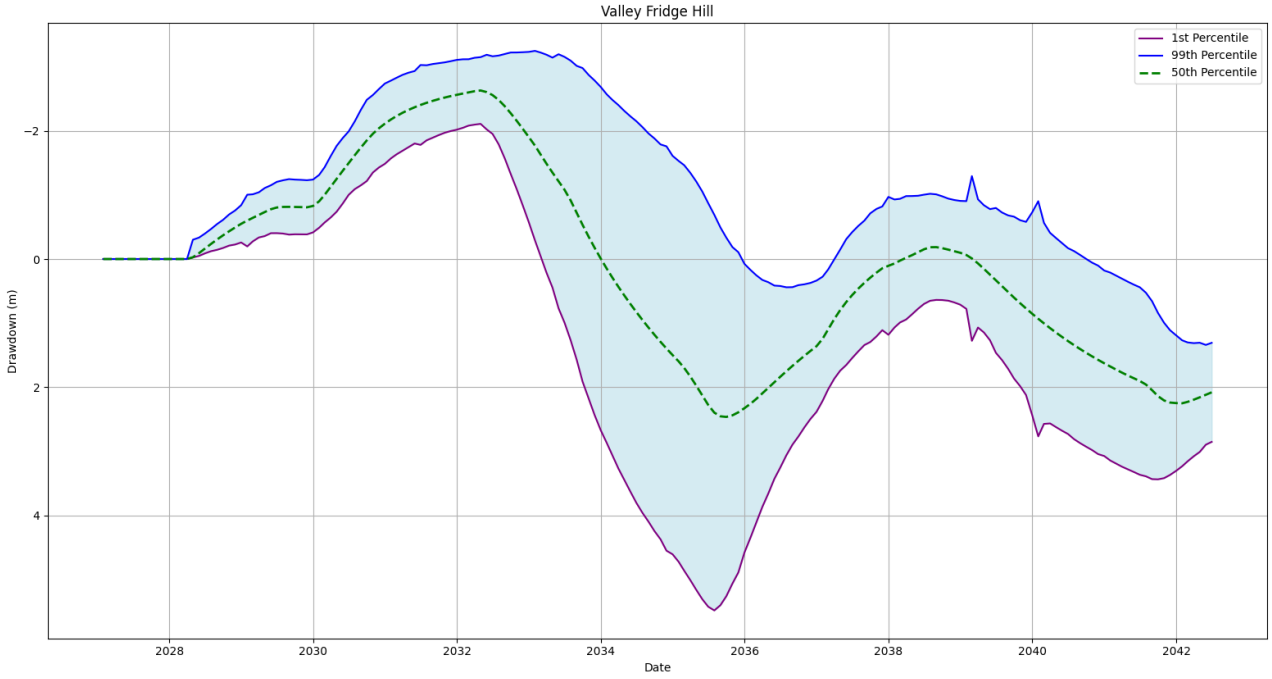

Figure E-15 Predicted aquifer recovery at T15 (valley Fridge Hill)

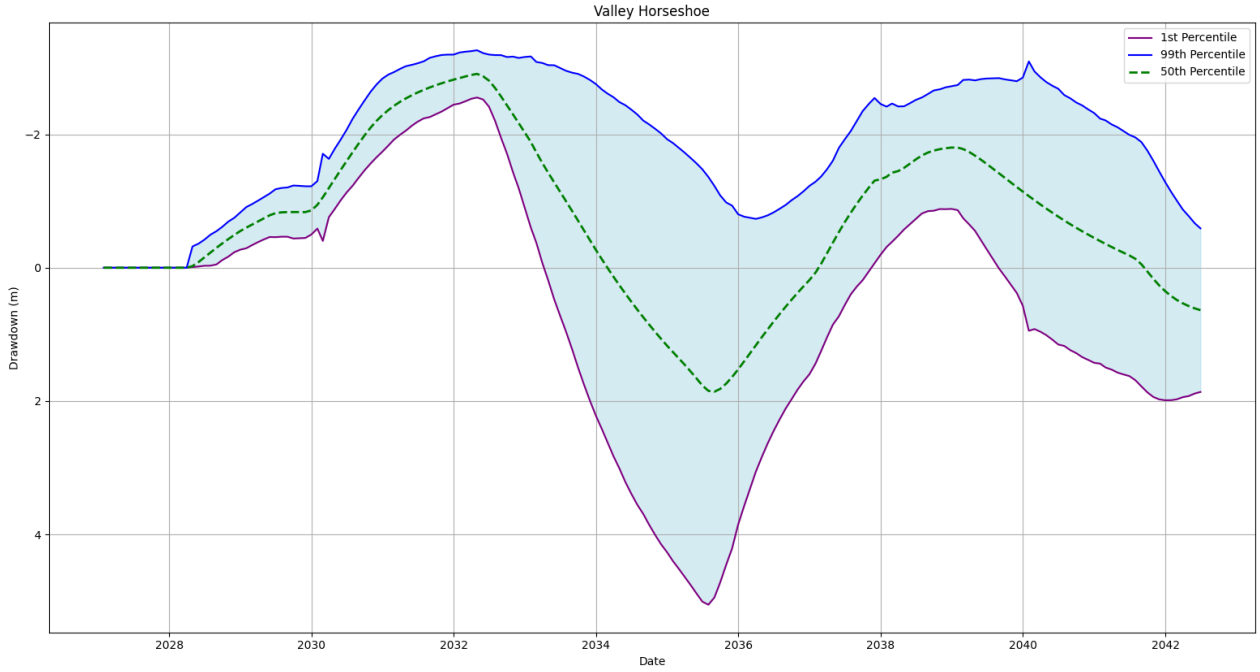

Figure E-16 Predicted aquifer recovery at T16 (valley Horseshoe)

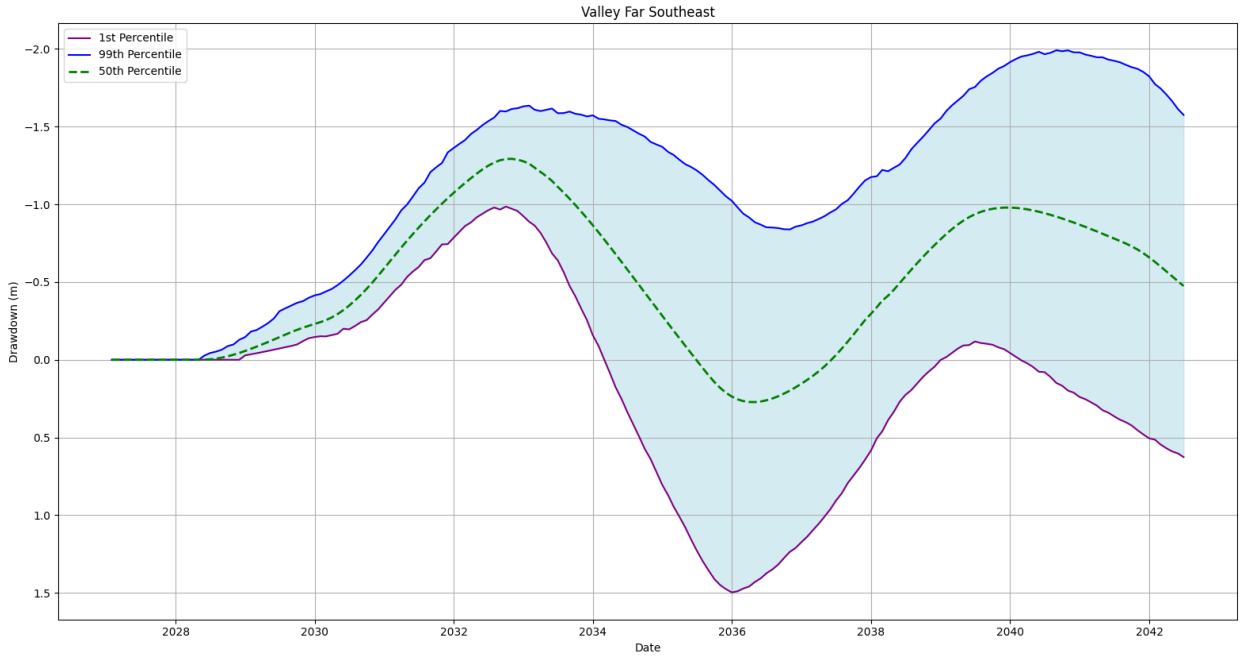

Figure E-17 Predicted aquifer recovery at T17 (valley Far Southeast)

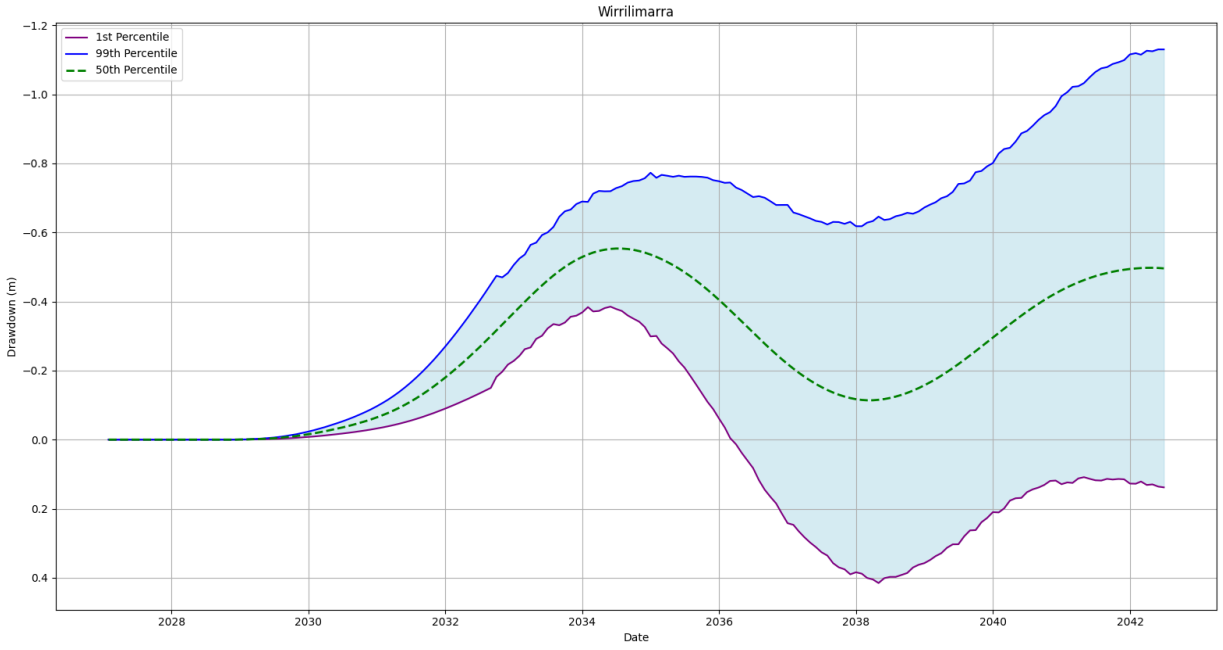

Figure E-18 Predicted aquifer recovery at T18 (Wirrilimarra area)